Towards a gene regulatory network for otic and epibranchial specification

Tambalo, Monica

Awarding institution:
King's College London

Towards a gene regulatory network for otic and epibranchial specification

by

Monica Tambalo

A thesis submitted to the King's College London's Higher Degree Office in partial fulfilment for the Degree of

Doctor of Philosophy

Department of Craniofacial Development and Stem Cell Biology
King's College London
London, UK, SE1 9RT

April 2015

Monica Tambalo, London. UK

ABSTRACT

Vertebrate sensory organs arise from the pre-placodal region (PPR) at the border of the neural plate, specified early during development. Differential activation of signalling pathways along the rostro-caudal axis patterns this territory to give rise to distinct placodes and ultimately to the olfactory epithelium, lens, inner ear and cranial ganglia. The aim of this project is to further investigate how sensory progenitor cells are restricted in fate to become specified as otic and epibranchial cells.

The otic placode is induced next to the developing hindbrain by a combination of FGF and WNT signalling, while the epibranchial placode is specified by sustained FGF signalling and BMPs. Downstream of these signals different transcription factors are activated sequentially to confer otic-epibranchial fate. However, their epistatic relationships and regulatory interactions are poorly understood. Gene regulatory networks (GRNs) are powerful tools to explain why cells behave the way they do and here I aim to uncover the network that controls otic-epibranchial specification. To this end, I have combined published data with results from new molecular screens to generate a preliminary GRN that contains around 50 otic and epibranchial specific transcription factors and their signalling inputs.

To establish the hierarchical interaction between all network components and their response to otic inducing signals I designed systematic perturbation experiments and exploited NanoString technology to quantify each component in the same tissue sample. Manipulation of signalling inputs reveals a temporal hierarchy of otic specification genes and points to a highly dynamic interaction between them. To identify new epistatic relationships among otic transcription factors, I employed loss-of-function approaches for key network components. In a complementary approach, I investigated the contribution of FGF on the otic chromatin landscape by ChIP-seq for histone modifications. Bioinformatic tools were used to interpret the data and regulatory elements for early FGF response genes were identified experimentally.

The emerging GRN will not only identify new key regulators for inner ear specification, but also the regulatory regions that integrate information to build a functional ear.

Table of contents

List of Figures

List of Tables

Acknowledgements

Four years in London, in CFD, and in the Streit lab… it has been a long but exciting journey. Not only I have learned how to open eggs (quickly and efficiently) but also how to think as a scientist. I met new people, and came into contact with many different cultures and habits that broadened my horizons.

Obviously this journey would have not been possible without the help and the support of my supervisor Prof Andrea Streit. I am very grateful to her for giving me this opportunity and for teaching me how to become a better scientist. I would also like to thank my second supervisor Albert Basson, Karen Liu's and Jeremy Green's groups as well as the UCL labs of Claudio Stern, Roberto Mayor and Paola Oliveri for the great discussions and their advice. A special thank also to our overseas collaborators in Marianne Bronner laboratory.

It has been a great pleasure to work in the Streit lab together with all the people who passed by during these years. We were relative small and became a big and tight-knit group, and I am really thankful to all of you. I like to acknowledge Timothy Grocott and Laura Lleras who first thought me how to work with eggs. I would like to thank Anneliese Norris and Mark Hintze, the 'small gang', for making the long hours spent at the microscope (dissecting small, almost invisible, tissues) become fun. Thanks to Jingchen Chen for teaching me a lot in the past years, to Maryam Anwar the best bioinformatician, to Ramya Ranganathan for her help and friendship, and to the more recent entries Mohi Ahmed, Ravindra Prajapati and Alice Gervasoni. It has been a great pleasure to work with all of you guys! I am also very grateful for the technical assistance of Ewa Kolano-Merlin, Fiorella Guerra, as well as former members' Annabelle Scott and Gael Molloy. Thanks to the whole CFD for the great moments in the past years, a special thanks to Angela and Rebecca for their precious help!

I would like to thank all my family and friends in Italy who, even if far away, have always helped me. There are also many new people I met in the UK who became very good friends. Finally, a special thanks to Margherita and Stefano for their love and support, this would have not been possible without you two!

Grazie di cuore a tutti!

Abbreviations

3D	Three-dimensional
ANOVA	ANalysis Of VAriance
ANR	Anterior Neural Ridge
AO	Area Opaca
aPPR	anterior Pre-Placodal Region
B	Border
BMP	Bone Morphogenic Protein
bp	base pair
CBP	CREB-binding protein
cDNA	complementary Deoxyribonucleic acid
ChIP	Chromatin immuno-precipitation
CHX	Cycloheximide
CNS	Conserved Non-coding Sequence
Cnt	Control
CREB	cAMP Response Element-binding protein
CTCF	CCCTC-binding factor
Dac	Dachshund
Dlx	Distal-less homeobox
DMSO	DiMethyl SulfOxide
DNA	Deoxyribonucleic acid
Epi	Epibranchial
ERK	Extracellular signalling-Regulating Kinase
eRNA	enhancer Ribonucleic Acid
EST	Expressed Sequence Tag
Etv	Ets Variant
Eya	Eyes absent
FC	Fold Change
FDR	False Discovery Rate
FGF	Fibroblast Growth Factor
FGFR	Fibroblast Growth Factor Receptor
Fox	Forkhead Box
GAPDH	GlycerAldehyde 3-Phosphate Dehydrogenase
Gbx	Gastrulation Brain Homeobox
GFP	Green Fluorescent Protein
GO	Gene Ontology
GRN	Gene Regulatory Network

H3K27ac	Histone H3 Lysine 27 acetylation
H3K27me3	Histone H3 Lysine 27 tri-methylation
H3K4me1	Histone H3 Lysine 4 mono-methylation
HAT	Histone acetyltransferases
HH	Hamburger and Hamilton
Hprt1	Hypoxanthine phosphoribosyltransferase 1
iAO	induced Area Opaca
Irx	Iroquois homeobox
MAPK	Mitogen-Activated Protein Kinase
mmV	Maxillomandibular trigeminal
MO	Morpholino
mRNA	mature RNA
Msx	Msh homeobox
NF	Neural Fold
NNE	Non-Neural Ectoderm
NP	Neural Plate
OEPD	Otic and Epibranchial Progenitor Domain
opV	ophthalmic trigeminal
OT	Otic
Otx	Orthodenticle homeobox
Pax	Paired box
PBS	Phosphate Buffered Saline
PCR	Polymerase Chain Reaction
PDGF	Platelet-Derived Growth Factor
PFA	Paraformaldehyde
Ph	Pharyngeal arch
Phox	Paired-like homeobox
PKC	Protein kinase C
pPPR	posterior Pre-Placodal Region
PPR	Pre-Placodal Region
qPCR	quantitative Polymerase Chain Reaction
RFP	Red Fluorescent Protein
RNA	Ribonucleic Acid
RPKM	Read Per Kilobase of exon per Million fragments mapped
Rplp1	Ribosomal protein large P1
rpm	rounds per minute
RT	Reverse Transcription
RT-qPCR	Reverse Transcription-quantitative Polymerase Chain Reaction

Sdha	Succinate dehydrogenase complex subunit A
siRNA	Small interfering RNA
Six	Sine oculis homeobox
So	Sine oculis
Soho	Sensory organ homeobox protein
Sox	SRY (sex determining region Y)-box
Spry	Sprouty homolog, antagonist of FGF signalling
ss	somite stage
Tcf	T-Cell-Specific Transcription Factor
TF	Transcription Factor
TFBS	Transcription Factor Binding Site
TGF	Transforming Growth Factor
Trig	Trigeminal
TSS	Transcription Start Site
VEGFA	Vascular Endothelial Growth Factor A
WNT	Wingless-type MMTV integration site family member

1. Introduction

1.1 The early steps of avian development

The domestic chicken (*Gallus gallus*) has been used as a model organism for embryological studies since ancient times. Eggs are widely available and embryos at a desired stage can be obtained by varying the time of incubation. Moreover, chicken embryos can be easily cultured inside or outside the egg and surgically manipulated (reviewed in Stern, 2005a). Since the molecular and biological processes of organ formation in chick are comparable to mammalian species, including humans, the chick embryo has been used for the present work as a model to study sensory organs and otic-epibranchial placode specification.

1.1.1 The blastula and gastrula stages in the avian embryo

Fertilisation of the chicken egg happens in the oviduct followed by secretion of the albumen and the shell to cover the egg. A common feature of birds, reptiles and fish is the discoidal meroblastic cleavage of the egg, where the embryo forms a disc of cells on top of the yolk, with cells initially open to the yolk (Bellairs et al., 1978). As the blastoderm grows, cells in the centre of the disc develop cell membranes and form the embryonic region of the embryo (area pellucida), while the yolk particle containing outer cells generate the extraembryonic area opaca. Initially, the epiblast is a single cell layer from which cells delaminate into the subgerminal cavity forming the hypoblast "islands" (Eyal-Giladi, 1984, Fabian and Eyal-Giladi, 1981, Kochav et al., 1980, reviewed in Stern and Downs, 2012). In the posterior part of the blastoderm a local thickening forms, known as Koller's sickle, which lies at the border between central epiblast and the posterior marginal zone in the area opaca (Koller, 1882, Callebaut and Van Nueten, 1994). Hypoblast cells spread forming a sheet, which expands anteriorly to cover the ventral side of the entire epiblast; this is subsequently displaced by a second layer, the endoblast (Eyal-Giladi et al., 1992, Bertocchini and Stern, 2002). The area opaca, hypoblast and endoblast cells will not contribute to the embryo proper, but form extraembryonic tissues.

As the endoblast forms, cells anterior to Koller's sickle accumulate in the lower layer forming a rod-like structure, the primitive streak, which is first visible at Hamburger and Hamilton stage 2 (Hamburger and Hamilton, 1951). During gastrulation, cells start to

ingress through the primitive streak into the blastocoel forming the endoderm and mesoderm (Eyal-Giladi et al., 1992, Bellairs, 1986). The primitive streak elongates and extends to around 60-70 percent of the total length of the area pellucida (from HH3 to HH4); the primitive groove appears at HH3^{+}. At HH4 the ingression of endodermal cells is complete, while mesodermal cells continue to ingress. At this stage, a thickening appears at the anterior end of the primitive streak forming the organiser, Hensen's node (Hensen, 1876). The avian node generates the axial mesoderm (notochord and prechordal mesoderm) and medial somites (Psychoyos and Stern, 1996) and is a crucial signalling centre for neural induction, patterning of the mesoderm and left-right axis formation.

1.1.2 The neurula stage in the avian embryo

Like the amphibian organizer Hensen's node secrets BMP antagonists (Chordin, Noggin and Follisatin) and the TGFβ ligand Nodal. The combination of both signals is important for neural induction (reviewed in Stern, 2005b). At neurula stage (HH5-6), mesodermal cells in the midline migrate anteriorly forming the head process and as Hensen's node regresses, the notochord starts to form and the embryonic axis is laid down in an anterior-posterior fashion. At this stage, differential gene expression subdivides the ectoderm into three domains from medial to lateral: the neural plate, the border region and the future epidermis (Garcia-Martinez et al., 1993, Hatada and Stern, 1994, Keller, 1975, Keller, 1976, Kimmel et al., 1990, Lawson, 1999). Cells in the border region are initially competent to give rise to neural, neural crest and sensory placodes precursors and non-neuron cell types (Basch et al., 2000, Bhattacharyya and Bronner-Fraser, 2008, Gallagher et al., 1996, Gallera and Ivanov, 1964, Groves and Bronner-Fraser, 2000, Hans et al., 2007, Koster et al., 2000, Kwon et al., 2010, Martin and Groves, 2006, Pieper et al., 2012, Selleck and Bronner-Fraser, 1995, Servetnick and Grainger, 1991, Storey et al., 1992, Streit et al., 1997, Waddington, 1934, Waddington, 1935, Waddington and Needham, 1936).

This study mainly focuses on the development of sensory placodes (also named cranial placodes). They will give rise to a diverse group of structures, contributing to the olfactory epithelium, eye, inner ear, distal portions of the cranial ganglia and, in fish and amphibians, to the lateral line. Cranial placodes form columnar epithelia next to the neural tube, they undergo epithelial-mesenchymal transition and then they contribute to the cranial sensory nervous system. They are neurogenic placodes with the exception of

the lens. Despite the differences of structures cranial placodes share high similarities early in development and they originate from a common progenitor domain (for review see: Schlosser, 2006, Streit, 2007, Grocott et al., 2012, Schlosser, 2010, Streit, 2008, Patthey et al., 2014). At HH6, sense placodes progenitors surround the neural plate in a horseshoe shape forming the pre-placodal region (PPR). At this stage the PPR is not uniquely composed of placode precursors but it is a mixture of neural crests, neural and epidermal cells. Subsequently, neural crest cells and sense placode precursors become progressively distinct. Within the PPR precursors for different sensory placodes are initially intermingled (Figure 1.1) and express a common set of genes (e.g. *Six1/4* and *Eya2*) (Ahrens and Schlosser, 2005, Bessarab et al., 2004, Esteve and Bovolenta, 1999, Ishihara et al., 2008b, Kobayashi et al., 2000, Litsiou et al., 2005, McLarren et al., 2003, Sato et al., 2010, Mishima and Tomarev, 1998, Pandur and Moody, 2000, Sahly et al., 1999, Ishihara et al., 2008a, Schlosser and Ahrens, 2004, Pieper et al., 2011). As somitogenesis starts (HH7-8) the lateral edge of the neural plate elevates forming the neural folds where neural crest cells begin to concentrate. At this point neural crest cells start to separate from the PPR (Bhattacharyya et al., 2004, Kozlowski et al., 1997, Streit, 2002).

The neural folds elevate further converging and fusing in the midline to form the neural tube. Neural crest cells begin to delaminate from the neural tube, migrate and contribute to a variety of structures (e.g. melanocytes, craniofacial cartilage and bone, muscles, peripheral nervous system and glia) (for review see: Betancur et al., 2010a, Sauka-Spengler and Bronner-Fraser, 2008). Around HH8 precursors for different sensory placodes start to separate until becoming fully restricted by HH15 (Streit, 2002, Bhattacharyya et al., 2004, Xu et al., 2008). However, a recent study has showed that there are no large-scale cell movements when the PPR segregates into different placodes in *Xenopus* (Pieper et al., 2011). The degree of overlap between sensory precursor cells and the extent of cell movements' contribution to placodes segregation are currently under debate. The main interest of this thesis is the specification of the otic placode, which is the first placode to become morphologically visible at HH10 at the level of rhombomeres 5 and 6, just anterior to the first somite (for review see Baker and Bronner-Fraser, 2001, Schlosser, 2010, Streit, 2007).

Even if the cranial placodes start to form at late neurula stages their induction begins much earlier. As described above, at early neurula stages genes expression and cell fate segregation define ectodermal domains. Expression of *Six* and *Eya* family members

marks the entire PPR region. In the next paragraphs I will revise the process of ectodermal regionalisation and specification of the pre-placodal region.

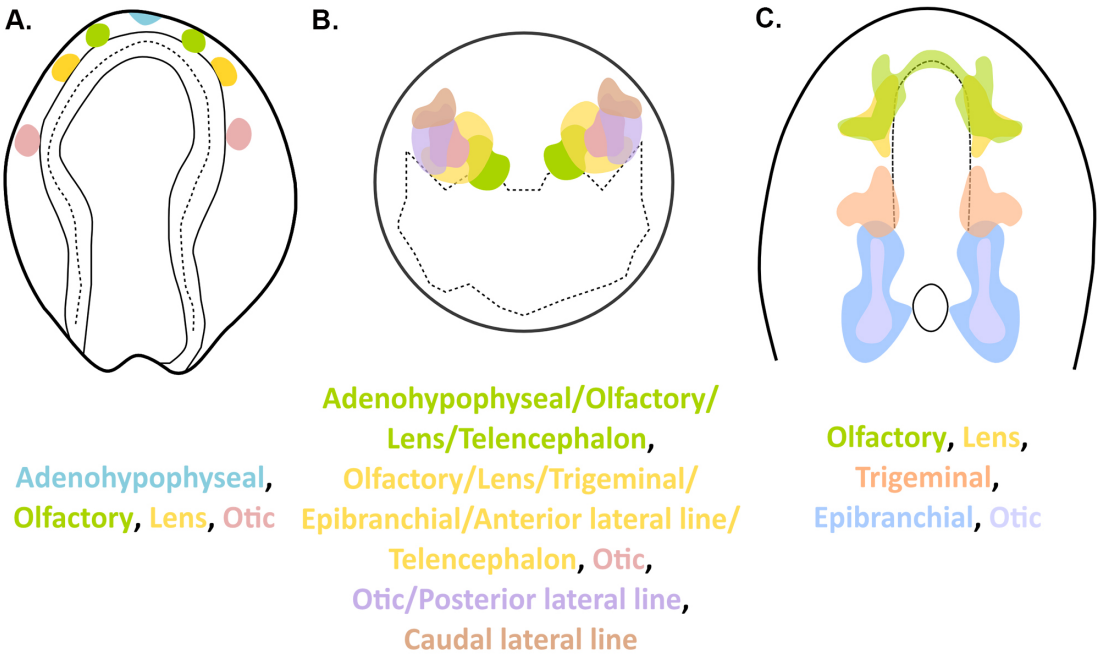

Figure 1.1 Fate maps of sensory placode precursors at mid gastrula or neural plate stages.
Schematic of the location on sense placode progenitors obtained from fate map studies in amphibian, fish and bird species. The location of the neural tube is shown with a dotted line. **(A)** Fate map of sensory placode progenitors of a neural plate stage salamander (*Ambystoma*) embryo (based on data from Carpenter, 1937). However, more recently in *Ambystoma* otic and lateral line placodes were found to originate from slightly more medial positions than what here represented (Northcutt, 1996). **(B)** Diagram showing the sense progenitors fate map of mid gastrula zebrafish embryo. (based on data from Kozlowski et al., 1997). **(C)** Schematic of a 0-1 somite stage chick embryo where the sensory precursors significantly overlap (based on data from: Bhattacharyya et al., 2004, Streit, 2002). Figure adapted from Schlosser (2006), Schlosser (2010).

1.2 Positioning sensory placode progenitors at the border of the neural plate

The subdivision of the ectoderm into distinct territories is a long, drawn out process that starts at pre-gastrula stages and continues until at least early neurula stages. Here, I will discuss the key events that position sensory progenitor cells at the border of the neural plate, including the signalling pathways and transcription factors that mediate this process of regionalisation. Although the anatomy of the early embryo and mode of gastrulation differs in different species, the general principles and gene expression domains are largely similar in chick, fish and *Xenopus*. Only few studies cover this early phase of development in mouse. Below I will mainly use the chick terminology, but include evidence from other species as relevant.

1.2.1 Regionalising the epiblast: signals and transcription factors

At blastula stages, the embryo proper (area pellucida in chick) is largely subdivided into two territories, identified by partially overlapping gene expression domains: pre-neural (e.g. *Sox3*, *Otx2*, *ERNI*, *Geminin*) (Bally-Cuif et al., 1995, Kroll et al., 1998, Papanayotou et al., 2008, Rex et al., 1997, Streit et al., 2000) and non-neural genes (e.g. *Dlx* genes, *Gata2/3*, *Msx1*, *Ap2*, *Foxi1/3*) (Brown et al., 2005, Hans et al., 2007, Hans et al., 2004, Hoffman et al., 2007, Knight et al., 2003, Li and Cornell, 2007, Luo et al., 2001a, Luo et al., 2001b, Matsuo-Takasaki et al., 2005, McLarren et al., 2003, Khatri et al., 2014, Khatri and Groves, 2013, Ohyama and Groves, 2004a, Papalopulu and Kintner, 1993, Pera and Kessel, 1999, Pera et al., 1999, Phillips et al., 2006, Pieper et al., 2012, Sheng and Stern, 1999, Streit and Stern, 1999, Suzuki et al., 1997, Woda, 2003, Yang et al., 1998). In the chick, pre-neural factors are enriched in the medial or central region of the epiblast, whereas non-neuronal transcripts are more abundant laterally (Figure 1.2).

Increasing evidence supports the idea that BMP and WNT signalling promote the expression of non-neural factors, while FGFs initiate pre-neural gene expression. The extraembryonic region and the non-neural ectoderm are sources of BMP and WNT factors (Skromne and Stern, 2001, Streit et al., 1998, Wilson et al., 2001). In *Xenopus*, inhibition of BMP in the animal cup favours neural differentiation, while its activation promotes epidermal fate (Hawley et al., 1995, Piccolo et al., 1996, Sasai et al., 1995, Wilson and Hemmati-Brivanlou, 1995, Xu et al., 1995). In addition, BMP regulates the expression of *Dlx5/6*, *Foxi1/3*, *Gata3* and *Ap2* genes. Misexpression of *BMP4* in the

animal blastoderm expands *Foxi1*, whereas overexpression of the BMP antagonist *Chordin* has the opposite effect (Matsuo-Takasaki et al., 2005, Kwon et al., 2010). BMP also positively regulates *Dlx3* and *Dlx5* (Feledy et al., 1999a, Luo et al., 2001a, Pera et al., 1999, Nguyen et al., 1998), *Gata2* (Kwon et al., 2010) and *Ap2* (Luo et al., 2003, Kwon et al., 2010) (Figure 1.4; Table 1.1). A two-phase model for BMP function has been recently proposed (Kwon et al., 2010). At late blastula stage, high levels of BMP establish the non-neural ectoderm; cells within this broad domain have both epidermal and pre-placodal potential. At late gastrula stage, expression of BMP antagonists at the border of the neural plate specifies the pre-placodal region (see below). The absence of BMP signalling is also required for formation of the neural plate. Furthermore, a combination of BMP and WNT signalling mediates *Gata2* and *Msx1* expression (Hong and Saint-Jeannet, 2007). In *Xenopus*, WNT signalling inhibits *Foxi1* and *Dlx3* (Beanan et al., 2000, Kwon et al., 2010, Matsuo-Takasaki et al., 2005, Pera et al., 1999, Suzuki et al., 1997, Wilson et al., 2001, Luo et al., 2003, Luo et al., 2002). In contrast, FGFs, emanated from the paraxial mesoderm and the organizer, seems to promote pre-neural gene expression. The chick hypoblast expresses *FGF8* and this has been linked to the initiation of *Sox3*, *ENRI* and *Geminin* in the overlying epiblast (Papanayotou et al., 2008, Streit et al., 2000, Albazerchi et al., 2007, for review see Wilson and Edlund, 2001). When the node is grafted in an ectopic position of the chick hypoblast *ERNI*, *Dlx5*, *Msx1*, *Sox2*, *Sox3* and *BMP4* are induced. The same genes, with the exception of BMP4, are ectopically expressed when FGF8 beads are located into the area opaca of a gastrula stage chick embryo (Litsiou et al., 2005, Streit et al., 2000, Streit and Stern, 1999). On the contrary, inhibition of FGF signalling by SU5402 causes the loss of the border genes *ERNI* and *Sox3* (Streit et al., 2000). Hence, prior to gastrulation, the antagonistic interplay of FGF and WNT/BMP signalling initially divides the epiblast into pre-neural and non-neural territories.

These two large overlapping domains become further subdivided during gastrulation as the primitive streak and neural plate form. Non-neural genes *Gata2/3* and *Foxi1/3* become restricted laterally whereas *Ap2*, *X-Dlx3* and *Dlx5/6* expression touch the neural plate (Figure 1.2) (Khudyakov and Bronner-Fraser, 2009, Feledy et al., 1999b, Kwon et al., 2010, Luo et al., 2001b, Pieper et al., 2012, Streit, 2002, Woda, 2003). The expression of these genes is conserved across species with some exceptions: chick *Dlx3*, unlike the fish and *Xenopus* homologues, is expressed similar to pre-neural genes, whereas expression of chick *Dlx5/6* is comparable to *X-Dlx3* and zebrafish *Dlx3b/4b* (Khudyakov

and Bronner-Fraser, 2009, Luo et al., 2001b, Pera and Kessel, 1999, Kaji and Artinger, 2004). Likewise, genes later confined to neural crest cells are initially present in the pre-neural territory (e.g. *n-Myc* and *Pax3/7*) (Khudyakov and Bronner-Fraser, 2009), suggesting that the neural crest and the pre-neural lineage may share a common regulation. Additional genes start to be expressed in the prospective neural region: *Zic1-5* (Elms et al., 2004, Elms et al., 2003, Gamse and Sive, 2001, Inoue et al., 2007, Merzdorf, 2007, Mizuseki et al., 1998, Nakata et al., 1997, Nakata et al., 1998), chick *Dlx3* (Khudyakov and Bronner-Fraser, 2009), *Sall1* (Bohm et al., 2008, Sweetman et al., 2005) and *Sall4* (Barembaum and Bronner-Fraser, 2007) (Figure 1.2). Furthermore, signals from the organiser promote neural induction and the definitive neural marker *Sox2* starts to be expressed exclusively in the neural plate (Rex et al., 1997, Streit et al., 1997, Uchikawa et al., 2003). At late gastrulation, the territory between neural and non-neuronal domain is named the 'neural plate border' (Moury and Jacobson, 1989, Streit and Stern, 1999, Zhang and Jacobson, 1993), where precursors for neural, neural crest, placodes and epidermis are intermingled (Ezin et al., 2009, Fernandez-Garre et al., 2002, Garcia-Martinez et al., 1993, Hatada and Stern, 1994, Puelles et al., 2005). A key event that will lead to *Six* and *Eya* expression is the induction of *Irx1*; in *Xenopus Irx1* is negatively regulated by BMP and positively by WNT and FGF signalling (Bellefroid et al., 1998, Glavic et al., 2004, Gomez-Skarmeta et al., 2001, Khudyakov and Bronner-Fraser, 2009, Goriely et al., 1999).

1.2.2 Transcription factor function in border specification

While different signalling pathways regulate the expression of transcription factors, these factors themselves play and important role for positioning the neural plate border.

Members of the *Msx* and *Dlx* family are initially induced by BMP and seem to restrict neural fate to the medial territory, the developing neural plate. Dlx family members antagonise neural plate formation while promoting neural plate border fate (Kaji and Artinger, 2004, McLarren et al., 2003, Sato et al., 2010, Solomon and Fritz, 2002, Woda, 2003). In zebrafish, Dlx3b/4b loss-of-function experiments affect the specification of the pre-placodal region and also sensory placodes are affected, while Dlx3b overexpression expands the PPR (Solomon and Fritz, 2002, Kaji and Artinger, 2004). A similar function has been reported for *Xenopus* Dlx3; its overexpression expands the border region at the expense of the neural plate, whereas misexpression of a repressive form of Dlx3 causes

the loss of border fate (Woda, 2003). In chick, overexpression of Dlx5 promotes the border markers *Msx1*, *BMP4* and the pre-placodal gene *Six4*, while it reduces *Sox2* and *Sox3* expression (McLarren et al., 2003). Recently, Dlx5 has been shown to directly regulate *Six1* through binding to its rostral enhancer (Sato et al., 2010) suggesting that in addition to playing a role in setting up the neural plate border, it may also directly regulate pre-placodal fate.

Moreover, Dlx proteins function during neural crest development but their role is complex. In *Xenopus*, *Dlx* genes present differences in their expression: *Dlx5* is expressed in epidermis, PPR and neural crest, while *Dlx3* is not present in neural crest cells (Luo et al., 2001b). Overexpression of Dlx3 causes inhibition of neural crest markers, while Dlx5 appears not to affect neural crest formation (Luo et al., 2001b). More recently, both Dlx3 gain- and loss-of-function decrease the level of neural crest gene expression (Pieper et al., 2012). Evidence in zebrafish suggests that Dlx3b/4b function non-cell autonomously in neural crest development (Kaji and Artinger, 2004). Overall these observations suggest that the level of Dlx protein is important for normal neural crest formation.

Like Dlx genes, the transcription factor *Msx1* has been positioned downstream of BMP signalling and it is involved in epidermal specification at the expense of neural differentiation (Suzuki et al., 1997, Ishimura et al., 2000, Yamamoto et al., 2000, Tribulo et al., 2003). *Msx1* is also important for neural crest development; its overexpression is sufficient to induce the expression of neural crest markers (Phillips et al., 2006, Monsoro-Burq et al., 2005, Tribulo et al., 2003). A complex interaction between Msx1 and Dlx proteins seems to take place, where *Msx1* reduction helps to restore pre-placodal fate in zebrafish *Dlx3b/4b* morphants (Phillips et al., 2006). Their reciprocal interaction seems to refine the neural plate border region: Msx1 favours the epidermal fate and neural crest and represses pre-placodal fate, while Dlx genes promote PPR and inhibits neural differentiation. Thus, it is possible that Dlx and Msx genes mutually antagonise each other to position the neural plate border.

Like Msx and Dlx family members, Foxi1/3 is important for the repression of the neural fate and the promotion of non-neuronal genes. In frog and zebrafish, *in vivo* inhibition of *Foxi1a* suppresses the expression of the epidermal marker *keratin* and *X-Dlx3*, while simultaneously causing expansion of the neural territory with an enlargement of *Sox2* expression (Matsuo-Takasaki et al., 2005, Kwon et al., 2010). Foxi1a function also seems

to be required for neural crest cell specification, possibly as a consequence of its role in setting up then neural-non-neural border (Matsuo-Takasaki et al. (2005). Recently, chick *Foxi3* expression was reported in the neural plate border (Khatri et al., 2014, Khatri and Groves, 2013). Here, *Foxi3* electroporation induced ectopic *Dlx5* expression and vice versa, suggesting the presence of a positive feedback loop between Foxi3 and Dlx5 (Khatri et al., 2014). Additional cross-regulation between the non-neuronal genes has been reported: in zebrafish, Gata3 and Ap2 regulates *Dlx3*, whereas in *Xenopus* Dlx3 and Gata2 positively regulate each other and also are required for *Dlx5* and *Foxi1a* expression (Kwon et al., 2010, Pieper et al., 2012). These evidences point to the importance of positive feedback loops in maintaining their expression and to a role of these genes as competence factors for placodal specification (see below).

Finally, the combination of Pax3 and Zic1 also antagonise neural specification in the posterior portion of the non-neural ectoderm since their knockdown expands the neural plate marker *Sox2* (Hong and Saint-Jeannet, 2007). Furthermore, together they promote neural crest fate, while Zic1 alone is positioned upstream of *Six1* (Hong and Saint-Jeannet, 2007, Plouhinec et al., 2014).

Together, this evidence points to a scenario where non-neuronal genes play a crucial role in restricting the neural plate and act in complex feedback loops to promote their own expression and maintain non-neural identity. It is still not clear how these non-neuronal proteins, which are mainly known as transcriptional activators, mediate such repression. It is plausible that they promote intermediate, yet unidentified, transcriptional repressors that in turn block neural fate. Dissection of the precise molecular cascade of such early events needs to be addressed in more detail, as does the question of whether the neural factors in turn repress non-neuronal cell fates. The main interactions are summarised in the gene regulatory network in Figure 1.4 and Table 1.1.

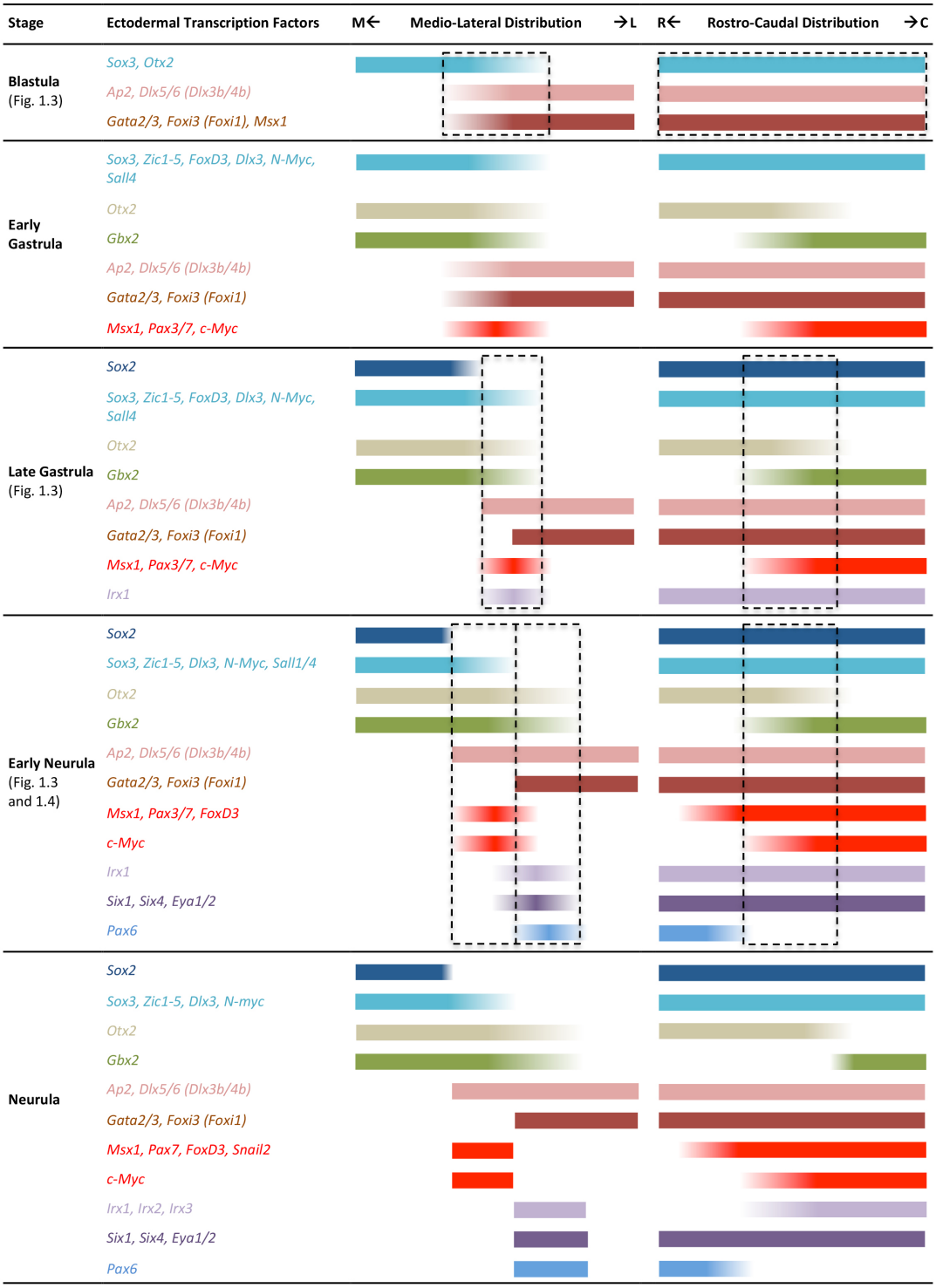

Figure 1.2 Spatial and temporal distinct ectodermal gene expression from blastula to neurula stages.

Transcription factors expressions from blastula to neurula stages along the medio-lateral and rostro-caudal axes are summarised here. TFs are organised into groups depending on their domain of expression and colour-coded. The dashed boxes indicate the regulatory network described in Figure 1.4 and Figure 1.6. Note: Ap2 is used as generic symbol for Ap2 family members, Dlx5/6 refers to chick and mouse whereas Dlx3b/4b to zebrafish, similarly Foxi3 is the chick and mouse name and Foxi1 is related to zebrafish (see text). Figure adapted from Grocott et al. (2012).

1.3 The Pre-placodal region (PPR)

At early neurula stages sensory placode progenitors and neural crest cells continue to be mixed at the border of the neural plate, but begin to segregate over time. Neural crest cells become confined to the neural folds, whereas placode precursors remain in the non-neural ectoderm outside the neural plate in the pre-placodal region (Bhattacharyya et al., 2004, Kozlowski et al., 1997, Streit, 2002, Xu et al., 2008). At PPR stage, placode precursors share common features and will differentiate and segregate to form individual sensory placodes only later in development (Bhattacharyya et al., 2004, Bhattacharyya and Bronner, 2013, Streit, 2002, Xu et al., 2008, Whitlock and Westerfield, 2000). The emerging model from the literature envisions that sensory placode precursors are induced by common inputs, express a common set of factors and possess similar characteristics (for review see Baker and Bronner-Fraser, 2001, Grocott et al., 2012, Schlosser, 2010, Streit, 2007, Schlosser, 2006, Streit, 2008). In the next section the evidence supporting this model will be discussed.

1.3.1 Properties of pre-placodal cells

Jacobson first formulated the hypothesis of a pre-placodal region in 1960s (Jacobson, 1963b, Jacobson, 1963c, Jacobson, 1963a, see also Torres and Giraldez, 1998). Performing classical embryological experiments he identified a horseshoe-shaped region at the border of the neural plate as the domain generating sensory placodes and defined potential inducing tissues (see below), as well as the time of placode commitment in newt (*Taricha torosa*). Rotating the placode domain along the rostro-caudal axis, Jacobson showed that initially placode precursors are competent to form any placode: when the PPR is rotated at early neural stages, cells will acquire placodal fate according to their new location. However, when the same experiment is performed at late neural stages PPR cells appear to be determined and develop according to their original fate independent of their new location (Jacobson, 1963c). Although not discussed specifically in these publications, these experiments were the first to put forward the notion that precursors for all placodes may share a common developmental history and that the PPR is a zone of unique competence. Morphological evidence also suggests that the PPR is a unique region: in amphibians and fish the PPR is visible as a thickening of the epithelium around the neural plate (Verwoerd and van Oostrom, 1979, Miyake, 1997). In other species, however such thickening is not present (Northcutt and Brandle, 1995, Schlosser and

Northcutt, 2000, Couly and Le Douarin, 1985). However, extensive fate map studies point to a corresponding location around the neural plate where sensory placode precursors lie (Xu et al., 2008, Whitlock and Westerfield, 2000, Streit, 2002, Kozlowski et al., 1997, Hatada and Stern, 1994, Bhattacharyya et al., 2004, Pieper et al., 2011).

At the transcriptional level PPR cells express a common set of genes, making them molecularly distinct from their neighbours (Figure 1.2). Importantly, members of the *Six* (*Six1* and *Six4*) and *Eya* (*Eya1* in *Xenopus* and zebrafish; *Eya2* in chick) families are expressed in a horseshoe domain in the entire PPR playing a central role in sensory placode formation (Ahrens and Schlosser, 2005, Bessarab et al., 2004, Esteve and Bovolenta, 1999, Ishihara et al., 2008b, Kobayashi et al., 2000, Litsiou et al., 2005, McLarren et al., 2003, Sato et al., 2010, Mishima and Tomarev, 1998, Pandur and Moody, 2000, Sahly et al., 1999, Ishihara et al., 2008a, Schlosser and Ahrens, 2004). The same *Six* and *Eya* genes will remain expressed in the sensory placodes (Bessarab et al., 2004, Esteve and Bovolenta, 1999, Ghanbari et al., 2001, Ishihara et al., 2008b, Kobayashi et al., 2000, Laclef et al., 2003, Oliver et al., 1995b, Ozaki et al., 2001a, Sahly et al., 1999, Ishihara et al., 2008a, Schlosser and Ahrens, 2004, Xu et al., 1997). The function of the Six/Eya core network will be discussed in section 1.3.4.

It is evident from the literature that cells need to acquire pre-placodal identity in order to contribute to placode formation (Martin and Groves, 2006). For example, while presumptive otic and trigeminal ectoderm is able to upregulate the otic/epibranchial marker *Pax2* if cultured in the presence of FGF2, anterior epiblast from $HH3^{+}$-4 chick embryos (tissue that never gives rise to placodes) does not (Martin and Groves, 2006). However, if anterior epiblast is first transplanted to the pre-placodal region, it starts to express the PPR genes *Eya2* and *Dlx* genes; if then cultured with FGF2 it turns on placode markers (Martin and Groves, 2006). In *Xenopus*, zebrafish and mouse overexpression of *Sox3*, *Six3* and *Pax6* can induce ectopic lenses, however only in the context of the anterior PPR (Altmann et al., 1997, Chow et al., 1999, Koster et al., 2000, Lagutin et al., 2001, Oliver et al., 1996). Likewise, overexpression of Spalt4 within, but not outside the pre-placodal ectoderm, induces ectopic otic gene expression and invagination to form an otic vesicle (Barembaum and Bronner-Fraser, 2007). Overall, these experiments highlight the importance of a "PPR state" for placode development and suggest a two-step model where cells first need to acquire PPR fate before they are committed to a placode identity.

An additional property of PPR cells is that independently of their anterior-posterior location they are initially specified as lens (Bailey et al., 2006). When different portions of the PPR are cultured in isolation they initiate a set of lens markers (*Pax6*, *L-Maf* and *δ-crystallin*) irrespective of their initial rostro-caudal level. FGFs appear to play a crucial role in repression of lens fate (Bailey et al., 2006, Lleras-Forero et al., 2013). The addition of FGF8 supresses *Pax6* expression and promotes the olfactory gene *GnRH1* (Bailey et al., 2006), while FGF signalling in the posterior PPR facilitates otic-epibranchial development (Lleras-Forero et al., 2013, Martin and Groves, 2006). Thus, lens seems to be the ground state of all pre-placodal cells and differential signalling along the anterior-posterior axis supresses lens fate, while allowing other placodes to develop.

In conclusion, cells need to become molecularly specified as PPR in order to give rise to sensory placodes. Inductive signals in the embryo are thereafter required to differentiate the individual placodes.

1.3.2 Signalling upstream of PPR induction

How is the pre-placodal ectoderm established in the developing embryo? Here, I will review the PPR-inducing tissues and the signals involved (Figure 1.3). Jacobson's original tissue recombination experiments suggest that signals from all tissues surrounding the PPR are required for its induction, as well as for induction of individual placodes. His experiments showed that signals from the endoderm are responsible for olfactory formation, while mesoderm-derived signals are required for lens and otic placodes, and also signals from the neural tube are required for placodes development (Jacobson, 1963a, Jacobson, 1963b). However, these experiments did not address specifically PPR induction due to the lack of a specific read out. More recently, the availability of molecular markers, both for the PPR and individual placodes, has allowed this issue to be assessed in depth.

The neural plate identity is established prior to the PPR and occupies the ectoderm medial to it. It therefore represents a candidate tissue to induce PPR in a planar fashion. Indeed, neural plate grafts into competent ectoderm induces ectopic *Six1* expression in *Xenopus* (Glavic et al., 2004, Ahrens and Schlosser, 2005, Woda, 2003) and in chick (Litsiou et al., 2005). However, the neural plate lacks the ability to induce genes like *Eya2* and *Six4* in chick, and unlike in frogs *Six1* is first induced in the graft itself, and only after long-term

exposure in the host ectoderm (Litsiou et al., 2005). These results suggest that additional signals are likely to play a role in PPR induction. In *Xenopus*, while the dorso-lateral mesoderm underling the PPR is not sufficient to induce *Six1* in competent belly ectoderm, it is required for proper *Six1* expression since its removal leads to reduction of *Six1* (Ahrens and Schlosser, 2005). Likewise, in chick lateral head mesoderm is also needed for PPR specification, and in addition is sufficient to induce the full set of PPR markers (*Six1*, *Six4* and *Eya2*) when grafted in a competent extraembryonic region (Litsiou et al., 2005). Finally, in chick anterior-mesendoderm in the midline is required for *Six1* and *Eya2* expression, as well as for the anterior PPR markers *Pax6*, *pNoc*, and *SSTR5* (Lleras-Forero et al. 2013); this finding is in agreement with Jacobson's tissue recombination experiments showing that endodermal signals are important for anterior PPR formation (Jacobson, 1963b, Jacobson, 1963a). Even if differences are observed between chick and frog it is evident that both tissues are crucial for PPR induction.

Concerning the signalling pathways mediating PPR induction, the same signalling pathways involved in the early ectodermal patterning (see section 1.2.1) are repeatedly used to impart PPR fate. When FGF is inhibited mesoderm and neural plate grafts are not able to upregulate pre-placodal genes suggesting that FGF is required for proper PPR induction (Ahrens and Schlosser, 2005, Litsiou et al., 2005). In chick, inhibition of FGF signalling by electroporation of a dominant-negative form of *FGFR1* causes expansion of the neural crest markers *Msx1* and *BMP4* into the PPR (Stuhlmiller and Garcia-Castro, 2012). Furthermore, FGF is sufficient to induce a subset of PPR genes: FGF8-coated beads induce *Eya2* in chick extraembryonic ectoderm, but are not sufficient for *Six1/4* (Litsiou et al., 2005). Comparably, in frog *FGF8*-injected animal caps, when grafted into the belly ectoderm, are not able to expand endogenous *Six1* (Ahrens and Schlosser, 2005). Interestingly, FGF signalling only seems to be required to initiate PPR induction, but is not necessary to complete it: when FGF is inhibited 5 hours after a graft of mesoderm into competent ectoderm PPR continues normally. Together these results indicate that while FGF signalling plays an important role, additional signals must mediate PPR formation.

Among these signals is the BMP pathway: treatment of zebrafish embryos with dorsomorphin, a pharmaceutical inhibitor of BMP, leads to loss of PPR fate (Kwon et al., 2010) and misexpression of BMP antagonists expands the PPR domain both in chick and frog but it is not sufficient for PPR induction (Ahrens and Schlosser, 2005, Glavic et al.,

2004, Litsiou et al., 2005, Brugmann et al., 2004). These findings suggest the requirement of a combination of signals for PPR formation. Indeed, in *Xenopus* ectopic FGF8 expression in the ventral ectoderm together with BMP inhibitors can induce *Six1* (Ahrens and Schlosser, 2005). However, the equivalent experiment in chick embryo does not lead to *Six1* induction; therefore additional factors are likely to play a role in birds (Litsiou et al., 2005). The discrepancy between the two systems may be due to technical differences, differences in stages used or to species-specific mechanisms of PPR induction.

The WNT pathway is a good candidate to regulate PPR formation. In birds, WNT ligands seem to surround the PPR; they are expressed in the lateral mesoderm next to the PPR and in the trunk mesoderm posterior to it (WNT8c; Litsiou et al., 2005), in the trunk ectoderm (WNT6; Garcia-Castro et al., 2002, Schubert et al., 2002) and in the neural folds (WNT1; Chapman et al., 2004, Galli et al., 2014) (Figure 1.3). Misexpression of WNT antagonists, *Crescent* and *Frzb1*, leads to expansion of the pre-placodal domain in both *Xenopus* and chick (Brugmann et al., 2004, Litsiou et al., 2005). In contrast, when WNT is activated ectopically in the PPR the sensory precursors markers *Six1*, *Six4* and *Eya2* are lost whereas the neural crest genes *Pax7* and *Slug* are gained (Litsiou et al., 2005, Brugmann et al., 2004). Thus, WNT signalling is important to delimit the pre-placodal territory and to distinguish sensory placode precursors from neural crest cells. In chick, only the combination of FGF signalling with WNT and BMP antagonists is able to induce PPR markers (Litsiou et al., 2005) suggesting that the combination of all three pathways is critical for PPR formation. Recently, neuropeptide signalling has been associated with anterior PPR development, in particular inhibition of somatostatin signalling in chick and zebrafish leads to *Eya2* reduction within the PPR (Lleras-Forero, 2011, Lleras-Forero et al., 2013). Thus, signals in addition to well-known developmental pathways may also play an important role in PPR specification.

The first model for PPR induction in chick was proposed by Litsiou and colleages in 2005 (Litsiou et al., 2005) and this is briefly summarised here (Figure 1.3). After the regionalisation of the ectoderm and the specification of the neural plate border (see section 1.2) the same signals are reused to specify the pre-placodal ectoderm. WNT signalling emanating from the lateral and posterior mesoderm, from the neural folds and from the trunk acts to limit the PPR (Garcia-Castro et al., 2002, Litsiou et al., 2005, Schubert et al., 2002). BMP signalling is present in the lateral ectoderm and cooperates in restricting the PPR fate (Fainsod et al., 1994, Faure et al., 2002, Liem et al., 1995, Streit

et al., 1998, Streit and Stern, 1999). The mesoderm underlying the PPR is a source of FGF ligands and of WNT and BMP antagonists (Ogita et al., 2001, Ohuchi et al., 2000, Shamim and Mason, 1999, Lunn et al., 2007, Stuhlmiller and Garcia-Castro, 2012) and these signals seem to protect the overlying ectoderm from inhibitory influences (BMP, WNT) and are crucial for specification of sensory precursors cells through the activation of *Six* and *Eya* genes. In addition, WNT and BMP signals appear to mediate the segregation of neural crest and sensory precursors cells. In a first phase, FGF induces the border region in which neural crest and placodes are intermingled (see section 1.2.1). In a second phase, WNT and BMP specify neural crest cells (Litsiou et al., 2005, Stuhlmiller and Garcia-Castro, 2012, Patthey et al., 2008, Steventon et al., 2009, Steventon and Mayor, 2012, LaBonne and Bronner-Fraser, 1998, Mayor et al., 1997, Monsoro-Burq et al., 2005, Villanueva et al., 2002). In summary, high levels of WNT and BMP signalling at the edge of the neural plate promote neural crest specification, whereas repression of the same pathways is required to allow sensory placode formation (for review see Betancur et al., 2010a, Grocott et al., 2012).

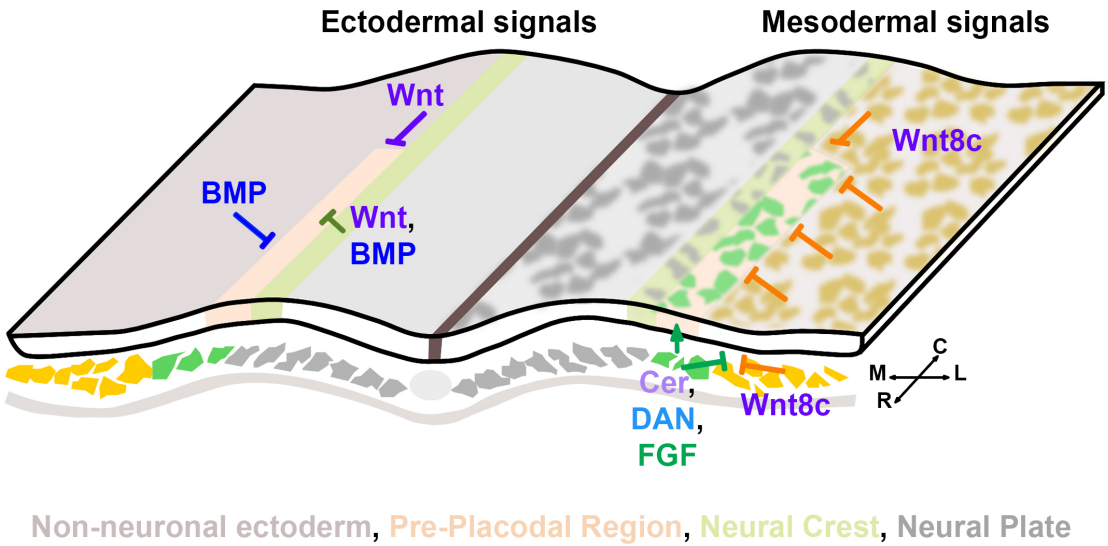

Figure 1.3 Inductive signals that position the PPR in the cranial ectoderm.
Schematic of a section through a neurula stage chick embryo, the rostro-caudal (R-C) and medio-lateral (M-L) orientation are indicated with arrows in the corner on the right. The ectodermal signals are represented in the left whereas on the right are the mesodermal signals. The pre-placodal region (light orange) is specified next to the neural crest cells (yellow-green) at the border of the neural plate (grey). The PPR is induced by FGF and the WNT (Cer) and BMP (DAN) antagonists, which are present in the cranial paraxial mesoderm (green). WNT signalling (violet) from the lateral and posterior mesoderm (yellow, right) works together with WNTs from the trunk ectoderm (left) to limit PPR fate. Additionally, BMP from the lateral ectoderm (taupe) prevents lateral expansion of the PPR in the non-neuronal ectoderm. Figure adapted from Litsiou et al. (2005).

1.3.3 Transcriptional upstream regulators of the Six and Eya network

The specification of the neural plate border is a crucial upstream event for PPR specification: factors expressed in this domain are among the upstream regulators of *Six* and *Eya*. Pre-neural and non-neural transcription factors, together with the specific border gene *Irx1*, are located upstream of *Six* and *Eya* family genes. Here, I briefly summarise the key inputs (Figure 1.3; Figure 1.4 and Table 1.1).

The non-neuronal transcription factors Dlx, Ap2, Foxi1/3 and Gata2/3 are important for the establishment of the sensory precursors domain. At late neurula stage, Dlx family members continue to antagonise the neural fate (Luo et al., 2001b, McLarren et al., 2003, Pieper et al., 2012, Woda, 2003) and promote the expression of pre-placodal genes. Misexpression of *Dlx5* in chick leads to upregulation of *Six4* in the non neural ectoderm and neural plate, while the crest gene *Slug* is repressed (McLarren et al., 2003). A similar

function is reported in frog, where misexpression of a repressive form of *Dlx3* or its knockdown causes a reduction of pre-placodal markers (Luo et al., 2001b, Pieper et al., 2011, Woda, 2003). Zebrafish mutants for Dlx3b/4b (b380 mutants) present a loss of the PPR followed by impaired development of the otic and olfactory placodes (Solomon and Fritz, 2002). A similar phenotype is observed upon Dlx3b/4b knockdown (Esterberg and Fritz, 2009, Kaji and Artinger, 2004, Solomon and Fritz, 2002). Additionally, the relative amount of Dlx and Msx proteins seems to be critical for correct PPR specification: in b380 zebrafish morphants where Msx genes are also knocked-down normal placode development is restored (Phillips et al., 2006). In this context it is interesting that an anterior pre-placodal enhancer (Six1-14) has been identified recently (Sato et al., 2010). Dlx5 and Msx1 directly bind to this enhancer and act as activator and repressor, respectively (Sato et al., 2010). This provides the first insight into the direct regulation of Six1. For review on the complex function of Dlx proteins during PPR and neural crest development see Grocott et al. (2012). The transcription factors Ap2, Foxi1/3 and Gata2/3 are also implicated in sensory precursors specification: in frog morpholino knockdown of these factors, individually or in combinations, causes abrogation of *Six1/4* and *Eya1* expression (Kwon et al., 2010, Pieper et al., 2012). While Dlx and Ap2 factors are also required for neural crest fate, Foxi and Gata proteins exclusively promote PPR formation. Overall, members of Dlx, Ap2, Foxi and Gata families play a crucial role in positioning the boundary between neural and non-neural territories and are important for PPR formation.

Another category of genes involved in PPR specification includes the neural crest transcription factors c-Myc, Pax3 and Msx1. c-Myc appears to regulate both PPR and neural crest cell development; cMyc knockdown in *Xenopus* results in the loss of both cell types (Bellmeyer et al., 2003). However, Pax3 and Msx1 act as repressors of the placodes. *Pax3* is induced by WNT signalling and in *Xenopus* it has been demonstrated to be a *Six1* repressor (Monsoro-Burq et al., 2005, Hong and Saint-Jeannet, 2007). The direct repression of *Six1* by Msx1 has been described above; in addition *Msx1* is a target of BMP signalling (Suzuki et al., 1997, Yamamoto et al., 2000, Maeda et al., 1997). It is likely that WNT through Pax3 and BMP through Msx1 repress *Six1* expression in the crest domain at neurula stages, therefore preventing expansion of the pre-placodal region.

An interesting cooperation is observed between Pax3 and Zic1 at the neural plate border. In *Xenopus*, Zic1 alone is able to promote *Six1* and *Eya1*, whereas when *Zic1* is

overexpressed together with *Pax3* this induction is lost and neural crest markers are upregulated (Hong and Saint-Jeannet, 2007, Monsoro-Burq et al., 2005). Contradictory results point to a positive regulation of *Six1* by Zic1 (Hong and Saint-Jeannet, 2007, Li and Cornell, 2007) as well as the opposite scenario (Brugmann et al., 2004). It is possible that the amount of Zic1 and Pax3 is critical in determining neural crest versus PPR induction (Hong and Saint-Jeannet, 2007), as well as the exact cellular context and timing of induction. Lastly, the specific neural plate border gene *Irx1* is expressed in the PPR just prior to the emergence of *Six/Eya* genes (Figure 1.2) (Glavic et al., 2004, Gomez-Skarmeta et al., 2001, Goriely et al., 1999, Khudyakov and Bronner-Fraser, 2009). Irx1 has been shown to regulate *Six1* positively; in *Xenopus* XIro1 overexpression induces *Six1*, while its downregulation causes *Six1* reduction (Glavic et al., 2004).

The role of neural genes in PPR formation is not fully established from the literature. In *Xenopus*, Sox3 promotes Sox2 expression, while overexpression of both Sox2 and Sox3 induces *Zic1* and *Geminin* (Rogers et al., 2009). However, placode-specific genes have not been analysed. In medaka, Sox genes positively regulate *Six1* and when misexpressed ectopic placodes form within the PPR (Koster et al., 2000). Additional investigations are required to accurately describe the role of Sox genes in early specification of pre-placodal cells.

In conclusion, Dlx, Ap2, Foxi and Gata family members appear to act as competence factors required cell-autonomously for PPR fate. Additionally, Zic1 and Irx1 also promote *Six1* expression. However, Msx1 and Pax3 promote neural crests and prevent the expansion of the pre-placodal domain. So far the enhancer associated with Six1 is uniquely active in the anterior portion of the PPR and only Dlx5 and Msx1 have been identified as direct regulators. To gain insight the molecular regulation of Six and Eya genes further investigations are required including the identification of the enhancer responsible for posterior *Six1* expression together with its interacting transcription factors. Direct versus indirect PPR regulators can only be separated after enhancer characterisation and lead to the improvement of the current network upstream of Six and Eya (Figure 1.4 and Table 1.1).

1.3.4 The role of Six and Eya family members in PPR formation

Placodal progenitors are molecularly distinct from the neural and non-neural cells because at neurula stages they express a unique set of genes: *Six* and *Eya* family members (Ahrens and Schlosser, 2005, Bessarab et al., 2004, Esteve and Bovolenta, 1999, Ishihara et al., 2008a, Kobayashi et al., 2000, Litsiou et al., 2005, McLarren et al., 2003, Mishima and Tomarev, 1998, Sato et al., 2010, Pandur and Moody, 2000). Additional factors are expressed in the PPR; although they are not specific to the PPR, they are yet important for restricting *Six* and *Eya* expression as described above (see section 1.3.3).

Six and Eya genes were initially identified in *Drosophila* as *sine oculis* (*So*) and *eyes absent* (*Eya*), respectively. In the fly they are required for normal eye development. The transcription factor *So* (Six homologue) cooperates with *eyes absent* (Eya homologue), *eyeless* (*Ey*; Pax homologue) and *dachshund* (*Dac*; Dach homologue) to form the fly eye. When misexpressed in the antenna or leg imaginal disks they act synergistically to form an ectopic eye (Bonini et al., 1997, Halder et al., 1998, Shen and Mardon, 1997, Chen et al., 1997). In contrast, loss of function mutants for So and Eya present complete or partial loss of the eye (Chen et al., 1997, Cheyette et al., 1994, Mardon et al., 1994, Pignoni et al., 1997a, Pignoni et al., 1997b, Serikaku and O'Tousa, 1994). Indeed, biochemical evidence indicates that So and Eya form a protein complex that functions as an activator to regulate retinal development (Giot et al., 2003, Jemc and Rebay, 2007, Pappu et al., 2005, Pauli et al., 2005, Pignoni et al., 1997a, Tanaka-Matakatsu and Du, 2008, Zhang et al., 2006). Recent findings point to a model where So also acts as a repressor, important for the inhibition of the antenna selector gene *Cut*. Therefore, in early phases of eye development repression of non-retinal genes seems to be necessary to allow eye formation (Anderson et al., 2012). Additionally, Drosophila *So* is located downstream of Ey (Pax6 homologue) and cooperates with Eya to promote *Dac* expression, together they form a regulatory loop which finally leads to eye development (Anderson et al., 2012, Chen et al., 1997, Shen and Mardon, 1997).

Homologues of the Drosophila Six (So, Optix and D-Six4) and Eya genes have been characterised in humans, mouse, chick and fish as well as in invertebrates. In vertebrates, six Six genes (Six1-6) and four Eya genes (Eya1-4) have been reported (for review see: Hanson, 2001, Donner and Maas, 2004, Wawersik and Maas, 2000). Members of the Six family present two conserved domains: a Six domain at the N-terminus involved in

protein-protein interaction and a homeodomain (HD) of 60 amino acids at the C-terminal for DNA binding (Pignoni et al., 1997a, Kobayashi et al., 2001, Ohto et al., 1999). Six factor function can vary from a repressor, when interacting with Groucho or Dach, to an activator, when associated with Eya (Kenyon et al., 2005a, Kenyon et al., 2005b, Rayapureddi et al., 2003, Li et al., 2003, Tessmar et al., 2002, Tootle et al., 2003, Zhu et al., 2002). Eya proteins also contain a number of conserved domains: an EYA domain at C-terminus of 217 amino acids is important for the interaction with Six and Dach, while at the N-terminus two proline-serine-threonine (PST) stretches are required for transactivation (Li et al., 2003, Rayapureddi et al., 2003, Tootle et al., 2003). The PST domain possesses phosphatase activity and this is important for switching the function of the Six-Eya-Dach complex from repressor to activator. Additionally, Dach and Eya can interact with CREB-binding protein (CBP), which functions as a histone acetyltransferase, possibly helping in the promotion of target genes transcription (Ikeda et al., 2002, Li et al., 2003).

Similar to Drosophila, in vertebrates Six and Eya genes play a crucial role in sense organ development: they are important for PPR specification and later for sensory placode development. Early in development, Six and Eya specify pre-placodal cells at the border of the neural plate. Misexpression of Six1/Eya2 promotes PPR fate, by upregulating *Six4*, at the expense of epidermis and neural crest (Christophorou et al., 2009, Brugmann et al., 2004). In contrast, knockdown or misexpression of a constitutive repressive from of *Six1* causes a loss of PPR fate (Brugmann et al., 2004, Christophorou et al., 2009). Unlike in the fly network, where the Pax6 homologue eyeless is upstream of *So* and *Eya*, in vertebrates it seems that Pax6 lies downstream of the Six/Eya cassette. This inversed network may explain why in chick misexpression of Six/Eya in competent ectoderm is not able to induce mature ectopic placodes (Christophorou et al., 2009), while in fly So and Eya are sufficient to induce ectopic eyes (Bonini et al., 1997, Halder et al., 1998, Shen and Mardon, 1997, Chen et al., 1997). When Six and Eya are knocked-down or mutated the development of all sense organs, the eye, ear and olfactory epithelium, as well as of the cranial ganglia is impaired (Chen et al., 2009, Christophorou et al., 2009, Friedman et al., 2005, Konishi et al., 2006, Kozlowski et al., 2005, Laclef et al., 2003, Li et al., 2003, Ozaki et al., 2004, Xu et al., 1999, Zou et al., 2006, Zheng, 2003, Zou et al., 2004, Ikeda et al., 2007). In Six1 and Eya1 knockouts mice the epibranchial placode is affected, hence the cranial sensory ganglia fail to develop and apoptosis is increased (Zou et al., 2004). In addition, in Six1 knockout mice the inner ear and nose are severely

affected together with defects in the craniofacial skeleton, and thymus and kidney are missing (Ozaki et al., 2004, Ikeda et al., 2007, Laclef et al., 2003, Zheng, 2003). Six4, which present a similar expression as *Six1*, is not essential for mouse embryonic development (Ozaki et al., 2001a). Functional redundancy with other Six genes could explain the absence of phenotypes in Six4 mice mutants; indeed double knockout of Six1 and Six4 augments the trigeminal defects observed in Six1 mutants (Konishi et al., 2006). Among the other family members, Six3 misexpression causes formation of ectopic optic vesicles in medaka and mouse (Lagutin et al., 2001, Oliver et al., 1996) and an expansion of the lens territory in chick (Liu et al., 2006). Furthermore, when Six3 is depleted, in mouse brain and lens development is affected (Lagutin et al., 2003, Liu et al., 2006). Six6 knockout mice present a hypoplastic hypophysis and retina (Li et al., 2002). When Six6 (XOptx2) is overexpressed in *Xenopus* increase in cell proliferation causes enlargement of the eye (Zuber et al., 1999). Additionally, Six5 mice mutants develop cataracts (Klesert et al., 2000, Sarkar et al., 2000).

Finally, human mutations in Eya1, Six1 and Six5 have been associated with Branchio-Oto-Renal syndrome (BOR), which is characterised by branchial, hearing and renal defects, while other patients present late-onset deafness and lens cataract (Abdelhak et al., 1997, Azuma et al., 2000, Johnson et al., 1999, Ruf et al., 2004, Schonberger et al., 2005, Wayne et al., 2001, Winchester et al., 1999, Zhang et al., 2004, Hoskins et al., 2007, Pham et al., 2005, Krug et al., 2011, Song et al., 2013). Additionally, Six3 mutations cause holoprosencephaly and microphthalmia and most of the cases are associated with cyclopia (Pasquier et al., 2000, Wallis et al., 1999), while in humans Six6 haploinsufficiency causes bilateral anophthalmia, the optic nerve and chiasma are absent and hypophysis defects (Gallardo et al., 1999).

It is therefore clear that Six and Eya genes are critical for the specification of sensory precursor cells, but also play a role in later sense organ development. However, their pan-placodal function cannot explain the differentiation of individual placodes and additional factors must work in parallel or downstream to regionalise the pre-placodal region and define the identify of distinct sensory placodes (Figure 1.6).

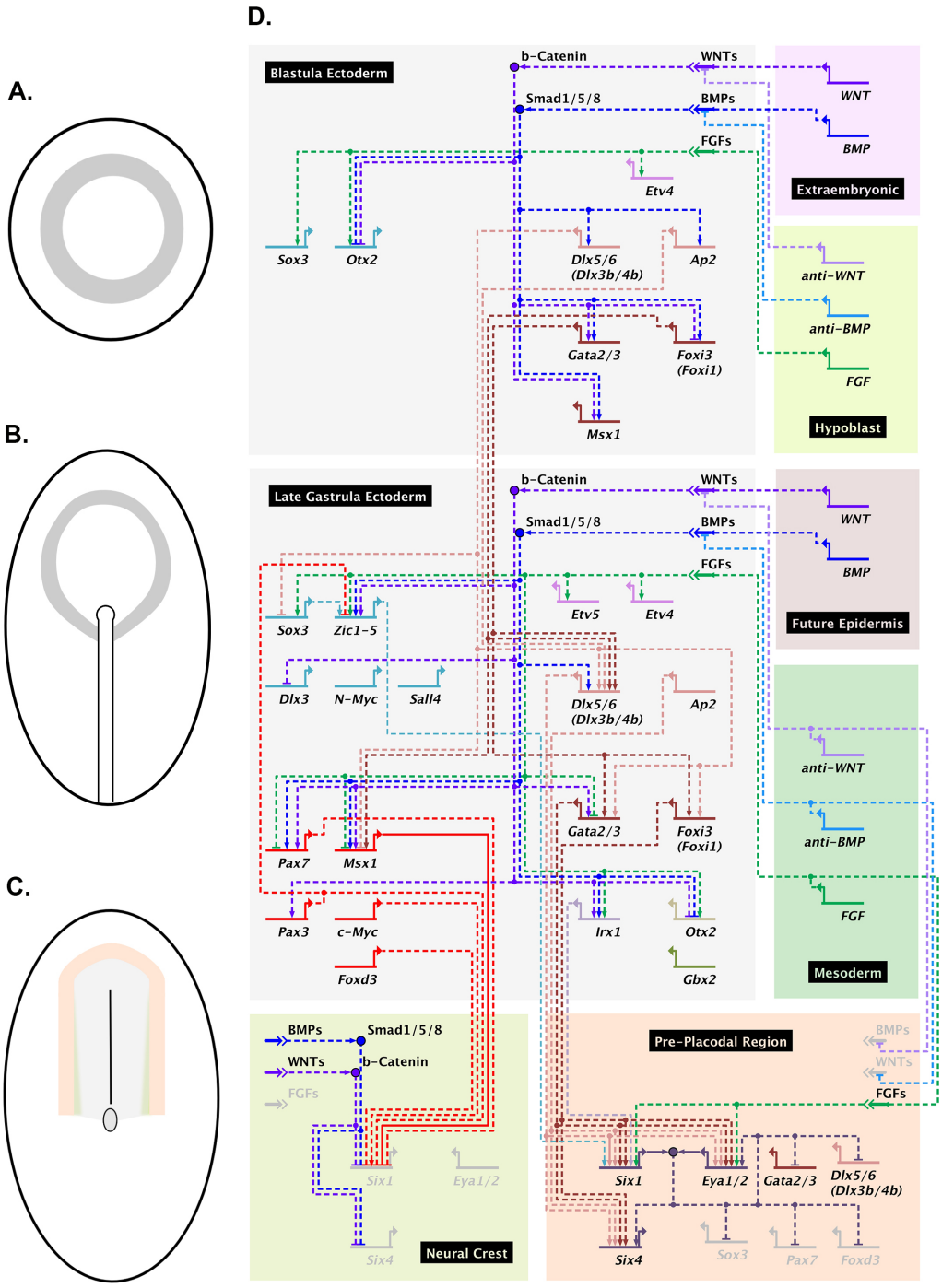

Figure 1.4 Gene regulatory network involved in PPR specification.
The main interactions involved in regionalisation of the ectoderm and specification of the PPR are summarised in a gene regulatory network from blastula to neurula stage. **(A-C)** Diagrams on the left represent the corresponding stages in the chick embryo. Different regions are colour-coded: in grey is the border domain, in light orange the PPR and in yellow-green the neural crests. **(D)** In the pre-streak ectoderm (blastula) gene expression is restricted by signals from the hypoblast and extraembryonic region. During gastrulation the early expressed genes in turn regulate a second group of genes at the border of the neural palate. At neurula stage, *Six* and *Eya* genes start to be expressed exclusively in the PPR, while they are repressed in neural crest cells. References for each interaction are reported in Table 1.1. Gene symbols are colour-coded as in Figure 1.2 accordingly to their expression domain. In the network a solid line represents experimentally verified direct interactions whereas dashed line indicates that such information is yet not available. Figure adapted from Grocott et al. (2012).

1.4 Regionalisation of the PPR

Although the entire PPR appears to have common features, it expresses *Six* and *Eya* genes homogenously and lens is the ground state of all sensory placodes, rostro-caudal patterning is early established within the PPR as it is specified. Recently, the characterisation of a specific anterior Six1 enhancer (Six1-14) points to a complex differential anterior to posterior regulation of *Six1* (Sato et al., 2010).

Otx2 and *Gbx2* are among the earliest genes to be regionally restricted, where *Otx2* is expressed in the anterior and *Gbx2* in the posterior PPR (Figure 1.2) (Acampora et al., 2001, Acampora et al., 1995, Bally-Cuif et al., 1995, Li et al., 2009, Simeone et al., 1992, Simeone et al., 1993, Tour et al., 2001, von Bubnoff et al., 1996). *Otx2* and *Gbx2* transcripts initially slightly overlap to form a boundary at neurula stage both in frog and chick (Steventon et al., 2012). The two-homeobox transcription factors mutually repress each other in the pre-placodal region as well as the mid-hindbrain boundary (MHB) (Steventon et al., 2012, Castro et al., 2006, Hidalgo-Sanchez et al., 1999, Katahira et al., 2000, Broccoli et al., 1999, Glavic et al., 2004, Joyner et al., 2000, Liu and Joyner, 2001, Millet et al., 1999, Wassarman et al., 1997). Additionally, activation of Otx2 targets is required for conferring anterior placode character (olfactory, lens and trigeminal placodes), whereas Gbx2 functions in the specification of the posterior otic and epibranchial domain (Steventon et al., 2012). Together, these findings suggest that the *Otx/Gbx* boundary could be a mechanism involved in rostro-caudal pattering of the entire ectoderm.

During somitogenesis, the PPR is further regionalised as evidenced by the appearance of genes differentially expressed along the rostro-caudal axis. Ultimately, this may lead to the formation of individual placodes each expressing a unique set of genes. The restricted expression of many factors in *Xenopus* has been reviewed in much detail by Schlosser (2006). Members of the paired-box family of transcription factors (*Pax* genes) correspond to PPR sub-domains with distinct fates with *Pax6* being expressed most anteriorly, followed by *Pax3* and finally *Pax2/8*. In the next paragraphs I will summarise the early steps of placode segregation and highlight the key events leading to differential Pax genes expression. In particular, I will be concentrating on the formation of the otic and epibranchial placodes; the details of their specification will be reviewed in sections 1.9 and 1.10 (Figure 1.7 and Table 1.1).

1.5 Cranial sensory placode and their derivatives

After the specification of the pre-placodal region sensory precursors segregate and form cranial placodes, which are visible as epithelial thickening next to the neural tube (Figure 1.5 B). The different placodes contribute, together with neural crest, to sensory organs (nose, eyes, inner ear and lateral line), the adenohypophysis and to the cranial sensory ganglia (Figure 1.5 C). A variety of cell types will originate from sensory placodes: neuroendocrine and endocrine cells, ciliated sensory receptors, sensory neurons, glia, and other supporting cells. The adenohypophysis and lens are non-neurogenic placodes, while cells in the remaining placodes undergo epithelial-mesenchymal transition, delaminate and form sensory neurons, or secretory cells or glia. After epithelial thickening, placodes which contribute to sense organs invaginate and form vesicles or pits, whereas cells in placodes contributing to cranial sensory ganglia (epibranchial and trigeminal) only delaminate and form neurons (for review see: Baker and Bronner-Fraser, 2001, Schlosser, 2006, Schlosser, 2010, Streit, 2008, Webb and Noden, 1993). Thanks to fate map studies the location of each placode has been described (Bhattacharyya et al., 2004, Carpenter, 1937, Couly and Le Douarin, 1985, D'Amico-Martel and Noden, 1983, Kozlowski et al., 1997, Streit, 2002, Whitlock and Westerfield, 2000, Xu et al., 2008, D'Amico-Martel, 1982, D'Amico-Martel and Noden, 1980, Eagleson et al., 1995, Eagleson et al., 1986, Rawles, 1936, Tam, 1989, Bhattacharyya and Bronner, 2013, Pieper et al., 2012, Modrell et al., 2014), their rostro-caudal position is reported in Figure 1.5 B.

The presumptive hypophyseal placode is located at the most rostral part of the neural ridge outside the neural plate and give rises to the adenohypophysis (or anterior pituitary), which is an endocrine organ involved in the regulation of several physiological processes comprising stress, growth, reproduction and lactation. Then, the olfactory placode is positioned next to the future olfactory bulb, undergoes complex morphogenetic processes to form the olfactory epithelium lining the nasal cavity and will produce different cell types including olfactory neurons, stem cells able to regenerate during lifetime and migratory neurons that finally localise in the brain. The non-neurogenic lens placode is located lateral to the diencephalon and next to the optic vesicles. It generates the crystalline lens of the eye composed of lens fibres and epithelial cells. More caudally, next to the midbrain, are positioned the ophthalmic and maxillomandibular trigeminal placodes. They are neurogenic patches from which neuroblasts delaminate to form the distal portion of the V^{th} trigeminal ganglia, which provides somatosensory innervation to

the face (D'Amico-Martel and Noden, 1983, Schlosser and Northcutt, 2000). In addition, the proximal parts of these ganglia as well as the glial cells have neural crest origin. Trigeminal neurons in mammals are responsible for pain, touch, and temperature sensations in the face; additionally they have some motility functions (biting, swallowing). The ophthalmic ganglion innervates eyeball, eye muscles, lacrimal gland, conjunctiva, the nose and the skin of the head. The maxillar nerve innervates the upper teeth, palate and pharynx while the mandibular nerve innervates the lower teeth, gums, mastication muscles, the floor of the oral cavity, and the mucosa of the tongue (Baker and Bronner-Fraser, 2001). At the level of the hindbrain (rhombomeres 5 and 6) are located the otic and epibranchial placodes. The complex structure of the inner ear arises from a simple epithelium: the otic placode (Figure 1.5 B-C and Figure 1.7 A-C), which invaginates to form an otic cup, and later closes giving rise to the otic vesicle; for more details see section 1.8. The epibranchial placodes, located lateral to the otic (Figure 1.5 B-C and Figure 1.7 A-C), generate the distal part of the VIIth, IXth and Xth cranial nerves, and similar to the trigeminal ganglion, neural crest cells also form the proximal part of each ganglion (for review see Baker and Bronner-Fraser, 2001). Lastly, in aquatic vertebrates (amphibians and fish), the pre- and post-otic lateral line placodes (Figure 1.1 B) generate neurons and sensory cells which give rise to a sensory system able to detect movements in the water and electric fields along the entire body (for review see Piotrowski and Baker, 2014).

In the next paragraphs I will review the more relevant interactions and the signals implicated in the specification of the cranial sensory placodes. Finally, I will describe in more details the epibranchial and otic placodes derivatives as well as the gene network involved in their regulation.

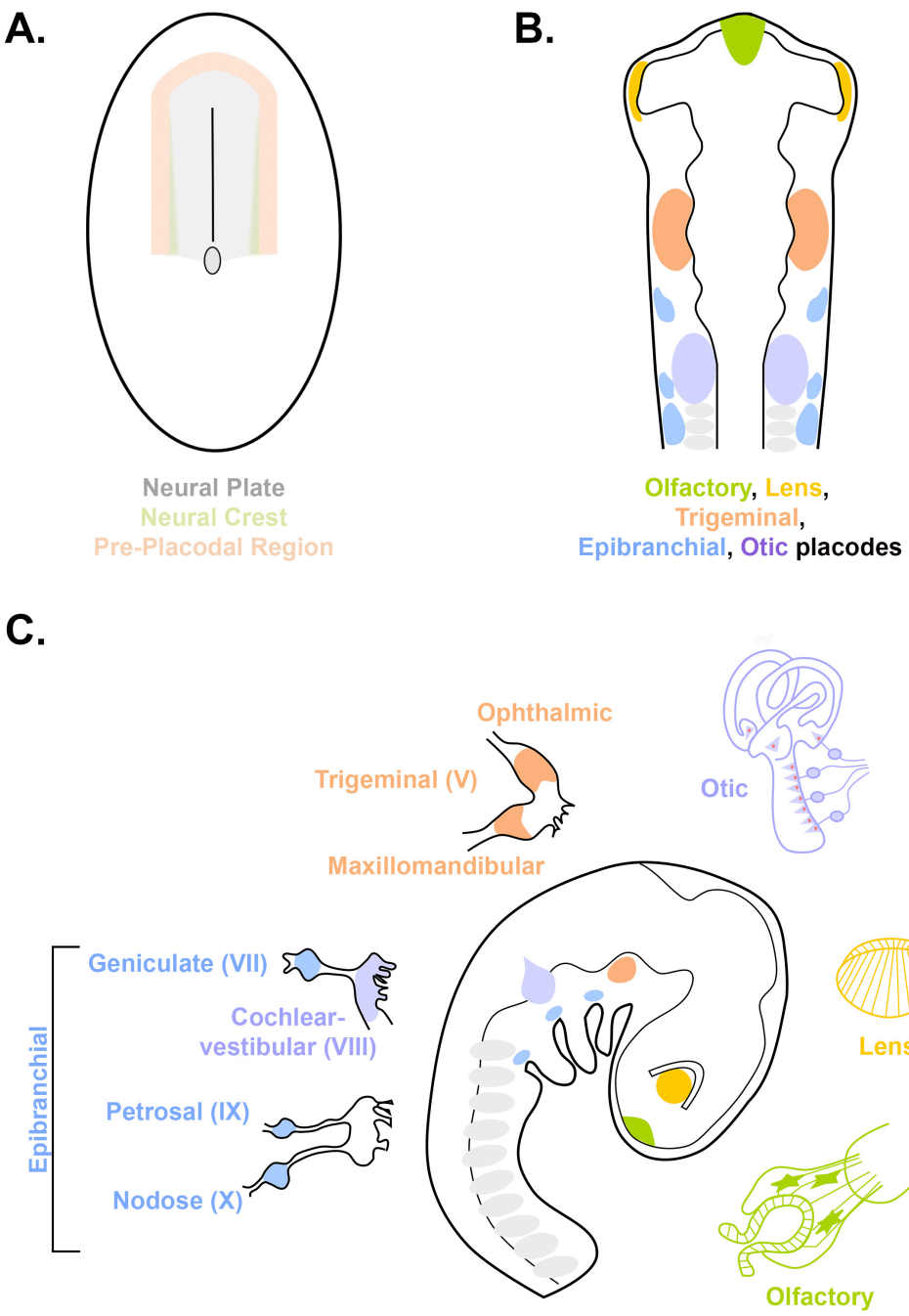

Figure 1.5 From the PPR to sensory placode derivatives.
(A) At head fold stage (HH6) the pre-placodal region (light orange) is molecularly distinct to the rest of the ectoderm. The PPR is specified at the border of the neural plate (grey) and neural crest (yellow-green). At this stage the boundaries between each territories are not very well defined and progenitors for each cell population are intermingled. Precursors for all sensory placodes are present in the PPR. **(B)** Schematic of a 10- 11-somite stage chick embryo. At this stage individual placodes are morphologically distinct as ectodermal thickening and are located at different rostro-caudal location in the developing head. Note: the adenohypophyseal placode is not represented in this drawing; it lies in the ventral midline. **(C)** The diagram shows a 3-day-old chick embryo with the sensory placodes highlighted. The correspondent placodal derivatives at later stages are represented and are colour-coded according to their placodal origin. Figure adapted from Grocott et al. (2012).

1.6 The anterior PPR: adenohypophysis, olfactory and lens placodes

Classical fate map analysis in *Xenopus*, zebrafish and chick has traced the origin of the anterior sensory placodes (adenohypophysis, olfactory and lens) to the more rostral portion of the PPR (Bhattacharyya et al., 2004, Bhattacharyya and Bronner, 2013, Dutta et al., 2005, Kozlowski et al., 1997, Pieper et al., 2012). These findings suggest that concomitant with PPR induction lineage bias towards a specific placodal fate is already implemented. Such early patterning of the PPR seems to correlate with the presence of genes strongly enriched in this PPR portion. In addition to *Otx2* (see section 1.4), *Pax6* (Bailey et al., 2006), *Pitx3* (Dutta et al., 2005), *Six3* (Liu et al., 2006), the neuropeptide *Nociceptin* and a receptor for somatostatin *SSTR5* (Lleras-Forero et al., 2013) are anteriorly localised. As described above Otx2 plays an important role in repressing *Gbx2* and therefore defining the anterior PPR. Otx2 is also associated with lens, olfactory and trigeminal placode formation. In *Xenopus*, misexpression of a constitutive repressive form of Otx2 prevents anterior placode development, however *Otx2* is not sufficient for ectopic induction of these placodes (Steventon et al., 2012). Therefore, additional factors must be required (Figure 1.6 C).

At early neurula stages, the paired-box gene *Pax6* starts to be expressed anteriorly, being the first Pax gene to be expressed in the head (Bailey et al., 2006, Zygar et al., 1998, Li et al., 1994). Some of the signals inducing Pax6 expression have been recently characterised: in chick and zebrafish, *Pax6* expression is lost when Nociceptin (Noc) or Somatostatin (SST) signalling is inhibited and eye development is impaired (Lleras-Forero et al., 2013). The source of SST is the midline mesoderm and indeed its ablation leads to loss of anterior placode character. In contrast, *Noc* is expressed in the anterior PPR itself and the posterior head mesoderm appears to prevent its expression in the caudal pre-placodal ectoderm (Lleras-Forero et al., 2013). In addition to *Pax6*, SST induces *Noc* in the overlying ectoderm, however Noc alone is unable to rescue the loss of *Pax6* in the absence of SST signalling. Thus, the two-neuropeptide pathways act in parallel and are both required for *Pax6* expression and normal lens development (Lleras-Forero et al., 2013). Although some of the signals upstream of *Pax6* have been characterised, little is known about the transcription factors that regulate its expression at PPR stages. Despite the identification of several enhancers no pre-placodal enhancer has been identified so far (Bhatia et al., 2014, Williams et al., 1998). *Pax6* regulation through Six1 has been described in chick where electroporation of a constitutive repressive form

of Six1 causes loss of *Pax6* expression (Christophorou et al., 2009). At the present it is unclear whether it is a direct or indirect regulation; therefore additional effort is required to characterize the early regulation of *Pax6* (Figure 1.6 and Table 1.1).

Local signalling sources are important for the segregation from the anterior PPR of the adenohypophysis, olfactory and lens placodes. The midline is a source of hedgehog signalling and promotes the formation of the adenohypophysis. Additionally, hedgehog represses lens and olfactory specification (Dutta et al., 2005, Herzog et al., 2004, Karlstrom et al., 1999, Kondoh et al., 2000, Sbrogna et al., 2003, Varga et al., 2001, Zilinski et al., 2005). In parallel to hedgehog, FGF3 from the diencephalon is also required for adenohypophysis formation; in zebrafish mutants for the FGF3 ligand (lia/FGF3 morphants) the pituitary fails to form (Herzog et al., 2004) (Figure 1.6 B).

Regarding the segregation between lens and the olfactory placode FGFs from the anterior neural ridge induce olfactory specification, while repressing lens. Ectopic FGF8 represses *Pax6* expression *in vivo*, and similarly PPR explants cultured with FGF8 lose the lens specification (Bailey et al., 2006). Furthermore, Pax6 and Dlx5 are important for the segregation of both placodes. Initially co-expressed in the anterior PPR, *Pax6* and *Dlx5* become complementary expressed in the future lens and olfactory placode, respectively (Bhattacharyya et al., 2004). FGF8, while repressing *Pax6*, promotes *Dlx5* expression (Bailey et al., 2006) and if Dlx5 is misexpressed in the lens territory *Pax6* is lost and the lens is smaller (Bhattacharyya et al., 2004). Thus, local FGF signalling promotes *Dlx5* expression, which in turn represses lens fate facilitating the segregation of both placodes. Pax6 maintain its own expression (Ashery-Padan et al., 2000) and activates downstream targets important for lens development. Additionally, Six3 maintains *Pax6* expression in the lens placode by directly binding to Pax6 lens enhancer (Pax6-EE; Liu et al., 2006) (Figure 1.2). Finally, these lead to the segregation of the lens and olfactory placodes (Figure 1.5).

As described above, experiments in chick indicate that the entire PPR initially has lens as 'ground state'(Bailey et al., 2006) raising the question of how in the embryo *Pax6* is exclusively expressed in the anterior PPR. Signalling factors like FGFs and WNTs are good candidates to mediate this process being present in posterior head mesoderm and in the neural plate. WNT signalling has been implicated in rostro-caudal pattering of the neural plate (for review see: Cavodeassi and Houart, 2012, Wilson and Houart, 2004) as

well as in establishing neural crest cells, which are not found at the most anterior edge of the neural plate (Carmona-Fontaine et al., 2007, Heisenberg et al., 2001, Kim et al., 2000, Li et al., 2009, Patthey et al., 2008, van de Water et al., 2001, Villanueva et al., 2002, Hollyday et al., 1995). Posterior enriched genes like *Gbx2* and *Irx1-3* have been linked to WNT signalling and are similarly important for anterior-posterior patterning the neural plate (Gomez-Skarmeta et al., 2001, Li et al., 2009, Braun et al., 2003, Itoh et al., 2002, Kiecker and Niehrs, 2001, Rhinn et al., 2009) as well as the PPR (Steventon et al., 2012). Moreover, WNT signalling activates *Pax3* (Canning et al., 2008, Lassiter et al., 2007), the paired-box gene expressed in the trigeminal placode, which in turn inhibits *Pax6* (Wakamatsu, 2011). As a consequence the ophthalmic trigeminal region becomes *Pax6* free (Figure 1.6 and Table 1.1). WNT signalling continues to inhibit *Pax6* even at later stages, limiting its expression to the lens placode (Grocott et al., 2011, Smith et al., 2005). Thus, WNT signalling, probably through these three factors, confines *Pax6* to the anterior portion of the PPR and lens territory. WNT antagonists present in the mesoderm underlying the anterior PPR (as described above in sections 1.2.1 and 1.3.2), in the anterior neural plate itself, and later in the lens territory (Grocott et al., 2011, Machon et al., 2010) allow lens morphogenesis to occur. In addition, FGF also suppress *Pax6* expression allowing the development of other placodes, like the olfactory, trigeminal, otic and epibranchial fate (Bailey et al., 2006, Freter et al., 2008, Maroon et al., 2002, Martin and Groves, 2006, Phillips et al., 2001, Urness et al., 2010, Wright and Mansour, 2003, Yang et al., 2013, Ladher et al., 2000, Nechiporuk et al., 2007, Nechiporuk et al., 2005, Nikaido et al., 2007, Sun et al., 2007) (Figure 1.6 and Table 1.1). While WNT signalling continues to repress lens (Grocott et al., 2011, Smith et al., 2005), FGF from the optic vesicle later promotes lens placode formation (Faber et al., 2001, Vogel-Hopker et al., 2000).

1.7 The intermediate PPR: the trigeminal placode

During development, the trigeminal placode is characterised by the expression of *Pax3*, which starts in the avian embryo at around 8 somites, later than the other family members, while in *Xenopus* it appears slightly earlier (Dude et al., 2009, Pieper et al., 2011, Schlosser and Ahrens, 2004, Stark et al., 1997). Prior to the appearance of *Pax3* some ophthalmic trigeminal (opV; profundal in anamniotes) precursors are *Pax6+* (Xu et al., 2008, Bailey et al., 2006, Bhattacharyya et al., 2004), while some maxillomandibular trigeminal (mmV; trigeminal in anamniotes) precursors are *Pax2+* (Xu et al., 2008),

while the majority of the mmV do not express any Pax gene. In anamniotes like *Xenopus* mmV/trigeminal precursors express *Pax6* at early stages and are located anterior to the profundal placode (Pieper et al., 2011). Since specific molecular markers have not been identified for the mmV/trigeminal placode very little is know about its specification.

It is not surprising that in the opV placode, when *Pax3* starts to be expressed, *Pax6* is lost as both factors mutually repress each other (Wakamatsu, 2011). An important upstream regulator of *Pax3* is Six1: in chick misexpression of a constitutive repressive form of Six1 causes loss of *Pax3* expression in the trigeminal domain (Christophorou et al., 2009). In Six1/Six4 double knockout mice even if the trigeminal neurons are generated they eventually die by programmed cell death (Konishi et al., 2006), again pointing to the upstream requirement of Six genes for *Pax3* expression. Additionally, Otx2 is necessary for *Pax3* but it appears not to be sufficient to drive *Pax3* expression ectopically in a competent ectoderm (Steventon et al., 2012). The key role of this Pax gene in trigeminal placode formation has been described in mouse, where Pax3 mutants (Splotch) present a smaller ophthalmic nerve due to the inability of the trigeminal placode to form (Serbedzija and McMahon, 1997). Moreover, misexpression of Pax3 itself in the head ectoderm is sufficient for the induction of opV markers (e.g. *FGFR4* and *Ngn2*), not for neuronal differentiation, suggesting the requirement of additional factors (Dude et al., 2009). Pax3 is also able to regulate *Eya2* and its own expression (Dude et al., 2009), and when misexpressed in the otic and epibranchial territory *Pax2* is downregulated and the otic vesicle fails to close (Dude et al., 2009). Thus, cross-repression between Pax genes is a recurrent mechanism important for the specification of individual placodes (Figure 1.6 and Figure 1.7).

The induction of Pax3+ cells in the opV is mediated by several signals emanating from neighbouring tissues (Figure 1.6 B). WNTs from the neural plate (Carmona-Fontaine et al., 2007, Heisenberg et al., 2001, Kim et al., 2000, Li et al., 2009, Patthey et al., 2008, van de Water et al., 2001, Villanueva et al., 2002, Hollyday et al., 1995) seem to play an important role. In chick, inhibition of canonical WNT signal causes the failure of cells to either maintain or adopt trigeminal character (Lassiter et al., 2007). However, WNT signalling is not sufficient to induce *Pax3* in a competent ectoderm (Lassiter et al., 2007), therefore additional factors must cooperate with WNT. It is likely that FGFs from the neural tube fulfil this role (Canning et al., 2008, Lassiter et al., 2009, Shigetani et al., 2000). The importance of WNT signalling in trigeminal development is evident also in

mammals: mouse mutants for WNT1$^{-/-}$ and WNT1$^{-/-}$; WNT3$^{-/-}$ double knockouts present a drastic reduction of the ophthalmic nerve (Ikeya et al., 1997). In addition, TGF-β family members BMPs emanate from the dorsal neural tube and later from neural crest derivatives; they have also been implicated in trigeminal induction: in frog BMP4 has the ability to induce *Pax3* ectopically (Rossi et al., 2008). Studies of dlx3b and dlx4b zebrafish mutants reveal that these factors contribute in a non-cell autonomous way to promote trigeminal identity via BMP activation (Kaji and Artinger, 2004). Lastly, PDGF signalling has been implicated in trigeminal induction: its receptor *PDGF receptor β* is expressed before the onset of *Pax3* (McCabe and Bronner-Fraser, 2008). *In vitro* and *in vivo* inhibition of PDGF signalling leads to *Pax3* reduction, while its overexpression increases the number of *Pax3* positive cells in the trigeminal region as well the number of neurons are in the condensing ganglia (McCabe and Bronner-Fraser, 2008) (Figure 1.6 B, E and Table 1.1). Thus, multiple signalling inputs have been associated with trigeminal opV development, however detailed understanding is still missing. Furthermore, the absence of mmV specific markers leaves open the question of how such a domain is induced and specified.

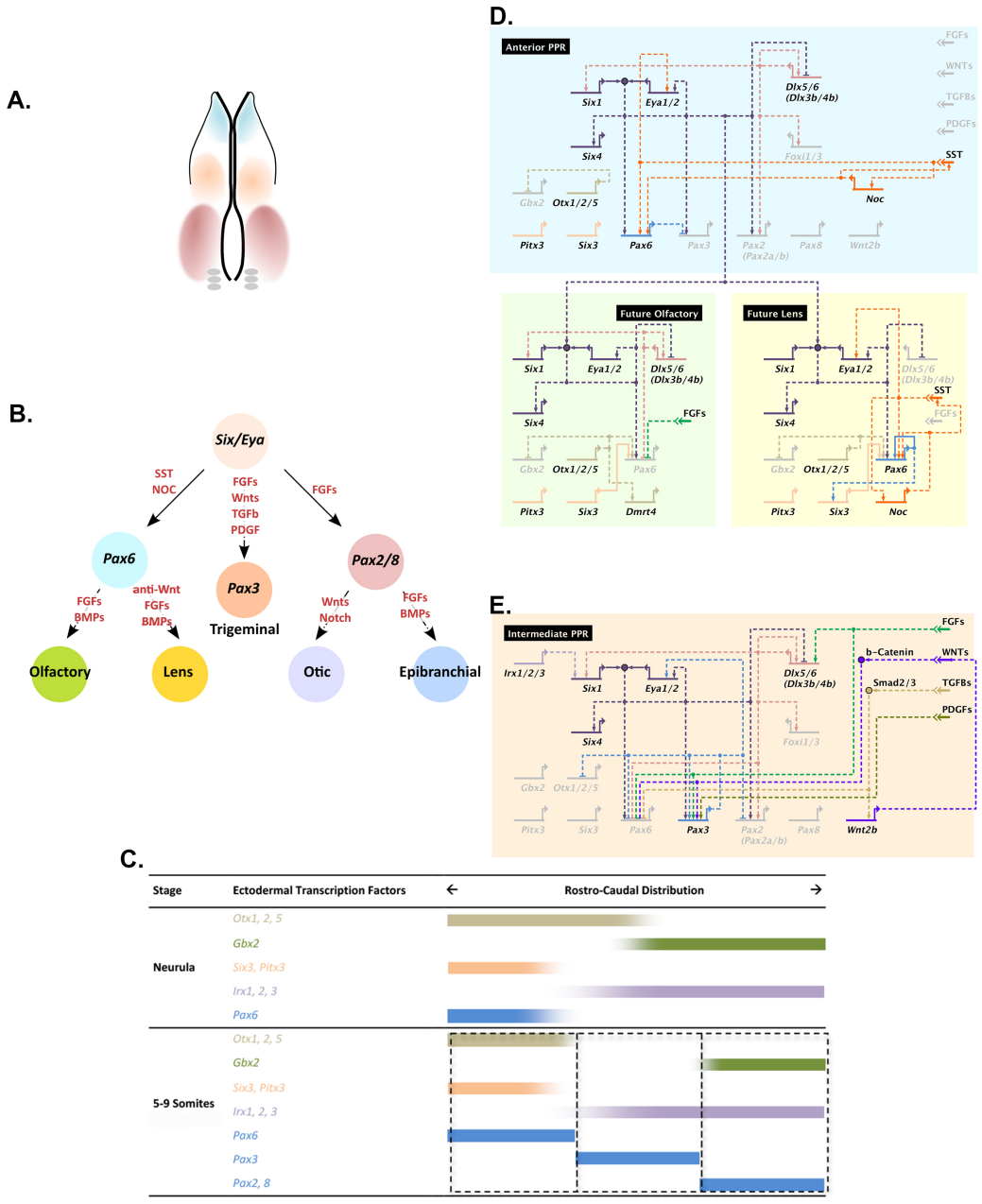

Figure 1.6 Regionalisation of the PPR and differentiation of the olfactory, lens and trigeminal placodes.

(A) Schematic of a chick embryo at 5-somite stage. Sensory organ progenitors are differentiated in: anterior (light blue), intermediate (orange) and posterior (pink) PPR domains. **(B)** Differential signals will induce the formation of distinct sensory placodes. A cell expressing *Six/Eya* genes depending on its rostro-caudal location in the embryo will undertake different fate paths. Cells located in the anterior PPR (light blue) will first express *Pax6* and later contribute to the olfactory (light green) or to the lens (yellow) placode. A cell in an intermediate position will express *Pax3* and form the trigeminal placode. Lastly, more posterior part of the PPR will express *Pax2/8* and differentiate into an otic (violet) or epibranchial (blue) placode. **(C)** Diagram showing differential transcription factors expression along the rostro-caudal axis at neurula and 5- 9-somite stage. **(D)** Gene network summarising the main interactions and signals restricting cells towards an anterior PPR fate and its later subdivision in olfactory or lens placodes. **(E)** Gene network promoting trigeminal fate. References for each interaction are reported in Table 1.1. In the network solid lines represent experimentally verified direct interactions, for the remaining dashed lines such information is yet not available. Figure adapted from Grocott et al. (2012).

1.8 The otic and epibranchial placodes

The main focus of my PhD thesis is the development of the otic and epibranchial placodes, therefore I will review the main aspects of their development in the next sections, giving an overview of the gene network emerging from the literature.

As mentioned above, the epibranchial placodes give rise to the distal part of the VIIth, IXth and Xth cranial nerves (Figure 1.5 C). The epibranchial placodes are the geniculate, petrosal and nodose. The geniculate placode, associated with the first branchial cleft, generates the geniculate ganglion and the distal parts of the VIIth cranial nerve and mainly innervates taste buds. In non-teleost fish the geniculate placode contributes to the spiracular organ and in birds to the paratympanic organ (for review see Baker and Bronner-Fraser, 2001). The petrosal placode is related to the second branchial cleft and generates the glossopharyngeal ganglion and the distal part of the IXth cranial nerve. Finally, the nodose placode, which is associated to the third branchial cleft, will give rise to the nodose ganglion and the distal part of the IXth cranial nerve. Fish, amphibians, and birds, extra nodose ganglia form above the more posterior branchial clefts (D'Amico-Martel and Noden, 1983, Landacre, 1912, Northcutt and Brandle, 1995, Schlosser and Northcutt, 2000, Yntema, 1937, Yntema, 1943). Together the petrosal and nodose ganglia innervate taste buds, the heart and visceral organs (for review see Baker and Bronner-Fraser, 2001) (Figure 1.5 and Figure 1.7 A-C).

The inner ear has a complex 3D structure involved in the transduction of sound and balance. It is composed of the cochlea involved in auditory perception and the vestibular sensory organs (semicircular canals and the vestibule) important for balance. The inner ear is composed of many different cell types, each important for a specific function, and their specification must be exquisitely coordinated with morphogenesis during development. Among them: hair cells are the mechano-receptors that convert the auditory or balance inputs in electrical signals, bipolar sensory neurons innervate the hair cells and transmit information to neurons in the vestibular and auditory nuclei in the brain stem, supporting cells, which vary in morphology and function, in general they are important as scaffold for the ear epithelium (e.g. pillar cells form a fluid-filled tunnel between the inner and outer hair cells, Deiters' cells are specialised supporting cell located in the organ of Corti that surrounds the outer hair cells etc.), and endolymph-secreting cells that maintain the correct composition of ions important for hearing and balance (for review

see: Fekete and Wu, 2002, Kelley, 2006, Forge and Wright, 2002). The entire inner ear develops from the otic placode (Figure 1.5 and Figure 1.7 A-C). As development progresses, the otic placode invaginates to form the otic cup, which closes to form the otic vesicle. The otic vesicle is a pseudo-stratified epithelium with an ellipside shape, which undertakes extensive proliferative growth and differentiation that results in the formation of the otocyst. Finally, the otocyst undergoes complex morphogenetic events that lead to the formation of the inner ear (for review see: Groves and Fekete, 2012, Bok et al., 2007).

1.8.1 Competence, specification, commitment and induction of the otic placode

To start understanding the process of otic specification is crucial to appreciate which tissues are competent to form the otic placode, how and when the otic placode is specified and committed, and finally which tissues are able to induce it (for review see: Cotanche and Kaiser, 2010, Corwin, 1992). The specific signals involved in otic and epibranchial induction will be summarised later in sections 1.9.1 and 1.10.1.

1.8.2 Which tissues are competent to form an otic placode?

In developmental biology the term *competence* refers to the ability of a tissue to adopt a specific fate when exposed to the appropriate environment. Such experiments generally require grafting of a test tissue into the region that usually adopts the fate to be assessed. Early last century, experiments in amphibians demonstrated that at early gastrula stages both the head and trunk ectoderm are competent to form the otic placode, however this ability is progressively restricted to the head ectoderm (Jacobson, 1963c, Yntema, 1933, Kaan, 1926) and at neurula stages seems to correspond to the PPR (Gallagher et al., 1996, Torres and Giraldez, 1998). At this stage, PPR rotation experiments along the rostro-caudal axis (see section 1.3.1) provide evidence that the anterior PPR is able to form an otic placode (Jacobson, 1963c) suggesting that the entire PPR is competent to acquire otic fate. In *Triton*, the limb bud is also competent to form an otic-like structure up to tailbud stages (Kaan, 1926) although the significance of this finding remains unclear. Moreover, in *Xenopus* FGF2 or 3 beads implanted at early neurula plate stage in the trunk ectoderm can induce the formation of ectopic otic vesicle (Lombardo et al., 1998, Lombardo and Slack, 1998).

In avian embryos, quail ectoderm from different locations was grafted into the presumptive otic territory of chick hosts and its ability to form an otic vesicle and to express otic markers was tested (Groves and Bronner-Fraser, 2000). The anterior epiblast from a stage HH3-4 embryo is competent to express otic markers (e.g. *Pax2*, *Notch*, *Sox3* and *BMP7*), to form an otic placode and cells can differentiate to form at least to one otic vesicle cell type (Groves and Bronner-Fraser, 2000). In addition, the head ectoderm, which normally forms the trigeminal placode, and the trunk ectoderm are competent and are able to express *Pax2* when grafted into the otic territory, but this ability declines with age and is lost by the 10-somite stage (Groves and Bronner-Fraser, 2000). It has also been shown that when the otic ectoderm is ablated neighboring tissue can regenerate it; this ability is lost after placode invagination (Kaan, 1926, Yntema, 1933). Thus, the evidence from different species shows that initially a broad area of ectoderm is competent to form an otic placode but this property declines with age; finally only the head ectoderm and PPR is competent.

1.8.3 When is the ectoderm specified to give rise to the otic placode?

The next question is when is the ectoderm specified as otic placode. A tissue is *specified* to a particular fate only if it is able to adopt such fate in a neutral environment, deprived of any inducing signals. However, such tissue could still be able to respond to inductive cues, for example when grafted elsewhere or when exposed to signalling molecules it may still adopt an alternative fate. Classically specification was addressed by the ability of a tissue to acquire specific morphological characteristics. Based on morphology in axolotl and Xenopus the presumptive otic ectoderm is specified at neurula stages (Gallagher et al., 1996, Yntema, 1939), but it is not the case in salamander (Jacobson, 1963a). The identification of molecular markers has helped to address the question of tissue specification. In chick, presumptive otic ectoderm from different stages was cultured in isolation and the otic markers *Pax2* and *BMP7* were used to assess otic specification (Groves and Bronner-Fraser, 2000). Otic explants from a 5-6-somite stage embryo are specified with the respect to *Pax2* expression, whereas they are specified to express *BMP7* at 7-8-somites (Groves and Bronner-Fraser, 2000). Thus, specification to express a specific marker seems to coincide with the time when this marker is first expressed *in vivo*. In contrast, the otic epithelium already seems programmed for neurogenesis long before neuroblasts are generated normally: from HH9 onwards otic

explants cultured in isolation generate neurons after 2.5 days, while *in vivo* neurogenesis only begins at HH13 (Adam et al., 1998).

1.8.4 When is the ectoderm committed to otic fate?

A tissue is *committed* to a particular fate when it adopts such fate regardless of the environment. To test otic commitment the prospective otic ectoderm was isolated and transplanted into ectopic locations of a host. As above, the expression of otic markers and/or formation of an otic vesicle were assessed. Experiments performed in the early 1900s in salamanders show that the ectoderm is committed to form a placodal thickening at early somites stages, when the prospective otic domain is grafted anterior or lateral of the endogenous territory (Ginsburg, 1946, Ginsburg, 1995, Yntema, 1933, Yntema, 1939). However, if the same tissue is grafted into the limb, i.e. a more challenging environment, otic placode commitment is first seen around the 7-somite stage (Ginsburg, 1946, Ginsburg, 1995, Yntema, 1933, Yntema, 1939). In anurans, when the otic territory is grafted to the flank ectoderm, it is already committed at neurula stages (Ginsburg, 1995, Sidorov, 1937, Zwilling, 1941). Experiments in chick not only evaluate commitment by assessing vesicle formation but also by expression of the otic marker *Pax2*. When the presumptive otic ectoderm from a 9-10 somite stage donor is grafted into the lateral trunk, it is able to form a $Pax2^{+}$ epithelial vesicle (Groves and Bronner-Fraser, 2000, Herbrand et al., 1998). Commitment as otic vesicle, able to form hair cells, is only detected after 18-22 somite stage (Swanson et al., 1990, Waddington, 1937). It appears that the stage of otic commitment varies slightly across species, but clearly depends on the site of grafting. When grafted close to the normal otic domain grafts tend to develop into otic structures more easily than in more remote territories such as the limb. Overall, when assessing commitment it is important to consider the criteria used and which stage of normal otic development they represent. Together, determination of specification and commitment provide clues to the beginning and end of otic induction: at the time of specification the placode must have received at least some inducing signals, while when committed inducing signals are no longer necessary to support otic fate.

1.8.5 Which tissues mediate otic induction?

When studying the development of a tissue it is important to identify the inductive source driving fate restriction. *Induction* is defined as “the interaction between an inducing and

responding tissue that alters the path of differentiation of the responding tissue" (Jacobson and Sater, 1988, Gurdon, 1987). The responding tissue has been characterised with the experiments described above leaving the question of which is/are the otic inducing tissue/s. Classic experiments largely depending on assessing tissue morphology were performed in the beginning of the 20th century, while more recently thanks to the availability of otic markers and molecular approaches otic inducing tissues have been characterised in more depth. It is likely that tissues near the otic placode have inducing abilities; therefore the underlying mesoderm was among the first candidates to be tested.

In *Xenopus*, an ectopic otic vesicle is induced by the anterior lateral mesoderm when it is grafted into competent belly ectoderm (Albaum and Nestler, 1937, Holtfreter, 1933, Raven and Kloos, 1945, Zwilling, 1941). Additionally, a graft of axial mesoderm induces a mixture of otic and neuronal cells in ventral ectoderm making it difficult to distinguish primary and secondary effects (Raven and Kloos, 1945, Borghese, 1942). The cardiac mesoderm together with the underlying endoderm also has the ability to induce an otic-like structure when grafted into a naïve placodal ectoderm, but it is not clear if host cells contribute to the vesicle (Jacobson, 1963a). Equivalent experiments in fish give comparable results: if the axial mesoderm is grafted into the gastrula ectoderm an otic vesicle is induced (Eakin, 1939). Moreover, when positioned in the prospective forebrain at gastrula stage both otic and neural tissues are induced (Woo and Fraser, 1997).

In complementary approaches, physical or genetic tissue ablation experiments revealed whether or not a particular tissue is required for otic development. Zebrafish mutants with defects in axial or cephalic mesoderm, acerebellar (ace) and one-eye pinhead (oep), exhibit delayed onset of otic vesicle formation (Mendonsa and Riley, 1999, Gritsman et al., 1999, Zhang et al., 1998). However, since these mutants present a variety of phenotypes the otic defect may be an indirect consequence of an earlier defect. Similarly, zebrafish embryos injected with ace or oep morpholinos show a delay in otic induction and present smaller otic vesicles (Phillips et al., 2001, Leger and Brand, 2002). Thus, although otic development is delayed in the absence of mesoderm, the otic placode still forms suggesting that in fish the mesoderm is not required for otic induction.

In birds the scenario is different: when the cranial paraxial mesoderm is removed between 0-3 somite stage the otic placode does not form (Orts et al., 1971) and the otic markers *Pax2*, *Sox3* and *Gata3* are not expressed (Kil et al., 2005). However, if the same

mesoderm is ablated after the 5-somite stage, otic development is not compromised (Kil et al., 2005). Thus, it appears that at least in chick the 0-4 somite stage is a critical time window, when the pre-placodal ectoderm requires inducing signals from the underling mesoderm to form an otic placode. Replacement of the paraxial mesoderm with mesoderm from more anterior or posterior location does not restore otic development (Kil et al., 2005), suggesting that the otic inducing ability is a unique property of the paraxial mesoderm. However, the paraxial mesoderm alone is not sufficient to induce otic identity in competent ectoderm of a gastrula stage host embryo (Kil et al., 2005). However, when the same mesoderm was grafted into the pre-placodal region at midbrain levels (future trigeminal) *Pax2+* cells and formation of columnar epithelium is detected (Kil et al., 2005). Thus, the paraxial mesoderm is required for otic induction in chick, but it can induce an otic placode only in a domain specified as PPR. Thus, it is clear that the mesoderm plays an important role in otic induction in a variety of species, however it is unlikely that it is the only source of inducing signals.

Several lines of evidence link the hindbrain, in particular rhombomeres 5 and 6, to otic induction. The hindbrain has otic inducing ability in amphibians when grafted into competent ectoderm (Albaum and Nestler, 1937, Gorbunova, 1939, Harrison, 1945, Stone, 1931). More recently, in zebrafish hindbrain grafts can also induce host-derived otic vesicles when placed into the ventral ectoderm but not when located in the forebrain (Woo and Fraser, 1998). Although the hindbrain seems to have the ability to induce otic tissue increasing evidence suggests that it is not necessary for otic placode formation. Hindbrain ablation in amphibians and birds does not affect otic placode formation (Giraldez, 1998, Jacobson, 1963a, Levi-Montalcini, 1946, Schmalhausen, 1940, Trampusch, 1941, Waddington, 1937). However, even if the hindbrain was removed it is possible that it regenerates to some extent; therefore additional evidence is required to confirm its otic inducing ability. Vitamin A deficient quail embryos, which lack rhombomeres 5 and 6, have normal otic vesicles and otic markers are expressed (Kil et al., 2005). Likewise, zebrafish embryos with hindbrain defects (e.g. valentiono morphants lacking rhombomeres 5 and 6 or Pbx2/4 mutants in which the entire hindbrain adopts rhombomeres 1 identity) present normal otic vesicles, but exhibit defects in otic vesicle patterning (Mendonsa and Riley, 1999, Whitfield et al., 1996, Kwak et al., 2002, Waskiewicz et al., 2002). Thus, signals from the hindbrain, in particular from rhombomers 5/6, do not seem to be required for otic induction.

However, patterning of the otic vesicle appears to depend on hindbrain derived signals. In mouse, *Kreisler*, Hoxa1 or Hoxb1 mutants show hindbrain defects as well as ear phenotypes: otic placode formation is normal but later the ears lack the cochlea and vestibule (Gavalas et al., 1998, Deol, 1964, Deol, 1966a, Deol, 1966b, Deol and Lane, 1966, Ruben, 1973, Sadl et al., 2003, Choo et al., 2006, Mark et al., 1993, McKay et al., 1996, Pasqualetti et al., 2001). In addition, when the hindbrain is rotated along the antero-posterior axis the rostro-caudal patterning of the otic vesicle is not affected. In contrast, when the hindbrain is rotated along the dorso-ventral axis patterning of the otic vesicle is defective (Bok et al., 2005). It seems therefore that the hindbrain is required for late steps of otic development and is important for patterning the otic vesicle.

The above section summarises the relative roles of mesoderm and hindbrain in otic induction. Both tissues possess some inducing ability: when grafted ectopically each is able to induce an otic-like structure. However, while the mesoderm is required for early otic induction the hindbrain seems to be necessary for late patterning of the future inner ear. When uncommitted prospective otic ectoderm is cultured together with the mesoderm or hindbrain, this ectoderm does not express high levels of otic markers, while if combined with both tissues strong expression of *Pax2*, *Nkx5.1* and *Soho-1* is induced coinciding with thickening of the epithelium (Ladher et al., 2000). Therefore, signalling cues from both the mesoderm and hindbrain are likely to cooperate during otic induction. The nature of the signalling involved in this process will be further discussed in the following sections (see sections 1.9.1 and 1.10.1).

Lastly, the endoderm underling the cranial paraxial mesoderm has an indirect involvement in otic induction (Ladher et al., 2005). Ablation of cranial endoderm in HH5 chick embryo causes hypoplastic or absent otic placode with a severe loss of *Pax2* expression on the operated side (Ladher et al., 2005). The role of the cranial endoderm appears to be indirect by instructing the overlaying mesoderm to produce signalling molecules required for otic induction (Ladher et al., 2005).

Thus, a complex model of otic induction emerges where three different tissues are involved. First, at neurula stage the endoderm instructs the overlying mesoderm to express FGF, which in turn induces otic features in the adjacent ectoderm. Secondly, the hindbrain contributes to the process of otic specification and inner ear patterning. The

molecular details of this model will be summarised in sections 1.9.1 and 1.10.1 (for review see Ladher et al., 2010).

1.9 Induction of the otic and epibranchial progenitor domain (OEPD)

After the specification of the pre-placodal region and its early regionalisation (see sections 1.3 and 1.4) local signals induce cells in the posterior PPR to become specified as otic-epibranchial progenitors and only subsequently otic and epibranchial placodes segregate. At this stage otic and epibranchial precursors are intermingled in a common progenitor domain (Otic and Epibranchial Progenitor Domain: OEPD; also named PPA: Posterior Placode Area) (for review see Ladher et al., 2010) located close to the hindbrain and posteriorly delimited by the first somite. Additionally, in amniotes the paratympanic placode may originate from the OEPD since it is located in very close proximity to the first epibranchial placode (O'Neill et al., 2012). In aquatic vertebrates the OEPD may also contain anterior lateral line precursors (D'Amico-Martel and Noden, 1983, McCarroll et al., 2012, Satoh and Fekete, 2005), which later form mechano- and electroreceptors to detect mechanic disturbances and electric fields in the water, respectively (for review see: Piotrowski and Baker, 2014, Schlosser, 2010). The OEPD is characterised by the expression of two paired-box genes *Pax2* and *Pax8* in a variety of species, and these are considered to be among the first markers of this domain (McCarroll et al., 2012, Heller and Brandli, 1999, Nornes et al., 1990, Krauss et al., 1991, Pfeffer et al., 1998, Terzic et al., 1998, Hutson et al., 1999, Hidalgo-Sanchez et al., 2000, Burton et al., 2004, Christophorou et al., 2010, Lawoko-Kerali et al., 2002, McCauley and Bronner-Fraser, 2002, Streit, 2002, Ohyama and Groves, 2004b, Li et al., 2004, Hans et al., 2004, Mackereth et al., 2005, Sanchez-Calderon et al., 2005, Aghaallaei et al., 2007, Bassham et al., 2008). However, in chick and possibly other sauropsides, *Pax8* has been lost because of genomic rearrangements (Christophorou et al., 2010, Freter et al., 2012). Their importance in the formation of a functional ear together with their integration in the otic gene network will be described later (see section 1.9.2). In the next paragraphs I will summarise the process of OEPD induction and the genes involved in this fate restriction.

1.9.1 OEDP induction by FGF signalling

The cranial paraxial mesoderm is required for otic development and has been identified as one of the otic inducing tissues (see section 1.8.5). The main signalling pathway initiating

OEPD induction is FGF, which is associated with the mesoderm. Expression of *FGF* ligands is dynamic, initially emanating from the endoderm and later from the mesoderm and hindbrain (for review see: Ladher et al., 2010, Ohyama et al., 2007). The exact member of the FGF family implicated in OEPD induction differs in different species (for review see: Schimmang, 2007, Ladher et al., 2010) (Figure 1.7 B).

In zebrafish, expression of *FGF3*, *FGF8* and *FGF10b* is detected in tissues correlated with otic induction. At 75% epiboly *FGF3* is present in the pre-placodal ectoderm and later, at 80% epiboly, it becomes expressed in the cranial paraxial mesoderm as well as in the fish analogue of rhombomere 4 (Maroon et al., 2002, Nechiporuk et al., 2007, Phillips et al., 2001, Leger and Brand, 2002, Liu et al., 2003, Maves et al., 2002). *FGF8* is expressed in a similar fashion; at 80% epiboly it is weakly expressed in the mesoderm to become strongly enriched during early somitogenesis and it is also present in the hindbrain (Nechiporuk et al., 2005, Nikaido et al., 2007, Phillips et al., 2001, Maves et al., 2002, Walshe et al., 2002). Recently, *FGF10b* has been identified to be present at tail bud stage in the cranial mesoderm underneath the prospective epibranchial placode, lateral to the otic domain (Maulding et al., 2014). For a review on inner ear development in zebrafish and details on FGF ligands expression see Whitfield et al. (2002). *FGF3* and *FGF8* are also found in medaka and are expressed in a similar fashion to their zebrafish homologues (Aghaallaei et al., 2007, Hochmann et al., 2007). The FGF downstream target *Etv4* (or *Pea3*) and *Etv5* (or *Erm*) are expressed in close association with the source of FGF8 (Roehl and Nusslein-Volhard, 2001). In *Xenopus* the same ligands are present: *FGF3* is strongly expressed in the posterior hindbrain (Lombardo et al., 1998), whereas *FGF8* at late gastrula stages is expressed in the paraxial mesoderm and later in the future midbrain-hindbrain boundary, pharyngeal arches and the otic placode (Fletcher et al., 2006). Thus, *FGF3* and *FGF8* are expressed in the hindbrain and the cranial paraxial mesoderm close to where the OEPD is induced.

In birds, extensive expression characterisation of *FGF* ligands in chick highlighted *FGF8*, *FGF3* and *FGF19* as main candidates for otic development (Paxton et al., 2010, Karabagli et al., 2002). During neurulation (HH6), *FGF8* is present in the endoderm underlying the cranial paraxial mesoderm and around 5-somite stage it is expressed in the pharyngeal endoderm (Ladher et al., 2005, Stolte et al., 2002, Karabagli et al., 2002). *FGF3* and *FGF19* are co-expressed: at late neurula stage (HH6-7) in the cranial paraxial mesoderm and from 3- 4-somite stage they are present in the hindbrain corresponding to

rhombomere 4-5-6 (Kil et al., 2005, Ladher et al., 2000, Ladher et al., 2005, Paxton et al., 2010, Mahmood et al., 1995). Similar to *FGF8*, *FGF3* is expressed in the pharyngeal endoderm from 5-somite stage (Mahmood et al., 1995) and followed by *FGF19* at around 6-somite stage (Ladher et al., 2000, Wright et al., 2004). Concomitant to the appearance of *FGF* ligands in the pharyngeal endoderm the cranial paraxial mesoderm loses FGF expression, which is crucial in the diversification of otic and epibranchial placodes (see section 1.10). The OEPD expresses several FGF receptors with high enrichment of *FGFR1* (Lunn et al., 2007, Walshe and Mason, 2000, Nishita et al., 2011); moreover otic and epibranchial cells show activated ERK1/2 and ERK/MAP kinase responsive genes, like *Etv4* and *Etv5*, a read out of FGF activity (Lunn et al., 2007).

Similar to the avian scenario, in mouse three ligands are detected: *FGF8*, *FGF10* and *FGF3* (for review see: Schimmang, 2007, Ladher et al., 2010). In mouse *FGF8* expression is more complicated than in chick; its expression relevant for otic development is in the endoderm, the mesoderm and the pre-placodal ectoderm before the formation of the otic placode at E8 (0-somite stage) (Ladher et al., 2005, Crossley and Martin, 1995). Later, *FGF8* is present in the pharyngeal endoderm (Crossley and Martin, 1995). Between 0 to 4 somites, *FGF10* is also detected in the anterior and ventral mesoderm and from 5 somites in the hindbrain next to the developing otic placode (Alvarez et al., 2003, Wright and Mansour, 2003). Lastly, *FGF3* appears in the hindbrain and PPR from 3-somite stage onwards (Alvarez et al., 2003, Mahmood et al., 1995, McKay et al., 1996, Wright and Mansour, 2003). Thus, FGFs are present in OEDP inducing tissues before the onset of OEPD markers and in general FGF expression in the cranial paraxial mesoderm precedes that in the hindbrain.

Since FGF signalling is present at the right time and place, it is a good candidate to mediate OEPD formation and therefore it has been extensively studied in the past decade (for review see Schimmang, 2007). In zebrafish, loss-of-function experiments for FGF3 and FGF8 by genetic deletion or by morpholino injection lead to a reduction or loss of otic markers and of the otic vesicle (Maroon et al., 2002, Leger and Brand, 2002, Liu et al., 2003, Phillips et al., 2001). FGF10b was only identified recently and, when knocked down affects later steps of otic and epibranchial formation causing a failure of otic cells to accumulate and a mild defect in epibranchial placode formation (Maulding et al., 2014). Acerebellar (ace) mutants, who lack functional FGF8, have a small otic vesicle with typically only one otolith, abnormal semi-circular canals and some behavioural

defects that are linked to the auditory-vestibular and lateral line system (Leger and Brand, 2002, Phillips et al., 2001). Additionally, early OEPD markers (e.g. *Pax2*, *Pax8*, *Dlx3*, *Eya1* and *Six4*) are expressed in a smaller domain in ace mutants (Leger and Brand, 2002, Phillips et al., 2001). Furthermore, when wild-type cells are transplanted into the hindbrain primordium of ace mutants the otic phenotype is rescued (Leger and Brand, 2002). Thus FGF8 is crucial for early OEPD induction. In zebrafish, loss of *FGF3* causes a milder otic phenotype whereas knockdown of FGF3 in ace mutants or MO-mediated knockdown of both ligands show a more drastic loss of otic vesicle (Liu et al., 2003, Maroon et al., 2002, Phillips et al., 2001, Solomon et al., 2004). Similarly, inhibition of FGF receptors using SU5402 blocks otic development and results in the absence of the otic markers *Pax2*, *Pax8*, *Dlx3* and *Spry4* (Leger and Brand, 2002, Maroon et al., 2002, Solomon et al., 2004).

In chick, siRNA-mediated FGF8 knockdown in the endoderm, causes loss of OEPD induction associated with *Pax2* downregulation (Ladher et al., 2005). Importantly, this phenotype can be rescued by FGF19-coated beads, and FGF8 induces *FGF19* expression in a mesoderm explant (Ladher et al., 2005); therefore FGF8 acts as an upstream inducer of mesodermal *FGF19* (for review see Ladher et al., 2010). In addition to FGF, WNT signalling is also associated to otic placode formation. In chick, *WNT8c* is expressed in the hindbrain next to the developing otic primordium (Paxton et al., 2010). Vitamin A-deficient quail embryos have been used to address the function of the hindbrain during otic induction; even though *FGF19*, *FGF3* and *WNT8c* hindbrain expression shifts caudally, the otic placode is still induced in the correct position because the mesodermal expression of *FGF19* is unaffected (Kil et al., 2005). This suggests that FGFs and WNTs from the hindbrain are not required for otic induction. However, loss of *FGF3* function using siRNA at HH8 blocks the transition from otic placode to otic vesicle (Zelarayan et al., 2007), implying a later function of FGFs in progression of otic development (see section 1.10.1). Unfortunately, in chick other studies of individual FGF ligands are still missing. Nevertheless, general inhibition of the pathway leads first to loss of OEPD specification and second of otic and epibranchial placodes (Martin and Groves, 2006, Abello et al., 2010, Yang et al., 2013).

In mouse, single and double knockouts for FGF ligands and receptors have been used to address the role of FGF in otic development. Homozygous mutants for *FGF8* are embryonic lethal (Meyers et al., 1998), while conditional deletion of FGF8 in the otic

vesicle, do not show a severe otic phenotype (Ladher et al., 2005, Zelarayan et al., 2007). Similarly, *FGF3* and *FGF10* knockouts form an otic vesicle although it is reduced in size (Alvarez et al., 2003, Ohuchi et al., 2000, Pauley et al., 2003, Wright and Mansour, 2003). The mild otic phenotype of the single mutants can be explained by the redundancy of the different ligands. Indeed double mutants for FGF3/FGF10 (Alvarez et al., 2003, Wright and Mansour, 2003, Zelarayan et al., 2007, Urness et al., 2010) and FGF3/FGF8 (FGF8 conditional allele) (Ladher et al., 2005, Zelarayan et al., 2007) present a severe otic phenotype. Additionally, in humans homozygous mutations in *FGF3* gene have been related to syndromic deafness and patients lacking the inner ear almost completely (Tekin et al., 2007). This finding suggests an early role of FGF3 in human inner ear development. Loss-of-function of FGF receptor 2 (FGFR IIIb), the receptor of FGF3 and FGF10, causes formation of a smaller otic vesicle (Pirvola et al., 2000). Thus, there is overwhelming evidence that inhibition of FGF signalling in vertebrates leads to otic defects.

On the other hand, gain-of-function experiments corroborate the key role of FGFs in OEPD formation. In zebrafish, wild-type embryos treated with retinoic acid, which in turn expands *FGF3* and *FGF8* expression in the hindbrain, leads to an expansion of the OEPD and induction of ectopic otic vesicles (Phillips et al., 2001). Similarly, misexpression of *FGF3* or *FGF8* is sufficient to expand the *Pax8*/*Pax2* domain and induce ectopic otic vesicle (Phillips et al., 2004, Hans et al., 2007, Padanad et al., 2012). Both in zebrafish and in medaka injection of *FGF8* mRNA produce an ectopic otic vesicle (Bajoghli et al., 2004, Solomon et al., 2004). The otic inducing ability of FGF is also conserved in frog, where ectopic placement of an FGF3-coated bead gives rise to an additional otic vesicle (Lombardo et al., 1998). In chick, misexpression of FGF3 leads to ectopic otic vesicle formation *in vivo* (Vendrell et al., 2000, Zelarayan et al., 2007) and lastly, also in mouse FGF10 is sufficient for otic placode formation (Alvarez et al., 2003).

In vitro culture of pre-placodal ectoderm is a powerful assay to study otic induction and it has been extensively used in chick. It has been shown that FGF19 can induce *FGF3* and *Pax2* as well as *WNT8c* expression in ectodermal explants (Ladher et al., 2000). Moreover, only when explants are cultured in a media supplemented with FGF2, an FGF ligand with a wide range activity, they express high level of *Pax2* after 24 hours of culture (Martin and Groves, 2006). In summary, both gain and loss of function approaches in mammals, birds, frog and fish provide overwhelming evidence for an

important role of FGF signalling in OEPD induction as a prerequisite for otic placode formation.

FGF ligands signal through tyrosine kinase receptors (FGFRs); ligand binding to their extracellular domain triggers the receptor dimerisation, which in turn causes the transphosphorylation of intracellular tyrosine residues. These events lead to the cytoplasmic activation of the pathway and signal transduction can follow different routes: MAP kinase (or Ras/ERK) involved in proliferation and differentiation, the Atk pathway which mediates cell survival and the protein kinase C (PKC) associated with cell morphogenesis and migration (for review see Dorey and Amaya, 2010). Recently, the different branches of FGF signalling have been selectively inhibited *in vivo* and *in vitro* in chick. Only inhibition of the Ras/ERK pathway leads to loss of the otic placode and *Pax2*, *Spry4*, *Eph4* are drastically reduced (Yang et al., 2013). Thus, FGF signalling through MAPK promotes OEPD fate (Figure 1.7).

In conclusion, FGF signalling from different tissues is required and sufficient for otic development. A model summarising the role of FGFs in OEPD induction has been recently proposed by Ladher et al. (2010). At early neurula stages, FGF8 is secreted from the endoderm and induces FGF in the overlying mesoderm. Later at mid-neurula stages, mesodermal FGF triggers the induction of OEPD fate in the ectoderm as well as that of *WNT8* in the neural tube. As somitogenesis progresses, FGF signalling is lost from the mesoderm allowing hindbrain-derived WNT to promote otic placode formation, while FGF and BMP from the pharyngeal endoderm induce epibranchial placodes form the OEPD. Formation of the two separate placodes will be further discussed (see section 1.10; Figure 1.7).

1.9.2 From the PPR to the OEPD: a gene network prospective

Having summarised the evidence for FGF signalling in OEPD specification it is important to understand how it functions to restrict sensory progenitor fate to cells expressing *Pax2* and *Pax8*; special attention will be given to its downstream targets and how they are linked together in the process (Figure 1.7 and Table 1.1).

As already described in section 1.4, prior to *Six/Eya* expression the ectoderm already starts to be regionalised and several genes become enriched in the posterior PPR. Among

them are *Gbx2*, which restricts *Otx2* anteriorly (Acampora et al., 2001, Acampora et al., 1995, Bally-Cuif et al., 1995, Li et al., 2009, Simeone et al., 1992, Simeone et al., 1993, Tour et al., 2001, von Bubnoff et al., 1996), and members of the *Irx* family with an anterior limit more rostral to *Gbx2* (Bellefroid et al., 1998, Glavic et al., 2002, Gomez-Skarmeta et al., 2001, Goriely et al., 1999) (Figure 1.6 C). Additionally, *Dlx* (Dlx3b/4b in fish and Dlx5/6 in chick) and *Foxi* (Foxi1 in fish and Foxi3 in chick) family members become enriched in the posterior placode domain (Brown et al., 2005, Khatri et al., 2014, Khatri and Groves, 2013, Ohyama and Groves, 2004a, Solomon and Fritz, 2002, Nissen, 2003, Solomon, 2003, Solomon et al., 2003b). These genes form a regulatory network and collaborate with FGFs to induce *Pax2*, *Pax8*, *Sox3* and other otic and epibranchial genes (Hans et al., 2004, Khatri et al., 2014, Kwon et al., 2010, Nissen, 2003, Padanad et al., 2012, Padanad and Riley, 2011, Solomon, 2003). Therefore, cells expressing these genes will become molecularly distinct from their neighbours and have the ability to differentiate into otic, epibranchial and lateral line placodes (for review see: Grocott et al., 2012, Ladher et al., 2010, Ohyama et al., 2007, Schlosser, 2006, Schlosser, 2010, Chen and Streit, 2013).

The role of *Gbx2* has been recently addressed in frog showing a dual function as repressor of anterior PPR fate and promoter of OEPD (Steventon et al., 2012). *Gbx2* knockdown causes expansion of *Otx2*, whereas misexpression of a constitutive repressive form of *Gbx2* and its over-expression result in loss of *Otx2*, suggesting that Gbx2 actively represses Otx2 (Steventon et al., 2012). Absence of enhancers for these two genes still leaves open the question if such interaction is direct or mediated by intermediate factors. Later, loss of Gbx2 function results in loss of *Pax2* and *Pax8* OEDP expression (Steventon et al., 2012) suggesting that it functions as an activator of OEPD fate. However, *Gbx2* alone is not sufficient to drive induction of *Pax2/8* (Steventon et al., 2012); therefore other factors must cooperate with Gbx2 to confer an otic and epibranchial fate.

During epiblast regionalisation *Dlx* and *Foxi1/3* are regulated by BMP signalling (see section 1.2.1) whereas later they are induced by FGFs in the posterior PPR and OEPD (Hans et al., 2007, Hans et al., 2004, Nissen, 2003). Loss of Foxi1 function in zebrafish leads to a loss of *Six1* and of the OEPD markers *Pax8*, *Pax2a* and *Dlx3b* accompanied by a very severe otic phenotype, where the otic vesicle is absent or very small (Nissen, 2003, Solomon, 2003, Bricaud and Collazo, 2006). In medaka, combined misexpression of

Foxi1, *Dlx3b* and *FGF8* leads to ectopic activation of otic genes and ectopic otic vesicles (Aghaallaei et al., 2007).

Both in chick and mouse *Foxi3* is expressed in equivalent domains as the fish *Foxi1*: at gastrula stage it is present in the non-neural ectoderm, at neurula stages it is enriched in the posterior PPR to become OEPD specific and then restricted to the developing epibranchial and trigeminal placodes (Khatri et al., 2014, Khatri and Groves, 2013, Ohyama and Groves, 2004a). Recent experiments in chick showed that misexpression of *Foxi3* alone is not sufficient to confer competence to respond to FGFs to ectodermal cells and to turn-on otic genes (Khatri et al., 2014). In contrast, Foxi3 knockdown causes loss of *Pax2* and *Foxg1* expression; however Foxi3 is not required for PPR specification (*Six1*, *Eya2*), the expression of the non-neural gene *Gata3* and the response to FGFs as evidenced by the continued expression of *Etv4* (Khatri et al., 2014). Even though Foxi3 is not required for *Six/Eya* expression it seems to be sufficient to induce them when misexpressed. Finally, although *Foxi3* is expressed prior to pre-placodal *Six/Eya* these factors regulate *Foxi3* expression suggesting a complex regulatory relationship among these genes (Khatri et al., 2014).

Recently, an otic enhancer for Six1 (Six1-21) has been identified and it presents two Foxi binding sites which, when mutated cause decreased enhancer activity (Sato et al., 2012). This finding corroborates the possibility of a positive feedback loop between Six1 and Foxi. On the other hand, the absence of Foxi enhancers leaves open the question whether Six1 directly regulates *Foxi3* (see Chapter 6). *Foxi1/3* and *Dlx3b/5* also mutually regulate each other in a positive feedback loop (Khatri et al., 2014, Pieper et al., 2011, Solomon, 2003). In addition, fish Dlx genes regulate their own expression (Aghaallaei et al., 2007, Solomon and Fritz, 2002) and in chick *Dlx5* and *6*, are co-expressed with *Dlx3* in the developing otic domain (Brown et al., 2005, Pera and Kessel, 1999, Khudyakov and Bronner-Fraser, 2009). Zebrafish mutants and morpholino knockdown experiments show that Dlx3b/4b also lies upstream of *Pax8* and *Pax2* (Hans et al., 2004, Solomon and Fritz, 2002, Solomon et al., 2004). Therefore, it is likely that FGF signalling acts through Foxi and Dlx genes to activate *Pax2* and *-8* in the otic and epibranchial domain. While Dlx genes remain expressed in the otic region (Brown et al., 2005, Khudyakov and Bronner-Fraser, 2009, Pera and Kessel, 1999), *Foxi* become expressed in the epibranchial placode (Khatri et al., 2014, Khatri and Groves, 2013, Ohyama and Groves, 2004a). Indeed, Foxi1/3 seems to promote epibranchial fate since its downregulation leads to loss of *Sox3*,

a well-established epibranchial marker (Sun et al., 2007). Thus, Dlx and Foxi family members initially work together to specify the OEPD, however later they play different roles in the segregation of otic versus epibranchial placodes (see section 1.10).

The development of the otic and epibranchial placodes is associated with two pair-box genes: Pax2 and Pax8 (Bouchard et al., 2010, Burton et al., 2004, Christophorou et al., 2010, Nechiporuk et al., 2007, Torres et al., 1996). In *Xenopus*, zebrafish and mouse *Pax8* is expressed prior to *Pax2* in the OEPD (Heller and Brandli, 1999, Pfeffer et al., 1998), while in chick *Pax8* is absent from its genome (Christophorou et al., 2010, Freter et al., 2012). In zebrafish, when Pax2a, Pax2b and Pax8 are knocked down only a small otic placode forms and degenerates over time (Hans et al., 2004, Mackereth et al., 2005) suggesting that early OEPD formation occurs normally whereas later otic development is compromised. Pax8 is upstream of the two duplicated zebrafish *Pax2* genes (*Pax2a* and *Pax2b*): loss of Pax8 causes reduction of *Pax2* genes (Hans et al., 2004, Mackereth et al., 2005). Pax2 mutant mice present a malformed cochlea and endolymphatic duct and the absence of the saccule (Burton et al., 2004, Torres et al., 1996). In contrast, Pax8 knockout mice do not have an ear phenotypes, while Pax2/Pax8 double mutants do form an otic vesicle, but arrest inner ear development thereafter (Bouchard et al., 2010). The crucial function of Pax2 for normal auditory function is highlighted by the fact that human patients with sensorineuronal deafness carry mutations in the Pax2 locus (Sanyanusin et al., 1995a, Favor et al., 1996, Schimmenti et al., 1997, Sanyanusin et al., 1995b).

A peculiar scenario is present in birds and reptiles where chromosomal rearrangements caused the loss of the Pax8 locus (Christophorou et al., 2010, Freter et al., 2012). Therefore it is possible to study the function of Pax2 in chick excluding any redundancy. In chick, loss of Pax2 function causes a reduction of the otic genes *Eya1* and *Gata3* and failure of placodal thickening due to absence of cell elongation (Christophorou et al., 2010). However, OEPD formation is not affected (Christophorou et al., 2010, Freter et al., 2012). Ectopic *Pax2* is able to activate adhesion molecules but alone is not sufficient to induce otic markers (Christophorou et al., 2010). Recently Pax2 function has been further investigated in chick. After Pax2 loss and gain of function otic and epibranchial markers are not affected (e.g. *Dlx5*, *Foxi2* and *Sox3*) but reduction of *Pax2* seems to decrease the number of cycling cells in the OEPD; therefore less progenitors contribute to the otic and epibranchial placodes (Freter et al., 2012). Overall, Pax2 does not function by

itself in establishing the OEPD but it could be involved in maintaining the otic and epibranchial together with other factors (Figure 1.7 and Table 1.1). Additionally, Pax2 regulates cell shape characteristic for placodes and it maintains cycling OEPD progenitors.

Similar to the anterior Pax genes, *Pax2* expression is under the control of Six/Eya: misexpression of a constitutive repressive form of Six1 in chick and Six1 knockdown in zebrafish leads to loss of *Pax2* (Bricaud and Collazo, 2006, Christophorou et al., 2009). Pax2b and Pax8 morpholino injection in zebrafish reduces *Six1* expression (Bricaud and Collazo, 2006). The otic enhancer for Six1 (Six1-21) presents a Pax binding site that when mutated causes decreased enhancer activity (Sato et al., 2012) raising the possibility of a positive feedback loop between Six1 and Pax2 which may maintain cells specified as otic. Additionally, Pax proteins repress each other: a mutual repression between Pax2 and Pax3 has been shown in the chick otic placode (Dude et al., 2009). As described above, absence of FGF signalling leads to loss of *Pax2* and *Pax8* genes in a variety of species and pre-placodal ectodermal explants when cultured in a FGF supplemented media turn on *Pax2* (Martin and Groves, 2006) (Figure 1.7 and Table 1.1). However, wheatear this is a direct or indirect event remain to be investigated (see Chapter 5).

Spalt4 (or Sall4) has been identified as an important factor taking part in otic vesicle formation. This transcription factor is broadly expressed in the chick epiblast to become restricted to the neural plate and PPR at neurula stages. Later *Spalt4* is present in the olfactory, lens and otic placodes (Barembaum and Bronner-Fraser, 2007). Misexpression of *Spalt4* is sufficient to induce invagination of the ectoderm and formation of a vesicle expressing otic markers. The level of *Spalt4* seems to be crucial since both its up- and down-regulation leads to otic defects (Barembaum and Bronner-Fraser, 2007). Additionally, identification of a Spalt4 enhancer (CR-F fragment) revealed that it is directly regulated by the FGF mediating factor Etv4 and Pax2 (Barembaum and Bronner-Fraser, 2010). FGF2-coated beads can induce both *Spalt4* expression and its enhancer in a competent ectoderm (Barembaum and Bronner-Fraser, 2007, Barembaum and Bronner-Fraser, 2010). Thus FGF, probably through Etv4, regulates *Spalt4* (Figure 1.7 and Table 1.1). In mouse, inactivation of Spalt4 leads to deafness that seems to be associated to conductive hearing loss, but further studies are required for exclude sensorineuronal deafness (Warren et al., 2007). In humans mutation in the Spalt4 locus are associated with

Okihiro syndrome, an autosomal dominant condition characterised by deafness in combination with eye movement and renal defects (Kohlhase et al., 2005).

In the otic-epibranchial region multiple genes are co-expressed. *Foxg1*, a telencephalon marker, starts to appear in the otic placode at around 10-11 somites and becomes later strongly expressed in the entire otic vesicle (Khatri et al., 2014). A similar expression pattern has been described in mouse (Hebert and McConnell, 2000) where Foxg1 is required for otic morphogenesis and innervation of the vestibular system (Hwang et al., 2009). Furthermore, it is regulated by FGFs (Urness et al., 2010, Yang et al., 2013) but lies downstream of Foxi3 (Khatri et al., 2014).

In chick, *Sox8* and *cMyb* are expressed in the OEPD and together with Etv4 they directly regulate *Sox10* expression, which appears in the otic territory around HH10. All three factors bind to the otic enhancer of Sox10 (Betancur et al., 2011) pointing to an early function of these genes in the otic network. *Gata3*, which is initially confined to the non-neural ectoderm, becomes enriched in the OEPD at 6-7 somite stage and it will remain expressed in the otic placode in chick (Sheng and Stern, 1999, Lillevali et al., 2007). A similar expression profile is found in mouse (Lawoko-Kerali et al., 2002, Lawoko-Kerali et al., 2004, Lillevali et al., 2004, Lillevali et al., 2007) and Gata3 loss-of-function leads to morphogenetic defects in the otic placode, which appears to be divided into a thicker ventral and thinner dorsal part leading to aberrant otic invagination (Lillevali et al., 2006) (Figure 1.7 and Table 1.1).

In summary, localised signalling, restriction of gene expression and mutual repression of Pax genes are key mechanisms providing spatial information to sensory progenitors along the rosto-caudal axis and allowing the specification of the posterior placodal area. Early in development, *Foxi* and *Dlx* genes are confined to the posterior PPR. They are proposed to act as competence factors, conferring the ability to respond to OEPD inducing signals emanating from cranial paraxial mesoderm and the hindbrain. Activation of *Pax2* and *Pax8* occurs rapidly downstream of FGF, with Foxi and Dlx as intermediate factors; further downstream a large group of factors emerges that cooperate to confer OEPD identity. These interactions are summarised in a gene network (Figure 1.7 and Table 1.1).

1.10 Diversification of the otic and epibranchial placodes

In order for the otic and epibranchial placode to form cells need to become distinct and segregate. The differential activity of WNT and Notch versus FGF and BMP play a crucial role in the differentiation between otic and epibranchial, respectively (for review see: Chen and Streit, 2013, Ladher et al., 2010). The function of these signals together with the genes that become differentially expressed in these two resolving domain will be here summarised.

1.10.1 Differential roles of WNT, Notch, FGF and BMP signalling in the segregation of otic and epibranchial placodes

Both FGF and WNT ligands from the hindbrain are important for otic induction (see sections 1.8.5 and 1.9.1) (Jayasena et al., 2008, Ladher et al., 2000, Nechiporuk et al., 2007, Ohyama et al., 2006, Urness et al., 2010, Park and Saint-Jeannet, 2008, Rhinn et al., 2005). Since the hindbrain is the source of WNT signalling, cells in its close proximity are exposed to high levels, while more lateral cells receive little or no canonical WNT. Indeed, in mouse the TCF/LacZ reporter line shows WNT activity in the medial OEPD, but not in the lateral domain (Ohyama et al., 2006). Conditional deletion of β-catenin in Pax2+ cells leads to expansion of epidermal markers (e.g. *Foxi2*) at the expense of otic fate (e.g. *Pax2*, *Pax8* and *Dlx5*), while β-catenin activation in Pax2+ cells results in the opposite phenotype (Ohyama et al., 2006). These findings suggest that WNT activity promotes otic fate in OEPD cells.

In agreement with the mouse data, activation of canonical WNT signalling in chick does not affect otic placode formation, but inhibits epibranchial development (*Foxi2* and *Phox2b*). Conversely its inhibition prevents the expression of the otic markers *Soho1* and *Nkx5.1* but does not compromise OEPD *Pax2* and *Foxi2* expression (Freter et al., 2008). Likewise, in zebrafish WNT stimulation leads to high levels of *Pax2a* (a feature characteristic for otic cells, while epibranchial cells only show low levels of Pax2a expression) and more cells appear to become committed to an otic fate (McCarroll et al., 2012) (Figure 1.7 and Table 1.1). Hindbrain derived WNT also promotes otic fate in frog embryos (Park and Saint-Jeannet, 2008). Therefore, high levels of WNT signalling are crucial to promote otic character, whereas its absence favours epibranchial and epidermal fates.

Importantly, the expression of WNT ligands in the hindbrain is under the control of FGFs. In chick, ectodermal explants express *WNT8a* in the presence, but not in the absence of FGF19 (Ladher et al., 2000) and in mice loss of the FGF antagonists Spry1 and Spry2 enlarges *WNT8a*, while *Foxi2* is reduced (Rogers et al., 2011). In contrast, in FGF3$^{-/-}$; FGF10$^{-/-}$ mutants the expression of *WNT8a* is reduced and as a consequence these embryos lack the OEPD and epidermal genes are expanded (Urness et al., 2010). Thus, these findings position the FGF pathway upstream of WNT signalling during otic induction.

As already mentioned WNT signalling promotes otic fate by enhancing the expression of genes like *Dlx5*, *Pax2*, *Pax8* and *Gbx2* (Ohyama et al., 2006). Notch components (e.g. *Jag1*, *Notch1*, *Hes1/5*) are expressed in the chick otic placode at around HH12 (Groves and Bronner-Fraser, 2000, Paxton et al., 2010) and are present in mouse from E8.5 onwards, are also induced by WNT (Jayasena et al., 2008). Similar to the phenotypes observed after WNT modulation, activation of Notch in the *Pax2+* domain leads to expansion of the otic placode at the expense of epibranchial/epidermal fate, while the opposite is true for loss of Notch signalling (Jayasena et al., 2008). Both pathways appear to have partially overlapping functions: both regulate *Pax8* independently, affect thickening of the placode and repress *Foxi2*, while genes like *Pax2*, *Gbx2* and *Dlx5* are uniquely regulated by WNT (Jayasena et al., 2008). Conditional overexpression of Notch augments TCF/Lef reporter activity in the otic placode (Jayasena et al., 2008). Thus, it is clear that a cross talk between WNT and Notch pathways takes place: WNT positively activates a set of otic genes and Notch factors (*Jag1*, *Notch1* and *Hes1*), which in turn promotes otic placode formation and WNT activity itself. The interplay between both pathways appears to be a conserved mechanism in other systems, like the intestine (for review see Watt et al., 2008) (Figure 1.7 and Table 1.1). In the context of ear development, it is likely that the feedback between WNT and Notch locks cells in an otic state in the medial OEPD.

While the otic and epibranchial placodes share a common origin and both require FGFs, shortly after OEPD specification they develop independently. Otic precursors will become independent of FGFs whereas epibranchial cells require sustained FGF signalling (Freter et al., 2008, Nechiporuk et al., 2007, Nikaido et al., 2007, Sun et al., 2007, McCarroll and Nechiporuk, 2013). FGF signalling emanates from the pharyngeal endoderm, which is brought into contact with the lateral portion of the OEPD (for review

see Ladher et al., 2010). Sustained FGF activity increases genes like *Phox2b,* thus promoting epibranchial development, while inhibiting otic fate by downregulation of *Soho1* and *Nkx5.1* (Freter et al., 2008). In zebrafish and chick, endodermal FGFs promote epibranchial fate also by inducing *Sox3* expression (McCarroll and Nechiporuk, 2013, Nikaido et al., 2007, Abello et al., 2010). The pharyngeal endoderm is also a source of BMPs. In chick *BMP7* is found to be expressed and when inhibited the epibranchial neurons fail to form, whereas BMP7 addition to ectodermal explants induces their formation (Begbie et al., 1999). *BMP2b* and *BMP5* are found in the pharyngeal endoderm in zebrafish and they play a similar role in the induction of *Phox2b* and promotion of epibranchial neurogenesis (Holzschuh et al., 2005). Manipulation of BMP signalling does not affect the development of any other placodes (trigeminal, otic and later line) (Holzschuh et al., 2005). Only few epibranchial markers have been characterised so far hence a precise time-resolution of the differentiation between the two placodes remains elusive (Figure 1.7 and Table 1.1).

The evidences summarised above point to a model where the interplay of multiple signals is required to segregate otic, epibranchial and epidermal cells from the common precursor domain, the OEPD. Mesodermal FGFs control *WNT8* expression in the hindbrain, which is crucial in the determination of the otic character in the medial portion of the OEPD. Additionally WNT inhibits epibranchial and epidermal fates. A positive feedback between WNT and Notch signalling ensures otic commitment. More laterally, the OEPD comes in close contact with the pharyngeal endoderm, which through FGFs and BMPs stabilise epibranchial fate and promote neurogenesis.

1.10.2 The gene network differentiating the otic and epibranchial placode

The complex role of signalling pathways in promoting otic versus epibranchial segregation has been described above; in addition epistatic interactions between transcription factors need to be considered to fully recapitulate this process (Figure 1.7 and Table 1.1).

In zebrafish, differential regulation of *Pax2* level along the medial-lateral OEPD seems to be crucial to differentiate between both placodes. At OEPD stages *Pax2* is homogenously expressed throughout the epithelium, while later medial OEPD cells gain high *Pax2* whereas lateral cells express lower levels (McCarroll et al., 2012). The combination of

Pax2a/8 gain- and loss-of-function experiments reveals that high level of *Pax2a/8* promotes otic fate, while low levels favour the differentiation of epibranchial cells. In addition to the already mentioned role of FGFs in induction OEPD-specific *Pax2* (see section 1.9), WNT signalling mediates high level of *Pax2a*/8 expression in the medial OEPD (McCarroll et al., 2012) (Figure 1.7 and Table 1.1). The importance of *Pax2* levels has recently been highlighted in the chick, however the interpretation of the results remains ambiguous. Both inhibition and up-regulation of *Pax2* leads to some extent of otic and epibranchial repression as evidenced by *Soho1*, *Foxg1* and *Phox2a* downregulation. However, other otic and epibranchial markers are not affected (e.g. *Dlx5*, *Foxi2* and *Sox3*) (Freter et al., 2012).

The general OEDP genes Dlx5 (Dlx3b/4b) and Foxi play different roles in otic and epibranchial differentiation. Dlx3b/4b is able to initiate otic induction even in the absence of *Foxi1* and gives sensory competence to cells in the medial OEPD (Hans et al., 2013). Additionally, Foxi1 loss-of-function in *no soul* zebrafish mutants affects neuronal OEPD derivatives and abrogates *Phox2a* and *Sox3* expression in the epibranchial domain (Lee, 2003, Sun et al., 2007). Taken this together with the early function of Foxi1 in the PPR (see section 1.3.3 and 1.9.2) it is possible that Foxi1 provides neuronal competence for OEPD-neuronal progenitors. Thus, Dlx genes promote otic differentiation, whereas Foxi family members support epibranchial fate decision (Figure 1.7 and Table 1.1).

Together with high level of *Pax2* and *Dlx5* (*Dlx3b/4b*) the otic placode starts to express two homeobox transcription factors: *Soho1* and *Nkx5.1*, which are both induced by WNT signalling (Freter et al., 2008). *Soho1* (sensory organ homeobox-1) is one of the first genes to be expressed in newly formed otic placode from around 9- 10-somite stage in the chick embryo (Deitcher et al., 1994, Freter et al., 2008, Kiernan et al., 1997). It is important to notice that at this stage the otic placode is already committed to form hair cells and neurons (Freter et al., 2008, Adam et al., 1998). Additionally, Nkx5.1 (H6 family homeobox 3; also known as Hmx3) is a transcription factor involved in neuronal differentiation and is required for inner ear development. In fish, it is co-expressed with *Soho1* in the otic vesicle (Adamska et al., 2000, Adamska et al., 2001). Its function has been studied mainly in mice and zebrafish where after Nkx5.1 knockout the inner ear vestibular structures do not form properly (Hadrys et al., 1998, Wang and Lufkin, 2005, Wang et al., 1998).

In the epibranchial placode *Foxi* family members are coexpressed with *Sox3* and *Phox2a* and *b*, while they are downregulated in the medial OEPD. In chick, *Sox3* is initially expressed in a broad area in the lateral OEPD at the 10-11-somite stage to become later restricted to four patches marking the epibranchial placodes (Abu-Elmagd et al., 2001). Both chick and zebrafish loss of *Sox3* abrogates neurogenesis (Tripathi et al., 2009, Dee et al., 2008). However, when epibranchial cells initiate neurogenesis they progressively lose *Sox3* and gain expression of *NeuroD* and *Phox2a*. Overexpression of Sox3 causes defects in neuroblast migration and abnormal epithelium morphology (Abu-Elmagd et al., 2001). Sox3 appears to be a competence factor required for proper neurogenesis but later epibranchial cells need to downregulate it to become fully differentiated. Additionally, two paired homeodomain transcription factors are expressed in the epibranchial placodes: *Phox2a* is expressed in epibranchial neuroblasts before and during delamination and *Phox2b* is present in delaminating neuroblasts (Begbie, 2002). In Phox2a$^{-/-}$ mutant mice the expression of *Phoxb2* is lost in epibranchial neuroblasts and while placodal morphogenesis is not affected, continued neuroblast specification is (Pattyn et al., 1997, Pattyn et al., 1999, Pattyn et al., 2000) (Figure 1.7 and Table 1.1). Therefore, *Phox2a* appears to be upstream of *Phox2b* and they play a role in neuronal differentiation (for a detailed discussion see Ladher et al. (2010)).

In combination with differentially expressed genes there are factors like *Six1*, *Eya1* and *Sox10* that are commonly expressed in both placodes and recently their enhancers have been identified. Two Six1 regulatory elements drive activity in both the otic and epibranchial placodes (Six1-12 and Six1-21). Only Six1-21 has been analysed in more detail; it presents Sox, Six, Foxi, Pax, TCF/Lef1 and E-box binding sites that once mutated decrease reporter activity (Sato et al., 2012). Combination of these factors is likely to drive both otic and epibranchial activity; however it is not entirely clear if each transcription factor contributes to both or only one. *Eya1* expression is under the control of multiple enhancers: two elements drive both otic and epibranchial activity (CS1-3 and CS1-5) and two additional enhancers regulate otic expression (CS1-23 and CS1-26). The regulatory element CS1-5 has been analysed in detail pointing to the function of TCF/Lef1 as positive regulator and Sox genes (e.g. Sox10) as possible repressors (Ishihara et al., 2008b). However, further analyses are required to determine if the identified factors regulate the transcription of Eya1 *in vivo*.

Sox10, which belongs to SoxE family together with Sox8 and Sox9, is expressed in the developing otic and epibranchial domain from around the 10-somite stage in chick (Betancur et al., 2010b, Barembaum and Bronner-Fraser, 2007). Three regulatory elements have been identified with some otic activity (Sox10E1, Sox10E2 and Sox10L8), among them Sox10E2 appears to have the highest ability to drive GFP in the otic placode (Betancur et al., 2010b, Betancur et al., 2011). Morpholino knockdown of Etv4, Sox8 and cMyb inhibits *Sox10* expression and additionally blocks enhancer activity (Betancur et al., 2011) suggesting that these factors directly regulate otic *Sox10* expression. How *Sox10* is regulated in the epibranchial placode still needs to be addressed (Figure 1.7 and Table 1.1).

In conclusion, the otic and epibranchial placodes originate from a common region, the OEPD, and along their developmental path they progressively differentiate by the interplay between signalling and restriction of gene expression. The key events governing such differentiation process are summarised in a gene network (Figure 1.7 and Table 1.1).

1.11 Insight into human deafness and the usage of auditory stem cells as a possible therapy

Worldwide approximately 70 million people are affected by some kind of hearing loss and around half of these cases have genetic origin, whereas the remaining are associated with environmental causes or trauma (Tekin et al., 2001). Hearing impairment is a very common congenital disease; in fact around 1.64 babies per 1000 births are born deaf (Morton, 1990). Genetic hearing loss in around 80% of the cases is non-syndromic, where deafness is not associated with any other features. Around 60-75% is autosomal recessive, of the remaining cases 20-30% are autosomal dominant and around 2% are associated with mitochondrial mutations or X-linked. Human hearing loss in a large proportion of the cases is progressive with variable onset. Almost 90% of the people affected by hearing loss present sensorineural defects, associated with loss of sensory hair cells and auditory neurons. The genetics of deafness is very complex and heterogeneous, where mutation in the same gene can give rise to a wide spectrum of clinical phenotypes. Although in the past decades new genes have been associated with deafness, in 25% of the cases the causes remain still unknown (for review see: Angeli et al., 2012, Steel and Brown, 1996). The majority of the genes identified play a role in late auditory processes, whereas very little is known about the genes that act early in this process. Several

developmental genes have been associated with deafness such as Pax2, Spalt4 and Six and Eya genes. Even if Six and Eya have been associated with branchio-oto-renal (BOR) syndrome and branchio-otic (BOS) syndrome about 30% of the patients do not show any mutations in these genes (Smith, 1993). This may suggest that other factors, acting up or downstream Six and Eya, could be involved. Therefore, it is very important to improve the knowledge of genes possibly involved in inner ear development and their function, this would be extremely helpful for genetic diagnosis.

In mammals, the progenitors of inner ear sensory cells are only produced during embryogenesis and at early postnatal stages. This makes hearing loss irreversible since damaged or lost cells cannot be replaced. At the present there are no medical treatment for deafness, although in patients with a functional nerve the sensory activity of the inner ear can be replaced by a cochlear implant. On the contrary, when the auditory nerve function is impaired only recently brainstem implant have been developed but this requires complicate brain surgery (Medina et al., 2014). Since in the current society the average age increases continuously the impact of age-related hearing loss also increases rapidly making it an imminent problem to address.

The knowledge of stem cell biology can provide some hopes for deafness treatment. Several possibilities can be pursued: sensory regeneration can be stimulated *in vivo* or the lost/damaged cells could be replaced by transplantation. The latter can be achieved by developing *in vitro* protocols to produce hair cells and neurons from stem cells. A protocol has been developed to differentiate human embryonic stem cells (hESCs) into hair-like-cells and sensory neurons by using the signals involved during otic development (Chen et al., 2012, Oshima et al., 2010, Ronaghi et al., 2014). Developing these protocols heavily relied on the knowledge generated through developmental biology approaches and animal model systems. hESCs are initially treated with FGFs to induce otic fate and upregulate *Pax2* and *Pax8*. Further differentiation then leads to neuro- and epithelial-like progenitors, which can be differentiated into neurons or sensory hair cells. Otic neuroprogenitors when transplanted into an auditory nerve injury model engraft and differentiate and improve the auditory response (Chen et al., 2012). Recently, mouse embryonic stem cells have also been differentiated into inner ear cells in 3D culture (Koehler and Hashino, 2014, Koehler et al., 2013). The same signalling used early in development to pattern the epiblast, differentiate the PPR and finally induce an otic placode were used to obtain hair-like-cells and sensory neurons in a dish. From an

ectoderm-like-structure a pre-placodal epithelium will form mainly under FGFs regulation and presence of BMP inhibitors, after OEPD induction WNT will drive otic prosensory vesicle formation and finally an inner ear organoid. The resulting hair cells are functional and form synapses with sensory neurons also originating from the culture (Koehler and Hashino, 2014, Koehler et al., 2013). The establishment of an *in vitro* model for inner ear differentiation is a very powerful tool to further understand inner ear development; differentiate hair cells and sensory neurons for transplantation and as a model for studying human deafness.

The progress recently made in the field of inner ear differentiation may provide a huge breakthrough for deafness treatment. However, more advances and knowledge is required in order to translate these preliminary studies into therapeutic treatments for patients. Indeed, deepening the understanding of inner ear development and the genetic of its formation are crucial points that will help to perfect *in vitro* hair cell differentiation and will also improve the diagnosis of genetic forms of hearing loss.

1.12 Aims of the project

This work aims to understand the molecular events of otic and epibranchial induction using chick as model system. In the first instance, it is crucial to identify the genes expressed during PPR and otic-epibranchial development. To establish a genetic hierarchy among such potential players I tested their epistatic relationship using functional experiments. Finally, the role of FGF signalling in OEPD induction and the chromatin state of the responding genes were investigated.

The main biological questions that I attempt to answer are:

- Which are the genes expressed in the pre-placodal region?
- Which are the transcription factors expressed during the transition from OEPD to otic and epibranchial segregation?
- Which and when are genes induced by FGFs during OEPD induction? Which are the direct and indirect targets?
- Does the chromatin state and/or the regulatory regions driving FGF target gene expression change during FGF induction?

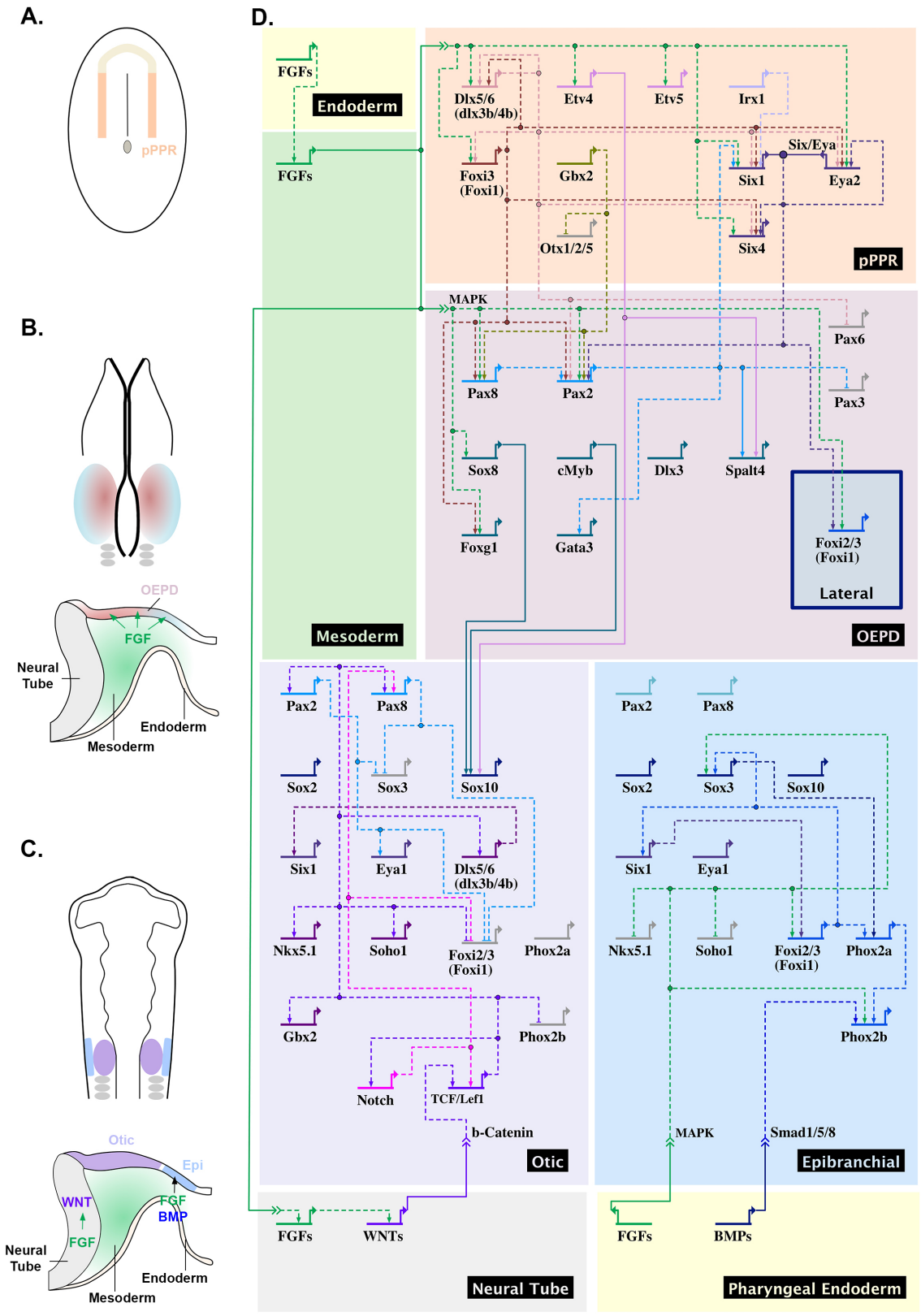

Figure 1.7 Gene network regulating the segregation of the otic and epibranchial placode.

Figure 1.7 Gene network regulating the segregation of the otic and epibranchial placode.

The main interactions involved in the specification of the otic and epibranchial domain (OEPD) and later in the segregation of the otic and epibranchial placodes are summarised in a gene regulatory network. **(A-C)** Diagrams on the left represent the corresponding stages in the chick embryo. **(A)** Neurula stage chick embryo where the posterior PPR (pPPR) is highlighted in orange. **(B)** The OEPD (pink and blue) is specified at around 5-somite stage in chick; Foxi3 (Foxi1) is expressed in the more lateral domain (light blue). FGFs from the mesoderm (green) induce expression of OEPD genes in the overlaying ectoderm. **(C)** At around 11-somite stage the otic (violet) and the epibranchial (light blue) are segregated. FGF in the neural tube (grey) promotes WNT signalling, which in turns favours the otic fate. The pharyngeal endoderm (light yellow) is brought in contact with the more lateral part of the OEPD and thanks to FGF and BMP helps in the formation of the epibranchial placode. **(D)** The main interactions present in the posterior part of the PPR are recapitulated at the top. Posterior PPR transcription factors together with FGFs from the mesoderm promotes OEPD genes, among them *Pax2/8*. In the last portion of the network are summarised the main interactions taking place from 11- to 15-somite stage. WNT and Notch signalling cooperate to promote otic fate while more laterally FGF and BMP promote the epibranchial fate. References for each interaction are reported in Table 1.1. Gene symbols are colour-coded accordingly to their expression domain. In the network solid lines represent experimentally verified direct interactions whereas dashed line indicates that such information is yet not available.

Table 1.1 Interactions from PPR to otic and epibranchial specification.

Source	Interaction	Target	System	Evidence
Interactions from blastula to neurula stages				
FGF	**Promotes**	**Sox3**	Chick	(Albazerchi et al. 2007; Streit et al. 2000; Wilson et al. 2001)
Dlx5 (Dlx3b/4b), Dlx3, Six1/Eya2	**Repress**	**Sox3**	Chick, *Xenopus*	(McLarren et al. 2003; Pieper et al. 2012; Woda 2003)
BMP, FGF, Wnt	**Promote**	**Zic1-5**	*Xenopus*	(Hong and Saint-Jeannet 2007; Monsoro-Burq et al. 2005)
Pax3	**Represses**	**Zic1-5**	*Xenopus*	(Hong and Saint-Jeannet 2007)
BMP, Wnt	**Promote**	**Pax7**	Chick	(Litsiou et al. 2005; Patthey et al. 2008)
FGF, Six1/Eya2	**Repress**	**Pax7**	Chick	(Christophorou et al. 2009; Stuhlmiller and Garcia-Castro 2012)
Wnt	**Promotes**	**Pax3**	*Xenopus*	(Bang et al. 1997; Hong and Saint-Jeannet 2007)
BMP, Foxi3 (Foxi1), Wnt	**Promote**	**Msx1**	Chick, *Xenopus*	(Hong and Saint-Jeannet 2007; Matsuo-Takasaki et al. 2005; Suzuki et al. 1997; Wilson et al. 2001)
Dlx5 (Dlx3b/4b), FGF	**Repress**	**Msx1**	Chick	(McLarren et al. 2003; Stuhlmiller and Garcia-Castro 2012)
Ap2, BMP, Dlx5 (Dlx3b/4b), Foxi3 (Foxi1), Gata2/3	**Promote**	**Dlx5 (Dlx3b/4b)**	Chick, *Xenopus*	(Kwon et al. 2010; Luo et al. 2001b; Luo et al. 2001a; Matsuo-Takasaki et al. 2005; McLarren et al. 2003; Pieper et al. 2012)
Six1/Eya2	**Represses**	**Dlx5 (Dlx3b/4b)**	Chick, *Xenopus*	(Brugmann et al. 2004; Christophorou et al. 2009)
BMP	**Promotes**	**Ap2**	*Xenopus* zebrafish	(Kwon et al. 2010; Luo et al. 2002)
BMP, Dlx5 (Dlx3b/4b), Gata2/3, Wnt	**Promote**	**Gata2/3**	Chick, *Xenopus*	(Kwon et al. 2010; McLarren et al. 2003; Pieper et al. 2012; Wilson et al. 2000; Wilson et al. 2001)
FGF, Six1/Eya2	**Repress**	**Gata2/3**	Chick	(Christophorou et al. 2009; Stuhlmiller and Garcia-Castro 2012)
BMP, Dlx5 (Dlx3b/4b), Gata2/3	**Promote**	**Foxi3 (Foxi1)**	*Xenopus*	(Kwon et al. 2010; Matsuo-Takasaki et al. 2005; Pieper et al. 2012)
Wnt	**Represses**	**Foxi3 (Foxi1)**	*Xenopus*	(Matsuo-Takasaki et al. 2005)
BMP, FGF, Wnt	**Promote**	**Irx1**	*Xenopus*	(Bellefroid et al. 1998; Glavic et al. 2004; Gomez-Skarmeta et al. 2001)
FGF	**Promotes**	**Otx2**	Chick	(Albazerchi et al. 2007; Wilson et al. 2001)
BMP, Wnt	**Repress**	**Otx2**	Chick	(Albazerchi et al. 2007; Wilson et al. 2001)
Ap2, c-Myc, Dlx5/6 (Dlx3a/4b)*, FGF, Foxi3 (Foxi1), Gata2/3, Irx1, Zic1-5	**Promote**	**Six1**	Chick, medaka, *Xenopus*, zebrafish	(Aghaallaei et al. 2007; Ahrens and Schlosser 2005; Bellmeyer et al. 2003; Brugmann et al. 2004; Esterberg and Fritz 2009; Glavic et al. 2004; Hong and Saint-Jeannet 2007; Kwon et al. 2010; Litsiou et al. 2005; Pieper et al. 2012; Sato et al. 2010*; Solomon

				and Fritz 2002; Woda 2003)
BMP, Foxd3, Msx1*, Pax3, Pax7, Wnt	Repress	Six1	Chick, *Xenopus*, zebrafish	(Ahrens and Schlosser 2005; Brugmann et al. 2004; Hong and Saint-Jeannet 2007; Kwon et al. 2010; Litsiou et al. 2005; Phillips et al. 2006; Sato et al. 2010*)
Ap2, Dlx5/6 (Dlx3a/4b), FGF, Foxi3 (Foxi1), Gata2/3, Six1/Eya2	Promote	Eya1/2	Chick, medaka, zebrafish	(Christophorou et al. 2009; Esterberg and Fritz 2009; Kwon et al. 2010; Litsiou et al. 2005; Pieper et al. 2012; Solomon and Fritz 2002)
BMP, Wnt	Represses	Eya1/2	Chick, *Xenopus*, zebrafish	(Brugmann et al. 2004; Kwon et al. 2010; Litsiou et al. 2005)
Ap2, Dlx5/6 (Dlx3a/4b), FGF, Foxi3 (Foxi1), Gata2/3, Six1/Eya2	Promote	Six4	Chick, *Xenopus*, Zebrafish	(Christophorou et al. 2009; Esterberg and Fritz 2009; Kwon et al. 2010; Litsiou et al. 2005; McLarren et al. 2003; Pieper et al. 2012)
BMP, Wnt	Repress	Six4	Chick, *Xenopus*, zebrafish	(Brugmann et al. 2004; Kwon et al. 2010; Litsiou et al. 2005)
Six1/Eya2	Represses	Foxd3	*Xenopus*	(Brugmann et al. 2004)
Regionalization of the PPR				
Otx1/2/5	Represses	Gbx2	*Xenopus*	(Steventon et al. 2012)
Otx1/2/5	Promotes	Dmrt4	*Xenopus*	(Steventon et al. 2012)
SST	Promotes	Noc	Chick	(L. Lleras-Forero et al. 2013)
Noc	Promotes	SST	Chick	(L. Lleras-Forero et al. 2013)
Pax6*, Noc, Otx1/2/5, Six1/Eya2, Six3*, SST	Promote	Pax6	Chick, mouse	(Ashery-Padan et al. 2000*; Christophorou et al. 2009; W. Liu et al. 2006*; L. Lleras-Forero et al. 2013; Steventon et al. 2012)
Dlx5/6 (Dlx3b/4b), FGF, Pax3, TGFβ, Wnt	Repress	Pax6	Chick, mouse	(Bailey et al. 2006; Bhattacharyya et al. 2004; Grocott et al. 2011; Smith et al. 2005; Wakamatsu 2011)
Pax6	Promotes	Six3	Mouse	(Ashery-Padan et al. 2000)
FGF, Pax3, PDGF, Six1/Eya2, Wnt	Promote	Pax3	Chick	(Canning et al. 2008; Christophorou et al. 2009; Dude et al. 2009; Lassiter et al. 2007; McCabe and Bronner-Fraser 2008)
Pax6	Represses	Pax3	Chick	(Wakamatsu 2011)
Pax3, SST	Promote	Eya2	Chick	(Dude et al. 2009; L. Lleras-Forero et al. 2013)
Pax3	Represses	Otx1/2/5	*Xenopus*	(Steventon et al. 2012)
TGFβ	Promotes	Wnt2b	Chick	(Grocott et al. 2011)
Interactions within the posterior PPR				
Dlx5/6 (Dlx3b/4b), FGF, Foxi1/3	Promote	Dlx5/6 (Dlx3b/4b)	Chick, *Xenopus*, zebrafish	(Aghaallaei et al. 2007; Bailey et al. 2006; Hans et al. 2004; Hans et al. 2007; Khatri et al. 2014;

				Litsiou et al. 2005; Nissen 2003; Pieper et al. 2012; Solomon and Fritz 2002; Solomon et al. 2003)
Dlx5/6 (Dlx3b/4b), FGF	**Promote**	**Foxi3 (Foxi1)**	Chick, *Xenopus*, Zebrafish	(Hans et al. 2004; Hans et al. 2007; Khatri et al. 2014; Nissen 2003; Phillips et al. 2004; Pieper et al. 2012; Solomon 2003)
FGF	**Promotes**	**Etv5**	Chick, *Xenopus*, zebrafish	(Kwon et al. 2010; Lunn et al. 2007; Raible and Brand 2001; Roehl and Nusslein-Volhard 2001)
FGF	**Promotes**	**Etv4**	Chick, zebrafish	(Lunn et al. 2007; Raible and Brand 2001; Roehl and Nusslein-Volhard 2001)
Gbx2	**Represses**	**Otx1/2/5**	*Xenopus*	(Steventon et al. 2012)
Dlx5/6 (Dlx3b/4b), FGF, Foxi3 (Foxi1), Irx1	**Promote**	**Six1**	Chick, *Xenopus*, Zebrafish	(Ahrens and Schlosser 2005; Glavic et al. 2004; Khatri et al. 2014; Pieper et al. 2012; Woda 2003)
Dlx5/6 (Dlx3b/4b), FGF, Foxi3 (Foxi1), Six1/Eya2	**Promote**	**Eya1/2**	Chick, medaka zebrafish	(Christophorou et al. 2009; Esterberg and Fritz 2009; Khatri et al. 2014; Kwon et al. 2010; Leger and Brand 2002; Litsiou et al. 2005; Pieper et al. 2012)
Dlx5/6 (Dlx3b/4b), FGF, Foxi3 (Foxi1), Six1/Eya2	**Promote**	**Six4**	Chick, *Xenopus*, zebrafish	(Altmann et al. 1997; Christophorou et al. 2009; Esterberg and Fritz 2009; Kwon et al. 2010; Leger and Brand 2002; McLarren et al. 2003)
Interactions from PPR to OEPD stage				
FGF	**Through**	**MAPK**	Chick	(Yang et al. 2013)
FGF, Gbx2, Foxi3 (Foxi1)	**Promote**	**Pax8**	*Xenopus*, zebrafish	(Hans et al. 2004; Leger and Brand 2002; Mackereth et al. 2005; Nissen 2003; Padanad and Riley 2011; Padanad et al. 2012; Park and Saint-Jeannet 2008; Phillips et al. 2001; Phillips et al. 2004; Solomon et al. 2003; Steventon et al. 2012)
Dlx5/6 (Dlx3b/4b), Gbx2, Foxi3 (Foxi1), FGF, Six1/Eya, Pax8	**Promote**	**Pax2**	Chick, mouse, *Xenopus*, zebrafish	(Bricaud and Collazo 2006; Christophorou et al. 2009; Freter et al. 2008; Hans et al. 2004; Hans et al. 2007; Khatri et al. 2014; Ladher et al. 2000; Ladher et al. 2005; Leger and Brand 2002; Mackereth et al. 2005; Maroon et al. 2002; Martin and Groves 2006; Padanad and Riley 2011; Padanad et al. 2012; Phillips et al. 2004; Solomon and Fritz 2002; Solomon et al. 2004; Steventon et al. 2012; Sun et al. 2007; Wright and Mansour 2003)
Pax2	**Represses**	**Pax3**	Chick	(Dude et al. 2009)
Dlx5/6 (Dlx3b/4b)	**Represses**	**Pax6**	Chick	(Bhattacharyya et al. 2004)
Pax2	**Promotes**	**Six1**	Zebrafish	(Bricaud and Collazo 2006)

FGF	Promotes	Sox8	Chick	(Yang et al. 2013)
FGF, Foxi3 (Foxi1), Pax2	Promotes	Foxg1	Chick, mouse	(Freter et al. 2012; Khatri et al. 2014; Urness et al. 2010; Yang et al. 2013)
Pax2*, Etv4*	Promote	Spalt4	Chick	(Barembaum and Bronner-Fraser 2010)
Pax2	Promotes	Gata3	Chick	(Christophorou et al. 2010)
FGF, Six1/Eya2	Promotes	Foxi2/3 (Foxi1)	Chick, zebrafish	(Khatri et al. 2014; Padanad et al. 2012)
Interaction between endoderm, mesoderm and neural plate				
FGF (endoderm)	Promotes	FGF (mesoderm)	Chick	(Ladher et al. 2005)
FGF	Promotes	Wnt	Chick, mouse, zebrafish	(Ladher et al. 2000; Phillips et al. 2004; Rogers et al. 2011)
Interactions in the otic & epibranchial placodes				
Wnt	Promotes	TCF/Lef1	Mouse	(Ohyama et al. 2006)
Wnt	Promotes	Notch	Mouse	(Jayasena et al. 2008)
Notch	Promotes	TCF/Lef1	Mouse	(Jayasena et al. 2008)
Wnt	Promote	Pax2	Chick, mouse, zebrafish	(Freter et al. 2008; McCarroll et al. 2012; Ohyama et al. 2006)
Notch, Wnt	Promotes	Pax8	Mouse, *Xenopus*, zebrafish	(Jayasena et al. 2008; McCarroll et al. 2012; Ohyama et al. 2006; Park and Saint-Jeannet 2008; Phillips et al. 2004)
Etv4*, cMyb*, Sox8*	Promote	Sox10	Chick	(Betancur et al. 2011*)
Pax2	Promotes	Eya1	Chick	(Christophorou et al. 2010)
Dlx5/6 (Dlx3b/4b)	Promotes	Six1	Medaka	(Aghaallaei et al. 2007)
Wnt	Promotes	Dlx5/6 (Dlx3b/4b)	Mouse	(Ohyama et al. 2006)
Wnt	Promotes	Gbx2	Mouse	(Ohyama et al. 2006)
Wnt	Promotes	Nkx5.1	Chick	(Freter et al. 2008)
FGF	Represses	Nkx5.1	Chick	(Freter et al. 2008)
Pax2, Wnt	Promotes	Soho1	Chick	(Freter et al. 2008; Freter et al. 2012)
FGF	Represses	Soho1	Chick	(Freter et al. 2008)
FGF, Six1	Promote	Foxi2/3 (Foxi1)	Chick, mouse, zebrafish	(Bricaud and Collazo 2006; Freter et al. 2008; Khatri et al. 2014; Rogers et al. 2011)
Notch, Pax2, Pax8, Wnt	Repress	Foxi2/3 (Foxi1)	Mouse, zebrafish	(Freter et al. 2008; Jayasena et al. 2008; Ohyama et al. 2006; Padanad and Riley 2011)
FGF, Foxi2/3 (Foxi1)	Promote	Sox3	Chick, zebrafish	(Abello et al. 2010; McCarroll and Nechiporuk 2013; Nikaido et al. 2007; Sun et al. 2007)
Pax2, Pax8	Repress	Sox3	Zebrafish	(Padanad and Riley 2011)

Foxi2/3 (Foxi1), Pax2, Sox3	**Promotes**	**Phox2a**	Chick, zebrafish	(Abu-Elmagd et al. 2001; Freter et al. 2012; Lee 2003)
BMP, FGF, Foxi2/3 (Foxi1), Phox2a	**Promote**	**Phox2b**	Chick, mouse, zebrafish	(Freter et al. 2008; Holzschuh et al. 2005; Pattyn et al. 1997)
Wnt	**Represses**	**Phox2b**	Chick	(Freter et al. 2008)

The table summarises the interactions described in the text and the related references. Gene's names are colour-coded using the same colour as in the networks and refer to chick nomenclature; in the case of different names used in other species they were reported in brackets. Experimentally verified direct enhancer regulations are marked (*).

2. Materials and Methods

2.1 Embryo isolation

Fertile chick eggs, from Winter and Steward Farms (UK), were incubated at 38°C in a humid incubator and left to develop for appropriate time to reach the desired stage, based on Hamburger and Hamilton (Hamburger and Hamilton, 1951). To isolate the embryos the shell was removed using blunt forceps and the excess of albumin removed from the half shell. The yolk was rotated until the embryo was positioned in the centre and using scissors the vitelline membrane was cut in a square around the embryo. With the help of a spoon the embryo was isolated and immersed in a dish with phosphate buffered saline (PBS) solution, when used for fixing, or with Tyrode's solution (137mM NaCl, 2.7mM KCl, 320μM $NaH_2PO_4.2H_2O$, 5.6mM glucose) for further manipulations. The embryos were carefully detached from the vitelline membrane and cleaned using a Pasteur pipette. At this point the embryos were ready for fixation (see section 2.7) or dissections (see section 2.5) for explants or tissue collection for molecular procedures. The embryological procedures were carried out using a dissecting microscope with transmitted or top light (Olympus SZ60).

2.2 New culture and filter culture

For *in vivo* electroporation the embryos were cultured according to a modified version of New's method (New, 1955) by Stern and Ireland (1981) or on Whatman filter rings (Chapman et al., 2001).

2.2.1 New Culture

The shell of the egg was removed as described above (see section 2.1); the thick albumin was discarded however the liquid part was collected in a beaker. The yolk was immersed in a large Pyrex dish filled with Pannet-Compton (PC) saline (82.8mM NaCl, 8.3mM KCl, 2.8mM $CaCl_2.2H_2O$, 2.5mM $MgCl_2.6H_2O$, 8mM $Na_2HPO_4.2H_2O$, 7.2mM $NaH_2PO_4.2H_2O$). The rest of the thick albumin was carefully removed from the yolks with the help of blunt forceps or Pasteur pipette; the yolk was rotated so that the embryo was visible on its top. Subsequently the yolk was cut just below the equator using sharp

scissors. Using fine forceps the vitelline membrane with the embryos was gently removed from the rest of the yolk. A glass ring (diameter: 1.5-2.5 cm; height: 3-4mm) was then positioned on top of the membrane with the embryo at the centre (ventral side facing upwards). With the help of the fine forceps the edges of the vitelline membrane were wrapped around the ring. A watch glass was then immersed in the PC solution; the ring with the membrane was slid on top of the glass, and finally removed from the Pyrex dish. Under the dissecting microscope, the edges of the membrane were folded around the ring to make the membrane flat. Any excess of membrane was trimmed and the embryo cleaned from any remaining yolk by gently blowing some solution with a Pasteur pipette. The embryo was kept immersed in few millilitres of PC solution and kept in a humid environment for few hours before further manipulation. This procedure was performed mainly for embryos at early streak stages (from HH3+ to HH5).

2.2.2 Whatman filter ring culture

The method of the filter culture (Chapman et al., 2001) substitutes the glass ring required for New culture with a square of filter paper (Whatman no. 1–5) presenting a hole in its centre. The hole was made using a single-hole paper puncher (hole of about 7.5mm and filter square of 1.5x1.5cm); the paper was autoclaved. The filter paper provides an optimal material for attachment of the vitelline membrane and offers support to maintain the membrane under tension. The egg was opened and the albumin removed as described for New culture. After having rotated the yolk to visualise the embryo the excess of albumin was further cleaned using some tissue paper. Important for a good adherence to the filter, the membrane needs to be dried well. The filter was then placed on top of the vitelline membrane with the embryo in the centre of the hole. After pushing the edges of the filter square down slightly, the vitelline membrane was cut around the filter paper using scissors. With forceps, the filter was gently pulled away from the yolk in a slight oblique orientation. The filter with the embryo attached was then immerse in a petri dish containing Tyrode's solution and the residual yolk was removed with a Pasteur pipette under the microscope. The filter culture can be left in Tyrode's solution for a maximum of half an hour, if left longer the membrane starts to detach from the filter. The embryos cultured with this method were mainly used for electroporation (see section 2.3). From neurulation stage (HH6) embryos show a high survival rate after electroporation using this method. In contrast, at gastrulation/early neural plate stages (HH3-HH5) electroporated embryos survive better in New culture.

2.3 Electroporation

In the chick embryo is possible to introduce morpholinos or DNA plasmids using the electroporation technique. The embryos were prepared as described in sections 2.2.1 and 2.2.2. They were then transferred into an electroporation chamber (Filter culture chamber: 2x2mm platinum electrode) ventral side facing upwards. DNA [general DNA mixture: 3 μg/μl reporter DNA (pTK Citrine/Cherry) and 1.5 μg/μl pCAB RFP/GFP in H_2O, 0.1% fast green] or MO (variable MO concentration, 0.1% fast green plus 50ng/μl pCAB vector used as a carrier; for MOs concentrations see Table 2.1) was injected by air pressure between the vitelline membrane and the dorsal side of the embryo using pulled glass needles. Subsequently, a platinum electrode (2x1 mm) was carefully placed above the target area at a minimum distance from the embryo. Current was then applied (5 pulses at 4V for 50ms with intervals of 750ms) using Intracel TSS20 OVODYNE pulse generator. The embryos were then placed into a petri dish (35mm diameter) containing 1ml of albumin collected during culture preparation. The lid of the dish was sealed with a drop of albumin; embryos were placed in an incubator at 38°C until they reached the desired stage. They were then further processed for fixation and *in situ* hybridisation, tissue collection or imaging.

Table 2.1 Morpholinos used for Pax2, Pea3, Sox8 and Sox10 *in vivo* knockdown

	Sequence	[MO]	Reference
Cnt*	5'CCTCTTACCTCAGTTACAATTTATA 3'	1mM	(Lleras-Forero et al., 2013)
Pax2	5'GCGGACTCGCCCTTACCTGTTTATG 3'	0.7mM	(Christophorou et al., 2010, Mende et al., 2008)
Etv4 (Pea3)	5'CTGCTGGTCCACGTACCCCTTCAT 3'	1.5mM	(Barembaum and Bronner-Fraser, 2010)
Sox8	5'CTCCTCGGTCATGTTGAGCATTTGG 3'	1mM	(Betancur et al., 2011)
Sox10	5'CATGGTGACTTCCTTCTTCTCAATT 3'	1.5mM	(Simoes-Costa et al., 2014)

*Standard control morpholino targeting β-globin RNA

2.4 *In vivo* drug treatment

To block FGF signalling SU5402 (Tocris Bioscience), which mainly inhibits tyrosine phosphorylation of FGFR1 (Mohammadi et al., 1997), was used. SU5402 was diluted in dimethyl sulfoxide (DMSO, Sigma) at a stock concentration of 10mM. Embryos were prepared using New culture (see section 2.2.1) were carefully removed from the membrane, placed in a petri dish, and incubated for 1 hour at room temperature in PC solution, containing DMSO (control; 1:1000) or 20µM SU5402. Subsequently, embryos were rinsed in PC and cultured at the following drug concentrations: SU5402 (20µM) or DMSO (1:1000). The drug was added to the albumin for the culture. 1µl of PC solution plus drug was also added on top of the embryo. The embryos were generally cultured from HH4-5 to HH7, around 6-8 hours, and fixed for *in situ* hybridisation.

2.5 Tissue dissection

To isolate specific tissues (posterior PPR, otic tissue ss5-6, ss8-9, ss11-12) the embryos were isolated from the egg (see section 2.1) and collected in Tyrode's solution. The embryo was pinned in four corners, ventral side upwards, in a Sylgard-coated petri dish containing Tyrode's solution. The mesendoderm, in the region to be dissected, was scored using a fine syringe needle (3mm, 30 half gauge; BD Microlance^{TM}3); to facilitate the dissociation of these tissues from the ectoderm few drops of dispase (working concentration of 0.1µg/ml; diluted in Tyrode's solution) were used. Finally, mesendoderm layers were removed, the ectoderm was cut and transferred to a dish with clean Tyrode's solution using a 20µl pipette and kept on ice for few hours until further processed. Tissues were used for culturing (see section 2.6) or collected for quantitative mRNA analysis (see sections 2.10, 2.11 and 2.12).

2.6 Explant cultures

The tissue of interest was isolated, as described in section 2.5, and processed for culture. For long cultures (6, 12, 24 hours) the tissue was cultured in collagen drops, however for shorter time points (3 and 6 hours) the tissue was left floating in the culture medium. The collagen was obtained by collecting collagen fibres from rat-tails in 50µl of water and 120µl of acetic acid. The collagen was left to dissolve over night on a rotating platform at 4°C. The next day 30 minutes spinning at 10,000g was performed; the supernatant was

collected whereas the pellet was re-suspended in water and acetic acid and a second precipitation was carried out. Collagen mix (Table 2.2) was prepared by mixing collagen with Medium 199 (Sigma), L-glutamine (Invitrogen), NaHCO3, Penicillin/Streptomycin (Invitrogen) and N2 supplement (GIBCO). The acidic pH keeps the collagen in solution; only with the addition of 1M NaOH it starts to solidify (Table 2.2). The collagen mix was kept on ice to prevent solidification. Explants were prepared as hanging drops. Initially, they were equilibrated with collagen medium (0.5ml medium in a petri dish), and then they were picked up in 10µl fresh collagen medium and placed on the lid of a petri dish lid. The lid was turned up-side-down and placed on top of a petri dish containing some water to provide humid environment, and drops were left to solidify for 15-30 minutes at 38°C. After the collagen had set, each drop was transferred using fine forceps into a 4-well plate containing 0.5ml of liquid medium (Table 2.2). In the case of floating explants, the tissue were first transferred into 0.5ml of culture medium with a small volume of culture medium and moved to a new well containing fresh medium in order to avoid contamination of the final culture medium with saline solution (condition used summarised in Table 2.3). The explants were incubated in a humidified CO_2 incubator (5%) at 37°C. After incubation the explants were fixed in 4% PFA for *in situ* hybridisation or dissected out of the collagen, using 3mm fine needles, and transferred to a PCR tube. For NanoString and RT-qPCR analysis the tissue was lysed in 5µl of lysis buffer (RNAqueous-Micro Kit, Ambion, see sections 2.10 and 2.11); for ChIPseq they were crossed linked following the protocol described in section 2.13.1. Finally, the tissues were snap frozen in liquid nitrogen and kept at -80°C until further processing.

Table 2.2 Solutions used for collagene-explant cultures

	Standard		FGF2 supplement		DMSO or SU5402 supplement	
	Collagen solution	**Liquid medium**	**Collagen solution**	**Liquid medium**	**Collagen solution**	**Liquid medium**
Collagen	700µl	-	700µl	-	700µl	-
Medium 199 (10x stock)	100µl	100µl	100µl	100µl	100µl	100µl
$NaHCO_3$ (11g/l stock)	100µl	100µl	100µl	100µl	100µl	100µl
L-Glutamine (200mM stock)	10µl	10µl	10µl	10µl	10µl	10µl
Penicillin/Streptomycin (100x stock)	10µl	10µl	10µl	10µl	10µl	10µl
N2 supplement (100x stock)	10µl	10µl	10µl	10µl	10µl	10µl
FGF2 (10µg/ml)	-	-	25µl	25µl	-	-
DMSO or SU5402 (10mM)	-	-	-	-	1µl	1µl
H_2O	63µl	770µl	38µl	745µl	62µl	769µl
NaOH (1M stock)	7µl	-	7µl	-	7µl	-
Total	**1000µl**	**1000µl**	**1000µl**	**1000µl**	**1000µl**	**1000µl**

Table 2.3 Culture medium used for 3 and 6 hours floating explants culture

	Standard	FGF2	CHX	CHX + FGF2
Medium 199 (10x stock)	100µl	100µl	100µl	100µl
$NaHCO_3$ (11g/l stock)	100µl	100µl	100µl	100µl
L-Glutamine (200mM stock)	10µl	10µl	10µl	10µl
Penicillin/Streptomycin (100x stock)	10µl	10µl	10µl	10µl
N2 supplement (100x stock)	10µl	10µl	10µl	10µl
FGF2 (10µg/ml)	-	25µl	-	25µl
CHX (10mM)	-	-	1µl	1µl
H_2O	770µl	745µl	769µl	744µl
Total	**1000µl**	**1000µl**	**1000µl**	**1000µl**

2.7 Whole mount *in situ* hybridisation

2.7.1 Preparation of Digoxigenin (DIG) – labelled riboprobes

Expressed sequence tags (ESTs) for the genes of interest, obtained from Source Bioscience, were used to make antisense probes (pBlueScript II SK vector, see Table 2.4). In other cases the plasmid with the gene of interest was obtained from different sources (Table 2.5). The identity of the plasmids was verified by sequencing (DBS Genomics, Durham University; SourceBioscience Sequencing, Cambridge). The insert was amplified by PCR using M13 Forward and M13 Reverse primers and Taq DNA polymerase (see Table 2.6 for composition and condition of the PCR reaction). To check the amplified product, an aliquot ($1/20^{th}$) of the PCR reaction was analysed by agarose gel electrophoresis. Antisense DIG-labelled probes were generated using the required enzyme, for ESTs T3 RNA-polymerase (Promega) was used. The transcription reactions were set up according to Table 2.7 and incubated for 2 hours at 37°C in the thermal cycler. 1µl of RQ1 DNase (RNase free, Promega) was added for 30 minutes at 37°C to remove the DNA template. To verify size and quantity of transcribed product an aliquot ($1/20^{th}$) was checked by agarose gel electrophoresis. The transcription reaction was made up to the volume of 80µl with nuclease-free water, precipitated using $1/10^{th}$ volume 4M LiCl and 2.5 volumes 100% ethanol and incubated overnight at -20°C or for 1 hour at -

80°C. After maximum speed centrifugation the pellet was recovered and washed in 300µl of 70% ethanol. A second centrifugation and ethanol wash was performed (50µl 100% ethanol). The pellet was then dried and dissolved in 80µl nuclease-free water. To further purify the probe, the transcript was precipitated a second time. Finally, the pellet was dissolved in 100µl of nuclease-free water at 65°C for 15 minutes. The probe was then denatured for 3 minutes at 95°C and cooled on ice for 5 minutes. After a brief centrifugation, 10 volumes of hybridisation buffer was added to the probe and stored at -20°C.

Table 2.4 Expression sequence tag (EST) information

Gene name	EST number	Insert size (bp)
Transcription Factors		
AATF	ChEST771e20	920
ADNP2	ChEST215f16	799
BCL7A	ChEST587h8	535
BCL11A	ChEST779p23	802
BCLAF1	ChEST662a16	730
DBX2	ChEST766g23	776
DLX6	ChEST406p23	793
E2F8	ChEST353j4	697
EAF2	ChEST150c24	638
EZH2	ChEST766d20	676
FLL4	ChEST433o1	815
FOXM1-AUTO1	ChEST977e16	795
FOXN2	ChEST534i24	792
FUBP1	ChEST478l21	782
HIF1A	ChEST282l1	630
HMGXB4	ChEST426k11	967
HSF2	ChEST436g19	737
LMX1A	ChEST609m14	726
LZTR1	ChEST589b12	495
MIER1	ChEST98k16	1059
MLLT10	ChEST1013a1	710
MORC2	ChEST972d11	707
MTA3	ChEST312g1	791
MYNN	ChEST536f8	1014
N-MYC	ChEST379n6	675
NFKB1	ChEST491b16	837
NIF3L1	ChEST45a16	1112
NPAS3	ChEST860p24	800
NR2F2	ChEST848j5	802
NSD1	ChEST995e21	815
POGZ-AUTO1	ChEST151l19	640

PSIP1	ChEST272n8	914
RCOR3	ChEST900m8	744
RERE	ChEST764l24	724
RRN3	ChEST522o13	852
RYBP	ChEST268o3	841
SOX8	ChEST706o2	778
SOX11	ChEST781p14	680
SOX13	ChEST437d11	788
SP4	ChEST535j5	693
STOX2	ChEST851g13	1500
TAF4B	ChEST912h16	907
TBPL1	ChEST72h9	747
TGIF2	ChEST692l13	621
TOX3	ChEST1009p6	983
TRIM24	ChEST401k15	977
VGLL2	ChEST976p9	657
YEATS4	ChEST9i5	756
ZBTB16	ChEST1038b13	594
ZFP161	ChEST309m24	869
ZIC1-AUTO	ChEST459n6	793
ZFHX3	ChEST472l4	733
ZNF217-AUTO1	ChEST192n15	820
ZNF462	ChEST236b12	920
Signalling Molecules		
CXCL14	ChEST896P24	1200
HOMER2	ChEST795g2	846
KREMEN1-LIKE	ChEST751a10	1100
LRP11	ChEST661h3	710
Chromatin modifying enzymes		
CHD7	ChEST757h23	901
DNMT3A	ChEST425j12	890
DNMT3B	ChEST405f22	820
SETD2	ChEST525a17	790
WHSC1	ChEST899n11	860

Table 2.5 Plasmids details for making DIG-antisense riboprobes

Gene	Vector	RNA polymerase
BLIMP1 (Dr Annabelle Scott)	TOPO pCR2.1	T7
ETV4 (Barembaum and Bronner-Fraser, 2010)	pBlueScript II SK	T3
ETV5 (Marianne Bronner)	pBlueScript II SK	T3
FOXI3 (Khatri and Groves, 2013)	pBlueScript II SK	T3
GBX2	///	T3
HEY1 (Anya Winkler)	pBlueScript II SK	T3
HEY2 (Anya Winkler)	pDK101	T7
PAX2 (Martyn Goulding)	pBlueScript II SK	T3
SP8 (Joy Richman)	pCR II Topo	SP6
TCF4	pGEM-T-Easy	SP6

Table 2.6 Composition and condition of the PCR reaction

PCR composition	
5x GoTaq Buffer (Promega)	**2µl**
dNTP Mix (10mM each) (Roche)	**0.2µl**
M13 Forward Primer (10µM)	**1µl**
M13 Reverse Primer (10µM)	**1µl**
GoTaq DNA Polymerase (5µg/µl) (Promega)	**0.2µl**
Plasmid DNA (1µg/µl)	**0.5µl**
Nuclease-free H_20	**5.1µl**
Total	**10µl**
PCR condition	
1. 95°C for 3 minutes **2.** 95°C for 1 minute **3.** 55°C for 1 minute **4.** 72°C for 1 minute **5.** Go to 2, 24 more times **6.** 72°C for 10 minutes **7.** 4°C	

Table 2.7 Transcription reaction mix for RNA polymerase

Transcription composition	
Templete DNA (PCR product)	**0.5µl**
Nuclease-free H_20	**13µl**
5xTranscription Buffer (Promega)	**5µl**
DTT (100mM) (Promega)	**2.5µl**
10x DIG-UTP Labelling Mix (Roche)	**2.5µl**
1-2mg/µl RNasin (Promega)	**0.5µl**
RNA polymerase (T3, T7 or SP6) (Promega)	**1µl**
Total	**25µl**

2.7.2 Whole mount *in situ* hybridisation

Chick embryos were collected as described in section 2.1, and fixed in paraformaldehyde with 2mM EGTA (Sigma) in PBS, for 4 hours at room temperature or over night at 4°C. After the fixation they were stored in 100% methanol at -20°C for maximum one week. Embryos were re-hydrated in decreasing concentration (75%, 50%, 25%) of methanol in PTW (PBS with 0.1% Tween-20, BDH) and washed twice in PTW for 10 minutes. Embryos older than 2 days were bleached for 1 hour in 6% H_2O_2 in PTW, and then rinsed in PTW three times for ten minutes. The embryos were incubated with proteinase K (10µg/ml, Sigma) according to their stage: HH4-7 for 16 minutes, HH8-10 for 20 and older stages for 30 minutes. Explants were treated with proteinase K for 5 minutes. They were briefly washed in PTW and incubated with post-fixing solution (4% formaldehyde in PTW and 0.1% glutaraldehyde) for 30 minutes at room temperature. They were rinsed first with PTW and then with hybridisation solution [50% formamide (BDH), 1.3X SSC (Sodium Chloride Sodium Citrate, BHD), 5mM EDTA (pH 8.0), 50µg/ml yeast RNA (Promega), 2mg/l Tween-20 (100%, BDH), 5mg/ml CHAPS (10%, Sigma), 100µg/ml Heparin (Sigma)]. Embryos were pre-hybridised in fresh hybridisation solution for 2 hours at 70°C, and then eventually stored at -20°C. The hybridisation solution was then replaced with pre-warmed DIG-labelled antisense probe and incubated at 70°C overnight. The next day, embryos were washed at 70°C in hybridisation solution (3x30 minutes) and 20 minutes with 1:1 hybridisation solution: Tris-buffered saline containing 1% Tween-20 (TBST; 0.05M Tris, 0.15M NaCl, 1% Tween-20). After two 15-30 minutes TBST washes at room temperature, the embryos were incubated for 3 hours in blocking buffer [5% heat inactivated sheep serum (Sigma), 1mg/ml BSA (Sigma) in TBST]. The solution was then replaced with anti-DIG antibody solution (0.2/0.4µg/ml sheep IgG-AP, Roche, diluted in 1:5000 blocking buffer) and incubated overnight at 4°C. Non-bound antibodies were

removed by all day TBST washing. Embryos were then incubated twice for 10 minutes in developing buffer NTMT [5M NaCl, 2M Tris-HCl (pH 9.5), 2M $MgCl_2$, 1% Tween-20] and then with NTMT containing NBT (Nitro Blue Tetrazolium, Sigma) and BCIP (5-Bromo-4 Chloro-3 Indodyl Phosphate, Sigma) as substrates [4.5µl NBT, 50mg/ml in 70% N,N-Dimethylformamide (DMF); 3.5µl BCIP, 50mg/ml in 100% DMF, per 1.5ml of NTMT]. Embryos were protected from light and left at room temperature until a dark blue colour had developed. Stained embryos were washed several times in PBS and then stored in 4% PFA at 4°C. Pictures were acquired with an Olympus SZX12 dissecting microscope and an AxioCam HR digital camera.

2.7.3 Wax sectioning

For wax sectioning, embryos were first incubated in absolute methanol for 10 minutes at room temperature and then in propan-2-ol for 5 minutes. They were incubated at 60°C for 30 minutes in 1:1 tetrahydronapthalene:wax and three times in wax. Subsequently, the embryos were placed into a mould and covered with wax. After hardening overnight at 4°C, embryos were processed for 12 µm sections using a Leica RM2245 microtome. Section de-waxing was performed using Histoclear (two washes of 10 minutes) and mounted using DPX (Solmedia Laboratory Suppliers) medium. Sections were viewed with a Zeiss Axiovert 200M inverted microscope and photographed using AxioCam HR digital camera.

2.8 Photography

Photographs of the whole embryos, after *in situ* hybridisation, were taken using an Olympus S2X12 microscope and AxioCam HR digital camera (Axiovision software). Wax sections were viewed under a Zeiss Axiovert 200M inverted microscope and photographed using AxioCam HR digital camera. Electroporated embryos were analysed using the same inverted microscope and photographed using a Hamamatsu C4742-9S camera (Digital Pixel software). Image processing was performed using ImageJ 1.480 and Adobe® Photoshop® CS6 (Adobe). Adobe® Photoshop was used to create montages and assembling the final figures.

2.9 mRNA extraction and cDNA preparation

To quantify gene expression mRNA was extracted and reverse transcribed to cDNA. Posterior PPR explants or otic tissues (see section 2.5), from 5 to 15 tissues per sample, were lysed in a total of 100µl lysis buffer and processed for mRNA extraction. A column based kit was use to extract the RNA (RNAqueous-Micro Kit, Ambion). The RNA was eluted in 10µl elution buffer and RNA concentration and purity was measured with NanoDrop 2000 (Thermo Scientific). To remove the genomic DNA samples were treated with DNase (30min at 37°C): 0.5µl RQ DNAse, 1µl 10X DNase Buffer (RNase free, Promega), RNA (equal amount of RNA was used across the same experiment) and water for a total volume of 10µl. 1µl of RQ1 RNase-Free DNase (Promega) was added for 10 minute at 65°C to inactivate the DNase. The RNA was then divided into two samples: 8.5µl for reverse transcription (RT) and 2.5µl were processed without enzyme (no-RT). Initially, random primers were added to the samples and incubated at 70°C to melt any secondary structure; then the remaining reaction components were added and processed for reverse transcription as described in Table 2.8. A simple PCR reaction was performed to check the efficiency of the reaction using primers for GAPDH. The cDNA was stored at -20°C until used for RT-qPCR.

Table 2.8 Reverse transcription

	RT	**no-RT**
RNA	8.5µl	2.5µl
Random primers (20µg) (Promega)	1.0µl	1.0µl
H_2O	2.5µl	8.5µl
	70°C 5 min on ice	
M-MLV RT 5XBuffer (Promega)	5.0µl	5.0µl
dNTPs Mix (10mM each) (Roche)	1.25µl	1.25µl
RNasin (Promega)	0.5µl	0.5µl
M-MLV RT (Promega)	1µl	-
H_2O	5.25µl	6.25µl
	37°C 60 min 75°C 10min 4°C (Hot lid kept at 40°C)	

2.10 Quantitative PCR (RT-qPCR)

Gene expression level was quantified by RT-qPCR using the QIAGEN Rotor Gene Q. Primers for the genes of interest were designed using tools available from IDT (http://eu.idtdna.com/scitools/Applications/RealTimePCR) and Sigma-Aldrich (http://www.oligoarchitect.com), and tested by PCR on cDNA obtained from whole embryo. When possible primers were designed spanning exons to avoid amplification of genomic DNA. For each RT-qPCR reaction: 1ng of cDNA was used together with 5µl of SensiMix™ SYBER kit (BIOLINE), primers (see Table 2.9 for sequences), at a final concentration of 2µM, and water for a final volume of 10µl. At least two biological replicates per condition were processed and, for each individual gene, three technical replicates were preformed. The no-RT samples were also analysed and a water control was included, where no cDNA was added to the reaction. For the set of posterior PPR explant experiments standard curves were also included (see below). A maximum of 72 reactions were possible to process together, so for each set of experiment the reactions were divided into few consecutive runs. The program used is summarised in Table 2.10. Additionally, the melting curve of the amplified products was measured during the RT-qPCR run.

Table 2.9 Primers used for RT-qPCR

Gene	Primers	Amplification size	
		cDNA (bp)	gDNA (bp)
AXIN2	F 5'-CCCCTACCATGTGAGTTCTG-3' R 5'-TCTTGCTCCCAATTCTGTACG-3'	149	5141
BLIMP1	F 5'-GGAGGCTGATTTCGAAGAGAAG-3' R 5'-CAAAGCGTGTTCCTTTTGGG-3'	191	6816
CITED2	F 5'-GACTGATTCCACCGCCAC-3' R 5'-TCATGTGTTCCGCCATCTC-3'	72	629
CXCL14	F 5'-CGAGTATGGAAGGAGAAG-3' R 5'-TGTCTTATGTCTGTGAGAG-3'	130	1250
DLX6	F 5'-GGCTATTCCCACTGGTAC-3' R 5'-GTCTCGGACAGTTCACAT-3'	75	75
ETV4	F 5'-AGTTCCTTGTGGCTCTATTGG-3' R 5'-TTGTCGTAGTTCATGGCTGG-3'	148	453
ETV5	F 5'-CAATTTGTCCCAGATTTCCAGTC-3' R 5'-GCACTTGTCTCCGTAGCTG-3'	147	4024

EYA2	F 5'-CTAGGCACTGTCTTCCCAATC-3' R 5'-TTCCTCTTCAACACCATCTCC-3'	135	922
FLL4	F 5'-AATGAAGTGGGAGTGGATGAG-3' R 5'-CACATTCGTTTGGCTGAAGG-3'	136	6010
FOXI3	F 5'-TGCCTACTACAGCTCCTT-3' R 5'-TACACCTCCGTTCCATCT-3'	114	114
GAPDH	F 5'-TCTCTGGCAAAGTCCAAGTG-3' R 5'-TCACAAGTTTCCCGTTCTCAG-3'	135	496
GBX2	F 5'-AAGAAGTACCTCTCGCTGAC-3' R 5'-CATTTGGCTCGCCTGTTC-3'	101	101
GPR160	F 5'-TGGTCTACAGATCCATTTGTCAG-3' R 5'-ATCAAAGTACACATAGCCCTAGC-3'	150	150
HEY2	F 5'-CTTGACTGAAGTTGCGAGGTA-3' R 5'-AGGTGCTGAGATGGGACA-3'	91	91
HPRT	F 5'-AATTATGAAGGGCATGGGAGG-3' R 5'-GACTTGTCACTGTTTCTGTTCAG-3'	120	5111
IRX3	F 5'-AAGGGTGAGAAGATCATG-3' R 5'-GTCATCTTGTTCTCCTTC-3'	110	110
LMX1A	F 5'-CTCTACTGCAAGCTGGACTAC-3' R 5'-TGTTGCGTGGTCAGGATG-3'	144	20714
LMX1B	F 5'-TCTGACCCCTCCACAAATGC-3' R 5'-GGTTTCCTACCCTAGCCTGC-3'	155	1162
NR2F2	F 5'- GCATGTCGACTCCGCAGAA-3' R 5'-GCACACTGTGACTTCTCCTGTA-3'	117	1046
PAX2	F 5'-ATCTGCGACAACGACACGGTCC-3' R 5'-GCTGGGCACGATAGTATGTCCTGG-3' (Yang1 et al., 2013)	83	25460
PAX6	F 5'-TCCTGATGTGTTTGCGAGAG-3' R 5'-CACCCATCTGTTGCTTTTCG-3'	140	257
PTPRU	F 5'-GAAGACCCTCCGTAACTACAAG-3' R 5'-CAAACCCTAAGCAAACCTCTG-3'	149	1354
RERE	F 5'-AGGAGTTGCTTCCGAATAAGG-3' R 5'-GCTCAAATCCAAGAATTCGCTG-3'	200	25298
RPLP1	F 5'-TCTACTCCGCCCTCATTCTC-3' R 5'-GCTCCTACGTTGCAGATGAG-3'	380	380
SDHA	F 5'-GCTGTACATCTGCTCACACTAG-3' R 5'-CTCTCCACGACATCCTTCTG-3'	149	1380
SIX1	F 5'-TACATAGCGGACGGTGAT-3' R 5'-AATAACGACAGTGGAGAAGG-3'	93	93
SOX10	F 5'-GAAGTAACAAGAGCAAACCCC-3' R 5'-CCGCTCTGCCTCTTCAATAAAG-3'	190	1072
SOX13	F 5'-TGAGCTGTGAGATGGACGG-3' R 5'-GCTTCTCCTGGTTCGTCATC-3'	198	2278
SSTR5	F 5'-TCAGAAAGTCCTTTGCCTCC-3' R 5'-GTTCTCTTGCCTGTGTTCAATG-3'	73	73
TCF4	F 5'-CAGGAACTATGGAGATGGGACT-3' R 5'-AACCCTGCAAATTCGAGTCTC-3'	158	35079

VGLL2	F 5'-TGCGTCCTCTTCACCTACTTC-3' R 5'-GGTAGGTGCTGTTCCAAAAGG-3'	193	1388
ZBTB16	F 5'-CACAGCGGTATGAAGACGTAC-3' R 5'-CGGCCATGTCTGTACCAG-3'	193	32223
ZFHX3	F 5'-AGATCTTCACCATCCGCAAG-3' R 5'-TGCTGGAAAACGGTACTCG-3'	192	41382

Housekeeping genes

Table 2.10 RT-qPCR condition

RT-qPCR condition
1. 95°C for 10 minutes
2. 95°C for 15 seconds
3. 60°C for 20 seconds
4. 72°C for 20 seconds
5. Go to 2, 40 more times
6. 72°C for 10 minutes

2.10.1 The standard curve method

The standard curves method was used to determine PCR efficiency and sensitivity of the assay, taking into account primers and reverse transcription variables (for review see Dorak, 2006). Purified PCR products of specific genes were amplified from cDNA and used as defined template amount. Subsequently, five dilutions were prepared: 10^{-3}pg, 10^{-4}pg, 10^{-6}pg, 10^{-7}pg and 10^{-8}pg; Ct values obtained ranged from 5 to 35. The concentration of tested genes was determined by interpolation with the standard curve (as example see Figure 2.1 B). GAPDH, SDHA and HRPT were used as housekeeping genes; the expression values of all three genes were averaged and used as normaliser value. Concerning the test-genes, their expression values were averaged between technical replicates and successively averaged between biological replicates. Relative level of expression was calculated dividing the averaged test-gene expression by the normaliser. Finally, the fold difference between the treated and untreated sample was calculated, 1.5 was used as cut-off for upregulated genes and 0.25 for downregulated. P-value was calculated using un-paired t-test.

2.10.2 The ΔΔCt method

In the cases where the RT-qPCR was used in parallel to other validation methods the simpler, but less accurate, method of the ΔΔCt was used to analyse differences in expression level. This method is based on the assumption that all the reactions have 100% efficiency. An arbitrary threshold of 0.01 (exponential phase of amplification) was used to determine the Ct values of all the reactions. Three equations were used to calculate the ratio of gene expression. The normaliser value was calculated as described above; similarly cut-off and p-values were adopted (see section 2.10.1).

Equation 1 $\Delta \boldsymbol{Ct} = \boldsymbol{Ct}\,(\boldsymbol{test\ gene}) - \boldsymbol{Ct}\,(\boldsymbol{normalizer})$

Equation 2 $\Delta\Delta \boldsymbol{Ct} = \Delta \boldsymbol{Ct}\,(\boldsymbol{treated\ sample}) - \Delta \boldsymbol{Ct}\,(\boldsymbol{control\ sample})$

Equation 3 $\boldsymbol{R} = \boldsymbol{2}^{(-\Delta\Delta \boldsymbol{Ct})}$

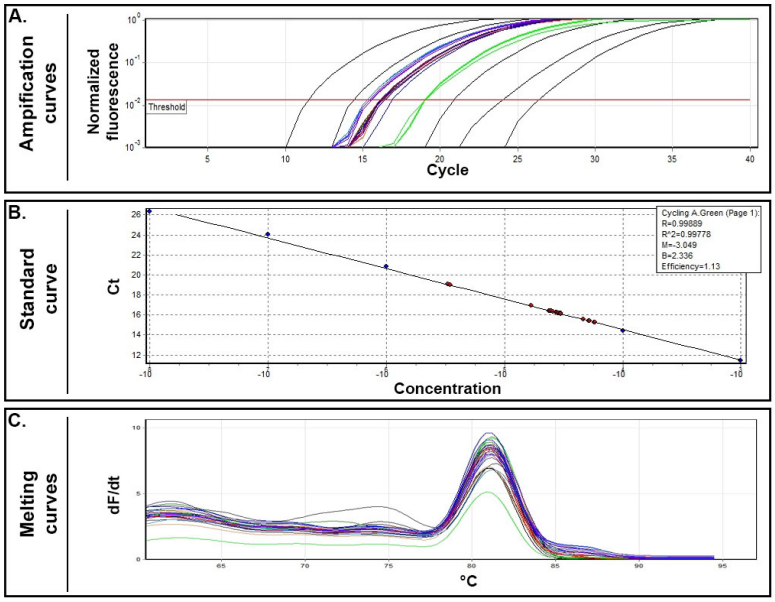

Figure 2.1 Example of data analysis for the housekeeping gene GAPDH.
Example of the data collected for the genes analysed by RT-qPCR. **(A)** PCR amplification curves have an exponential profile, in black the curves from the 5 dilution series of defined template amount and in colours (blue, green, red and violet) the test samples. A threshold was established from the QIAGEN Rotor Gene Q software (red line). **(B)** A standard curve, obtained by plotting the log-transformed Ct values of the serial dilution (blue dots). Slope of standard curve of -3.3 represents 100% efficiency (a range between -3.6 and -3.0 was usually obtained; in the case of GAPDH M=-3.049). Concentration of each test sample was calculated based on the standard curve (red dots). **(C)** Melting curve of the amplified products was measured during the RT-qPCR run. Presence of a single pick represents amplification of a single PCR product.

2.11 NanoString nCounter analysis

Posterior PPR tissue was dissected and cultured as explained in section 2.6, lysed and stored at -80°C until processed for NanoString. Hybridisation reactions were performed according to nCounter Gene Expression Assay Manual. The total RNA was hybridised with the capture and reporter probes by incubation at 65°C for 16 to 18 hours. Using the NanoString Prep Station the excess of unbound capture and reporter probes were removed, the purified ternary complexes were immobilised to the imaging surface. The cartridge was immediately analysed by the NanoString nCounter, counting 600 fields of view for each reaction (Figure 2.2) (Fortina and Surrey, 2008, Geiss et al., 2008).

Data analysis was performed following the nCounter Data Analysis Guidelines. In brief, the NanoString code set contains positive and negative controls (control sequences with no homology to any known organisms) that were used as normaliser. The positive controls are used to take into account differences in hybridisation, purification and binding efficiency. The counts for the positive controls were summed together to estimate the overall hybridisation efficiency and recovery for each individual lane. The individual positive control sums were averaged together; the initial positive sum for each column was then divided by the averaged value, creating a normalisation factor for each lane. The count of each gene in a particular lane was multiplied by the normalisation factor creating a background corrected value. Negative controls are also present in the probe set and were used to remove possible background reads. The average of the negative counts was summed to its standard deviation; this value was then subtracted from the background corrected value giving the final detected mRNA count. To consider differences in amounts of starting material total mRNA present in each sample was calculated and used to further normalise the data. Was noticed that only after this step the housekeeping genes show comparable levels across different samples. For each set of experiments three replicates were processed and their average value was used. Fold difference between treated and control sample was calculated (1.5 cut-off for upregulated and 0.25 for downregulated genes) and together with p-value (un-paired t-test; p-value$\leq$0.05) used to identify the significant up or downregulated genes.

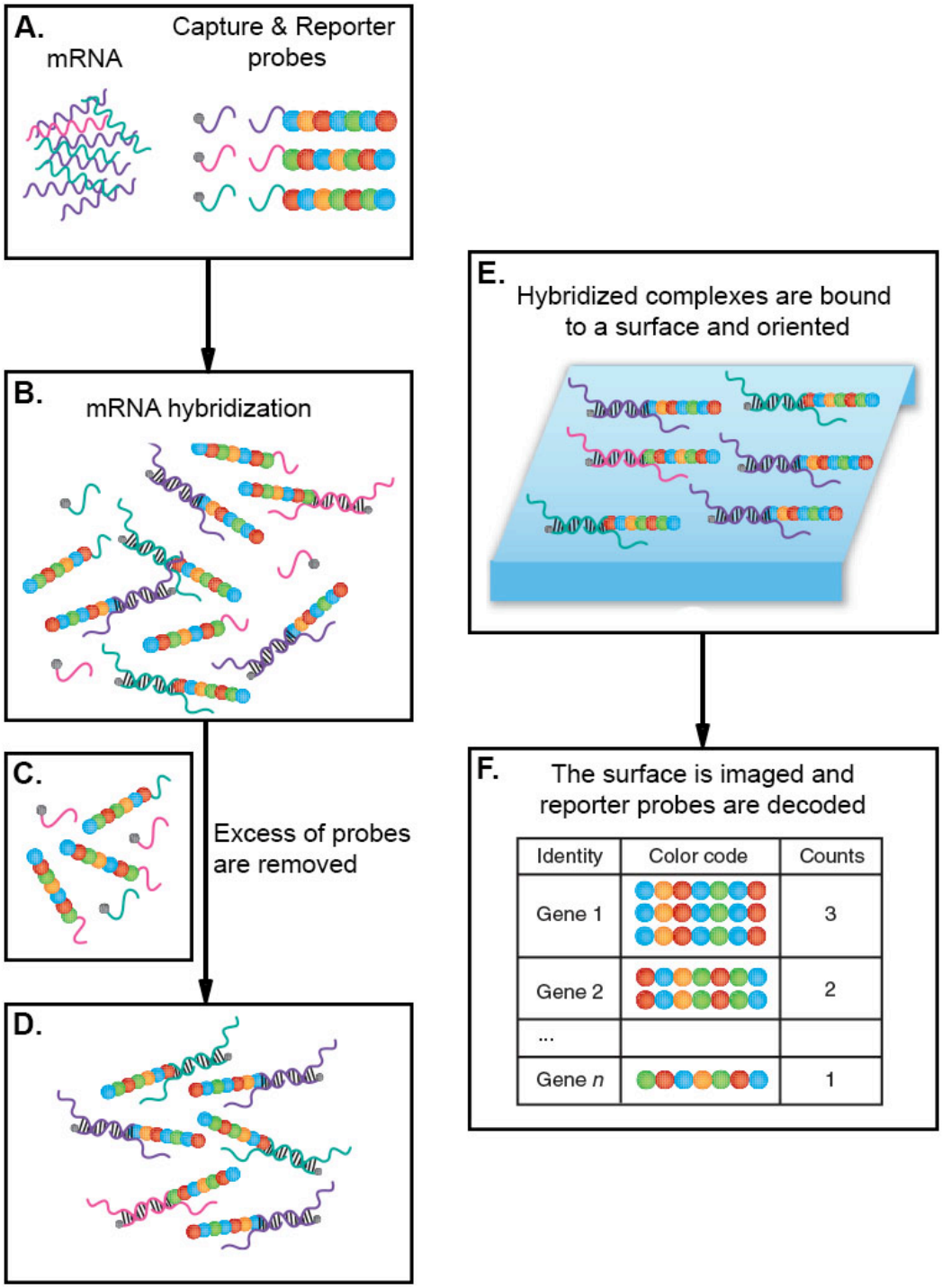

Figure 2.2 Schematic of the NanoString nCounter gene expression analysis.
(A) The mRNAs are directly mixed with the NanoString code set (reporter and capture probes). After the hybridisation **(B)** the excess of unbound probes is removed **(C-D)**. The purified ternary complexes are bound to the surface of a cartridge **(E)** and imaged. The numbers of reporter probes, representing individual copies of mRNA, are counted for each gene. Figure adapted from Fortina and Surrey (2008).

2.12 mRNA-seq and downstream bioinformatics analysis

2.12.1 RNA isolation, library preparation and next generation sequencing

After dissecting around 100 pieces of otic tissue for each stage (ss5-6, ss8-9 and ss11-12) cells were lysed (lysis buffer from RNAqueous-Micro Kit, Ambion) and the RNA was isolated as described in seciton 2.9. Additionally, ss3 whole embryos were processed for transcriptome analysis as control sample. RNA concentration and purity was verified with NanoDrop 2000 (Thermo Scientific). RNA integrity was assessed by Agilent Bioanalyser (Agilent technologies) using the Agilent RNA 6000 Nano Kit (Agilent technologies). All samples had an RNA Integrity Number (RIN) grater than 8. Sequence libraries were prepared with TrueSeq RNA Sample Preparation V2 kit (Illumina). The NGS libraries were sequenced with Illumina HiSeq 2000 (Illumina) with 50 cycles from single end. Library preparation and deep sequencing was performed in the Division of Biology, California Institute of Technology, USA.

2.12.2 Downstream bioinformatics analysis: sequence alignment and identification of enriched genes

To assess the sequence quality the mRNA-seq reads were scanned with FastQC (Andrews, 2010). Mispriming during reverse transcription may affect the accuracy of the first nucleotide of each read, therefore it was trimmed. The reads obtained were aligned with TopHat 2 (v2.0.7) to the last version of the chicken genome (Galgal4.71). Gene annotations from ensembl (Galgal4.71.gtf) and gene references (refGene) acquired from UCSC table browser were used to assemble the transcriptome profile of each sample using the software Cufflinks (v2.1.1). All the annotations were merged in a unique file and the number of reads at each genomic location was normalised using Cuffdiff (v2.1.1). The normalised count of reads RPKM (Reads Per Kilobase of exon per Million fragments mapped) was obtained for each gene and the final count was converted in a table format by easyRNASeq (v2.1.0) (Delhomme et al., 2012). DEseq (v1.16.0) (Anders and Huber, 2010) was used to identify genes enriched in the otic domain relative to the whole embryo. Cuts off of 4 RPKM and of 300 of the normalised count from DEseq were used to define otic expressed genes. In addition, a gene was considered to be enriched in the developing otic placode when the fold change between the otic sample and the whole embryo was ≥1.5; fold change was calculated using DEseq. Functional annotation of the

enriched genes was performed using DAVID (DAVID Bioinformatics Resources 6.7) (Huang da et al., 2009a, Huang da et al., 2009b). Otic enriched transcription factors were extracted and further analysed.

2.13 Chromatin immuno-precipitation (ChIP)

2.13.1 Cell dissociation and crosslinking

The tissue of interest was collected, as described in section 2.5, in a 1.7ml low binding tube (Costar). 0.5ml of Nuclei Extraction Buffer (NEB; Table 2.11) were added to the tissues and subsequently transferred to a pre-cooled 1ml dounce homogeniser. For all the passages low-retention tips (Advantip, Hamilton) or p1000 reach tips (ART molecular bio products, Fischer Scientific) were used to reduce material loss. The tissues were then homogenised by 20 strokes using a loose pestle. 488µl of homogenate was transferred to a new low binding tube. 12.16µl of 37% formaldehyde (Sigma) was added for cross-linking proteins and DNA. The tube was left rotating at room temperature for exactly 9 minutes. To stop cross-linking, 71.5µl of 1M glycine was added for 5 minutes at room temperature. The sample was then spun at 4000g at 4°C for 4 minutes, the supernatant was discarded and the pellet washed using pre-cooled PBS supplemented with Protease Inhibitor (PI) (10ml 1XPBS, 10µl 1M DTT, 10µl 200mM PMSF and 1 PI Mini tablet*). Three consecutive washes were performed; particular care was taken to avoid disturbing the pellet. After the last wash the pellet was snap frozen in liquid nitrogen and stored at -80°C.

2.13.2 Optimisation of chromatin sonication

To optimise the sonication around three neural tubes (100,000 to 200,000 cells) were collected from HH10-12 embryos. After cell dissociation and cross-linking (see section 2.13.1) the pellet was re-suspended in cold and freshly prepared NEB and transferred in 1ml dounce homogeniser. Cells were homogenised on ice by 20 strokes using a tight pestle. The homogenate was transferred to a new low binding tube and then spun at maximum speed (20,000g) for 1 minute at 4°C. The supernatant was discarded and the pellet washed with cold PBS/PI. After a second spin the pellet was re-suspended in 120µl of SDS lysis buffer (Table 2.12), after the addition of 20µl 7xPI the tube was placed on

ice at a 10° angle for around 1 hour to lyse the sample. Just prior to sonication 280µl of ChIP dilution buffer without Triton x-100 (Table 2.13) was added and mixed by slowly pipetting up and down. Extra care was taken to remove any bubbles; this is a critical step that may influence sonication efficiency. The samples were placed on ice and sonicated using a probe sonicator (SONICS, Vibra Cell™). Several conditions were tested to optimise the procedure, and finally 12 cycles were used (15 seconds on and 30 seconds off) at 40% amplitude. Using this condition DNA fragments obtained were less than 1000bp in size with the majority between 600 and 200bp (Figure 6.1, Appendix 9.3). Thereafter, 42µl of 10% Triton x-100 was added to the sample and spun for 10 minutes at 4°C at top speed. The supernatant (410µl) was transferred to a screw cap tube and then supplemented with 6µl of 0.5M EDTA and 17µl of 20% SDS. To reverse cross-link the chromatin, the sample was incubated over-night at 65°C on a thermo mixer at 400rpm.

The following day 450µl of 1x TE were added together with 18µl of RNAse A (10mg/ml, Sigma) to dilute the SDS and incubated at 37°C for one hour. Next, 18µl proteinase K (10mg/ml, Sigma) were added and the samples were incubated at 55°C for an hour. 900µl of phenol: chloroform: isoamyl alcohol was added to each sample, samples were vortexed for 30 seconds and spun at room temperature at maximum speed for 10 minutes. Approximately 900µl of the top aqueous phase were transferred to a new tube. To precipitate the chromatin 1ml of pure ethanol (molecular grade, Sigma) was added together with 99µl of 3M sodium acetate (pH 5.5) and 1.5µl of glycogen (20mg/ml, Thermo Scientific); the samples were left to precipitate at -80°C for around one hour. The samples were then spun at maximum speed in a pre-cooled centrifuge (4°C) for one hour. The supernatant was discarded and the pellet washed with 1ml of 70% ethanol for 10 minutes at maximum speed. The pellet was fully dried and dissolved in 12µl of molecular biology grade water (Fisher Scientific). To verify the sonication profile 3µl 1.5x loading dye was added to the samples and they and 1µl of 100bp ladder was run on a 1% agarose gel (60 Volts for 5 minutes and 120 Volts for one hour).

Table 2.11 Composition of Nuclei Extraction Buffer (NEB)

	Volume	Final concentration
10% NP-40	250µl	0.5%
10% Triton X-100	125µl	0.25%
1M Tris-HCl (pH 7.5)	50µl	10mM
100mM $CaCl_2$	150µl	3mM
1.5M Sucrose	833.3µl	0.25M
1M DTT	5µl	1mM
200mM PMSF	5µl	0.2mM
7x Protease Inhibitor (PI)*	750µl	1X
H_2O	2831.7µl	-
Total	**5000µl**	

***** 1 Mini tablet (Complete ULTRA Tablets, EDTA-free; Roche) in 1.5ml of molecular water

Table 2.12 Composition of SDS lysis buffer

Stock solution	Volume	Final concentration
20% SDS	500µl	1%
1M Tris-HCl (pH 8)	500µl	50mM
0.5M EDTA	200µl	10mM
H_2O	7371µl	-
Total	**10ml**	

Table 2.13 Composition of ChIP dilution buffer without Triton x-100

(A) ChIP dilution buffer without Triton x-100 stock solution

Stock solution	Volume	Final concentration
20% SDS	5µl	0.01%
1M Tris-HCl (pH 8)	167µl	16.7mM
0.5M EDTA	24µl	1.2mM
5mM NaCl	334µl	167mM
H_2O	7940µl	-
Total	**10ml**	

(B) Supplementation of ChIP dilution buffer without Triton x-100

Stock solution	Volume
ChIP dilution buffer w/o Triton x-100	847µl
200mM PMSF	2µl
1M DTT	1µl
7xPI	150µl
Total	**1000µl**

2.13.3 Chromatin immuno-precipitation (ChIP) for histone modifications

For each antibody used for immune-precipitation (IP) 100µl of well-vortexed Dynal magnetic beads (Protein A, Novex Life Technologies) were added to a low binding tube using a wide bore tip (ART molecular bio products, Fischer Scientific). The beads were then incubated with 1ml of blocking buffer (1X PBS with 0.5% BSA, filter sterilised) and left rotating at room temperature for 2 minutes. Using a magnetic stand the beads were collected on one side of the tube by leaving the stand horizontal for 3 minutes, this allows easy removal of the supernatant, for which p1000 reach tips were used (ART molecular bio products, Fischer Scientific). The beads were washed two more times following the same procedure. After the final wash, they were re-suspended in 250µl blocking buffer and the respective antibody was added (for details in antibody concentration and reference see Table 2.14). Antibody and beads were incubated overnight rotating at 4°C. To remove the un-coupled antibody the beads were washed for three times as previously described using 1ml of blocking buffer. All steps were performed in the cold room at 4°C. Finally, beads were re-suspended in 100µl of blocking buffer.

The tissue of interest (neural tube or pPPR cultured for 6 hours with or without FGF2) was homogenised and cross-linked (section 2.13.1). The pellet, stored at -80°C, was thawed on ice and processed as described in section 2.13.2. When the chromatin was used for immuno-precipitation, the protocol described in section 2.13.2 was followed up to the sonication step, afterwards 42µl of 10% Triton x-100 were added and the sample was span. Thereafter, 410µl supernatant were transferred to a new chilled low binding tube and 1ml of ChIP dilution buffer with Triton x-100 (Table 2.15) was added. Samples were spun again at maximum speed for 10 minutes at 4°C. 900µl of the supernatant were combined with the supernatant collected from the previous spin. The sonicated chromatin was gently mixed and evenly divided such that each IP, in a specific experiment, contains

the same amount of starting material. Importantly 1/10th of the chromatin was kept and stored at -80°C as input (control sample). The tubes containing chromatin and beads (conjugated with each specific antibody) were incubated overnight on a rotor at 4°C.

As described above, the next day tubes where placed on a pre-chilled magnetic stand and left in a horizontal position for 3 minutes to allow bead collection. The supernatant was carefully discarded using a p1000 reach tip; tips were changed between each tube to avoid any possible cross-contamination. Beads were then washed with 1ml freshly prepared RIPA buffer (Table 2.16) to remove any unbound chromatin. The tubes were mixed gently to obtain a uniform suspension and left rotating for 3 minutes. Thereafter beads were left to collect for 3 minutes and the supernatant was removed. A total of nine washes were performed. After the final wash, the beads were re-suspended in 1ml of TE/NaCl buffer (Table 2.17). After 3 minutes on the rotor the homogenous mix was carefully transferred to a new chilled low binding tube, trying to avoid any material loss. This step is important to reduce any non-specific background. The supernatant was discarded using the procedure previously described, and an extra TE/NaCl wash was performed. The supernatant was completely discarded by adding a spinning step (1000g for 3 minutes at 4°C); the excess of the buffer was removed using a p10 filter tip. All the above steps were performed in the cold room at 4°C.

Finally, the chromatin was eluted in 220µl ChIP elution buffer (Table 2.18) and incubated at 65°C for 15 minutes on a thermo mixer at 1,400 rpm. The tubes were centrifuged for 1 minute at 16,000g at room temperature and 200µl of the pellet was very carefully transferred to a screw cap tube, avoiding pipetting any beads. Samples were then incubated at 65°C overnight on a thermo mixer at 400rpm for reverse cross-link the protein and the chromatin. The input, which had been stored at -80°C, was thawed on ice and 3 volumes of elution buffer was added. Similarly, the input was transferred to a screw cap tube and reverse cross-linked.

On the last day of the protocol, 200µl 1xTE were added together with 8µl of RNAse A (10mg/ml) to each sample and incubated at 37°C for one hour. Next, 8µl of Proteinase K (10mg/ml) were added for one hour at 55°C. Purification of the chromatin was performed by adding 400µl of phenol: chloroform: isoamyl alcohol, fully vortexed and the phase separated by spinning (15 minutes at maximum speed at room temperature). 380µl of the top phase, containing the pulled down chromatin, was transferred to a fresh low binding tube and, 1140µl of ethanol plus 42µl 3M sodium acetate (pH 5.5) and 1.5µl glycogen

(20mg/ml) were added. Chromatin was precipitated at -80°C for one hour and spun at maximum speed for one hour at 4°C. After the supernatant was discarded, the pellet was washed in 70% ethanol and spun (10 minutes maximum speed). The pellets were left to air dry completely and were dissolved in 10µl molecular grade water when used for RT-qPCR runs (for antibody validation see section 2.13.4) or in 60µl for linear amplification (see section 2.13.5).

Table 2.14 References and concentrations for the antibodies used for ChIP

Antibodies	Company	Amount used	Volume added
Rabbit anti-IgG	Millipore (CA92590)	5µg	5µl
Rabbit anti-H3K4me1	Diagenode (pAB194-050)	2.5µg	2.7µl
Rabbit anti-H3K27ac	Abcam (ab4729)	2.5µg	2.8µl
Rabbit anti-H3K27me3	Cell signalling (C36B11)	-	2.5µl

Table 2.15 Composition of ChIP dilution buffer with Triton x-100

(A) ChIP dilution buffer with Triton x-100 stock solution

Stock solution	Volume	Final concentration
20% SDS	5µl	0.01%
1M Tris-HCl (pH 8)	167µl	16.7mM
0.5M EDTA	24µl	1.2mM
5mM NaCl	334µl	167mM
H_2O	6830µl	-
Total	**10ml**	

(B) Supplementation of ChIP dilution buffer without Triton x-100

Stock solution	Volume
ChIP dilution buffer w Triton x-100	737µl
200mM PMSF	2µl
1M DTT	1µl
7xPI	150µl
10% Triton x-100	110µl
Total	**1000µl**

Table 2.16 Composition of the washing buffer RIPA

Stock solution	Volume	Final concentration
1M Hepes-KOH (pH8)	2.5ml	50mM
5M LiCl	5.0ml	500mM
0.5M EDTA	0.1ml	1mM
10% NP-40	5ml	1%
10% Na-deoxycholate*	3.5ml	0.7%
1 Maxi tablet of PI	-	-
H_2O	33.9ml	-
Total	**50ml**	

*Na- deoxycholate is highly unstable therefore the RIPA buffer was freshly made

Table 2.17 Composition of TE/NaCl buffer

Stock solution	Volume	Final concentration
10x TE	1ml	1x
5M NaCl	0.1ml	50mM
H_2O	8.9ml	-
Total	**10ml**	

Table 2.18 Composition of ChIP elution buffer

Stock solution	Volume	Final concentration
1M Tris-HCl (pH 8)	2.5ml	50mM
0.5M EDTA	1.0ml	10mM
20% SDS	2.5ml	1%
H_2O	41.5ml	-
Total	**50ml**	

2.13.4 qPCR for ChIP validation

To validate antibody specificity neural tubes from stage HH10-12 embryos were dissected and processed for ChIP-qPCR. Known active and repressed genes and enhancer regions were selected (Figure 6.1) and specific primers were designed (Table 2.20). The ChIPed chromatin was used to set up a qPCR experiment (Table 2.19). After analysing the profile of amplification an arbitrary threshold of 0.01 was used to extract the corresponded Ct values. For each condition three technical replicates were setup and their

average value was calculated. The ΔΔCt was calculated comparing the average value of each antibody, for each primer pair, against the input as described in the following equations. Since 1/10 of the chromatin was used for the input a dilution factor of 10 was introduced in the first equation (Equation 4).

Equation 4 $$\Delta Ct = [Ct\ (input) - \log_2 10]\ - Ct\ (test\ antibody)$$

Equation 5 $$\Delta\Delta Ct = 2^{(-\Delta Ct)}$$

The percentage of enrichment of each antibody compared to the input, obtained from Equation 5, was used to analyse the profile of pull-down at each tested region. Standard error of the mean (Equation 6) and standard error (Equation 7) were calculated; the standard error was used for the error bars in the chart.

Equation 6 $$SEM = StDev/\sqrt{n}$$ (StDev= Standard Deviation; n= number replicates)

Equation 7 $$SE = \log_e 2 * \Delta\Delta Ct * \sqrt{(SEM\ test\ antibody)^2 + (SEM\ input)^2}$$

Table 2.19 ChIP-qPCR

ChIP-qPCR composition	
ChIPed chromatin	**0.5µl**
SYBER green master mix (Roche)	**5µl**
Forward Primer (2µM)	**1.25µl**
Reverse Primer (2µM)	**1.25µl**
Nuclease-free H_20	**2µl**
Total	**10µl**
PCR condition	
1. 95°C for 10 minutes **2.** 95°C for 10 seconds **3.** 60°C for 30 seconds **4.** 72°C for 30 seconds **5.** Go to 2, 4 for 40 times **6.** 72°C for 5 minutes Melting temperature 60°C to 95°C; 1°C each step	

Table 2.20 Primers used for ChIP-qPCR

Gene	Primers
SOX2_N2	F 5'-CGGCACACGCACTCTTAT-3' R 5'-AGATTGGTTACTGGCAGGTT-3'
SOX2_N4	F 5'-CCTACCTCCTCGCTTCCAA-3' R 5'-GGCATAGCATCCAACCTAAGTAAG-3'
SOX2_P	F 5'-TACATTCAAACTACTTTAGCC-3' R 5'-TAATCCATCAGCGAAGAG-3'
SOX3_P	F 5'-TCTCCAAACCGACCCATTA-3' R 5'-GCATTTGATTGACGGGCTATA-3'
GATA2_P	F 5'-CAGAGGATGAAGGGTAATACAGG-3' R 5'-TGTCTTTGTGATATGGTTCGGG-3'
SPALT4_E	F 5'-GAGTTTGAAGGGATAAGGGAAGAT-3' R 5'-GTCTGAGAAGCCTTACCTGAG-3'

2.13.5 Amplification of the ChIPed chromatin and Next Generation Sequencing

In order to obtain sufficient material for Next Generation Sequencing a step of linear amplification was performed after chromatin immuno-precipitation. The amplification was carried out as described in the protocol published by Adli and Bernstein (2011).

A two stages protocol was performed; here the main steps are summarised. In the first step (stage A) the DNA was primed using primer1 (5′-GACATGTATCCGGATGTNNNNNNNNN-3′; HPLC purified, IDT) and the Sequenase enzyme. Three cycles were performed; the enzyme was repeatedly added each time and the PCR cycler lid was turned off since the Sequenase is not thermo stable (Table 2.21). To remove the excess of primer1 3µl ExoSAP-IT were added to each sample and they were incubated at 37°C for 15 minutes. Subsequently, ExoSAP-IT was heat inactivated by incubation at 80°C for 15 minutes. Finally, the stage A product was diluted four times by adding 45µl of water.

Thereafter linear amplification was carried out (stage B) using primer2 (5′-GACATGTATCCGGATGT-3′; HPLC purified, IDT) and Phusion enzyme for a total of 15 cycles (Table 2.22). For each sample four stage B reactions were set up. The PCR products were purified using a PCR purification kit (mini elute kit from Qiagen) and eluted twice (25µl followed by 20µl) in molecular grade water. The fragment size and concentration were estimated using Agilent Bioanalyser and compared with the unamplified DNA (see Appendix 9.3). The amplified chromatin was immediately send

for library preparation and then used for pair end sequencing. The library preparation was performed by Tony Brooks (Sequencing Applications Specialist, UCL Genomics, Institute of Child Health) following the protocol used for nano-ChIP-seq (Adli and Bernstein, 2011), with the exception that only 12 cycles were used in the PCR amplification. Details for stock solutions and materials used for the ChIP protocol are summarised in Table 2.23.

Table 2.21 Stage A: Sequenase priming reaction

Sequenase priming reaction	
ChIPed chromatin	**7µl**
5x Sequenase buffer	**2µl**
Primer1 (4µM)	**1µl**
Total	**10µl**
Stage A reaction mix	
5x Sequenase buffer	**1µl**
dNTPs (3mM)	**1.5µl**
DTT (0.1M)	**0.75µl**
BSA (10 mg/ml)	**1.5µl**
Sequenase enzyme (13 U/µl)	**0.3µl**
Total	**5.05µl**
Stage A cycling conditions	
1. 98°C for 2 minutes **2.** 8°C for 1 minutes **3.** Add 5.05µl reaction mix **4.** 8°C for 2 minutes **5.** 16°C for 1 minutes **6.** 22°C for 1 minutes **7.** 28°C for 1 minutes **8.** 36°C for 30 seconds **9.** 36.5°C for 1 minutes **10.** 37°C for 8 minutes **11.** Go to cycle 1, repeat for 3 times **12.** 4°C	

Table 2.22 Stage B: amplification

Stage B reaction mix	
Stage A diluted product	**15µl**
5x GC reaction buffer	**10µl**
dNTPs (10mM)	**2µl**
Primer2 (10µM)	**1µl**
100% DMSO	**1µl**
Nuclease-free H_20	**20µl**
Phusion enzyme (2 U/µl)	**1µl**
Total	**50µl**

Stage B cycling conditions
1. 98°C for 2 minutes
2. 88°C for 10 seconds
3. 55°C for 30 seconds
4. 60°C for 30 seconds
5. 72°C for 20 seconds
6. 72°C for 10 minutes
7. Go to cycle 2, repeat for 15 times
8. 4°C

Table 2.23 General stock solution and equipment used for ChIP protocol

Stock solutions and material for ChIP
1. 37% formaldehyde solution (stored at room temperature in the dark, Sigma)
2. 1 M glycine (0.22µm filtered sterilise, aliquoted and stored at -20° C, Sigma)
3. 1 M DTT (0.22µm filtered sterilise, aliquoted and stored at -20° C)
4. 1.5M Sucrose (0.22µm filtered sterilise, aliquoted and stored at -20° C, Sigma)
5. 0.2 M PMSF (dissolved in ethanol, filtered sterilise 0.22µm, aliquoted and stored at -20° C, Gibco BRL)
6. Protease inhibitor tablet (PI) (Complete, Mini, EDTA-free- Prepared 7X stock solution by dissolving 1 tablet in 1.5ml of molecular water. The stock solution is stable for at least 12 weeks at -15 to -25° C, Roche)
7. 1M Tris-HCl pH 7.5 and pH 8.0 (autoclaved, stored at room temperature, Sigma)
8. 1M Hepes-KOH pH 8 (0.22µm filtered sterilise, stored at 4° C, free acid Omni Pure)
9. 5M NaCl (autoclaved, stored at room temperature, Sigma)
10. 5M LiCl (autoclaved, stored at room temperature, Sigma)
11. 0.1M $CaCl_2$ (0.22µm filtered sterilise, stored at room temperature, BDH AnalaR)
12. 10X TE (100mM Tris-HCl pH8, 10mM EDTA)
13. 20% SDS (0.22µm filtered sterilise, stored at room temperature, BDH AnalaR)
1. 0.5 M EDTA pH 7.5 (autoclaved, stored at room temperature, BDH AnalaR)

2. 10% Triton X-100 (0.22µm filtered sterilise, stored at room temperature, BDH AnalaR)
3. 10% NP-40 (0.22µm filtered sterilise, stored at 4° C, Fluka Biochemica)
4. 10 mg/ml RNAse A (Invitrogen)
5. 20 mg/ml Proteinase K (Roche)
6. BSA (molecular biology grade, Sigma)
7. 20µg/µl Glycogen (molecular biology grade, Thermo Scientific)
8. 1 ml all glass dounce homogenizer sets (loose pestles (A) and tight pestle (B), Kontes Kimble)
9. Low-retention tip (1000µl, Hamilton Advantip)
10. Wide-bore tips (200µl, ART molecular bio products, Fischer Scientific)
11. 1.7 ml low-binding tubes (DNAase, RNAase free, Costar)
12. Molecular biology grade water (DNAase, RNAase free, Fisher Scientific)
13. Dynabeads protein A (magnetic beads, Novex life technologies)
14. Magnetic stand (Eppendorf)
15. Na-Deoxycholate (Sigma)
16. Complete ULTRA Tablets (mini and maxi) EDTA-free Protease Inhibitor (Roche)
17. 3M Sodium acetated PH 5.5 (molecular biology grade, Ambion)
18. Ultra-pure PCI (phenol: chloroform: isoamyl alcohol PH 8.0, Sigma)
19. Reach tips (1000µl, ART molecular bio products, Fischer Scientific)
20. Filter tips (p1000, p200 and p10, Star lab)
21. Screw cap tube (1.7ml, Sarstedt)

Stock solutions and material for amplification

1. Ultra-pure PCI (phenol: chloroform: isoamyl alcohol PH 8.0, Sigma)
2. RNase solution (20 mg/ml, Invitrogen)
3. Sequenase enzyme Kit (Version 2.0, U.S. Biochemical)
4. dNTP mix (Invitrogen)
5. BSA (10 mg/ml; NEB)
6. DTT (0.1 M stock, Invitrogen)
7. Primer1 (4µM): 5'-GACATGTATCCGGATGTNNNNNNNNN-3' (HPLC purified, IDT)
8. ExoSAP-IT (U.S. Biochemical)
9. Phusion polymerase (NEB, provided with 100% DMSO, 5× GC buffer)
10. Primer2 (10µM stock): 5'-GACATGTATCCGGATGT-3' (HPLC purified, IDT)
11. MinElute PCR purification kit (Qiagen)
12. Nuclease-free water (Fisher Scientific)
13. Strip PCR tube (0.2ml, Star lab)
14. Filter tips (p1000, p200 and p10, Star lab)

Equipment

1. Thermo mixer (Mixing block, Bioer, Alpha laboratories)
2. Thermo cycler (Gene pro, Bioer, Alpha laboratories)
3. Centrifuge (Eppendorf, 5415R)
4. Probe Sonicator (SONICS, Vibra Cell TM)

2.13.6 Bioinformatics analysis of the ChIP-seq data

To assess sequence quality the ChIP-seq reads were scanned with FastQC (Andrews, 2010). The amplification steps of the nano-ChIP-seq protocol are reported to produce high mismatch at the first 9 bases, probably due to imperfect hybridisation of random primers (Adli and Bernstein, 2011). Therefore 9bp at the 5' were trimmed. Additionally, a few bases at the 3' end were trimmed where the sequence quality was poor (Appendix 9.3). The reads were aligned using Novoalign (Novocraft 2.08.01) to the last version of the chicken genome (Galgal4.71). Uniquely aligned sequences (Appendix 9.3) were used for peak calling using the software Homer (Heinz et al., 2010). Statistically significant peaks were defined by several parameters: 1) fold enrichment over Input ≥1.5; 2) False Discovery Rate (FDR) ≤0.01; 3) since histone peaks cover broad regions a minimum size of the peaks was set at 750bp (arbitrary value set based on histone mark Tag distribution); 4) a minimal distance of 300bp was used to identify separate peaks. In order to predict regions devoid of all histone marks all the reads files were merged together and peak calling was performed as described above. Thereafter, enhancers were predicted: 1) considering regions lacking histone marks; 2) such regions should be flaked by two H3K27ac peaks and 3) H3K27me3 peaks should not be present. The retrieved putative enhancers were annotated, using the Homer function 'annotatePeaks', to the nearest gene according to the gene annotation file used for mRNA-seq analysis (see section 2.12.2). The distributions of annotate reads (Tag distribution) around the transcription start side or the centre of putative enhancers was performed using the Homer function 'annotatePeaks'. The analysis described above was performed independently for the –FGF and +FGF ChIP-seq samples. Common versus unique putative enhancers from FGF treated and untreated samples were identified using the R package 'ChIPpeakAnno'. Correlation between putative enhancers and gene level of expression from mRNA-seq was performed using the Wilcoxon test in R. The function of genes with an associated enhancer was annotated using DAVID (DAVID Bioinformatics Resources 6.7) (Huang da et al., 2009a, Huang da et al., 2009b). This bioinformatics analyses was performed by Maryam Anwar.

2.14 Putative enhancer cloning in the pTK reporter vector

Fragments of the putative enhancers, identified with the bioinformatics pipeline described above, were retrieved from UCSC genome browser and specific primers were designed

using the IDT primer quest tool (http://eu.idtdna.com/PrimerQuest; primer listed in (Table 2.24). The putative elements were amplified from chick genomic DNA using the PCR conditions reported in Table 2.25. To sub-clone the enhancer from the initial full-length fragment, additional primers were designed in the desired location (Table 2.24). The PCR product was run on a gel and the specific band was cut and purified (Agarose gel DNA extraction kit, Roche). The pTK vector was linearised using the blunt-end restriction enzyme SmaI at 25 °C overnight. The linearised vector was purified and tailed with dTTP by using goTag DNA Polymerase (Promega) and dTTP, for 2 hours at 72°C. Ligation takes advantage of the fact that during PCR goTag DNA Polymerase adds dATP to each ends of the fragment, thus generating ends complementary to the dT-tailed vector. Ligation was set up using: linearised vector, purified PCR fragment, 1µl 10x T4 DNA ligase Buffer (Promega) and 1µl T4 DNA ligase enzyme (Promega). A 1:1 molar ratio of vector and PCR product was found to be the optimal ratio for this kind of ligations. The reaction was incubated over night at 16°C. 3-5µl ligation were transformed into 50-100µl DH5α competent cells. After adding DNA, the cells were kept on ice for 25 minutes, incubated at 42°C for 30 seconds and re-placed on ice for 2 minutes. 600µl LB were added to the tube and the cells were incubated for 1 hour at 37°C shaking at 225 rpm. The tube was then spun at maximum speed, approximately 500µl supernatant were discarded; the pellet was re-suspended and plated on a LB agar plate with ampicillin (100µg/ml). Plates were then incubated at 37°C overnight and the following day bacteria colonies were screened. 5-10 colonies were picked using a yellow tip and screened by colony PCR. The tip was scraped at the bottom of a 0.2µl tube and the exact same tip was put into 3-5ml LB plus ampicillin media. PCR mixture (Table 2.25) was added to each tube and the PCR was performed as described in Table 2.25; the product size was visualised by gel electrophoresis. 2-3 colonies with the correct insert were grown overnight at 37°C and the plasmids were purified with a miniprep kit (peqGOLD miniprep kit, Peqlab). The correct insert was further verified by sequencing. High concentration of plasmid DNA was obtained by midiprep (peqGOLD XChange Plasmid midiprep, Peqlab) and was later used for *in vivo* electroporation (see section 2.3).

2.15 Transcription factor binding site analysis

Enhancers from ChIP-seq were scanned for transcription factor binding sites (TFBSs) using a customised library containing enriched TFs in the PPR, otic, lens and trigeminal placodes (expression data from molecular screens) using RSAT (Foxi3 E1, Foxi3 E2). A

z-score of 6 and above was used to identify significant binding sites from Clover. Binding sites for a single transcription factor (e.g. Ap1) were analysed using RSAT as it reports individual occurrences of each TF in provided sequences. Co-occurrence of TF binding motifs in ChIP-seq enhancers was done in R by clustering enhancers based on TFBS data from RSAT. This bioinformatics analyses was performed by Maryam Anwar.

Table 2.24 Primers for putative enhancer cloning

Gene	Primers	Size	Coordinates
Foxi3 E1	F 5'-CTCATTATCCCAGCTCCCTCCT-3' R 5'-GCAGGCAAACCTTGTGGAAAC-3'	3660	Chr4: 85593696-85597534
Foxi3 E1.A	F 5'-CTCATTATCCCAGCTCCCTCCT-3' R 5'-GATCAGATTGCACCTGCCTAA-3'	1883	Chr4: 85593696-85595578
Foxi3 E1.B	F 5'-AGCTGCGATTTCATGCTTAAC-3' R 5'-GCAGGCAAACCTTGTGGAAAC-3'	2204	Chr4: 85595331-85597534
Foxi3 E1 NFR	F 5'-AAGGAACTTGGGCAGGATG-3' R 5'-GAGTTCGTTCAGGAAAGACAGA-3'	1992	Chr4: 85594801-85596939
Foxi3 E1.C	F 5'-TCTGACATTTCATCATGGCTTCA-3' R 5'-CCCTTCTTGTTGTTGTTGTGT-3'	962	Chr4: 85595131-85596131
Foxi3 E1.D	F 5'- TCTGACATTTCATCATGGCTTCA-3' R 5'- GGTCATCTGAATGACAACTGTCTC-3'	610	Chr4: 85595131-85595778
Foxi3 E2	F 5'-GCCTTGTATGGATGTTGCTGGA-3' R 5'-AGCTGGTGAACTCAATGGTGATG-3'	3450	Chr4: 85610429-85613878
Foxi2 E2.A	F 5'-GCCTTGTATGGATGTTGCTGGA-3' R 5'-CAGACGGAGGATGCTGTAATG-3'	982	Chr4: 85610395-85611376
Foxi2 E2.CNS	F 5'-TTTGGCCCTGTTCAAATGG-3' R 5'-CAGTTTGTTGATACCTTCAGTGT-3'	497	Chr4: 85611274-85611770
CXCL14 E1	F 5'-AGCCTACCAGTTGTCCTAGA-3' R 5'-CACAGTGTATTGCTTGGCTTT-3'	1651	Chr13: 14642163-14643893
SPRY1 E1	F 5'-CTGCCAGCTGTTTCCATTTC-3' R 5'-CTGGGCTGCATGTTGTATTTC-3'	1493	Chr4: 52750797-52752350
SPRY1 E2	F 5'-CTGTACATTTCATGCCCTAAGC-3' R 5'-TTTCCCTATTCTGCCTTCCTC-3'	853	Chr4: 52760097-52761083
SPRY1 E3	F 5'-CCTCTGATTGCTCACAGCTT-3' R 5'-TTTCCTCTGTGCCTTTGGAC-3'	778	Chr4: 52764665-52765503
SPRY2 E2	F 5'-GCAAGAGTTACATTTAAGACCCTTAG-3' R 5'-TGCCAAGATGAACTGTCTCTC-3'	853	Chr1: 151929286-151931013
SPRY2 E4	F 5'-ACTAGTAGTAGCATACACACAAAGAG-3' R 5'-AGCTCAAGATCAGCACAAACTA-3'	778	Chr1: 152018235-152019860
HESX1 E1	F 5'-GAGACCCTTCAACTTACCAATCT-3' R 5'-GATCCCAGTATCTGAGTGCTTC-3'	1260	Chr12: 8580923-8582319
SOX13 E1	F 5'-GAACAAAGGACCAAAGAGAGGA-3' R 5'-AACTGAGCAAATTGTGGTTCTG-3'	1178	Chr26: 1632057-1633251
PAX6 E1	F 5'-CCTGCAATCCTTCCCAATCT-3' R 5'-AATTAAGACTAGTCGCCCAACC-3'	1691	Chr5: 5247319-5249078

GATA3 E5	F 5'-CTTTAGAAATACCCAAACTTGCAGA-3' R 5'-CTGATTATACCTGACATAACCCACT-3'	675	Chr1: 4596414-4597191

Table 2.25 Composition and condition of the PCR reaction for enhancer cloning

PCR composition	
5x GoTaq Buffer (Promega)	**10µl**
dNTP Mix (10mM each) (Roche)	**1µl**
Forward Primer (10µM)	**1.25µl**
Reverse Primer (10µM)	**1.25µl**
goTaq DNA Polymerase (5µg/µl) (Promega)	**0.25µl**
genomic DNA (100ng/µl)	**2µl**
Nuclease-free H_20	**34.25µl**
Total	**50µl**
PCR condition	
8. 95°C for 3 minutes **9.** 95°C for 10 seconds **10.** 60°C for 45 seconds **11.** 72°C for 4 minute **12.** Go to 2, 29 more times **13.** 72°C for 10 minutes **14.** 4°C	

3. Identification of novel genes in the pre-placodal region and early otic placode

3.1 Introduction

The process of PPR and otic specification is complex and so far poorly understood. While some molecular players are known many new factors and their interactions still need to be identified. As previously described, surrounding tissues play an important role in PPR induction: e.g. the mesoderm underneath the PPR induces the expression of *Six1, -4* and *Eya2* in a naïve region that normally never forms placodes (Litsiou et al., 2005). However, does the induced PPR have properties identical to the endogenous PPR? The PPR is normally specified as lens (Bailey et al, 2006) and is the only region responsive to placode inducing signals (Martin and Groves, 2006). However, the induced area opaca (iAO), if cultured in a neutral media, will not develop to express any lens marker (e.g. *Pax6*) nor will it respond to FGF signalling and express any otic marker (e.g. *Pax2)* (Christophorou, 2008). This suggests that the endogenous PPR has some additional characteristics not present in the induced tissue. To identify the missing factors involved in PPR specification a microarray screen was designed (Christophorou, 2008). Four different tissues were compared: non-induced area opaca (AO), mesoderm induced area opaca (iAO), anterior and posterior PPR (aPPR, pPPR; Figure 3.1).

For each cell population (AO, iAO, aPPR, pPPR) three biological replicates were performed and hybridised to chick Affymetrix microarrays. The initial downstream analysis was performed using Genespring GX (analysis carried out by Dr David Chambers; MRC Centre for Developmental Neurobiology). Biological replicates were normalised to take into account unequal RNA amounts and detection efficiency across different chips (Quackenbush, 2001, Quackenbush, 2002); the raw value of each gene was divided by the mean raw value of all genes on the chip. To visualise the quality of each sample the normalised values were plotted on a logarithmic scale; most values centre around 1 for all 12 arrays (Figure 3.2). Subsequently, a second step of normalisation was performed, by calculating the average normalised value between the three biological replicates. These values were then used to compare gene expression across samples.

The Affymetrix chip contains a total of 38,535 probes; of these around 12,000 probes were found to be expressed at a not appreciable level in any cell population and therefore considered to be absent. To identify genes with robust changes from the remaining probes a 2-fold change was used as cut off. 10,621 genes met this criterion and they were processed for one-way ANOVA analysis (ANalysis Of VAriance) to identify significant changes. This resulted in a total of 3,471 probes showing significant changes across at least two cell populations with a p-value ≤ 0.05 (Figure 3.3).

To assess the reliability of the data the behaviour of known genes was assessed. The level of expression of some of these genes is shown in Figure 3.4 A. The pre-placodal marker *Eya2* is strongly expressed in the entire PPR, as expected. In addition, it is highly induced by the head mesoderm, being expressed at a low level in the control area opaca and presenting an up-regulation only after induction by the mesoderm as previously shown by Litsiou et al. (2005) and Christophorou (2008). An anterior PPR marker, *Pax6*, is enriched in the anterior part of the PPR (Bailey et al., 2006); in contrast *Gbx2* is more strongly expressed in the posterior PPR (Steventon et al., 2012) and it is also present in the induced area opaca. *Sox3* is normally expressed in the neural plate and in the PPR albeit at lower level; it is weakly induced by the mesoderm (Litsiou et al., 2005). Finally, the neural crest marker *Pax7* is almost absent from all the four groups in accordance with published data (Litsiou et al., 2005). In conclusion, the microarray data have a good quality and reproduce findings reported in the literature.

Among the 3,471 enriched genes only 2,402 were successfully annotated and processed for further analysis. Furthermore, it is important to note that some genes known to be present in the PPR and placodal tissues are absent from the Affimetrix microarray e.g. Dlx5, Six1, Six4, Pax2 and Gata3, raising the possibility that some information will be missed. The successfully annotated genes were classified according to their molecular function using gene ontology terms. The publicly available Gene Set Enriched Analysis (GSEA) tool was used to categorise genes according to their function (Subramanian et al., 2007, Subramanian et al., 2005). Only around 1,900 genes presented a match with annotated terms and only around 1,000 were significantly associated with gene ontology terms (Figure 3.4 B).

The ultimate aim of the project is to establish a gene network for early otic specification and to identify the major transcriptional regulators. Therefore, it is necessary to focus on

classes of molecules involved in transcriptional regulation and to identify those transcripts that are specifically expressed in placodal cells. Thus, in this chapter I will describe the identification of the temporal and spatial expression patterns of selected transcripts as a basis to establish their hierarchy during otic placode induction.

3.2 Clustering of genes with a similar expression profile across cell population and identification of syn-expression groups

To further understand the process of PPR and early otic specification I decided to focus mainly on i) transcription factors, as first players in gene regulation; ii) chromatin remodelling molecules involved in gene activation and repression (overall around 100 genes have been associated with transcription regulation, Figure 3.4 B); and iii) a few factors involved in intercellular communication. Among these categories around 80 genes were selected from the microarray (90% transcription factors, 6% chromatin enzymes and 4% signalling molecules) and displayed as a heat map using R gplots tool (heatmap.2 function). A false colour image was generated and genes were clustered according to their expression values across all samples. The dendrogram highlights genes with similar behaviour (Figure 3.5). The comparison of expression level across the four-cell population is important to highlight factors differentially expressed in the PPR and/or induced by the mesoderm (Figure 3.1 B). As mentioned above the presence and behaviour of the known genes is important to ensure the reliability of the clusters.

Pax6, an anterior PPR marker, is grouped together with seven other genes (light blue cluster). Among them are *SSTR5* and *pNoc*, a neuropeptide receptor and neuropeptide expressed in a domain overlapping with *Pax6* and known Pax6 up-stream regulators (Lleras-Forero, 2011, Lleras-Forero et al., 2013). Likewise, *Follistatin-like 4*, a TGFβ superfamily inhibitor, is expressed in the anterior neural plate and PPR (Lleras-Forero, 2011). *Dlx6* in addition is specifically expressed in the anterior PPR in chick (Brown et al., 2005) (Figure 3.9 A-C). Finally, *Eya2* also clusters together with anterior PPR genes, probably because it is more abundant anteriorly than posteriorly at neurula stage (Ishihara et al., 2008a). Within this cluster there is some variability since *Pax6*, *SSTR5*, *Follistatin-like 4* and *Dlx6* are not induced by the cranial paraxial mesoderm whereas *pNoc* and *Eya2* are. Thus, genes in this group are potential new markers of the anterior PPR (Figure 3.9A-C).

A small cluster of six molecules represents genes highly enriched in the posterior PPR, from where the trigeminal, otic and epibranchial placodes originate (green). Among them *Gbx2* is a known posterior PPR and otic marker (Steventon et al., 2012, Li et al., 2009, Tour et al., 2001, von Bubnoff et al., 1996, Paxton et al., 2010, Niss and Leutz, 1998, Su and Meng, 2002). *Irx2*, a transcription factor of the Irx family, is strongly expressed in the posterior PPR and later in the otic region (Goriely et al., 1999, Glavic et al., 2002, Gomez-Skarmeta et al., 2001, Khudyakov and Bronner-Fraser, 2009) and *Lmx1b* has also been associated with otic development (Abello et al., 2010). Additionally, my expression data (see below) support enrichment of the transcription factor *Yeast4* in the posterior domain of the PPR (Figure 3.8), although it is later restricted to the neural tube, as well as enrichment of the histone methyltransferase *Setd2* in the future otic domain (Figure 3.11). A second small cluster, includes genes related to otic development e.g. *Sox8* (Betancur et al., 2011, Sinkkonen et al., 2011, Guth et al., 2010, Sock et al., 2001, Bell et al., 2000, O'Donnell et al., 2006) (see Chapter 4) and *Etv5* (Lunn et al., 2007, Chotteau-Lelievre et al., 1997, Roehl and Nusslein-Volhard, 2001, Znosko et al., 2010, Munchberg et al., 1999, Chotteau-Lelievre et al., 2001, Raible and Brand, 2001). *Homer2*, which is included in this cluster, is identified as a new PPR and otic marker (Figure 3.12). Genes in these two clusters appear to be induced by signals from the mesoderm, as they are expressed in the induced area opaca.

A large cluster contains genes expressed in anterior and relatively enriched in the posterior PPR. The mesoderm underling the pre-placodal region induces the majority of them. Expression pattern of some of these genes will be discussed in more detail in following paragraphs.

The cluster of five genes, highlighted in purple at the top of the heatmap, is the only group of genes expressed in the endogenous PPR and not induced by the mesoderm, and therefore might be important to confer intrinsic PPR properties. Among them *Zic1* and *Sox2* are expressed initially in the entire PPR and later restricted to the neural plate (Khudyakov and Bronner-Fraser, 2009, Rex et al., 1997, Uchikawa et al., 2003, Streit et al., 1997, Uwanogho et al., 1995, Mizuseki et al., 1998, Okuda et al., 2006, McMahon and Merzdorf, 2010, Nagai et al., 1997, Nakata et al., 1998, Fujimi et al., 2006); *Otx2* is initially expressed widely in the epiblast including neural and placode precursors, but then is more confined anteriorly, complementary to *Gbx2* (Steventon et al., 2012, Li et al., 2009, Tour et al., 2001, von Bubnoff et al., 1996, Paxton et al., 2010, Niss and Leutz,

1998, Su and Meng, 2002). *Six3* and *Hesx1* (*Ganf*) behaviour from the microarray screen seems not to be in line with their spatial expression in the embryo, since they are weakly expressed in the anterior neural plate, and only later, in chick development, they will appear in sensory placodes (Bovolenta et al., 1998, Chapman, 2003).

In conclusion, cluster analysis reveals relativly small groups of transcripts with similar expression profiles across the four cell populations examined, which are in line with their expression reported in the literature, with a few exceptions.

3.3 Classification of genes accordingly to their spatial and temporal expression

However, the microarray data cannot provide information on spatial distribution of transcripts; e.g. they do not allow a distinction between genes specific to the PPR and those expressed in multiple territories within the ectoderm (e.g. PPR, neural plate, neural crest and epidermis). Therefore the heatmap information is limited to the four-cell population used in the screen. For example, from the microarray analysis a transcript could be identified as expressed in the PPR but it could be ubiquitously expressed in the ectoderm, hence unlikely to play a specific role in PPR or placodes specification. Therefore, I decided to assess the spatial-temporal expression of transcripts for which no expression patterns had been described in the chick. This analysis not only provides novel expression data, but based on the timing of expression also predicts their possible hierarchy and reduces the number of genes to be analysed further.

To add spatial and temporal information I analysed the expression of about 60 factors by *in situ* hybridisation at different stages of chick development (from HH4- to HH9) screening the majority of genes contained in the heatmap (Figure 3.5). The following broad expression domains were considered: anterior versus posterior embryonic regions, medial versus lateral territories and different germ layers (see Appendix 9.1, Figure 9.1). The genes characterised can be categorised into 4 main classes: ubiquitously expressed in the ectoderm (9 genes), genes enriched in the neural plate and PPR (18 genes), transcripts highly expressed in the neural plate (22 genes) and lastly genes restricted to the PPR (5 genes). The remaining genes have weak expression or cannot be detected in the ectoderm at all, these could be due to poor *in situ* probes or they could be false positive from the microarray screen. The summary of these expression patterns together with the known

PPR and otic genes are listed in Appendix 9.1. The following section describes some examples for each class.

The transcription factors *Bclaf1*, *Aatf1* and *FoxM1* are examples of the first category of ubiquitously expressed genes (Figure 3.6). Overall they are broadly present in the ectoderm from gastrulation stage onwards, where they are expressed in the neural plate (NP), the border of the neural plate containing a mixture of future neural, neural crest, placode and epidermal cells (B), and the non-neural ectoderm (NNE) domains. They maintain a broad expression throughout the stages analysed. This category of genes is unlikely to be specifically involved in the process of PPR formation.

A second class includes genes mainly present in the neural plate and border region; generally these transcripts are excluded from (or only weakly expressed) in the more lateral non-neural ectoderm, the future epidermis. Trim24, Znf462 and Mta3 represent members of this group (Figure 3.7). *Trim24* is excluded from the non-neural ectoderm from gastrulation stages onwards (Figure 3.7 A), whereas *Znf462* and *Mta3* are initially more broadly expressed (Figure 3.7 D, G). As neurulation begins they all become enriched in the neural and PPR, making them an interesting category to further study.

A third group comprises molecules initially expressed in the neural plate and PPR that become restricted to the neural plate domain during somitogenesis. *Nsd1*, *Yeast4* and *Tbpl1* are good examples for this expression profile (Figure 3.8). They are expressed in a relativly extended region between gastrulation and neurulation (Figure 3.8 A, B, D, E, G, H) and subsequently switched off from the medio-lateral region and enriched in the neural plate (Figure 3.8 C, F, I). Likewise, the genes in this class may be important players in the specification of neural and PPR precursors.

Lastly, only three new genes were found to be restricted to the PPR; the transcription factors *Dlx6* and *Nfkb1* and the scaffold protein *Homer2* (see section 3.6). *Dlx6*, similar to *Dlx5* (McLarren et al., 2003, Khudyakov and Bronner-Fraser, 2009, Streit, 2002, Luo et al., 2001b, Quint et al., 2000, Brown et al., 2005, Yang et al., 1998), is strongly expressed in the anterior part of the PPR from where lens and trigeminal placodes will develop (Figure 3.9 A-C). A more broad ectodermal expression is shown for *Nfkb1* (Figure 3.9 D) at gastrulation stage. However, as neurulation starts, it becomes restricted to the PPR with a high enrichment in the more anterior domain (Figure 3.9 E-F). This confirms the

microarray data, where both genes are enriched in the anterior PPR (see Figure 3.5). The expression pattern of a new PPR marker will be discussed in more details in the session 3.6.

In conclusion, the majority of the genes here analysed are expressed in the neural plate and border/PPR region. This suggests that early in development neural and sensory placodal precursors may share common properties. Furthermore, new specific PPR genes have been identified. Overall, the *in situ* screen reflects the trend observed from the microarray and, by adding a deeper layer of information, is crucial for the identification of new putative players in the process of PPR specification.

3.4 Characterisation of the expression of the transcription factors *Hmgxβ4*, *Hsf2* and *Mynn*

Based on the *in situ* hybridisation screen new molecules have been identified as enriched in the PPR and in the otic and epibranchial domain. In particular, three transcription factors (*Hmgxβ4*, *Hsf2* and *Mynn*) have emerged.

In the chick embryo, *Hmgxβ4* and *Hsf2* are present in the neural plate and border domain during gastrulation and neurulation (Figure 3.10 A, a', B, b', F, f', G, g'). During somitogenesis, they are strongly expressed in the neural plate and are enriched in two patches close to the hindbrain where the otic-epibranchial placode domain forms (OEPD; Figure 3.10 C, D, H). Later, at the otic cup stage, *Hmgxβ4* is strongly enriched (Figure 3.10 E) whereas *Hsf2* is weakly expressed (Figure 3.10 J) in the otic placode. The *in situ* hybridisation patterns described here are supported by the expression levels determined by the microarray screen and the otic transcriptome analysis (see Chapter 4).

Lastly, the transcription factor Mynn (BTP/POZ zinc finger also known as Zbtb31) functions as a transcriptional activator and repressor (Melnick et al., 2000, Melnick et al., 2002). It has been implicated in gene expression at the neuromuscular junctions (Alliel et al., 2000, Cifuentes-Diaz et al., 2004). During chick development, *Mynn* is expressed in neural and border region (Figure 3.10 K, k', L, l') and it is later present in the otic cup (Figure 3.10 O). The microarray data confirm *Mynn* enrichment in the posterior pre-placodal region (Figure 3.10 P), however, mRNA-seq based transcriptome analysis shows much lower expression levels when compared to the previous two genes (Figure 3.10 Q).

In conclusion, the three transcription factors *Hmgxβ4*, *Hsf2* and *Mynn* were identified from the array screen as not induced by the mesoderm (not enriched in the iAO), but enriched in the posterior PPR. The *in situ* expression analysis largely confirms their presence in the pre-placodal ectoderm and OEPD, making them putative players in otic development.

3.5 Spatio-temporal expression of four chromatin modifying enzymes

The microarray screen identified four chromatin-modifying enzymes as mesoderm-induced and enriched in the posterior PPR. I therefore analysed their expression using *in situ* hybridisation (Figure 3.11 U). Two of them, Setd2 and Whsc1, are histone methyltransferases associated with active and inactive chromatin, respectively. Setd2 specifically methylates lysine-36, while and Whsc1 methylates lysine-27 of histone H3. The other two molecules, Dnmt3a and -b, are *de novo* DNA methylases related to heterochromatin and have recently been implicated in neural crest development (Hu et al., 2012, Jacques-Fricke et al., 2012, Martins-Taylor et al., 2012).

As expected, these genes are ubiquitously expressed (Figure 3.11) at early stages as well as at late somitogenesis. In fact, during gastrulation and after the 10-somite stage they are widely present in the ectoderm (Figure 3.11 A, B, E, F, G, J, K, L, O, P, Q, T). However, during the beginning of somitogenesis two of them, *Setd2* and *Dnmt3b*, become restricted to the neural plate (Figure 3.11 C, R), whereas *Whsc1* and *Dnmt3a* are also expressed in the pre-placodal region (Figure 3.11 H, M). Later, when the otic vesicle starts to invaginate, they are all expressed in the placode, although *Dnmt3a* and *-b* seem to be present at a higher level, both from the *in situ* expression and mRNA-seq data (Figure 3.11 O, T, V).

Together, these results suggest a possible role of these enzymes in the regulation of the chromatin landscape during otic development and may therefore be involved in fine-tuning gene expression in this region.

3.6 Homer2: a new PPR and otic marker

Homer2 belongs to the Homer family of scaffold proteins involved in several cellular processes: calcium homeostasis, clustering and trafficking of proteins at the plasma

membrane, cytoskeletal reorganisation and interaction with the transcription factors mediating their nuclear localisation (for review see Foa and Gasperini, 2009). Interestingly, Homer3 is able to bind Pax6, an anterior PPR specific factor crucial for lens and olfactory development (Ashery-Padan et al., 2000, Collinson et al., 2000, Quinn et al., 1996, Grindley et al., 1997), and mediates its translocation to the nucleus (Cooper and Hanson, 2005).

From the microarray screen *Homer2* was identified as induced by the mesoderm and enriched in the posterior pre-placodal region (Figure 3.12 H). Remarkably, *Homer2* is expressed in a horseshoe shape in the ectoderm marking the entire PPR domain (Figure 3.12 A, a', B, b', C, c'), similarly to the PPR markers *Six* and *Eya*. Later, it becomes restricted to the otic-epibranchial domain (OEPD) and the olfactory placode (Figure 3.12 E, F). It remains expressed in the otic vesicle as it forms and is strongly present in the developing brain (Figure 3.12 G). mRNA-seq analysis confirms the strong otic enrichment of *Homer2* (Figure 3.12 I). Thus, Homer2 represents a new marker of pre-placodal cells and of the otic and olfactory region. However, its function during vertebrate development remains to be elucidated.

3.7 Discussion

The main aim of this initial work was to identify new genes specific to placode progenitors and the future otic placode, which may in turn be involved in specification of these fates. One of the purposes of the screen was to identify new genes present in the PPR and possibly involved in its specification. Overall, the epistatic regulation of Six/Eya and in general the genetic of PPR specification is poorly understood. Only few up-stream regulators of Six/Eya have been identified so far (see section 1.3.3) and only an anterior PPR enhancer and its direct regulators has been described for Six1 (Sato et al., 2010). Therefore, the identification of genes early induced by the mesoderm could help in finding potential PPR inducer factors that might be located up-stream of Six/Eya in the hierarchy. Additionally, analysing the transcriptome of the anterior versus posterior pre-placodal ectoderm would help in understanding the process of rostro-caudal regionalisation of the PPR. Particular interest was given to genes enriched in the posterior PPR and in their potential late expression in the otic placode domain, since they could possibly function in early otic induction. Finally, thanks to the complementation of the microarray with an *in situ* hybridisation screen new genes expressed in the PPR and otic,

as well as few new PPR markers, were identified. The *in situ* hybridisation analysis provided more detailed information about when and where differentially regulated genes are expressed in the developing chick embryo. Around 60 transcripts were analysed and their expression pattern was characterised (Appendix 9.1).

Nine genes are present in a broad domain within the ectoderm; this ubiquitous expression makes them unlikely to be crucial players of PPR specification. Interestingly however, at gastrulation stages the vast majority of genes examined are expressed in both the neural and pre-placodal field. During somitogenesis, a subclass of them, around 20, remains expressed in both territories, whereas the other 20 become exclusively restricted to the neural plate. Thus, although the screen was originally designed to identify PPR specifiers, the presence of a vast group of transcripts marking the PPR as well as the young neural plate raises the possibility that both domains share common properties. Indeed, increasing experimental evidence supports this idea: a graft of Hensen's node, the source of neural inducing signals, induces a similar set of genes as the PPR-inducing mesoderm (Trevers, Hintze and Stern; personal communication). These findings suggest that to some extent, both inducing tissues initiate a similar cellular state. This "state" may define common progenitors for the central nervous system and placode lineage and the cohort of genes induced may function to specify such common progenitor.

Since most genes analysed here are expressed prior to PPR formation they may be an important part of the upstream network that regulates the expression of the PPR-specific genes Six1/4 and Eya2. Only very few genes identified here show a similar expression profile to these PPR markers. The transcription factors *Dlx6* and *Nfkb1* are strongly enriched in the anterior PPR, making them good candidates for lens and olfactory specification. So far, the only gene to have the characteristic horseshoe shape expression surrounding the neural plate is *Homer2*, a scaffold protein mainly being involved in postsynaptic activities (Brakeman et al., 1997, Xiao et al., 1998, Shiraishi et al., 1999). Its restricted expression suggests a possible role in PPR specification, however so far functional studies have not been performed.

Concomitant with its induction, the PPR undergoes the process of regionalisation along the anterior-posterior axis and ultimately individual sensory placodes will emerge (Acampora et al., 2001, Acampora et al., 1995, Bally-Cuif et al., 1995, Li et al., 2009, Simeone et al., 1992, Simeone et al., 1993, Tour et al., 2001, von Bubnoff et al., 1996,

Steventon et al., 2012) (for review see: Grocott et al., 2012, Schlosser, 2006). How pluripotent PPR cells become restricted to their ultimate fate is not been fully understood. The array and *in situ* screens also provide some insight into this process by revealing genes differentially expressed in the anterior versus posterior PPR. *Dlx6* and *Nfkb1* are specifically enriched in the anterior PPR, and therefore they may be important in lens and/or olfactory specification. To further understand how cells become committed to an otic fate, particular attention was paid to genes enriched in the posterior PPR and/or in the otic placode.

Several transcription factors (*Hsf2*, *Hmgxβ4* and *Mynn*) were found to be expressed in two patches close to the hindbrain where the otic domain will form. Of particular interest, *Hsf2* and *Hmgxβ4* are enriched in the more posterior part of the PPR, they are not strongly induced by the mesoderm and they present a similar expression profile in chick embryos (Figure 3.10 A-J, P). Furthermore, they have an analogous trend of expression from the mRNA-seq datasets: they are expressed in the otic domain at somites 5-6 and 11-12; and at a weaker level at somites 8-9, probably because at this stage their expression is restricted to a portion of the placode (Figure 3.10 D, J, Q). In addition, they both are highly present in the whole embryo (Figure 3.10 Q), reflected by their expression in multiple domains in the ectoderm. The first transcription factor, Hsf2 (heat shock factor 2), is involved in activation of gene expression after stress response as well as being a regulator of constitutive gene expression (Wilkerson et al., 2007). Hsf2 is involved in maintaining the c-Fos promoter in a permissive state (Wilkerson et al., 2007) allowing rapid transcription of the target gene when necessary. c-Fos forms, together with c-Jun, the Ap1 complex which can bind to a consensus DNA sequence and activate the expression of Ap1-responding genes (Glover and Harrison, 1995, Neuberg et al., 1989). ERK/MAP kinase, downstream of FGF, can regulate c-Jun/c-Fos activity by phosphorylation (Lopez-Bergami et al., 2007, Gruda et al., 1994, Hurd et al., 2002). Given the importance of FGF signalling in early induction of the OEPD (for review see: Schimmang, 2007, Ladher et al., 2010) and the key role of c-Fos and c-Jun in the pathway, the presence of the c-Fos regulator *Hsf2* in the otic primordium can be functionally relevant for otic fate determination. In the context of the liver it has also been demonstrated to be a WNT target (Kavak et al., 2010). In addition, other members of this family have been associated with sensory organs development: Hsf4 is important for the lens differentiation (Fujimoto et al., 2004, Min et al., 2004), while and Hsf1 participates in olfactory neurogenesis (Takaki et al., 2006). The second transcription factor, Hmgxβ4

(also known as Hmg2l1), is composed of a single high mobility group (HMG); it is a sequence-specific DNA binding protein, similarly to other members of the family like TCF/Lef1 (van de Wetering et al., 1991) and Sox proteins (Pevny and Lovell-Badge, 1997, Wegner, 1999). Hmgxβ4 has been shown to be a negative regulator of WNT signalling (Yamada et al., 2003). However, its expression has not been fully characterised. WNT signalling function in a later phase of otic development, by promoting the otic versus the epibranchial cells (for review see Ladher et al., 2010; see section 1.11), thus the presence of a WNT repressor could modulate WNT response within the OEPD and otic placode.

The chromatin modifiers (*Setd2*, *Whsc1*, *Dnmt3a* and *-b*), here investigated, even if broadly expressed during chick development are strongly present in the otic vesicle; these molecules could be involved in remodelling the chromatin state in crucial loci. In general, the deposition of methylation at the lysine 36 of histone 3 by Setd2 has been associated with intronic region and it is coupled with RNA-polymerase (de Almeida et al., 2011), however its function in embryonic development has not been investigated (Hu et al., 2010). Hemizygous deletion of the distal short arm of chromosome 4 (4p16.3), in which Whsc1 locus is present, leads to Wolf–Hirschhorn syndrome (WHS) a malformation syndrome associated with craniofacial phenotypes, mental retardation and deafness (Stec et al., 1998, Battaglia et al., 1999, Wieczorek et al., 2000, Bergemann et al., 2005). The role of Whsc1 in otic development and its possible relation with deafness remains to be addressed. The function of Dnmt3a and -b has been recently investigated and related to neural crest development. When Dnmt3a is knockdown in chick the expression of the neuronal genes *Sox2* and *Sox3* expands at the expenses of neural crest markers. The association of Dnmt3a with Sox2 and 3 promoters, and their subsequent methylation, results in gene repression. Therefore, it has been proposed to function as a molecular switch, promoting neural crest and repressing neuronal fate (Hu et al., 2012). Similarly, Dnmt3b mediates methylation in human embryonic stem cells (hESCs) and it is crucial for the regulation of neuronal and neural crest genes (Martins-Taylor et al., 2012). However, in mouse Dnmt3b does not appear to be necessary for cranial neural crest development, while the neural crest phenotypes observed have been mainly associated with its function in other linages (e.g. branchial arch and mesoderm) that interact with neural crest (Jacques-Fricke et al., 2012). It is possible that de novo methytransferase also function in the otic in a similar fashion by specifically repressing non-otic genes.

Lastly, *Homer2* is the only gene here identified to have a very restricted expression profile and it is strongly enriched in the developing otic placode. Homer proteins have at the N-terminal an enabled/vasodilator-stimulated phosphoprotein homology domain (EVH1), which defines the Homer family (Beneken et al., 2000), and at the C-terminal a coiled-coil (CC) domain (for review see Shiraishi-Yamaguchi and Furuichi, 2007). Through the EVH1 domain, Homer binds to different classes of proteins that include: synaptic signalling ligands, anchoring proteins and transcription factors (for review see Foa and Gasperini, 2009); remarkably Homer3 has been shown to bind to Pax6 and to promote its nuclear translocation (Cooper and Hanson, 2005). It is therefore possible that Homer2 could bind to otic transcription factors, possibly Pax2, and might contribute to otic specification. Functional experiments are required to establish the role of Homer2 in PPR and otic development.

Although the microarray was originally designed to analyse the early steps of PPR specification, it has also revealed new putative regulators of otic fate. Subsequently, mRNA-seq was performed to gain more insight into the changes during otic development (see Chapter 4). These screens complement each other, and together with the literature, will provide an overall picture of the genes expressed from PPR precursors to otic cells.

In conclusion, this chapter further characterised some of the molecules expressed in the developing PPR including a large number of novel genes. The next step aims to positioning these new factors together with established PPR and otic specifiers into a preliminary gene regulatory network. To identify their position in the hierarchy the system will be perturb and co-behaving genes will be positioned closely in the network (see Chapter 5).

A.

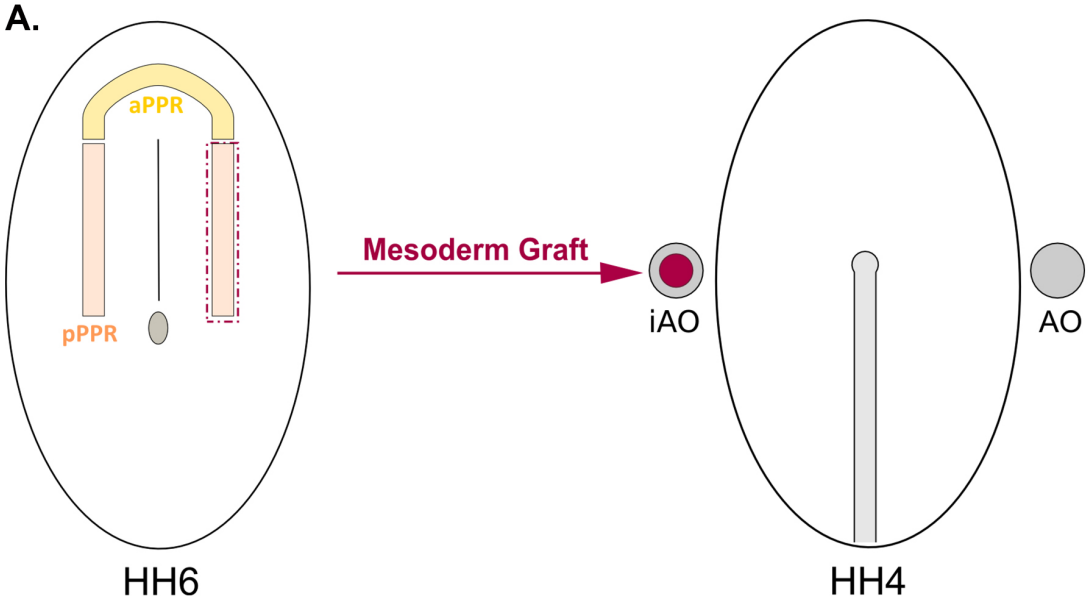

B.

	aPPR	pPPR	AO	iAO
Endogenous PPR genes	+	+	-	-
Mesodermal induced PPR genes	+	+	-	+
aPPR genes	+	-	-	+/-
pPPR genes	-	+	-	+/-
Inhibitory genes	-	-	+	+

Figure 3.1 Design of a microarray screen to identify new genes involved in PPR and otic placode specification.

(A) Illustration representing the design of the screen. The head mesoderm (purple dotted line) underling the posterior PPR (orange) is a source of FGF and WNT and BMP antagonists. HH6 mesoderm (purple) was grafted in the extra-embryonic region (grey dot) of a stage HH4 embryo. The embryo was then cultured for 12 hours (by which time *Six1/4* and *Eya2* are induced) and four domains were dissected and analysed by microarray. The non-induced extra-embryonic region (AO, grey dot) was used as control and compared with the mesoderm-induced area opaca (iAO, grey + purple dots); anterior (yellow) and posterior (orange) PPR were collected from HH6 embryos.

(B) Table summarising expression profiles relevant to PPR specification. Genes present exclusively in the anterior and posterior PPR could be candidate for the specification of the entire pre-placodal region. Genes additionally enriched in the iAO are likely to be induced by the signals present in the head mesoderm. Factors upregulated in the anterior PPR (aPPR) could be involved in the specification of anterior placodes (lens and olfactory) and they might be inhibitors of the posterior PPR fate. The ones enriched in the posterior PPR (pPPR) could be candidate as otic specifiers. Lastly, genes present in the AO and iAO and absent from the PPR could act as inhibitors of PPR specification.

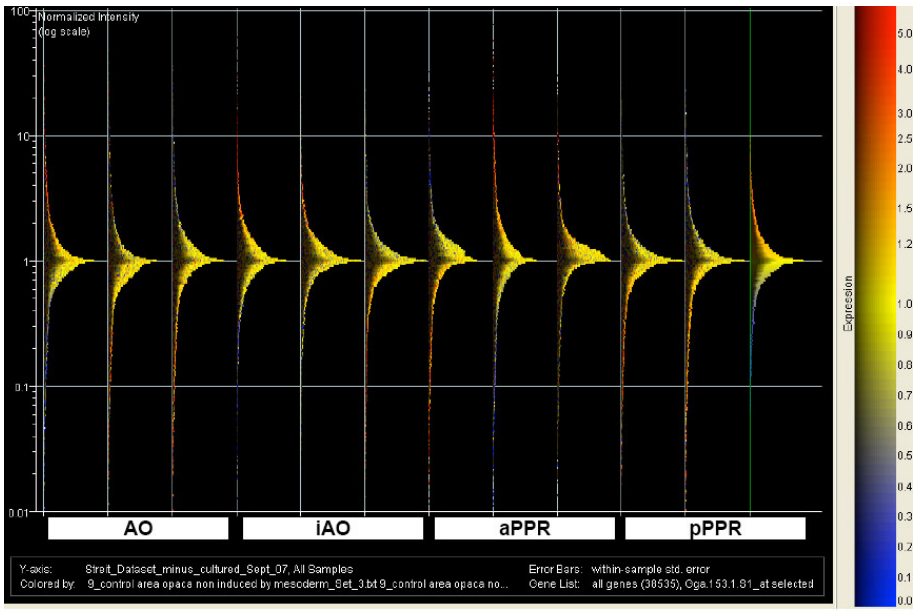

Figure 3.2 Distribution of normalised values for each biological replicate.
Normalised values for all the genes in the array were plotted on a logarithmic scale; three replicates for each cell population are illustrated for a total of 12 diagrams. The distribution is cantered around 1.

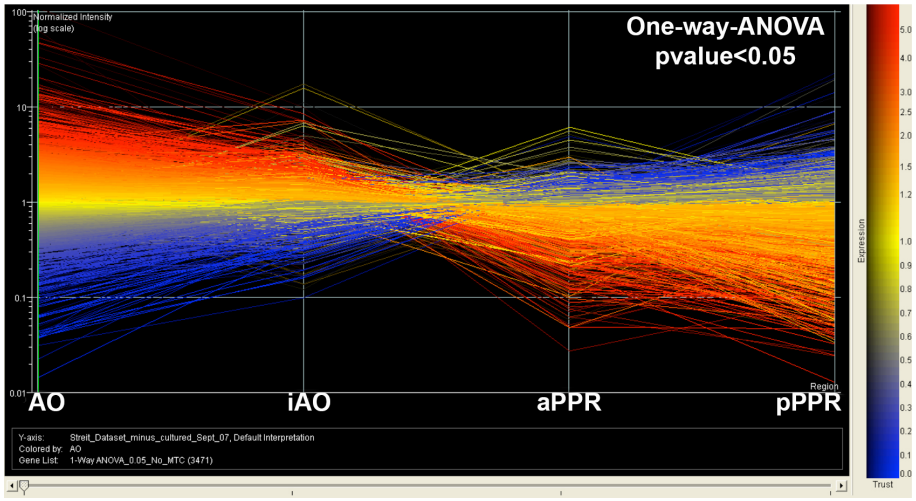

Figure 3.3 Transcripts with significant changes.
A one-way ANOVA analysis identified 3,741 transcripts with a significant, 2-fold change (p-value≤0.05) in expression level in at least one cell population. The different lines represent genes with variation in expression between tissues. The coloured lines refer to the level of expression in the area opaca: red represents strongly expressed genes and the blue low expressing genes.

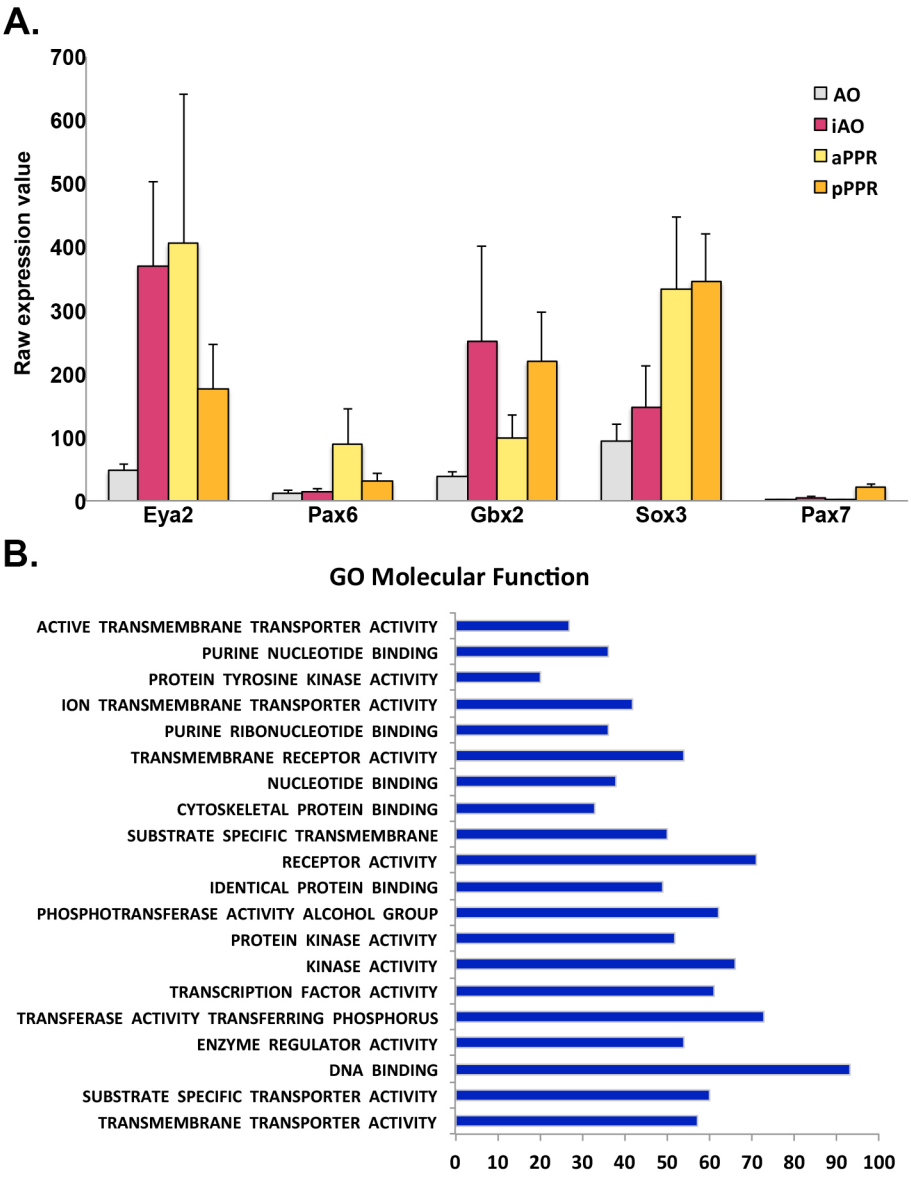

Figure 3.4 Analysis of microarray data.

(A) Plots of the raw expression values of five known genes across the four-cell populations. Gene expression profiles in the microarray correspond to their experimentally verified behaviour. AO: area opaca (grey); iAO: induced area opaca (magenta); aPPR: anterior PPR (yellow); pPPR: posterior PPR (oragnge). Error bars rapresent the standard error of the mean.

(B) Bar plot for gene ontology (GO) molecular function. 19 GO terms were found significantly associated with the genes identified in the microarray. Particular interest was given to the genes related to transcription regulation. The analysis was performed using Gene Set Enriched Analysis (GSEA) tool.

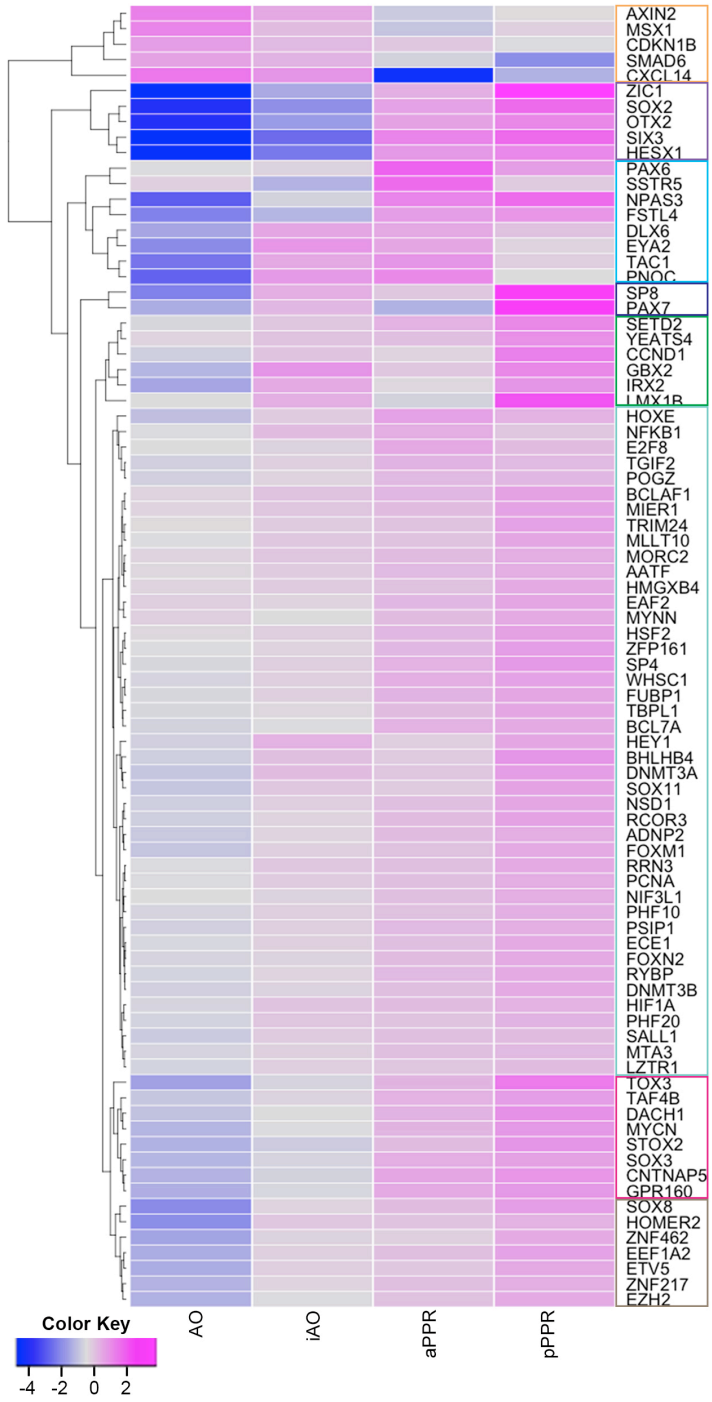

Figure 3.5 Hierachical cluster analysis of 84 transcripts.
The log2 of gene expression level for each cell population (AO, iAO, aPPR, pPPR) was plotted in the heatmap. Low level of expressions are represented with a blue gradient, intermediate level in grey and high level in magenta (colour key). A dendrogram, on the left side, shows the clusters of co-behaving genes; colour boxes highlight the eight main clusters identified.

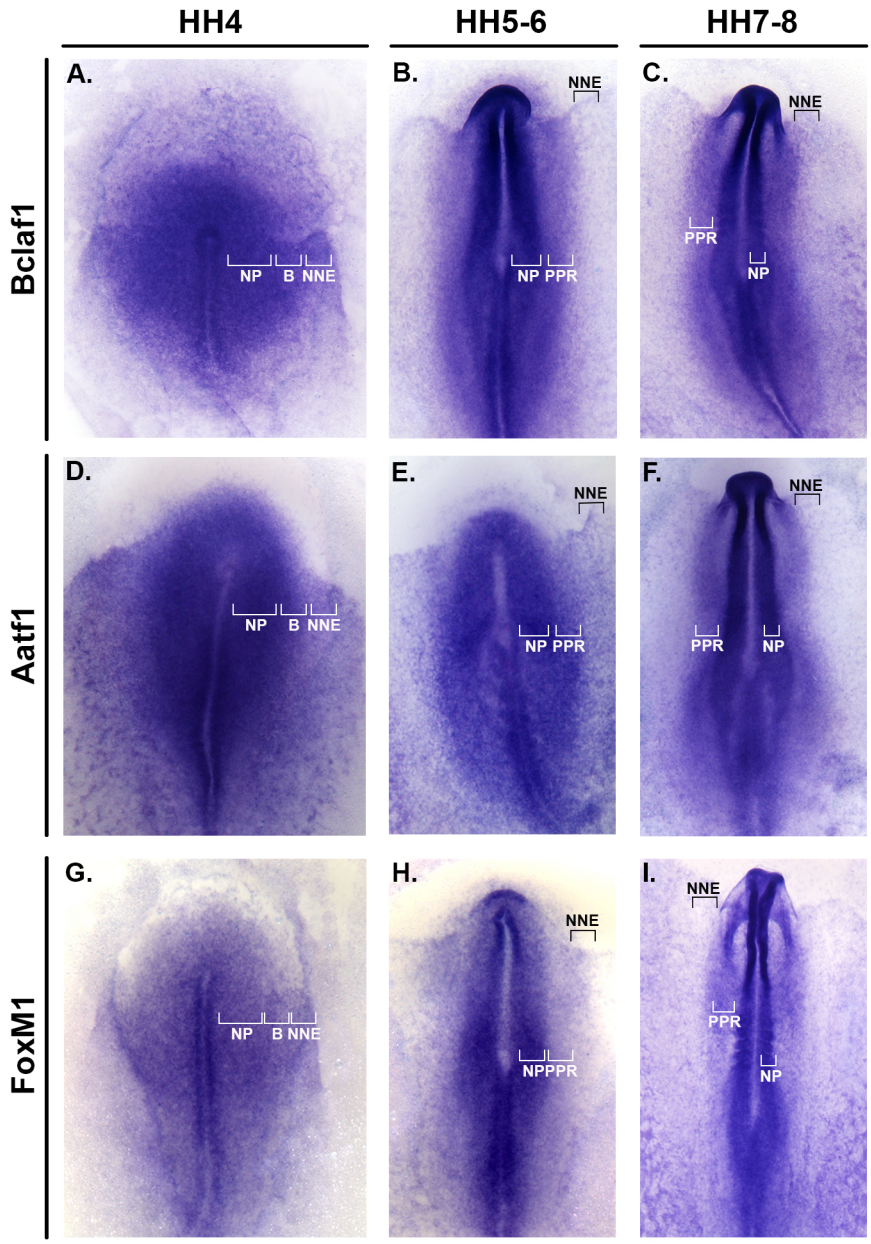

Figure 3.6 Ubiquitously expressed transcripts.
Expression profiles of *Bclaf1* **(A-C)**, *Aatf1* **(D-F)** and *FoxM1* **(G-I)** are examples of broadly expressed genes in the ectoderm. They are expressed in the neural plate (NP), border region (B) and non-neural ectoderm (NNE) during gastrulation (HH4; **A**, **D**, **G**) and at neurula stage (HH5-6; **B**, **E**, **H**). Expression in the mesodermal wings suggests their presence also in the mesoderm and possibly endoderm. Furthermore, during somitogenesis (HH7-8; **C**, **F**, **I**) they remain expressed broadly in the ectoderm. Neural plate (NP); border region (B); non-neural ectoderm (NNE); pre-placodal region (PPR).

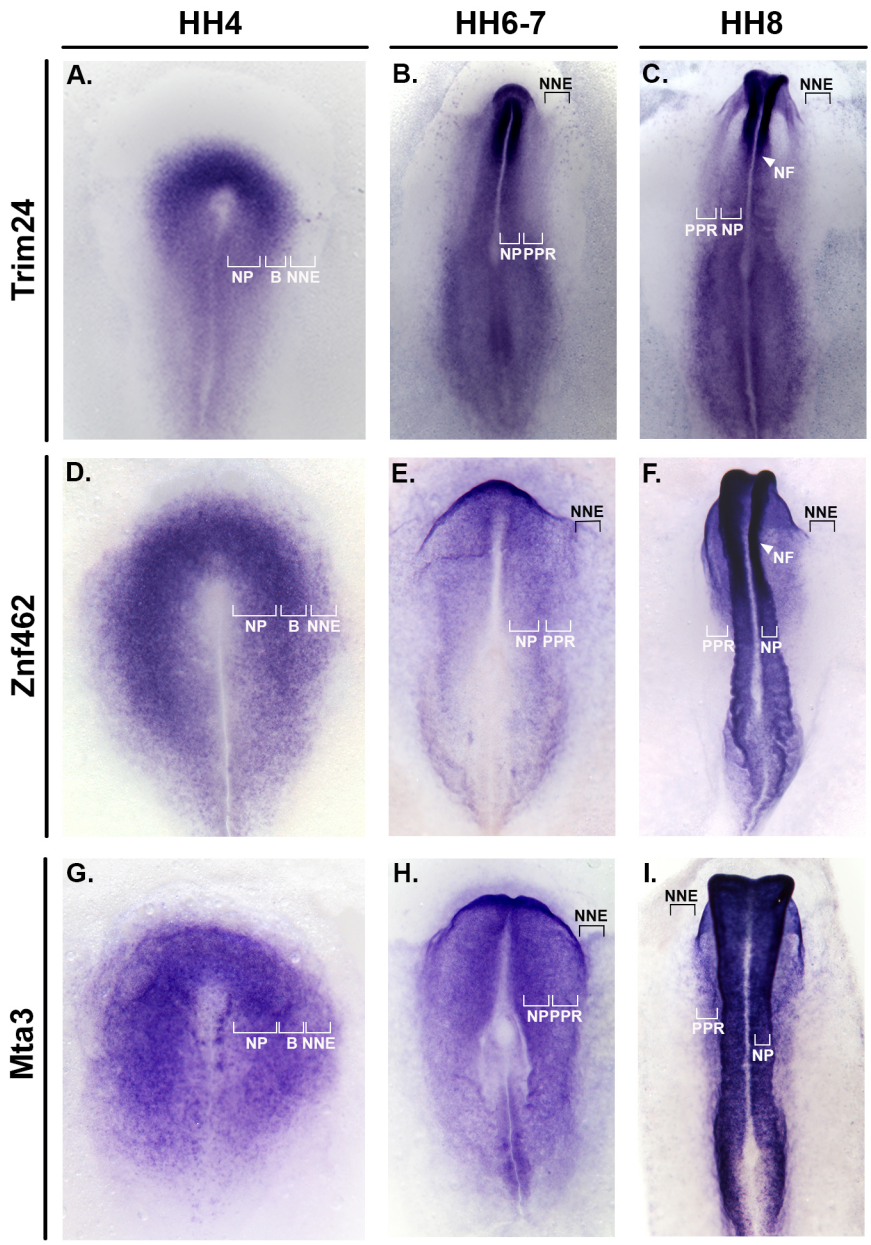

Figure 3.7 Neural plate and pre-placodal region expressed transcripts.
Expression profiles of *Trim24* **(A-C)**, *Znf462* **(D-F)** and *Mta3* **(G-I)** are examples of genes enriched in the neural plate and pre-placodal region (PPR). *Trim24* expression is restricted to the neural plate (NP) and border region (B) at gastrulation stages (**A-C**). Around stage HH8 it is expressed mainly in the neural plate, in particular enriched anteriorly, and weakly in the future placodal domains (PPR; **C**). It is also possible *Trim24* is expressed in the paraxial mesoderm. *Znf462* and *Mta3* are expressed quite broadly in the ectoderm at gastrulation (**D**, **G**) and later become restricted to the neural plate and PPR (**F**, **I**). All of them are clearly not expressed in the non-neuronal ectoderm (NNE) at somitogenesis (**C**, **F**, **I**). Neural plate (NP); border region (B); non-neural ectoderm (NNE); pre-placodal region (PPR); neural fold (NF).

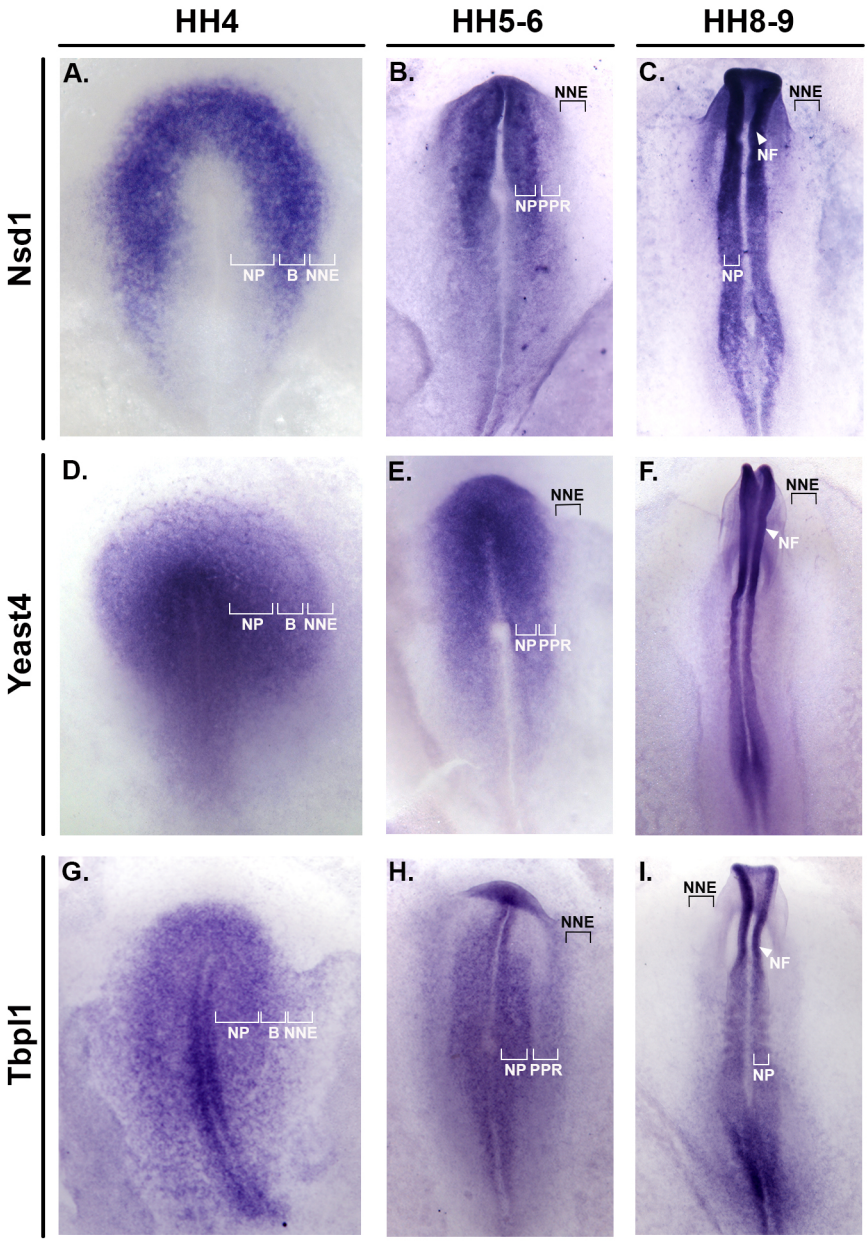

Figure 3.8 Some transcripts become restricted to the neural plate.
Nsd1 **(A-C)**, *Yeast4* **(D-F)** and *Tbpl1* **(G-I)** are broadly expressed in the ectoderm: neural plate (NP), border region (B) and non-neural ectoderm (NNE) at gastrulation (HH4; **A**, **D**, **G**). *Nsd1* and *Tbpl1* remain expressed in the three domains also at neurulation (HH5-6; **B**, **H**) whereas *Yeast4* appears to be restricted to the neural plate (NP) and PPR (**E**). Later, at somitogenesis all three genes will be exclusively expressed in the neural plate (NP) and neural fold (NF) and excluded from the placodes (HH7-8; **C**, **F**, **I**).

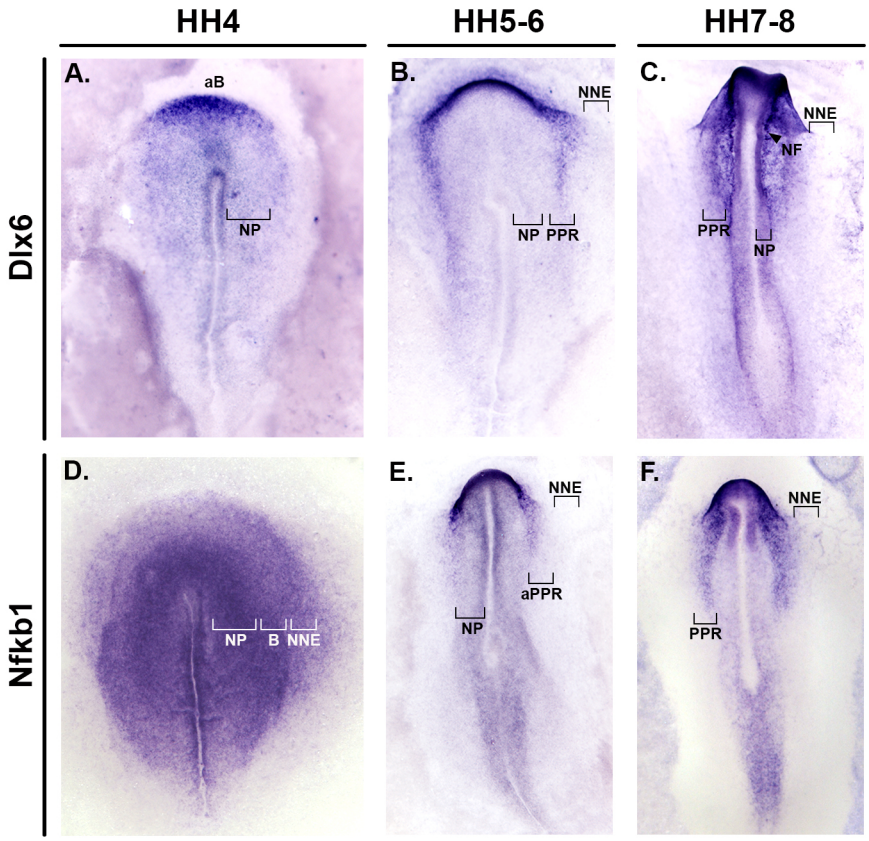

Figure 3.9 Some transcription factors are restricted to the PPR.
Dlx6 **(A-C)**, *Nfkb1* **(D-F)** are restricted to the PPR region at neural stage (HH6; **B**, **E**). (**A**) At gatrulation (HH4), *Dlx6* is mainly expressed in the anterior future PPR (anterior Border, aB) and weakly in the neural plate (**B**). Later, it is expressed in the entire PPR, remaining more strongly enriched in anteriorly. At somitogenesis, *Dlx6* is expressed in the anterior placodal domains (lens and trigeminal) as well as the neural crest region (neural fold: NF). (**D**) At gastrulation *Nfkb1* is broadly expressed in the entire ectoderm (neural plate: NP; border region: B; non-neural ectoderm: NNE). (**E-F**) Shortly thereafter, it becomes mainly restricted to the anterior PPR.

Figure 3.10 Expression of the transcription factors Hmgxβ4, Hsf2 and Mynn from gastrulation to early somitogenesis.
Expression of the transcription factors: *Hmgxβ4* (**A**-**E**, **a'**, **b'**), *Hsf2* (**F**-**J**, **f'**, **g'**) and *Mynn* (**K**-**O**, **k'**, **l'**) at different developmental stages. At gastrulation (HH4; **A**, **a'**, **F**, **f'**, **K**, **k'**) from left to right the ectoderm is subdivided in: neural plate (NP), border region (B) and non neural ectoderm (NNE). At neurulation (HH5-6; **B**, **b'**, **G**, **g'**, **L**, **l'**) the pre-placodal region (PPR) is specified. During somitogenesis (HH7-8; **C**, **H**, **M**; HH9-10; **D**, **I**, **N**) the otic-epibranchial placodal domain (OEPD) is highlighted. Later, when the otic placode (OT) starts to invaginate (HH11-12; **E**, **J**, **O**) a section of the placode is showed in the insert. (**P**) Normalised expression values in the four cell populations are shown in the bar chart. AO: area opaca (grey); iAO: induced area opaca (magenta); aPPR: anterior PPR (yellow); pPPR: posterior PPR (orange). (**Q**) Levels of expression from the mRNA-seq summarise the genes behaviour during otic placode development (whole embryo in grey; ss5-6 in light pink; ss8-9 in pink; ss11-12 in violet).

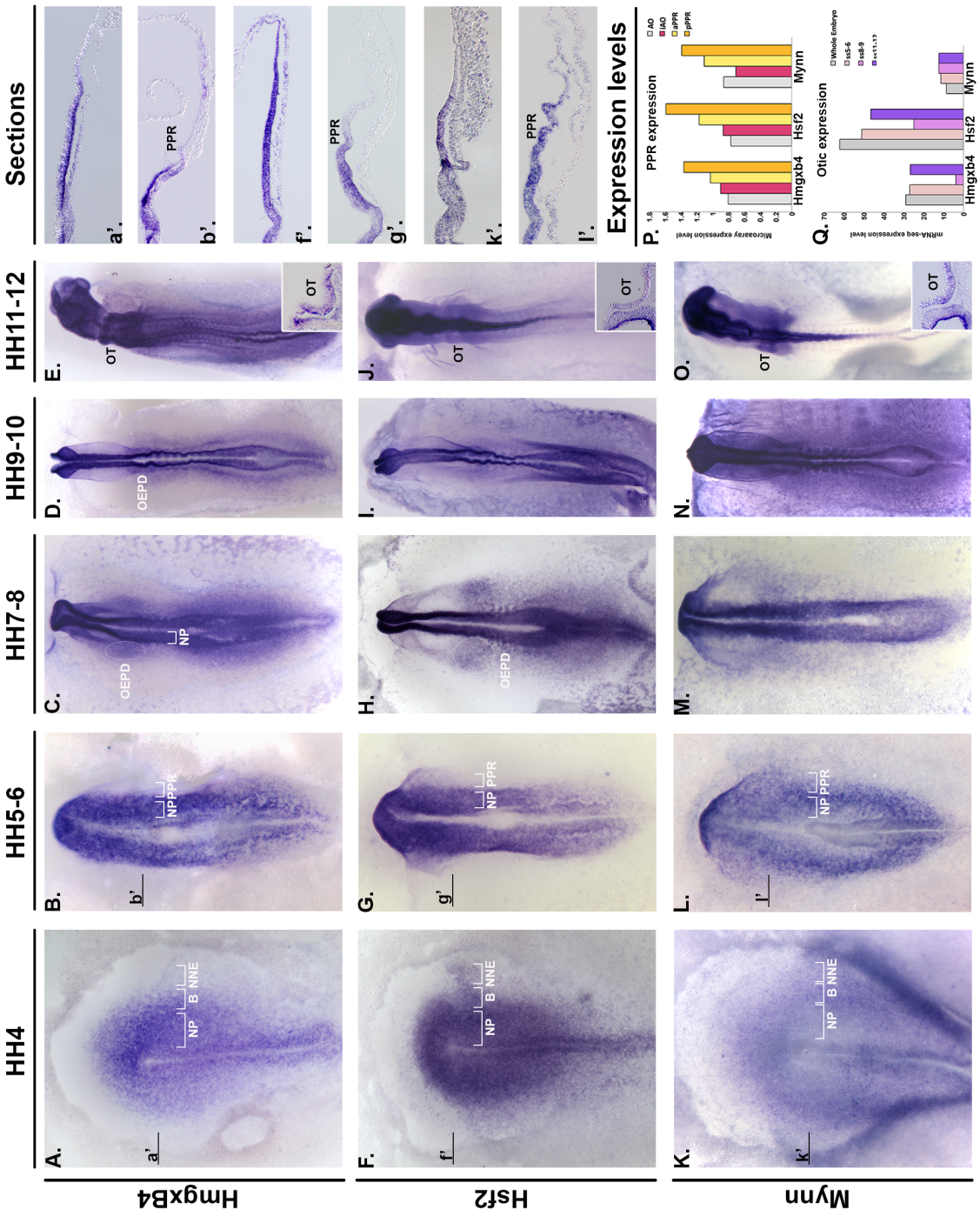

Figure 3.10 Expression of the transcription factors Hmgxβ4, Hsf2 and Mynn from gastrulation to early somitogenesis.

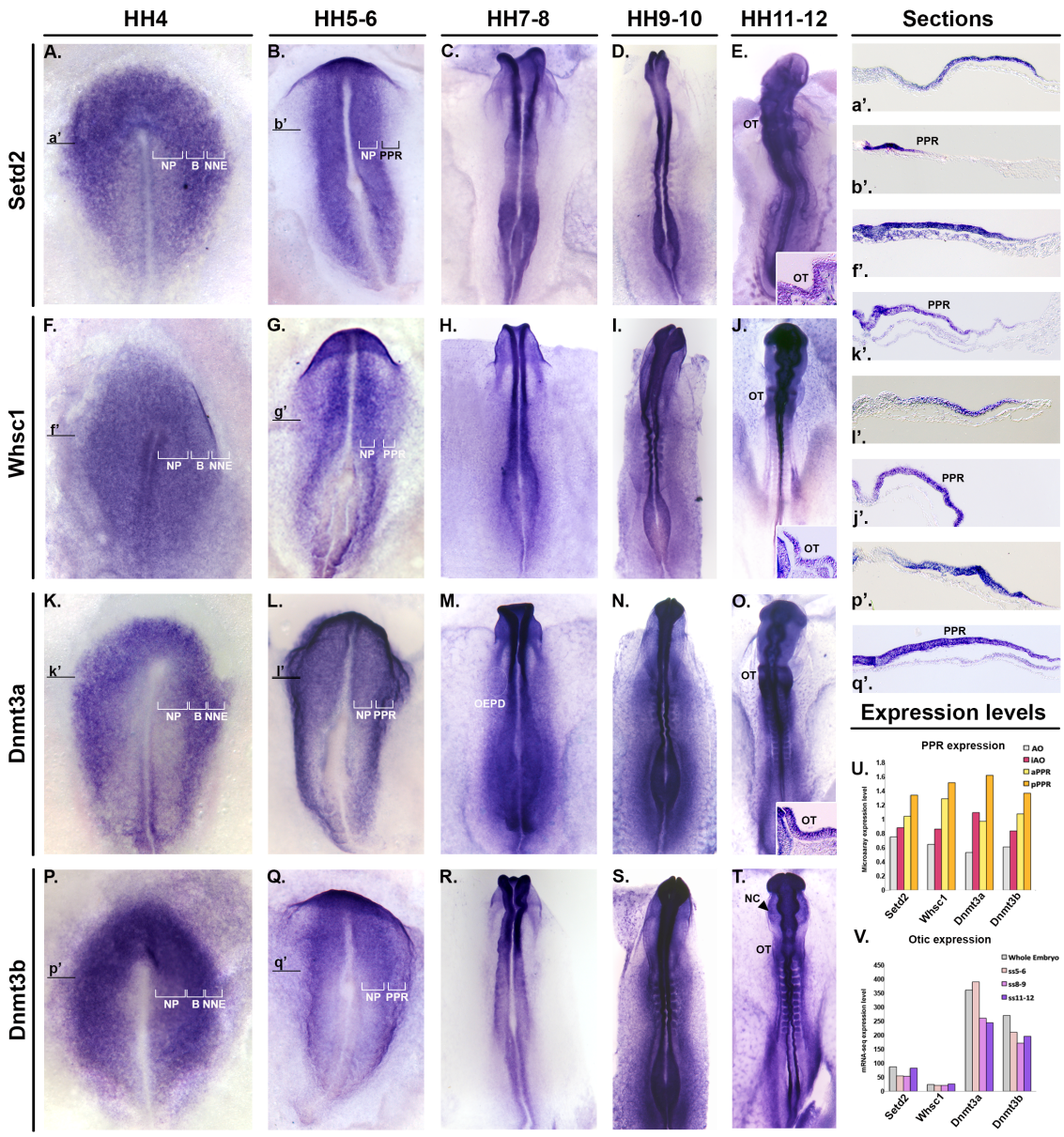

Figure 3.11 Expression of the chromatin remodellers *Setd2*, *Whsc1*, *Dnmt3a* and *Dnmt3b* from gastrulation to early somitogenesis.

Expression of the chromatin modifier enzymes: *Setd2* (**A**-**E**, **a'**, **b'**), *Whsc1* (**F**-**J**, **f'**, **g'**), *Dnmt3a* (**K**-**O**, **k'**, **l'**) and *Dnmt3b* (**P**-**T**, **p'**, **q'**) at different developmental stages. At gastrulation (HH4; **A**, **a'**, **F**, **f'**, **K**, **k'**, **P**, **p'**) from left to right the ectoderm is subdivided in: neural plate (NP), border region (B) and non neural ectoderm (NNE). At neurulation (HH5-6; **B**, **b'**, **G**, **g'**, **L**, **l'**, **Q**, **q'**) the pre-placodal region (PPR) is specified. During somitogenesis (HH7-8; **C**, **H**, **M**, **R**; HH9-10; **D**, **I**, **N**, **S**) the otic-epibranchial placodal domain (OEPD) is highlighted. Later, when the otic placode (OT) starts to invaginate (HH11-12; **E**, **J**, **O**, **T**) a section of the placode is showed in the insert. Expression of *Dnamt3b* in the neural crest (NC) is showed with an arrowhead. (**U**) Normalised expression values in the four-cell populations are shown in the bar chart. AO: area opaca (grey); iAO: induced area opaca (magenta); aPPR: anterior PPR (yellow); pPPR: posterior PPR (orange). (**V**) Levels of expression from the mRNA-seq summarise the genes behaviour during otic placode development (whole embryo in grey; ss5-6 in light pink; ss8-9 in pink; ss11-12 in violet).

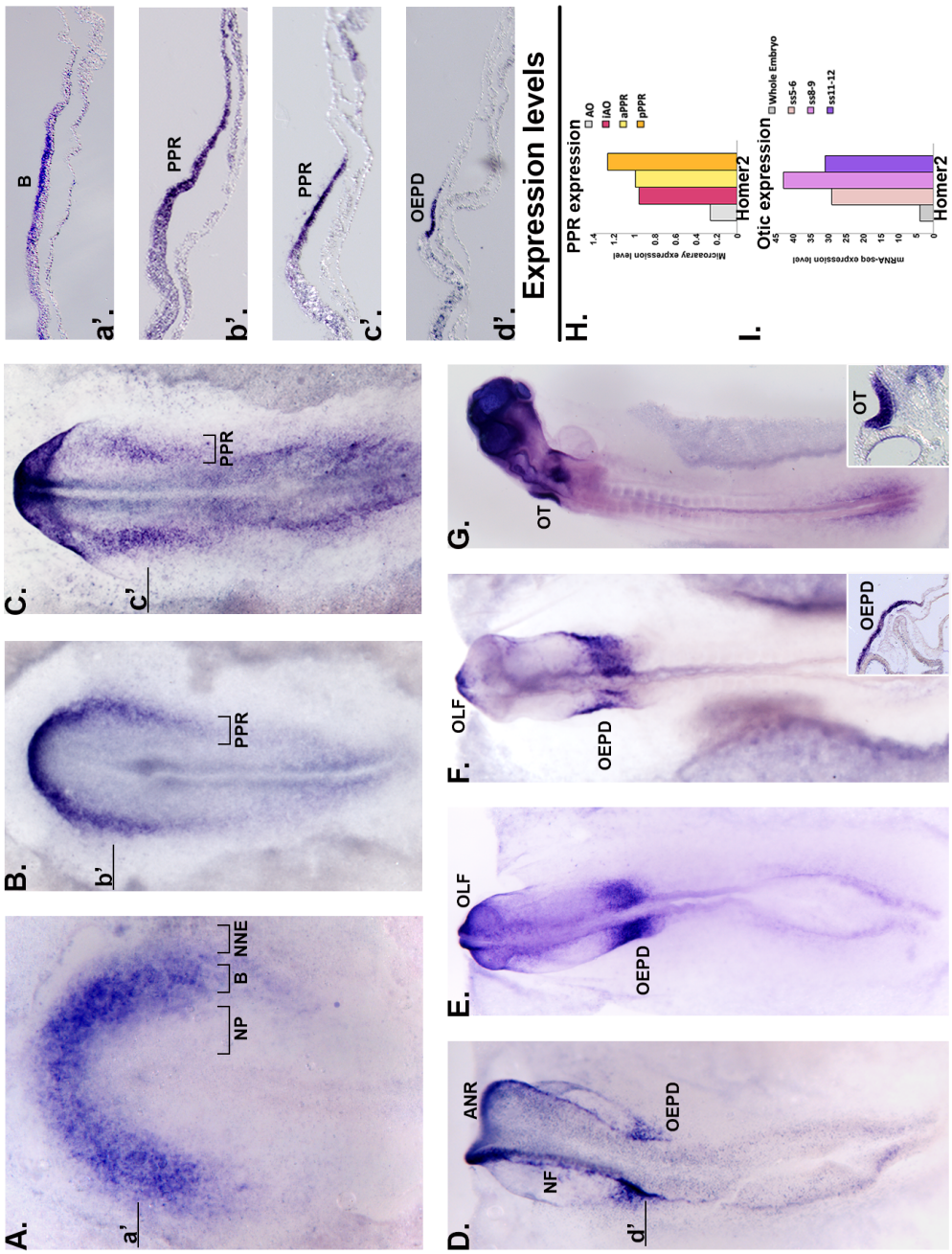

Figure 3.12 Expression of *Homer2* a new marker of the PPR and otic placode.
(**A**, **a'**) *Homer2* is restricted to the border region (B) already at gastrulation (HH4) being absent from the neural plate (NP) and non-neural ectoderm (NNE). As the head fold starts to form *Homer2* is expressed in a horseshoe shape in the entire PPR (HH6; **B**, **b'**; HH7 **C**, **c'**). (**D**, **d'**) At the beginning of somitogenesis, *Homer2* becomes restricted to the otic-epibranchial domain (OEPD) and it is also present in the neural folds (NF) and anterior neural ridge (ANR). (**E**, **F**) Later in somitogenesis it remains expressed in the OEPD and in the olfactory placode (OLF). The insert in (**F**) shows *Homer2* mRNA in the otic and epibranchial domain. (**G**) At around HH12 *Homer2* is strongly expressed in the invaginating otic placode (OT) and also in the brain. (**H**) Normalised expression values in the four cell populations are shown in the bar chart. AO: area opaca (grey); iAO: induced area opaca (magenta); aPPR: anterior PPR (yellow); pPPR: posterior PPR (orange). (**I**) Levels of expression from the mRNA-seq summarise the gene behaviour during otic placode development (whole embryo in grey; ss5-6 in light pink; ss8-9 in pink; ss11-12 in violet).

4. Genome-wide transcriptome analysis reveals novel regulatory connections in the developing ear

4.1 Introduction

In the previous chapter, I described the identification of new pPPR-specific genes that are expressed prior to proper otic placode specification. While a number of transcription factors present in the otic and epibranchial placodes have been identified, many players remain to be discovered (see section 1.9 and 1.10). This chapter uses mRNA-seq to identify novel otic genes to refine the hierarchy of otic commitment.

Specification of otic precursors, induction and patterning of the placode are critical steps that require temporal and spatial integration of different signals and transcription factors. This process is initiated by FGFs inducing the OEPD, from which both the ear and the epibranchial ganglia arise. The OEPD is subsequently refined by a combination of WNT and Notch signalling in response to which cells begin to express a series of transcription factors that imbue the otic placode with its characteristic identity, while sustained FGF and additional BMP signalling promote epibranchial cells (for review see: Ladher et al., 2010, Ohyama et al., 2007) (see section 1.10, Figure 1.7 and Table 1.1). Some of the earliest known transcription factors in the otic placode include *Foxi3* (zebrafish *Foxi1*), *Dlx* genes, *Pax2/8, Foxg1, Spalt* and *Gata3*, followed by *Eya1*, *Gbx2*, *Nkx5.1, Soho1, Sox10, Sox3* and *Phox2* (Adamska et al., 2000, Adamska et al., 2001, Barembaum and Bronner-Fraser, 2007, Barembaum and Bronner-Fraser, 2010, Betancur et al., 2011, Bouchard et al., 2010, Christophorou et al., 2010, Economou et al., 2013, Esterberg and Fritz, 2009, Feng and Xu, 2010, Freter et al., 2012, Friedman et al., 2005, Hans et al., 2007, Hans et al., 2013, Hidalgo-Sanchez et al., 2000, Hwang et al., 2009, Kaji and Artinger, 2004, Khatri et al., 2014, Khatri and Groves, 2013, Lawoko-Kerali et al., 2002, Lawoko-Kerali et al., 2004, Lillevali et al., 2007, Lillevali et al., 2004, Ohyama and Groves, 2004a, Ohyama and Groves, 2004b, Padanad and Riley, 2011, Pattyn et al., 1997, Pauley et al., 2006, Solomon et al., 2003a, Steventon et al., 2012, Zou et al., 2006, Abu-Elmagd et al., 2001). However, these are far from complete, the epistatic relationship of these factors is not well established and the function of only a relatively small number of genes has been characterised in detail. To date only few genes that show differential expression in the otic and epibranchial placode have been identified, leaving open the question of how and when they become molecularly distinct during development. Thus,

an otic and epibranchial gene regulatory network (GRN) will clarify how distinct differentiation programs are activated in the OEPD and how this leads to diversification into specialised cells.

To expand the knowledge of potential regulators and their role within the otic and epibranchial gene network, the ear transcriptome was analysed by mRNA-seq, from OEPD to invaginating otic cup stages. The results reveal hundreds of novel genes, as well as nearly all known otic genes, which are enriched in the developing otic and epibranchial placode as well as new factors exclusively expressed in one of the two. Functional analysis reveals novel connections between known otic regulators and these novel genes, thus allowing elaboration of the otic GRN. The results offer a panoramic view of the transcriptional landscape of the early developing ear and identify new links in the gene regulatory network controlling its formation.

This work has been carried out as collaboration project and different people contributed to the work: Dr Jingchen Chen, Dr Annabelle Scott and Chia-Li Liao (King's College London), Dr Meyer Barembaum and Dr Marcos Simões-Costa (Marianne Bronner Laboratory, California Institute of Technology).

4.2 Identification of genes enriched in otic and epibranchial cells

The progressive commitment of ectodermal cells toward an otic identity occurs gradually, via a series of complex and not well-understood regulatory interactions. Transplantation experiments in avian embryos have shown that otic specification begins around 5-somite stage (ss), but that, by the 10-somite stage, the otic ectoderm is already committed to an otic fate, to invaginate and to form an otic vesicle (Groves et al., 2000). To examine the steps leading up to this cell fate decision, three stages of otic development were selected for genome-wide transcriptome analysis: 5-6ss, 8-9ss, and 11-12ss, corresponding to the otic-epibranchial domain, the otic placode, and the invaginating otic placode stage, respectively (Figure 4.1 A-D). The ectoderm lateral to the hindbrain corresponding to the presumptive otic region was carefully dissected, separated from the underlying mesoderm by mild enzymatic digestion, and dissociated. RNA was extracted from the placodal cell population and reverse transcribed; cDNA was amplified using a linear amplification system and used for sequencing library preparation (see section 2.12.1). Library

preparation and sequencing was carried out in the California Institute of Technology with the contribution of Dr Marcos Simões-Costa.

The mRNA-seq results were compared with whole embryos (3ss) mRNAs to identify transcripts that were enriched in the otic placode cells. Several hundred genes were found to be enriched at 5-6ss (1201), 8-9ss (1079), and 11-12ss (1315) (Figure 4.1; Figure 4.2). Some of these are expressed in a stage-specific manner while others are present at all stages examined, as illustrated in the Venn diagram (Figure 4.1 E-F). For example, 481 genes are commonly enriched among all the three stages, while 335, 188, and 394 genes are enriched uniquely at 5-6ss, 8-9ss and 11-12ss, respectively (Figure 4.1 E). The remaining enriched genes were similar between two of the three stages (Figure 4.1 E).

4.3 Biological pathway analysis at different stage of otic development

To gain insight into the biological meaning of these enriched genes, functional annotation was performed to identify gene ontology (GO) terms enriched in each data set using four categories: biological process, molecular function, cellular component and signalling pathway. Several GO terms are over-represented at all three stages (Figure 4.1 G; Figure 4.2 B, D, F), including 'phosphatase activity' and 'protein domain specific-binding' representing more general cellular functions like dephosphorylation and protein-protein interactions. Interestingly, 'WNT receptor signalling' is highly enriched in all three data sets, consistent with its well-known involvement in otic commitment (Freter et al., 2008, Ladher et al., 2000, McCarroll et al., 2012, Ohyama et al., 2006). Other GO terms are shared by two different stages (Figure 4.1 G; Figure 4.2 B, D, F). While 'epithelium development' is significantly enriched at the 5-6ss and 8-9ss, 'inner ear and ear development' is highly associated with 8-9ss and 11-12ss. This likely reflects progressive commitment of cells toward ear identity, whereas the placode at earlier stages retains plasticity in terms of cell fate, but is clearly classified as epithelium.

This analysis also reveals the dynamic and repeated use of signalling pathways as cells transit from otic-epibranchial progenitor to committed otic cells. While all three stages are associated with WNT signalling and share the expression of a vast group of WNT related genes (e.g. *Fzd1*, *Fzd3*, *Ptpru, Ldb1* and *Tcf4*) they differ by the expression of few factors (e.g. *Ror2*, *Fzd4* and *Mitf*). Additionally, Notch activity is highly enriched in early otic-epibranchial precursors and in late otic cells, but not at intermediate stages. Notch

signalling is known to promote otic commitment at placode stages (Abello et al., 2007, Groves and Bronner-Fraser, 2000, Jayasena et al., 2008), however its early role remains to be elucidated. Interestingly, a cohort of Notch associated genes are shared by the two time points (e.g. *Jag1* and *-2*, *Dtx2* and *-4*, *Lfng*) whereas the membrane-bound protein *NUMB* is exclusively enriched at 5-6ss and the histone acetyltransferase (HAT) *Kat2a* and *–b* are uniquely found at 11-12ss. Finally, functional annotation also reveals the potential role of novel signals during otic development: the VEGF pathway is significantly enriched at ss8-9; however it has never been associated with otic fate determination.

The presence of gene ontologies uniquely associated with particular stages is of particular significance. At 5-6ss, the term 'apical part of cell' is overrepresented, indicating that many cells at this stage are polarised, as might be reflected by expression of genes such as *NUMB* and *Par6* (Figure 4.1 G and Figure 4.2 B). The expression of 'plasma membrane' genes indicates that many genes encoding signalling receptors and transport machinery are present at this stage. Consistent with this, several signalling pathways also are enriched, such as Notch signalling, calcium signalling and WNT receptor signalling pathways (Figure 4.1 G and Figure 4.2 B). Moreover, genes encoding adhesion molecules and adherents junction are enriched, coherent with on-going active cellular rearrangements at OEPD stage. The enrichment of 'Golgi apparatus' genes at 8-9ss demonstrates that active protein transport or protein modification could take place at this stage. The correct localisation and modification of proteins may be critical for establishment of cell identity.

Distinct to the 11-12ss are high levels of genes associated with transcriptional regulation and tissue organisation as evidenced by enrichment of 'transcription regulation activity', 'extracellular matrix' and 'focal adhesion' genes. Spatiotemporal transcriptional regulation may be required for establishment of the polarity of invaginating otic vesicle, whereas adhesion and extracellular matrix molecules are likely important for its morphogenesis. The association of Notch signalling pathway at this stage is consistent with the known role of Notch in the medial placode (Abello et al., 2007, Groves and Bronner-Fraser, 2000, Jayasena et al., 2008).

The interrogation of the different transcriptome data sets highlighted new processes and genes that might be important for the formation of ear. Thus, this analysis is the starting point for future functional studies.

4.4 Transcriptome analysis reveals novel otic transcriptional regulators

To elaborate the otic GRN, identification of novel putative transcription factors from the genes found enriched in the developing ear is of crucial importance. 70 to 100 known or putative transcription factors were identified for each stage (Figure 4.3). Almost all previously known otic transcription factors are found in the dataset, including *Pax2, Eya1*, *Gata3, Sox10, Soho1, Gbx2*, etc. (Figure 4.3). 45 transcription factors were enriched in all three stages, while 13, 8 and 40 were unique to 5-6ss, 8-9ss, and 11-12ss, respectively (Figure 4.1 and Figure 4.3).

In order to compare the level of expression of the 127 annotated transcription factors, found to be enriched at least at one stage, the log2 of the fpkm (Fragments Per Kilobase Of Exon Per Million Fragments Mapped) values were plotted in a heatmap (Figure 4.4). Seven main clusters were identified based on their dynamic expression profiles. A first cluster contains genes expressed at a moderate level constantly present across different stages, among them *Etv4/5*, *Foxp4*, *Foxg1*, *Irx1/5/6*, *Sox10*, *Dlx6*, *Soho1* etc. *Irx4* clusters by itself since it is expressed at low level at 5-6ss then it rises at 8-9ss to decrease again. The third cluster is composed of many known OEPD factors (e.g. *Eya2*, *Foxi3*, *Gbx2*, *Gata3*, *Pax2*, *Six1* and *Sox8*) expressed at high level throughout otic development. Genes presenting an intermediate or low level of expression with an increase towards 11-12ss are present in cluster number four and five, respectively. The sixth cluster is composed of genes expressed at relative low level with a slight rise at the last stage. Finally, cluster seven is distinguished by the presence of transcription factors present at a low level at 5-6ss and 8-9ss that significantly increases at 11-12ss (Figure 4.4). Overall, mRNA-seq data points to a high dynamic expression of transcription factors during otic development with an enrichment in transcription factors around 11-12ss.

Since many of these transcription factors have not been described before in chick a subset of novel genes, for a total of 38, was validated by *in situ* hybridisation and qPCR. These results show that most of them are true positives, being expressed in the presumptive otic tissue. As highlighted by the mRNA-seq levels (Figure 4.4), the expression of these

transcription factors is highly dynamic in time and space. For example, *Sox13, Zbtb16* and *Lmx1a* begin to be expressed at 5-6ss and they persist in the otic placode until at least the 12ss (Figure 4.5 A-F). This is consistent with their level of expression detected by mRNA-seq (Figure 4.4 red asterisks). In contrast, *Zfhx3*, *RERE* and *Tcf4* (*Tcf7l2*) are not prominently expressed in the otic territory until the 9ss (Figure 4.5 G-L), while the expression of *Nr2f2* and *Vgll2* is not present in the otic region but rather restricted to the epibranchial placode at the later time point (Figure 4.5 O-R). Distinct from the others, *Blimp1* transcripts are initially present broadly at the 5ss, but then become confined to the epibranchial placode after the 9ss (Figure 4.5 M-N). These results were corroborated by RT-qPCR. Genes not expressed or expressed weakly at the 5-6ss did not show statistically significant fold enrichment relative to the 3ss whole embryo, while at the 11-12ss, all transcripts tested are highly enriched (Figure 4.6). These RT-qPCR results generally confirm the trend of enrichment profiles obtained form mRNA-seq (Figure 4.6). In total 27 genes were confirmed to be expressed in the developing otic, the genes described above are restricted to the otic and/or epibranchial placode while the remaining were broadly present in the entire head ectoderm. 11 genes were not detected by *in situ* hybridisation; this may be due to false positives retrieved from mRNA-seq or poor *in situ* probes therefore requiring additional validations. The large *in situ* hybridisation screen was performed by Dr Annabelle Scott and Chia-Li Liao.

In conclusion, thanks to the mRNA-seq transcriptome analysis new markers of the early otic and epibranchial domain, invaginating otic and epibranchial placode were identified. Having found new transcription factors differentially expressed during otic and epibranchial development is of crucial importance for better understanding of the otic gene network.

4.5 Testing GRN connections: effects of loss of known otic transcription factors, Etv4, Pax2, and Sox8, on novel targets

To establish regulatory connections during the process of otic development, three transcription factors (Etv4, Pax2 and Sox8), that are early expressed in the OEPD, were knockdown and the effects on the novel otic transcription factors identified in the mRNA-seq dataset were examined. *Etv4* is a known target of FGF shown to be expressed prior to gastrulation in the epiblast and then it becomes enriched in the posterior PPR and OEDP from neurula stage (Lunn et al., 2007). Given its early presence in the otic and

epibranchial region it was postulated to play an important role in establishing the domain. Further analysis on Etv4 involvement in OEPD formation will be discussed in the next chapter (see Chapter 5). *Pax2* is one of the earliest markers of the OEPD starting to be expressed at 4- 5-somite stage and it is involved in placode formation (Christophorou et al., 2010, Groves and Bronner-Fraser, 2000, Streit, 2002, Freter et al., 2012). Lastly, *Sox8* is expressed at OEPD stage and has been located upstream of Sox10, binding to its otic enhancer (Betancur et al., 2011); however its function during otic development has not been deeply investigated. In order to gain insight the relation of these known otic genes to the newly identified transcription factors, they were knockdown by morpholino electroporation at HH6-7 and otic gene expression was assessed at 11-12ss.

Initially, the change in level of expression of the nine new otic transcription factors (Figure 4.5) plus *Sox10*, *Pax2* and *Splat4* was analysed by RT-qPCR. Around ten otic tissues electroporated with Etv4, Pax2, Sox8 or control morpholino were collected and retro-transcribed to cDNA (Figure 4.7 A-C). To establish how Etv4, Sox8 and Pax2 affect the level of expression test morpholino electroporation was compared to the level of expression in the control sample, using the ΔΔCt method (see section 2.10.2). At the present only one biological replicate, consisting of ten individual tissues, was analysed by RT-qPCR by performing three technical replicates. Etv4 and Pax2 has been shown to regulate Spalt4 through its enhancer (Barembaum and Bronner-Fraser, 2010). Indeed, Pax2 loss leads to significant decrease in *Splat4* (Pax2 MO: -1.72, p-value=0.01) whereas Etv4 knockdown causes only a mild decrease (Etv4 MO: -1.13, p-value=0.58) (Figure 4.7 D). Since the effect of Pax2 and Etv4 loss-of-function has not been previously investigated it is possible that the two factors differentially contribute to the level of *Spalt4* expression. Additionally, Sox8 and Etv4 are direct regulators of Sox10 otic enhancer, both affecting the expression of *Sox10* in the otic domain (Betancur et al., 2011). Etv4 and Sox8 morpholino electroporations cause a decrease in Sox10 level of expression but do not fully meet the strict set criteria (Etv4 MO: -1.43, p-value=0.065; Sox8 MO: -1.49, p-value=0.042) (Figure 4.7 D). Overall, the trend observed by RT-qPCR reflects the literature data therefore it can be used as first screen to identify new interactions. Using the same procedure expression level of the nine newly identified transcription factors was assessed. Etv4 loss significantly affects three genes (*Blimp1*, *Tcf4* and *Pax2*), whereas Pax2 and Sox8 seem to be regulating a vaster group of genes (Figure 4.7 D). Pax2 causes loss of: *Sox13*, *Zfhx3*, *Blimp1*, *Lmx1a*, *Vgll2*, *Zbtb16*, *Tcf4* and *Splat4*; however its own transcript is increased in level (Figure 4.7 D), probably due

to a compensatory effect. Sox8 appears to be upstream of: *Sox13*, *Zfhx3*, *Tcf4* and *Pax2* (Figure 4.7 D). Since the RT-qPCR was not performed across different biological replicates the results could be strongly influenced by the variability of the electroporation, the amount of morpholino introduced in each cell, and the size of the dissection. Therefore, the putative interactions were further validated by *in situ* hybridisation. The results were used as a guide to further verify the interactions starting by the significant changing genes and extending it to few others.

After loss of Sox8, *Pax2* (n=5/7), *Zbtb16* (n=8/9) are downregulated on the morpholino-treated compared to the control side of the same embryo (Figure 4.8 I-J). Additionally, *Tcf4* (n=12/19) and *Zfhx3* (n=4/6) appear to be downregulated (data not showed). In contrast, after Sox8 knockdown there is an expansion in the expression of *Blimp1* (n=7/11) from the epibranchial towards the dorsal otic ectoderm compared to the control side (Figure 4.8 K). Likewise, in the absence of Sox8 *Sox13* appears to be expanded anteriorly (n=10/12) (Figure 4.8 L). Sections will be performed to further verify and clarify the phenotype. Thus, Sox8 function is required for the expression of most new otic transcription factors, while seems to restrict the epibranchial marker *Blimp1*. A different behaviour is found for *Sox13*, being probably repressed by Sox8.

After knockdown of the FGF downstream effector Etv4, the expression of *Pax2* (n=8/12) and *Zbtb16* (n=6/6) is reduced (Figure 4.8 M-N). *Tcf4* (n=8/10) expression is also affected (data not shown), while *Sox13* (n=2/8) (Figure 4.8 O) and *Zfhx3* (n=2/5) are occasionally decreased. *Vgll2* was also analysed but sections of the otic are required for interpreting the possible phenotype (Figure 4.8 P). Etv4 is therefore responsible for the regulation of a restricted cohort of otic genes.

Lastly, the loss of Pax2, one of the earliest genes labelling otic-epibranchial progenitors, affects both OEPD and epibranchial genes. The newly identified OEPD marker *Lmx1a* (n=4/4) and *Zbtb16* (n=3/4) are drastically reduced after Pax2 knockdown (Figure 4.8 E, e', F, f'), while Pax2 is not affecting *Sox13* expression (n=4/4) (data not shown). In addition, the lateral expression of the epibranchial genes *Blimp1* (n=3/4) and *Vgll2* (n=6/7) is decreased (Figure 4.8 G, g', H, h'). Thus, Pax2 is regulating both cell fates.

In conclusion, the three factors appear to regulate different cohort of genes therefore they are differentially contributing to the otic and epibranchial specification process.

4.6 Discussion

Specification of the ear and segregation of otic from epibranchial precursors within a common progenitor domain requires signalling events as well as transcriptional regulation. WNT signalling from the adjacent hindbrain (Ohyama et al, 2006) and Notch signalling in the medial region of the common domain mutually regulate each other to mediate and stabilise the formation of the otic placode (Jayasena et al, 2008) (see section 1.10). Concomitantly, FGF signalling from the underlying endoderm induces the formation of the epibranchial placode from the lateral portion of the same placodal domain (Freter et al, 2008). In addition to these signalling pathways, dozens of transcription factors are expressed during this process. However, the acquisition of otic and epibranchial fates remains poorly understood. A study in zebrafish shows that differential *Pax2* levels in medial and lateral portions of the common otic-epibranchial domain are associated with specification of their respective fates (Figure 4.9; Figure 1.7); such high levels of *Pax2* on the medial side establish otic fate while low levels on the lateral side maintain epibranchial fate (McCarroll et al, 2012).

The transcriptome analysis by mRNA-seq has identified hundreds of genes enriched in the otic region during the process of commitment toward otic fate. Functional annotation reveals several known biological processes/functions that are enriched during the process of commitment to otic identity. These include pathways involved in epithelial development at early stages, and inner ear development at later stage. Known signalling pathway components, like WNT and Notch signalling pathways, are expressed at elevated levels. These results reveal high expression of genes associated with VEGF pathway whose function has not been previously implicated in ear development. Additionally, there is enrichment of genes associated with protein dephosphorylation, an important mechanism of rapidly regulating protein function. One example is *Eya*, a phosphatase expressed in the otic tissue (Ishihara et al., 2008a, Kozlowski et al., 2005, Xu et al., 1997), which transactivates the transcription factor Six via dephosphorylation (Li et al., 2003, Rayapureddi et al., 2003, Tootle et al., 2003). Another example is apical protein genes, enriched at 5-6ss, that may be responsible for initiating otic commitment by deposition of apical proteins like NUMB and Par6, whose asymmetric localisation often leads to cell fate diversification from a common progenitor fate (for review see: Gulino et al., 2010, Etienne-Manneville and Hall, 2003). Furthermore, high levels of genes associated with Golgi activity including protein transport or protein post-modification at

8-9ss, would suggest that correct protein localisation and post-modification are required to stabilise cell identity. Finally, otic fate is determined by forming a tightly connective epithelium, the otic placode, as corroborated by the enrichment of cell adhesion molecules at the 11-12ss.

Importantly, a dramatic increase in the number of transcription regulators expressed at the 11- 12-somite stage was observed, suggesting that further cell differentiation into multiple cell types requires precise transcriptional control. At this stage, dozens of novel otic transcription factors were identified however their functions remain to be clarified. Based on analysis of transcript levels and localisation pattern, these transcripts exhibit dynamic spatiotemporal expression, despite the relatively short time frame during which otic commitment occurs in the chicken embryo. The transcription factors *Lmx1a*, *Sox13*, *Zbtb16* and *Tcf4* are more strongly enriched in the medial otic placode; conversely *Blimp1*, *Nr2f2* and *Vgll2* are expressed in the lateral epibranchial domain. A homogenous expression was found for *RERE* and *Zfhx3* across the two areas (Figure 4.5 and Figure 4.9). Thus, new transcription factors differentially expressed in the two segregating placodes could be playing a role in cell fate determination (Figure 4.9 A).

The investigation of the upstream regulation of newly identified factors points to differential roles of Etv4, Sox8 and Pax2 in otic and epibranchial formation. The downstream FGF factor Etv4 seems to be regulating exclusively otic factors at the tested stage (Figure 4.9 B). However, it is well established that FGF plays a crucial role in the segregation of the two placodes by promoting the epibranchial fate (Abello et al., 2010, Freter et al., 2008, McCarroll and Nechiporuk, 2013, Nikaido et al., 2007). Several hypothesises could be formulated to explain this apparent inconsistency: it is possible that Etv4 has a second function later in development in the maintenance of epibranchial genes, or the other member of the family, Etv5, could be the main mediator of the epibranchial fate downstream of FGF otherwise it is possible that Etv4 is not upstream of the epibranchial genes here tested but it could be promoting epibranchial fate via different factors (e.g. *Sox3* and *Phox2*).

The early OEPD marker Pax2 appears to be upstream of several otic and epibranchial genes, since in its absence markers of both placodes become downregulated (Figure 4.9 B). The function of Pax2 has been recently assessed in different organisms. As mentioned above, in zebrafish *Pax2* is homogenously expressed in the OEPD, later in development

medial cells will have high level of *Pax2* while lateral cells will express it at lower levels (Figure 4.9 A). Both *Pax2a/8* gain- and loss-of-function experiments demonstrated that high level of *Pax2a/8* promotes otic fate decision whereas low-level favours the epibranchial (McCarroll et al., 2012). In the same year, Pax2 function as also been further investigated in chick, where both inhibition and up-regulation of *Pax2* leads to repression of otic and epibranchial genes (*Soho1*, *Foxg1* and *Phox2a*) whereas other factors were not affected (*Dlx5*, *Foxi2* and *Sox3*) (Freter et al., 2012) (Figure 1.7). Consistently with the here presented findings, it appears that the level of *Pax2* is crucial for the regulation of a subset of otic and epibranchial genes but it is not differentially promoting the two cell fates.

Sox8 has been recently identified to be expressed in the otic and directly regulating *Sox10* through binding to its enhancer (Betancur et al., 2011), apart from this its function in otic development has not been investigated so far. The results here summarised point to a key role of Sox8 in otic versus epibranchial development. Sox8 seems to act early, being an upstream regulator of *Pax2*, and favouring the otic against epibranchial fate, as in its absence expression of otic genes is repressed, while epibranchial genes expand (Figure 4.9 B). Sox8 has been described to mainly function as a transcriptional activator. Therefore it is likely to be indirectly repressing the epibranchial fate through intermediate repressors. Since the here highlighted importance of Sox8 in cell fate decision, its function will be further analysed by screening its ability to regulate other known and newly identified genes using the NanoString platform. Hopefully, this will further clarify its role in the otic and epibranchial GRN.

Downstream of Sox8, three transcription factors could potentially work as repressors: Zbtb16, Tcf4 and Zfhx3. Zbtb16 (also known as Plzf) is highly regulated, being promoted by Etv4, Sox8 and Pax2, and can function as a repressor by recruiting the histone deacetylase HDAC4 (Chauchereau et al., 2004). The member of the Tcf family, Tcf4 can function as a transcriptional repressor or activator in the presence of β-catenin (CTNNB1) (for review see: Forrest et al., 2014). Thus, prior to WNT onset in the otic it could function as a repressor preventing epibranchial genes to expand in the otic domain. Corroborating this hypothesis, Tcf4 binding site was identified in one of the newly described Foxi3 enhancer where it could function in preventing Foxi3 expression in the otic (see section 6.7). At 11-12ss both Zbtb16 and Tcf4 are highly enriched medially in the otic domain therefore could be good candidate in the cell-autonomous repression of

epibranchial genes in the otic placode. Thus, absence of Sox8 would cause reduction of these two factors, which in turn would remove the repression on Blimp1 allowing its expansion. Furthermore, Zfhx3 (or Atbf1) functions as repressor and since it is expressed both in the otic and epibranchial it could be involved in fine tuning Blimp1 levels. To establish the exact function of these newly identified genes further studies will need to be carried out. Additionally, exploiting the regulatory elements driving Blimp1 epibranchial expression would help in the precise identification of its direct positive and negative regulators.

The presence of some inconsistency between the RT-qPCR results and the *in situ* hybridisation data can be mainly attributed to the dissection process. Even mild differences in dissection of the otic domain with the respect of the medio-lateral and rostro-causal axis could significantly affect the final RT-qPCR readouts. In the case of gene expansion the size of dissection becomes crucial and this phenotype could be easily miss-interpreted. *In situ* hybridisation results were considered to be more reliable and therefore were used to build the GRN (Figure 4.9 B). Implementation of the n number, section of the otic placode and test of few other possible downstream targets will help in the corroboration of the here presented network.

In summary, the otic and epibranchial transcriptome analysis of three developmental time points reveals a dynamic shift in gene distribution during the process of commitment of ectoderm to an otic placode/vesicle fate. Most notably, there was a gradual transition of enriched genes from 'epithelium development' to 'inner ear development'. Therefore, it was hypothesised that this dynamic change of transcript expression drives the specification of otic/epibranchial progenitors toward otic fate producing the base for further functional studies.

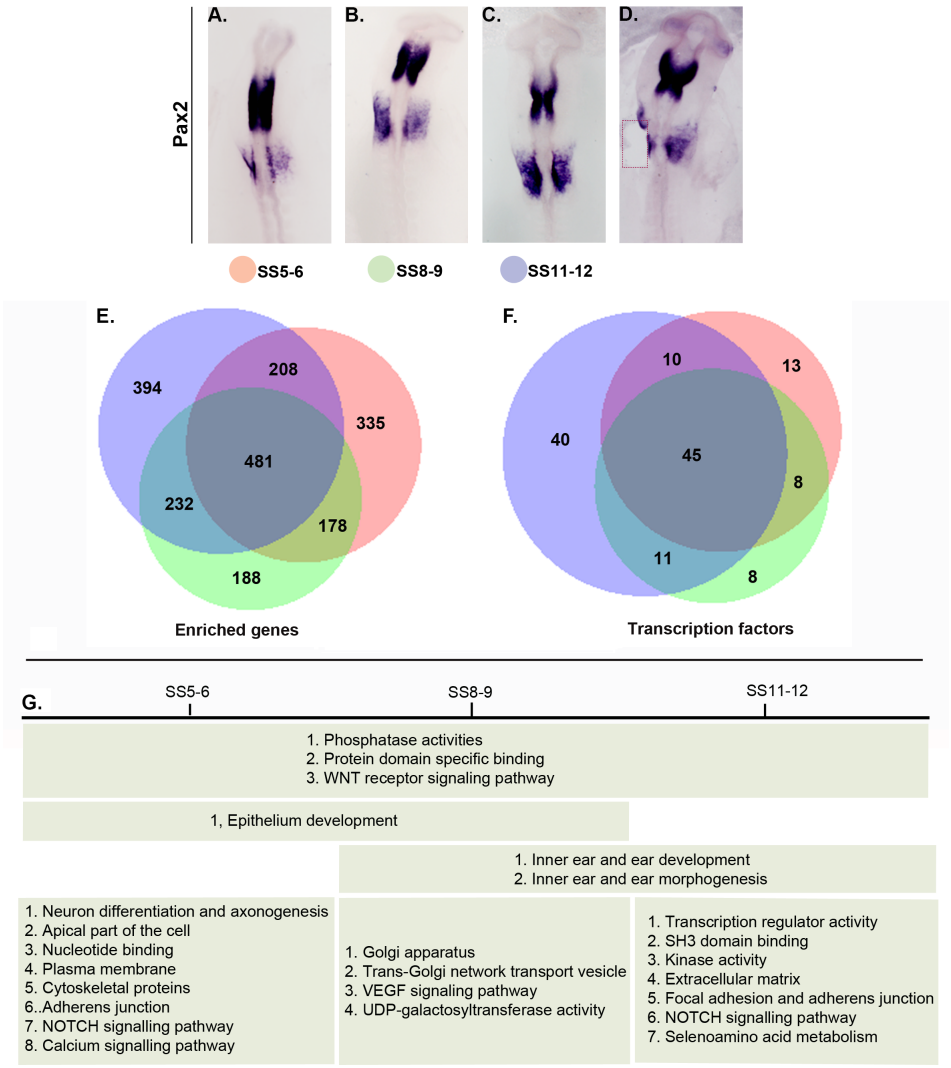

Figure 4.1 Summary of the enriched genes and their related function at different stages of otic development.

(A-D) *Pax2* expression has been used as a landmark to guide otic dissection. *Pax2* is expressed in the entire OPED at 5-6ss **(A)** and it remains expressed during otic development at 8-9ss **(B)** and 11-12ss. *Pax2* expression domain is next to the hindbrain and rostral to the first somite, and has a length of approximately 1/3 of cranial neural tube along A-P axis. The position of Pax2-positive area is estimated and carefully dissected without including undesired regions. **(D)** Example of a dissected tissue on the left side (red box). **(E-F)** Summary of enriched genes at the different stages. The numbers of common and unique enriched genes **(E)** and of transcription factors **(F)** among the three stages are shown in the Venn diagram. **(G)** Summary of the analysis of the enriched GO functional terms associated with common and unique genes across three different stages. 5-6ss orange; 8-9ss green; 11-12ss blue. The bioinformatics analysis of the mRNA-seq data sets has been carried out by Dr Jingchen Chen.

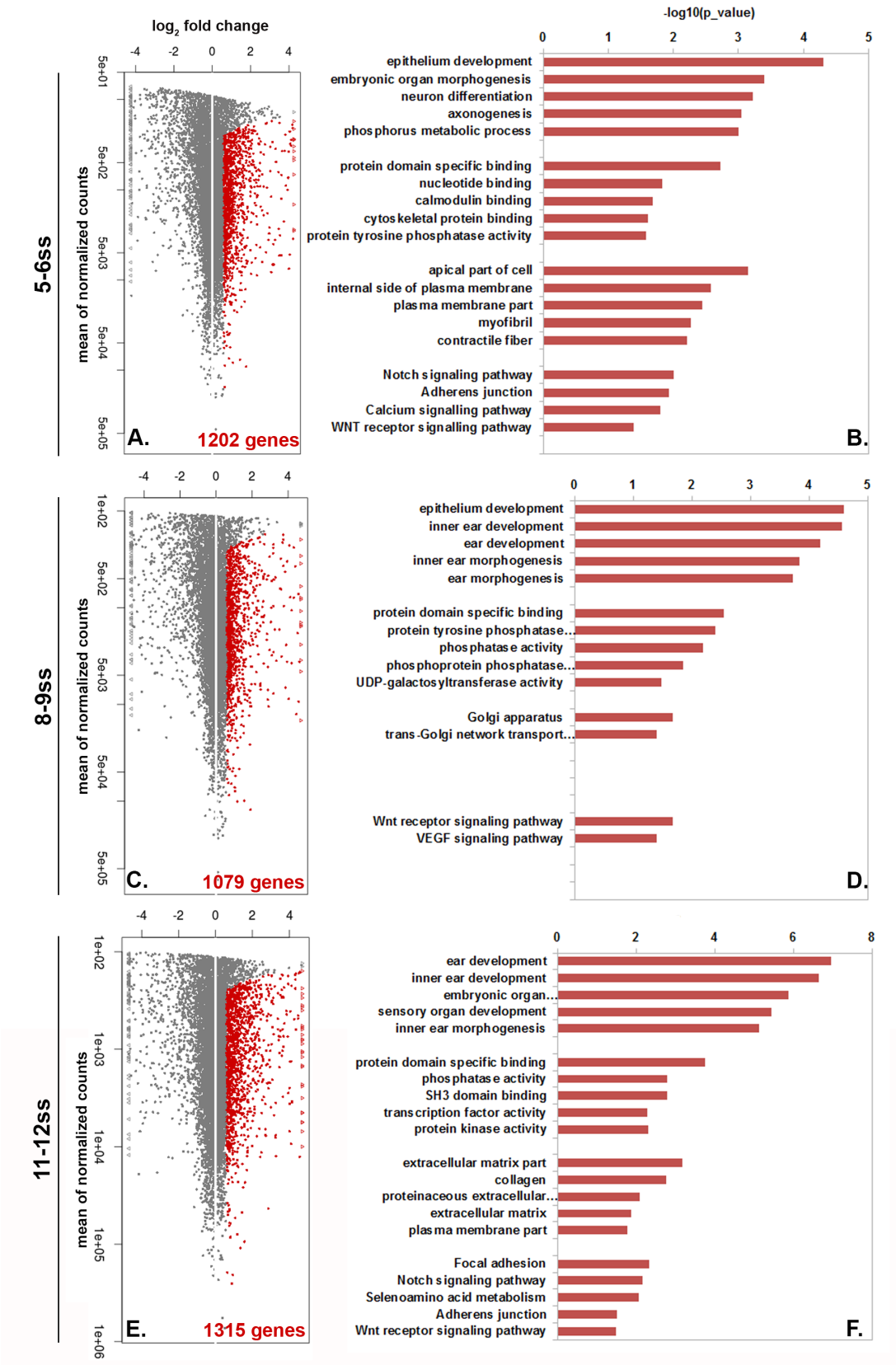

Figure 4.2 Identification of enriched genes and their relative enrichment analysis.

Figure 4.2 Identification of enriched genes and their relative enrichment analysis.
(A, C, E) Plots showing the profile of transcript enriched in the otic placode (5-6ss, 8-9ss and 11-12ss) versus whole embryo of 3ss. Genes with fold enrichment ≥ 1.5 and with count above 300 are highlighted in red. **(B, D, F)** GO terms associated with enriched genes at each stage were annotated. For each stage four groups of terms were considered: biological processes, molecular function, cellular component and signalling pathway. In each category the top 5 over-represented terms with a p-value ≤ 0.05 are listed. The bioinformatics analysis of the mRNA-seq data sets has been carried out by Dr Jingchen Chen.

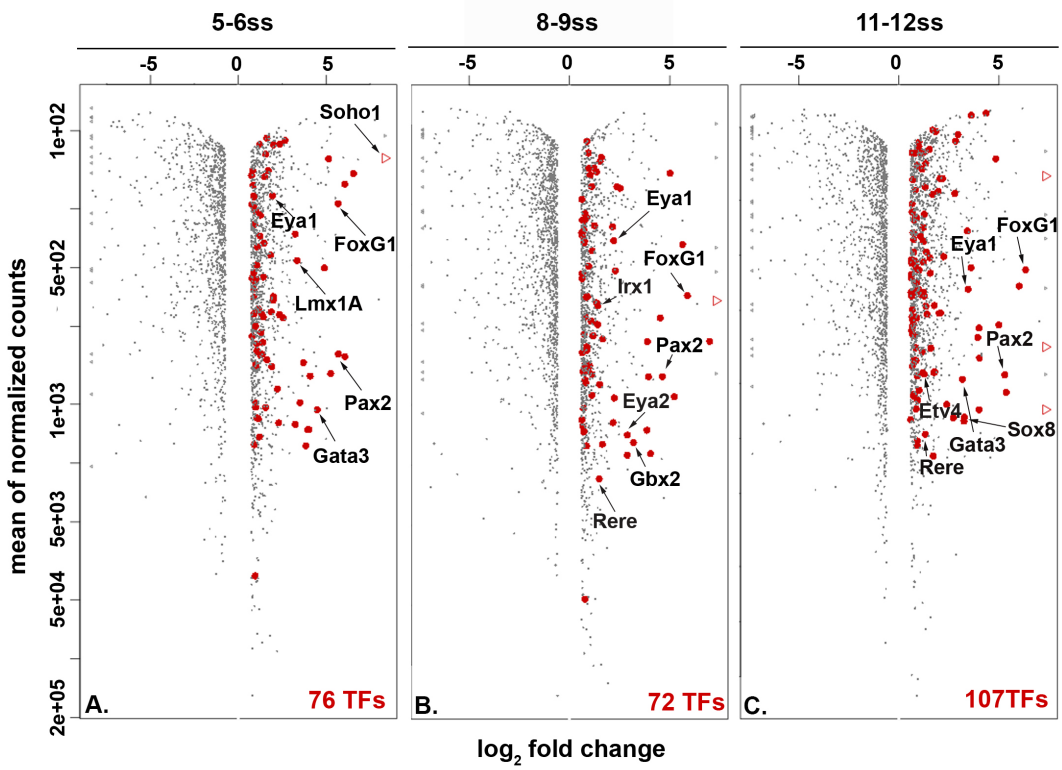

Figure 4.3 Enriched transcription factors during otic development.
Among the enriched genes 76, 72 and 107 transcription factors are present at 5-6ss **(A)**, 8-9ss **(B)** and 11-12ss **(C)**, respectively. Transcription factors are highlighted in red and some of the know TFs are pointed out as examples.

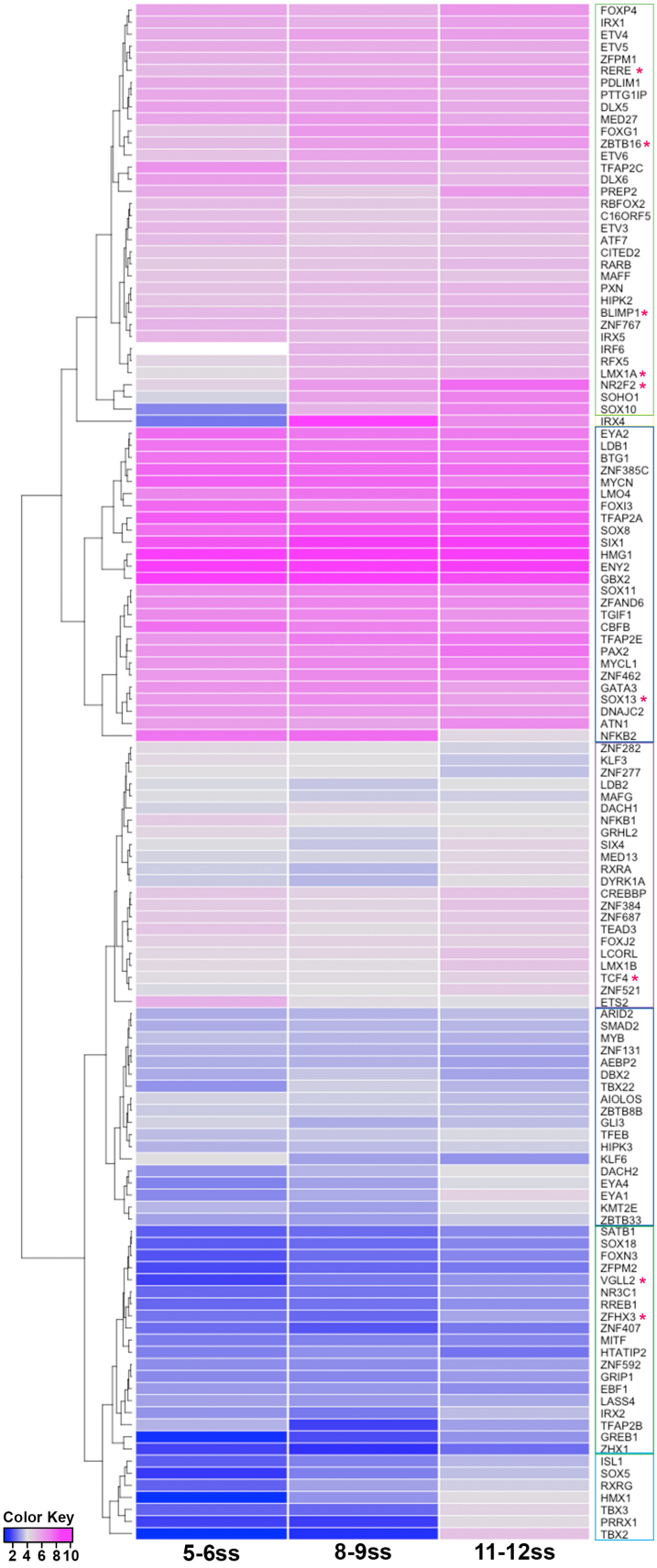

Figure 4.4 Clustering of transcription factors based on their dynamic expression during otic development.

Level of expression of 127 transcription factors at 5-6ss, 8-9ss and 11-12ss is reported in a heatmap. The level of expression of each gene has been calculated as the log2 of the fpkm value detected by mRNA-seq. A blue colour is associated with low level whereas magenta indicates high level of expression (Colour key bottom left). TFs are clustered in 7 main groups according to their dynamic expression during otic development (coloured boxes). Newly identified otic and epibranchial markers are highlighted with a red asterisk.

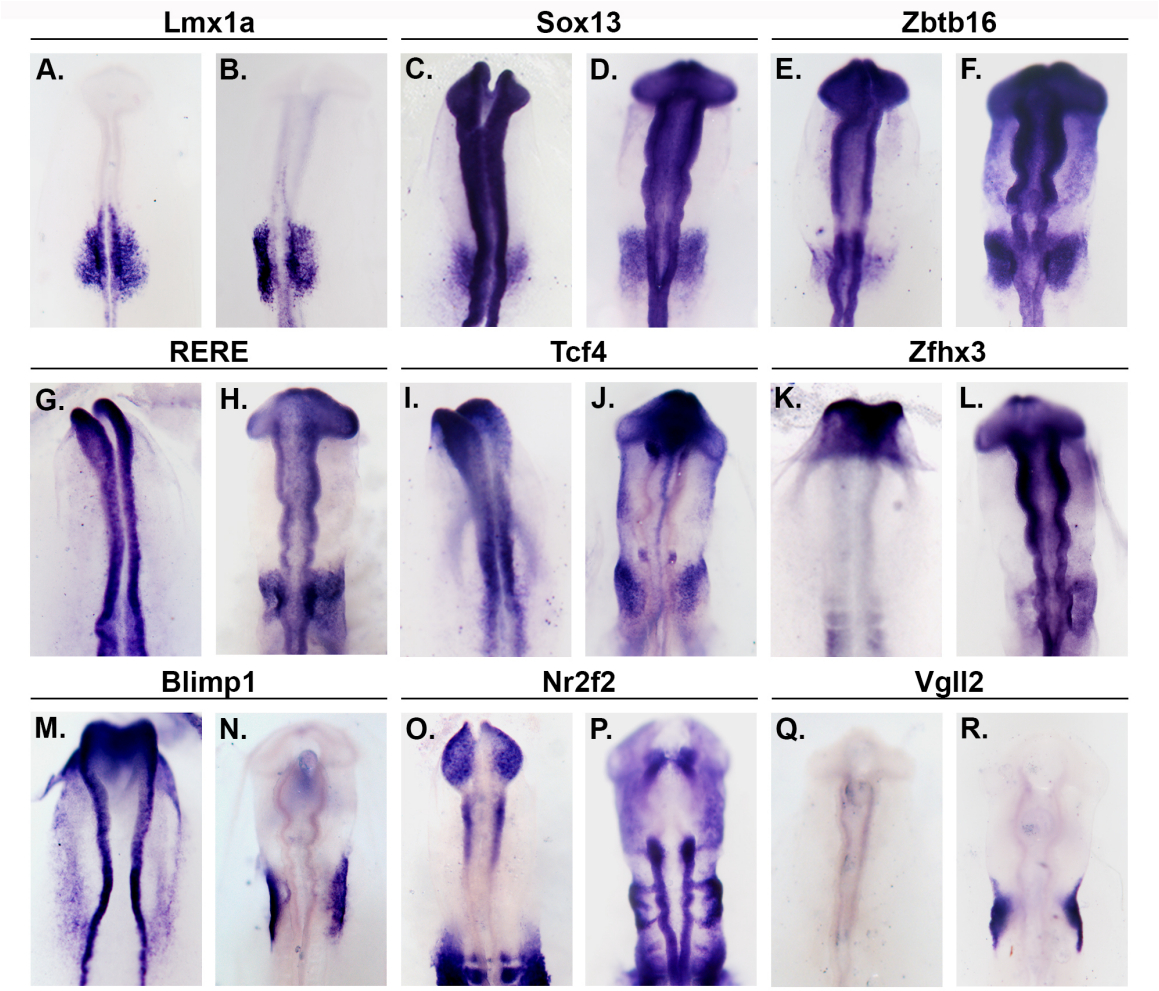

Figure 4.5 Diverse expression patterns of enriched otic and epibranchial transcription factors.
Lmx1a **(A-B)**, *Sox13* **(C-D)** and *Zbtb16* **(E-F)** are expressed in a wide domain in the entire OEPD and remain present at later stages. *RERE* **(G-H)**, *Tcf4* **(I-J)** and *Zfhx3* **(K-L)** are not present early in the OEPD but they are strongly enriched in the otic placode at around 11-12ss. *Blimp1* **(M-N)** in initially enriched in the lateral portion of the OEPD to become strongly expressed in the epibranchial placode. *Nr2f2* **(O-P)** and *Vgll2* **(Q-R)** are turned on later at 11-12ss in the epibranchial domain.

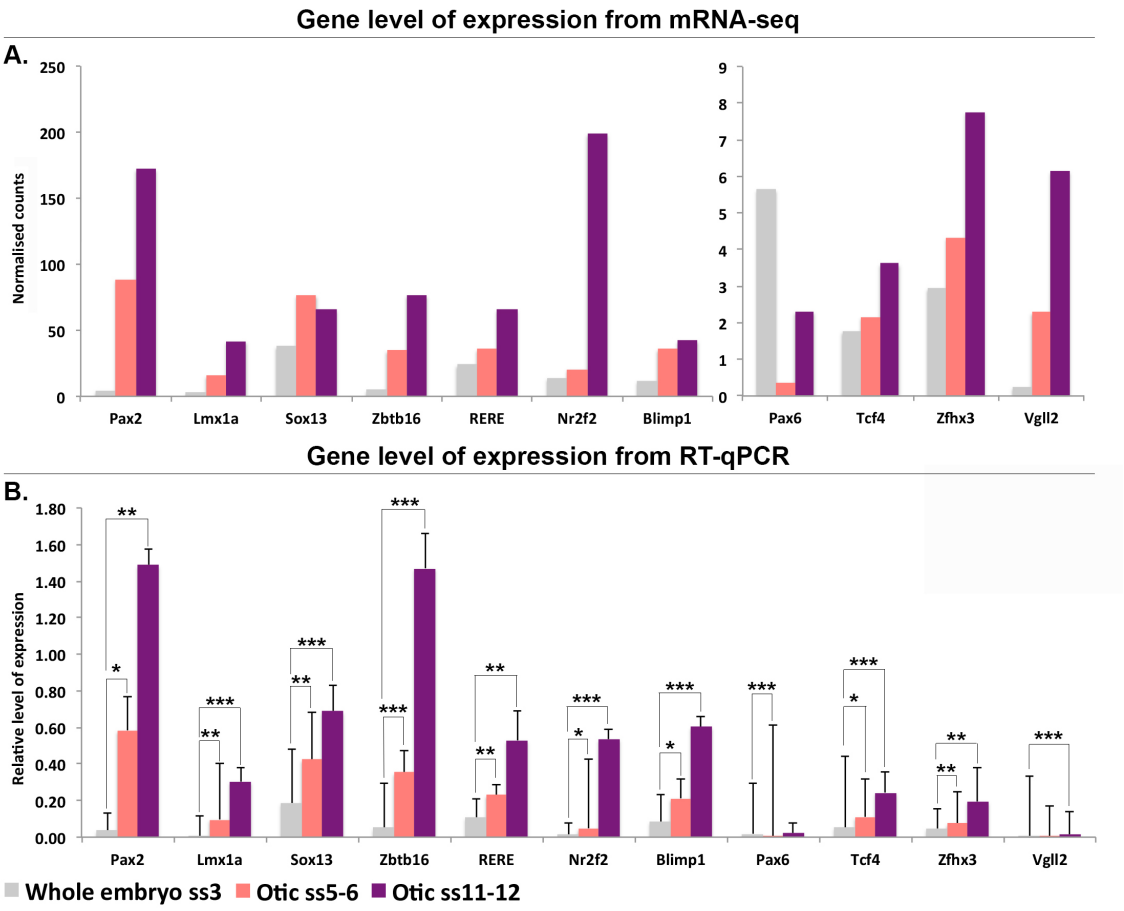

Figure 4.6 Quantification of the level of the newly identified otic transcription factors.

Level of expression of the newly identified factors together with the lens marker *Pax6* and OEPD marker *Pax2* was measured by RT-qPCR **(B)** and compared to the respective levels detected by mRNA-seq **(A)**. ss5-6 (pink) and ss11-12 (violet) were analysed, gene expression level in the otic placode was compared to the expression in the ss3 whole embryo (grey). mRNA-seq and RT-qPCR data show a similar trend for the majority of the analysed genes, corroborating each other. Statistically significant fold enrichments are labelled with an asterisk: *** p-value≤0.001, ** p-value≤0.01 and * p-value≤0.05.

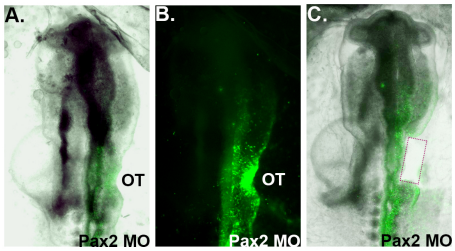

D.

Symbol	ETV4 MO		
	Test MO /Control MO	pvalue	In situ
SOX13	-1.204879516	0.20001934	No change
ZFHX3	-1.258951078	0.42923491	No change
RERE	-1.14781401	0.50384689	
NR2F2	-1.039259226	0.75867613	
BLIMP1	-2.151817247	0.03867232	Not tested
LMX1A	-1.036860799	0.86696444	
SOX10	-1.432851293	0.06579212	Enh
VGLL2	-1.711849126	0.1140255	?
ZBTB16	-1.244490792	0.16880889	Yes
TCF4	-2.197031501	0.00534436	Yes
PAX2	-1.908213006	0.01797597	Yes
SPLAT4	-1.137254825	0.58065262	Enh

Symbol	PAX2 MO			SOX8 MO		
	Test MO /Control MO	pvalue	In situ	Test MO /Control MO	pvalue	In situ
SOX13	-1.823444977	0.00822436	No	-1.681792831	0.02325495	Expansion
ZFHX3	-1.725084064	0.00467124	No	-3.286761258	0.0234089	Yes
RERE	-1.183724489	0.29687319		1.057018041	0.94939328	
NR2F2	-1.565546833	0.05262366		1.066832243	0.87745966	
BLIMP1	-1.670175839	0.0490418	Yes	-1.643380629	0.08692925	Expansion
LMX1A	-1.765405993	0.01428232	Yes	-1.021012126	0.91351854	
SOX10	-1.245449622	0.14847658		-1.4913994	0.04236952	Enh
VGLL2	-1.51221856	0.04703078	Yes	-1.810849523	0.07910742	?
ZBTB16	-1.561933827	0.01720304	Yes	-1.378723669	0.04611344	Yes
TCF4	-2.163449332	0.00161272	Not tested	-2.361985323	0.00610278	Yes
PAX2	4.102964486	0.00146911		-2.271008858	0.00600036	Yes
SPLAT4	-1.721102874	0.0104511	Enh	-1.09682498	0.4447501	

Upregulated genes FD >= 1.5
Downregulated genes FD <= -1.5
pavlue <= 0.05

Figure 4.7 Effects of Etv4, Pax2 and Sox8 knockdown analysed by RT-qPCR.
Embryos were electroporated on one side where the otic region was targeted **(A-B)**. The otic region was carefully dissected (red box) and processed for RT-qPCR **(C)**. **(D)** RT-qPCR analysis after Etv4, Pax2 and Sox8 knockdown. The level of expression of the gene of interest was compared between the test and the control morpholino; a fold changes threshold of -1.5 and +1.5 was used together with a p-value≤ 0.05 to define the affected genes. The short listed genes were successively tested by *in situ* hybridisation to verify the possible link. The last column (in situ) summarises the results so far obtained (Figure 4.8). 'Yes' means that the interaction has been validated by *in situ* hybridisation whereas a 'No' means that such difference was not observed. The presence of question marks indicates that additional validation and embryo sectioning are required to validate the presumptive interactions. In few cases an expansion in the size of gene expression was observed ('Expansion') and in few others no difference was found between the internal control and test side ('No change'). Etv4 and Pax2 has been identified to directly regulate Spalt4 enhancer (Barembaum and Bronner-Fraser, 2010), additionally Etv4 and Sox8 regulate Sox10 otic enhancer (Betancur et al., 2011). Only Pax2 knockdown significantly affects *Splat4* expression while the remaining show a trend of downregulation; these links are marked with 'Enh'. Finally, 'no tested' means that a particular interaction has not yet been validated.

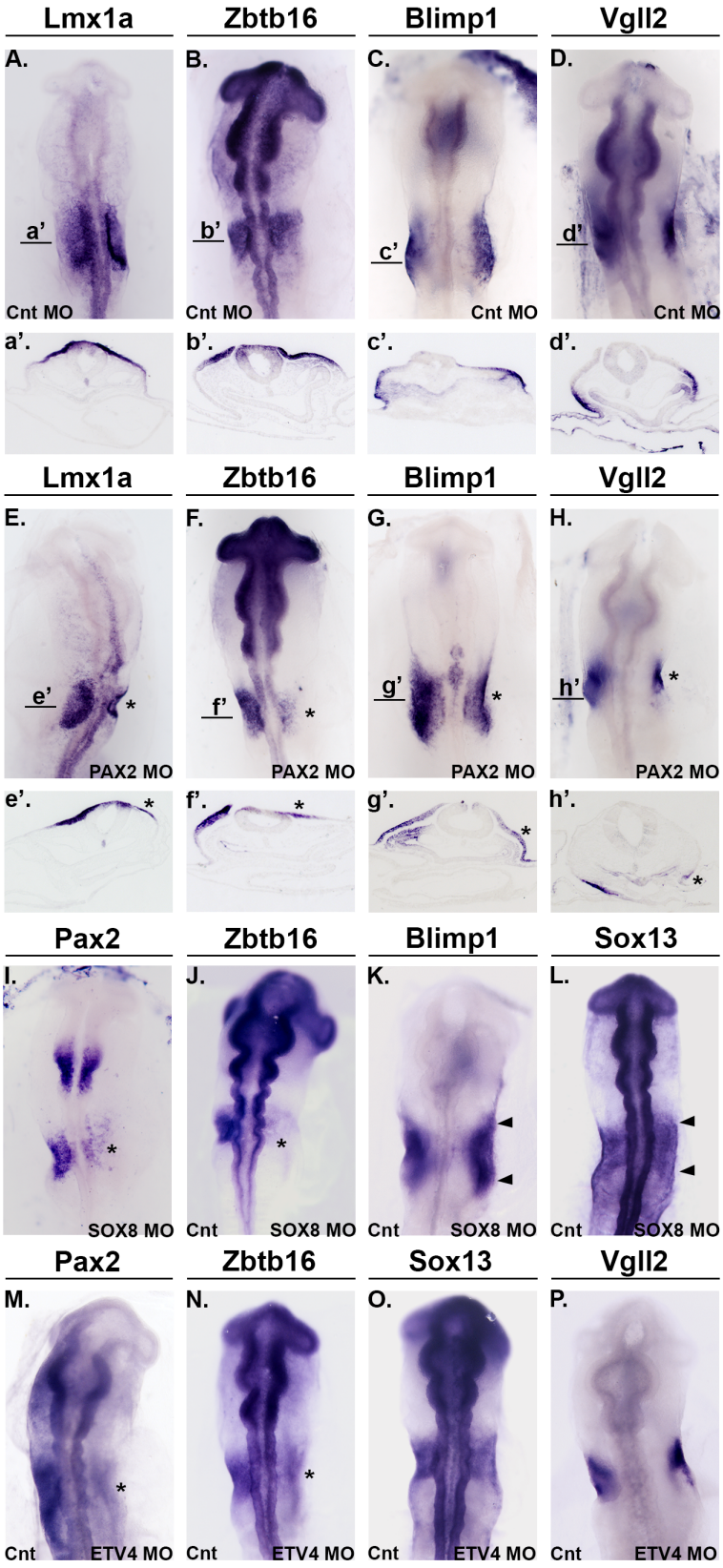

Figure 4.8 Effects of Etv4, Pax2 and Sox8 knockdown analysed by *in situ* hybridisation.
(A-D) Control morpholino electroporation in half side of the embryo (see example Figure 4.7 A-C); expression of *Lmx1a* **(A, a')**, *Zbtb16* **(B, b')**, *Blimp1* **(C, c')** and *Vgll2* **(D, d')** is comparable in the electroporated and not electroporated side. **(E-H)** Pax2 knockdown causes loss of placode thickening and of *Lmx1a* **(E, e')**, *Zbtb16* **(F, f')** expression (asterisk). Pax2 affects also the epibranchial expression of *Blimp1* **(G, g')** and *Vgll2* **(H, h')** (asterisk). **(a'-h')** A representative section at the level of the otic placode is showed for each gene. **(I-P)** Electoporation of Sox8 and Etv4 morpholino was performed in the right side whereas as internal control the left side was electroporated with control morpholino. Dr Meyer Barembaum executed these electroporations and respective *in situ* hybridisation. **(I-L)** Sox8 knockdown reduces the level of *Pax2* **(I)** and *Zbtb16* **(J)** expression (asterisk). However, it seems to enlarge *Blimp1* **(K)** and *Sox13* **(L)** expression (arrow heads); otic sections are required to further confirm the phenotype. **(M-P)** Etv4 loss causes absence of *Pax2* **(M)** and *Zbtb16* **(N)** expression (asterisk), while *Sox13* **(O)** and *Vgll2* **(P)** appears not to be affected.

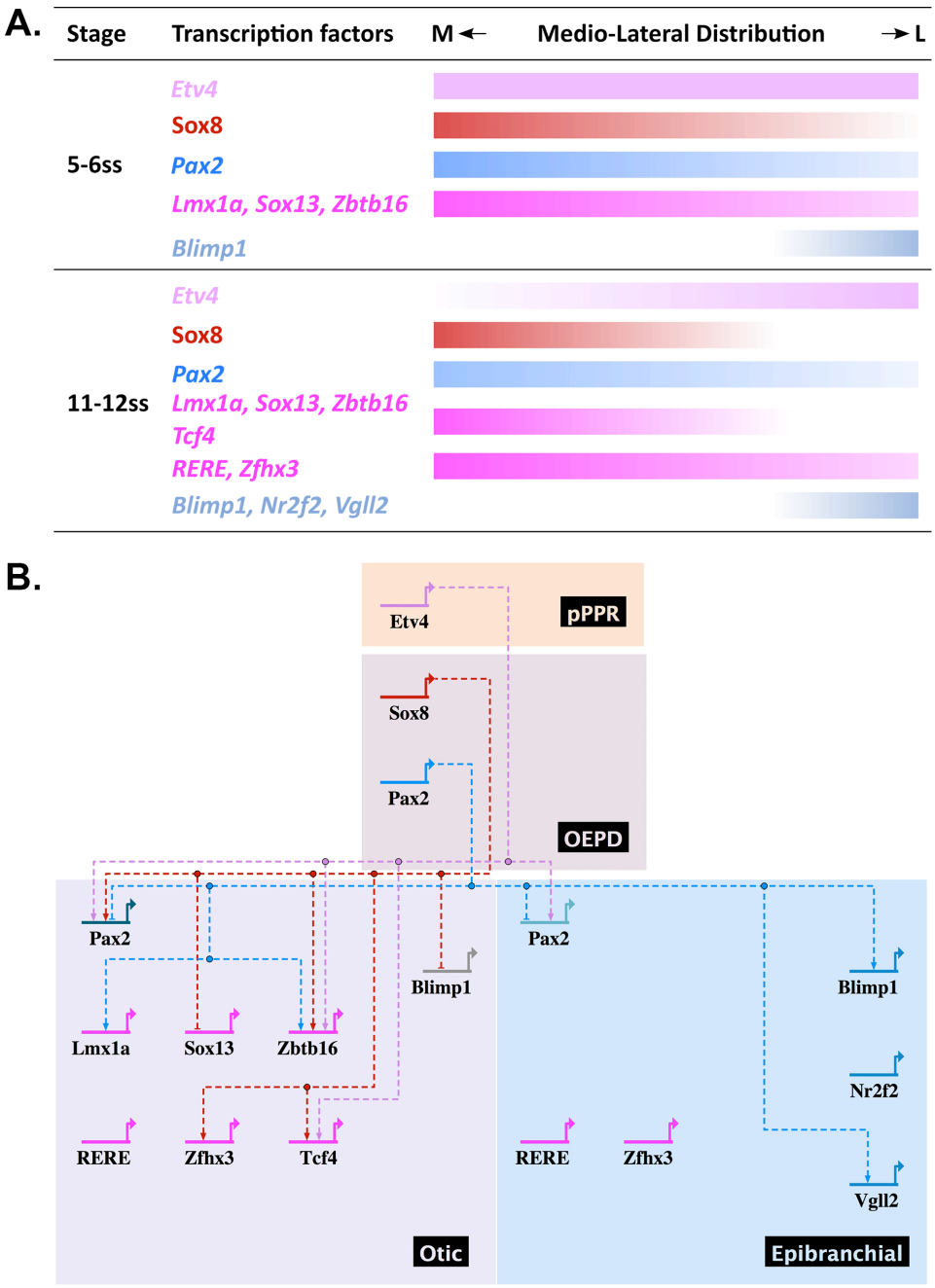

Figure 4.9 Summary of the expression pattern of the newly identified transcription factors and their upstream regulations.

(A) Diagram showing the medio-lateral expression within the otic domain of *Etv4*, *Pax2* and *Sox8* and the newly identified transcription factors. The OEPD domain at 5-6ss presents a homogenous expression of the majority of the genes, with the exception of *Blimp1*, which is enriched laterally. As the otic and epibranchial placode segregates a subset of transcription factors become complementary expressed: *Sox8, Pax2*, *Lmx1a*, *Sox13*, *Zbtb16* and *Tcf4* show enrichment in the medial portion while *Etv4*, *Blimp1*, *Nr2f2* and *Vgll2* are more abundant laterally. **(B)** Illustration of the here identified interactions between Etv4 (pink), Sox8 (red) and Pax2 (sky blue) the new otic and epibranchial transcription factors. The presence of dotted lines indicates that there is no evidence suggesting a direct regulation. Posterior PPR (pPPR) orange; OEPD pink; Otic violet; Epibranchial blue.

5. Transcriptional hierarchy downstream of FGF signalling during otic and epibranchial induction

5.1 Introduction

At neural palte stages precursors of different sense organs are intermingled in a common progenitor domain, the pre-placodal region. Cells within this domain share common features: they express general PPR markers (Six/Eya genes) and their ground state is lens placode (Bailey et al., 2006). As development progresses, regionalisation of the PPR is apparent by differential expression of transcription factors (e.g. *Pax6* in the lens territory, *Pax3* in the trigeminal region and *Pax2* in the OEPD) and signals along the anterior-posterior axis induce different cell fates (for review see Grocott et al., 2012; see section 1.4). The combination of transcription factors expressed seems to impact on cell identity resulting in the specification of individual sensory placodes. Embryological experiments have shown that the initial source for otic/epibranchial-inducing signals is the paraxial mesoderm underlying the posterior PPR (Kil et al., 2005, Albaum and Nestler, 1937, Borghese, 1942, Eakin, 1939, Gritsman et al., 1999, Holtfreter, 1933, Jacobson, 1963a, Ladher et al., 2000, Leger and Brand, 2002, Mendonsa and Riley, 1999, Orts et al., 1971, Phillips et al., 2001, Raven and Kloos, 1945, Woo and Fraser, 1997, Zhang et al., 1998, Zwilling, 1941). FGF signalling from this mesoderm and later from the hindbrain (as reviewed in Ladher et al., 2010, Ohyama et al., 2007, Schimmang, 2007) is the main factor mediating the induction of OEPD-specific genes. A variety of FGF ligands have been identified in different species: *FGF3* and *FGF8* in zebrafish (Leger and Brand, 2002, Liu et al., 2003, Maroon et al., 2002, Phillips et al., 2001), *FGF10* and *FGF3* in mouse (Wright and Mansour, 2003, Urness et al., 2010, Ladher et al., 2005) and *FGF3* and *FGF19* in the chicken embryo (Karabagli et al., 2002, Kil et al., 2005, Ladher et al., 2000, Ladher et al., 2005), and they function in a similar fashion. Inhibition of FGF signalling in different species has confirmed its function in otic development. In zebrafish, FGF3 or FGF8 loss-of-function leads to reduction or loss of otic markers and of the otic vesicle (Maroon et al., 2002, Leger and Brand, 2002, Liu et al., 2003, Phillips et al., 2001, Solomon et al., 2004). Likewise, inhibition of FGF receptors using SU5402 in zebrafish embryo blocks otic formation and the otic markers *Pax2*, *Pax8*, *Dlx3* and *Spry4* are absent (Leger and Brand, 2002, Maroon et al., 2002, Solomon et al., 2004). *FGF3* and *FGF10* knockout mice form an otic vesicle but it is reduced in size (Alvarez et

al., 2003, Ohuchi et al., 2000, Pauley et al., 2003, Wright and Mansour, 2003). Double mutants for FGF3/FGF10 (Alvarez et al., 2003, Wright and Mansour, 2003, Zelarayan et al., 2007, Urness et al., 2010) and FGF3/FGF8 (FGF8 conditional allele) (Ladher et al., 2005, Zelarayan et al., 2007) depict a more severe phenotype; thus FGF ligands have redundant functions in mouse. Additionally, loss of FGF receptor 2 (FGFR IIIb), the receptor of FGF3 and FGF10, give rise to a smaller otic vesicle (Pirvola et al., 2000). In chick, *FGF8* endodermal knockdown by siRNA causes loss of OEPD induction and *Pax2* downregulation that can be rescued by an FGF19 bead (Ladher et al., 2005). FGF8 in the endoderm induces FGF19 that in turn promotes otic fate (for review see Ladher et al., 2010). *FGFR1* is highly expressed at OEPD stages and otic and epibranchial cells show activated ERK1/2 and ERK/MAP kinase responsive genes (Lunn et al., 2007). Furthermore, in chick specific inhibition of the ERK/MAP kinase pathway leads to loss of the OEPD marker *Pax2* and prevents placode formation (Yang et al., 2013). Together, these data show that FGF is a potent inducer of OEPD fate, and point to the importance of ERK/MAP kinase branch of the pathway. Importantly however, only cells that have first acquired PPR identity are able to respond to induction by FGF (Martin and Groves, 2006) suggesting a two-step model for otic and epibranchial specification.

Despite the importance of FGF signalling in OEPD induction only a small set of factors has clearly been associated with this process and the overall gene network downstream of FGF has not been characterised in detail. Materna and Oliveri (2008) and Streit et al. (2013) described the general workflow to assemble a high-resolution gene network. After having dissected the developmental process of interest over time, the next step is to identify all possible players, determine their expression profiles and use perturbation experiments to asses their epistatic relationship and hierarchy. In Chapter 3 and 4, I have described the identification of many network components using microarray and mRNA-seq approaches and their temporal and spatial expression profiles during PPR and otic placode formation. In this chapter, I will use perturbation experiments at different time points, followed by quantitative methods to measure the behaviour of all network components and thus to examine the earliest response to FGF signalling during the transition from posterior PPR cells to OEPD. This will position genes into a hierarchy, determine FGF target genes and establish epistatic relationships among some of the crucial components. Thus, the overall aim of this chapter is to unravel the dynamic and complex events downstream of FGF signalling and to construct a basic network for OEPD specification.

5.2 Establishing the assay for *in vitro* otic induction

Since tissue interactions *in vivo* are complex and the function of a single signal is difficult to assess, I used a well-established *in vitro* assay to determine the response of the posterior PPR (Figure 5.1 A orange domain), a region comprising the prospective trigeminal placode and the OEPD, to FGF signalling. In chick, FGF19 from the head mesoderm is the main FGF ligand to act as OEPD inducing signals; however it is FGF2 that better mimics FGF activity *in vitro* (Martin and Groves, 2006). The competence of trigeminal ectoderm to respond to FGF signalling is similar to that of the prospective OEPD itself (Yang et al., 2013) and therefore these tissues were combined for the *in vitro* assay. The posterior PPR was isolated from the 0-somite stage (HH6) to minimise the presence of early otic placode transcripts and cultured in isolation in the absence or presence of the FGF2 ligand. Explants were cultured for 6, 12 or 24 hours to identify the dynamic changes of gene expression and to position responsive genes into a temporal hierarchy.

Although the majority of experiments was analysed using NanoString, it was important to confirm the reliability of the assay and to compare results obtained by *in situ* hybridisation (as in previous studies: Martin and Groves, 2006, Yang et al., 2013) with results obtained by NanoString. Tissues treated with or without FGF for 6, 12 and 24 hours were processed for *Pax2 in situ* hybridisation, one of the OEPD earliest markers. After 6 hours 80% of the FGF2-treated tissues express *Pax2* (n=4/5; Figure 5.2 B, I, J) compared to untreated explants where no *Pax2* expression was detected (n=0/4; Figure 5.2 A, I, J). Surprisingly, after 12 hours not only FGF2-treated (100% n=13/13; Figure 5.2 D, F, I, J), but also control tissues express some *Pax2* (62% n=5/8; Figure 5.2 C, E, I, J). However, overall the number of $Pax2^{+}$ cells per explant seems smaller and the percentage of positive explants is less. After 24 hours, 71% of the FGF2-exposed tissues express *Pax*2 (n=10/14; Figure 5.2 H, I, J), while in the controls *Pax2* was not detected (n=0/8; Figure 5.2 G, I, J). Thus, although control tissues express some *Pax2* after 12 hours of culture they lose this expression after longer culture (24 hours). Martin and Groves (2006) did not analyse in details the dynamic of *Pax2* expression in control and FGF2-treated tissues. The results I have obtained highlight the importance of considering the dynamic of FGF response, and show that pPPR cells may already have autonomous tendency to become OEPD, but they require sustained FGF to fully embark this fate.

The same experiments were analysed by NanoString (see below) and compared with the results described above. Comparison of the percentages of *Pax2* positive tissues (Figure 5.2 I) and the expression levels obtained by NanoString for each time point (Figure 5.2 J) shows very consistent outcomes: the dynamic changes of *Pax2* expression is highly comparable. Furthermore, the high sensitivity of the NanoString platform and the usage of biological replicates provide good confidence in the results obtained.

5.3 Design of the NanoString probe sets and NanoString data analysis

To characterise the response of pPPR cells to FGF signalling, two different NanoString probe sets were generated. Downstream analysis of the microarray screen identified new factors that may be involved in PPR and OEPD specification (see Chapter 3). Together with data from the literature a list of 126 genes (PPR NanoString probe set) was obtained comprising new and known PPR and otic transcripts, transcripts specific for other placodes as well as the neural plate and neural crest, read-outs for various signalling pathways and housekeeping genes. More recently, an otic NanoString probe set was designed based on transcriptome profiling of the placode at different stages (see Chapter 4). Like the first probe set, it contains: known and newly identified otic and epibranchial transcription factors, chromatin modifiers present in the otic domain identified by the mRNA-seq screen, olfactory, lens and trigeminal markers, neural crest, neuronal genes, cell adhesion molecules, read-outs for various signalling pathways and housekeeping genes, for a total of 221 genes (otic NanoString probe set). The presence of different categories of genes in the probe sets is important for analysing how FGF influence fate decision and if modulates other signalling pathways during time. Presence of FGF read-outs helped in controlling the correct activation or inhibition of the pathway. Overall, the NanoString probe sets are a useful tool to study how FGF affects cell fate decision and time course experiment helped in positioning genes in a temporal hierarchy.

On average 10 tissues were collected per sample and three experimental replicates where used for each condition. The NanoString platform allows quantification of gene expression changes more accurately than *in situ* hybridisation and is comparable to RT-qPCR (Geiss et al., 2008), thus providing semi-quantitative measurements. The data analysis was performed as reported in section 2.11. The NanoString code set contains internal standard control, positive and negative, which were used as normaliser. The positive controls are used to take into account differences in hybridisation, purification

and binding efficiency. The counts for the positive controls were summed together to estimate the overall hybridisation efficiency and recovery for each lane. In order to normalise the data across different experiments the individual positive control sums were averaged together; the initial positive sum for each column was then divided by the averaged value, creating a normalisation factor for each lane. The count of each gene in a particular lane was multiplied by the normalisation factor creating a background corrected value. Negative controls are also present in the probe set used to remove possible background reads. The average of the negative counts was summed to its standard deviation; this value was then subtracted from the background corrected value giving the final detected mRNA count. Genes with a count below 50 were considered as not expressed in the tissues. Additionally, to take in account differences in amounts of starting material total mRNA present in each sample was calculated and used to further normalise the data; only after this step housekeeping genes showed comparable levels across different samples. For each set of experiments three replicates were processed and their average value was calculated. Fold difference between treated and control sample was calculated (1.5 cut-off for upregulated and 0.25 for downregulated genes) and together with p-value (un-paired t-test; p-value≤0.05) used to identify the significant up or downregulated genes.

Thus, the NanoString platform allow to quantify the expression level of many genes at the same time using a small amount of starting material, which are major advantages over RT-qPCR and *in situ* hybridisation. Furthermore, performance of triplicates allows the determination of statistically significant changing genes. Comparison of *Pax2* expression by *in situ* hybridisation and NanoString results are highly comparable (Figure 5.2) giving good confidence on the results. Therefore the NanoString was used as method to analyse change on gene expression after FGF perturbation.

5.4 FGF signalling is sufficient to induce otic and epibranchial genes at the expenses of the anterior PPR

To establish the temporal response of posterior PPR cells to FGF signalling the NanoString platform was used as tool to quantify changes in gene expression. Around 10 pPPR tissues (HH6) were dissected per each sample and cultured in isolation with or without FGF2 ligand. Explants were cultured for 6, 12 or 24 hours to identify the temporal response to FGF signalling during otic development.

In Table 5.1 are summarised the genes up or downregulated at the different time points. In particular, after 6 hours, thanks to the analysis using the PPR and otic NanoString probe sets, a large group of genes was found to be upregulated (Figure 5.3 A-D; Appendix 9.2 Table 9.2). Among them posterior PPR and OEPD genes appear to be positively upregulated at this early time point: *Foxi3* (as also reported by Khatri et al., 2014), *Gbx2* (Yang et al., 2013), *Sox13* and *Pax2* (Figure 5.3 and Figure 5.4). The chemokine *Cxcl14*, initially identified in the molecular screen carried out by Lleras-Forero (2011), is expressed in the more posterior part of the pre-placodal region and after the otic vesicle formation it appears to be enriched at the posterior tip of the otic (Figure 5.4 C, D). This molecule is among one of the more strongly upregulated genes by FGF, highlighting a potential role for the chemokine signalling during otic placode formation (see section 6.4). Late known otic and epibranchial factors also appear under FGF control at this early time point: *Soho-1* (Kiernan et al., 1997), *Hesx1* (Abe et al., 2006), *Foxg1* (Yang et al., 2013), *Hoxb1* (Paxton et al., 2010), *Hey2* (Doetzlhofer et al., 2009) and *EphA4* (Baker and Antin, 2003); some of them have already been associated with FGF signalling. In addition, several molecules associated with chromatin regulation identified by molecular screens (see Chapter 3 and 4) are under FGF control at the early tested time point (*Arid3a*, *Bax1a*, *Cbx4*, *Chd7* and *Setd2*). After 12 hours the transcriptional repressor *Sall1*, which is expressed in the otic and epibranchial placodes at HH11 (Sweetman et al., 2005), becomes upregulated by FGF. While *Gbx2* and *Foxi3* remain upregulated in the +FGF2 explants but they are not anymore significant (Table 5.1; Appendix 9.2 Table 9.4). Interestingly genes like N*ociceptin* (Noc), an early Pax6 regulators (Lleras-Forero, 2011, Lleras-Forero et al., 2013; Figure 5.3 G-H), and *Follistatin like 4* (Fstl4) (Lleras-Forero, 2011; Figure 5.3) are downregulated after 6 hours and later (24 hours) will become enriched in the treated sample. This is in line with their expression profile in the embryos, where they are expressed in the anterior PPR at neurula stage and will be later present in the otic vesicle (Lleras-Forero, 2011, Lleras-Forero et al., 2013; Figure 5.4 O-P). As expected, some of the known ERK/MAP kinase targets are strongly regulated by FGF (*Etv4*, *Etv5*, *Spry1* and *2*; Figure 5.3 A-D). It is important to notice that Etv4, Spry1 and 2 are only present in the otic probe set while Etv5 is present also in the PPR NanoString probe set.

An aspect not investigated in the literature is the role of FGF signalling in gene downregulation during OEPD formation. To answer this question, the counterpart of genes highly expressed in the control tissues and present at a lower level in the FGF

treated sample were analysed. A large majority of the genes suppressed by FGF are strongly expressed in the anterior PPR, where the lens and olfactory placodes will form (Figure 5.3). Among them: *Pax6* (Figure 5.4 M-N), *SSTR5* (Lleras-Forero, 2011, Lleras-Forero et al., 2013), *Dlx3* (Khudyakov and Bronner-Fraser, 2009), *Dlx5* (McLarren et al., 2003), *Dlx6* (Figure 3.9), *Gpr160* (Figure 5.4 Q-R) and *Kremen1* (*Krm1*; Figure 5.4 S-T). Furthermore, the non-neurunal genes *Gata2/3* are also repressed by FGF (Figure 5.3 C-D, G-H; Figure 5.4 W-X).

Since Pax genes play a crucial role in sensory organs development and the lens placode has been reported to be the ground state of all PPR cells (Bailey et al., 2006) the relation between *Pax2* and *Pax6* expression upon FGF treatment was further examined. *Pax2*, as described above (see section 5.2), is strongly present in +FGF sample although the control tissues present a spike in its expression after 12 hours (Figure 5.5 A). An opposite behaviour was observed for *Pax6*, being strongly expressed in the untreated PPR (Figure 5.5 B) and present at a low level after FGF treatment. Other Pax genes (*Pax3* and *Pax7*), involved in sensory organs specification, are not expressed in the examined tissues (see Appendix 9.2). Comparison of *Pax2-Pax6* level of expression in the two conditions revealed that *Pax6* is predominant on *Pax2* in the control sample (Figure 5.5 C), being expressed at a high level at all the three time points. In contrary, FGF is promoting very quickly *Pax2* expression and repressing *Pax6* (Figure 5.5 D). Further corroborating the idea that FGF signalling is promoting the otic and epibranchial fate and is doing that also by downregulating expression of lens genes.

Furthermore, FGF seems to modulate other signalling pathways. The WNT target *Lef1* (Figure 5.4 U-V) is initially upregulated by FGF signalling but after 24 hours it will become, together with *Axin2,* downregulated (Figure 5.3 C-H). Retinoic acid associated genes are under FGF control at 6 hours: *Retinoic Acid Inducer 1* (*Rai1*), which regulates transcription through chromatin remodelling, is upregulated whereas *Retinoic Acid Receptor beta* (*Rarb*) and a member of the retinoid X receptor (*RXRG*) are repressed. Thus, FGF appears to differentially control genes associated with other signalling pathway.

General PPR markers like *Six1*, *Six4* and the newly identified *Homer2* are similarly expressed in the control and treated tissues, only at the late time point of 24 hours *Six1* and *Homer2* become enriched in the +FGF2 sample, probably correlating with their late

otic enrichment (Sato et al., 2012; Figure 3.12) (Appendix 9.2 Table 9.5). FGF treatment did result in *Eya2* up regulation, but this trend was not significant (except in the 6 hours otic probe set) (Figure 5.3 and Table 5.1). It is also important to point out that the majority, 86, 101 and 81 genes at 6, 12 and 24 hours, respectively and 178 for the otic NanoString probe set, did not present any variations (Appendix 9.2). This suggests that only subsets of genes are under FGF control during otic induction.

The overall picture reveals a highly dynamic network, in which at each time point a cohort of genes is regulated and only a subset of them will remain under FGF dependence constantly (Figure 5.3 and Table 5.1). As expected, some of the known ERK/MAP kinase targets are strongly regulated by FGF (*Etv4*, *Etv5*, *Spry1* and *2*; Figure 5.3), as are known pPPR and OEPD transcripts including *Pax2*. The emerging model points to an overall upregulation of the OEPD fate at the expenses of the more anterior PPR fate.

Table 5.1 Genes up and downregulated after FGF2 treatment

6h (PPR NanoString probe set)	
FC≥1.5; P-value ≤ 0.05	*Cxcl14*, *Hey2*, *Gbx2*, *Hesx1*, *Etv5*, *Foxi3*
FC≥1.5	*BMP4*, *Chd7*, *Eya2*, *Hey1*, *Ing5*, *Mllt10*, *Pax2*, *Tbx1*, *Zhx2*, *Zic3*, *Znf462*
FC≤0.25; P-value ≤ 0.05	*Ptpru*, *Gpr160*, *SSRT5*, *Fstl4*, *Irx3*
FC≤0.25	*Axin2*, *Dlx3/5/6*, *Gata2/3*, *Irx2*, *Lmx1b*, *Lrp11*, *Otx2*, *Pax6*, *Noc*, *Six3*, *Sox9/10*, *Stox2*, *Tbx3*, *Zic1*
6h (otic NanoString probe set)	
FC≥1.5; P-value ≤ 0.05	*Arid3a*, *Baz1a*, *BMP4*, *Cbx4*, *Ccnd1*, *Cxcl14*, *EphA4*, *Ets2*, *Etv4/5*, *Eya2*, *Ezrin*, *Foxi3*, *Foxp1*, *Fzd7*, *Gbx2*, *Hesx1*, *Hoxb1*, *Id1*, *Klf7*, *Lef1*, *Msi1*, *N-Myc*, *Pax2*, *Rai1* and *Raldh2*, *Sema4d*, *Setd2*, *Snail1*, *Soho1*, *Sox13*, *Spry1/2*, *SSTR2*
FC≥1.5	*Chd6, En2, FGF16, Foxd3*, *Gli3*, *HoxA1*, *Sip1*
FC≤0.25; P-value ≤ 0.05	*Dlx5/6*, *FGFR3*, *Gata2/3*, *Krm1*, *Pax6*, *Rarb*, *RXRG*
FC≤0.25	*Snail2, Vgll2*
12h (PPR NanoString probe set)	
FC≥1.5; P-value ≤ 0.05	*Cxcl14*, *Etv5*, *Foxg1*, *Hesx1*, *Hey2*, *Sall1*
FC≥1.5	*BMP4*, *Dbx2*, *Foxi3*, *Gbx2*, *Hey1*
FC≤0.25; P-value ≤ 0.05	*Axin2*, *Irx3*, *Krm1*, *Lef1*, *Sox9*
FC≤0.25	*Cntnap5*, *Cxxc6l*, *Dlx5/6*, *Gata2*, *Geminin*, *Gpr160, N-Myc*
24h (PPR NanoString probe set)	
FC≥1.5; P-value ≤ 0.05	*Bcl2*, *BMP4*, *Ccnd1*, *Chd7*, *Cited2*, *Cxcl14*, *Etv5*, *Fstl4*, *Pax2*, *Noc*, *Ptpru*, *Setd2*
FC≥1.5	*Dbx2*, *Eya2*, *Foxi3*, *Gbx2*, *Hesx1*, *Hey1/2*, *Homer2*, *Irx2*, *Six1*, *Six3*, *Sox2*, *Tbx1/3, Znf423*
FC≤0.25; P-value ≤ 0.05	*Gata2*, *Irx3*, *Krm1*, *Lef1*, *Pax6*, *Sox10, Zfhx1b*
FC≤0.25	*Axin2*, *Dlx3/5/6*, *Keratin19*, *Lrp11*, *Mef2d*, *Otx2*, *Sox9, Zic1*

(FC: Fold Change)

5.5 FGF signalling is required for expression of otic and epibranchial genes

After having investigated the sufficiency of FGF signalling in OEPD induction the next question to address is whether FGF is also required and, if so, for which transcripts. To answer this again an *in vitro* assay was used, which allows inhibition of FGF signalling in the OEPD specifically, without interfering with the development of other tissues. The prospective OEPD was dissected together with the underlying mesoderm, which is the source of FGF during the early steps of otic induction (Kil et al., 2005, Paxton et al., 2010, Ladher et al., 2005). SU5402 was used to block FGFR signalling and gene expression was compared with DMSO-treated controls. It has previously been reported that *Pax2* expression in the OEPD is dependent on FGF signalling (Abello et al., 2010, Yang et al., 2013) and this was confirmed here after visualising *Pax2* using *in situ* hybridisation (Figure 5.6). Thus, the assay is suitable to determine the requirement of FGF signalling during OEPD induction.

FGF signalling was inhibited for 6, 12 and 24 hours using the drug SU5402 and gene level of expression was compared by NanoString with DMSO control explants. FGF seems to be sufficient to regulate a vast group of OEDP genes however, only a subset of them, does require the signalling to be expressed. The FGF downstream transcription factor *Etv5* is significantly downregulated at all the investigated time points, suggesting it requires sustained FGF to be expressed. The posterior PPR and OEPD genes *Cxcl14*, *Foxi3*, *Gbx2* and the otic gene *Hesx1* have the tendency to be downregulated; however their significance varies over time (Figure 5.7; Table 5.2; see Appendix 9.2). The PPR marker and later otic gene *Eya2* is significantly downregulated after 6 and 24 hours. Additionally, *Homer2* is induced by FGF only after 24 hours of culture and it also depends on FGF at this time point (Figure 5.7; Table 5.2; see Appendix 9.2 Table 9.8). Members of the Sox family appear to require FGF from the mesoderm to be expressed at late time points: *Sox10* is downregulated after 12 hours while *Sox3* at 24 (Figure 5.7; Table 5.2; see Appendix 9.2 Table 9.7 and 9.8). After 24 hours of culture, a large group of genes are downregulated (10 significantly and 30 with a p-value>0.05) (Table 5.2; see Appendix 9.2 Table 9.8); among them: *Sox3*, *Irx1*, *Lmx1b* and *Tbx1* are expressed in the otic placode and it has already been shown that they require FGF signalling *in vivo* (Abello et al., 2010, Yang et al., 2013). *Pax2* is downregulated after SU5402 treatment but does not seem to be highly significant (Table 5.2; see Appendix 9.2).

On the other side, the lens marker *Pax6* appears also to require FGF to be repressed in the pre-placodal ectoderm after 6 hours of treatment. FGF is also necessary for lowering the expression of the non-neuronal markers *Gata2* (12 and 24 hours) and *Keratin19* (24 hours). Furthermore, at early and late time points the WNT target *Axin2* and *Cited2* are upregulated in the absence of FGF (Figure 5.7; Table 5.2; see Appendix 9.2).

The above experiments show that among the earliest responsive genes to FGF are *Foxi3* and *Gbx2*; likewise *Pax2* has previously been reported to be FGF dependent. To test if FGF is similarly required *in vivo*, HH4-5 embryos were cultured with DMSO or 20μM SU5402 for around 10 hours and expression of *Foxi3* and *Gbx2* was assessed by *in situ* hybridisation. As a positive control *Pax2* expression was analysed after culturing HH6 embryos in the presence or absence of SU5402 overnight. Reduction or loss of *Foxi3* expression is observed in 56% of the cases (n=9/16; Figure 5.8 A-C). It has been recently reported that *Foxi3* is mainly regulated by signals from the hypoblast and its expression is not affected by mesoderm ablation (Khatri et al., 2014). It is possible that the variability of the phenotype observed is related to the starting stages since embryos were used not prior to gastrulation. *Gbx2* expression is specifically lost in the posterior PPR in 85% of the cases (n=6/7), whereas it is not affected in the neural plate (Figure 5.8 D-F, d'-f'). As previously reported (Yang et al., 2013, Abello et al., 2010), *Pax2* requires FGF expression *in vivo* and its expression is strongly compromised in the absence of FGF (n=5/6; Figure 5.8 G-I).

In conclusion, only a subgroup of the genes that can be induced by FGF signalling require the pathway to be active in order to be maintained or repressed in the OEPD explants. *Etv5*, *Cxcl14*, *Foxi3*, *Gbx2*, *Pax2* and *Homer2* are induced by FGF but importantly they also require the activity of the signalling to be maintained in the pre-otic ectoderm. On the other side, *Pax6*, *Gata2* and *Axin2* need low level of FGF signalling to be expressed while a high level repress them. Regarding the remaining FGF induced or repressed genes other signalling pathways present in the mesoderm could be cooperating with FGF to modulate their expression.

Table 5.2 Genes up and downregulated after SU5402 treatment

6h (PPR NanoString probe set)	
FC≥1.5; P-value ≤ 0.05	*Axin2*, *Cited2*, *Pax6*
FC≥1.5	*Foxm1*, *Gata2*, *Sox2/3*, *Zic1*
FC≤0.25; P-value ≤ 0.05	*Cxcl14*, *Dlx6*, *Etv5*, *Eya2*, *Foxi3*, *Hesx1*
FC≤0.25	*Eya1*, *Gbx2*, *Hey2*, *Hsf2*, *Irx1*, *Pax2*, *Noc*, *Six3*, *Tbx1/3*
12h (PPR NanoString probe set)	
FC≥1.5; P-value ≤ 0.05	*Erni*, *Gata2*
FC≥1.5	*Keratin19*, *Krm1*, *Six3*, *Zic1*
FC≤0.25; P-value ≤ 0.05	*Etv5*, *Gbx2*, *Sox10*
FC≤0.25	*Cxcl14*, *Dbx2*, *Dlx6*, *Eya2*, *Foxi3*, *Foxm1, Gpr160*, *Hesx1*, *Hey1/2*, *Pax2*, *Noc, Tbx1*
24h (PPR NanoString probe set)	
FC≥1.5; P-value ≤ 0.05	*Cited2*, *Dach1*, *Gata2*, *Keratin19*
FC≥1.5	*Axin2*, *BMP4*, *Cdkn1b*, *Dlx3*, *Erni*, *Hey2*, *Krm1*, *Tbx3*
FC≤0.25; P-value ≤ 0.05	*Etv5*, *Eya2*, *Gbx2*, *Hesx1*, *Homer2*, *Lrp11, Pcna*, *Sox3*, *Tox3*, *Zhx2*
FC≤0.25	*Aatf*, *Cntnap5*, *Dbx2*, *Dlx6*, *Dnajc1*, *Fstl4, Foxi3*, *Foxm1*, *Geminin*, *Gpr160*, *Hsf2*, *Irx1/2, Lmx1b*, N-Myc, *Otx2*, *Pax2/6*, *Pdl14*, *Psip1, Six3*, *Sox2/10*, *Sp4*, *Tbx1*, *Whsc1*, *Zfhx1b, Zic2/3*, *Znf462*

(FC: Fold Change)

5.6 Difference between mesoderm derived FGF and FGF2

In vivo, the head mesoderm is the initial source of the OEPD inducing signal FGF. It is FGF2 that recapitulates this activity *in vitro*, at least partially. Do they both have the same activity or are there any differences? To address this question I compared the level at which key genes are induced in both conditions. The average expression level at each time point was log2 transformed and depicted as a heat map using R gplots tool (heatmap.2 function). A false colour image was generated using a gradient from blue to red representing low to high expression values, respectively (Figure 5.9).

When gene expression level is compared between the four-cell populations it is possible to notice that the trend is generally conserved. In particular when comparing

corresponding samples: the two conditions (the pre-placodal ectoderm without FGF (Cnt) and the SU5402 treatment) where the explants are depleted of FGF signalling and the remaining two (PPR treated with FGF (+FGF2) and control DMSO sample) with active FGF. A closer look, however, reveals that the mesodermal FGF is inducing/maintaining gene expression mildly compared to FGF2. This could be estimated by the colour in the heatmap (Figure 5.9) and more precisely by the level of expression reported in Appendix 9.2. As example could be used *Etv5* that is induced by FGF2 with an average relative value of 0.007, similarly the mesoderm upregulates *Etv5* but only to the level of 0.002 (Figure 5.9; Appendix 9.2). This seems also to be the case for other OEPD genes (*Cxcl14*, *Gbx2*, *Foxi3*, *Eya2*, *Hesx1* and *Pax2*). In particular, *Pax2* is very mildly induced by the mesoderm especially after 24 hours where its level is around 0.001 compared to 0.01 after culturing in the presence of FGF2. Probably related to such low level of *Pax2*, after 24 hours of treatment, the level of *Pax6* seems to be rising up to a relative level of 0.002 (Appendix 9.2).

Inversely, genes like *Axin2*, *Lef1*, *Irx3*, *Gata2* and *Keratin19* are more expressed when the mesoderm is present. This could indicate that even if FGF is contributing to their level of expression (see sections 5.4 and 5.5) additional signals from the mesoderm could be involved in modulating their presence in the pre-otic ectoderm.

The picture that emerges shows quite a complex gene regulation where FGFs seem to play a crucial role but probably other uncharacterised signals from the mesoderm and or signals from the neural tube need to be present in order to fully establish the OEPD fate.

5.7 FGF directly positively regulates *Etv4* and *Etv5* and negatively *Pax6*

The results described above clearly show that the early response to FGF signalling during OEPD induction. However, they do not address which transcripts are direct FGF targets. In the first instance, genes significantly upregulated by FGF signalling after 6 hours are good candidates as direct FGF targets. I therefore investigated if they are regulated by FGF more rapidly. Their expression was analysed by RT-qPCR after 3 hours' culture in the presence or absence of FGF2. The trend of response is very similar to that demonstrated by Nanostring analysis (see above). *Etv4*, *Etv5*, *Cxcl14*, *Gbx2*, *Foxi3* and *Pax2* are significantly induced by FGF already after 3 hours, while *Pax6* and *Cited2*

showed a significant downregulation. In contrast, *SSTR5* expression does not change (Figure 5.10 A).

To exclude the possibility that regulation of the above factors occurs through intermediate players, the same experiment was carried out in the presence of translation inhibitors. 10μM of cycloheximide (CHX) (Palmeirim et al., 1997) was used to block protein synthesis and the expression levels of the same transcripts were evaluated by RT-qPCR. Among the positively regulated genes only *Etv4* and *Etv5* appear to be direct FGF targets (Figure 5.9 B), while *Pax6* seems to be the only direct target negatively regulated (Figure 5.9 B) by FGF.

It is therefore likely that the remaining factors are under the control of direct FGF targets e.g. Etv4. To test this hypotesy a loss-of-function approach was designed: a morpholino (MO) tageting Etv4 was used to knockdown its expression (Barembaum and Bronner-Fraser, 2010) and the expression of *Gbx2* and *Pax2* was evaluated by *in situ* hybridisation. These experiments were performed by our collaborator Meyer Barembaum (Division of Biology, California Institute of Technology, Los Angeles, US). Control and Etv4 MOs were electroporated into opposite sides of HH3-4 embryos for Gbx2 and HH6 for Pax2 analyis. At HH6-7, *Gbx2* expression is abolished on the experimental side, but maintained on the contralateral control side (100% n=7/7; Figure 5.9 C). Likewise, at HH12, *Pax2* expression is reduced in the otic region in the Etv4 MO, but not in the control MO electroporated side (Figure 5.9 D). These results suggest that both Gbx2 and Pax2 are regulated by Etv4, which in turn is downstream of FGF signalling.

In summary, the results described above suggest that during OEPD induction FGF signalling controls a very small set of genes directly including Etv4 and -5, and Pax6. The activation or repression of the remaining FGF targets is likely to be mediated by intermediate factors like Etv4.

5.8 Discussion

In this chapter I have investigated the response of FGF signalling in early otic and epibranchial induction. The data here summarised show that FGF promotes only a small set of genes, and I have identified some of its immediate targets. While FGF clearly promotes OEPD character, FGF inhibition demonstrates FGF requirement for only a

subset of genes. In addition to promoting otic identity, FGF mediates lens repression, the ground state of placode precursors (Bailey et al., 2006). Overall, these results reveal that FGF is dynamically regulating a small cohort of gene expression during OEPD development and disentangle the hierarchy downstream of FGF signalling during otic and epibranchial induction.

5.8.1 The role of FGF in induction of otic and epibranchial fate

The role of FGF signalling in otic and epibranchial specification has been intensively studied as a paradigm for cell fate induction. It is evident from the literature that the FGF pathway plays a crucial role in OEPD formation. As previously described (see sections 1.9.1 and 5.1), inhibition of FGF signalling in zebrafish (Maroon et al., 2002, Leger and Brand, 2002, Liu et al., 2003, Phillips et al., 2001, Solomon et al., 2004), in single and double FGF mice mutants (Alvarez et al., 2003, Ohuchi et al., 2000, Pauley et al., 2003, Wright and Mansour, 2003, Ladher et al., 2005, Urness et al., 2010, Zelarayan et al., 2007, Pirvola et al., 2000) and in chick (Ladher et al., 2005, Abello et al., 2010, Yang et al., 2013) has demonstrated how in its absence the otic placode does not properly form. Additionally, FGF gain of function has showed that only pre-placodal cells respond to FGF signalling and start to be specified as otic and epibranchial (Martin and Groves, 2006). Several otic marker have been linked to FGF signalling and recently, thanks to molecular screens, an increasing set of genes has been correlated to FGF (Urness et al., 2010, Yang et al., 2013). However, all these studies mostly investigated late events, no immediate targets have been identified, and the sequence of events is not clear. Several genes identified by Yang et al. (2013) appear to be under FGF control also in the here presented work. The same factors (*Sprys*, *Etv4/5*, *Gbx2, Pax2* and *Foxg1*) are shown also to be downstream of FGF signalling in the mouse (Urness et al., 2010) and some of them have been associated with inner ear phenotypes (Ohyama et al., 2007, Christophorou et al., 2010, Torres et al., 1996, Hans et al., 2004, Rogers et al., 2011, Burton et al., 2004, Padanad and Riley, 2011, Pauley et al., 2006). Using careful analysis of the temporal response to FGF, I have mapped the genetic hierarchy downstream of FGF signalling (summarised in Figure 5.11). This analysis reveals that only a small set of transcripts is initiated rapidly, many of which are broadly expressed in the OEPD (e. g. *Erv4/5*, *Spry1/2*, *Foxi3*, *Gbx2*, *Pax2*, *Sox13*). Thus, as suggested previously (Ladher et al., 2000, Ladher et al., 2005, Martin and Groves, 2006, for review see Schimmang, 2007, Urness

et al., 2010, Yang et al., 2013) FGF signalling promotes OEPD fate, while transcription factors induced later may represent indirect FGF targets. More extensive work is required to further characterise if, among the newly identified FGF responsive genes (data obtained from otic NanoString probe set), any are direct targets. Additionally, at the present only *Gbx2* and *Pax2* have been linked to the direct target Etv4 (Figure 5.11). A possibility to implement this knowledge is to analyse in larger scale, maybe by using the NanoString platform, the effect of protein synthesis inhibition and the effect of Etv4 knock down and of any other direct target (e.g. Etv5). Another possibility to establish the links between the downstream-FGF targets is to identify their regulatory elements and the possible transcription factor binders (see Chapter 6). Overall, these approaches will implement the hierarchy I have described with this work.

New otic and epibranchial transcripts have only been analysed at the earliest time point of 6 hours. There is no evidence that FGF preferentially promote one cell fate versus the other at this early stage. Later, sustained FGF together, with the absence of WNT, is known to be crucial for the epibranchial segregation from the otic (for review see Ladher et al., 2010, Ohyama et al., 2007). Interestingly, *Kremen 1*, which cooperates with Dkk1 to block WNT (Davidson, 2002, Nakamura et al., 2008, Mao et al., 2002), is repressed by FGF; similarly in zebrafish tailbud FGF has been showed to inhibit transcription of the WNT inhibitors Dkk1 (Stulberg et al., 2012). This could explain the concomitant upregulation of the WNT target *Lef1* in the FGF treated tissue at the early time point of 6 hours. However, *Lef1* is dynamically regulated by FGF, being first up and then, together with *Axin2*, downregulated. Up to date, few points of positive cross talk between FGF and WNT have been described (for review see Pownall and Isaacs, 2010) but there are no relevant studies describing a negative role of FGF signalling on WNT targets. It is possible that long exposure to FGF might mimic the *in vivo* requirement of sustained FGF activity for the epibranchial placode. Further experiments are required to disentangle this aspect. Epibranchial markers and their relation with FGF require to be investigated at later time points. Additionally, systematic manipulation of the WNT signalling could help to further clarify this process.

I have here highlighted the downregulation of *Pax6* and other anterior PPR genes by FGF in the otic context (Figure 5.11). It has already been shown that FGF can inhibit *Pax6* expression both *in vitro* and *in vivo*; when an FGF8 bead is located close to the lens territory *Pax6* is repressed. Additionally, pre-placodal ectodermal explants treated with

FGF8 transiently represses *Pax6* while promoting the olfactory fate (e.g. *Foxg1* and *GnRH*) (Bailey et al., 2006). During otic development FGF plays a similar role, it is repressing anterior PPR fate and I showed that it is directly downregulating *Pax6*. A possibility is that Ap1 binding sites are present in the anterior PPR Pax6 regulatory element, and Ap1 could directly repress *Pax6* upon FGF stimulation by recruiting co-repressors (Mittelstadt and Patel, 2012, Lim et al., 2012). In general, the repression of *Pax6* by FGF could be a mechanism repetitively used in sensory organs development to bypass the lens ground state.

5.8.2 OEPD induction by mesoderm-derived FGF signalling

The paraxial mesoderm underlying the future otic placode has been identified as the main tissue necessary for OEPD induction. In the zebrafish mutants *no tail (ntl)* and *one-eye pinhead (oep)*, which lack cranial mesoderm, induction of early OEPD markers (e.g. *Pax8*) is severely affected (Mendonsa and Riley, 1999). Similarly, in chick ablation of the mesoderm underlying the otic placode prevents *Pax2* expression (Kil et al., 2005). These experiments also showed that otic fate becomes independent of mesodermal signals after the 5-somite stage. This is consistent with the thereafter otic and epibranchial segregation; thus the cranial paraxial mesoderm is required for OEPD formation and provides a strong source of inducing cues.

In recombinant explants, otic induction in competent ectoderm is only observed in the presence of both mesoderm and hindbrain, after around 36 hours' culture (Ladher et al., 2000). Here I show that when posterior PPR and mesoderm are co-cultured for 24 hours OEPD markers are only mildly upregulated when compared to the strength of induction observed after FGF2 treatment. It is important to notice that FGF2 was reported to be the only FGF ligand, among the screened ones, to induce *Pax2* expression in explants (Martin and Groves, 2006). The peculiarity of FGF2 is its ability to activate all the four FGF receptors, possibly meaning that multiple receptors are involved in OEPD induction. It is also possible that the expression of FGF ligands is not maintained in isolated mesoderm and additional signals, e.g. from the underlying endoderm, are required. Indeed, endoderm-derived FGF8 appears to be necessary for mesodermal FGF expression (Ladher et al., 2005).

Alternatively, it is possible that mesoderm-derived FGF signalling (FGF19 in chick, FGF10 in mouse) by itself is not sufficient to induce the full otic programme. In both chick and mouse FGF3 from the hindbrain is a good candidate to cooperate with mesodermal signals (Ladher et al., 2000, Alvarez et al., 2003, Mahmood et al., 1995, McKay et al., 1996, Wright and Mansour, 2003, Kil et al., 2005, Ladher et al., 2005, Paxton et al., 2010). In chick, loss of FGF3 by siRNA at HH8 blocks the transition from otic placode to otic vesicle (Zelarayan et al., 2007, Freter et al., 2008), while FGF3 knockout mice form a smaller otic vesicle compared to wild-type animals (Alvarez et al., 2003, Wright and Mansour, 2003). Double mutants for FGF3/FGF10 (Alvarez et al., 2003, Wright and Mansour, 2003, Zelarayan et al., 2007, Urness et al., 2010) and FGF3/FGF8 (Ladher et al., 2005, Zelarayan et al., 2007) have a severe otic phenotype, corroborating the idea of multiple FGF ligands working together in otic development.

Classical experiments have demonstrated that both the mesoderm (Albaum and Nestler, 1937, Holtfreter, 1933, Raven and Kloos, 1945, Zwilling, 1941, Borghese, 1942, Jacobson, 1963a) and the hindbrain (Woo and Fraser, 1998, Albaum and Nestler, 1937, Gorbunova, 1939, Harrison, 1945, Stone, 1931) have the ability to ectopically induce an otic vesicle when grafted in a competent ectoderm. Additionally, fish mutants with defects in the head mesoderm present only a delay in otic vesicle formation (Mendonsa and Riley, 1999, Gritsman et al., 1999, Zhang et al., 1998). In chick if the mesoderm is ablated between 0-3 somite stage the otic placode does not form (Orts et al., 1971, Kil et al., 2005), while if the same mesoderm is removed after 5-somite stage otic development is not compromised (Kil et al., 2005). Overall, these would suggest that even if the mesoderm is involved in OEPD induction it is not a strong signalling centre and it requires additional sources (e.g. hindbrain) to robustly commit cells towards an otic and epibranchial fate.

5.8.3 FGF signalling regulates only few factors directly during OEPD induction

In the context of otic development the precise molecular mechanism downstream of FGF signalling has not been investigated in great detail. The ERK/MAP kinase branch of the FGF pathway has been associated with otic induction (Yang et al., 2013). FGF stimulation in turn induces ERK phosphorylation that subsequently translocate to the nucleus to drive gene expression. In the nucleus, active ERK phosphorylates several transcriptional regulators (e.g. c-Jun and c-Fos) that lead to rapid induction of immediate

targets. MAP kinases can phosphorylate c-Jun and c-Fos kinase activity (Monje et al., 2003, Leppa et al., 1998), which after phosphorylation can form the heterodimer complex Ap1; this is one of the main mechanisms by which FGF seems to activate gene expression directly.

Beside Ap1, primary targets of FGF signalling are the Ets transcription factors (e.g. Etv4, Etv5, Etv1 etc.) (Sharrocks, 2001) and ATF/CREB proteins (for review see Dailey et al., 2005). In the otic context, I have shown that FGF signalling seems only to activate *Etv4* and *Etv5* directly: their expression is upregulated even in the presence of translation inhibitors suggesting that no intermediate factors are involved. In contrast, other early FGF targets require intermediate protein synthesis to be significantly upregulated in the pre-placodal ectoderm after FGF2 treatment. Etv4 knockdown confirms that *Gbx2* and *Pax2*, two transcripts induced after 6 hours of FGF2 exposure, are indeed downstream of Etv4. To populate the network further, similar epistatic relationships must be investigated in more details (Figure 5.11). In analogy, in other contexts Ets transcription factors are crucial mediators of FGF signalling. An example is the zebrafish work where simultaneous knockdown of Etv4, Etv5 and Etv1 highly resemble the phenotype of FGF mutants (Znosko et al., 2010). A different study in chick shows that Etv4 is the main mediator of FGF signalling in the hindbrain (Weisinger et al., 2010). Thus, it is likely that Ets family members are key mediator of FGF signalling during otic development.

Overall, these considerations point to a model in which signalling input activates only a few factors directly, while a second cohort of genes is indirectly activated downstream of FGF. At present it cannot be excluded that Ap1 cooperates with additional partners to drive otic gene expression successfully. To resolve this issue and to clarify which transcription factors exactly promote otic gene activation downstream of FGF, it is important to identify the regulatory elements that control their expression. Identification of the interacting factors will disentangle the network architecture downstream of FGF.

An important aspect involved in gene expression regulation and modulation is the state of the chromatin: its compaction and presence or absence of histone modification. It is now well established that relaxed chromatin, where histone tails are enriched in acetylation (e.g. H3K27ac) and depleted in methylation (e.g. H3K27me3), is a permissive state that allows transcription to occur. Such chromatin features have never been explored in the context of otic and epibranchial development. It is therefore possible that some extent of

the here-described downstream regulation by FGF may function by modulation of the chromatin state. A recent study associates FGF signalling to mechanisms that regulate chromatin organisation. In chick during neural tube development FGF signalling is high in the stem zone, located caudally in the tail, where it compacts the chromatin of not-transcribed genes (*Pax6* and *Irx3*). In the neural tube, where FGF is absent, the same loci are in a permissive state and therefore genes transcription occurs (Patel et al., 2013). The hypothesis of a role of FGF signalling in chromatin regulation will be further investigated and described in the next chapter.

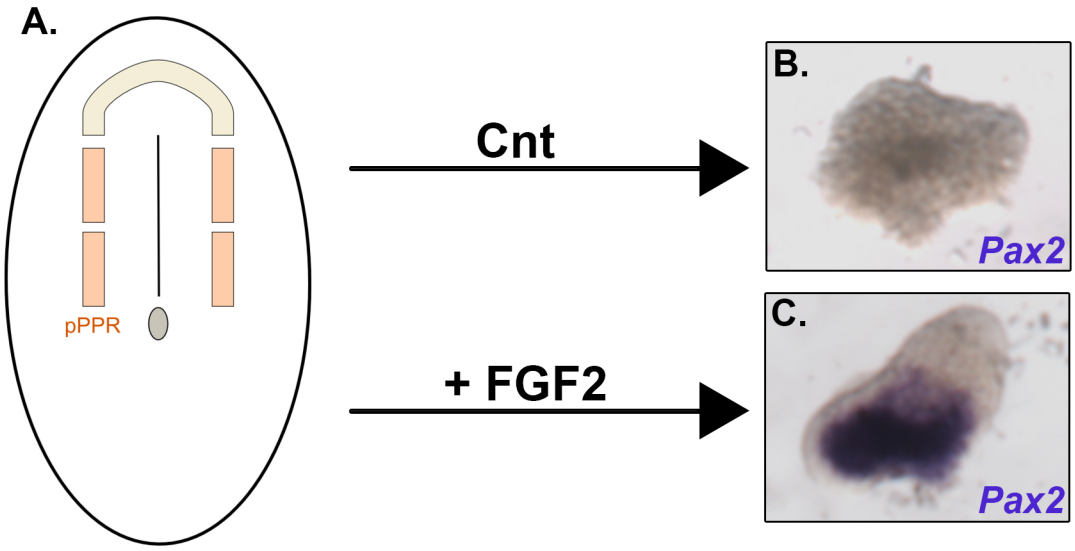

Figure 5.1 Sustained expression of the otic-epibranchial marker *Pax2* in the presence of FGF2.
(A) Schematic of a HH6 chick embryo; the pre-placodal region is highlighted: anterior PPR in yellow and posterior PPR (future trigeminal, epibranchial and otic cells) in orange. **(B)** Dissected pPPR cultured in isolation will not express any *Pax2*. **(C)** Addition of FGF2 to the culture medium leads to *Pax2* regulation already after 6 hours.

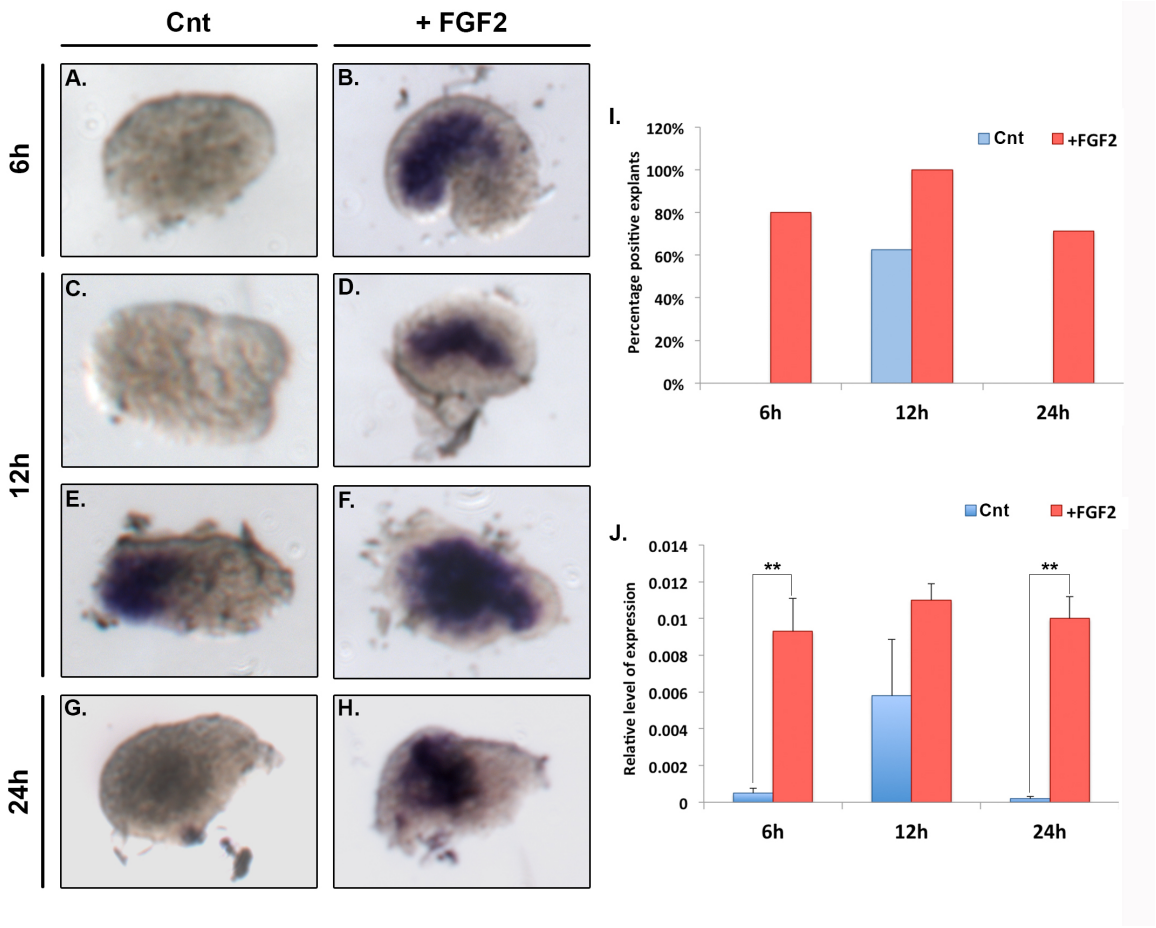

Figure 5.2 Comparison of changes in *Pax2* levels assessed by *in situ* hybridisation and quantified by NanoString.

pPPR was cultured for 6 **(A-B)**, 12 **(C-F)** and 24 hours **(G-H)**. In control explants **(A, C, E, G)**, without FGF2 addition *Pax2* is only present in 60% of explants at the 12 hours time point **(E)**. Addition of FGF2 strongly promotes *Pax2* expression **(B, D, F, H)**. **(I)** Percentage of *Pax2* expressing explants was quantified and plotted in a bar chart; blue: control explants, red: FGF2-treated explants. **(J)** The same experiments were performed in triplicates and assessed by NanoString; the relative level of *Pax2* expression was plotted; blue: control explants, red: FGF2-treated explants. Error bars represent the standard error; statistically significant fold enrichments are labelled with an asterisk: *** p-value≤0.001, ** p-value≤0.01 and * p-value≤0.05.

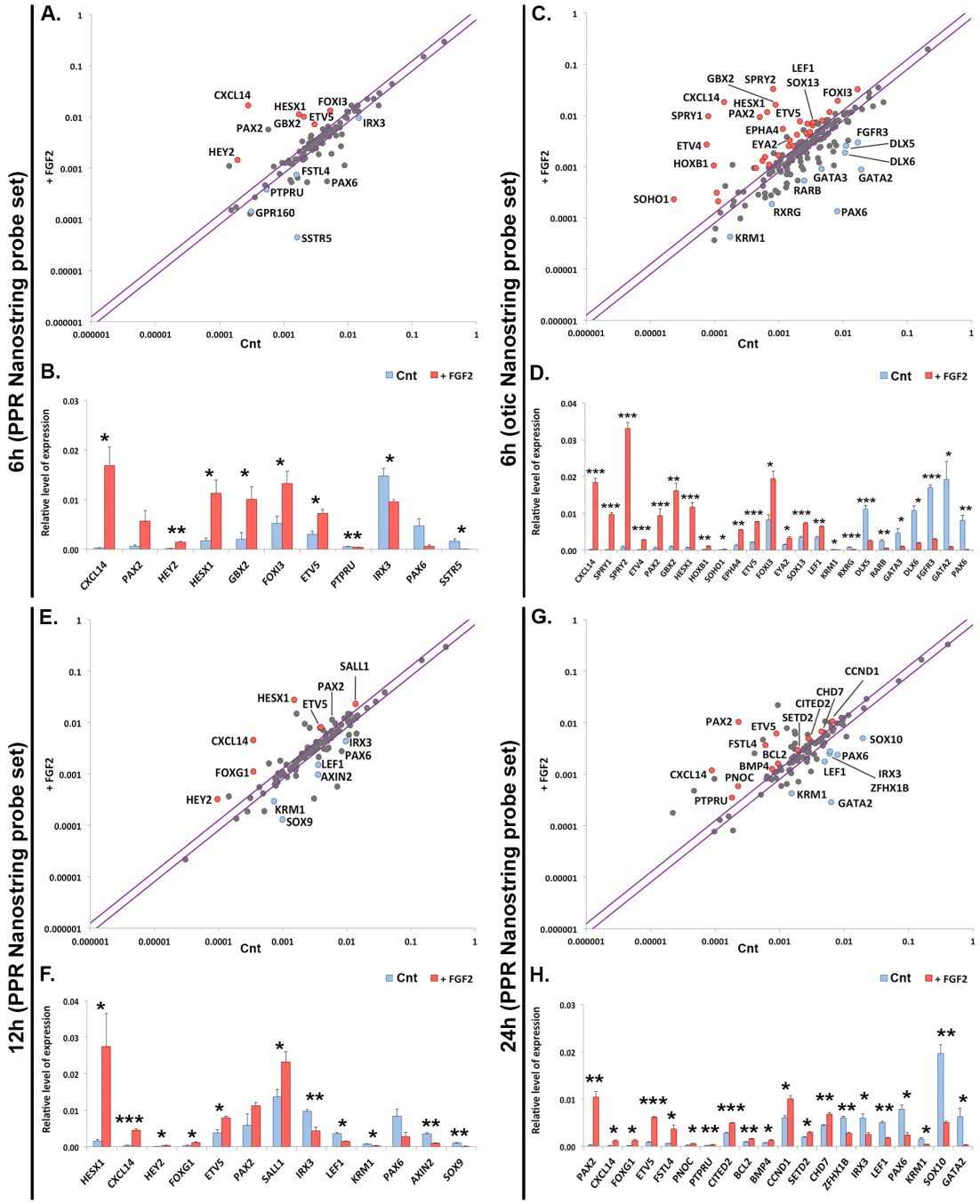

Figure 5.3 FGF2-regulated transcripts in pPPR explants at 6, 12 and 24 hours after treatment.

Figure 5.3 FGF2-regulated transcripts in pPPR explants at 6, 12 and 24 hours after treatment.

(A, C, E, F) The average relative expression level of control (Cnt; x axis) and treated (+FGF2; y axis) samples were log10 transformed and plotted in a diagram. A 1.5 and 0.25-fold change was used as threshold (purple lines); transcripts with less fold-change lie on the diagonal (grey dots). Significantly up- and downregulated genes are shown in red and blue, respectively (p-value<0.05). **(B, D, F)** Bar chart showing only transcripts with significant changes with controls in blue and FGF2-treated in red. **(A-B, C-D)** Comparison of results obtained using the PPR and otic NanoString probe set shows a robust correlation. In a few cases, higher significance is detected in the otic probe set (Appendix B). Error bars represent the standard error. Asterisks (***, ** and *) indicate significant differences (0.001, 0.01 and 0.05, respectively).

Figure 5.4 Expression pattern of some of the new factors early regulated by FGF.

The known FGF target *Etv4* is expressed in the entire OEPD at HH8 **(A)** and is later (HH11) enriched in the epibranchial domain **(B)**. The chemokine ligand *Cxcl14* is present in the posterior PPR at HH6 (pPPR; **C**) and is restricted to the ectoderm surrounding the otic placode at HH11 with a strong enrichment at its posterior tip **(D)**. *Foxi3* is expressed in the entire posterior PPR at HH7 **(E),** but is later progressively lost from the otic domain to remain expressed in the epibranchial and trigeminal placodes **(F)**. *Gbx2* labels the early OEPD at HH7 **(G)** and the medial-posterior edge of the otic placode at HH11 **(H)**. *Sox13* is expressed in all sensory placode progenitors at HH6 **(I)** and is strongly enriched in the otic and epibranchial placode as well as in the neural tube at HH11 **(J)**. **(K-L)** *Pax2*, a well known otic and epibranchial marker, is present in the entire OEPD. In contrast, *Pax6* is initially expressed in the anterior PPR **(M)** and becomes restricted to the lens region **(N)**. *Follistatin like 4* is initially expressed in the anterior PPR and neural plate **(O)** and appears in the otic placode only around the 12-somite stage **(P)**. The G protein-coupled receptor 16 (*Gpr160*) is restricted to the anterior PPR at HH6 **(Q)** and becomes enriched in the neural tube **(R)**. **(S-T)** *Kremen1*, a WNT inhibitor, is strongly expressed in the neural plate and at a lower level in the OEPD at HH6 and HH9. **(U-V)** The WNT target *Lef1* is not expressed in the PPR at HH6, but found at the anterior and posterior tip of the otic vesicle at HH12 **(V)**. **(W-X)** *Gata2* labels the non-neuronal ectoderm at HH6, but is almost absent from the embryo at HH11. Anterior PPR: aPPR; posterior PPR: pPPR; otic-epibranchial progenitor domain: OEPD; lens: L; neural crest: NC; non-neuronal ectoderm: NNE. Note: Fsl4, Gpr160 and Krm1 were firstly identified by Lleras-Forero (2011).

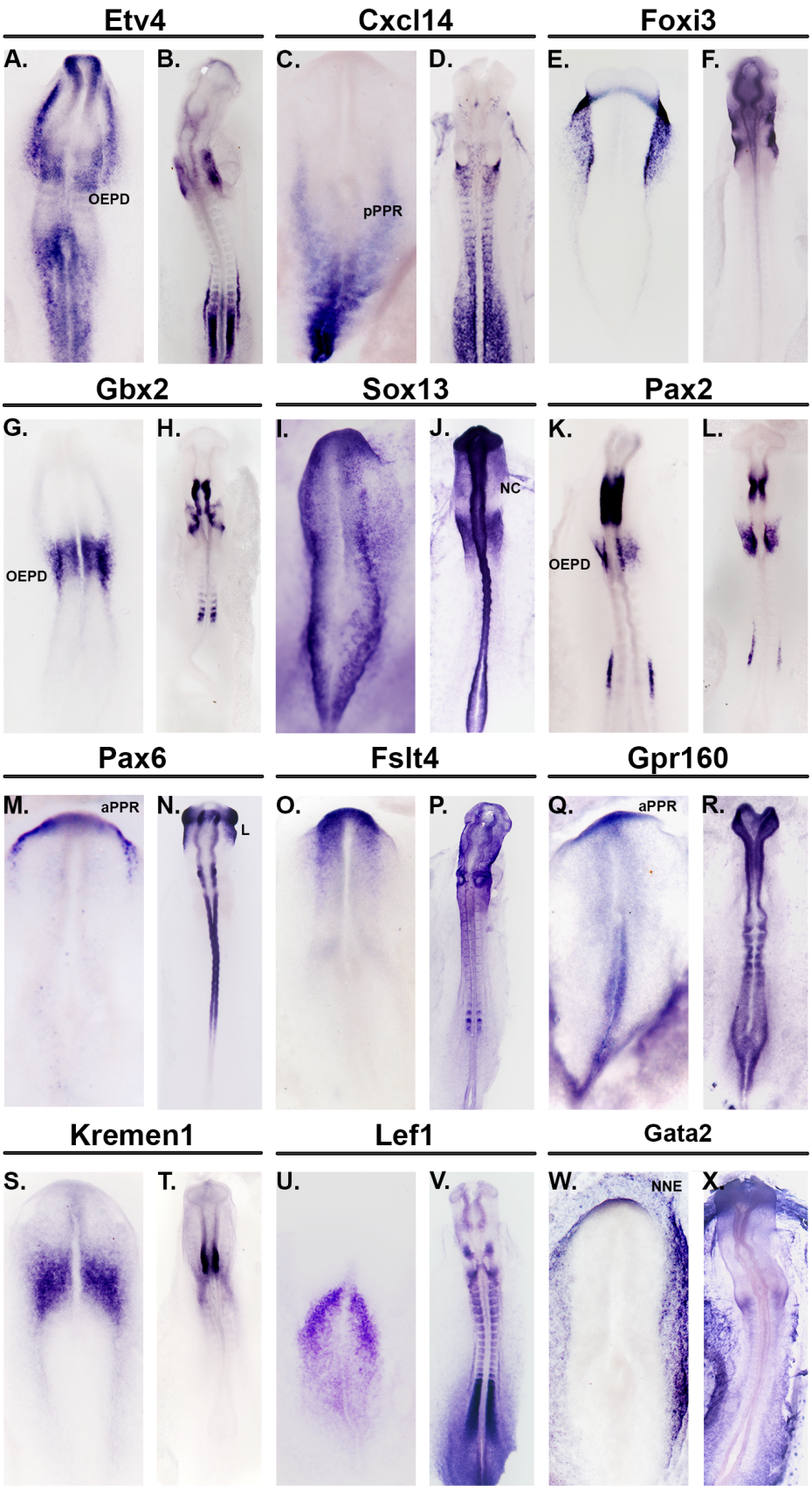

Figure 5.4 Expression pattern of some of the new factors early regulated by FGF.

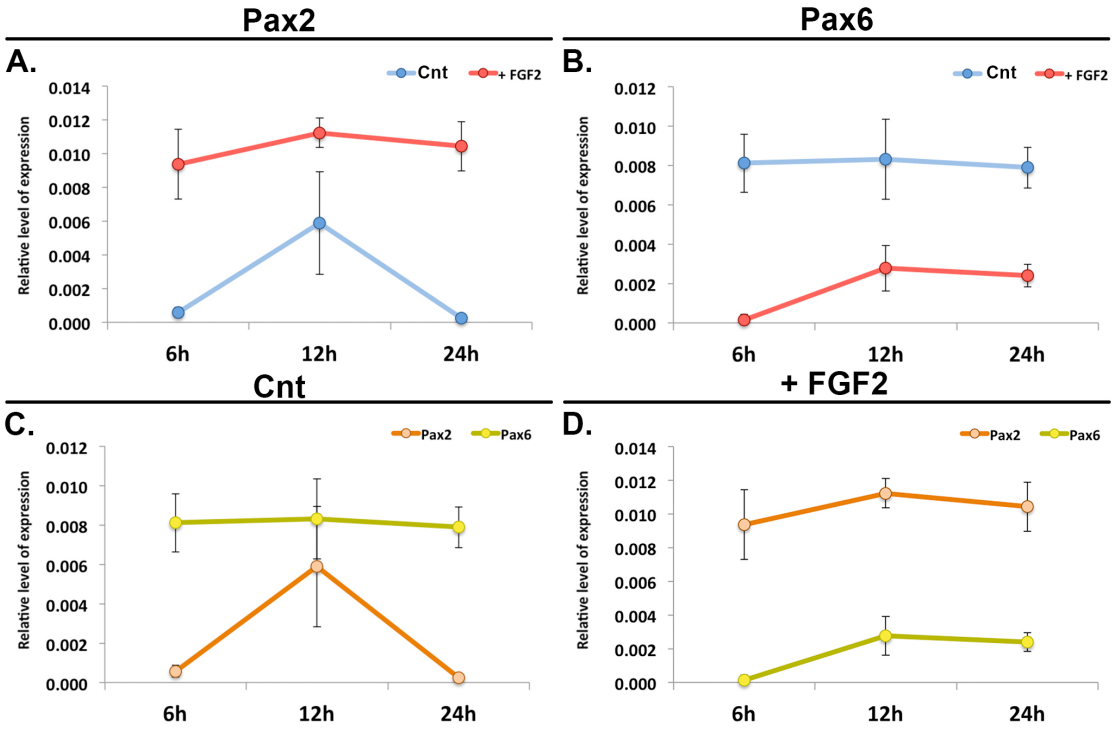

Figure 5.5 FGF treatment promotes *Pax2* expression and strongly reduces *Pax6*. **(A)** *Pax2* is highly expressed in the pre-placodal ectoderm after FGF treatment (red). However, in untreated sample (Cnt) it is not expressed, except for a spike after 12 hours' culture (blue). **(B)** *Pax6* shows the opposite behaviour being expressed at high levels in the absence of FGF2 (blue), but reduced in its presence. **(C-D)** Comparison of *Pax2* (orange) and *Pax6* (yellow) levels reveals the dominance of *Pax6* in the untreated sample **(C)** whereas *Pax2* is expressed at much higher levels after FGF treatment **(D)**.

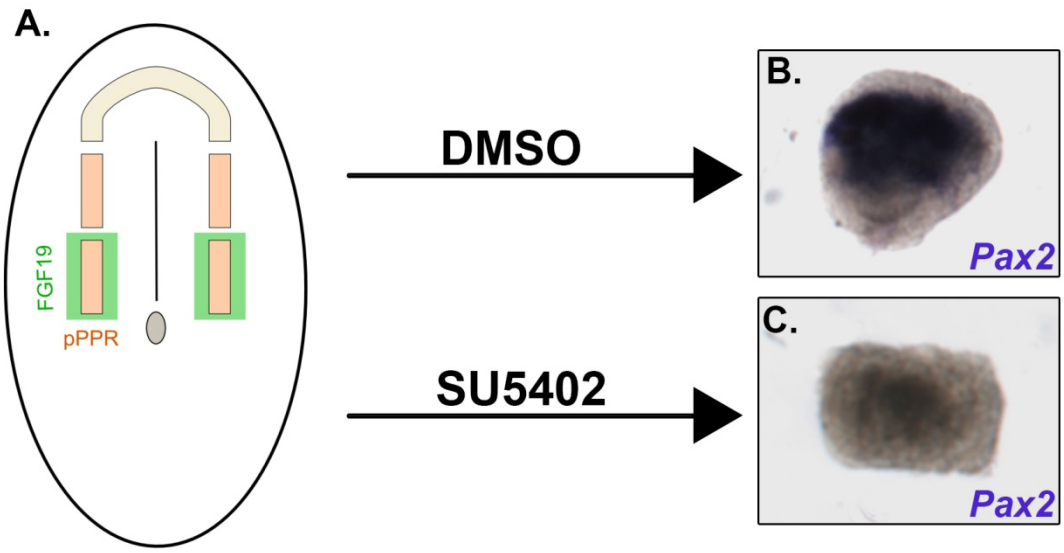

Figure 5.6 Inhibition of FGF signalling from the mesoderm is used as an assay to identify which genes require FGF for their expression.
(A) Schematic of a HH6 embryo where the pre-placodal region is highlighted: anterior PPR in yellow and posterior PPR in orange. The cranial paraxial mesoderm is the source of FGF signalling, mainly FGF19 in chick (green). Dissected pPPR and underlying mesoderm were cultured. **(B)** In the control condition (DMSO) *Pax2* was induced. **(C)** Inhibition of FGF by SU5042 abrogates *Pax2* expression.

Figure 5.7 Identification of the genes that require FGF signalling to be expressed in the OEPD.
(A, C, E) The average of relative level of expression of the control (DMSO; x axis) and treated (SU5402; y axis) samples were log10 transformed and compared. Purple lines represent the fold change threshold of 1.5 and 0.25 used to define changing genes. Molecules with no change in level of expression remain in the diagonal line (grey dots). In blue (upregulated; negatively regulated by FGF) and red (downregulated; positively regulated by FGF) colours are highlighting the significant changing genes (p-value<0.05). **(B, D, F)** Additionally, the significant factors are plotted in a bar chart where the SU5402 is in blue and DMSO in red. Error bar represents the standard error. Asterisks (***, ** and *) indicate significant differences (0.001, 0.01 and 0.05 respectively).

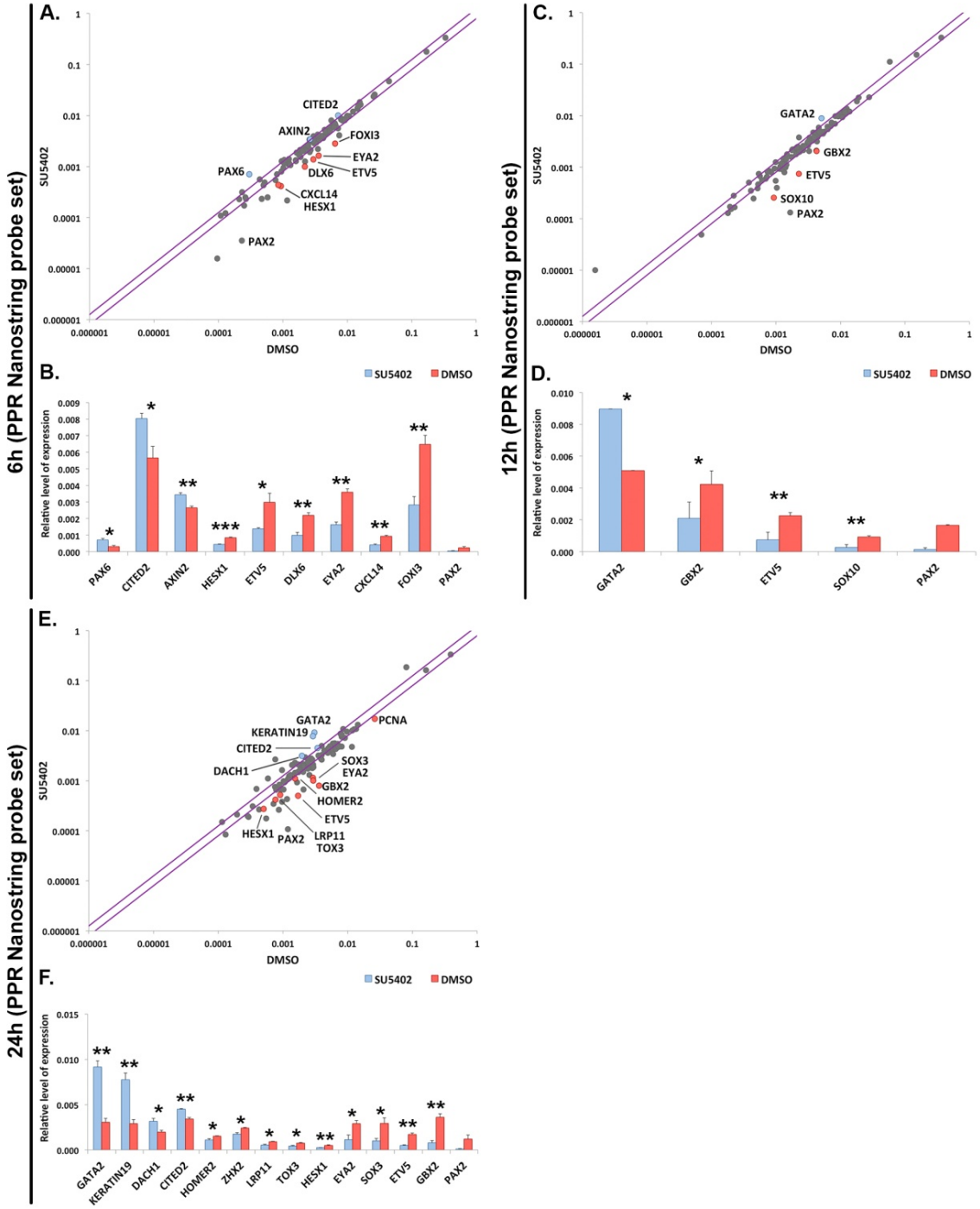

Figure 5.7 Identification of the genes that require FGF signalling to be expressed in the OEPD.

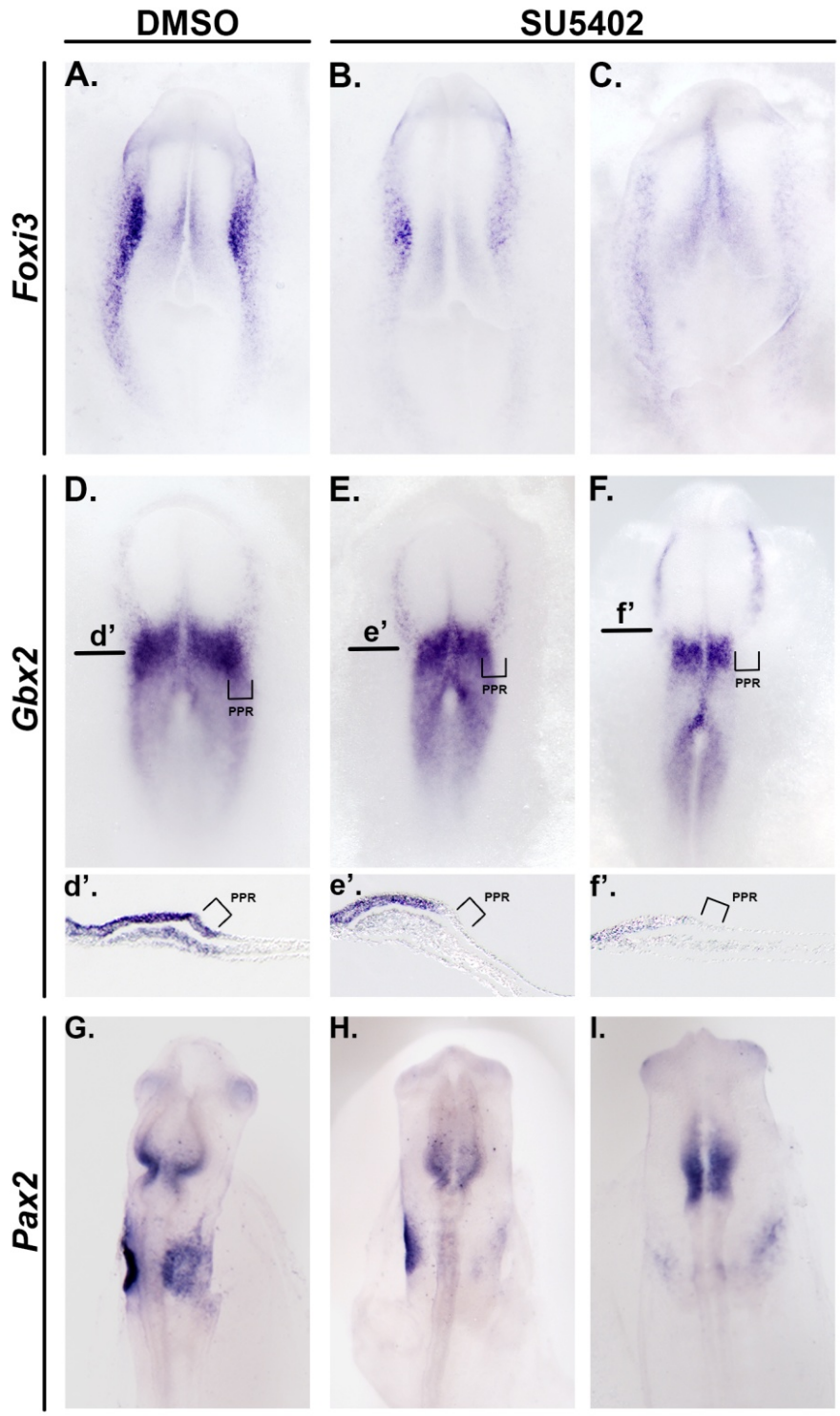

Figure 5.8 *In vivo* requirement of FGF signalling for the expression of *Foxi3*, *Gbx2* and *Pax2*.

(A-C) *Foxi3* in the control condition (**A**; DMSO) is expressed in the posterior PPR. After inhibition of FGF signalling *Foxi3* is reduced **(B)** or almost lost **(C)** in the pre-placodal progenitors in the 56% of the cases (n=9/16). **(D-F)** *Gbx2* is expressed in the neural plate, mesoderm and OEPD **(D, d')**. However, after SU5402 treatment its expression is lost from the PPR **(E, e', F, f')**. **(G)** *Pax2* expression in the otic and epibranchial region is compromised upon FGF inhibition **(H-I)**.

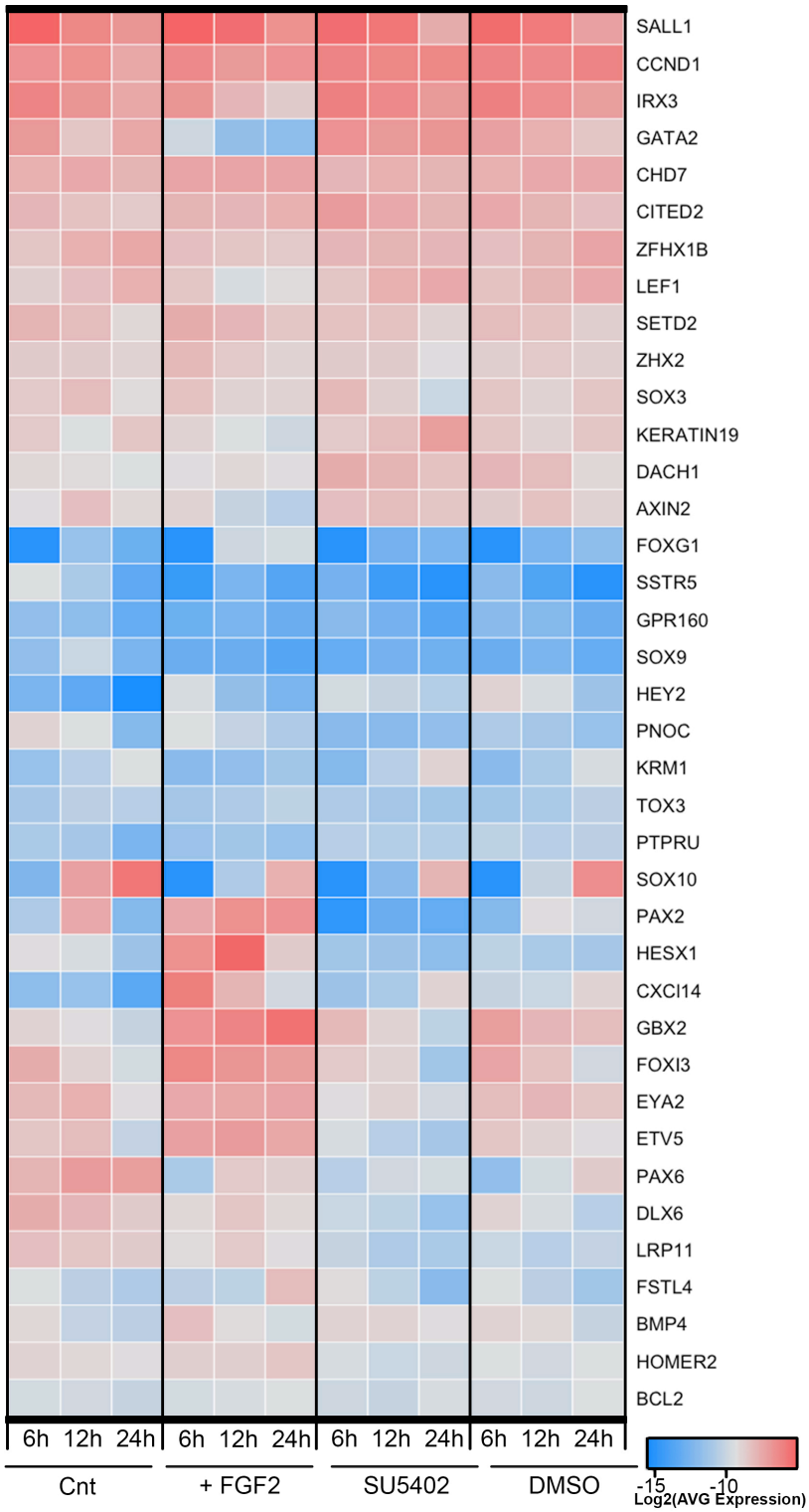

Figure 5.9 Comparative analysis of the induction ability between FGF2 and the mesodermal FGF.

The expression levels of the 38 genes, significantly regulated by FGF at least in one time point, were plotted in a heat map. The average of the expression level of three biological replicates was log2 transformed and visualised using a gradient of blue to red colour. The bottom of the scale (blue) represents low level of expression however a red colour would indicate higher expression. For each manipulation (Cnt, +FGF2, SU5402 and DMSO) the level at three different time points are plotted (6, 12, and 24 hours).

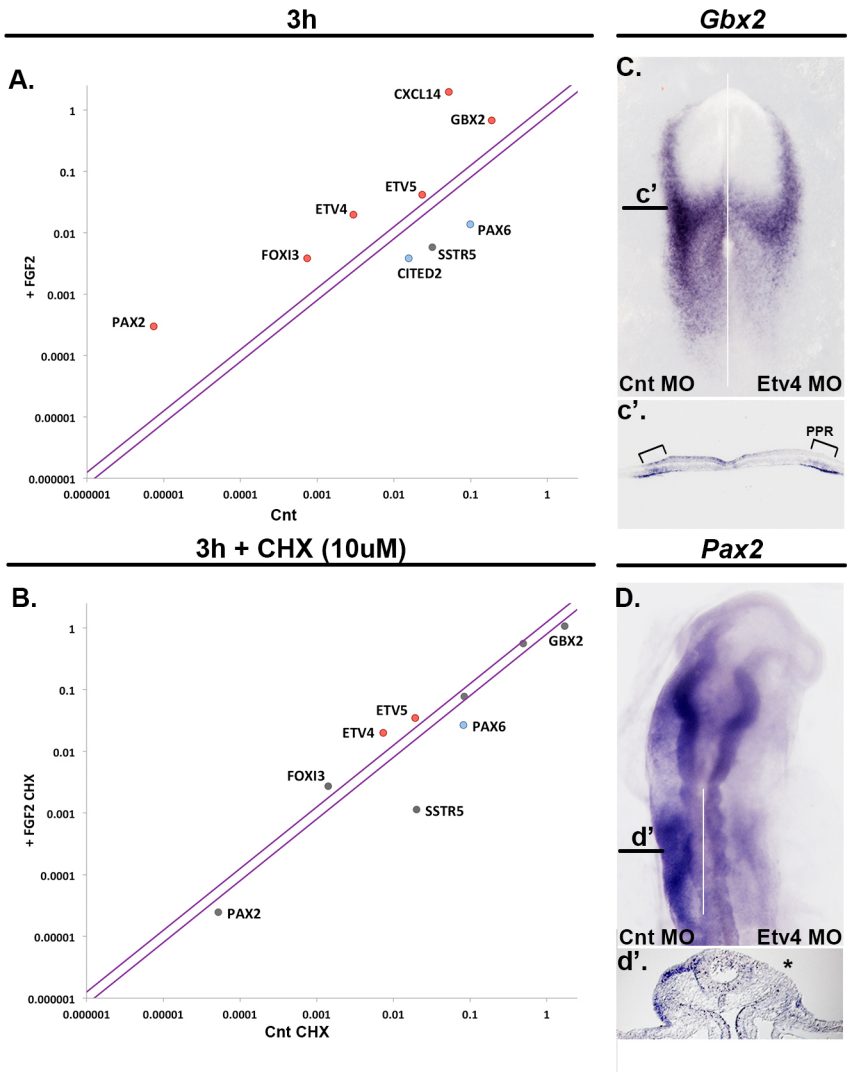

Figure 5.10 Identification of the direct targets downstream of FGF signalling and some of their potential downstream targets.

(A) Gene level of expression in the untreated versus FGF treated samples (3 hours of culture) was quantified by RT-qPCR. Normalised levels of expression were log10 transformed and plotted (Cnt in the x and +FGF and y axis). **(B)** Samples treated with cycloheximide (CHX), with or without FGF, were similarly analysed. Purple lines represent the fold change threshold of 1.5 and 0.25 used to define changing genes. In red and blue are represented significantly up and downregulated genes, respectively (p-value<0.05). **(C, c', D, d')** Embryos were electroporated on the left with control MO and on the right side with Etv4 MO. **(C, c')** *Gbx2* is specifically lost in the PPR in the Etv4 MO side. **(D, d')** Furthermore, knockdown of Etv4 leads to a loss of *Pax2* in the left side.

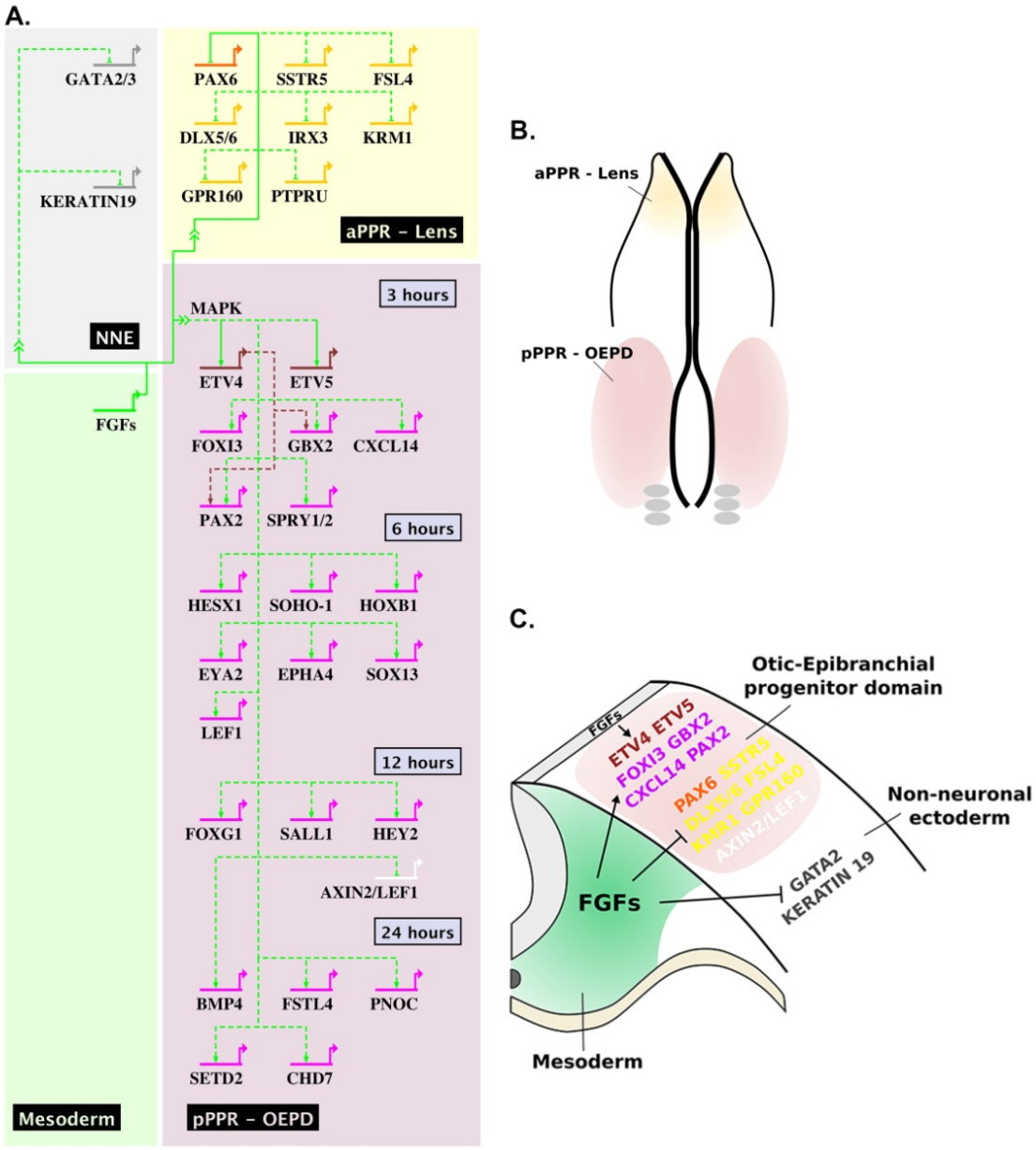

Figure 5.11 Hierarchy downstream of FGF signalling and a model for otic induction. **(A)** Summary of the downstream hierarchy of FGF build from experimental data and drawn using Biotapestry. FGF, mainly from the mesoderm (green region), is positively regulating gene expression in the pPPR – OEPD (pink region) by activation of the MAPK branch of the pathway. However, Axin2 and Lef1 would be repressed by the signalling (white gene). The pPPR – OEPD is divided in sub-regions (3, 6, 12 and 24 hours) to visualise the temporal cascade of gene activation. Solid lines represent the direct upregulation of *Etv4* and *Etv5*. Subsequently Etv4 has been showed to regulate *Gbx2* and *Pax2* (bordeaux dotted lines). Concomitantly FGF is repressing the expression of non-neuronal (grey region) and anterior PPR - Lens genes (yellow region). *Pax6* is directly regulated by FGF and is here showed in orange. **(B)** Schematic of a 3-4 somites embryo head where the lens domain is in yellow and the OEPD in pink. **(C)** Transverse section across the OEPD shows the mesoderm (green) as main source of FGF but some contribution could derive also from the neural tube (light grey). The pink domain represents the OEPD where otic and epibranchial genes are positively regulated (bordeaux and magenta genes) whereas anterior PPR genes and Axin2/Lef1 are inhibited (orange/yellow and white, respectively). Laterally to the OEPD non-neuronal genes are also downregulated.

6. Variation in the chromatin signature upon FGF stimulation reveals OEPD enhancer

6.1 Introduction

The epigenetic state of cells is a crucial aspect in fate decisions that impacts on the level of gene expression. In particular, regulatory elements need to become available for transcription factor binding to control downstream activation or repression of key molecules involved in cell fate determination. It is now clear that specific histone modification correlate with active enhancer regions and that these vary during development, contributing to gene regulation (Asp et al., 2011, Bonn et al., 2012, Buecker and Wysocka, 2012, Ernst et al., 2011, Heintzman et al., 2009, Heintzman et al., 2007, Kharchenko et al., 2011). Specific features have been strongly linked with active enhancers: acetylation of histone 3 lysine-27 (H3K27ac) (Creyghton et al., 2010, Kharchenko et al., 2011, Rada-Iglesias et al., 2012, Rada-Iglesias et al., 2011, Zentner et al., 2011), recruitment of p300 (Visel et al., 2009), low nucleosome density (Boyle et al., 2008) and recently expression of RNA transcripts (eRNA) (Kim et al., 2010, Wang et al., 2011). Additionally, H3K4 mono-methylation (H3K4me1) is associated with both active and poised enhancers although not all active elements necessarily present such marks (Creyghton et al., 2010). In contrast, enhancer inactivation strongly correlates with the deposition of tri-methylation histone-3 lysine-27 (H3K27me3) (Rada-Iglesias et al., 2011, Heintzman et al., 2007, Zentner et al., 2011). The epigenetic state that regulates enhancer and how this correlates with ratio of gene expression is complex, however increasing evidence points to a crucial role of H3K27ac as determinant factor marking active enhancers.

A key question in developmental biology is how cells become progressively committed to their ultimate fate, and instructions from their environment are known to play a crucial role in this process. How such environmental cues (e.g. signalling pathways) act at the transcriptional level has been subject of many studies, however how such signals affect the chromatin landscape has not been explored in depth.

The importance of FGF signalling in otic and epibranchial commitment has been investigated in the previous chapter (see Chapter 5), which dissected the transcriptional cascade downstream of FGF. An intriguing possibility is that the FGF pathway not only

controls gene expression through its transcriptional effectors, but also affects the epigenetic landscape of its target genes by modifying the chromatin state. The main aim of this chapter is to investigate this possibility at the genome-wide level. The epigenetic state of prospective otic and epibranchial cells, cultured in the presence or absence of the FGF2 ligand, was profiled by ChIP for histone modifications followed by sequencing (ChIP-seq). Finally, to gain insight into the regulation of FGF response genes their putative enhancers were identified, tested for *in vivo* activity and their molecular regulation was determined. Overall, this work highlights a dynamic scenario where FGF signalling seems to affect deposition of H3K27ac marks around some of its response genes and thus influences the activation of specific enhancers.

Part of this work was performed in collaboration with Ramya Ranganathan (validation of ChIP antibody), Dr Jingchen Chen (validation of ChIP antibody and performance of ss5-6 ChIP-seq) and Maryam Anwar, who performed most of the ChIP-seq bioinformatics analysis.

6.2 Validation of ChIP for histone modifications as a tool to uncover the chromatin state

The aim of this chapter is to analyse changes in the chromatin state in posterior PPR cells after FGF stimulation, by comparing FGF2 treated and corresponding untreated samples. The first step was to reproduce the nano-ChIP protocol reliably (Adli and Bernstein, 2011) and to verify the specificity of each antibody (anti-H3K4me1, anti-H3K27ac and anti-H3K27me3) (see section 2.16). Neural tube of HH10-12 chick embryos was chosen as tissue for this validation since several active enhancers have been described and can serve as positive controls (Figure 6.1 A SOX2_N2 and SOX2_N4; Uchikawa et al., 2003). In addition, a Spalt4 otic enhancer (Figure 6.1 A; Barembaum and Bronner-Fraser, 2010) should be inactive or poised in neural tube cells. Promoters of the neural gene Sox2 and non-neuronal gene Gata2 were also analysed.

Sonicated neural tube chromatin (Figure 6.1 B), with a high percentage of fragments between 600 and 200bp, was processed for immuno-precipitation (IP) using antibodies against H3K4me1 (generally enriched at enhancer level), H3K27ac (flanking active enhancers) and H3K27me3 (deposited around poised/inactive enhancers) (Figure 6.1 C).

Unfortunately, the H3K4me3 antibody (marker of active promoter) did not work in my hands and is therefore not presented here.

After IP with the above antibodies the chromatin was analysed by qPCR using primers for active and inactive enhancers as well as promoters to test the ability of antibodies to pull down specific chromatin regions (Figure 6.1 D). The %IP was calculated in order to analyse the percentage of pull down of each antibody at a given location. In this method, the qPCR signals derived from the ChIP samples are divided by the qPCR values obtained from the input sample, an aliquot of the sonicated chromatin, and adjusted to account for input dilution (Haring et al., 2007; see section 2.13.4). The comparison of a positive versus a negative region would determine if the pull-down is significant and not just background. It is expected that anti-H3K27ac precipitates enhancers, while anti-H3K27me3 precipitates inactive regions and anti-H3K4me1 is a general enhancer mark able to pull down active and poised regions. With an average of 2.9% input the anti-H3K4me1 antibody shows a low pull down efficiency, but nonetheless appears to be enriched at the level of active enhancers. Anti-H3K27ac antibody shows an average pull down of 10.89% input, being strongly enriched at the level of Sox2 promoter (Figure 6.1 D SOX2_P) and at its active regulatory elements (Figure 6.1 D SOX2_N2 and SOX2_N4). With an average pull down of 7.76% input anti-H3K27me3 presents an opposite behaviour, which shows enrichment around repressed regions (Figure 6.1 D SPALT4_E and GATA2_P). Analysis of each domain reveals that the active enhancer SOX2_N4 shows relatively more H3K27ac than H3K27me3, whereas the inactive element SPALT4_E shows equal levels of both marks. Thus, the distribution of histone marks observed after ChIP is overall in agreement with the enhancer activity described *in vivo*.

Since the starting material for ChIP is extremely limited, the nano-ChIP protocol described by Adli and Bernstein (2011) includes a step of linear amplification in order to obtain sufficient DNA for deep sequencing. Therefore a second step of validation was used to verify that the amplification step does not introduce any major bias into the profiles. Any drastic variation would affect the interpretation of the final data giving low reliability to the assay. Generally, the H3K27ac mark is enriched at the level of active regions (Figure 6.1 E SOX2_P, SOX2_N2 and SOX2_N4) however H3K27me3 is present in the negative regions (Figure 6.1 E GATA2_P and SPALT4_E). In such negative regions the situation is not straightforward because H3K27ac and H3K27me3

are both present and generally H3K27ac is slightly more abundant. However the presence of both marks will be interpreted as repressive state. Similar analysis will be the base of the genome wide bioinformatics strategy that will be used.

Thus histone-modification antibodies were validated and hence used to investigate the chromatin landscape upon FGF treatment.

6.3 Performance of nano-ChIP-seq for histone modifications to analyse the chromatin landscape after FGF stimulation

A challenging question is whether FGF signalling influences gene expression by affecting the chromatin landscape of some of its key targets. Furthermore, to gain insight into the gene network downstream of FGF it is crucial to identify the regulatory elements for some downstream targets. Therefore, having validated the nano-ChIP protocol I proceeded to investigate the distribution of histone marks (H3K4me1, H3K27ac and H3K27me3) in posterior pre-placodal ectoderm cultured for 6 hours in the absence or presence of FGF2.

The amplified ChIPed DNA was then used for library preparation and sent for 100bp paired end sequencing. The quality of each sample was assessed by various methods. The sonication profile and concentration was evaluated using Aligent Bioanalyser for pre- and post-amplified samples as well as after library preparation (see Appendix 9.3). Sequencing quality was examined using FastQC (version 0.10.01); the summary of these quality controls is reported in Appendix 9.3. FastQC provides a quality control report, which can identify issues that had originated during the sequencing or during the step of library preparation. Various parameters are analysed by the FastQC software, for example: pre base sequence quality gives an overview of the quality range values across all bases at each position, per base sequence content analysis the proportion of each base in the sequences, per base N content plots the percentage of uncalled bases (N) across the whole sequence and overrepresented sequences analyse if a single sequence is overrepresented in the set, giving an indication of possible library contamination (Andrews, 2010). Since the amplification steps of the nano-ChIP-seq protocol can produce high mismatch at the first 9 bases, they were trimmed as suggested by Adli and Bernstein (2011); a few more base pairs were removed as required, if sequence quality was poor (see Appendix 9.3). Trimmed sequences were aligned to the latest version of the

chick genome (galGal4 November 2011). DNA sequencing library complexity is defined as the amount of uniquely aligned DNA molecules and it varies depending on the genome size and type of peak (broad-peak for histone modification requires deeper sequencing compared to transcription factors sharp-peak); more than 10 million uniquely aligned reads were obtained for all the samples in the experiment (accurate counts are reported in Appendix 9.3) which was sufficient for peak calling. Overall the quality of the ChIP-seq data is in line with the standard reported in the literature (for review see Furey, 2012) and therefore the data were used for downstream analysis.

Uniquely aligned sequences were used for peak calling using the software Homer (Heinz et al., 2010). The software package identifies genomic regions where the sequence distribution (also called ChIP-seq tags) is greater than expected by chance. 'Putative' peaks are then compared to the Input tag distribution. Four parameters were used to identify statistically significant peaks: 1) fold enrichment over Input ≥1.5; 2) False Discovery Rate (FDR) ≤0.01; 3) since histone peaks cover broad regions a minimum size of the peaks was set to 750bp; 4) a minimal distance of 300bp was used to identify separate peaks. After having identified peaks for each histone modification, enhancers were predicted considering: 1) regions lacking histone marks; 2) such regions should be flanked by two H3K27ac peaks and 3) they should be deprived of H3K27me3 peak. Finally, the retrieved putative enhancers were annotated to the nearest gene. For more details on the ChIP-seq data analysis see section 2.13.6.

In order to gain insight on the distribution of the histone modification, the average tag distribution of H3K4me1, H3K27ac and H3K27me3 was plotted cantered to the transcription-start site (TSS) of the nearest gene (Figure 6.2). Among the histone modifications, H3K4me3 is highly enriched around the transcription start site, whereas H3K4me1 is present downstream towards the gene body (Figure 6.2; orange line). Additionally, H3K27ac is associated with actively transcribed genes and it is present at the TSS (Figure 6.2; green line) while repressed/poised genes present H3K27me3 (Figure 6.2; grey line) (for review see Kimura, 2013). Thus, the histone mark distribution obtained from the control and +FGF2 ChIP-seq is in line with the literature.

Below, I will present a more careful analysis of the epigenetic state at specific loci.

6.4 Dynamic distribution of H3K27ac upon FGF2 treatment

Analysis of histone mark distribution upon FGF stimulation reveals an interesting behaviour. In particular, acetylation of H3K27 is highly dynamic and seems to respond to FGF treatment.

H3K27ac peaks in control and FGF2 treated samples were annotated to the nearest gene for a total of 13,637 genes associated to at least one H3K27ac peak. To assess if after FGF stimulation there is any variation in the distribution of H3K27ac the number of H3K27ac peaks associated to the control and +FGF sample were compared by calculating the difference between the two. Genes presenting a variation of 2 or more peaks were further analysed. After FGF treatment 1,278 genes present an increase in H3K27ac whereas only half (652) show a decrease in acetylation. To understand the biological function of these two gene sets, their functional annotation was performed using the online tool DAVID 6.7 (Huang da et al., 2009b). In particular gene ontology for biological processes, molecular functions and signalling pathways enrichment analysis was performed. This reveals that genes showing increased acetylation after FGF treatment are significantly correlated with terms related to sensory organ and otic/inner ear development (Figure 6.3 A), and to protein kinase and MAPK pathways, as well as cytokine signalling. This correlates well with the experimental paradigm of FGF treatment, and with the result that the cytokine Cxcl14 is strongly upregulated in the presence of FGF elsewhere (see Chapter 5) and changes its epigenetic marks (see below). In contrast, genes associated with less acetylation upon FGF exposure only correlate to general biological terms (Figure 6.3 B) and TGFβ and WNT signalling. While in both groups the molecular function of genes is related to DNA binding and transcriptional regulation. This analysis provides good confidence in the results obtained.

Transcriptional gene regulation downstream of FGF has been discussed in the previous chapter (see Chapter 5), which identified up and down-regulated transcripts. The question arises whether the same genes show a relative change in their level of acetylation. Such genes were therefore analysed further, the difference between the numbers of H3K27ac peaks in +FGF versus –FGF was plotted (Figure 6.3 C). In general, a good correlation is observed between up-regulated gene and an increase of H3K27ac levels, and vice versa (Figure 6.3 C red and blue dots). However, a large group of factors were found to have un-relevant variation in acetylation levels between the two conditions (Figure 6.3 C grey

dots). After 6 hours of FGF treatment, it appears that Pax genes (Pax2 and Pax6) do not present any major variation in H3K27ac distribution even if they are differentially expressed across sample. This would suggest that only a subset of FGF-responding genes might be subject to epigenetic changes.

To better illustrate acetylation changes a few example gene loci are shown in Figure 6.4. Spry1 and -2 are very strongly upregulated by FGF and are known to be immediate FGF-response genes (Ozaki et al., 2001b, Chambers and Mason, 2000, Minowada et al., 1999). They are the two genes with the greatest changes in acetylation genome wide. Around the Spry1 transcription start site (TSS) 38 H3K27ac peaks are found in +FGF sample compared to just 3 in the control. Similarly, Spry2 shows 28 peaks exclusively found in the treated tissue (Figure 6.4 A-B). The chemokine Cxcl14 shows a smaller increase and only 4 additional H3K27ac peaks are found close to the TSS (Figure 6.4 C-D). Foxi3 shows a similar profile with an additional 5 peaks detected upon FGF treatment (Figure 6.4 E). Dlx5/6 show the opposite behaviour, the level of acetylation upon FGF stimulation is decreased (quantified as 4 peaks; Figure 6.4 F). Furthermore, Gata2/3, Fstl4 and Axin2 are among the transcriptionally downregulated genes presenting a decrease in H3K27ac (Figure 6.3 B). By analysing the other histone marks distribution it was noticed that they vary slightly, but are far less striking than H3K27ac.

In conclusion, upon 6 hours of FGF stimulation variation in gene expression level was observed (see Chapter 5), and concomitant with this a subgroup of genes also present variation in the acetylation of lysine-27 on histone-3. The difference in H3K27ac correlates well with changes in the transcriptional activation or repression of the majority of these genes. However, whether this difference in acetylation is a cause or a consequence of change in gene level has not been addressed.

6.5 Genome wide identification of regions with enhancer features

The next step was to identify regions with the epigenetic features of regulatory elements, specifically enhancers. Enhancers are crucial for fine-tuning gene expression and their function is critical during embryonic development. It is now clear that specific epigenetic features mark active enhancers (see section 6.1). H3K4me1 is a pioneer modification placed in a genomic window where subsequently markers of active enhancer (i.e. H3K27ac) will be deposited (Creyghton et al., 2010, Rada-Iglesias et al., 2011, Wamstad

et al., 2012). However, presence of H3K27me3 has been associated with repressed enhancer states (for review see: Calo and Wysocka, 2013, Maston et al., 2012). With this in mind, the ChIP-seq data were examined to identify regions characterised by such marks.

The focus was mainly given to regions flanked by two peaks of H3K27ac and depleted of H3K27me3. As an example, the genomic region 5' of the Foxi3 TSS presents features of a putative enhancer. Interestingly this element is exclusively identified after FGF treatment (Figure 6.5 A; this element will be discussed in section 6.7). To obtain a general idea of how histone marks are scattered around putative enhancer elements their distribution was plotted centred on the middle of such domains. Overall all three marks investigated show a bimodal distribution (Figure 6.5 B) in line with what reported in the literature (Kimura, 2013).

The putative enhancer regions were annotated to the nearest TSS; at this point distal enhancers were not considered. The total number of putative enhancer elements was counted; both samples share a total of 808 enhancers, among them an element associated with Pax6. However, they present a high number of unique elements: 2,451 genomic regions are uniquely identified in control tissue (e.g. Gata2 and 3), while 2,883 are only present in FGF-treated posterior PPR cells (e.g. Spry1 and 2, Cxcl14 and Foxi3).

To assess whether enhancer-association, in the presence or absence of FGF treatment, reflects gene expression levels of the same genes in the normal posterior PPR and OEPD (obtained from mRNA-seq), correlation between both was determined using the Wilcoxon test. Both control and treated samples correlate well with pPPR gene expression levels, with a p-value= $7.55e^{-12}$ and p-value= $4.5e^{-11}$, respectively. When considering the full set of enhancer both correlate to the OEPD transcriptome data set with a p-value of 0.01, while when unique control enhancers are considered the p-value drops to 0.25 and for the +FGF to 0.15. It would appear that common enhancers between the two samples are contributing to improve the correlation. Overall, after FGF treatment it seems that regions with enhancer feature are changing and less high expressed pPPR genes are associated to an enhancer but after only 6 hours of treatment the chromatin state does not fully recapitulate the transcriptional profile of an endogenous otic-epibranchial domain.

To further gain insight the potential function of the genes associated with putative enhancers functional annotation was carried out using DAVID 6.7 as describe above. The biological function related to inner ear development is significantly correlated only to genes with FGF responding elements, whereas terms related to general sensory organ formation and eye development are associated to both ChIP-seq data sets. There is a high overlap between the terms associated to the distribution of H3K27ac (Figure 6.3 A, B) and the ones related to putative enhancers. Again, the MAPK pathway is exclusively associated to the +FGF ChIP-seq (Figure 6.5 D, E) suggesting a good correlation with the biology of the experiment.

Overall, the identification of putative regulatory elements points to a complex picture where the genomic landscape is dynamically modified by FGF signalling. FGF may mark genomic regions as enhancers to allow transcription.

6.6 *In vivo* activity of putative enhancer regions

The presence of the histone mark H3K27ac is a good indication of a transcriptionally active chromatin region (for review see: Calo and Wysocka, 2013, Kimura, 2013, Maston et al., 2012). However, to identify enhancers reliably H3K27ac is usually combined with other features (e.g. p300 DNA binding and enhancer RNAs). In the chick p300 antibodies do not perform well in nano-ChIP experiments (Tatjana Sauka-Spengler, personal communication). Additionally *in vivo* test is required to clearly identify the active elements.

In chick it is possible to rapidly examine potential enhancer activity by electroporation. The candidate regions were cloned from chick genome and inserted into a plasmid containing the putative enhancer upstream of a minimal promoter and a GFP cassette (ptk-Citrine). In order to check the quality of the electroporation, a plasmid where a constitutive active promoter drives RFP (pCAB RFP) was co-electroporated. If a putative element is active *in vivo*, it will cooperate with the minimal promoter and allow transcription of GFP/Citrine, hence green fluorescence will be detected when and where the enhancer is active. With this in mind, the ectoderm of chick embryos were electroporated at early gastrula stage (HH3+/4) and enhancer activity analysed the next day at early somitogenesis (HH6 onwards); alternatively the embryos were electroporated at HH6-7 and monitored several times in the following day. Since I was interested in

identifying otic enhancers, embryos with a wide ectodermal and OEPD electroporation (red fluorescence) were analysed and green fluorescence was checked in the prospective otic region as well as other sensory placodes.

Genes expressed at OEPD stage and/or responsive to FGF (Spry1, Spry2, Cxcl14, Foxi3, Hesx1, Sox13, Gata3 and Pax6) were used for an initial screen where *in vivo* enhancer activity was tested. Their putative enhancers identified from control and + FGF ChIP-seq were compared to the endogenous putative enhancers identified from a ChIP-seq performed at 5- 6-somite stage (Dr Jingchen Chen). Additionally, conservation across species using classical alignment method and putative transcription factors binding sites were taken into account. In total 12 elements were selected for validation and their features are summarised in Table 6.1. The sequence flanked by two H3K27ac peaks was selected and cloned into the ptk-Citrine reporter vector and successively tested by *in vivo* electroporation. Reporter activity was analysed at various stages mainly focusing between HH8 to HH12.

Of the putative enhancers tested only few show reporter activity *in vivo* (Figure 6.6 and Figure 6.7). Cxcl14 E1 seems to be a weak enhancer, active mainly at the edge of the neural tube at HH9-10; additionally, a few cells close to the otic placode appear to be GFP positive at later stages (Figure 6.6 D-F). Two Foxi3 associated elements show temporally and spatially distinct activity and will be discussed in the next section 6.7. The remaining putative elements are not functional *in vivo* at the stages tested (few selected examples in Figure 6.6).

Thus, the initial *in vivo* validation reveals that only around 25% of the genomic regions flanked by H3K27ac peaks and depleted of H3K27me3 seem to be active in the otic territory at the tested stages. Several possibilities need to be taken into account for future validations: the initially selected domain could be too small especially where several putative enhancers are located close one to an other, it is also possible that the time window analysed needs to be extended, and weak activity might be difficult to detect etc. These considerations will be taken into account for further validations.

Table 6.1 Summary of selected putative enhancers form Cnt and +FGF ChIP-seq

Spry1	
E1 (Chr4: 52750797-52752350)	+FGF ChIP-seq; Relevant TFBS: Ap1, Gata3, Sall1, Sox2/3
E2 (Chr4: 52760097-52761083)	+FGF ChIP-seq; Relevant TFBS: Irx2/4/5, Lmx1a/b, Sall1, Six1, Sox8/13, Tead1
E3 (Chr4: 52764665-52765503)	+FGF and ss5-6 ChIP-seq; Relevant TFBS: CREB, Gata3, Six1, Sox2
Spry2	
E2 (Chr1: 151929286-151931013)	+FGF ChIP-seq; cross-species conservation; Relevant TFBS: Ap1, HoxA, Irx2/4/5, Lmx1a/b, Nr2f2, Six4, Sox2/13, CREB
E4 (Chr1: 152018235-152019860)	+FGF ChIP-seq; Relevant TFBS: Ap1, Gata3, HoxA, Lmx1a/b, Pax2, Sall1, Six4, Sox3/5/8/13
Cxcl14	
E1 (Chr13: 14642163- 14643893)	+FGF and ss5-6 ChIP-seq; Relevant TFBS: Ap1, HoxA, Lmx1a/b, Pax2, Six1/4, Sall1, Sox2/5/8/13
Sox13	
E2 (Chr26: 1632057-1633251)	+FGF and ss5-6 ChIP-seq; cross-species conservation; Relevant TFBS: Ap1, Sox3/5/8/13
Hesx1	
E1 (Chr12: 8580923-8582319)	+FGF ChIP-seq; Relevant TFBS: Ap1, Etv4/5, Gata3, Sox2/3/5/8/13
Pax6	
E1 (Chr5: 5247319-5249078)	Cnt and +FGF ChIP-seq; cross-species conservation; Relevant TFBS: Dlx5, Gata3, Lmx1a/b, Nfkb1, Nr2f2, Sall1, Six1/4, Sox5
Gata3	
E5 (Chr1: 4596414-4597191)	Cnt ChIP-seq; Relevant TFBS: Gata3, Irx2/4/5, Lmx1a/b, Sall1, Six1, Sox2/3/5/8/13

6.7 The complexity of *Foxi3* expression is recapitulated by two spatially and temporal distinct enhancers

While ChIP-seq is a useful way to identify putative enhancer regions, ultimately their activity must be tested *in vivo*. ChIP-seq identified two active elements in proximity of the Foxi3 transcription-start site (TSS) and their differential activity was analysed further.

Foxi3 transcript is enriched in the posterior part of the PPR (HH6-7; Figure 5.4), and is later present in the trigeminal-otic-epibranchial region to become restricted to the epibranchial and trigeminal placodes only (HH12; Figure 5.4). Later, *Foxi3* will be mainly expressed in the pharyngeal arches (Khatri and Groves, 2013). When histone mark distribution is analysed around the Foxi3 TSS three discrete regions (E0, E1, E2; Figure 6.7 red elements) can be identified as putative enhancers. In addition, in the endogenous OEPD (ss5-6) the same domains have enhancer characteristics (ChIP-seq experiment carried out by Dr Jingchen Chen; Figure 6.7 magenta elements). The ChIP-seq data were complemented by analysis of cross-species conservation (predictions carried out by Maryam Anwar); this reveals the presence of conserved elements at the level of E1 and E2 (Figure 6.7 black elements). Therefore, these two putative enhancers were selected for further investigation, cloned into a reporter vector (ptk-Citrine) and assessed for *in vivo* activity. Initially a larger region identified by the OEPD ChIP-seq was used for these experiments. The ectoderm of early gastrula (HH3+/4) and neurula (HH6-7) stage embryos were electroporated, with the control RFP plasmid and the reporter Citrine vector containing the putative enhancer element, and fluorescent was assessed the following day.

The first element (Foxi3 E1; Chr4:85593696-85597534) located downstream of the Foxi3 TSS (Figure 6.7) shows reporter activity from early somitogenesis stages (HH7; Figure 6.8 D) and remains active in the OEPD up to HH9 (Figure 6.8 E-F). Thereafter, its activity decreases progressively to be completely lost around HH12 (Figure 6.8 G-H). To determine which portion of the 3.8kb fragment is minimally required it was divided in half; both sequences lost completely activity (Figure 6.8 B E1.A and E1.B) pointing to the presence of a crucial domain in its centre. Therefore a 2kb region in the centre of the original piece was sub-cloned, and it reported activity similar to the original E1 (Figure 6.8 B E1.C). Similarly, further reduction of the enhancer size maintains its activity (Figure 6.8 B E1.D and E1.E). At this point, the shortest sequence tested is 600bp long

(E1.E) and contains the vast majority of transcription factor binding sites. Binding site analysis, using RSAT tool (performed by Maryam Anwar), revealed the presence of Sall1, Tead1, Otx2, Dmbx1/Otx3, Pax2, SoxD (Sox5, Sox6 and Sox13) and SoxE (Sox8, Sox9 and Sox10) motives (Figure 6.9). These transcription factors are therefore good candidates to regulate the spatial and temporal activity of Foxi3 E1. Furthermore, two Ap1 binding sites are present one at the 5' end of E1.C and one at the 3' of the original piece E1, linking this element to FGF signalling. However, removal of the Ap1 binding site does not diminish reporter activity since the 610bp element (E1.E) has a similar activity to the full length E1.

A second putative enhancer element (Foxi3 E2) was identified based on the ChIP-seq data from OEPD stages that lies upstream to the Foxi3 TSS (Figure 6.7). A large domain of 3.7kb (Chr4:85610429-85613878) was initially cloned into a reporter vector. Around the centre of the large element 300bp were found to be conserved across-species, this piece was extended of 100bp at each extremity for a total of 511bp (E2.CNS Figure 6.10 B) and sub-cloned. Additionally, a sequence of 982bp at the 5' of Foxi3 E2 was tested (E2.A Figure 6.10 B). The full element Foxi3 E2, as well as the conserved domain (E2.CNS), showed *in vivo* activity while E2.A was not functional (Figure 6.10 B). This second Foxi3 enhancer shows a strong activity in the trigeminal placode from HH9 (Figure 6.10 C-E), while earlier in development is not functional. Later, it will also recapitulate the *Foxi3* expression in the pharyngeal streams and similar to the late Foxi3 expression it is not active in the otic (Figure 6.10 F) (Khatri and Groves, 2013). The conserved element was scanned by RSAT tool (performed by Maryam Anwar) for transcription factors binding sites using a customised library containing PPR, otic and other sensory placodes transcription factors (see section 2.15). Several putative binding sites were identified: Rxra, Cited2, Tcf4, Nr2f2, Otx2 and two Six1 (Figure 6.11) Relevant to sensory organ development two Six1 binding sites were found and additionally the transcriptional repressor Tcf4, only expressed in the otic placode (Figure 4.5), could be important to prevent *Foxi3* expansion in the otic domain. Mutagenesis and functional experiments will be performed to validate these hypotheses.

ChIP–seq from endogenous OEPD (ss5-6) and +FGF2 treated posterior PPR helped to identify two Foxi3 enhancers. They present enhancer features only upon FGF stimulation and they are functional *in vivo*. These two elements are spatially and temporally distinct and they are able to recapitulate *Foxi3* expression pattern. At the present predictions of

putative binding sites highlighted several transcription factors that could directly regulate Foxi3 (Figure 6.9, Figure 6.11 and Figure 6.12), however further experiments are required to validate these hypothesis.

6.8 Discussion

In this chapter I have described a first attempt to investigate the role of FGF signalling in modulating the epigenetic state of otic and epibranchial cells during development. Histone modification marking transcriptional active and repressed chromatin was analysed on a genome wide level. Particular attention was given to the dynamics of H3K27ac, which correlates well with gene expression levels in the OEPD. Strikingly, acetylation around the TSS of FGF up-regulated genes is significantly enriched within only 6 hours of FGF exposure. Recently, dynamic changes in H3K27ac have been analysed upon VEGFA treatment and 1 hour of stimulation appears to be sufficient for changes in acetylation (Zhang et al., 2013). Additionally, the distribution of histone marks was interrogated to predict the position of putative enhancer regions, and few of such regulatory elements were tested *in vivo*. Two spatially and temporally distinct Foxi3 enhancers, unique to the +FGF condition, were identified and their upstream regulation is currently under investigation. Overall, after FGF stimulation some chromatin changes appear, however if they are a cause or consequence of gene expression remain to be address.

6.9 Dynamic H3K27ac signature correlates with the transcriptional response to FGF

The role of signalling cues in the regulation of the epigenetic state of cells has not been explored in depth. Here, otic and epibranchial induction was used as a paradigm to study how signalling can influence cell fate by altering the chromatin modification.

After FGF stimulation otic and epibranchial genes become strongly upregulated, while anterior pre-placodal and non-neural genes decrease in expression levels (see Chapter 5). This poses the question of whether such variation correlates with changes in the chromatin landscape. This point was exploited by preforming ChIP-seq for histone modifications (H3K4me1, H3K27ac and H3K27me3). Upon FGF treatment of posterior PPR cells, dynamic variation in H3K27ac deposition was noticed in the vicinity of FGF-responsive genes (e.g. Spry1, Spry2, BMP4, Cxcl14, Foxi3, Hesx1; see Chapter 5; Figure

6.3). Similarly, in a recent study highly dynamic H3K27ac was associated to VEGFA signalling during endothelial development (Zhang et al., 2013). The authors showed that one hour of induction is sufficient to increase H3K27ac level at specific loci and that this is associated to increased gene expression. They also show that the dynamic of H3K27ac is associated with p300, which is functionally required for the deposition of this marks, and impacts on regulation of gene expression by VEGFA (Zhang et al., 2013).

The histone acetyltransferase, which acetylates lysine-27 of histone 3, is p300/CREB (for review see Holmqvist and Mannervik, 2013, Karamouzis et al., 2007). Its enzymatic activity can be modulated by post-translational modifications and, in particular, phosphorylation strongly influences CREB function. Phosphorylation of CREB Ser-133 by MAP kinase stimulates CREB activity (Ait-Si-Ali et al., 1999). Zhang and colleagues recently demonstrated that inhibition of p300/CREB leads to a drastic loss of the dynamic deposition of H3K27ac upon VEGFA treatment (Zhang et al., 2013). In addition, phosphorylated c-Jun and c-Fos can interact with CREB and enhance its function (Chen et al., 2004). The Ap1 complex (composed of c-Jun and c-Fos) is among the transcription factors (TFs) responsible for recruiting p300/CREB to specific DNA regions and c-Jun seems to be required for CREB recruitment in response to VEGFA. Interestingly, VEGFA signalling does not affect nucleosome deposition, but exclusively the acetylation mark (Zhang et al., 2013).

Overall, it is likely that activation of the FGF pathway plays a similar role in the process of otic induction. It is conceivable a scenario where in pre-placodal cells the chromatin is accessible (nucleosome free regions) at specific genomic locations; only cells in the posterior PPR will be sensing FGF signalling that downstream would enhance p300/CREB activity. PPR and early OEPD transcription factors would be recruiting the enzyme to specific location allowing deposition of the acetylation mark hence boosting gene transcription. Overall, such mechanism could explain the process of dynamic deposition of H3K27ac and would point to a putative role of p300/CREB in otic development. At the present *in vivo* proofs are missing to corroborate this hypothesis.

6.10 Exploiting histone mark distribution to identify enhancers active *in vivo*

The present work is one of the first attempts to analyse histone mark distribution in chick cells using a genome wide approach. In the past decade enhancers have been extensively

identified on a genome wide scale by different features: the putative element is usually flanked by H3K27ac and nucleosome free, p300 is found bound to the enhancer, and short RNAs are transcribed at the level of the enhancer (eRNAs) (for review see: Calo and Wysocka, 2013, Kimura, 2013, Maston et al., 2012). Anti-histone modification antibodies routinely used in mammalian species have never been used systematically in chick and several difficulties were encountered during their validation. Unfortunately, a ChIP quality p300 antibody has not yet been identified (Dr. T. Sauka-Spengler, personal communication), which would simplify enhancer discovery considerably. Therefore the limitation of the system influences the quality of genome wide analysis. Even though the increase in H3K27ac marks correlates well with an increase in gene expression upon FGF treatment, the identification of enhancers that are active *in vivo* still has room for improvement. In fact, only 25% of putative enhancers identified by ChIP-seq using the current bioinformatics pipeline are active in the embryo at the tested stages.

Several possibilities could improve the identification of *in vivo* active enhancers. Experimental identification of nucleosome free regions correlated with the presence of histone marks will help to decrease the number of false positive. Optimisation of H3K4me1 mark discovery and its co-occurrence with H3K27ac will also improve enhancer retrieval. Additionally, the nano-ChIP-seq protocol introduces a step of linear amplification that can introduce some bias in the data. In particular over amplification of the input could affect the identification of significant peaks and therefore affect the analysis.

Another feature of regulatory elements is that they are often highly conserved across the animal kingdom. At this point conservation has not been explored for all ChIP-seq identified putative enhancers; however in the future prediction of such conserved regions using classical alignment (ECR Browser) and nonalignment-based tools (EDGI/DReive) (Sosinsky et al., 2007) will be performed for all FGF responsive genes. This has been very successful for example for Foxi3; initially enhancers were predicted by Maryam Anwar using both methods and these were later associated to ChIP-seq data. The combination of both approaches allowed the discovery of two active elements. In addition, prediction of CTCF binding sites (Khan et al., 2013) as putative insulator regions may help to identify the boundaries for the position of putative enhancers with respect to the gene of interest, and therefore help associating transcripts with their putative enhancers.

Improving ChIP-seq analysis mainly by adding downstream bioinformatics prediction will potentially help to increase the percentage of *in vivo* functional enhancers. This will be an important data source to be interrogated for further studies inner ear development.

6.11 Dissection of Foxi3 regulation

While investigating FGF responsive enhancers two spatially and temporally distinct Foxi3 regulatory elements where identified and their upstream regulation was studied.

Foxi3 transcript is present broadly in the PPR (HH5-6) and then it becomes restricted to the otic and epibranchial domain, until 8- 9-somite stage when it is downregulated from this domain and becomes expressed in the trigeminal placode. Later, *Foxi3* is expressed in the ectoderm and endoderm of the pharyngeal arches (Khatri and Groves, 2013). The expression pattern of Foxi3 correlates well with the activity of the two enhancers here identified. The first element (Foxi3 E1) is first detected around the 2- 3-somite stage (HH7-8) in the OEPD and decreases progressively to be switched off at HH11-12. While the second sequence (Foxi3 E2) is active from 8- 9-somite stage in the trigeminal placode and it remains active later in the pharyngeal arches (Figure 6.8 and Figure 6.10).

Activity of the first element (Foxi3 E1) is first detected in the OEPD and it is later switched-off. Transcription factor binding site analysis of the 610bp element, sufficient to drive reporter expression, reveals sites for several factors. Members of the Sox gene family (in particular Sox8 and Sox13) may control Foxi3 E1 activity. *Sox8* is early expressed in the posterior PPR and remains expressed in the OEPD (Barembaum and Bronner-Fraser, 2010; Mark Hintze unpublished). Similarly, *Sox13* was recently identified as a new OEPD factor (Figure 4.5) but is expressed early in the PPR (Figure 5.4). Given their early presence in pre-placodal cells Sox8 and Sox13 could be good candidates for Foxi3 E1 regulation. Additionally, Pax2 binding sites were identified. However, since Foxi3 E1 and Foxi3 transcripts are active prior to *Pax2* expression it is unlikely that Pax2 plays a crucial role in Foxi3 initiation, but rather in its maintenance in the OEPD. Further experiments, including gene knockdowns, will be necessary to firmly link these TFs with Foxi3 E1 activity. Tead1, a factor associated to the Hippo pathway, also is a hypothetical regulator of Foxi3 E1. Its expression profile has not been investigated in chick, although significant levels of *Tead1* transcript are identified by mRNA-seq (in the posterior PPR tissue and otic placode). In future, *Tead1* expression

will need to be analysed further by *in situ* hybridisation. The presence of a binding site for the transcriptional repressors Otx2/Otx3 could be important for preventing enhancer activity in the anterior PPR. *Otx2* is expressed in the anterior PPR (Bally-Cuif et al., 1995, Steventon et al., 2012) and it is important for PPR regionalisation, forming a boundary with Gbx2 (Steventon et al., 2012), while *Otx3* expression has not been characterised but it is probably similar to Otx2. Thus, Otx factors could be repressing *Foxi3* in the anterior PPR via its early enhancer. Remarkably, Foxi3 E1 contains two binding sites for the transcriptional repressor Sall1 (Figure 6.9), which starts to be expressed in the OEPD at the time when Foxi3 E1 is switched off (Sweetman et al., 2005). Sall1 repressor activity is associated with recruitment of histone deacetylases (HDACs) to specific genomic loci (Kiefer et al., 2002). Hence Sall1 may mediate the removal of active marks like H3K27ac and shut down Foxi3 E1 activity. Furthermore, *Sall1* expression in the anterior PPR (Hintze, unpublished) may prevent ectopic activation of Foxi3 anteriorly. Lastly, two Ap1 motives are present one at the 5' and one 3' end of Foxi3 E1; Ap1, as described above, has been implicated in the recruitment of p300/CREB to specific genomic location, which in turn, leads to deposition of active marks like H3K27ac. Although Ap1 binding sites are not required for Foxi3 E1 activity it is possible that endogenously, in the context of chromatin in cells poised to adopt otic/epibranchial fate, Ap1 is functionally important. A summary of the hypothesised Foxi3 E1 regulation is summarised in Figure 6.12.

The second regulatory element for Foxi3 (Foxi3 E2) active *in vivo* is predominantly activated in the trigeminal placode. TF binding site analysis for Foxi3 E2 CNS (511bp) reveals few possible upstream regulators and among them Six1 appears to be the main candidate, presenting two binding sites. Mis-expression of *Six1/Eya2* is sufficient for ectopic *Foxi3* expression (Khatri et al., 2014); it remains to be explored whether this is also true for activation of Foxi3 E2. Additionally, a motif for Cited2 is present which is a factor able to bind and transactivate Cbp/p300 (Yahata, 2000, Bhattacharya et al., 1999). Even if Cited2 has been mainly been associated with heart development, Cited2 knockout mice present defects in cranial ganglia (Bamforth et al., 2001). In chick, Cited2 is broadly expressed in the ectoderm and mesendoderm during gastrulation and neurulation, during somitogenesis it appears to be expressed in the head ectoderm but this needs to be further investigated (Schlange et al., 2000). Therefore it is possible that Cited2 helps in the recruitment of p300 to Foxi3 E2, which could acetylate the enhancer and hence promote is activation. FGF signalling appears to be important for marking this enhancer as an

active element, this seems in contradiction with the absence of otic activity for Foxi3 E2.CNS. The presence of a binding site for the otic transcriptional repressor Tcf4 (Figure 4.5) could explain this apparent ambiguity and Tcf4 could inhibit *Foxi3* in the otic domain. The possible regulation of Foxi3 E2 has been summarised in Figure 6.12.

In order to validate these putative interactions transcription factor binding sites will be ablated from the enhancer sequence and enhancer activity will be addressed thereafter. If a binding site is functionally important the hypothesis is that the enhancer activity would be affected: the fluorescent signal will decrease or increase in case of a positive or a negative link, respectively. Additionally, loss- and gain-of-function of the putative direct regulators can be performed, and enhancer activity as well *Foxi3* expression can be assessed. Overall, the combination of these experiments will establish which of the putative interactions summarised in Figure 6.12 are functionally important.

This first attempt to dissect the molecular regulation of an FGF responsive gene can be considered as a pioneer work that will be extended in the future to any newly identified enhancers. The combination of these types of studies will help in building a high-resolution network for otic and epibranchial cell fate decisions.

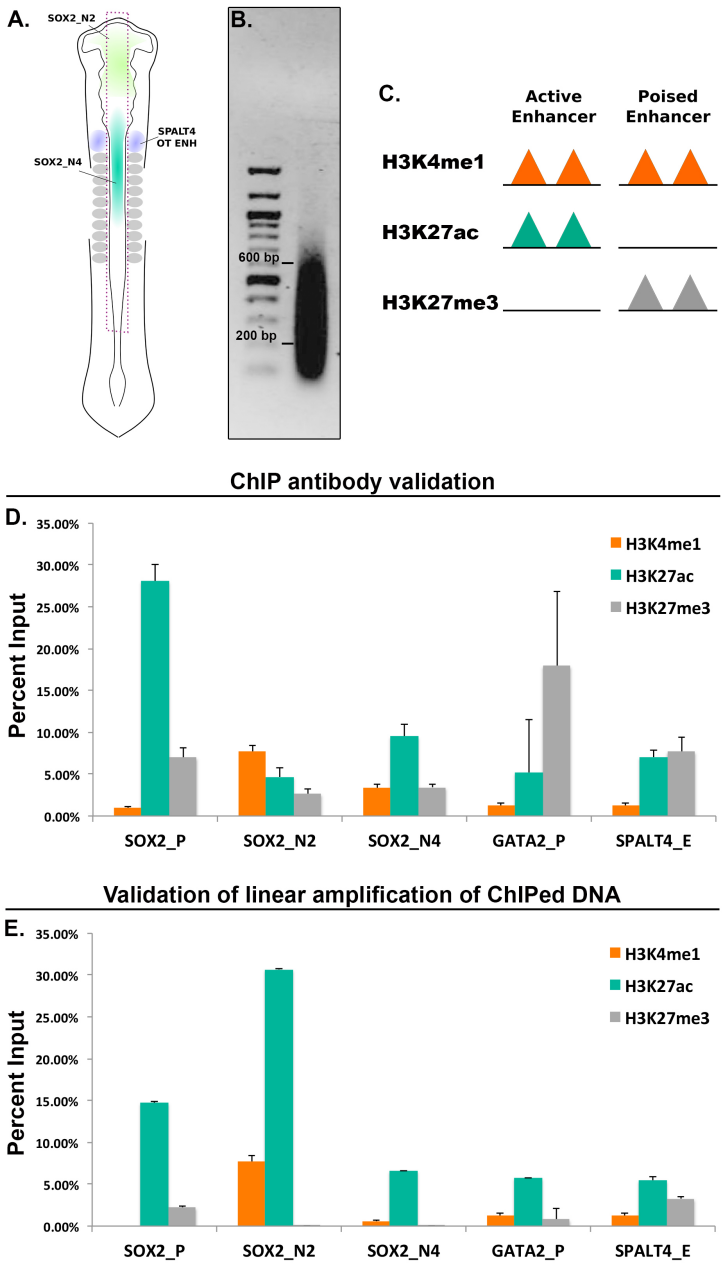

Figure 6.1 Validation of anti-H3K4me1, anti-H3K27ac and anti-H3K27me3 antibodies and the nano-ChIP protocol by ChIP-qPCR.

(A) Schematic of a HH11 chick embryo: the neural tube was dissected (purple dotted line) and processed for ChIP of histone modifications. SOX2_N2 (light green) and SOX2_N4 (dark green) are active in the neural tube (Uchikawa et al., 2003). SPALT4 OT ENH (violet) is active in the otic placode, but not in the neural tube (Barembaum and Bronner-Fraser, 2010). **(B)** Example of a sonication profile: the majority of DNA fragments lie between 200 and 600bp. Note the absence of any genomic DNA or large genomic fragments. DNA appears slightly over-sonicated (fragments <200bp), but at an acceptable level. **(C)** Summary of the marks present at the level of active and poised enhancers. H3K4me1 (orange) is present in both enhancer states. Usually, H3K27ac (green) is predominant in active region whereas H3K27me3 (grey) is enriched in inactive enhancers. **(D)** Bar diagram for ChIP-qPCR data illustrating the antibody pull down efficiency. The data represents the relative fold enrichment of each antibody (anti-H3K4me1 in blue, anti-H3K27ac in red and anti-H3K27me3 in grey) calculated against the sonicated chromatin without any immune-precipitation (Input sample). Specific primers were used to investigate ChIP around the Sox2 promoter (SOX2_P), Sox2 enhancers (SOX2_N2 and SOX2_N4), Gata2 promoter (GATA2_P) and Spalt4 otic enhancer (SPALT4_E). **(E)** Chart summarising the validation of linear amplification of ChIPed DNA. After the ChIP protocol a first round of qPCR was performed **(D)** and subsequently the same ChIPed DNA was amplified and analysed as described above. The profiles of each gene were compared against the un-amplified ones to check if any major bias was introduced. Even tough the two profiles are not identical, active and inactive regions can be still distinguished. Therefore since overall interpretation seems not to be strongly affected the protocol was used for ChIP-seq. The error bars represent the standard error.

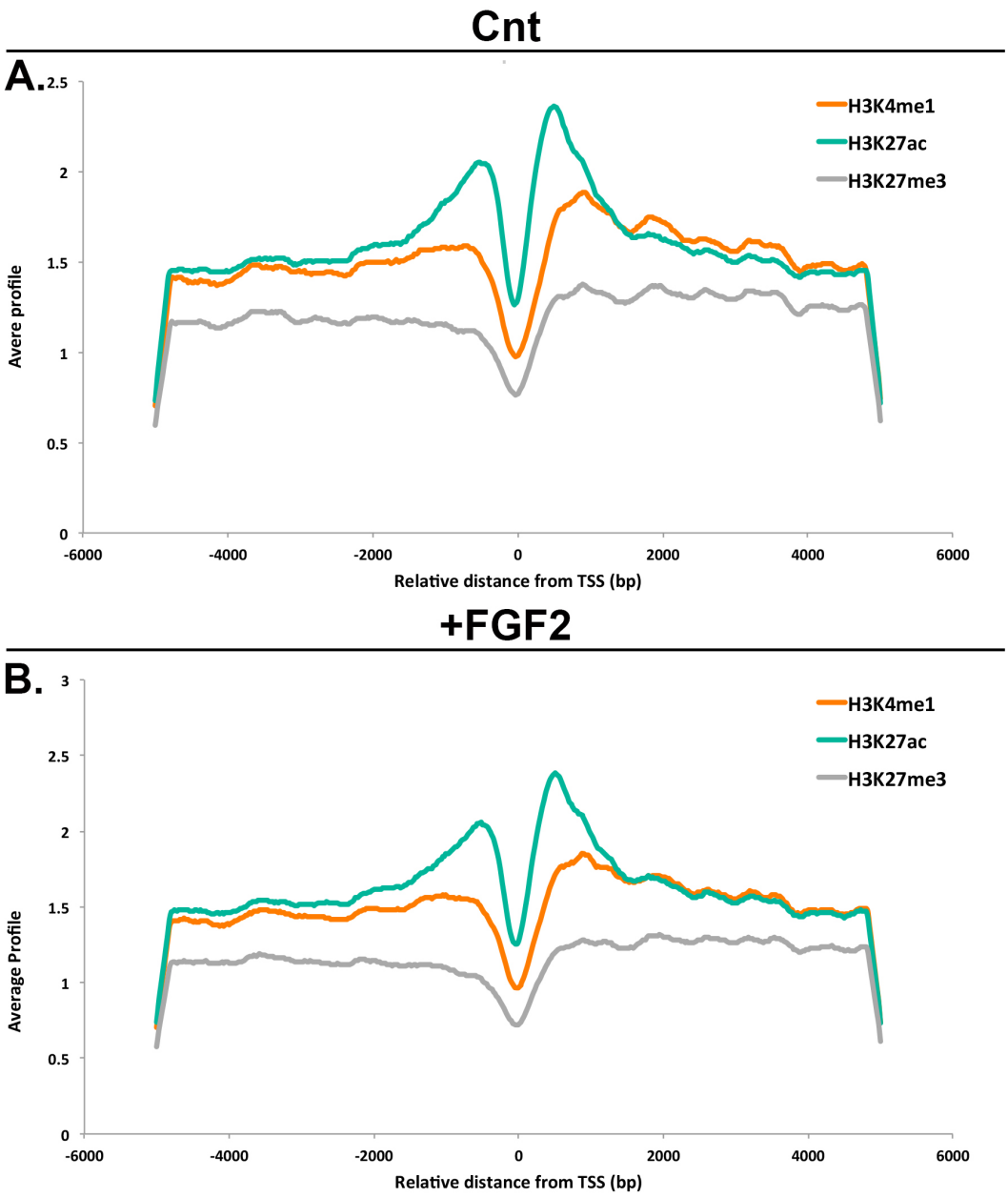

Figure 6.2 H3K4me1, H3K27ac and H3K27me3 density distribution around the transcription start site (TSS).

Average density distribution around the TSS for each histone mark (H3K4me1, H3K27ac and H3K27me3). **(A)** Control untreated sample; **(B)** FGF-treated tissue. The x-axis represents the relative distance from the TSS (zero) in base pair. The y-axis represents the average density of each antibody at each given location. Maximal H3K27ac density occurs closer to the TSS compared to H3K4me1 and H3K27me3.

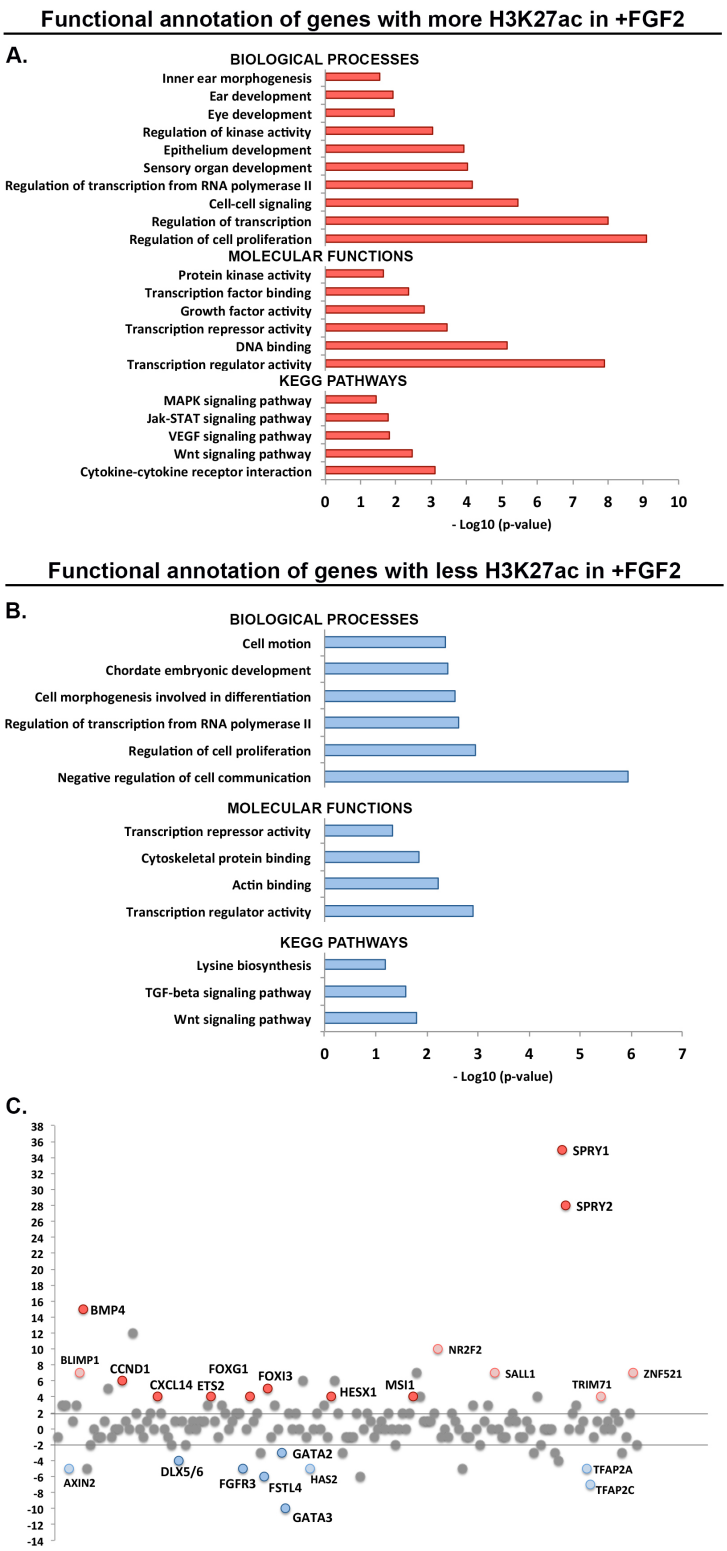

Figure 6.3 Functional annotation of genes with variation in H3K27ac after FGF stimulation.

Gene ontology annotation of genes associated with more (**A**; red) or less (**B**; blue) H3K27ac upon treatment with FGF2. Relevant terms for biological process, molecular function and KEGG pathway are plotted. Y-axis: –Log10(p-value) indicates the significance of the correlation. **(C)** Quantification of the H3K27ac abundance for genes analysed by NanoString. The y-axis represents the difference in number of H3K27ac peaks between +FGF and –FGF sample. Arbitrary the differences of two peaks were considered insignificant (horizontal grey lines). Genes in red and blue are significantly up- (red) or downregulated (blue) by FGF, whereas genes in light red and blue are not significant. Overall a good correlation is observed.

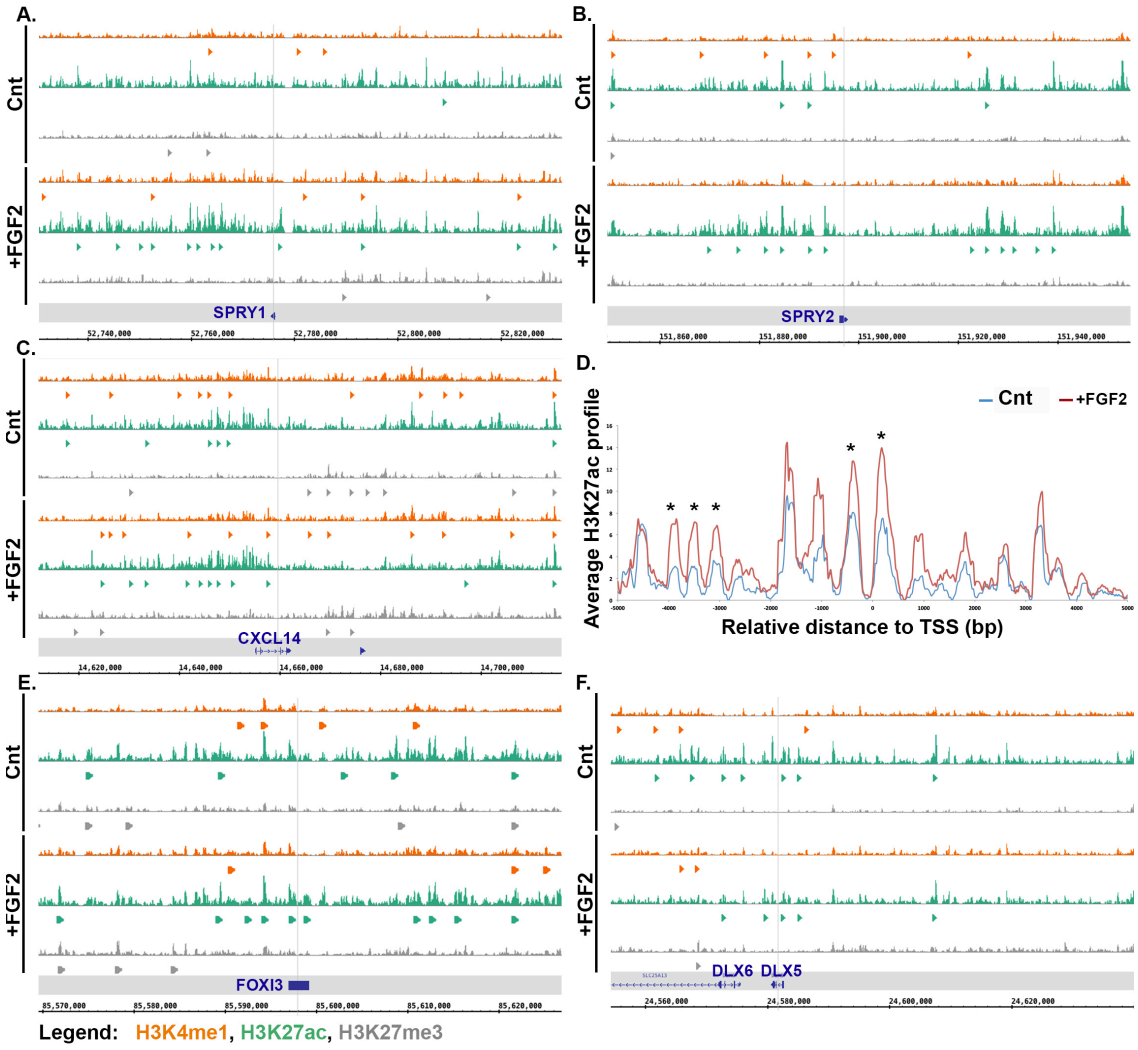

Figure 6.4 Histone mark distribution around selected FGF response genes.
H3Kme1 (orange), H3K27ac (green) and H3K27me3 (grey) distributions around the following loci: Spry1 **(A)**, Spry2 **(B)**, Cxcl14 **(C)**, Foxi3 **(E)** and Dlx5/6 **(F).** Tracks show the comparison of control (Cnt) and +FGF ChIP-seq data for each gene. For each histone mark the first track represents aligned sequence distribution, whereas in the second line triangles represent the statistically significant peaks identified after comparison with the input sample. **(D)** As example the comparison between Cnt (blue) and +FGF (red) H3K27ac density distribution around Cxcl14 TSS have been plotted. After FGF stimulation in four positions (asterisks) in four positions more H3K27ac is detected. Asterisks are positioned close to regions where significant peaks were found.

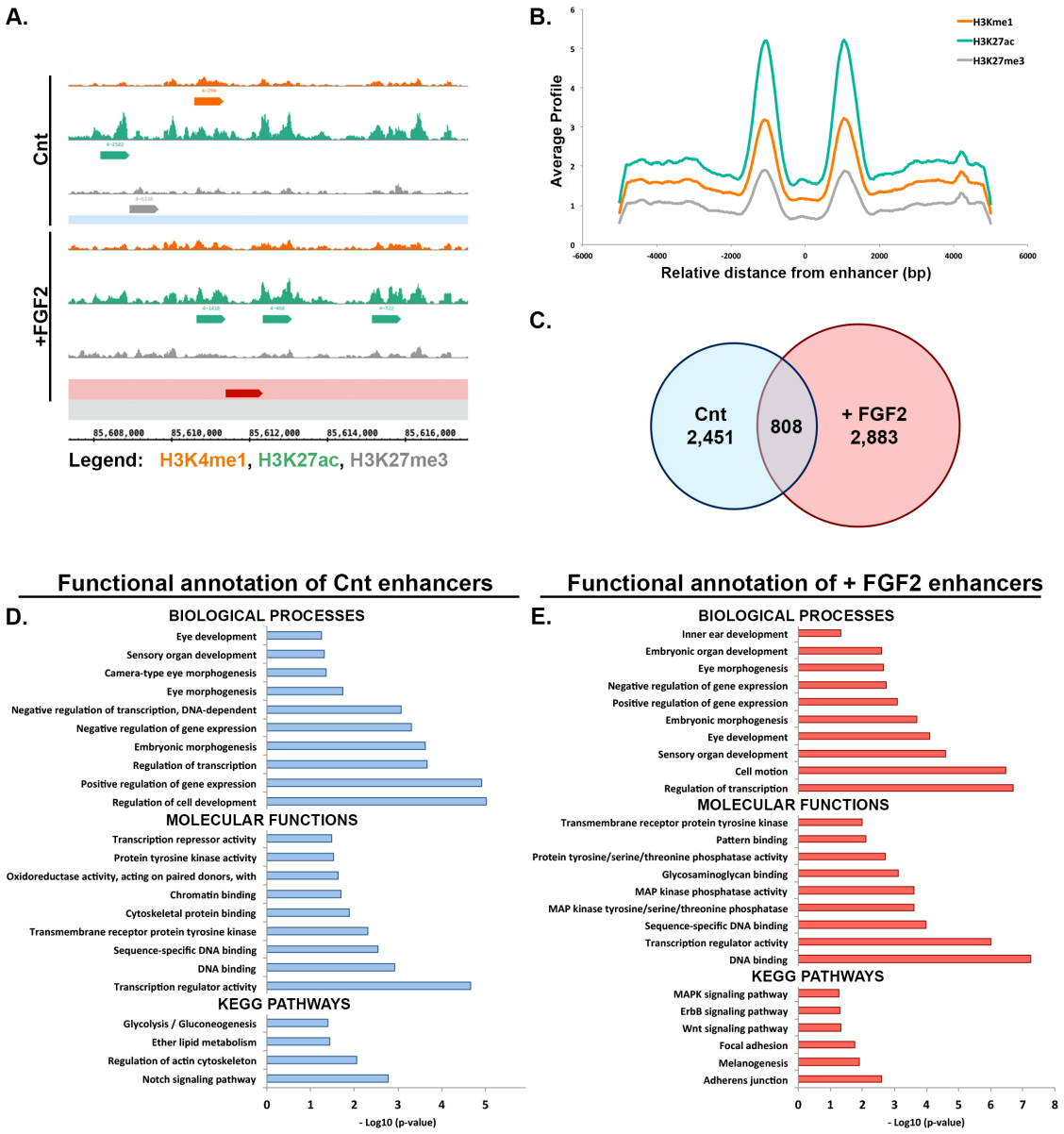

Figure 6.5 Annotation of the regions with enhancer features.
(A) Example region located at the 5'of the Foxi3 TSS. Presence of H3K27ac double peaks (green) and absence of H3K27me3 (grey) identify a putative enhancer region (red) only after FGF stimulation. **(B)** Average histone mark density distribution centred on the putative enhancer region shows a bimodal distribution (H3K4me1 in orange, H3K27ac in green and H3K27me3 in grey). **(C)** Diagram representing unique elements for control (blue; 2,451) and +FGF (red; 2,883) ChIP-seq data sets. 808 putative enhancers are in common between both experiments. Functional annotation of genes associated with a putative enhancer in the control (**D**; blue) and +FGF (**E**; red) treated sample. Relevant terms for biological process, molecular function and KEGG pathway are plotted. y-axis: –Log10(p-value) indicates the significance of the correlation.

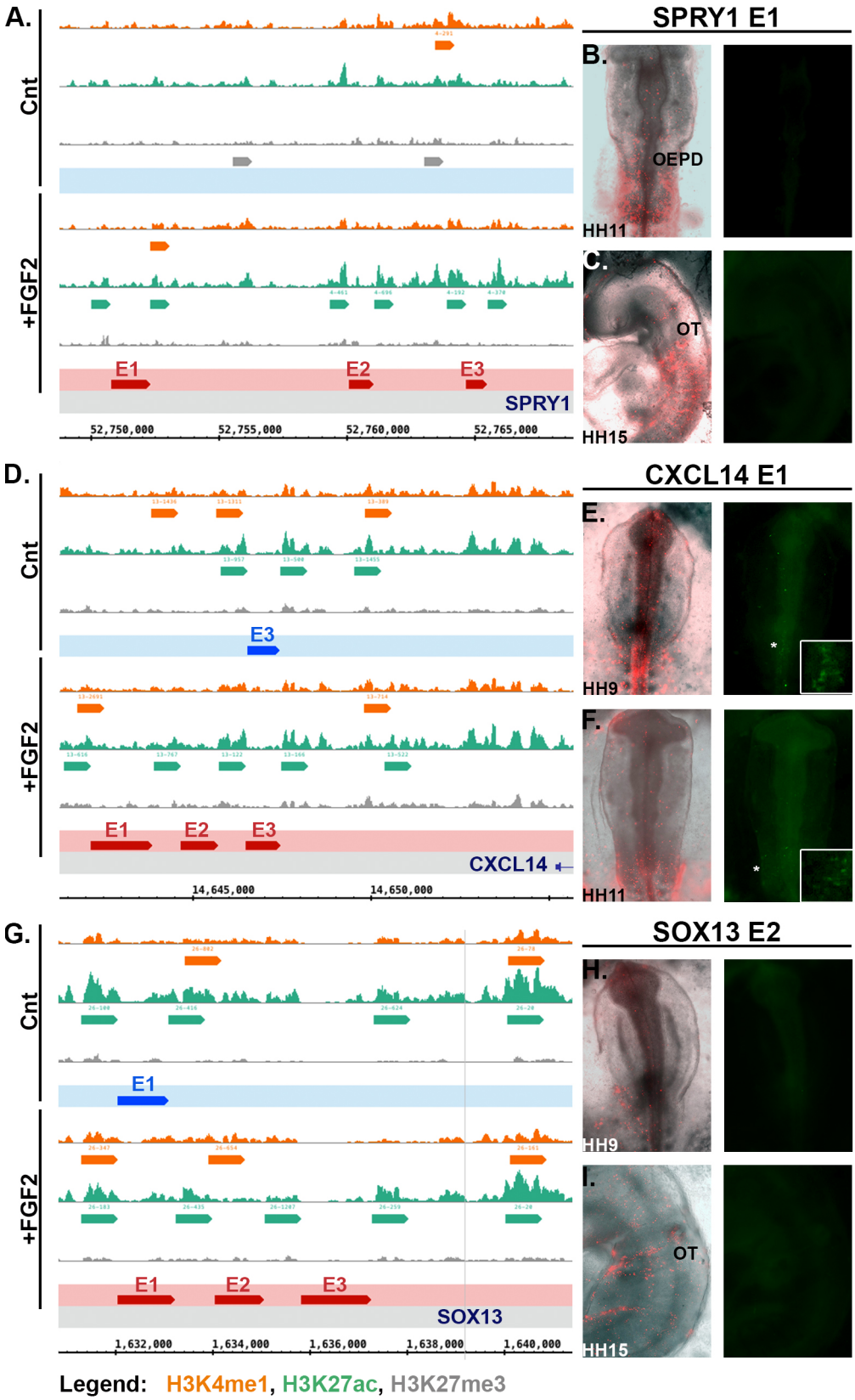

Figure 6.6 ***In vivo*** **activity of putative enhancer regions.**

Figure 6.6 *In vivo* activity of putative enhancer regions.
The chromatin landscape around Spry1 **(A)** Cxcl14 **(D)** and Sox13 **(G)**. Distribution of H3Kme1 (orange), H3K27ac (green) and H3K27me3 (grey); rectangles represent the statistically significant peaks. Putative enhancers are highlighted in blue for control and red for +FGF. **(B-C)** Spry1 E1 does not show any activity between HH11 and HH15. The red fluorescence is used as control for the electroporation while the green fluorescence is sign for enhancer activity. **(E-F)** Cxcl14 E1 shows week activity in the neural tube close to the otic region (HH9) and in some otic cells at HH11. Asterisks indicate the positive regions, which is magnified in the inset. **(H-I)** The Sox13 E2 unique to +FGF is not active at the stages examined (HH9 to HH15).

Figure 6.7 Genomic location of Foxi3 enhancers identified from the ChIP-seq.
At the 3' of the Foxi3 TSS two elements are uniquely identified in the +FGF ChIP-seq (E0 and E1 in red). Additionally a larger domain (magenta), partially overlapping the two segments, is considered to be an enhancer in the endogenous OEPD (ChIP-seq ss5-6). A third element (E2 in red) is present at the 5' end of the gene. This element is also identified in the endogenous OEPD (magenta). Evolutionary conserved elements (CNS) identified by classical alignment (ECR Browser) and nonalignment-based (DReiVe) (Sosinsky et al., 2007) methods are shown as black rectangles. H3K4me1 (orange), H3K27ac (green) and H3K27me3 (grey).

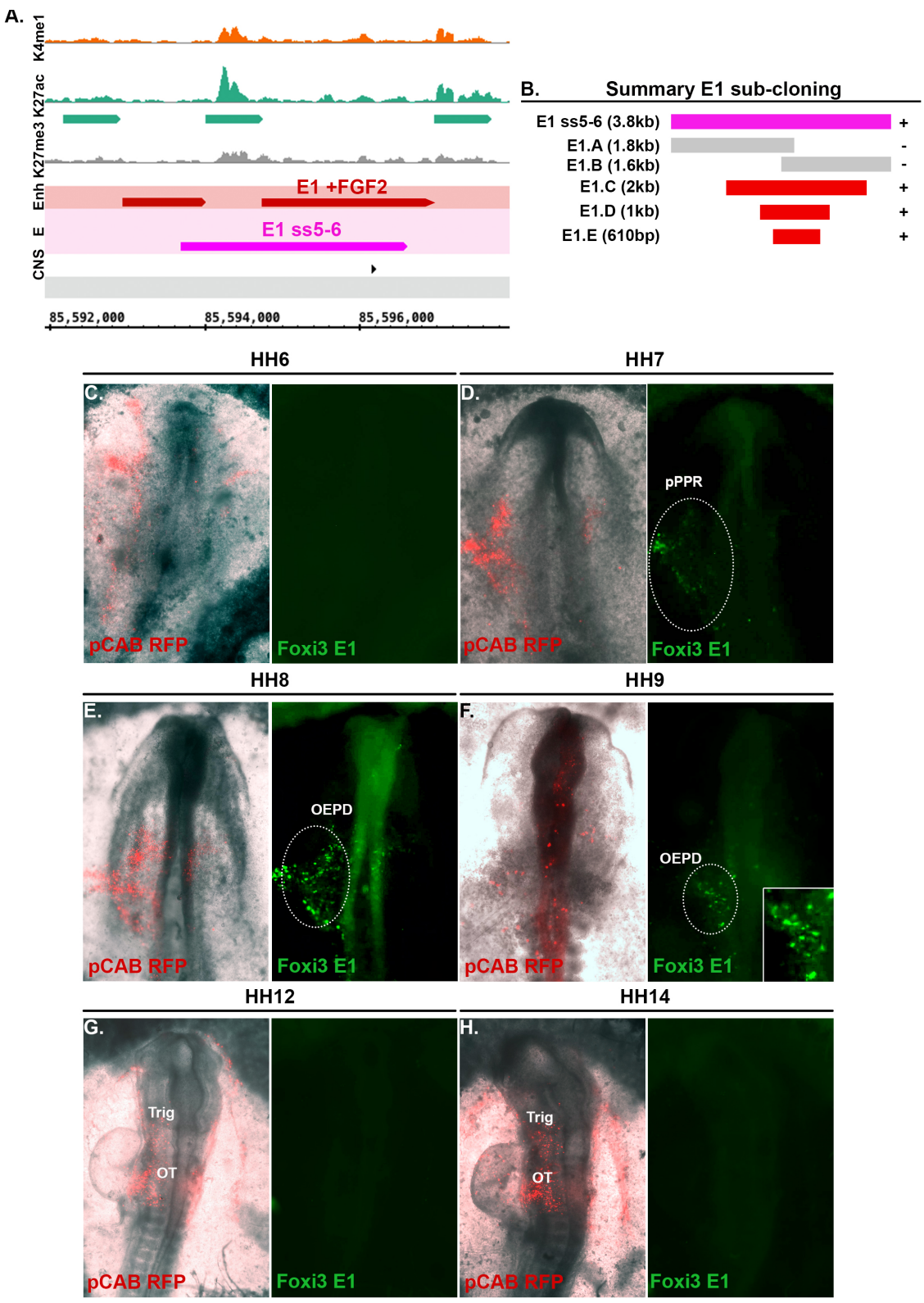

Figure 6.8 Foxi3 E1 is active at the time of OEPD induction.

Figure 6.8 Foxi3 E1 is active at the time of OEPD induction.
(A) Enlarged view of the histone mark distributions around Foxi3 E1 (Figure 6.7). **(B)** Summary of various sub-clones of Foxi3 E1 and their in vivo activity. E1 ss5-6 (3.8kb; magenta) is the longest fragment and is active in the OEPD. E1.A and E1.B divide E1 ss5-6 into two fragments are not active. E1.C, E1.D and E1.F are shorter versions of E1 ss5-6 with the central portion maintained intact. These three sequences show similar activity to the original clone E1 ss5-6. Characterisation of the *in vivo* activity of the Foxi3 E1 enhancer. pCAB-RFP vector has been used as positive control for the electroporation while the Foxi3 E1 has been inserted in a pkt-Citrine vector and green fluorescent is a mark of enhancer activity **(C-D)** A few GFP+ cells were first identified at HH7 in the posterior PPR (pPPR). **(E-F)** The enhancer shows activity in the entire OEPD between HH8-9 and it becomes inactive around HH12 **(G-H)**. The enhancer appears to be specific to the OEPD since other electroporated regions, e.g. neural tube in F, do not present any green fluorescence.

A. **Foxi3 E1.E (610bp) Chr4:85595131-85595778**

1	AAGCGCATGAATGTCATCTGACATTTCATCATGGCTTCATTATATTTTGG	**50**
51	ATCAGGCCAGTGGTTCATCTTGCATTACTGCCATATACACGTTAAGCATG	**100**
101	TAGCCAGTGAAGAGGCACTGCATCACAGTGCCAATGATATTGTTTTCTGA	**150**
151	ATAGCCTGCAGGGATGGCCTTACATCATGCAAGATGCATACACAGTTAAT	**200**
201	AGCTGCGATTTCATGCTTAACTTCAGTGTTGATGTTACATTCCTCTGGAA	**250**
251	GAAATTTATACTTATGTTCCATGGCTGCACGTGGAGCCCAGCAAACAACG	**300**
301	TATGCAAACAGCAAGAACTGGGGATTAATGGTTTTGCATAAGGGATGCTG	**350**
351	AAGGAAAGATTCTCTGTAGTGTGTTTATGGTGGAGGGCTCAGCCTGGCCT	**400**
401	GCCAAGTGACCAGTCTGACTTCTCATTTTAGGCAGGTGCAATCTGATCTG	**450**
451	AAAAAGTAACTTGCAAAATGGATGAGGGTCGAGGCAGCCAAGCTCAGCCT	**500**
501	TGCTCCTCCTCTCCCCCCCTGCTTGCCGGCGCTGTGCTGGAACCAGCCCT	**550**
551	GCTTCTTTTCCTTTTGCAAGCTTTTATTATTTTGACTAAACCAGGCTGAA	**600**
601	AAGAGACAGTTGTCATTCAGATGACC	**610**

B.

TF	Strand	Start	End	Sequence	P-value
TEAD1	D	85595366	85595377	TACATTCCTCTG	7.10E-07
Otx2	D	85595447	85595463	ACTGGGGATTAATGGTT	1.40E-05
SALL1	R	85595701	85595712	AAATAATAAAAG	3.10E-05
Pax-2	D	85595300	85595318	TTACATCATGCAAGATGCA	3.70E-05
Pax-2	D	85595193	85595211	GTTCATCTTGCATTACTGC	4.40E-05
Otx3	D	85595446	85595462	AACTGGGGATTAATGGT	5.50E-05
Tcfap2b/2c	D	85595282	85595295	TAGCCTGCAGGGAT	6.30E-05
SALL1	R	85595386	85595397	ACATAAGTATAA	6.70E-05
SoxD	R	85595264	85595279	CAGAAAACAATATCAT	6.80E-05
SoxE	D	85595700	85595716	GCTTTTATTATTTTGAC	0.045

Figure 6.9 Sox8, Sall1, Otx2/3 and Tead1 are putative regulators of the early expression of Foxi3.
(A) The 600bp of Foxi3 E1.D presents several significant transcription factor-binding sites for genes expressed during sensory organ development; different TFBS are highlighted in different colours. **(B)** Combination of RSAT and Clover analysis is summarised including the p-values associated to each motive.

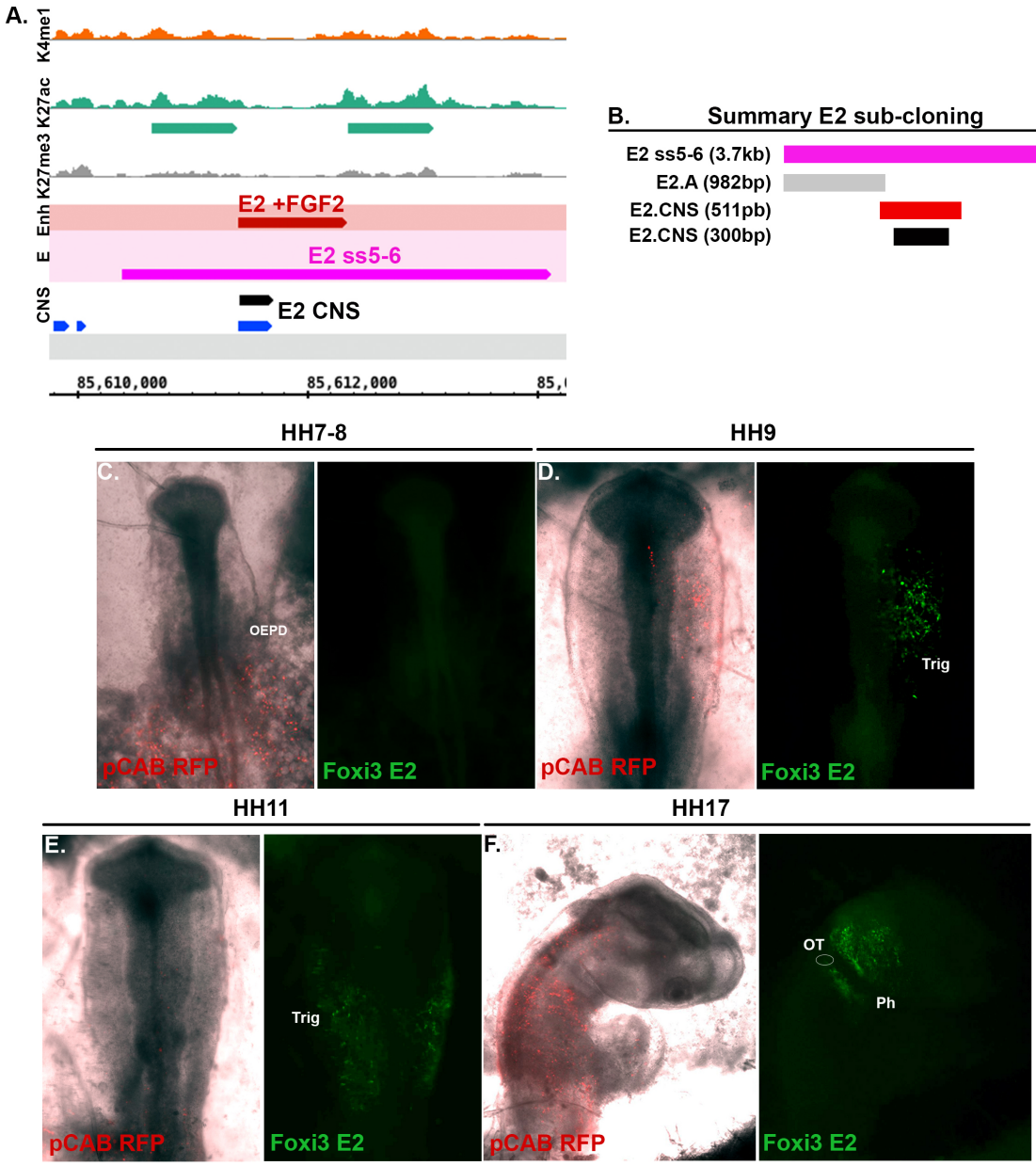

Figure 6.10 Foxi3 E2 is active in the trigeminal domain accounting for the late phase of *Foxi3* expression.

(A) Enlargement of the mark distributions around Foxi3 E2 (Figure 6.7). **(B)** Summary of the sub-cloning reporter activity. E2 ss5-6 (3.7kb; magenta), considered as full length, is active in the trigeminal. E2.A (982bp; grey) excludes the conserved element and does not show any activity. E2 CNS (511bp; red), containing the 300bp of the conserved element (black), is sufficient to drive GFP expression. Characterisation of the *in vivo* activity of the Foxi3 E2 enhancer. **(C-D-E)** GFP+ cells were first identified at HH9 in the trigeminal placode (Trig). **(F)** At around HH17 the enhancer remains active in the pharyngeal arches (Ph). The otic vesicle (OT; highlighted with a circle) has been widely electroporated but no reporter activity is detected. Overall the activity of Foxi3 E2 recapitulates the late expression of *Foxi3*.

A. **Foxi3 E2.CNS (511bp) Chr4: 85611260-85611770**

```
1    TTTGGCCCTGTTCAAATGGCTGGGAATGTTGTTAATCACTCAGTAGAGCC  50
51   ACTGCCTGCGTTTCATTCCCAGGAGGCACCTTCCCAGCTCTCATGCCATT  100
101  ACAGCATCCTCCGTCTGTCATCGCGCTGGTCCTTGGGAGCGAGGGACGAG  150
151  CGGCTTCATCCTTCTTCCTCTAAACGCTTCATCAGCCGCTCCCCTGAAAA  200
201  CTGTAAATAAAGGCCGCTGGGGATAGCTTTTCTGCTTGACCCCTCACCTG  250
251  AAATGAAAATAGAGGTGGCTGGATTTCATCCTGATGTGGAGCTCCTTCCC  300
301  GGGCCGGCTCTTTCCCGTCACTGTTGACAGTTACCTGCCAAGCCCCATGG  350
351  TTACCTTTGATTTCGCCGTAATGATATCTCAGTACTTAGGATGGCTCTGG  400
401  GCTCATAATCCTCTCTGCAGCCTTAACCAATTTATGGGTAACCTGAGAGC  450
451  AGGCTCTCGCTTCCTCGTGATTTTGCCTCTTGTTAAATACACTGAAGGTA  500
501  TCAACAAACTG                                          511
```

B.

TF	Strand	Start	End	Sequence	P-value
RXRA	D	85611491	85611508	CTGCTTGACCCCTCACC	3.20E-06
SIX1	R	85611626	85611633	CGTAATGATATCTCAGT	9.70E-06
CITED2	R	85611580	85611595	AGGTAACTGTCAACAG	4.60E-05
TCF4	D	85611609	85611625	GTTACCTTTGATTTCGC	7.30E-05
NR2F2	R	85611492	85611507	GGTGAGGGGTCAAGCA	8.30E-05
SIX1	D	85611651	85611667	CTGAAGGTATCAACAAA	8.50E-05
OTX2	R	85611659	85611675	AGAGAGGATTATGAGCC	9.40E-05

Figure 6.11 Six1, Cited2 and Tcf4 are among the putative regulators of the late expression of *Foxi3*.
(A) The 511bp of Foxi3 E2.CNS presents several significant transcription factor-binding sites for genes expressed during sensory organ development; different TFBS are highlighted in different colours. **(B)** Combination of RSAT and Clover analysis is summarised including the p-values associated to each motive.

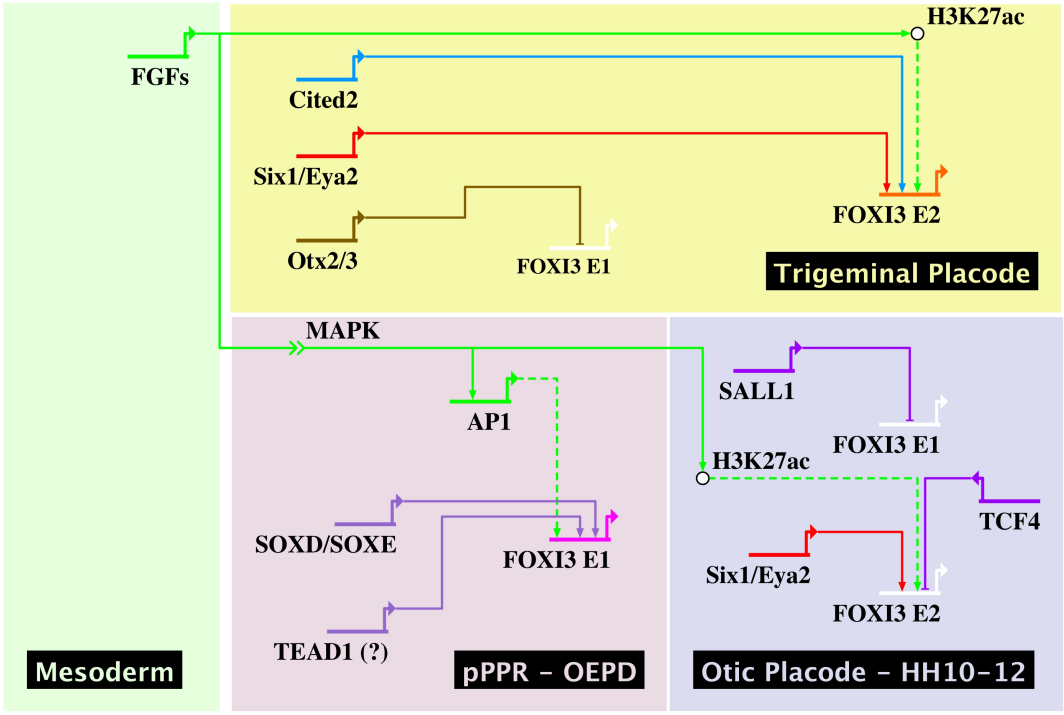

Figure 6.12 Putative molecular regulation of Foxi3 through its two regulatory elements.

The expression of *Foxi3* in the OEPD from HH7 to HH8+ can be recapitulated by the activity of Foxi3 E1. Transcription factor binding sites analysis pointed to SoxD (Sox13) and SoxE (Sox8) as possible positive regulators as well as Tead1, but since its expression has not been analysed in chick it need further validation. Additionally, two Ap1 binding sites are present but they are not functionally important for enhancer report activity (dashed line). In the anterior PPR Foxi3 E1 is not active and this could be due to the presence of the repressor Otx2/3. At around HH9 Foxi3 E1 becomes inactive, presence of the repressor *Sall1* in the OEPD could mediate its shout-down. Later, *Foxi3* becomes expressed in the trigeminal placode and it is clear form the otic domain. Active in the trigeminal from HH9 the second Foxi3 enhancer (E2) could be the main element regulating the late expression of *Foxi3*. Mainly Six1 could be driving Foxi3 E2 activity in the trigeminal. However, in the otic domain even if *Six1* is present the enhancer is inactive. This could be mediated by the otic repressor Tcf4. Foxi3 E2 appears to have enhancer features only after FGF treatment (dashed line), and the increase in acetylation could be mediated by the recruitment of p300 by Cited2 which presents a binding site in the enhancer.

7. Discussion

The main goal of this work is to further characterise the process of otic and epibranchial development. The first step towards their specification is the formation of a common sensory precursor domain (PPR). Remarkably, despite the diversity of sense organs, their progenitors arise from a common domain in the ectoderm (Bhattacharyya et al., 2004, Kozlowski et al., 1997, Pieper et al., 2012, Xu et al., 2008, Streit, 2002) and they share common features (Bailey et al., 2006, Martin and Groves, 2006) (for review see: Grocott et al., 2012, Schlosser, 2006, Schlosser, 2010, Streit, 2008). The second step requires the induction of a common otic-epibranchial domain (OEPD), marked by the expression of *Pax2*, which lies anterior to the first somite (McCarroll et al., 2012, Ohyama and Groves, 2004b, Streit, 2002). Later, the otic and epibranchial placodes segregate to give rise to the entire inner ear and the VIIth, IXth and Xth cranial nerves, respectively (for review see: Chen and Streit, 2013, Ladher et al., 2010).

In this thesis, new factors expressed at different phases of otic development have been identified and integrated in the existing gene network. Furthermore, the role of FGF signalling in OEPD induction has been studied in detail.

7.1 Towards the formation of the pre-placodal region

Recently, PPR development has been investigated more extensively; however the PPR transcriptome remains to be characterised together with a high-resolution gene network for PPR regulation.

Studies in different organisms have identified FGFs together with WNT and BMP antagonists as some of the key signals that induce the PPR (Ahrens and Schlosser, 2005, Brugmann et al., 2004, Glavic et al., 2004, Kwon et al., 2010, Litsiou et al., 2005, Stuhlmiller and Garcia-Castro, 2012). While the source of these inducing signals has not been established in all species, the underlying head mesoderm has been implicated (Ahrens and Schlosser, 2005, Jacobson, 1963b, Jacobson, 1963a, Litsiou et al., 2005, Lleras-Forero et al., 2013) and this mesoderm is able to induce *Six1, -4* and *Eya2* in a competent ectoderm that normally never forms placodes (Litsiou et al., 2005). However, the "induced PPR" differs from the endogenous domain and does not posses all PPR characteristics: it is not specified as lens and does not respond to otic inducing signals

(Christophorou, 2008). These findings suggest that some crucial factors that determine the properties of the endogenous PPR are absent from the induced tissue. One of the aims of the microarray screen described here was to identify such differences. Several Sox family members (*Sox2*, *Sox3*, *Sox8* and *Sox11*), *Zic1/2*, *Otx2*, *Six3* and the newly characterised transcription factors *Trim24*, *Hsf2*, *Mynn* and *Hmgxβ4* are among the genes found to be expressed in the endogenous PPR but not strongly induced by the mesoderm. Some of these genes (e.g. Sox2/3, Zic1/2 and Otx2) are known to play a crucial role in pre-placodal cell specification while the remaining factors are good candidates to be involved in PPR formation.

Among the head mesoderm induced genes, many are expressed during gastrulation, prior to PPR formation, and are present in the border as well as the neural plate. This observation implies that the neural plate and the border derivatives (PPR and neural crest) share common features early in development and that their initial induction involves some common steps. Indeed, new evidence supports this hypothesis: similarly to the mesoderm graft, Hensen's node, the source of neural inducing signals FGFs, TGF β and BMP antagonists (for review see Stern, 2005b), promotes the expression of a similar set of factors (Trevers, Hintze and Stern; personal communication). Thus, a scenario emerges in which both placode and neural inducing tissues generate a 'common state' from which subsequently central nervous system, neural crest and placode lineages diverge.

In response to PPR-inducing signals a number of transcription factors are initiated in a strict temporal sequence (Hintze, personal communication), which reflects their temporal appearance in the normal embryo. I will discuss briefly those factors known to influence PPR formation. At gastrula stage pre-neural and non-neural genes overlap in an ectodermal domain named the 'border' of the neural plate. By the end of gastrulation, an increasing number of transcripts are specifically expressed in different regions subdividing the ectoderm into three partially overlapping territories: the neural plate (*Sox2*, *Sox3*), the border region (*Irx1*, *Msx1*, *Pax3/7*, *cMyc*) and the non-neural ectoderm (*Dlx*, *Ap2*, *Foxi1/3* and Gata2/3) (for review see: Grocott et al., 2012, Schlosser, 2006, Streit, 2007). At this stage the border region is composed of a mixture of neural, PPR, neural crest and epidermal cells (Ezin et al., 2009, Fernandez-Garre et al., 2002, Garcia-Martinez et al., 1993, Hatada and Stern, 1994). Neural and non-neural transcription factors work together with neural crest and border genes to establish the PPR. Dlx, Ap2, Foxi1/3 and Gata2/3 are among the non-neuronal transcription factors required for the

expression of the PPR-specific transcripts of the *Six* and *Eya* families, and when they are lost sensory placode identity is compromised (Luo et al., 2001b, McLarren et al., 2003, Pieper et al., 2012, Woda et al., 2003, Esterberg and Fritz, 2009, Kaji and Artinger, 2004, Kwon et al., 2010, Sato et al., 2010, Solomon and Fritz, 2002). In addition, neural crest genes are also involved in PPR specification: c-Myc is present at the border of the neural plate and PPR fate (Bellmeyer et al., 2003), while Pax3 and Msx1 repress sensory placode development and promote neural crest (Monsoro-Burq et al., 2005, Hong and Saint-Jeannet, 2007, Maeda et al., 1997, Suzuki et al., 1997, Yamamoto et al., 2000). The expression of *Irx1* in the neural plate border is important for PPR formation, it is expressed just prior to *Six/Eya* (Glavic et al., 2004, Gomez-Skarmeta et al., 2001, Goriely et al., 1999, Khudyakov and Bronner-Fraser, 2009) and it positively regulates *Six1* (Glavic et al., 2004). Lastly, neural genes and their function in PPR formation have not been addressed fully and further investigation is required. However, one study in *Xenopus* suggests that the neural plate expressed transcription factor *Sox2* represses *Six1* (Brugmann et al., 2004). In contrast, members of the Six and Eya families are necessary to establish PPR identity and for normal development of all sensory placodes (Chen et al., 2009, Christophorou et al., 2009, Friedman et al., 2005, Konishi et al., 2006, Kozlowski et al., 2005, Laclef et al., 2003, Li et al., 2003, Ozaki et al., 2004, Xu et al., 1999, Zou et al., 2006, Zheng, 2003, Zou et al., 2004, Ikeda et al., 2007). For example, while lack of Six1 expands neural crest and neural gene expression, its overexpression alone or together with Eya1/2 leads to repression of these genes. Thus, negative cross regulation between neural, neural crest and PPR transcription factors sharpens gene expression boundaries and thus segregates cells of different fates at the neural plate border.

Six and *Eya* family members are specifically expressed in the PPR, marking the entire domain. However, simultaneously rostro-caudal patterning is initiated as evidenced by the regionalised expression of transcription factors. For instance, *Otx2* is enriched anteriorly, while *Gbx2* is a posterior gene; they inhibit each other establishing a first diversification between anterior and posterior PPR cells similar to their role in the central nervous system (Acampora et al., 2001, Acampora et al., 1995, Bally-Cuif et al., 1995, Li et al., 2009, Simeone et al., 1992, Simeone et al., 1993, Steventon et al., 2012, Tour et al., 2001, von Bubnoff et al., 1996). Likewise, members of the *Irx* family and *Six3* subdivide the PPR into different anterior-posterior domains (Bovolenta et al., 1998, Oliver et al., 1995a, Seo et al., 1998, Zhou et al., 2000, Bellefroid et al., 1998, Goriely et al., 1999). It is tempting to speculate that, as in the brain, they also allocate different cell fates to placodal

cells. The microarray screen conducted here also reveals new differentially expressed factors; among them the neuropeptide *Nociceptin* and the neuropeptide receptor *SSTR5* (Lleras-Forero et al., 2013), which have been implicated in anterior PPR specification. In addition, the arrays together with the *in situ* hybridisation screen have identified the new PPR specific factor *Homer2*, as well as new anterior PPR markers *Dlx6* and *Nfkb*. However, their precise role in PPR development remains to be established.

In summary, the microarray screen provides a rich resource of new players in PPR formation including potential upstream regulators of the Six and Eya network and factors that may impart regional character to placode progenitors. Moreover, it reveals an unexpected commonality between placode and neural induction, suggesting that before cells become committed to either fate they pass through a 'common state' from which they diverge later.

7.2 Towards a gene regulatory network for otic and epibranchial specification

7.2.1 Role of FGF signalling in OEPD induction

FGF signalling plays a critical role in OEPD induction and it has been used as a paradigm to study cell fate induction. Studies in different species have demonstrated that FGF is required for OEPD formation. Inhibition of FGF leads to small otic vesicles and expression of OEPD markers are reduced or lost (Alvarez et al., 2003, Ohuchi et al., 2000, Pauley et al., 2003, Wright and Mansour, 2003, Ladher et al., 2005, Urness et al., 2010, Zelarayan et al., 2007, Pirvola et al., 2000, Abello et al., 2010, Ladher et al., 2000, Yang et al., 2013, Leger and Brand, 2002, Liu et al., 2003, Maroon et al., 2002, Phillips et al., 2001, Solomon et al., 2004). Gain-of-function experiments in frog, zebrafish and chick support the importance of FGFs in OEDP formation. Misexpression of FGF leads to an enlargement of the *Pax8*/*Pax2* expressing domain and the formation of ectopic otic vesicles (Phillips et al., 2001, Hans et al., 2007, Padanad et al., 2012, Phillips et al., 2004, Bajoghli et al., 2004, Solomon et al., 2004, Lombardo et al., 1998, Vendrell et al., 2000, Zelarayan et al., 2007).

In vitro culture of pre-placodal ectoderm is a powerful assay to study otic induction and it has been used in chick to establish the inducing potential of FGF. Only pre-placodal cells

are able to respond to FGF signalling by expressing the OEPD marker *Pax2* (Martin and Groves, 2006). More recently, a microarray screen identified a larger set of FGF responding genes after 24 hours' treatment and associated the ERK/MAP kinase branch of the FGF pathway with OEPD induction (Yang et al., 2013). However, the sequence of events downstream of FGF remains unclear. The present work has positioned several transcription factors and OEPD markers into a hierarchy downstream of FGF by analysing different time points (6, 12 and 24 hours of culture) after FGF exposure (Figure 5.11). A small set of transcripts is induced rapidly, and many of them are broadly expressed in the OEPD (e. g. *Etv4/5*, *Spry1/2*, *Foxi3*, *Gbx2*, *Pax2*, *Sox13*). Of the tested factors, only *Etv4* and *Etv5* are direct FGF targets. In turn, morpholino knockdown of Etv4 reduces both *Gbx2* and *Pax2* expression, suggesting that FGF regulates these genes indirectly via Etv4 (Figure 7.1). Thus, possibly Etv4 and Etv5 are the most important mediators of the FGF response.

Another important property of FGF during sensory placodes induction is its ability to repress the lens specification, which has been shown to be the ground state of all PPR cells (Bailey et al., 2006). In chick, FGF8 reduces lens specific *Pax6* expression while inducing olfactory markers (*Foxg1* and *GnRH*) (Bailey et al., 2006). Here, I show that FGF plays a similar role in the otic context: FGF represses anterior PPR fate by downregulating *Pax6*, *SSTR5* and other anterior genes. In fact, *Pax6* is directly repressed by FGF. Therefore, FGF signalling seems to have an important role in lens repression, while simultaneously allowing other sensory placodal fates.

The role of the mesoderm in OEPD induction is limited to a small time window. In fact, in chick when the cranial paraxial mesoderm is ablated between 0-3 somite stages the otic placode is compromised (Orts et al., 1971, Kil et al., 2005), while if the same mesoderm is removed after 5-somite stage the otic vesicle forms properly (Kil et al., 2005). Several lines of evidence from the literature suggest that FGFs from the mesoderm cooperate with FGFs from the hindbrain to promote OEPD e.g. FGF3 in chick and mouse (Ladher et al., 2000, Alvarez et al., 2003, Mahmood et al., 1995, McKay et al., 1996, Wright and Mansour, 2003, Kil et al., 2005, Ladher et al., 2005, Paxton et al., 2010, Freter et al., 2008, Urness et al., 2010, Zelarayan et al., 2007). In addition, otic induction is only observed in recombinant explants when both mesoderm and hindbrain are combined together (Ladher et al., 2000). Lastly, the only FGF ligand among the tested one able to strongly induce *Pax2* is FGF2, which has the characteristic of activating all FGF receptors

(Martin and Groves, 2006). Comparison between the inducing abilities of FGF2 and the mesoderm, by NanoString data analysis, further corroborates the idea that the mesoderm is not a strong signalling source for OEPD induction since it only weakly induces otic and epibranchial markers. Therefore it is likely that additional signals are needed to fully commit cells to an otic and epibranchial fate.

During development, signalling pathways alter gene expression through activation of transcription factors. Classically, FGF regulates cell fate determination by a series of cytoplasmic phosphorylation events that lead to ERK/MAP kinase phosphorylation. Phosphorilated ERK trans-locates to the nucleus where it phosphorylates members of the Ets family (e.g. c-Jun and c-Fos), which in turn regulate the expression of FGF target genes (for review see Dorey and Amaya, 2010). Only more recently signalling pathways have been linked to epigenetic changes at specific gene loci (Patel et al., 2013, Blythe et al., 2010, Mosimann et al., 2009, Wamstad et al., 2012). Zhang and colleagues have demonstrated that acetylation on the lysine-27 of histone-3, via p300, is dynamically deposited after VEGFA stimulation, which in turn increases gene expression (Zhang et al., 2013). Similarly in this work an increase in H3K27ac level is noticed upon FGF treatment at the locus of genes induced by FGF. The histone acetyltransferase involved in H3K27ac is p300/CREB (for review see: Holmqvist and Mannervik, 2013, Karamouzis et al., 2007), which can be stimulated by MAP kinase via phosphorylation (Ait-Si-Ali et al., 1999). Furthermore, Ap1 complex and Sox genes can recruit p300/CREB to specific genomic location (Furumatsu et al., 2005a, Furumatsu et al., 2005b, Tsuda et al., 2003, Chen et al., 2004, Zhang et al., 2013). Interestingly, these binding sites are abundant in the two FGF-unique enhancers associated to Foxi3 here described. It is possible to speculate that these factors recruit p300/CREB at these sequences, causing acetylation of the enhancers. This mechanism could regulate enhancer activation of other FGF-responding genes and it has also been demonstrated to function in endothelial cells (Zhang et al., 2013). Thus, signalling pathways may induce global epigenetic modifications to rapidly regulate transcription. However, at the present there are no evidences that the deposition of acetylation marks is functionally important for FGF-gene regulation in the otic context. A possibility to test the significance of the dynamic H3K27ac in the otic would be to treat the posterior PPR with FGF2 and simultaneously block the activity of histone acetyl-transferases (HATs). Anacardic acid can be used as a general inhibitor of HATs (Hemshekhar et al., 2012), while the drug C646 could serve to specifically block p300 (Zhang et al., 2013). If the acetylation is important FGF will be

no longer able to activate its targets after HATs inhibition. On the other side, if the deposition of H3K27ac is a secondary event of gene activation, the block of HATs activity will not have an early impact on OEPD genes. In the case where experimental evidences support the first scenario would be interesting to establish whether Ap1 is the key factor that binds to FGF-responsive genes and specifically recruits p300 at these loci. ChIP-qPCR could be used to assess if Ap1 and p300 are present together at the enhancers and promoter of FGF-regulated genes. Furthermore, the Ap1 complex could be disrupted (e.g. morpholino knock-down of c-Jun or c-Fos) and p300 recruitment assessed. Performing these type of experiments would help to characterise the contribution of epigenetics to the molecular cascade downstream of FGF signalling.

7.2.2 Implementation of the otic and epibranchial gene network and its relation with human deafness

In addition to FGF signalling, several transcription factors are required for OEPD specification and they function in a network to ultimately regulate cell fate decision. Posterior PPR genes (Gbx2, Irx, Dlx, Foxi3, Etv4/5) together with Six/Eya collaborate with FGF to mediate the expression of *Pax2*, *Pax8*, *Spalt4*, *Foxg1*, *Sox3* and to confer OEPD fate (Hans et al., 2004, Khatri et al., 2014, Kwon et al., 2010, Nissen et al., 2003, Padanad et al., 2012, Padanad and Riley, 2011, Solomon et al., 2003a, Steventon et al., 2012, Hans et al., 2007, Bricaud and Collazo, 2006, Aghaallaei et al., 2007, Khatri and Groves, 2013, Ohyama and Groves, 2004a, Pieper et al., 2011, Solomon and Fritz, 2002, Sun et al., 2007, Barembaum and Bronner-Fraser, 2010). In addition, *Sox8* (Betancur et al., 2011) and *Lmx1a*, *Sox13* and *Blimp1*, new transcription factors here identified, are expressed early in the OEPD (Figure 7.1). Since they early appearance in the OEPD, which resample *Pax2* expression, they could be contributing to instruct cells to become fully specified as otic or epibranchial.

The subsequent step is the segregation of the otic and epibranchial placodes. Cooperation of WNT and Notch signals fully commit cells to an otic fate, while sustained FGF and BMP induce the epibranchial placode (for review see: Chen and Streit, 2013, Ladher et al., 2010; see section 1.10.1). WNT signalling promotes otic fate by enhancing the expression of genes like *Dlx5*, *Pax2*, *Pax8*, *Gbx2*, *Soho1* and *Nkx5.1* and represses the epibranchial fate by negatively regulating *Foxi2/3* and *Phox2b* (Ohyama et al., 2006, Freter et al., 2008). Similar to WNT, Notch promotes the otic gene *Pax8* and represses the

epibranchial gene *Foxi2* (Jayasena et al., 2008). In addition to their overlapping function the two pathways positively regulate each other (Jayasena et al., 2008). However, FGF signalling from the pharyngeal endoderm is required to promote epibranchial fate by increasing *Phox2b* and *Sox3* expression and inhibits the otic genes *Soho1* and *Nkx5.1* (Freter et al., 2008, Nechiporuk et al., 2007, Nikaido et al., 2007, Sun et al., 2007, McCarroll and Nechiporuk, 2013). The pharyngeal endoderm is also a source of BMP (Begbie et al., 1999) which has been located upstream of *Phox2b* (Holzschuh et al., 2005). Furthermore, the mRNA-seq analysis has identified a number of new factors specific to the otic and epibranchial domains: *Tcf4* appears enriched in the otic placode, while *Blimp1*, *Nr2f2* and *Vgll2* are expressed more laterally. Their specific function has not yet been investigated.

This work highlights the importance of Sox8 as a key factor for otic development. *Sox8* is expressed in the otic field at 3 somite-stage and its morpholino knockdown causes a reduction in the thickening of the otic placode (data not shown) and mis-regulation of several otic and epibranchial genes. Sox8 functions upstream of *Pax2* and is required for otic fate: in its absence *Zbtb16*, *Zfhx3* and *Tcf4* expression is loss, while the expression of the epibranchial gene *Blimp1* is expanded. Sox8 appears to have a high position in the hierarchy however its function in the otic development has not been deeply investigated. Therefore, it would be interesting to further elucidate its role in otic and epibranchial fate decision.

Two paired-box genes (Pax2 and Pax8) are key factors in otic and epibranchial development. Mutations in the Pax2 locus have been associated with human sensorineuronal deafness (Sanyanusin et al., 1995a, Favor et al., 1996, Schimmenti et al., 1997, Sanyanusin et al., 1995b). In frog, fish and mouse *Pax8* is expressed prior to *Pax2* in the OEPD (Heller and Brandli, 1999, Pfeffer et al., 1998, Nornes et al., 1990, Krauss et al., 1991), while Pax8 is absent from the genome of reptiles and birds (Christophorou et al., 2010, Freter et al., 2012). The rapid induction of *Pax2* by FGF signalling (Martin and Groves, 2006, Urness et al., 2010, Yang et al., 2013 and the present work) is an indirect event mediated by Etv4 and possibly by other posterior PPR genes (e.g. Foxi3 and Gbx2). Loss of Pax2 in birds appears to affect both otic (e.g. *Lmx1a*, *Zbtb16*, *Soho1* and *Foxg1*) and epibranchial (e.g. *Blimp1*, *Vgll2* and *Phox2a*) genes (Freter et al., 2012; present work) (Figure 7.1). Thus, Pax2 key role as OEPD specifier is highlighted by the fact that many

inputs, both negative and positive, converge on Pax2, while many targets depend on its function.

To further characterise the process of otic specification, gene expression was analysed by mRNA-seq at different time points. Such genome wide analyses generate large datasets that need to be summarised in order to obtain a comprehensive picture. For this purpose reverse engineering approaches can be used to integrate expression datasets together with perturbation analysis data and infer the position of each gene in the network (for review see Epstein, 2009, Sakabe et al., 2012). The highlighted new hubs (e.g. Zbtb16, Lmx1a, Sox13) are likely to be key component in the network and might be important for ear formation. Thus, bioinformatics could be used to gain insight into the biological relevance of molecular screens.

The reconstruction of an up to date comprehensive gene regulatory network for otic and epibranchial precursors not only is a valuable resource that can be used for further studies but could also help in highlighting new candidate genes for human deafness. At present, more than a hundred human genomic loci have been associated with non-syndromic hearing loss. However, most of them are large genomic regions and only around 40 loci have been characterised at the mutational level (Van Camp and Smith, 2014 http://hereditaryhearingloss.org). Since for the vast majority identification of the causal gene is still missing it is important to identify new potential candidates. Molecular screen of genes expressed in different portions of the mouse inner ear at different stages has identified several new genes potentially associated with deafness loci (Sajan et al., 2007). Similarly, the molecular screens presented in this study can be used to extend the number of candidates. It is possible to systematically analyse the uncharacterised deafness loci and determine which early otic genes fall within such genetic intervals. Additionally, the ChIP-seq datasets for histone modification have helped in the identification of non-coding regions associated with ear genes. These chick genomic data can be converted to human coordinates and their relation to human deafness loci can be analysed. All together transcriptome analysis and ChIP-seq data could help in the identification of new deafness genes and the diagnosis of genetic forms of deafness in humans. Indeed, several of the newly identified genes are located in some of the known loci associated with hereditary hearing loss. The PPR and otic gene Homer2 as well as the epibranchial gene Nr2f2 are located in the autosomal dominant non-syndromic hearing loss locus DFNA30 (Mangino et al., 2001). Additionally, Lmx1a and the FGF-regulated chemokine Cxcl14 are related

to the dominant hearing loss loci DFNA49 and DFNA42, respectively (Moreno-Pelayo et al., 2003, Xia et al., 2002). The otic genes Zbtb16 and RERE are associated with the autosomal recessive non-syndromic hearing loss loci DFNB24 and DFNB96, respectively (Ansar et al., 2011, Khan et al., 2007). More systematic interrogation of the datasets is likely to increase the number of putative deafness related genes. However, the identification of genes early expressed in the otic placode and located in human deafness loci does not necessary mean that they are functionally important to build the inner ear. It is therefore important to test their function in otic development and in the adult inner ear.

Since cis-regulatory elements are important for the correct temporal and spatial expression of developmental genes it is likely that mutations at the enhancer level can also cause developmental defects. The SHH enhancer in the limb bud is a demonstration of this: point mutations in this element have been associated with the formation of extra digits (preaxial polydactyly) in humans (Lettice, 2003). At present few otic enhancers have been described in the literature and the histone ChIP-seq here presented is one of the first genome-wide studies aiming to characterise OEPD regulatory elements. Knowledge of the cis-regulatory regions is key for building a comprehensive gene network and understanding of how individual otic genes are regulated in time and space (e.g. Foxi3 enhancers and its upstream regulators, see Figure 6.12). After having identified otic enhancers the consequences of their loss or mutation can be studied *in vivo*. In the last few years the CRISPR/Cas9 system has been extensively used for gene editing across many species (for review see Marraffini and Sontheimer, 2010). This powerful technique could be potentially used to disrupt enhancer sequences *in vivo* and assess their function during otic development. Finally, the information about otic enhancers could be used as a guide to help in locating causative hearing loss mutations in humans (for review see Epstein, 2009, Sakabe et al., 2012).

Hearing impairment, especially in infants, can have dramatic consequences on social relationships and education of the individual. It is anticipated that around two thirds of hearing loss with childhood-onset have a genetic cause (Stamatiou and Stankovic, 2013). Despite the complexity and heterogeneity of the genetic of deafness, it is important to conduct genetic screens in order to identify babies with risk of developing hearing loss associated with a genetic cause. This not only would prepare families to the handicap but would also enable interventions, when possible (Hilgert et al., 2009). However, genetic screens cannot be reliably used until more is known about the function of the candidate

genes. It is therefore crucial to study the role of hearing loss genes in animal models. Ultimately, this knowledge could also be used for inner ear gene therapy. Gene therapy allows the specific manipulation of the causative genes by inhibition of the expression of a deleterious allele or by the introduction of a missing or downregulated gene. Even if progresses have recently been made, gene therapy is still not ready to make the transition from basic research to medicine. Some remaining issues regard safety, reliability and consistency of results from the introduction of exogenous genes in living ears. Additionally, the delivery of therapeutic agents requires invasive surgery (for review see Linden Phillips et al., 2013). However, encouraging progresses have been made towards treatment of hereditary inner ear defects in mice model for human deafness (for review see Fukui and Raphael, 2013).

In conclusion, a common region, the OEPD, gives rise to both the otic and epibranchial placodes, and along their developmental path they progressively differentiate by the mutual action of signalling and gene expression restriction. The literature based gene network was enriched with the new findings obtained from this thesis (Figure 7.1). This network recapitulates otic and epibranchial development, provides a guideline for future studies, and it could be used as a resource to identify new putative candidate genes for genetic forms of human deafness.

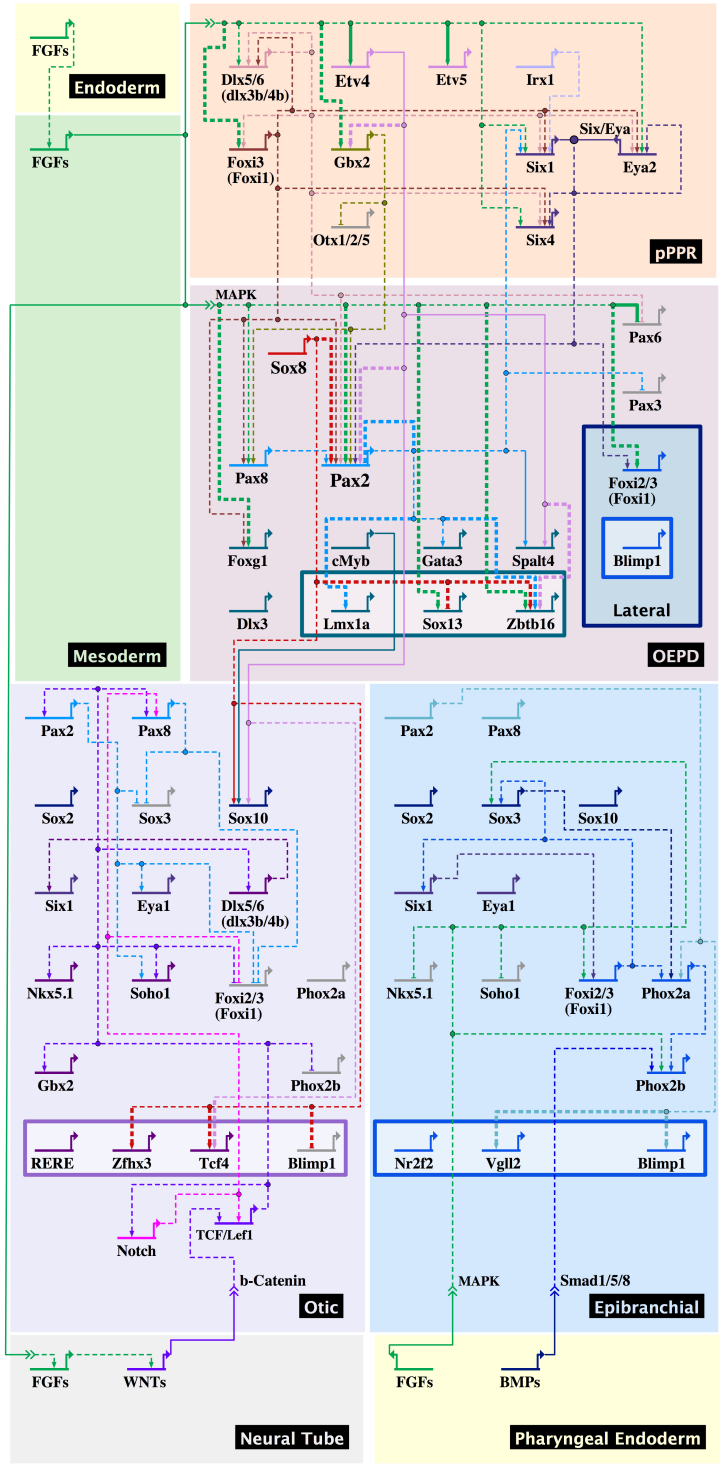

Figure 7.1 Implemented gene network regulating the segregation of the otic and epibranchial placode. The main interactions between transcription factors involved in the specification of the otic and epibranchial domain (OEPD), and later in the segregation of the otic and epibranchial placodes are summarised in a comprehensive gene regulatory network. At neurula stage in the posterior PPR (pPPR; orange) transcription factors regulate the onset of *Six/Eya*, as well as they initiate OEPD genes. The OEPD (pink and blue) is specified at around 5-somite stage in chick; *Foxi3* (Foxi1) and *Blimp1* are expressed in the more lateral domain (light blue). *Lmx1a*, *Sox13* and *Zbtb16* are newly identified OEPD genes. FGFs from the mesoderm (green) together with transcription factors promote expression of OEPD genes in the overlaying ectoderm. Sox8 appears to function upstream of *Pax2*, and positively regulates otic fate. Pax2 is regulated by several transcription factors, among them Etv4 mediates *Pax2* expression downstream of FGF. At around 11-somite stage the otic (violet) and the epibranchial (light blue) are segregated. FGF in the neural tube (grey) promotes WNT signalling, which in turns favours the otic fate. The pharyngeal endoderm (light yellow) is brought in contact with the more lateral part of the OEPD and thanks to FGF and BMP helps in the formation of the epibranchial placode. The last portion of the network summarises the main interactions taking place from 11- to 15-somite stage. *RERE*, *Zfhx3* and *Tcf4* are otic genes, while *Nr2f2* and *Vgll2* are epibranchial genes newly identified by the mRNA-seq. References for the interaction reported from the literature are presented in Table 1.1. Newly identified interactions and genes are here highlighted and refer to the present work (thick lines and genes in the boxes, respectively). Gene symbols are colour-coded accordingly to their expression domain. In the network solid lines represent experimentally verified direct interactions whereas dashed line indicates that such information is yet not available.

8. Bibliography

Abdelhak, S., Kalatzis, V., Heilig, R., Compain, S., Samson, D., Vincent, C., Weil, D., Cruaud, C., Sahly, I., Leibovici, M., Bitner-Glindzicz, M., Francis, M., Lacombe, D., Vigneron, J., Charachon, R., Boven, K., Bedbeder, P., Van Regemorter, N., Weissenbach, J. & Petit, C. 1997. A human homologue of the Drosophila eyes absent gene underlies branchio-oto-renal (BOR) syndrome and identifies a novel gene family. *Nat Genet,* 15**,** 157-64.

Abe, Y., Chen, W., Huang, W., Nishino, M. & Li, Y. P. 2006. CNBP regulates forebrain formation at organogenesis stage in chick embryos. *Dev Biol,* 295**,** 116-27.

Abello, G., Khatri, S., Giraldez, F. & Alsina, B. 2007. Early regionalization of the otic placode and its regulation by the Notch signaling pathway. *Mech Dev,* 124**,** 631-45.

Abello, G., Khatri, S., Radosevic, M., Scotting, P. J., Giraldez, F. & Alsina, B. 2010. Independent regulation of Sox3 and Lmx1b by FGF and BMP signaling influences the neurogenic and non-neurogenic domains in the chick otic placode. *Dev Biol,* 339**,** 166-78.

Abu-Elmagd, M., Ishii, Y., Cheung, M., Rex, M., Le Rouedec, D. & Scotting, P. J. 2001. cSox3 expression and neurogenesis in the epibranchial placodes. *Dev Biol,* 237**,** 258-69.

Acampora, D., Gulisano, M., Broccoli, V. & Simeone, A. 2001. Otx genes in brain morphogenesis. *Prog Neurobiol,* 64**,** 69-95.

Acampora, D., Mazan, S., Lallemand, Y., Avantaggiato, V., Maury, M., Simeone, A. & Brulet, P. 1995. Forebrain and midbrain regions are deleted in Otx2-/- mutants due to a defective anterior neuroectoderm specification during gastrulation. *Development,* 121**,** 3279-90.

Adam, J., Myat, A., Le Roux, I., Eddison, M., Henrique, D., Ish-Horowicz, D. & Lewis, J. 1998. Cell fate choices and the expression of Notch, Delta and Serrate homologues in the chick inner ear: parallels with Drosophila sense-organ development. *Development,* 125**,** 4645-54.

Adamska, Leger, S., Brand, M., Hadrys, T., Braun, T. & Bober, E. 2000. Inner ear and lateral line expression of a zebrafish Nkx5-1 gene and its downregulation in the ears of FGF8 mutant, ace. *Mech Dev,* 97**,** 161-5.

Adamska, Wolff, A., Kreusler, M., Wittbrodt, J., Braun, T. & Bober, E. 2001. Five Nkx5 genes show differential expression patterns in anlagen of sensory organs in medaka: insight into the evolution of the gene family. *Development Genes and Evolution,* 211**,** 338-349.

Adli, M. & Bernstein, B. E. 2011. Whole-genome chromatin profiling from limited numbers of cells using nano-ChIP-seq. *Nat Protoc,* 6**,** 1656-68.

Aghaallaei, N., Bajoghli, B. & Czerny, T. 2007. Distinct roles of Fgf8, Foxi1, Dlx3b and Pax8/2 during otic vesicle induction and maintenance in medaka. *Dev Biol,* 307**,** 408-20.

Ahrens, K. & Schlosser, G. 2005. Tissues and signals involved in the induction of placodal Six1 expression in Xenopus laevis. *Dev Biol,* 288**,** 40-59.

Ait-Si-Ali, S., Carlisi, D., Ramirez, S., Upegui-Gonzalez, L. C., Duquet, A., Robin, P., Rudkin, B., Harel-Bellan, A. & Trouche, D. 1999. Phosphorylation by p44 MAP Kinase/ERK1 stimulates CBP histone acetyl transferase activity in vitro. *Biochem Biophys Res Commun,* 262**,** 157-62.

Albaum, H. G. & Nestler, H. A. 1937. Xenoplastic ear induction between Rana Pipiens and Amblystoma Punctatum. *J Exp Zool* 1-35.

Albazerchi, A., Cinquin, O. & Stern, C. D. 2007. A new method to transfect the hypoblast of the chick embryo reveals conservation of the regulation of an Otx2 enhancer between mouse and chick extraembryonic endoderm. *BMC Dev Biol,* 7**,** 25.

Alliel, P. M., Seddiqi, N., Goudou, D., Cifuentes-Diaz, C., Romero, N., Velasco, E., Rieger, F. & Perin, J. P. 2000. Myoneurin, a novel member of the BTB/POZ-zinc finger family highly expressed in human muscle. *Biochem Biophys Res Commun,* 273**,** 385-91.

Altmann, C. R., Chow, R. L., Lang, R. A. & Hemmati-Brivanlou, A. 1997. Lens induction by Pax-6 in Xenopus laevis. *Dev Biol,* 185**,** 119-23.

Alvarez, Y., Alonso, M. T., Vendrell, V., Zelarayan, L. C., Chamero, P., Theil, T., Bosl, M. R., Kato, S., Maconochie, M., Riethmacher, D. & Schimmang, T. 2003. Requirements for FGF3 and FGF10 during inner ear formation. *Development,* 130**,** 6329-38.

Anders, S. & Huber, W. 2010. Differential expression analysis for sequence count data. *Genome Biol,* 11**,** R106.

Anderson, A. M., Weasner, B. M., Weasner, B. P. & Kumar, J. P. 2012. Dual transcriptional activities of SIX proteins define their roles in normal and ectopic eye development. *Development,* 139**,** 991-1000.

Andrews, S. 2010. FastQC: A quality control tool for high throughput sequence data. *Available online at:* http://www.bioinformatics.babraham.ac.uk/projects/fastqc.

Angeli, S., Lin, X. & Liu, X. Z. 2012. Genetics of hearing and deafness. *Anat Rec (Hoboken),* 295**,** 1812-29.

Ansar, M., Lee, K., Naqvi, S. K., Andrade, P. B., Basit, S., Santos-Cortez, R. L., Ahmad, W. & Leal, S. M. 2011. A new autosomal recessive nonsyndromic hearing impairment locus DFNB96 on chromosome 1p36.31-p36.13. *J Hum Genet,* 56**,** 866-8.

Ashery-Padan, R., Marquardt, T., Zhou, X. & Gruss, P. 2000. Pax6 activity in the lens primordium is required for lens formation and for correct placement of a single retina in the eye. *Genes Dev,* 14**,** 2701-11.

Asp, P., Blum, R., Vethantham, V., Parisi, F., Micsinai, M., Cheng, J., Bowman, C., Kluger, Y. & Dynlacht, B. D. 2011. Genome-wide remodeling of the epigenetic landscape during myogenic differentiation. *Proc Natl Acad Sci U S A,* 108**,** E149-58.

Azuma, N., Hirakiyama, A., Inoue, T., Asaka, A. & Yamada, M. 2000. Mutations of a human homologue of the Drosophila eyes absent gene (EYA1) detected in patients with congenital cataracts and ocular anterior segment anomalies. *Hum Mol Genet,* 9**,** 363-6.

Bailey, A. P., Bhattacharyya, S., Bronner-Fraser, M. & Streit, A. 2006. Lens specification is the ground state of all sensory placodes, from which FGF promotes olfactory identity. *Developmental Cell,* 11**,** 505-517.

Bajoghli, B., Aghaallaei, N., Heimbucher, T. & Czerny, T. 2004. An artificial promoter construct for heat-inducible misexpression during fish embryogenesis. *Dev Biol,* 271**,** 416-30.

Baker, C. V. & Bronner-Fraser, M. 2001. Vertebrate cranial placodes I. Embryonic induction. *Dev Biol,* 232**,** 1-61.

Baker, R. K. & Antin, P. B. 2003. Ephs and ephrins during early stages of chick embryogenesis. *Dev Dyn,* 228**,** 128-42.

Bally-Cuif, L., Gulisano, M., Broccoli, V. & Boncinelli, E. 1995. c-otx2 is expressed in two different phases of gastrulation and is sensitive to retinoic acid treatment in chick embryo. *Mech Dev,* 49**,** 49-63.

Bamforth, S. D., Braganca, J., Eloranta, J. J., Murdoch, J. N., Marques, F. I., Kranc, K. R., Farza, H., Henderson, D. J., Hurst, H. C. & Bhattacharya, S. 2001. Cardiac malformations, adrenal agenesis, neural crest defects and exencephaly in mice lacking Cited2, a new Tfap2 co-activator. *Nat Genet,* 29**,** 469-74.

Bang, A. G., Papalopulu, N., Kintner, C. & Goulding, M. D. 1997. Expression of Pax-3 is initiated in the early neural plate by posteriorizing signals produced by the organizer and by posterior non-axial mesoderm. *Development,* 124**,** 2075-85.

Barembaum, M. & Bronner-Fraser, M. 2007. Spalt4 mediates invagination and otic placode gene expression in cranial ectoderm. *Development,* 134**,** 3805-14.

Barembaum, M. & Bronner-Fraser, M. 2010. Pax2 and Pea3 synergize to activate a novel regulatory enhancer for spalt4 in the developing ear. *Dev Biol,* 340**,** 222-31.

Basch, M. L., Selleck, M. A. & Bronner-Fraser, M. 2000. Timing and competence of neural crest formation. *Dev Neurosci,* 22**,** 217-27.

Bassham, S., Canestro, C. & Postlethwait, J. H. 2008. Evolution of developmental roles of Pax2/5/8 paralogs after independent duplication in urochordate and vertebrate lineages. *BMC Biol,* 6**,** 35.

Battaglia, A., Carey, J. C., Cederholm, P., Viskochil, D. H., Brothman, A. R. & Galasso, C. 1999. Natural history of Wolf-Hirschhorn syndrome: experience with 15 cases. *Pediatrics,* 103**,** 830-6.

Beanan, M. J., Feledy, J. A. & Sargent, T. D. 2000. Regulation of early expression of Dlx3, a Xenopus anti-neural factor, by beta-catenin signaling. *Mech Dev,* 91**,** 227-35.

Begbie, J. 2002. Early Steps in the Production of Sensory Neurons by the Neurogenic Placodes. *Molecular and Cellular Neuroscience,* 21**,** 502-511.

Begbie, J., Brunet, J. F., Rubenstein, J. L. & Graham, A. 1999. Induction of the epibranchial placodes. *Development,* 126**,** 895-902.

Bell, K. M., Western, P. S. & Sinclair, A. H. 2000. SOX8 expression during chick embryogenesis. *Mech Dev,* 94**,** 257-60.

Bellairs, R. 1986. The primitive streak. *Anat Embryol (Berl),* 174**,** 1-14.

Bellairs, R., Lorenz, F. W. & Dunlap, T. 1978. Cleavage in the chick embryo. *J Embryol Exp Morphol,* 43**,** 55-69.

Bellefroid, E. J., Kobbe, A., Gruss, P., Pieler, T., Gurdon, J. B. & Papalopulu, N. 1998. Xiro3 encodes a Xenopus homolog of the Drosophila Iroquois genes and functions in neural specification. *EMBO J,* 17**,** 191-203.

Bellmeyer, A., Krase, J., Lindgren, J. & Labonne, C. 2003. The protooncogene c-myc is an essential regulator of neural crest formation in xenopus. *Dev Cell,* 4**,** 827-39.

Beneken, J., Tu, J. C., Xiao, B., Nuriya, M., Yuan, J. P., Worley, P. F. & Leahy, D. J. 2000. Structure of the Homer EVH1 domain-peptide complex reveals a new twist in polyproline recognition. *Neuron,* 26**,** 143-54.

Bergemann, A. D., Cole, F. & Hirschhorn, K. 2005. The etiology of Wolf-Hirschhorn syndrome. *Trends Genet,* 21**,** 188-95.

Bertocchini, F. & Stern, C. D. 2002. The hypoblast of the chick embryo positions the primitive streak by antagonizing nodal signaling. *Dev Cell,* 3**,** 735-44.

Bessarab, D. A., Chong, S. W. & Korzh, V. 2004. Expression of zebrafish six1 during sensory organ development and myogenesis. *Dev Dyn,* 230**,** 781-6.

Betancur, P., Bronner-Fraser, M. & Sauka-Spengler, T. 2010a. Assembling neural crest regulatory circuits into a gene regulatory network. *Annu Rev Cell Dev Biol,* 26**,** 581-603.

Betancur, P., Bronner-Fraser, M. & Sauka-Spengler, T. 2010b. Genomic code for Sox10 activation reveals a key regulatory enhancer for cranial neural crest. *Proc Natl Acad Sci U S A,* 107**,** 3570-5.

Betancur, P., Sauka-Spengler, T. & Bronner, M. 2011. A Sox10 enhancer element common to the otic placode and neural crest is activated by tissue-specific paralogs. *Development,* 138**,** 3689-98.

Bhatia, S., Monahan, J., Ravi, V., Gautier, P., Murdoch, E., Brenner, S., Van Heyningen, V., Venkatesh, B. & Kleinjan, D. A. 2014. A survey of ancient conserved non-

coding elements in the PAX6 locus reveals a landscape of interdigitated cis-regulatory archipelagos. *Dev Biol,* 387**,** 214-28.

Bhattacharya, S., Michels, C. L., Leung, M. K., Arany, Z. P., Kung, A. L. & Livingston, D. M. 1999. Functional role of p35srj, a novel p300/CBP binding protein, during transactivation by HIF-1. *Genes Dev,* 13**,** 64-75.

Bhattacharyya, S., Bailey, A. P., Bronner-Fraser, M. & Streit, A. 2004. Segregation of lens and olfactory precursors from a common territory: cell sorting and reciprocity of Dlx5 and Pax6 expression. *Dev Biol,* 271**,** 403-14.

Bhattacharyya, S. & Bronner, M. E. 2013. Clonal analyses in the anterior pre-placodal region: implications for the early lineage bias of placodal progenitors. *Int J Dev Biol,* 57**,** 753-7.

Bhattacharyya, S. & Bronner-Fraser, M. 2008. Competence, specification and commitment to an olfactory placode fate. *Development,* 135**,** 4165-77.

Blythe, S. A., Cha, S. W., Tadjuidje, E., Heasman, J. & Klein, P. S. 2010. beta-Catenin primes organizer gene expression by recruiting a histone H3 arginine 8 methyltransferase, Prmt2. *Dev Cell,* 19**,** 220-31.

Bohm, J., Buck, A., Borozdin, W., Mannan, A. U., Matysiak-Scholze, U., Adham, I., Schulz-Schaeffer, W., Floss, T., Wurst, W., Kohlhase, J. & Barrionuevo, F. 2008. Sall1, sall2, and sall4 are required for neural tube closure in mice. *Am J Pathol,* 173**,** 1455-63.

Bok, J., Bronner-Fraser, M. & Wu, D. K. 2005. Role of the hindbrain in dorsoventral but not anteroposterior axial specification of the inner ear. *Development,* 132**,** 2115-24.

Bok, J., Chang, W. & Wu, D. K. 2007. Patterning and morphogenesis of the vertebrate inner ear. *Int J Dev Biol,* 51**,** 521-33.

Bonini, N. M., Bui, Q. T., Gray-Board, G. L. & Warrick, J. M. 1997. The Drosophila eyes absent gene directs ectopic eye formation in a pathway conserved between flies and vertebrates. *Development,* 124**,** 4819-26.

Bonn, S., Zinzen, R. P., Girardot, C., Gustafson, E. H., Perez-Gonzalez, A., Delhomme, N., Ghavi-Helm, Y., Wilczynski, B., Riddell, A. & Furlong, E. E. 2012. Tissue-specific analysis of chromatin state identifies temporal signatures of enhancer activity during embryonic development. *Nat Genet,* 44**,** 148-56.

Borghese, E. 1942. Transplantation der chorda von neurulen unter die prasumptive rumpfepidermis mittlerer und spater gastrulen in verschiedener orientierung bei Triton. *Roux's Arch EntwMech***,** 53-82.

Bouchard, M., De Caprona, D., Busslinger, M., Xu, P. & Fritzsch, B. 2010. Pax2 and Pax8 cooperate in mouse inner ear morphogenesis and innervation. *BMC Dev Biol,* 10**,** 89.

Bovolenta, P., Mallamaci, A., Puelles, L. & Boncinelli, E. 1998. Expression pattern of cSix3, a member of the Six/sine oculis family of transcription factors. *Mech Dev,* 70**,** 201-3.

Boyle, A. P., Davis, S., Shulha, H. P., Meltzer, P., Margulies, E. H., Weng, Z., Furey, T. S. & Crawford, G. E. 2008. High-resolution mapping and characterization of open chromatin across the genome. *Cell,* 132**,** 311-22.

Brakeman, P. R., Lanahan, A. A., O'brien, R., Roche, K., Barnes, C. A., Huganir, R. L. & Worley, P. F. 1997. Homer: a protein that selectively binds metabotropic glutamate receptors. *Nature,* 386**,** 284-8.

Braun, M. M., Etheridge, A., Bernard, A., Robertson, C. P. & Roelink, H. 2003. Wnt signaling is required at distinct stages of development for the induction of the posterior forebrain. *Development,* 130**,** 5579-87.

Bricaud, O. & Collazo, A. 2006. The transcription factor six1 inhibits neuronal and promotes hair cell fate in the developing zebrafish (Danio rerio) inner ear. *J Neurosci,* 26**,** 10438-51.

Broccoli, V., Boncinelli, E. & Wurst, W. 1999. The caudal limit of Otx2 expression positions the isthmic organizer. *Nature,* 401**,** 164-8.

Brown, S. T., Wang, J. & Groves, A. K. 2005. Dlx gene expression during chick inner ear development. *J Comp Neurol,* 483**,** 48-65.

Brugmann, S. A., Pandur, P. D., Kenyon, K. L., Pignoni, F. & Moody, S. A. 2004. Six1 promotes a placodal fate within the lateral neurogenic ectoderm by functioning as both a transcriptional activator and repressor. *Development,* 131**,** 5871-81.

Buecker, C. & Wysocka, J. 2012. Enhancers as information integration hubs in development: lessons from genomics. *Trends Genet,* 28**,** 276-84.

Burton, Q., Cole, L. K., Mulheisen, M., Chang, W. & Wu, D. K. 2004. The role of Pax2 in mouse inner ear development. *Dev Biol,* 272**,** 161-75.

Callebaut, M. & Van Nueten, E. 1994. Rauber's (Koller's) sickle: the early gastrulation organizer of the avian blastoderm. *Eur J Morphol,* 32**,** 35-48.

Calo, E. & Wysocka, J. 2013. Modification of enhancer chromatin: what, how, and why? *Mol Cell,* 49**,** 825-37.

Canning, C. A., Lee, L., Luo, S. X., Graham, A. & Jones, C. M. 2008. Neural tube derived Wnt signals cooperate with FGF signaling in the formation and differentiation of the trigeminal placodes. *Neural Dev,* 3**,** 35.

Carmona-Fontaine, C., Acuna, G., Ellwanger, K., Niehrs, C. & Mayor, R. 2007. Neural crests are actively precluded from the anterior neural fold by a novel inhibitory mechanism dependent on Dickkopf1 secreted by the prechordal mesoderm. *Dev Biol,* 309**,** 208-21.

Carpenter, E. 1937. The head pattern in Amblystoma studied by vital staining and transplantation methods. *J. Exp. Zool.,* 75**,** 103-129.

Castro, L. F., Rasmussen, S. L., Holland, P. W., Holland, N. D. & Holland, L. Z. 2006. A Gbx homeobox gene in amphioxus: insights into ancestry of the ANTP class and evolution of the midbrain/hindbrain boundary. *Dev Biol,* 295**,** 40-51.

Cavodeassi, F. & Houart, C. 2012. Brain regionalization: of signaling centers and boundaries. *Dev Neurobiol,* 72**,** 218-33.

Chambers, D. & Mason, I. 2000. Expression of sprouty2 during early development of the chick embryo is coincident with known sites of FGF signalling. *Mech Dev,* 91**,** 361-4.

Chapman, S. C. 2003. Anterior identity is established in chick epiblast by hypoblast and anterior definitive endoderm. *Development,* 130**,** 5091-5101.

Chapman, S. C., Brown, R., Lees, L., Schoenwolf, G. C. & Lumsden, A. 2004. Expression analysis of chick Wnt and frizzled genes and selected inhibitors in early chick patterning. *Dev Dyn,* 229**,** 668-76.

Chapman, S. C., Collignon, J. & Schoenwolf, G. C. a. L., A. 2001. Improved method for chick whole-embryo culture using a filter paper carrier. *Dev. Dyn,* 220**,** 284–289.

Chauchereau, A., Mathieu, M., De Saintignon, J., Ferreira, R., Pritchard, L. L., Mishal, Z., Dejean, A. & Harel-Bellan, A. 2004. HDAC4 mediates transcriptional repression by the acute promyelocytic leukaemia-associated protein PLZF. *Oncogene,* 23**,** 8777-84.

Chen, B., Kim, E. H. & Xu, P. X. 2009. Initiation of olfactory placode development and neurogenesis is blocked in mice lacking both Six1 and Six4. *Dev Biol,* 326**,** 75-85.

Chen, J. & Streit, A. 2013. Induction of the inner ear: stepwise specification of otic fate from multipotent progenitors. *Hear Res,* 297**,** 3-12.

Chen, L. C., Chen, B. K., Chang, J. M. & Chang, W. C. 2004. Essential role of c-Jun induction and coactivator p300 in epidermal growth factor-induced gene expression of cyclooxygenase-2 in human epidermoid carcinoma A431 cells. *Biochim Biophys Acta,* 1683**,** 38-48.

Chen, R., Amoui, M., Zhang, Z. & Mardon, G. 1997. Dachshund and eyes absent proteins form a complex and function synergistically to induce ectopic eye development in Drosophila. *Cell,* 91**,** 893-903.

Chen, W., Jongkamonwiwat, N., Abbas, L., Eshtan, S. J., Johnson, S. L., Kuhn, S., Milo, M., Thurlow, J. K., Andrews, P. W., Marcotti, W., Moore, H. D. & Rivolta, M. N. 2012. Restoration of auditory evoked responses by human ES-cell-derived otic progenitors. *Nature,* 490**,** 278-82.

Cheyette, B. N., Green, P. J., Martin, K., Garren, H., Hartenstein, V. & Zipursky, S. L. 1994. The Drosophila sine oculis locus encodes a homeodomain-containing protein required for the development of the entire visual system. *Neuron,* 12**,** 977-96.

Choo, D., Ward, J., Reece, A., Dou, H., Lin, Z. & Greinwald, J. 2006. Molecular mechanisms underlying inner ear patterning defects in kreisler mutants. *Dev Biol,* 289**,** 308-17.

Chotteau-Lelievre, A., Desbiens, X., Pelczar, H., Defossez, P. A. & De Launoit, Y. 1997. Differential expression patterns of the PEA3 group transcription factors through murine embryonic development. *Oncogene,* 15**,** 937-52.

Chotteau-Lelievre, A., Dolle, P., Peronne, V., Coutte, L., De Launoit, Y. & Desbiens, X. 2001. Expression patterns of the Ets transcription factors from the PEA3 group during early stages of mouse development. *Mech Dev,* 108**,** 191-5.

Chow, R. L., Altmann, C. R., Lang, R. A. & Hemmati-Brivanlou, A. 1999. Pax6 induces ectopic eyes in a vertebrate. *Development,* 126**,** 4213-22.

Christophorou, N. 2008. The role of Eya2 and Six1 in early placode development. *A thesis submitted to the King's College London's Higher Degree Office in partial fulfilment for the Degree of Doctor of Philosophy.*

Christophorou, N. A., Bailey, A. P., Hanson, S. & Streit, A. 2009. Activation of Six1 target genes is required for sensory placode formation. *Dev Biol,* 336**,** 327-36.

Christophorou, N. A., Mende, M., Lleras-Forero, L., Grocott, T. & Streit, A. 2010. Pax2 coordinates epithelial morphogenesis and cell fate in the inner ear. *Dev Biol,* 345**,** 180-90.

Cifuentes-Diaz, C., Bitoun, M., Goudou, D., Seddiqi, N., Romero, N., Rieger, F., Perin, J. P. & Alliel, P. M. 2004. Neuromuscular expression of the BTB/POZ and zinc finger protein myoneurin. *Muscle Nerve,* 29**,** 59-65.

Collinson, J. M., Hill, R. E. & West, J. D. 2000. Different roles for Pax6 in the optic vesicle and facial epithelium mediate early morphogenesis of the murine eye. *Development,* 127**,** 945-56.

Cooper, S. T. & Hanson, I. M. 2005. A screen for proteins that interact with PAX6: C-terminal mutations disrupt interaction with HOMER3, DNCL1 and TRIM11. *BMC Genet,* 6**,** 43.

Corwin, J. T. 1992. Regeneration in the auditory system. *Exp Neurol,* 115**,** 7-12.

Cotanche, D. A. & Kaiser, C. L. 2010. Hair cell fate decisions in cochlear development and regeneration. *Hear Res,* 266**,** 18-25.

Couly, G. F. & Le Douarin, N. M. 1985. Mapping of the early neural primordium in quail-chick chimeras. I. Developmental relationships between placodes, facial ectoderm, and prosencephalon. *Dev Biol,* 110**,** 422-39.

Creyghton, M. P., Cheng, A. W., Welstead, G. G., Kooistra, T., Carey, B. W., Steine, E. J., Hanna, J., Lodato, M. A., Frampton, G. M., Sharp, P. A., Boyer, L. A., Young, R. A. & Jaenisch, R. 2010. Histone H3K27ac separates active from poised enhancers and predicts developmental state. *Proc Natl Acad Sci U S A,* 107**,** 21931-6.

Crossley, P. H. & Martin, G. R. 1995. The mouse Fgf8 gene encodes a family of polypeptides and is expressed in regions that direct outgrowth and patterning in the developing embryo. *Development,* 121**,** 439-51.

D'amico-Martel, A. 1982. Temporal patterns of neurogenesis in avian cranial sensory and autonomic ganglia. *Am J Anat,* 163**,** 351-72.

D'amico-Martel, A. & Noden, D. M. 1980. An autoradiographic analysis of the development of the chick trigeminal ganglion. *J Embryol Exp Morphol,* 55**,** 167-82.

D'amico-Martel, A. & Noden, D. M. 1983. Contributions of placodal and neural crest cells to avian cranial peripheral ganglia. *Am J Anat,* 166**,** 445-68.

Dailey, L., Ambrosetti, D., Mansukhani, A. & Basilico, C. 2005. Mechanisms underlying differential responses to FGF signaling. *Cytokine Growth Factor Rev,* 16**,** 233-47.

Davidson, G. 2002. Kremen proteins interact with Dickkopf1 to regulate anteroposterior CNS patterning. *Development,* 129**,** 5587-5596.

De Almeida, S. F., Grosso, A. R., Koch, F., Fenouil, R., Carvalho, S., Andrade, J., Levezinho, H., Gut, M., Eick, D., Gut, I., Andrau, J. C., Ferrier, P. & Carmo-Fonseca, M. 2011. Splicing enhances recruitment of methyltransferase HYPB/Setd2 and methylation of histone H3 Lys36. *Nat Struct Mol Biol,* 18**,** 977-83.

Dee, C. T., Hirst, C. S., Shih, Y. H., Tripathi, V. B., Patient, R. K. & Scotting, P. J. 2008. Sox3 regulates both neural fate and differentiation in the zebrafish ectoderm. *Dev Biol,* 320**,** 289-301.

Deitcher, D. L., Fekete, D. M. & Cepko, C. L. 1994. Asymmetric expression of a novel homeobox gene in vertebrate sensory organs. *J Neurosci,* 14**,** 486-98.

Delhomme, N., Padioleau, I., Furlong, E. E. & Steinmetz, L. M. 2012. easyRNASeq: a bioconductor package for processing RNA-Seq data. *Bioinformatics,* 28**,** 2532-3.

Deol, M. S. 1964. The Abnormalities of the Inner Ear in Kreisler Mice. *J Embryol Exp Morphol,* 12**,** 475-90.

Deol, M. S. 1966a. Influence of the neural tube on the differentiation of the inner ear in the mammalian embryo. *Nature,* 209**,** 219-20.

Deol, M. S. 1966b. The probable mode of gene action in the circling mutants of the mouse. *Genet Res,* 7**,** 363-71.

Deol, M. S. & Lane, P. W. 1966. A new gene affecting the morphogenesis of the vestibular part of the inner ear in the mouse. *J Embryol Exp Morphol,* 16**,** 543-58.

Doetzlhofer, A., Basch, M. L., Ohyama, T., Gessler, M., Groves, A. K. & Segil, N. 2009. Hey2 regulation by FGF provides a Notch-independent mechanism for maintaining pillar cell fate in the organ of Corti. *Dev Cell,* 16**,** 58-69.

Donner, A. L. & Maas, R. L. 2004. Conservation and non-conservation of genetic pathways in eye specification. *Int J Dev Biol,* 48**,** 743-53.

Dorak, M. T. 2006. Real-time PCR. *Taylor & Francis Group*.

Dorey, K. & Amaya, E. 2010. FGF signalling: diverse roles during early vertebrate embryogenesis. *Development,* 137**,** 3731-42.

Dude, C. M., Kuan, C. Y., Bradshaw, J. R., Greene, N. D., Relaix, F., Stark, M. R. & Baker, C. V. 2009. Activation of Pax3 target genes is necessary but not sufficient for neurogenesis in the ophthalmic trigeminal placode. *Dev Biol,* 326**,** 314-26.

Dutta, S., Dietrich, J. E., Aspock, G., Burdine, R. D., Schier, A., Westerfield, M. & Varga, Z. M. 2005. pitx3 defines an equivalence domain for lens and anterior pituitary placode. *Development,* 132**,** 1579-90.

Eagleson, G., Ferreiro, B. & Harris, W. A. 1995. Fate of the anterior neural ridge and the morphogenesis of the Xenopus forebrain. *J Neurobiol,* 28**,** 146-58.

Eagleson, G. W., Jenks, B. G. & Van Overbeeke, A. P. 1986. The pituitary adrenocorticotropes originate from neural ridge tissue in Xenopus laevis. *J Embryol Exp Morphol,* 95**,** 1-14.

Eakin, R. M. 1939. Regional determination in the development of the trout. *Roux's Arch. EntwMech.***,** 274-281.

Economou, A., Datta, P., Georgiadis, V., Cadot, S., Frenz, D. & Maconochie, M. 2013. Gata3 directly regulates early inner ear expression of Fgf10. *Dev Biol,* 374**,** 210-22.

Elms, P., Scurry, A., Davies, J., Willoughby, C., Hacker, T., Bogani, D. & Arkell, R. 2004. Overlapping and distinct expression domains of Zic2 and Zic3 during mouse gastrulation. *Gene Expr Patterns,* 4**,** 505-11.

Elms, P., Siggers, P., Napper, D., Greenfield, A. & Arkell, R. 2003. Zic2 is required for neural crest formation and hindbrain patterning during mouse development. *Dev Biol,* 264**,** 391-406.

Epstein, D. J. 2009. Cis-regulatory mutations in human disease. *Brief Funct Genomic Proteomic,* 8**,** 310-6.

Ernst, J., Kheradpour, P., Mikkelsen, T. S., Shoresh, N., Ward, L. D., Epstein, C. B., Zhang, X., Wang, L., Issner, R., Coyne, M., Ku, M., Durham, T., Kellis, M. & Bernstein, B. E. 2011. Mapping and analysis of chromatin state dynamics in nine human cell types. *Nature,* 473**,** 43-9.

Esterberg, R. & Fritz, A. 2009. dlx3b/4b are required for the formation of the preplacodal region and otic placode through local modulation of BMP activity. *Dev Biol,* 325**,** 189-99.

Esteve, P. & Bovolenta, P. 1999. cSix4, a member of the six gene family of transcription factors, is expressed during placode and somite development. *Mech Dev,* 85**,** 161-5.

Etienne-Manneville, S. & Hall, A. 2003. Cell polarity: Par6, aPKC and cytoskeletal crosstalk. *Curr Opin Cell Biol,* 15**,** 67-72.

Eyal-Giladi, H. 1984. The gradual establishment of cell commitments during the early stages of chick development. *Cell Differ,* 14**,** 245-55.

Eyal-Giladi, H., Anat, D. & Noa, H. 1992. The posterior section of the chick's area pellucida and its involvement in hypoblast and primitive streak formation. *Development,* 116**,** 819-830.

Ezin, A. M., Fraser, S. E. & Bronner-Fraser, M. 2009. Fate map and morphogenesis of presumptive neural crest and dorsal neural tube. *Dev Biol,* 330**,** 221-36.

Faber, S. C., Dimanlig, P., Makarenkova, H. P., Shirke, S., Ko, K. & Lang, R. A. 2001. Fgf receptor signaling plays a role in lens induction. *Development,* 128**,** 4425-38.

Fabian, B. & Eyal-Giladi, H. 1981. A SEM study of cell shedding during the formation of the area pellucida in the chick embryo. *J Embryol Exp Morphol,* 64**,** 11-22.

Fainsod, A., Steinbeisser, H. & De Robertis, E. M. 1994. On the function of BMP-4 in patterning the marginal zone of the Xenopus embryo. *EMBO J,* 13**,** 5015-25.

Faure, S., De Santa Barbara, P., Roberts, D. J. & Whitman, M. 2002. Endogenous patterns of BMP signaling during early chick development. *Dev Biol,* 244**,** 44-65.

Favor, J., Sandulache, R., Neuhauser-Klaus, A., Pretsch, W., Chatterjee, B., Senft, E., Wurst, W., Blanquet, V., Grimes, P., Sporle, R. & Schughart, K. 1996. The mouse Pax2(1Neu) mutation is identical to a human PAX2 mutation in a family with renal-coloboma syndrome and results in developmental defects of the brain, ear, eye, and kidney. *Proc Natl Acad Sci U S A,* 93**,** 13870-5.

Fekete, D. M. & Wu, D. K. 2002. Revisiting cell fate specification in the inner ear. *Curr Opin Neurobiol,* 12**,** 35-42.

Feledy, J. A., Beanan, M. J., Sandoval, J. J., Goodrich, J. S., Lim, J. H., Matsuo-Takasaki, M., Sato, S. M. & Sargent, T. D. 1999a. Inhibitory patterning of the anterior neural plate in Xenopus by homeodomain factors Dlx3 and Msx1. *Dev Biol,* 212**,** 455-64.

Feledy, J. A., Morasso, M. I., Jang, S. I. & Sargent, T. D. 1999b. Transcriptional activation by the homeodomain protein distal-less 3. *Nucleic Acids Res,* 27**,** 764-70.

Feng, Y. & Xu, Q. 2010. Pivotal role of hmx2 and hmx3 in zebrafish inner ear and lateral line development. *Dev Biol,* 339**,** 507-18.

Fernandez-Garre, P., Rodriguez-Gallardo, L., Gallego-Diaz, V., Alvarez, I. S. & Puelles, L. 2002. Fate map of the chicken neural plate at stage 4. *Development,* 129**,** 2807-22.

Fletcher, R. B., Baker, J. C. & Harland, R. M. 2006. FGF8 spliceforms mediate early mesoderm and posterior neural tissue formation in Xenopus. *Development,* 133**,** 1703-14.

Foa, L. & Gasperini, R. 2009. Developmental roles for Homer: more than just a pretty scaffold. *J Neurochem,* 108**,** 1-10.

Forge, A. & Wright, T. 2002. The molecular architecture of the inner ear. *Br Med Bull,* 63**,** 5-24.

Forrest, M. P., Hill, M. J., Quantock, A. J., Martin-Rendon, E. & Blake, D. J. 2014. The emerging roles of TCF4 in disease and development. *Trends Mol Med,* 20**,** 322-31.

Fortina, P. & Surrey, S. 2008. Digital mRNA profiling. *Nat Biotechnol,* 26**,** 293-4.

Freter, S., Muta, Y., Mak, S. S., Rinkwitz, S. & Ladher, R. K. 2008. Progressive restriction of otic fate: the role of FGF and Wnt in resolving inner ear potential. *Development,* 135**,** 3415-24.

Freter, S., Muta, Y., O'neill, P., Vassilev, V. S., Kuraku, S. & Ladher, R. K. 2012. Pax2 modulates proliferation during specification of the otic and epibranchial placodes. *Dev Dyn,* 241**,** 1716-28.

Friedman, R. A., Makmura, L., Biesiada, E., Wang, X. & Keithley, E. M. 2005. Eya1 acts upstream of Tbx1, Neurogenin 1, NeuroD and the neurotrophins BDNF and NT-3 during inner ear development. *Mech Dev,* 122**,** 625-34.

Fujimi, T. J., Mikoshiba, K. & Aruga, J. 2006. Xenopus Zic4: conservation and diversification of expression profiles and protein function among the Xenopus Zic family. *Dev Dyn,* 235**,** 3379-86.

Fujimoto, M., Izu, H., Seki, K., Fukuda, K., Nishida, T., Yamada, S., Kato, K., Yonemura, S., Inouye, S. & Nakai, A. 2004. HSF4 is required for normal cell growth and differentiation during mouse lens development. *EMBO J,* 23**,** 4297-306.

Fukui, H. & Raphael, Y. 2013. Gene therapy for the inner ear. *Hear Res,* 297**,** 99-105.

Furey, T. S. 2012. ChIP-seq and beyond: new and improved methodologies to detect and characterize protein-DNA interactions. *Nat Rev Genet,* 13**,** 840-52.

Furumatsu, T., Tsuda, M., Taniguchi, N., Tajima, Y. & Asahara, H. 2005a. Smad3 induces chondrogenesis through the activation of SOX9 via CREB-binding protein/p300 recruitment. *J Biol Chem,* 280**,** 8343-50.

Furumatsu, T., Tsuda, M., Yoshida, K., Taniguchi, N., Ito, T., Hashimoto, M., Ito, T. & Asahara, H. 2005b. Sox9 and p300 cooperatively regulate chromatin-mediated transcription. *J Biol Chem,* 280**,** 35203-8.

Gallagher, B. C., Henry, J. J. & Grainger, R. M. 1996. Inductive processes leading to inner ear formation during Xenopus development. *Dev Biol,* 175**,** 95-107.

Gallardo, M. E., Lopez-Rios, J., Fernaud-Espinosa, I., Granadino, B., Sanz, R., Ramos, C., Ayuso, C., Seller, M. J., Brunner, H. G., Bovolenta, P. & Rodriguez De Cordoba, S. 1999. Genomic cloning and characterization of the human homeobox gene SIX6 reveals a cluster of SIX genes in chromosome 14 and associates SIX6

hemizygosity with bilateral anophthalmia and pituitary anomalies. *Genomics,* 61**,** 82-91.

Gallera, J. & Ivanov, I. 1964. [Neurogenic Competence of the External Layer of the Chick Blastoderm as a Function of the 'Time' Factor]. *J Embryol Exp Morphol,* 12**,** 693-711.

Galli, L. M., Munji, R. N., Chapman, S. C., Easton, A., Li, L., Onguka, O., Ramahi, J. S., Suriben, R., Szabo, L. A., Teng, C., Tran, B., Hannoush, R. N. & Burrus, L. W. 2014. Frizzled10 mediates WNT1 and WNT3A signaling in the dorsal spinal cord of the developing chick embryo. *Dev Dyn,* 243**,** 833-43.

Gamse, J. T. & Sive, H. 2001. Early anteroposterior division of the presumptive neurectoderm in Xenopus. *Mech Dev,* 104**,** 21-36.

Garcia-Castro, M. I., Marcelle, C. & Bronner-Fraser, M. 2002. Ectodermal Wnt function as a neural crest inducer. *Science,* 297**,** 848-51.

Garcia-Martinez, V., Alvarez, I. S. & Schoenwolf, G. C. 1993. Locations of the ectodermal and nonectodermal subdivisions of the epiblast at stages 3 and 4 of avian gastrulation and neurulation. *J Exp Zool,* 267**,** 431-46.

Gavalas, A., Studer, M., Lumsden, A., Rijli, F. M., Krumlauf, R. & Chambon, P. 1998. Hoxa1 and Hoxb1 synergize in patterning the hindbrain, cranial nerves and second pharyngeal arch. *Development,* 125**,** 1123-36.

Geiss, G. K., Bumgarner, R. E., Birditt, B., Dahl, T., Dowidar, N., Dunaway, D. L., Fell, H. P., Ferree, S., George, R. D., Grogan, T., James, J. J., Maysuria, M., Mitton, J. D., Oliveri, P., Osborn, J. L., Peng, T., Ratcliffe, A. L., Webster, P. J., Davidson, E. H., Hood, L. & Dimitrov, K. 2008. Direct multiplexed measurement of gene expression with color-coded probe pairs. *Nat Biotechnol,* 26**,** 317-25.

Ghanbari, H., Seo, H. C., Fjose, A. & Brandli, A. W. 2001. Molecular cloning and embryonic expression of Xenopus Six homeobox genes. *Mech Dev,* 101**,** 271-7.

Ginsburg, A. S. 1946. Specific differences in the determination of the internal ear and other ectodermal organs in certain Urodela. . *C. R. (Dokl.) Acad. Sci. URSS***,** 557-560.

Ginsburg, A. S. 1995. Determination of the labyrinth in different amphibian species and its correlation with determination of the other ectoderm derivatives. *Roux's Arch Dev Biol***,** 351-358.

Giot, L., Bader, J. S., Brouwer, C., Chaudhuri, A., Kuang, B., Li, Y., Hao, Y. L., Ooi, C. E., Godwin, B., Vitols, E., Vijayadamodar, G., Pochart, P., Machineni, H., Welsh, M., Kong, Y., Zerhusen, B., Malcolm, R., Varrone, Z., Collis, A., Minto, M., Burgess, S., Mcdaniel, L., Stimpson, E., Spriggs, F., Williams, J., Neurath, K., Ioime, N., Agee, M., Voss, E., Furtak, K., Renzulli, R., Aanensen, N., Carrolla, S., Bickelhaupt, E., Lazovatsky, Y., Dasilva, A., Zhong, J., Stanyon, C. A., Finley, R. L., Jr., White, K. P., Braverman, M., Jarvie, T., Gold, S., Leach, M., Knight, J., Shimkets, R. A., Mckenna, M. P., Chant, J. & Rothberg, J. M. 2003. A protein interaction map of Drosophila melanogaster. *Science,* 302**,** 1727-36.

Giraldez, F. 1998. Regionalized organizing activity of the neural tube revealed by the regulation of lmx1 in the otic vesicle. *Dev Biol,* 203**,** 189-200.

Glavic, A., Gomez-Skarmeta, J. L. & Mayor, R. 2002. The homeoprotein Xiro1 is required for midbrain-hindbrain boundary formation. *Development,* 129**,** 1609-21.

Glavic, A., Maris Honore, S., Gloria Feijoo, C., Bastidas, F., Allende, M. L. & Mayor, R. 2004. Role of BMP signaling and the homeoprotein Iroquois in the specification of the cranial placodal field. *Dev Biol,* 272**,** 89-103.

Glover, J. N. & Harrison, S. C. 1995. Crystal structure of the heterodimeric bZIP transcription factor c-Fos-c-Jun bound to DNA. *Nature,* 373**,** 257-61.

Gomez-Skarmeta, J., De La Calle-Mustienes, E. & Modolell, J. 2001. The Wnt-activated Xiro1 gene encodes a repressor that is essential for neural development and downregulates Bmp4. *Development,* 128**,** 551-60.

Gorbunova, G. P. 1939. Concerning inductive capacity of medulla oblongata in embryos of amphibians. *Compt. Rend. Acad. Sci.U.R.S.S. ,* 23**,** 298-301.

Goriely, A., Diez Del Corral, R. & Storey, K. G. 1999. c-Irx2 expression reveals an early subdivision of the neural plate in the chick embryo. *Mech Dev,* 87**,** 203-6.

Grindley, J. C., Hargett, L. K., Hill, R. E., Ross, A. & Hogan, B. L. 1997. Disruption of PAX6 function in mice homozygous for the Pax6Sey-1Neu mutation produces abnormalities in the early development and regionalization of the diencephalon. *Mech Dev,* 64**,** 111-26.

Gritsman, K., Zhang, J., Cheng, S., Heckscher, E., Talbot, W. S. & Schier, A. F. 1999. The EGF-CFC protein one-eyed pinhead is essential for nodal signaling. *Cell,* 97**,** 121-32.

Grocott, T., Johnson, S., Bailey, A. P. & Streit, A. 2011. Neural crest cells organize the eye via TGF-beta and canonical Wnt signalling. *Nat Commun,* 2**,** 265.

Grocott, T., Tambalo, M. & Streit, A. 2012. The peripheral sensory nervous system in the vertebrate head: a gene regulatory perspective. *Dev Biol,* 370**,** 3-23.

Groves, A. K. & Bronner-Fraser, M. 2000. Competence, specification and commitment in otic placode induction. *Development,* 127**,** 3489-99.

Groves, A. K. & Fekete, D. M. 2012. Shaping sound in space: the regulation of inner ear patterning. *Development,* 139**,** 245-57.

Gruda, M. C., Kovary, K., Metz, R. & Bravo, R. 1994. Regulation of Fra-1 and Fra-2 phosphorylation differs during the cell cycle of fibroblasts and phosphorylation in vitro by MAP kinase affects DNA binding activity. *Oncogene,* 9**,** 2537-47.

Gulino, A., Di Marcotullio, L. & Screpanti, I. 2010. The multiple functions of Numb. *Exp Cell Res,* 316**,** 900-6.

Gurdon, J. B. 1987. Embryonic induction--molecular prospects. *Development,* 99**,** 285-306.

Guth, S. I., Bosl, M. R., Sock, E. & Wegner, M. 2010. Evolutionary conserved sequence elements with embryonic enhancer activity in the vicinity of the mammalian Sox8 gene. *Int J Biochem Cell Biol,* 42**,** 465-71.

Hadrys, T., Braun, T., Rinkwitz-Brandt, S., Arnold, H. H. & Bober, E. 1998. Nkx5-1 controls semicircular canal formation in the mouse inner ear. *Development,* 125**,** 33-9.

Halder, G., Callaerts, P., Flister, S., Walldorf, U., Kloter, U. & Gehring, W. J. 1998. Eyeless initiates the expression of both sine oculis and eyes absent during Drosophila compound eye development. *Development,* 125**,** 2181-91.

Hamburger, V. & Hamilton, H. L. 1951. A series of normal stages in the development of the chick embryo. *J Morphol,* 88**,** 49-92.

Hans, S., Christison, J., Liu, D. & Westerfield, M. 2007. Fgf-dependent otic induction requires competence provided by Foxi1 and Dlx3b. *BMC Dev Biol,* 7**,** 5.

Hans, S., Irmscher, A. & Brand, M. 2013. Zebrafish Foxi1 provides a neuronal ground state during inner ear induction preceding the Dlx3b/4b-regulated sensory lineage. *Development,* 140**,** 1936-45.

Hans, S., Liu, D. & Westerfield, M. 2004. Pax8 and Pax2a function synergistically in otic specification, downstream of the Foxi1 and Dlx3b transcription factors. *Development,* 131**,** 5091-102.

Hanson, I. M. 2001. Mammalian homologues of the Drosophila eye specification genes. *Semin Cell Dev Biol,* 12**,** 475-84.

Haring, M., Offermann, S., Danker, T., Horst, I., Peterhansel, C. & Stam, M. 2007. Chromatin immunoprecipitation: optimization, quantitative analysis and data normalization. *Plant Methods,* 3**,** 11.

Harrison, R. G. 1945. Relations of symmetry in the developing embryo. *Trans Conn Acad Arts Sci,* 36**,** 238-247.

Hatada, Y. & Stern, C. D. 1994. A fate map of the epiblast of the early chick embryo. *Development,* 120**,** 2879-89.

Hawley, S. H., Wunnenberg-Stapleton, K., Hashimoto, C., Laurent, M. N., Watabe, T., Blumberg, B. W. & Cho, K. W. 1995. Disruption of BMP signals in embryonic Xenopus ectoderm leads to direct neural induction. *Genes Dev,* 9**,** 2923-35.

Hebert, J. M. & Mcconnell, S. K. 2000. Targeting of cre to the Foxg1 (BF-1) locus mediates loxP recombination in the telencephalon and other developing head structures. *Dev Biol,* 222**,** 296-306.

Heintzman, N. D., Hon, G. C., Hawkins, R. D., Kheradpour, P., Stark, A., Harp, L. F., Ye, Z., Lee, L. K., Stuart, R. K., Ching, C. W., Ching, K. A., Antosiewicz-Bourget, J. E., Liu, H., Zhang, X., Green, R. D., Lobanenkov, V. V., Stewart, R., Thomson, J. A., Crawford, G. E., Kellis, M. & Ren, B. 2009. Histone modifications at human enhancers reflect global cell-type-specific gene expression. *Nature,* 459**,** 108-12.

Heintzman, N. D., Stuart, R. K., Hon, G., Fu, Y., Ching, C. W., Hawkins, R. D., Barrera, L. O., Van Calcar, S., Qu, C., Ching, K. A., Wang, W., Weng, Z., Green, R. D., Crawford, G. E. & Ren, B. 2007. Distinct and predictive chromatin signatures of transcriptional promoters and enhancers in the human genome. *Nat Genet,* 39**,** 311-8.

Heinz, S., Benner, C., Spann, N., Bertolino, E., Lin, Y. C., Laslo, P., Cheng, J. X., Murre, C., Singh, H. & Glass, C. K. 2010. Simple combinations of lineage-determining transcription factors prime cis-regulatory elements required for macrophage and B cell identities. *Mol Cell,* 38**,** 576-89.

Heisenberg, C. P., Houart, C., Take-Uchi, M., Rauch, G. J., Young, N., Coutinho, P., Masai, I., Caneparo, L., Concha, M. L., Geisler, R., Dale, T. C., Wilson, S. W. & Stemple, D. L. 2001. A mutation in the Gsk3-binding domain of zebrafish Masterblind/Axin1 leads to a fate transformation of telencephalon and eyes to diencephalon. *Genes Dev,* 15**,** 1427-34.

Heller, N. & Brandli, A. W. 1999. Xenopus Pax-2/5/8 orthologues: novel insights into Pax gene evolution and identification of Pax-8 as the earliest marker for otic and pronephric cell lineages. *Dev Genet,* 24**,** 208-19.

Hemshekhar, M., Sebastin Santhosh, M., Kemparaju, K. & Girish, K. S. 2012. Emerging roles of anacardic acid and its derivatives: a pharmacological overview. *Basic Clin Pharmacol Toxicol,* 110**,** 122-32.

Hensen, V. 1876. Beobachtungen uber die Befruchtung und Entwicklung des Kaninchens und Meerschweinchens. *Z. Anat. EntwGesch. ,* 1**,** 353-423.

Herbrand, H., Guthrie, S., Hadrys, T., Hoffmann, S., Arnold, H. H., Rinkwitz-Brandt, S. & Bober, E. 1998. Two regulatory genes, cNkx5-1 and cPax2, show different responses to local signals during otic placode and vesicle formation in the chick embryo. *Development,* 125**,** 645-54.

Herzog, W., Sonntag, C., Von Der Hardt, S., Roehl, H. H., Varga, Z. M. & Hammerschmidt, M. 2004. Fgf3 signaling from the ventral diencephalon is required for early specification and subsequent survival of the zebrafish adenohypophysis. *Development,* 131**,** 3681-92.

Hidalgo-Sanchez, M., Alvarado-Mallart, R. & Alvarez, I. S. 2000. Pax2, Otx2, Gbx2 and Fgf8 expression in early otic vesicle development. *Mech Dev,* 95**,** 225-9.

Hidalgo-Sanchez, M., Millet, S., Simeone, A. & Alvarado-Mallart, R. M. 1999. Comparative analysis of Otx2, Gbx2, Pax2, Fgf8 and Wnt1 gene expressions during the formation of the chick midbrain/hindbrain domain. *Mech Dev,* 81**,** 175-8.

Hilgert, N., Smith, R. J. & Van Camp, G. 2009. Forty-six genes causing nonsyndromic hearing impairment: which ones should be analyzed in DNA diagnostics? *Mutat Res,* 681**,** 189-96.

Hochmann, S., Aghaallaei, N., Bajoghli, B., Soroldoni, D., Carl, M. & Czerny, T. 2007. Expression of marker genes during early ear development in medaka. *Gene Expr Patterns,* 7**,** 355-62.

Hoffman, T. L., Javier, A. L., Campeau, S. A., Knight, R. D. & Schilling, T. F. 2007. Tfap2 transcription factors in zebrafish neural crest development and ectodermal evolution. *J Exp Zool B Mol Dev Evol,* 308**,** 679-91.

Hollyday, M., Mcmahon, J. A. & Mcmahon, A. P. 1995. Wnt expression patterns in chick embryo nervous system. *Mech Dev,* 52**,** 9-25.

Holmqvist, P. H. & Mannervik, M. 2013. Genomic occupancy of the transcriptional co-activators p300 and CBP. *Transcription,* 4**,** 18-23.

Holtfreter, J. 1933. Der Einfluss von Wirtsalter und verschiedenen Organbezirken auf die Differenzierung von angelagertem Gastrulaektoderm. . *Roux's Arch EntwMech***,** 619-775.

Holzschuh, J., Wada, N., Wada, C., Schaffer, A., Javidan, Y., Tallafuss, A., Bally-Cuif, L. & Schilling, T. F. 2005. Requirements for endoderm and BMP signaling in sensory neurogenesis in zebrafish. *Development,* 132**,** 3731-42.

Hong, C. S. & Saint-Jeannet, J. P. 2007. The activity of Pax3 and Zic1 regulates three distinct cell fates at the neural plate border. *Mol Biol Cell,* 18**,** 2192-202.

Hoskins, B. E., Cramer, C. H., Silvius, D., Zou, D., Raymond, R. M., Orten, D. J., Kimberling, W. J., Smith, R. J., Weil, D., Petit, C., Otto, E. A., Xu, P. X. & Hildebrandt, F. 2007. Transcription factor SIX5 is mutated in patients with branchio-oto-renal syndrome. *Am J Hum Genet,* 80**,** 800-4.

Hu, Strobl-Mazzulla, P., Sauka-Spengler, T. & Bronner, M. E. 2012. DNA methyltransferase3A as a molecular switch mediating the neural tube-to-neural crest fate transition. *Genes Dev,* 26**,** 2380-5.

Hu, M., Sun, X. J., Zhang, Y. L., Kuang, Y., Hu, C. Q., Wu, W. L., Shen, S. H., Du, T. T., Li, H., He, F., Xiao, H. S., Wang, Z. G., Liu, T. X., Lu, H., Huang, Q. H., Chen, S. J. & Chen, Z. 2010. Histone H3 lysine 36 methyltransferase Hypb/Setd2 is required for embryonic vascular remodeling. *Proc Natl Acad Sci U S A,* 107**,** 2956-61.

Huang Da, W., Sherman, B. T. & Lempicki, R. A. 2009a. Bioinformatics enrichment tools: paths toward the comprehensive functional analysis of large gene lists. *Nucleic Acids Res,* 37**,** 1-13.

Huang Da, W., Sherman, B. T. & Lempicki, R. A. 2009b. Systematic and integrative analysis of large gene lists using DAVID bioinformatics resources. *Nat Protoc,* 4**,** 44-57.

Hurd, T. W., Culbert, A. A., Webster, K. J. & Tavare, J. M. 2002. Dual role for mitogen-activated protein kinase (Erk) in insulin-dependent regulation of Fra-1 (fos-related antigen-1) transcription and phosphorylation. *Biochem J,* 368**,** 573-80.

Hutson, M. R., Lewis, J. E., Nguyen-Luu, D., Lindberg, K. H. & Barald, K. F. 1999. Expression of Pax2 and patterning of the chick inner ear. *J Neurocytol,* 28**,** 795-807.

Hwang, C. H., Simeone, A., Lai, E. & Wu, D. K. 2009. Foxg1 is required for proper separation and formation of sensory cristae during inner ear development. *Dev Dyn,* 238**,** 2725-34.

Ikeda, K., Ookawara, S., Sato, S., Ando, Z., Kageyama, R. & Kawakami, K. 2007. Six1 is essential for early neurogenesis in the development of olfactory epithelium. *Dev Biol,* 311**,** 53-68.

Ikeda, K., Watanabe, Y., Ohto, H. & Kawakami, K. 2002. Molecular Interaction and Synergistic Activation of a Promoter by Six, Eya, and Dach Proteins Mediated through CREB Binding Protein. *Molecular and Cellular Biology,* 22**,** 6759-6766.

Ikeya, M., Lee, S. M., Johnson, J. E., Mcmahon, A. P. & Takada, S. 1997. Wnt signalling required for expansion of neural crest and CNS progenitors. *Nature,* 389**,** 966-70.

Inoue, T., Ota, M., Mikoshiba, K. & Aruga, J. 2007. Zic2 and Zic3 synergistically control neurulation and segmentation of paraxial mesoderm in mouse embryo. *Dev Biol,* 306**,** 669-84.

Ishihara, T., Ikeda, K., Sato, S., Yajima, H. & Kawakami, K. 2008a. Differential expression of Eya1 and Eya2 during chick early embryonic development. *Gene Expr Patterns,* 8**,** 357-67.

Ishihara, T., Sato, S., Ikeda, K., Yajima, H. & Kawakami, K. 2008b. Multiple evolutionarily conserved enhancers control expression of Eya1. *Dev Dyn,* 237**,** 3142-56.

Ishimura, A., Maeda, R., Takeda, M., Kikkawa, M., Daar, I. O. & Maeno, M. 2000. Involvement of BMP-4/msx-1 and FGF pathways in neural induction in the Xenopus embryo. *Dev Growth Differ,* 42**,** 307-16.

Itoh, M., Kudoh, T., Dedekian, M., Kim, C. H. & Chitnis, A. B. 2002. A role for iro1 and iro7 in the establishment of an anteroposterior compartment of the ectoderm adjacent to the midbrain-hindbrain boundary. *Development,* 129**,** 2317-27.

Jacobson, A. G. 1963a. The Determination and Positioning of the Nose, Lens and Ear. I. Interactions within the Ectoderm, and between the Ectoderm and Underlying Tissues. *J Exp Zool,* 154**,** 273-83.

Jacobson, A. G. 1963b. The Determination and Positioning of the Nose, Lens and Ear. Ii. The Role of the Endoderm. *J Exp Zool,* 154**,** 285-91.

Jacobson, A. G. 1963c. The Determination and Positioning of the Nose, Lens and Ear. Iii. Effects of Reversing the Antero-Posterior Axis of Epidermis, Neural Plate and Neural Fold. *J Exp Zool,* 154**,** 293-303.

Jacobson, A. G. & Sater, A. K. 1988. Features of embryonic induction. *Development,* 104**,** 341-59.

Jacques-Fricke, B. T., Roffers-Agarwal, J. & Gammill, L. S. 2012. DNA methyltransferase 3b is dispensable for mouse neural crest development. *PLoS One,* 7**,** e47794.

Jayasena, C. S., Ohyama, T., Segil, N. & Groves, A. K. 2008. Notch signaling augments the canonical Wnt pathway to specify the size of the otic placode. *Development,* 135**,** 2251-61.

Jemc, J. & Rebay, I. 2007. Identification of transcriptional targets of the dual-function transcription factor/phosphatase eyes absent. *Dev Biol,* 310**,** 416-29.

Johnson, K. R., Cook, S. A., Erway, L. C., Matthews, A. N., Sanford, L. P., Paradies, N. E. & Friedman, R. A. 1999. Inner ear and kidney anomalies caused by IAP insertion in an intron of the Eya1 gene in a mouse model of BOR syndrome. *Hum Mol Genet,* 8**,** 645-53.

Joyner, A. L., Liu, A. & Millet, S. 2000. Otx2, Gbx2 and Fgf8 interact to position and maintain a mid-hindbrain organizer. *Curr Opin Cell Biol,* 12**,** 736-41.

Kaan, H. W. 1926. Experiments on the development of the ear of Amblystoma punctatum. *J Exp Zool***,** 13-61.

Kaji, T. & Artinger, K. B. 2004. dlx3b and dlx4b function in the development of Rohon-Beard sensory neurons and trigeminal placode in the zebrafish neurula. *Dev Biol,* 276**,** 523-40.

Karabagli, H., Karabagli, P., Ladher, R. K. & Schoenwolf, G. C. 2002. Comparison of the expression patterns of several fibroblast growth factors during chick gastrulation and neurulation. *Anat Embryol (Berl),* 205**,** 365-70.

Karamouzis, M. V., Konstantinopoulos, P. A. & Papavassiliou, A. G. 2007. Roles of CREB-binding protein (CBP)/p300 in respiratory epithelium tumorigenesis. *Cell Res,* 17**,** 324-32.

Karlstrom, R. O., Talbot, W. S. & Schier, A. F. 1999. Comparative synteny cloning of zebrafish you-too: mutations in the Hedgehog target gli2 affect ventral forebrain patterning. *Genes Dev,* 13**,** 388-93.

Katahira, T., Sato, T., Sugiyama, S., Okafuji, T., Araki, I., Funahashi, J. & Nakamura, H. 2000. Interaction between Otx2 and Gbx2 defines the organizing center for the optic tectum. *Mech Dev,* 91**,** 43-52.

Kavak, E., Najafov, A., Ozturk, N., Seker, T., Cavusoglu, K., Aslan, T., Duru, A. D., Saygili, T., Hoxhaj, G., Hiz, M. C., Unal, D. O., Birgul-Iyison, N., Ozturk, M. & Koman, A. 2010. Analysis of the Wnt/B-catenin/TCF4 pathway using SAGE, genome-wide microarray and promoter analysis: Identification of BRI3 and HSF2 as novel targets. *Cell Signal,* 22**,** 1523-35.

Keller, R. E. 1975. Vital dye mapping of the gastrula and neurula of Xenopus laevis. I. Prospective areas and morphogenetic movements of the superficial layer. *Dev Biol,* 42**,** 222-41.

Keller, R. E. 1976. Vital dye mapping of the gastrula and neurula of Xenopus laevis. II. Prospective areas and morphogenetic movements of the deep layer. *Dev Biol,* 51**,** 118-37.

Kelley, M. W. 2006. Regulation of cell fate in the sensory epithelia of the inner ear. *Nat Rev Neurosci,* 7**,** 837-49.

Kenyon, K. L., Li, D. J., Clouser, C., Tran, S. & Pignoni, F. 2005a. Fly SIX-type homeodomain proteins Sine oculis and Optix partner with different cofactors during eye development. *Dev Dyn,* 234**,** 497-504.

Kenyon, K. L., Yang-Zhou, D., Cai, C. Q., Tran, S., Clouser, C., Decene, G., Ranade, S. & Pignoni, F. 2005b. Partner specificity is essential for proper function of the SIX-type homeodomain proteins Sine oculis and Optix during fly eye development. *Dev Biol,* 286**,** 158-68.

Khan, M. A., Soto-Jimenez, L. M., Howe, T., Streit, A., Sosinsky, A. & Stern, C. D. 2013. Computational tools and resources for prediction and analysis of gene regulatory regions in the chick genome. *Genesis,* 51**,** 311-24.

Khan, S. Y., Ahmed, Z. M., Shabbir, M. I., Kitajiri, S., Kalsoom, S., Tasneem, S., Shayiq, S., Ramesh, A., Srisailpathy, S., Khan, S. N., Smith, R. J., Riazuddin, S., Friedman, T. B. & Riazuddin, S. 2007. Mutations of the RDX gene cause nonsyndromic hearing loss at the DFNB24 locus. *Hum Mutat,* 28**,** 417-23.

Kharchenko, P. V., Alekseyenko, A. A., Schwartz, Y. B., Minoda, A., Riddle, N. C., Ernst, J., Sabo, P. J., Larschan, E., Gorchakov, A. A., Gu, T., Linder-Basso, D., Plachetka, A., Shanower, G., Tolstorukov, M. Y., Luquette, L. J., Xi, R., Jung, Y. L., Park, R. W., Bishop, E. P., Canfield, T. K., Sandstrom, R., Thurman, R. E., Macalpine, D. M., Stamatoyannopoulos, J. A., Kellis, M., Elgin, S. C., Kuroda, M. I., Pirrotta, V., Karpen, G. H. & Park, P. J. 2011. Comprehensive analysis of the chromatin landscape in Drosophila melanogaster. *Nature,* 471**,** 480-5.

Khatri, S. B., Edlund, R. K. & Groves, A. K. 2014. Foxi3 is necessary for the induction of the chick otic placode in response to FGF signaling. *Dev Biol,* 391**,** 158-69.

Khatri, S. B. & Groves, A. K. 2013. Expression of the Foxi2 and Foxi3 transcription factors during development of chicken sensory placodes and pharyngeal arches. *Gene Expr Patterns,* 13**,** 38-42.

Khudyakov, J. & Bronner-Fraser, M. 2009. Comprehensive spatiotemporal analysis of early chick neural crest network genes. *Dev Dyn,* 238**,** 716-23.

Kiecker, C. & Niehrs, C. 2001. A morphogen gradient of Wnt/beta-catenin signalling regulates anteroposterior neural patterning in Xenopus. *Development,* 128**,** 4189-201.

Kiefer, S. M., Mcdill, B. W., Yang, J. & Rauchman, M. 2002. Murine Sall1 represses transcription by recruiting a histone deacetylase complex. *J Biol Chem,* 277**,** 14869-76.

Kiernan, A. E., Nunes, F., Wu, D. K. & Fekete, D. M. 1997. The expression domain of two related homeobox genes defines a compartment in the chicken inner ear that may be involved in semicircular canal formation. *Dev Biol,* 191**,** 215-29.

Kil, S. H., Streit, A., Brown, S. T., Agrawal, N., Collazo, A., Zile, M. H. & Groves, A. K. 2005. Distinct roles for hindbrain and paraxial mesoderm in the induction and

patterning of the inner ear revealed by a study of vitamin-A-deficient quail. *Dev Biol,* 285**,** 252-71.

Kim, C. H., Oda, T., Itoh, M., Jiang, D., Artinger, K. B., Chandrasekharappa, S. C., Driever, W. & Chitnis, A. B. 2000. Repressor activity of Headless/Tcf3 is essential for vertebrate head formation. *Nature,* 407**,** 913-6.

Kim, T. K., Hemberg, M., Gray, J. M., Costa, A. M., Bear, D. M., Wu, J., Harmin, D. A., Laptewicz, M., Barbara-Haley, K., Kuersten, S., Markenscoff-Papadimitriou, E., Kuhl, D., Bito, H., Worley, P. F., Kreiman, G. & Greenberg, M. E. 2010. Widespread transcription at neuronal activity-regulated enhancers. *Nature,* 465**,** 182-7.

Kimmel, C. B., Warga, R. M. & Schilling, T. F. 1990. Origin and organization of the zebrafish fate map. *Development,* 108**,** 581-94.

Kimura, H. 2013. Histone modifications for human epigenome analysis. *J Hum Genet,* 58**,** 439-45.

Klesert, T. R., Cho, D. H., Clark, J. I., Maylie, J., Adelman, J., Snider, L., Yuen, E. C., Soriano, P. & Tapscott, S. J. 2000. Mice deficient in Six5 develop cataracts: implications for myotonic dystrophy. *Nat Genet,* 25**,** 105-9.

Knight, R. D., Nair, S., Nelson, S. S., Afshar, A., Javidan, Y., Geisler, R., Rauch, G. J. & Schilling, T. F. 2003. lockjaw encodes a zebrafish tfap2a required for early neural crest development. *Development,* 130**,** 5755-68.

Kobayashi, M., Nishikawa, K., Suzuki, T. & Yamamoto, M. 2001. The homeobox protein Six3 interacts with the Groucho corepressor and acts as a transcriptional repressor in eye and forebrain formation. *Dev Biol,* 232**,** 315-26.

Kobayashi, M., Osanai, H., Kawakami, K. & Yamamoto, M. 2000. Expression of three zebrafish Six4 genes in the cranial sensory placodes and the developing somites. *Mech Dev,* 98**,** 151-5.

Kochav, S., Ginsburg, M. & Eyal-Giladi, H. 1980. From cleavage to primitive streak formation: a complementary normal table and a new look at the first stages of the development of the chick. II. Microscopic anatomy and cell population dynamics. *Dev Biol,* 79**,** 296-308.

Koehler, K. R. & Hashino, E. 2014. 3D mouse embryonic stem cell culture for generating inner ear organoids. *Nat Protoc,* 9**,** 1229-44.

Koehler, K. R., Mikosz, A. M., Molosh, A. I., Patel, D. & Hashino, E. 2013. Generation of inner ear sensory epithelia from pluripotent stem cells in 3D culture. *Nature,* 500**,** 217-21.

Kohlhase, J., Chitayat, D., Kotzot, D., Ceylaner, S., Froster, U. G., Fuchs, S., Montgomery, T. & Rosler, B. 2005. SALL4 mutations in Okihiro syndrome (Duane-radial ray syndrome), acro-renal-ocular syndrome, and related disorders. *Hum Mutat,* 26**,** 176-83.

Koller, C. 1882. Untersuchungen uber die Blatterbildung im Huhnerkeim. . *Arch. Mikr. Anat.,* 20**,** 174-211.

Kondoh, H., Uchikawa, M., Yoda, H., Takeda, H., Furutani-Seiki, M. & Karlstrom, R. O. 2000. Zebrafish mutations in Gli-mediated hedgehog signaling lead to lens transdifferentiation from the adenohypophysis anlage. *Mech Dev,* 96**,** 165-74.

Konishi, Y., Ikeda, K., Iwakura, Y. & Kawakami, K. 2006. Six1 and Six4 promote survival of sensory neurons during early trigeminal gangliogenesis. *Brain Res,* 1116**,** 93-102.

Koster, R. W., Kuhnlein, R. P. & Wittbrodt, J. 2000. Ectopic Sox3 activity elicits sensory placode formation. *Mech Dev,* 95**,** 175-87.

Kozlowski, D. J., Murakami, T., Ho, R. K. & Weinberg, E. S. 1997. Regional cell movement and tissue patterning in the zebrafish embryo revealed by fate mapping with caged fluorescein. *Biochem Cell Biol,* 75**,** 551-62.

Kozlowski, D. J., Whitfield, T. T., Hukriede, N. A., Lam, W. K. & Weinberg, E. S. 2005. The zebrafish dog-eared mutation disrupts eya1, a gene required for cell survival and differentiation in the inner ear and lateral line. *Dev Biol,* 277**,** 27-41.

Krauss, S., Johansen, T., Korzh, V. & Fjose, A. 1991. Expression of the zebrafish paired box gene pax[zf-b] during early neurogenesis. *Development,* 113**,** 1193-206.

Kroll, K. L., Salic, A. N., Evans, L. M. & Kirschner, M. W. 1998. Geminin, a neuralizing molecule that demarcates the future neural plate at the onset of gastrulation. *Development,* 125**,** 3247-58.

Krug, P., Moriniere, V., Marlin, S., Koubi, V., Gabriel, H. D., Colin, E., Bonneau, D., Salomon, R., Antignac, C. & Heidet, L. 2011. Mutation screening of the EYA1, SIX1, and SIX5 genes in a large cohort of patients harboring branchio-oto-renal syndrome calls into question the pathogenic role of SIX5 mutations. *Hum Mutat,* 32**,** 183-90.

Kwak, S. J., Phillips, B. T., Heck, R. & Riley, B. B. 2002. An expanded domain of fgf3 expression in the hindbrain of zebrafish valentino mutants results in mis-patterning of the otic vesicle. *Development,* 129**,** 5279-87.

Kwon, H. J., Bhat, N., Sweet, E. M., Cornell, R. A. & Riley, B. B. 2010. Identification of early requirements for preplacodal ectoderm and sensory organ development. *PLoS Genet,* 6**,** e1001133.

Labonne, C. & Bronner-Fraser, M. 1998. Neural crest induction in Xenopus: evidence for a two-signal model. *Development,* 125**,** 2403-14.

Laclef, C., Souil, E., Demignon, J. & Maire, P. 2003. Thymus, kidney and craniofacial abnormalities in Six1 deficient mice. *Mechanisms of Development,* 120**,** 669-679.

Ladher, R. K., Anakwe, K. U., Gurney, A. L., Schoenwolf, G. C. & Francis-West, P. H. 2000. Identification of synergistic signals initiating inner ear development. *Science,* 290**,** 1965-7.

Ladher, R. K., O'neill, P. & Begbie, J. 2010. From shared lineage to distinct functions: the development of the inner ear and epibranchial placodes. *Development,* 137**,** 1777-85.

Ladher, R. K., Wright, T. J., Moon, A. M., Mansour, S. L. & Schoenwolf, G. C. 2005. FGF8 initiates inner ear induction in chick and mouse. *Genes Dev,* 19**,** 603-13.

Lagutin, O., Zhu, C. C., Furuta, Y., Rowitch, D. H., Mcmahon, A. P. & Oliver, G. 2001. Six3 promotes the formation of ectopic optic vesicle-like structures in mouse embryos. *Dev Dyn,* 221**,** 342-9.

Lagutin, O. V., Zhu, C. C., Kobayashi, D., Topczewski, J., Shimamura, K., Puelles, L., Russell, H. R., Mckinnon, P. J., Solnica-Krezel, L. & Oliver, G. 2003. Six3 repression of Wnt signaling in the anterior neuroectoderm is essential for vertebrate forebrain development. *Genes Dev,* 17**,** 368-79.

Landacre, F. L. 1912. The epibranchial placodes of lepidosteus osseus and their relation to the cerebral ganglia. *The Journal of Comparative Neurology***,** 1-69.

Lassiter, R. N., Dude, C. M., Reynolds, S. B., Winters, N. I., Baker, C. V. & Stark, M. R. 2007. Canonical Wnt signaling is required for ophthalmic trigeminal placode cell fate determination and maintenance. *Dev Biol,* 308**,** 392-406.

Lassiter, R. N., Reynolds, S. B., Marin, K. D., Mayo, T. F. & Stark, M. R. 2009. FGF signaling is essential for ophthalmic trigeminal placode cell delamination and differentiation. *Dev Dyn,* 238**,** 1073-82.

Lawoko-Kerali, G., Rivolta, M. N. & Holley, M. 2002. Expression of the transcription factors GATA3 and Pax2 during development of the mammalian inner ear. *J Comp Neurol,* 442**,** 378-91.

Lawoko-Kerali, G., Rivolta, M. N., Lawlor, P., Cacciabue-Rivolta, D. I., Langton-Hewer, C., Van Doorninck, J. H. & Holley, M. C. 2004. GATA3 and NeuroD distinguish auditory and vestibular neurons during development of the mammalian inner ear. *Mech Dev,* 121**,** 287-99.

Lawson, K. A. 1999. Fate mapping the mouse embryo. *Int J Dev Biol,* 43**,** 773-5.

Lee, S. A. 2003. The zebrafish forkhead transcription factor Foxi1 specifies epibranchial placode-derived sensory neurons. *Development,* 130**,** 2669-2679.

Leger, S. & Brand, M. 2002. Fgf8 and Fgf3 are required for zebrafish ear placode induction, maintenance and inner ear patterning. *Mech Dev,* 119**,** 91-108.

Leppa, S., Saffrich, R., Ansorge, W. & Bohmann, D. 1998. Differential regulation of c-Jun by ERK and JNK during PC12 cell differentiation. *EMBO J,* 17**,** 4404-13.

Lettice, L. A. 2003. A long-range Shh enhancer regulates expression in the developing limb and fin and is associated with preaxial polydactyly. *Human Molecular Genetics,* 12**,** 1725-1735.

Levi-Montalcini, R. 1946. Ricerche sperimentali sulla determinazione del placode otico nell'embrione di pollo. *Rend Acad Naz Lincei Ser,* 1**,** 443-448.

Li, B., Kuriyama, S., Moreno, M. & Mayor, R. 2009. The posteriorizing gene Gbx2 is a direct target of Wnt signalling and the earliest factor in neural crest induction. *Development,* 136**,** 3267-78.

Li, H., Liu, H., Corrales, C. E., Mutai, H. & Heller, S. 2004. Correlation of Pax-2 expression with cell proliferation in the developing chicken inner ear. *J Neurobiol,* 60**,** 61-70.

Li, H. S., Yang, J. M., Jacobson, R. D., Pasko, D. & Sundin, O. 1994. Pax-6 is first expressed in a region of ectoderm anterior to the early neural plate: implications for stepwise determination of the lens. *Dev Biol,* 162**,** 181-94.

Li, W. & Cornell, R. A. 2007. Redundant activities of Tfap2a and Tfap2c are required for neural crest induction and development of other non-neural ectoderm derivatives in zebrafish embryos. *Dev Biol,* 304**,** 338-54.

Li, X., Oghi, K. A., Zhang, J., Krones, A., Bush, K. T., Glass, C. K., Nigam, S. K., Aggarwal, A. K., Maas, R., Rose, D. W. & Rosenfeld, M. G. 2003. Eya protein phosphatase activity regulates Six1-Dach-Eya transcriptional effects in mammalian organogenesis. *Nature,* 426**,** 247-54.

Li, X., Perissi, V., Liu, F., Rose, D. W. & Rosenfeld, M. G. 2002. Tissue-specific regulation of retinal and pituitary precursor cell proliferation. *Science,* 297**,** 1180-3.

Liem, K. F., Jr., Tremml, G., Roelink, H. & Jessell, T. M. 1995. Dorsal differentiation of neural plate cells induced by BMP-mediated signals from epidermal ectoderm. *Cell,* 82**,** 969-79.

Lillevali, K., Haugas, M., Matilainen, T., Pussinen, C., Karis, A. & Salminen, M. 2006. Gata3 is required for early morphogenesis and Fgf10 expression during otic development. *Mech Dev,* 123**,** 415-29.

Lillevali, K., Haugas, M., Pituello, F. & Salminen, M. 2007. Comparative analysis of Gata3 and Gata2 expression during chicken inner ear development. *Dev Dyn,* 236**,** 306-13.

Lillevali, K., Matilainen, T., Karis, A. & Salminen, M. 2004. Partially overlapping expression of Gata2 and Gata3 during inner ear development. *Dev Dyn,* 231**,** 775-81.

Lim, Y. M., Hayashi, S. & Tsuda, L. 2012. Ebi/AP-1 suppresses pro-apoptotic genes expression and permits long-term survival of Drosophila sensory neurons. *PLoS One,* 7**,** e37028.

Linden Phillips, L., Bitner-Glindzicz, M., Lench, N., Steel, K. P., Langford, C., Dawson, S. J., Davis, A., Simpson, S. & Packer, C. 2013. The future role of genetic screening to detect newborns at risk of childhood-onset hearing loss. *Int J Audiol,* 52**,** 124-33.

Litsiou, A., Hanson, S. & Streit, A. 2005. A balance of FGF, BMP and WNT signalling positions the future placode territory in the head. *Development,* 132**,** 4051-62.

Liu, A. & Joyner, A. L. 2001. EN and GBX2 play essential roles downstream of FGF8 in patterning the mouse mid/hindbrain region. *Development,* 128**,** 181-91.

Liu, D., Chu, H., Maves, L., Yan, Y. L., Morcos, P. A., Postlethwait, J. H. & Westerfield, M. 2003. Fgf3 and Fgf8 dependent and independent transcription factors are required for otic placode specification. *Development,* 130**,** 2213-24.

Liu, W., Lagutin, O. V., Mende, M., Streit, A. & Oliver, G. 2006. Six3 activation of Pax6 expression is essential for mammalian lens induction and specification. *EMBO J,* 25**,** 5383-95.

Lleras-Forero, L. 2011. Novel roles for neuropeptides in early sensory organ development. *A thesis submitted to the King's College London's Higher Degree Office in partial fulfilment for the Degree of Doctor of Philosophy*.

Lleras-Forero, L., Tambalo, M., Christophorou, N., Chambers, D., Houart, C. & Streit, A. 2013. Neuropeptides: developmental signals in placode progenitor formation. *Dev Cell,* 26**,** 195-203.

Lombardo, A., Isaacs, H. V. & Slack, J. M. 1998. Expression and functions of FGF-3 in Xenopus development. *Int J Dev Biol,* 42**,** 1101-7.

Lombardo, A. & Slack, J. M. 1998. Postgastrulation effects of fibroblast growth factor on Xenopus development. *Dev Dyn,* 212**,** 75-85.

Lopez-Bergami, P., Huang, C., Goydos, J. S., Yip, D., Bar-Eli, M., Herlyn, M., Smalley, K. S., Mahale, A., Eroshkin, A., Aaronson, S. & Ronai, Z. 2007. Rewired ERK-JNK signaling pathways in melanoma. *Cancer Cell,* 11**,** 447-60.

Lunn, J. S., Fishwick, K. J., Halley, P. A. & Storey, K. G. 2007. A spatial and temporal map of FGF/Erk1/2 activity and response repertoires in the early chick embryo. *Developmental Biology,* 302**,** 536-552.

Luo, T., Lee, Y. H., Saint-Jeannet, J. P. & Sargent, T. D. 2003. Induction of neural crest in Xenopus by transcription factor AP2alpha. *Proc Natl Acad Sci U S A,* 100**,** 532-7.

Luo, T., Matsuo-Takasaki, M., Lim, J. H. & Sargent, T. D. 2001a. Differential regulation of Dlx gene expression by a BMP morphogenetic gradient. *Int J Dev Biol,* 45**,** 681-4.

Luo, T., Matsuo-Takasaki, M. & Sargent, T. D. 2001b. Distinct roles for Distal-less genes Dlx3 and Dlx5 in regulating ectodermal development in Xenopus. *Mol Reprod Dev,* 60**,** 331-7.

Luo, T., Matsuo-Takasaki, M., Thomas, M. L., Weeks, D. L. & Sargent, T. D. 2002. Transcription factor AP-2 is an essential and direct regulator of epidermal development in Xenopus. *Dev Biol,* 245**,** 136-44.

Machon, O., Kreslova, J., Ruzickova, J., Vacik, T., Klimova, L., Fujimura, N., Lachova, J. & Kozmik, Z. 2010. Lens morphogenesis is dependent on Pax6-mediated inhibition of the canonical Wnt/beta-catenin signaling in the lens surface ectoderm. *Genesis,* 48**,** 86-95.

Mackereth, M. D., Kwak, S. J., Fritz, A. & Riley, B. B. 2005. Zebrafish pax8 is required for otic placode induction and plays a redundant role with Pax2 genes in the maintenance of the otic placode. *Development,* 132**,** 371-82.

Maeda, R., Kobayashi, A., Sekine, R., Lin, J. J., Kung, H. & Maeno, M. 1997. Xmsx-1 modifies mesodermal tissue pattern along dorsoventral axis in Xenopus laevis embryo. *Development,* 124**,** 2553-60.

Mahmood, R., Kiefer, P., Guthrie, S., Dickson, C. & Mason, I. 1995. Multiple roles for FGF-3 during cranial neural development in the chicken. *Development,* 121**,** 1399-410.

Mangino, M., Flex, E., Capon, F., Sangiuolo, F., Carraro, E., Gualandi, F., Mazzoli, M., Martini, A., Novelli, G. & Dallapiccola, B. 2001. Mapping of a new autosomal dominant nonsyndromic hearing loss locus (DFNA30) to chromosome 15q25-26. *Eur J Hum Genet,* 9**,** 667-71.

Mao, B., Wu, W., Davidson, G., Marhold, J., Li, M., Mechler, B. M., Delius, H., Hoppe, D., Stannek, P., Walter, C., Glinka, A. & Niehrs, C. 2002. Kremen proteins are Dickkopf receptors that regulate Wnt/beta-catenin signalling. *Nature,* 417**,** 664-7.

Mardon, G., Solomon, N. M. & Rubin, G. M. 1994. dachshund encodes a nuclear protein required for normal eye and leg development in Drosophila. *Development,* 120**,** 3473-86.

Mark, M., Lufkin, T., Vonesch, J. L., Ruberte, E., Olivo, J. C., Dolle, P., Gorry, P., Lumsden, A. & Chambon, P. 1993. Two rhombomeres are altered in Hoxa-1 mutant mice. *Development,* 119**,** 319-38.

Maroon, H., Walshe, J., Mahmood, R., Kiefer, P., Dickson, C. & Mason, I. 2002. Fgf3 and Fgf8 are required together for formation of the otic placode and vesicle. *Development,* 129**,** 2099-108.

Marraffini, L. A. & Sontheimer, E. J. 2010. CRISPR interference: RNA-directed adaptive immunity in bacteria and archaea. *Nat Rev Genet,* 11**,** 181-90.

Martin, K. & Groves, A. K. 2006. Competence of cranial ectoderm to respond to Fgf signaling suggests a two-step model of otic placode induction. *Development,* 133**,** 877-87.

Martins-Taylor, K., Schroeder, D. I., Lasalle, J. M., Lalande, M. & Xu, R. H. 2012. Role of DNMT3B in the regulation of early neural and neural crest specifiers. *Epigenetics,* 7**,** 71-82.

Maston, G. A., Landt, S. G., Snyder, M. & Green, M. R. 2012. Characterization of enhancer function from genome-wide analyses. *Annu Rev Genomics Hum Genet,* 13**,** 29-57.

Materna, S. C. & Oliveri, P. 2008. A protocol for unraveling gene regulatory networks. *Nat Protoc,* 3**,** 1876-87.

Matsuo-Takasaki, M., Matsumura, M. & Sasai, Y. 2005. An essential role of Xenopus Foxi1a for ventral specification of the cephalic ectoderm during gastrulation. *Development,* 132**,** 3885-94.

Maulding, K., Padanad, M. S., Dong, J. & Riley, B. B. 2014. Mesodermal Fgf10b cooperates with other Fgfs during induction of otic and epibranchial placodes in zebrafish. *Dev Dyn*.

Maves, L., Jackman, W. & Kimmel, C. B. 2002. FGF3 and FGF8 mediate a rhombomere 4 signaling activity in the zebrafish hindbrain. *Development,* 129**,** 3825-37.

Mayor, R., Guerrero, N. & Martinez, C. 1997. Role of FGF and noggin in neural crest induction. *Dev Biol,* 189**,** 1-12.

Mccabe, K. L. & Bronner-Fraser, M. 2008. Essential role for PDGF signaling in ophthalmic trigeminal placode induction. *Development,* 135**,** 1863-74.

Mccarroll, M. N., Lewis, Z. R., Culbertson, M. D., Martin, B. L., Kimelman, D. & Nechiporuk, A. V. 2012. Graded levels of Pax2a and Pax8 regulate cell differentiation during sensory placode formation. *Development,* 139**,** 2740-50.

Mccarroll, M. N. & Nechiporuk, A. V. 2013. Fgf3 and Fgf10a work in concert to promote maturation of the epibranchial placodes in zebrafish. *PLoS One,* 8**,** e85087.

Mccauley, D. W. & Bronner-Fraser, M. 2002. Conservation of Pax gene expression in ectodermal placodes of the lamprey. *Gene,* 287**,** 129-39.

Mckay, I. J., Lewis, J. & Lumsden, A. 1996. The role of FGF-3 in early inner ear development: an analysis in normal and kreisler mutant mice. *Dev Biol,* 174**,** 370-8.

Mclarren, K. W., Litsiou, A. & Streit, A. 2003. DLX5 positions the neural crest and preplacode region at the border of the neural plate. *Developmental Biology,* 259**,** 34-47.

Mcmahon, A. R. & Merzdorf, C. S. 2010. Expression of the zic1, zic2, zic3, and zic4 genes in early chick embryos. *BMC Res Notes,* 3**,** 167.

Medina, M., Di Lella, F., Di Trapani, G., Prasad, S. C., Bacciu, A., Aristegui, M., Russo, A. & Sanna, M. 2014. Cochlear implantation versus auditory brainstem implantation in bilateral total deafness after head trauma: personal experience and review of the literature. *Otol Neurotol,* 35**,** 260-70.

Melnick, A., Ahmad, K. F., Arai, S., Polinger, A., Ball, H., Borden, K. L., Carlile, G. W., Prive, G. G. & Licht, J. D. 2000. In-depth mutational analysis of the promyelocytic leukemia zinc finger BTB/POZ domain reveals motifs and residues required for biological and transcriptional functions. *Mol Cell Biol,* 20**,** 6550-67.

Melnick, A., Carlile, G., Ahmad, K. F., Kiang, C. L., Corcoran, C., Bardwell, V., Prive, G. G. & Licht, J. D. 2002. Critical Residues within the BTB Domain of PLZF and Bcl-6 Modulate Interaction with Corepressors. *Molecular and Cellular Biology,* 22**,** 1804-1818.

Mende, M., Christophorou, N. A. & Streit, A. 2008. Specific and effective gene knock-down in early chick embryos using morpholinos but not pRFPRNAi vectors. *Mech Dev,* 125**,** 947-62.

Mendonsa, E. S. & Riley, B. B. 1999. Genetic analysis of tissue interactions required for otic placode induction in the zebrafish. *Dev Biol,* 206**,** 100-12.

Merzdorf, C. S. 2007. Emerging roles for zic genes in early development. *Dev Dyn,* 236**,** 922-40.

Meyers, E. N., Lewandoski, M. & Martin, G. R. 1998. An Fgf8 mutant allelic series generated by Cre- and Flp-mediated recombination. *Nat Genet,* 18**,** 136-41.

Millet, S., Campbell, K., Epstein, D. J., Losos, K., Harris, E. & Joyner, A. L. 1999. A role for Gbx2 in repression of Otx2 and positioning the mid/hindbrain organizer. *Nature,* 401**,** 161-4.

Min, J. N., Zhang, Y., Moskophidis, D. & Mivechi, N. F. 2004. Unique contribution of heat shock transcription factor 4 in ocular lens development and fiber cell differentiation. *Genesis,* 40**,** 205-17.

Minowada, G., Jarvis, L. A., Chi, C. L., Neubuser, A., Sun, X., Hacohen, N., Krasnow, M. A. & Martin, G. R. 1999. Vertebrate Sprouty genes are induced by FGF signaling and can cause chondrodysplasia when overexpressed. *Development,* 126**,** 4465-75.

Mishima, N. & Tomarev, S. 1998. Chicken Eyes absent 2 gene: isolation and expression pattern during development. *Int J Dev Biol,* 42**,** 1109-15.

Mittelstadt, M. L. & Patel, R. C. 2012. AP-1 mediated transcriptional repression of matrix metalloproteinase-9 by recruitment of histone deacetylase 1 in response to interferon beta. *PLoS One,* 7**,** e42152.

Miyake, T., Von Herbing, I. H. And Hall, B. K. 1997. Neural ectoderm, neural crest, and placodes: contribution of the otic placode to the ectodermal lining of the embryonic opercular cavity in Atlantic cod (Teleostei). . *J.Morphol.* **,** 231-253.

Mizuseki, K., Kishi, M., Matsui, M., Nakanishi, S. & Sasai, Y. 1998. Xenopus Zic-related-1 and Sox-2, two factors induced by chordin, have distinct activities in the initiation of neural induction. *Development,* 125**,** 579-87.

Modrell, M. S., Hockman, D., Uy, B., Buckley, D., Sauka-Spengler, T., Bronner, M. E. & Baker, C. V. 2014. A fate-map for cranial sensory ganglia in the sea lamprey. *Dev Biol,* 385**,** 405-16.

Mohammadi, M., Mcmahon, G., Sun, L., Tang, C., Hirth, P., Yeh, B. K., Hubbard, S. R. & Schlessinger, J. 1997. Structures of the tyrosine kinase domain of fibroblast growth factor receptor in complex with inhibitors. *Science,* 276**,** 955-60.

Monje, P., Marinissen, M. J. & Gutkind, J. S. 2003. Phosphorylation of the Carboxyl-Terminal Transactivation Domain of c-Fos by Extracellular Signal-Regulated Kinase Mediates the Transcriptional Activation of AP-1 and Cellular

Transformation Induced by Platelet-Derived Growth Factor. *Molecular and Cellular Biology,* 23**,** 7030-7043.

Monsoro-Burq, A. H., Wang, E. & Harland, R. 2005. Msx1 and Pax3 cooperate to mediate FGF8 and WNT signals during Xenopus neural crest induction. *Dev Cell,* 8**,** 167-78.

Moreno-Pelayo, M. A., Modamio-Hoybjor, S., Mencia, A., Del Castillo, I., Chardenoux, S., Fernandez-Burriel, M., Lathrop, M., Petit, C. & Moreno, F. 2003. DFNA49, a novel locus for autosomal dominant non-syndromic hearing loss, maps proximal to DFNA7/DFNM1 region on chromosome 1q21-q23. *J Med Genet,* 40**,** 832-6.

Morton, N. E. 1990. Genetic linkage and complex diseases: A comment. *Genet. Epidemiol.,* 7.

Mosimann, C., Hausmann, G. & Basler, K. 2009. Beta-catenin hits chromatin: regulation of Wnt target gene activation. *Nat Rev Mol Cell Biol,* 10**,** 276-86.

Moury, J. D. & Jacobson, A. G. 1989. Neural fold formation at newly created boundaries between neural plate and epidermis in the axolotl. *Dev Biol,* 133**,** 44-57.

Munchberg, S. R., Ober, E. A. & Steinbeisser, H. 1999. Expression of the Ets transcription factors erm and pea3 in early zebrafish development. *Mech Dev,* 88**,** 233-6.

Nagai, T., Aruga, J., Takada, S., Gunther, T., Sporle, R., Schughart, K. & Mikoshiba, K. 1997. The expression of the mouse Zic1, Zic2, and Zic3 gene suggests an essential role for Zic genes in body pattern formation. *Dev Biol,* 182**,** 299-313.

Nakamura, T., Nakamura, T. & Matsumoto, K. 2008. The functions and possible significance of Kremen as the gatekeeper of Wnt signalling in development and pathology. *J Cell Mol Med,* 12**,** 391-408.

Nakata, K., Nagai, T., Aruga, J. & Mikoshiba, K. 1997. Xenopus Zic3, a primary regulator both in neural and neural crest development. *Proc Natl Acad Sci U S A,* 94**,** 11980-5.

Nakata, K., Nagai, T., Aruga, J. & Mikoshiba, K. 1998. Xenopus Zic family and its role in neural and neural crest development. *Mech Dev,* 75**,** 43-51.

Nechiporuk, A., Linbo, T., Poss, K. D. & Raible, D. W. 2007. Specification of epibranchial placodes in zebrafish. *Development,* 134**,** 611-23.

Nechiporuk, A., Linbo, T. & Raible, D. W. 2005. Endoderm-derived Fgf3 is necessary and sufficient for inducing neurogenesis in the epibranchial placodes in zebrafish. *Development,* 132**,** 3717-30.

Neuberg, M., Schuermann, M., Hunter, J. B. & Muller, R. 1989. Two functionally different regions in Fos are required for the sequence-specific DNA interaction of the Fos/Jun protein complex. *Nature,* 338**,** 589-90.

New, D. a. T. 1955. A New Technique for the Cultivation of the Chick Embryo in vitro. *J. Embryol. Exp. Morph.,* 3**,** 326-331.

Nguyen, V. H., Schmid, B., Trout, J., Connors, S. A., Ekker, M. & Mullins, M. C. 1998. Ventral and lateral regions of the zebrafish gastrula, including the neural crest progenitors, are established by a bmp2b/swirl pathway of genes. *Dev Biol,* 199**,** 93-110.

Nikaido, M., Doi, K., Shimizu, T., Hibi, M., Kikuchi, Y. & Yamasu, K. 2007. Initial specification of the epibranchial placode in zebrafish embryos depends on the fibroblast growth factor signal. *Dev Dyn,* 236**,** 564-71.

Nishita, J., Ohta, S., Bleyl, S. B. & Schoenwolf, G. C. 2011. Detection of isoform-specific fibroblast growth factor receptors by whole-mount in situ hybridization in early chick embryos. *Dev Dyn,* 240**,** 1537-47.

Niss, K. & Leutz, A. 1998. Expression of the homeobox gene GBX2 during chicken development. *Mech Dev,* 76**,** 151-5.

Nissen, R. M. 2003. Zebrafish foxi one modulates cellular responses to Fgf signaling required for the integrity of ear and jaw patterning. *Development,* 130**,** 2543-2554.

Nissen, R. M., Yan, J., Amsterdam, A., Hopkins, N. & Burgess, S. M. 2003. Zebrafish foxi one modulates cellular responses to Fgf signaling required for the integrity of ear and jaw patterning. *Development,* 130**,** 2543-54.

Nornes, H. O., Dressler, G. R., Knapik, E. W., Deutsch, U. & Gruss, P. 1990. Spatially and temporally restricted expression of Pax2 during murine neurogenesis. *Development,* 109**,** 797-809.

Northcutt, R. G. 1996. The origin of craniates: neural crest, neurogenic placodes, and homeobox genes. . *Isr. J. Zool. ,* 42.

Northcutt, R. G. & Brandle, K. 1995. Development of branchiomeric and lateral line nerves in the axolotl. *J Comp Neurol,* 355**,** 427-54.

O'donnell, M., Hong, C. S., Huang, X., Delnicki, R. J. & Saint-Jeannet, J. P. 2006. Functional analysis of Sox8 during neural crest development in Xenopus. *Development,* 133**,** 3817-26.

O'neill, P., Mak, S. S., Fritzsch, B., Ladher, R. K. & Baker, C. V. 2012. The amniote paratympanic organ develops from a previously undiscovered sensory placode. *Nat Commun,* 3**,** 1041.

Ogita, J., Isogai, E., Sudo, H., Sakiyama, S., Nakagawara, A. & Koseki, H. 2001. Expression of the Dan gene during chicken embryonic development. *Mech Dev,* 109**,** 363-5.

Ohto, H., Kamada, S., Tago, K., Tominaga, S. I., Ozaki, H., Sato, S. & Kawakami, K. 1999. Cooperation of six and eya in activation of their target genes through nuclear translocation of Eya. *Mol Cell Biol,* 19**,** 6815-24.

Ohuchi, H., Kimura, S., Watamoto, M. & Itoh, N. 2000. Involvement of fibroblast growth factor (FGF)18-FGF8 signaling in specification of left-right asymmetry and brain and limb development of the chick embryo. *Mech Dev,* 95**,** 55-66.

Ohyama, T. & Groves, A. K. 2004a. Expression of mouse Foxi class genes in early craniofacial development. *Dev Dyn,* 231**,** 640-6.

Ohyama, T. & Groves, A. K. 2004b. Generation of Pax2-Cre mice by modification of a Pax2 bacterial artificial chromosome. *Genesis,* 38**,** 195-9.

Ohyama, T., Groves, A. K. & Martin, K. 2007. The first steps towards hearing: mechanisms of otic placode induction. *Int J Dev Biol,* 51**,** 463-72.

Ohyama, T., Mohamed, O. A., Taketo, M. M., Dufort, D. & Groves, A. K. 2006. Wnt signals mediate a fate decision between otic placode and epidermis. *Development,* 133**,** 865-75.

Okuda, Y., Yoda, H., Uchikawa, M., Furutani-Seiki, M., Takeda, H., Kondoh, H. & Kamachi, Y. 2006. Comparative genomic and expression analysis of group B1 sox genes in zebrafish indicates their diversification during vertebrate evolution. *Dev Dyn,* 235**,** 811-25.

Oliver, G., Loosli, F., Koster, R., Wittbrodt, J. & Gruss, P. 1996. Ectopic lens induction in fish in response to the murine homeobox gene Six3. *Mech Dev,* 60**,** 233-9.

Oliver, G., Mailhos, A., Wehr, R., Copeland, N. G., Jenkins, N. A. & Gruss, P. 1995a. Six3, a murine homologue of the sine oculis gene, demarcates the most anterior border of the developing neural plate and is expressed during eye development. *Development,* 121**,** 4045-55.

Oliver, G., Wehr, R., Jenkins, N. A., Copeland, N. G., Cheyette, B. N., Hartenstein, V., Zipursky, S. L. & Gruss, P. 1995b. Homeobox genes and connective tissue patterning. *Development,* 121**,** 693-705.

Orts, F., Jimenez-Collado, L. & Jimenez-Collado, J. 1971. Regulation of the embryo after the extirpation of Hensen's node. Consequences on the differentiation of the otic placode. *Arch Anat Histol Embryol,* 54**,** 1-11.

Oshima, K., Shin, K., Diensthuber, M., Peng, A. W., Ricci, A. J. & Heller, S. 2010. Mechanosensitive hair cell-like cells from embryonic and induced pluripotent stem cells. *Cell,* 141**,** 704-16.

Ozaki, H., Nakamura, K., Funahashi, J., Ikeda, K., Yamada, G., Tokano, H., Okamura, H. O., Kitamura, K., Muto, S., Kotaki, H., Sudo, K., Horai, R., Iwakura, Y. & Kawakami, K. 2004. Six1 controls patterning of the mouse otic vesicle. *Development,* 131**,** 551-62.

Ozaki, H., Watanabe, Y., Takahashi, K., Kitamura, K., Tanaka, A., Urase, K., Momoi, T., Sudo, K., Sakagami, J., Asano, M., Iwakura, Y. & Kawakami, K. 2001a. Six4, a putative myogenin gene regulator, is not essential for mouse embryonal development. *Mol Cell Biol,* 21**,** 3343-50.

Ozaki, K., Kadomoto, R., Asato, K., Tanimura, S., Itoh, N. & Kohno, M. 2001b. ERK pathway positively regulates the expression of Sprouty genes. *Biochem Biophys Res Commun,* 285**,** 1084-8.

Padanad, M. S., Bhat, N., Guo, B. & Riley, B. B. 2012. Conditions that influence the response to Fgf during otic placode induction. *Dev Biol,* 364**,** 1-10.

Padanad, M. S. & Riley, B. B. 2011. Pax2/8 proteins coordinate sequential induction of otic and epibranchial placodes through differential regulation of foxi1, sox3 and fgf24. *Dev Biol,* 351**,** 90-8.

Palmeirim, I., Henrique, D., Ish-Horowicz, D. & Pourquie, O. 1997. Avian hairy gene expression identifies a molecular clock linked to vertebrate segmentation and somitogenesis. *Cell,* 91**,** 639-48.

Pandur, P. D. & Moody, S. A. 2000. Xenopus Six1 gene is expressed in neurogenic cranial placodes and maintained in the differentiating lateral lines. *Mech Dev,* 96**,** 253-7.

Papalopulu, N. & Kintner, C. 1993. Xenopus Distal-less related homeobox genes are expressed in the developing forebrain and are induced by planar signals. *Development,* 117**,** 961-75.

Papanayotou, C., Mey, A., Birot, A. M., Saka, Y., Boast, S., Smith, J. C., Samarut, J. & Stern, C. D. 2008. A mechanism regulating the onset of Sox2 expression in the embryonic neural plate. *PLoS Biol,* 6**,** e2.

Pappu, K. S., Ostrin, E. J., Middlebrooks, B. W., Sili, B. T., Chen, R., Atkins, M. R., Gibbs, R. & Mardon, G. 2005. Dual regulation and redundant function of two eye-specific enhancers of the Drosophila retinal determination gene dachshund. *Development,* 132**,** 2895-905.

Park, B. Y. & Saint-Jeannet, J. P. 2008. Hindbrain-derived Wnt and Fgf signals cooperate to specify the otic placode in Xenopus. *Dev Biol,* 324**,** 108-21.

Pasqualetti, M., Neun, R., Davenne, M. & Rijli, F. M. 2001. Retinoic acid rescues inner ear defects in Hoxa1 deficient mice. *Nat Genet,* 29**,** 34-9.

Pasquier, L., Dubourg, C., Blayau, M., Lazaro, L., Le Marec, B., David, V. & Odent, S. 2000. A new mutation in the six-domain of SIX3 gene causes holoprosencephaly. *Eur J Hum Genet,* 8**,** 797-800.

Patel, N. S., Rhinn, M., Semprich, C. I., Halley, P. A., Dolle, P., Bickmore, W. A. & Storey, K. G. 2013. FGF signalling regulates chromatin organisation during neural differentiation via mechanisms that can be uncoupled from transcription. *PLoS Genet,* 9**,** e1003614.

Patthey, C., Gunhaga, L. & Edlund, T. 2008. Early development of the central and peripheral nervous systems is coordinated by Wnt and BMP signals. *PLoS One,* 3**,** e1625.

Patthey, C., Schlosser, G. & Shimeld, S. M. 2014. The evolutionary history of vertebrate cranial placodes--I: cell type evolution. *Dev Biol,* 389**,** 82-97.

Pattyn, A., Goridis, C. & Brunet, J. F. 2000. Specification of the central noradrenergic phenotype by the homeobox gene Phox2b. *Mol Cell Neurosci,* 15**,** 235-43.

Pattyn, A., Morin, X., Cremer, H., Goridis, C. & Brunet, J. F. 1997. Expression and interactions of the two closely related homeobox genes Phox2a and Phox2b during neurogenesis. *Development,* 124**,** 4065-75.

Pattyn, A., Morin, X., Cremer, H., Goridis, C. & Brunet, J. F. 1999. The homeobox gene Phox2b is essential for the development of autonomic neural crest derivatives. *Nature,* 399**,** 366-70.

Pauley, S., Lai, E. & Fritzsch, B. 2006. Foxg1 is required for morphogenesis and histogenesis of the mammalian inner ear. *Dev Dyn,* 235**,** 2470-82.

Pauley, S., Wright, T. J., Pirvola, U., Ornitz, D., Beisel, K. & Fritzsch, B. 2003. Expression and function of FGF10 in mammalian inner ear development. *Dev Dyn,* 227**,** 203-15.

Pauli, T., Seimiya, M., Blanco, J. & Gehring, W. J. 2005. Identification of functional sine oculis motifs in the autoregulatory element of its own gene, in the eyeless enhancer and in the signalling gene hedgehog. *Development,* 132**,** 2771-82.

Paxton, C. N., Bleyl, S. B., Chapman, S. C. & Schoenwolf, G. C. 2010. Identification of differentially expressed genes in early inner ear development. *Gene Expr Patterns,* 10**,** 31-43.

Pera, E. & Kessel, M. 1999. Expression of DLX3 in chick embryos. *Mech Dev,* 89**,** 189-93.

Pera, E., Stein, S. & Kessel, M. 1999. Ectodermal patterning in the avian embryo: epidermis versus neural plate. *Development,* 126**,** 63-73.

Pevny, L. H. & Lovell-Badge, R. 1997. Sox genes find their feet. *Curr Opin Genet Dev,* 7**,** 338-44.

Pfeffer, P. L., Gerster, T., Lun, K., Brand, M. & Busslinger, M. 1998. Characterization of three novel members of the zebrafish Pax2/5/8 family: dependency of Pax5 and Pax8 expression on the Pax2.1 (noi) function. *Development,* 125**,** 3063-74.

Pham, Y. C., Man, N., Holt, I., Sewry, C. A., Pall, G., Johnson, K. & Morris, G. E. 2005. Characterisation of the transcription factor, SIX5, using a new panel of monoclonal antibodies. *J Cell Biochem,* 95**,** 990-1001.

Phillips, B. T., Bolding, K. & Riley, B. B. 2001. Zebrafish fgf3 and fgf8 encode redundant functions required for otic placode induction. *Dev Biol,* 235**,** 351-65.

Phillips, B. T., Kwon, H. J., Melton, C., Houghtaling, P., Fritz, A. & Riley, B. B. 2006. Zebrafish msxB, msxC and msxE function together to refine the neural-nonneural border and regulate cranial placodes and neural crest development. *Dev Biol,* 294**,** 376-90.

Phillips, B. T., Storch, E. M., Lekven, A. C. & Riley, B. B. 2004. A direct role for Fgf but not Wnt in otic placode induction. *Development,* 131**,** 923-31.

Piccolo, S., Sasai, Y., Lu, B. & De Robertis, E. M. 1996. Dorsoventral patterning in Xenopus: inhibition of ventral signals by direct binding of chordin to BMP-4. *Cell,* 86**,** 589-98.

Pieper, M., Ahrens, K., Rink, E., Peter, A. & Schlosser, G. 2012. Differential distribution of competence for panplacodal and neural crest induction to non-neural and neural ectoderm. *Development,* 139**,** 1175-87.

Pieper, M., Eagleson, G. W., Wosniok, W. & Schlosser, G. 2011. Origin and segregation of cranial placodes in Xenopus laevis. *Dev Biol,* 360**,** 257-75.

Pignoni, F., Hu, B., Zavitz, K. H., Xiao, J., Garrity, P. A. & Zipursky, S. L. 1997a. The eye-specification proteins So and Eya form a complex and regulate multiple steps in Drosophila eye development. *Cell,* 91**,** 881-91.

Pignoni, F., Hu, B. & Zipursky, S. L. 1997b. Identification of genes required for Drosophila eye development using a phenotypic enhancer-trap. *Proc Natl Acad Sci U S A,* 94**,** 9220-5.

Piotrowski, T. & Baker, C. V. 2014. The development of lateral line placodes: taking a broader view. *Dev Biol,* 389**,** 68-81.

Pirvola, U., Spencer-Dene, B., Xing-Qun, L., Kettunen, P., Thesleff, I., Fritzsch, B., Dickson, C. & Ylikoski, J. 2000. FGF/FGFR-2(IIIb) signaling is essential for inner ear morphogenesis. *J Neurosci,* 20**,** 6125-34.

Plouhinec, J. L., Roche, D. D., Pegoraro, C., Figueiredo, A. L., Maczkowiak, F., Brunet, L. J., Milet, C., Vert, J. P., Pollet, N., Harland, R. M. & Monsoro-Burq, A. H. 2014. Pax3 and Zic1 trigger the early neural crest gene regulatory network by the direct activation of multiple key neural crest specifiers. *Dev Biol,* 386**,** 461-72.

Pownall, M. E. & Isaacs, H. V. 2010. *FGF Signalling in Vertebrate Development*. San Rafael (CA).

Psychoyos, D. & Stern, C. D. 1996. Fates and migratory routes of primitive streak cells in the chick embryo. *Development,* 122**,** 1523-34.

Puelles, L., Fernandez-Garre, P., Sanchez-Arrones, L., Garcia-Calero, E. & Rodriguez-Gallardo, L. 2005. Correlation of a chicken stage 4 neural plate fate map with early gene expression patterns. *Brain Res Brain Res Rev,* 49**,** 167-78.

Quackenbush, J. 2001. Computational analysis of microarray data. *Nat Rev Genet,* 2**,** 418-27.

Quackenbush, J. 2002. Microarray data normalization and transformation. *Nat Genet,* 32 Suppl**,** 496-501.

Quinn, J. C., West, J. D. & Hill, R. E. 1996. Multiple functions for Pax6 in mouse eye and nasal development. *Genes & Development,* 10**,** 435-446.

Quint, E., Zerucha, T. & Ekker, M. 2000. Differential expression of orthologous Dlx genes in zebrafish and mice: implications for the evolution of the Dlx homeobox gene family. *J Exp Zool,* 288**,** 235-41.

Rada-Iglesias, A., Bajpai, R., Prescott, S., Brugmann, S. A., Swigut, T. & Wysocka, J. 2012. Epigenomic annotation of enhancers predicts transcriptional regulators of human neural crest. *Cell Stem Cell,* 11**,** 633-48.

Rada-Iglesias, A., Bajpai, R., Swigut, T., Brugmann, S. A., Flynn, R. A. & Wysocka, J. 2011. A unique chromatin signature uncovers early developmental enhancers in humans. *Nature,* 470**,** 279-83.

Raible, F. & Brand, M. 2001. Tight transcriptional control of the ETS domain factors Erm and Pea3 by Fgf signaling during early zebrafish development. *Mech Dev,* 107**,** 105-17.

Raven, D. P. & Kloos, J. 1945. Induction by medial and lateral pieces of the archenteron roof, with special reference to the determination of the neural crest. . *Acta Neerl Morphol* 348-362.

Rawles, M. E. 1936. *A study in the localization of organ-forming areas in the chick blastoderm of the head-process state*. Ph D, University of Chicago.

Rayapureddi, J. P., Kattamuri, C., Steinmetz, B. D., Frankfort, B. J., Ostrin, E. J., Mardon, G. & Hegde, R. S. 2003. Eyes absent represents a class of protein tyrosine phosphatases. *Nature,* 426**,** 295-8.

Rex, M., Orme, A., Uwanogho, D., Tointon, K., Wigmore, P. M., Sharpe, P. T. & Scotting, P. J. 1997. Dynamic expression of chicken Sox2 and Sox3 genes in ectoderm induced to form neural tissue. *Dev Dyn,* 209**,** 323-32.

Rhinn, M., Lun, K., Ahrendt, R., Geffarth, M. & Brand, M. 2009. Zebrafish gbx1 refines the midbrain-hindbrain boundary border and mediates the Wnt8 posteriorization signal. *Neural Dev,* 4**,** 12.

Rhinn, M., Lun, K., Luz, M., Werner, M. & Brand, M. 2005. Positioning of the midbrain-hindbrain boundary organizer through global posteriorization of the neuroectoderm mediated by Wnt8 signaling. *Development,* 132**,** 1261-72.

Roehl, H. & Nusslein-Volhard, C. 2001. Zebrafish pea3 and erm are general targets of FGF8 signaling. *Curr Biol,* 11**,** 503-7.

Rogers, A. a. M., Zhang, J. & Shim, K. 2011. Sprouty1 and Sprouty2 limit both the size of the otic placode and hindbrain Wnt8a by antagonizing FGF signaling. *Dev Biol,* 353**,** 94-104.

Rogers, C. D., Harafuji, N., Archer, T., Cunningham, D. D. & Casey, E. S. 2009. Xenopus Sox3 activates sox2 and geminin and indirectly represses Xvent2 expression to induce neural progenitor formation at the expense of non-neural ectodermal derivatives. *Mech Dev,* 126**,** 42-55.

Ronaghi, M., Nasr, M., Ealy, M., Durruthy-Durruthy, R., Waldhaus, J., Diaz, G. H., Joubert, L. M., Oshima, K. & Heller, S. 2014. Inner ear hair cell-like cells from human embryonic stem cells. *Stem Cells Dev,* 23**,** 1275-84.

Rossi, C. C., Hernandez-Lagunas, L., Zhang, C., Choi, I. F., Kwok, L., Klymkowsky, M. & Artinger, K. B. 2008. Rohon-Beard sensory neurons are induced by BMP4 expressing non-neural ectoderm in Xenopus laevis. *Dev Biol,* 314**,** 351-61.

Ruben, R. J. 1973. Development and cell kinetics of the kreisler (kr-kr) mouse. *Laryngoscope,* 83**,** 1440-68.

Ruf, R. G., Xu, P. X., Silvius, D., Otto, E. A., Beekmann, F., Muerb, U. T., Kumar, S., Neuhaus, T. J., Kemper, M. J., Raymond, R. M., Jr., Brophy, P. D., Berkman, J., Gattas, M., Hyland, V., Ruf, E. M., Schwartz, C., Chang, E. H., Smith, R. J., Stratakis, C. A., Weil, D., Petit, C. & Hildebrandt, F. 2004. SIX1 mutations cause branchio-oto-renal syndrome by disruption of EYA1-SIX1-DNA complexes. *Proc Natl Acad Sci U S A,* 101**,** 8090-5.

Sadl, V. S., Sing, A., Mar, L., Jin, F. & Cordes, S. P. 2003. Analysis of hindbrain patterning defects caused by the kreisler(enu) mutation reveals multiple roles of Kreisler in hindbrain segmentation. *Dev Dyn,* 227**,** 134-42.

Sahly, I., Andermann, P. & Petit, C. 1999. The zebrafish eya1 gene and its expression pattern during embryogenesis. *Dev Genes Evol,* 209**,** 399-410.

Sajan, S. A., Warchol, M. E. & Lovett, M. 2007. Toward a systems biology of mouse inner ear organogenesis: gene expression pathways, patterns and network analysis. *Genetics,* 177**,** 631-53.

Sakabe, N. J., Savic, D. & Nobrega, M. A. 2012. Transcriptional enhancers in development and disease. *Genome Biol,* 13**,** 238.

Sanchez-Calderon, H., Martin-Partido, G. & Hidalgo-Sanchez, M. 2005. Pax2 expression patterns in the developing chick inner ear. *Gene Expr Patterns,* 5**,** 763-73.

Sanyanusin, P., Mcnoe, L. A., Sullivan, M. J., Weaver, R. G. & Eccles, M. R. 1995a. Mutation of PAX2 in two siblings with renal-coloboma syndrome. *Hum Mol Genet,* 4**,** 2183-4.

Sanyanusin, P., Schimmenti, L. A., Mcnoe, L. A., Ward, T. A., Pierpont, M. E., Sullivan, M. J., Dobyns, W. B. & Eccles, M. R. 1995b. Mutation of the PAX2 gene in a family with optic nerve colobomas, renal anomalies and vesicoureteral reflux. *Nat Genet,* 9**,** 358-64.

Sarkar, P. S., Appukuttan, B., Han, J., Ito, Y., Ai, C., Tsai, W., Chai, Y., Stout, J. T. & Reddy, S. 2000. Heterozygous loss of Six5 in mice is sufficient to cause ocular cataracts. *Nat Genet,* 25**,** 110-4.

Sasai, Y., Lu, B., Steinbeisser, H. & De Robertis, E. M. 1995. Regulation of neural induction by the Chd and Bmp-4 antagonistic patterning signals in Xenopus. *Nature,* 376**,** 333-6.

Sato, S., Ikeda, K., Shioi, G., Nakao, K., Yajima, H. & Kawakami, K. 2012. Regulation of Six1 expression by evolutionarily conserved enhancers in tetrapods. *Dev Biol,* 368**,** 95-108.

Sato, S., Ikeda, K., Shioi, G., Ochi, H., Ogino, H., Yajima, H. & Kawakami, K. 2010. Conserved expression of mouse Six1 in the pre-placodal region (PPR) and identification of an enhancer for the rostral PPR. *Dev Biol,* 344**,** 158-71.

Satoh, T. & Fekete, D. M. 2005. Clonal analysis of the relationships between mechanosensory cells and the neurons that innervate them in the chicken ear. *Development,* 132**,** 1687-97.

Sauka-Spengler, T. & Bronner-Fraser, M. 2008. A gene regulatory network orchestrates neural crest formation. *Nat Rev Mol Cell Biol,* 9**,** 557-68.

Sbrogna, J. L., Barresi, M. J. & Karlstrom, R. O. 2003. Multiple roles for Hedgehog signaling in zebrafish pituitary development. *Dev Biol,* 254**,** 19-35.

Schimmang, T. 2007. Expression and functions of FGF ligands during early otic development. *Int J Dev Biol,* 51**,** 473-81.

Schimmenti, L. A., Cunliffe, H. E., Mcnoe, L. A., Ward, T. A., French, M. C., Shim, H. H., Zhang, Y. H., Proesmans, W., Leys, A., Byerly, K. A., Braddock, S. R., Masuno, M., Imaizumi, K., Devriendt, K. & Eccles, M. R. 1997. Further delineation of renal-coloboma syndrome in patients with extreme variability of phenotype and identical PAX2 mutations. *Am J Hum Genet,* 60**,** 869-78.

Schlange, T., Andree, B., Arnold, H. & Brand, T. 2000. Expression analysis of the chicken homologue of CITED2 during early stages of embryonic development. *Mech Dev,* 98**,** 157-60.

Schlosser, G. 2006. Induction and specification of cranial placodes. *Dev Biol,* 294**,** 303-51.

Schlosser, G. 2010. Making Senses: Development of Vertebrate Cranial Placodes. *International Review of Cell and Molecular Biology,* 283**,** 129-234.

Schlosser, G. & Ahrens, K. 2004. Molecular anatomy of placode development in Xenopus laevis. *Dev Biol,* 271**,** 439-66.

Schlosser, G. & Northcutt, R. G. 2000. Development of neurogenic placodes in Xenopus laevis. *J Comp Neurol,* 418**,** 121-46.

Schmalhausen, O. I. 1940. Development of ear vesicles in the absence of medulla oblongata in amphibians. *Compt. Rend. Acad. Sci.. U.R.S.S.,* 28**,** 277-280.

Schonberger, J., Wang, L., Shin, J. T., Kim, S. D., Depreux, F. F., Zhu, H., Zon, L., Pizard, A., Kim, J. B., Macrae, C. A., Mungall, A. J., Seidman, J. G. & Seidman, C. E. 2005. Mutation in the transcriptional coactivator EYA4 causes dilated cardiomyopathy and sensorineural hearing loss. *Nat Genet,* 37**,** 418-22.

Schubert, F. R., Mootoosamy, R. C., Walters, E. H., Graham, A., Tumiotto, L., Munsterberg, A. E., Lumsden, A. & Dietrich, S. 2002. Wnt6 marks sites of epithelial transformations in the chick embryo. *Mech Dev,* 114**,** 143-8.

Selleck, M. A. & Bronner-Fraser, M. 1995. Origins of the avian neural crest: the role of neural plate-epidermal interactions. *Development,* 121**,** 525-38.

Seo, H. C., Drivenes, Ellingsen, S. & Fjose, A. 1998. Expression of two zebrafish homologues of the murine Six3 gene demarcates the initial eye primordia. *Mech Dev,* 73**,** 45-57.

Serbedzija, G. N. & Mcmahon, A. P. 1997. Analysis of neural crest cell migration in Splotch mice using a neural crest-specific LacZ reporter. *Dev Biol,* 185**,** 139-47.

Serikaku, M. A. & O'tousa, J. E. 1994. sine oculis is a homeobox gene required for Drosophila visual system development. *Genetics,* 138**,** 1137-50.

Servetnick, M. & Grainger, R. M. 1991. Changes in neural and lens competence in Xenopus ectoderm: evidence for an autonomous developmental timer. *Development,* 112**,** 177-88.

Shamim, H. & Mason, I. 1999. Expression of Fgf4 during early development of the chick embryo. *Mech Dev,* 85**,** 189-92.

Sharrocks, A. D. 2001. The ETS-domain transcription factor family. *Nat Rev Mol Cell Biol,* 2**,** 827-37.

Shen, W. & Mardon, G. 1997. Ectopic eye development in Drosophila induced by directed dachshund expression. *Development,* 124**,** 45-52.

Sheng, G. & Stern, C. D. 1999. Gata2 and Gata3: novel markers for early embryonic polarity and for non-neural ectoderm in the chick embryo. *Mech Dev,* 87**,** 213-6.

Shigetani, Y., Nobusada, Y. & Kuratani, S. 2000. Ectodermally derived FGF8 defines the maxillomandibular region in the early chick embryo: epithelial-mesenchymal interactions in the specification of the craniofacial ectomesenchyme. *Dev Biol,* 228**,** 73-85.

Shiraishi, Y., Mizutani, A., Bito, H., Fujisawa, K., Narumiya, S., Mikoshiba, K. & Furuichi, T. 1999. Cupidin, an isoform of Homer/Vesl, interacts with the actin cytoskeleton and activated rho family small GTPases and is expressed in developing mouse cerebellar granule cells. *J Neurosci,* 19**,** 8389-400.

Shiraishi-Yamaguchi, Y. & Furuichi, T. 2007. The Homer family proteins. *Genome Biol,* 8**,** 206.

Sidorov, O. A. 1937. Transplantation in certain Anura of the auditory vesicle in diverse stages of its development in order to discover the moment of its determination and its influence on the mesenchyme. . *Russk Arkh Anat*

Simeone, A., Acampora, D., Gulisano, M., Stornaiuolo, A. & Boncinelli, E. 1992. Nested expression domains of four homeobox genes in developing rostral brain. *Nature,* 358**,** 687-90.

Simeone, A., Acampora, D., Mallamaci, A., Stornaiuolo, A., D'apice, M. R., Nigro, V. & Boncinelli, E. 1993. A vertebrate gene related to orthodenticle contains a homeodomain of the bicoid class and demarcates anterior neuroectoderm in the gastrulating mouse embryo. *EMBO J,* 12**,** 2735-47.

Simoes-Costa, M., Tan-Cabugao, J., Antoshechkin, I., Sauka-Spengler, T. & Bronner, M. E. 2014. Transcriptome analysis reveals novel players in the cranial neural crest gene regulatory network. *Genome Res,* 24**,** 281-90.

Sinkkonen, S. T., Starlinger, V., Galaiya, D. J., Laske, R. D., Myllykangas, S., Oshima, K. & Heller, S. 2011. Serial analysis of gene expression in the chicken otocyst. *J Assoc Res Otolaryngol,* 12**,** 697-710.

Skromne, I. & Stern, C. D. 2001. Interactions between Wnt and Vg1 signalling pathways initiate primitive streak formation in the chick embryo. *Development,* 128**,** 2915-27.

Smith, A. N., Miller, L. A., Song, N., Taketo, M. M. & Lang, R. A. 2005. The duality of beta-catenin function: a requirement in lens morphogenesis and signaling suppression of lens fate in periocular ectoderm. *Dev Biol,* 285**,** 477-89.

Smith, R. J. H. 1993. Branchiootorenal Spectrum Disorders. *In:* Pagon, R. A., Adam, M. P., Ardinger, H. H., Bird, T. D., Dolan, C. R., Fong, C. T., Smith, R. J. H. & Stephens, K. (eds.) *GeneReviews(R)*. Seattle (WA).

Sock, E., Schmidt, K., Hermanns-Borgmeyer, I., Bosl, M. R. & Wegner, M. 2001. Idiopathic weight reduction in mice deficient in the high-mobility-group transcription factor Sox8. *Mol Cell Biol,* 21**,** 6951-9.

Solomon, K. S. 2003. Zebrafish foxi1 mediates otic placode formation and jaw development. *Development,* 130**,** 929-940.

Solomon, K. S. & Fritz, A. 2002. Concerted action of two dlx paralogs in sensory placode formation. *Development,* 129**,** 3127-36.

Solomon, K. S., Kudoh, T., Dawid, I. B. & Fritz, A. 2003a. Zebrafish foxi1 mediates otic placode formation and jaw development. *Development,* 130**,** 929-40.

Solomon, K. S., Kwak, S. J. & Fritz, A. 2004. Genetic interactions underlying otic placode induction and formation. *Dev Dyn,* 230**,** 419-33.

Solomon, K. S., Logsdon, J. M., Jr. & Fritz, A. 2003b. Expression and phylogenetic analyses of three zebrafish FoxI class genes. *Dev Dyn,* 228**,** 301-7.

Song, M. H., Kwon, T. J., Kim, H. R., Jeon, J. H., Baek, J. I., Lee, W. S., Kim, U. K. & Choi, J. Y. 2013. Mutational analysis of EYA1, SIX1 and SIX5 genes and strategies for management of hearing loss in patients with BOR/BO syndrome. *PLoS One,* 8**,** e67236.

Sosinsky, A., Honig, B., Mann, R. S. & Califano, A. 2007. Discovering transcriptional regulatory regions in Drosophila by a nonalignment method for phylogenetic footprinting. *Proc Natl Acad Sci U S A,* 104**,** 6305-10.

Stamatiou, G. A. & Stankovic, K. M. 2013. A comprehensive network and pathway analysis of human deafness genes. *Otol Neurotol,* 34**,** 961-70.

Stark, M. R., Sechrist, J., Bronner-Fraser, M. & Marcelle, C. 1997. Neural tube-ectoderm interactions are required for trigeminal placode formation. *Development,* 124**,** 4287-95.

Stec, I., Wright, T. J., Van Ommen, G. J., De Boer, P. A., Van Haeringen, A., Moorman, A. F., Altherr, M. R. & Den Dunnen, J. T. 1998. WHSC1, a 90 kb SET domain-containing gene, expressed in early development and homologous to a Drosophila dysmorphy gene maps in the Wolf-Hirschhorn syndrome critical region and is fused to IgH in t(4;14) multiple myeloma. *Hum Mol Genet,* 7**,** 1071-82.

Steel, K. P. & Brown, S. D. 1996. Genetics of deafness. *Curr Opin Neurobiol,* 6**,** 520-5.

Stern, C. D. 2005a. The chick: a great model system becomes even greater. *Dev Cell,* 8**,** 9-17.

Stern, C. D. 2005b. Neural induction: old problem, new findings, yet more questions. *Development,* 132**,** 2007-21.

Stern, C. D. & Downs, K. M. 2012. The hypoblast (visceral endoderm): an evo-devo perspective. *Development,* 139**,** 1059-69.

Stern, C. D. & Ireland, G. W. 1981. An integrated experimental study of endoderm formation in avian embryos. *Anat Embryol (Berl),* 163**,** 245-63.

Steventon, B., Araya, C., Linker, C., Kuriyama, S. & Mayor, R. 2009. Differential requirements of BMP and Wnt signalling during gastrulation and neurulation define two steps in neural crest induction. *Development,* 136**,** 771-9.

Steventon, B. & Mayor, R. 2012. Early neural crest induction requires an initial inhibition of Wnt signals. *Dev Biol,* 365**,** 196-207.

Steventon, B., Mayor, R. & Streit, A. 2012. Mutual repression between Gbx2 and Otx2 in sensory placodes reveals a general mechanism for ectodermal patterning. *Dev Biol,* 367**,** 55-65.

Stolte, D., Huang, R. & Christ, B. 2002. Spatial and temporal pattern of Fgf-8 expression during chicken development. *Anat Embryol (Berl),* 205**,** 1-6.

Stone, L. S. 1931. Induction of the ear by the medulla and its relation to experiments of the lateralis system in amphibia. *Science* 74**,** 577.

Storey, K. G., Crossley, J. M., De Robertis, E. M., Norris, W. E. & Stern, C. D. 1992. Neural induction and regionalisation in the chick embryo. *Development,* 114**,** 729-41.

Streit, A. 2002. Extensive Cell Movements Accompany Formation of the Otic Placode. *Developmental Biology,* 249**,** 237-254.

Streit, A. 2007. The preplacodal region: an ectodermal domain with multipotential progenitors that contribute to sense organs and cranial sensory ganglia. *Int J Dev Biol,* 51**,** 447-61.

Streit, A. 2008. The cranial sensory nervous system: specification of sensory progenitors and placodes. *StemBook*.

Streit, A., Berliner, A. J., Papanayotou, C., Sirulnik, A. & Stern, C. D. 2000. Initiation of neural induction by FGF signalling before gastrulation. *Nature,* 406**,** 74-8.

Streit, A., Lee, K. J., Woo, I., Roberts, C., Jessell, T. M. & Stern, C. D. 1998. Chordin regulates primitive streak development and the stability of induced neural cells, but is not sufficient for neural induction in the chick embryo. *Development,* 125**,** 507-19.

Streit, A., Sockanathan, S., Perez, L., Rex, M., Scotting, P. J., Sharpe, P. T., Lovell-Badge, R. & Stern, C. D. 1997. Preventing the loss of competence for neural induction: HGF/SF, L5 and Sox-2. *Development,* 124**,** 1191-202.

Streit, A. & Stern, C. D. 1999. Establishment and maintenance of the border of the neural plate in the chick: involvement of FGF and BMP activity. *Mech Dev,* 82**,** 51-66.

Streit, A., Tambalo, M., Chen, J., Grocott, T., Anwar, M., Sosinsky, A. & Stern, C. D. 2013. Experimental approaches for gene regulatory network construction: the chick as a model system. *Genesis,* 51**,** 296-310.

Stuhlmiller, T. J. & Garcia-Castro, M. I. 2012. FGF/MAPK signaling is required in the gastrula epiblast for avian neural crest induction. *Development,* 139**,** 289-300.

Stulberg, M. J., Lin, A., Zhao, H. & Holley, S. A. 2012. Crosstalk between Fgf and Wnt signaling in the zebrafish tailbud. *Dev Biol,* 369**,** 298-307.

Su, Y. & Meng, A. 2002. The expression of gbx-2 during zebrafish embryogenesis. *Mech Dev,* 113**,** 107-10.

Subramanian, A., Kuehn, H., Gould, J., Tamayo, P. & Mesirov, J. P. 2007. GSEA-P: a desktop application for Gene Set Enrichment Analysis. *Bioinformatics,* 23**,** 3251-3.

Subramanian, A., Tamayo, P., Mootha, V. K., Mukherjee, S., Ebert, B. L., Gillette, M. A., Paulovich, A., Pomeroy, S. L., Golub, T. R., Lander, E. S. & Mesirov, J. P. 2005. Gene set enrichment analysis: a knowledge-based approach for interpreting genome-wide expression profiles. *Proc Natl Acad Sci U S A,* 102**,** 15545-50.

Sun, S. K., Dee, C. T., Tripathi, V. B., Rengifo, A., Hirst, C. S. & Scotting, P. J. 2007. Epibranchial and otic placodes are induced by a common Fgf signal, but their subsequent development is independent. *Dev Biol,* 303**,** 675-86.

Suzuki, A., Ueno, N. & Hemmati-Brivanlou, A. 1997. Xenopus msx1 mediates epidermal induction and neural inhibition by BMP4. *Development,* 124**,** 3037-44.

Swanson, G. J., Howard, M. & Lewis, J. 1990. Epithelial autonomy in the development of the inner ear of a bird embryo. *Dev Biol,* 137**,** 243-57.

Sweetman, D., Smith, T. G., Farrell, E. R. & Munsterberg, A. 2005. Expression of csal1 in pre limb-bud chick embryos. *Int J Dev Biol,* 49**,** 427-30.

Takaki, E., Fujimoto, M., Sugahara, K., Nakahari, T., Yonemura, S., Tanaka, Y., Hayashida, N., Inouye, S., Takemoto, T., Yamashita, H. & Nakai, A. 2006. Maintenance of olfactory neurogenesis requires HSF1, a major heat shock transcription factor in mice. *J Biol Chem,* 281**,** 4931-7.

Tam, P. P. 1989. Regionalisation of the mouse embryonic ectoderm: allocation of prospective ectodermal tissues during gastrulation. *Development,* 107**,** 55-67.

Tanaka-Matakatsu, M. & Du, W. 2008. Direct control of the proneural gene atonal by retinal determination factors during Drosophila eye development. *Dev Biol,* 313**,** 787-801.

Tekin, M., Arnos, K. S. & Pandya, A. 2001. Advances in hereditary deafness. *Lancet,* 358**,** 1082-90.

Tekin, M., Hismi, B. O., Fitoz, S., Ozdag, H., Cengiz, F. B., Sirmaci, A., Aslan, I., Inceoglu, B., Yuksel-Konuk, E. B., Yilmaz, S. T., Yasun, O. & Akar, N. 2007. Homozygous mutations in fibroblast growth factor 3 are associated with a new form of syndromic deafness characterized by inner ear agenesis, microtia, and microdontia. *Am J Hum Genet,* 80**,** 338-44.

Terzic, J., Muller, C., Gajovic, S. & Saraga-Babic, M. 1998. Expression of PAX2 gene during human development. *Int J Dev Biol,* 42**,** 701-7.

Tessmar, K., Loosli, F. & Wittbrodt, J. 2002. A screen for co-factors of Six3. *Mech Dev,* 117**,** 103-13.

Tootle, T. L., Silver, S. J., Davies, E. L., Newman, V., Latek, R. R., Mills, I. A., Selengut, J. D., Parlikar, B. E. & Rebay, I. 2003. The transcription factor Eyes absent is a protein tyrosine phosphatase. *Nature,* 426**,** 299-302.

Torres, M. & Giraldez, F. 1998. The development of the vertebrate inner ear. *Mech Dev,* 71**,** 5-21.

Torres, M., Gomez-Pardo, E. & Gruss, P. 1996. Pax2 contributes to inner ear patterning and optic nerve trajectory. *Development,* 122**,** 3381-91.

Tour, E., Pillemer, G., Gruenbaum, Y. & Fainsod, A. 2001. The two Xenopus Gbx2 genes exhibit similar, but not identical expression patterns and can affect head formation. *FEBS Lett,* 507**,** 205-9.

Trampusch, H. a. L. 1941. On Ear-induction. *Acta Neerl. Morph. Norm. Path.,* 4**,** 195-213.

Tribulo, C., Aybar, M. J., Nguyen, V. H., Mullins, M. C. & Mayor, R. 2003. Regulation of Msx genes by a Bmp gradient is essential for neural crest specification. *Development,* 130**,** 6441-52.

Tripathi, V. B., Ishii, Y., Abu-Elmagd, M. M. & Scotting, P. J. 2009. The surface ectoderm of the chick embryo exhibits dynamic variation in its response to neurogenic signals. *Int J Dev Biol,* 53**,** 1023-33.

Tsuda, M., Takahashi, S., Takahashi, Y. & Asahara, H. 2003. Transcriptional co-activators CREB-binding protein and p300 regulate chondrocyte-specific gene expression via association with Sox9. *J Biol Chem,* 278**,** 27224-9.

Uchikawa, M., Ishida, Y., Takemoto, T., Kamachi, Y. & Kondoh, H. 2003. Functional analysis of chicken Sox2 enhancers highlights an array of diverse regulatory elements that are conserved in mammals. *Dev Cell,* 4**,** 509-19.

Urness, L. D., Paxton, C. N., Wang, X., Schoenwolf, G. C. & Mansour, S. L. 2010. FGF signaling regulates otic placode induction and refinement by controlling both ectodermal target genes and hindbrain Wnt8a. *Dev Biol,* 340**,** 595-604.

Uwanogho, D., Rex, M., Cartwright, E. J., Pearl, G., Healy, C., Scotting, P. J. & Sharpe, P. T. 1995. Embryonic expression of the chicken Sox2, Sox3 and Sox11 genes suggests an interactive role in neuronal development. *Mech Dev,* 49**,** 23-36.

Van Camp, G. & Smith, R. J. H. 2014. Hereditary Hearing Loss Homepage.

Van De Water, S., Van De Wetering, M., Joore, J., Esseling, J., Bink, R., Clevers, H. & Zivkovic, D. 2001. Ectopic Wnt signal determines the eyeless phenotype of zebrafish masterblind mutant. *Development,* 128**,** 3877-88.

Van De Wetering, M., Oosterwegel, M., Dooijes, D. & Clevers, H. 1991. Identification and cloning of TCF-1, a T lymphocyte-specific transcription factor containing a sequence-specific HMG box. *EMBO J,* 10**,** 123-32.

Varga, Z. M., Amores, A., Lewis, K. E., Yan, Y. L., Postlethwait, J. H., Eisen, J. S. & Westerfield, M. 2001. Zebrafish smoothened functions in ventral neural tube specification and axon tract formation. *Development,* 128**,** 3497-509.

Vendrell, V., Carnicero, E., Giraldez, F., Alonso, M. T. & Schimmang, T. 2000. Induction of inner ear fate by FGF3. *Development,* 127**,** 2011-9.

Verwoerd, C. D. & Van Oostrom, C. G. 1979. Cephalic neural crest and placodes. *Adv Anat Embryol Cell Biol,* 58**,** 1-75.

Villanueva, S., Glavic, A., Ruiz, P. & Mayor, R. 2002. Posteriorization by FGF, Wnt, and retinoic acid is required for neural crest induction. *Dev Biol,* 241**,** 289-301.

Visel, A., Blow, M. J., Li, Z., Zhang, T., Akiyama, J. A., Holt, A., Plajzer-Frick, I., Shoukry, M., Wright, C., Chen, F., Afzal, V., Ren, B., Rubin, E. M. & Pennacchio, L. A. 2009. ChIP-seq accurately predicts tissue-specific activity of enhancers. *Nature,* 457**,** 854-8.

Vogel-Hopker, A., Momose, T., Rohrer, H., Yasuda, K., Ishihara, L. & Rapaport, D. H. 2000. Multiple functions of fibroblast growth factor-8 (FGF-8) in chick eye development. *Mech Dev,* 94**,** 25-36.

Von Bubnoff, A., Schmidt, J. E. & Kimelman, D. 1996. The Xenopus laevis homeobox gene Xgbx-2 is an early marker of anteroposterior patterning in the ectoderm. *Mech Dev,* 54**,** 149-60.

Waddington, C. H. 1934. Experiments on embryonic induction. Part I: The

competence of the extra-embryonic ectoderm. Part II: Experiments on coagu- lated organisers in the chick. Part III: A note on inductions by chick primitive streak transplanted to the rabbit embryo. *J. Exp. Biol.,* 11.

Waddington, C. H. 1935. The origin of competence for lens formation in the amphibia. *J. Exp. Biol.,* 8**,** 86-91.

Waddington, C. H. 1937. The determination of the auditory placode in the chick. *J Exp Biol***,** 232-239.

Waddington, C. H. & Needham, J. 1936. Evocation, individuation, and competence in amphibian organizer action. *Proc Kon Akad Wetensch Amsterdam,* 39**,** 887-891.

Wakamatsu, Y. 2011. Mutual repression between Pax3 and Pax6 is involved in the positioning of ophthalmic trigeminal placode in avian embryo. *Dev Growth Differ,* 53**,** 994-1003.

Wallis, D. E., Roessler, E., Hehr, U., Nanni, L., Wiltshire, T., Richieri-Costa, A., Gillessen-Kaesbach, G., Zackai, E. H., Rommens, J. & Muenke, M. 1999. Mutations in the homeodomain of the human SIX3 gene cause holoprosencephaly. *Nat Genet,* 22**,** 196-8.

Walshe, J., Maroon, H., Mcgonnell, I. M., Dickson, C. & Mason, I. 2002. Establishment of hindbrain segmental identity requires signaling by FGF3 and FGF8. *Curr Biol,* 12**,** 1117-23.

Walshe, J. & Mason, I. 2000. Expression of FGFR1, FGFR2 and FGFR3 during early neural development in the chick embryo. *Mech Dev,* 90**,** 103-10.

Wamstad, J. A., Alexander, J. M., Truty, R. M., Shrikumar, A., Li, F., Eilertson, K. E., Ding, H., Wylie, J. N., Pico, A. R., Capra, J. A., Erwin, G., Kattman, S. J., Keller, G. M., Srivastava, D., Levine, S. S., Pollard, K. S., Holloway, A. K., Boyer, L. A. & Bruneau, B. G. 2012. Dynamic and coordinated epigenetic regulation of developmental transitions in the cardiac lineage. *Cell,* 151**,** 206-20.

Wang, D., Garcia-Bassets, I., Benner, C., Li, W., Su, X., Zhou, Y., Qiu, J., Liu, W., Kaikkonen, M. U., Ohgi, K. A., Glass, C. K., Rosenfeld, M. G. & Fu, X. D. 2011. Reprogramming transcription by distinct classes of enhancers functionally defined by eRNA. *Nature,* 474**,** 390-4.

Wang, W. & Lufkin, T. 2005. Hmx homeobox gene function in inner ear and nervous system cell-type specification and development. *Exp Cell Res,* 306**,** 373-9.

Wang, W., Van De Water, T. & Lufkin, T. 1998. Inner ear and maternal reproductive defects in mice lacking the Hmx3 homeobox gene. *Development,* 125**,** 621-34.

Warren, M., Wang, W., Spiden, S., Chen-Murchie, D., Tannahill, D., Steel, K. P. & Bradley, A. 2007. A Sall4 mutant mouse model useful for studying the role of Sall4 in early embryonic development and organogenesis. *Genesis,* 45**,** 51-8.

Waskiewicz, A. J., Rikhof, H. A. & Moens, C. B. 2002. Eliminating zebrafish pbx proteins reveals a hindbrain ground state. *Dev Cell,* 3**,** 723-33.

Wassarman, K. M., Lewandoski, M., Campbell, K., Joyner, A. L., Rubenstein, J. L., Martinez, S. & Martin, G. R. 1997. Specification of the anterior hindbrain and establishment of a normal mid/hindbrain organizer is dependent on Gbx2 gene function. *Development,* 124**,** 2923-34.

Watt, F. M., Estrach, S. & Ambler, C. A. 2008. Epidermal Notch signalling: differentiation, cancer and adhesion. *Curr Opin Cell Biol,* 20**,** 171-9.

Wawersik, S. & Maas, R. L. 2000. Vertebrate eye development as modeled in Drosophila. *Hum Mol Genet,* 9**,** 917-25.

Wayne, S., Robertson, N. G., Declau, F., Chen, N., Verhoeven, K., Prasad, S., Tranebjarg, L., Morton, C. C., Ryan, A. F., Van Camp, G. & Smith, R. J. 2001. Mutations in the transcriptional activator EYA4 cause late-onset deafness at the DFNA10 locus. *Hum Mol Genet,* 10**,** 195-200.

Webb, J. F. & Noden, D. M. 1993. Ectodermal placodes: contributions to the development of the vertebrate head. *Am. Zool,* 33**,** 434-447.

Wegner, M. 1999. From head to toes: the multiple facets of Sox proteins. *Nucleic Acids Res,* 27**,** 1409-20.

Weisinger, K., Kayam, G., Missulawin-Drillman, T. & Sela-Donenfeld, D. 2010. Analysis of expression and function of FGF-MAPK signaling components in the hindbrain reveals a central role for FGF3 in the regulation of Krox20, mediated by Pea3. *Dev Biol,* 344**,** 881-95.

Whitfield, T. T., Granato, M., Van Eeden, F. J., Schach, U., Brand, M., Furutani-Seiki, M., Haffter, P., Hammerschmidt, M., Heisenberg, C. P., Jiang, Y. J., Kane, D. A., Kelsh, R. N., Mullins, M. C., Odenthal, J. & Nusslein-Volhard, C. 1996. Mutations affecting development of the zebrafish inner ear and lateral line. *Development,* 123**,** 241-54.

Whitfield, T. T., Riley, B. B., Chiang, M. Y. & Phillips, B. 2002. Development of the zebrafish inner ear. *Dev Dyn,* 223**,** 427-58.

Whitlock, K. E. & Westerfield, M. 2000. The olfactory placodes of the zebrafish form by convergence of cellular fields at the edge of the neural plate. *Development,* 127**,** 3645-53.

Wieczorek, D., Krause, M., Majewski, F., Albrecht, B., Horn, D., Riess, O. & Gillessen-Kaesbach, G. 2000. Effect of the size of the deletion and clinical manifestation in Wolf-Hirschhorn syndrome: analysis of 13 patients with a de novo deletion. *Eur J Hum Genet,* 8**,** 519-26.

Wilkerson, D. C., Skaggs, H. S. & Sarge, K. D. 2007. HSF2 binds to the Hsp90, Hsp27, and c-Fos promoters constitutively and modulates their expression. *Cell Stress Chaperones,* 12**,** 283-90.

Williams, S. C., Altmann, C. R., Chow, R. L., Hemmati-Brivanlou, A. & Lang, R. A. 1998. A highly conserved lens transcriptional control element from the Pax-6 gene. *Mech Dev,* 73**,** 225-9.

Wilson, P. A. & Hemmati-Brivanlou, A. 1995. Induction of epidermis and inhibition of neural fate by Bmp-4. *Nature,* 376**,** 331-3.

Wilson, S. I. & Edlund, T. 2001. Neural induction: toward a unifying mechanism. *Nat Neurosci,* 4 Suppl**,** 1161-8.

Wilson, S. I., Graziano, E., Harland, R., Jessell, T. M. & Edlund, T. 2000. An early requirement for FGF signalling in the acquisition of neural cell fate in the chick embryo. *Curr Biol,* 10**,** 421-9.

Wilson, S. I., Rydstrom, A., Trimborn, T., Willert, K., Nusse, R., Jessell, T. M. & Edlund, T. 2001. The status of Wnt signalling regulates neural and epidermal fates in the chick embryo. *Nature,* 411**,** 325-30.

Wilson, S. W. & Houart, C. 2004. Early steps in the development of the forebrain. *Dev Cell,* 6**,** 167-81.

Winchester, C. L., Ferrier, R. K., Sermoni, A., Clark, B. J. & Johnson, K. J. 1999. Characterization of the expression of DMPK and SIX5 in the human eye and implications for pathogenesis in myotonic dystrophy. *Hum Mol Genet,* 8**,** 481-92.

Woda, J. M. 2003. Dlx proteins position the neural plate border and determine adjacent cell fates. *Development,* 130**,** 331-342.

Woda, J. M., Pastagia, J., Mercola, M. & Artinger, K. B. 2003. Dlx proteins position the neural plate border and determine adjacent cell fates. *Development,* 130**,** 331-42.

Woo, K. & Fraser, S. E. 1997. Specification of the zebrafish nervous system by nonaxial signals. *Science,* 277**,** 254-7.

Woo, K. & Fraser, S. E. 1998. Specification of the hindbrain fate in the zebrafish. *Dev Biol,* 197**,** 283-96.

Wright, T. J., Ladher, R., Mcwhirter, J., Murre, C., Schoenwolf, G. C. & Mansour, S. L. 2004. Mouse FGF15 is the ortholog of human and chick FGF19, but is not uniquely required for otic induction. *Dev Biol,* 269**,** 264-75.

Wright, T. J. & Mansour, S. L. 2003. Fgf3 and Fgf10 are required for mouse otic placode induction. *Development,* 130**,** 3379-90.

Xia, J., Deng, H., Feng, Y., Zhang, H., Pan, Q., Dai, H., Long, Z., Tang, B., Deng, H., Chen, Y., Zhang, R., Zheng, D., He, Y. & Xia, K. 2002. A novel locus for autosomal dominant nonsyndromic hearing loss identified at 5q31.1-32 in a Chinese pedigree. *J Hum Genet,* 47**,** 635-40.

Xiao, B., Tu, J. C., Petralia, R. S., Yuan, J. P., Doan, A., Breder, C. D., Ruggiero, A., Lanahan, A. A., Wenthold, R. J. & Worley, P. F. 1998. Homer regulates the association of group 1 metabotropic glutamate receptors with multivalent complexes of homer-related, synaptic proteins. *Neuron,* 21**,** 707-16.

Xu, P. X., Adams, J., Peters, H., Brown, M. C., Heaney, S. & Maas, R. 1999. Eya1-deficient mice lack ears and kidneys and show abnormal apoptosis of organ primordia. *Nat Genet,* 23**,** 113-7.

Xu, P. X., Woo, I., Her, H., Beier, D. R. & Maas, R. L. 1997. Mouse Eya homologues of the Drosophila eyes absent gene require Pax6 for expression in lens and nasal placode. *Development,* 124**,** 219-31.

Xu, R. H., Kim, J., Taira, M., Zhan, S., Sredni, D. & Kung, H. F. 1995. A dominant negative bone morphogenetic protein 4 receptor causes neuralization in Xenopus ectoderm. *Biochem Biophys Res Commun,* 212**,** 212-9.

Xu, X., Dude, C. M. & Baker, C. V. 2008. Fine-grained fate maps for the ophthalmic and maxillomandibular trigeminal placodes in the chick embryo. *Dev Biol,* 317**,** 174-86.

Yahata, T. 2000. The MSG1 Non-DNA-binding Transactivator Binds to the p300/CBP Coactivators, Enhancing Their Functional Link to the Smad Transcription Factors. *Journal of Biological Chemistry,* 275**,** 8825-8834.

Yamada, M., Ohkawara, B., Ichimura, N., Hyodo-Miura, J., Urushiyama, S., Shirakabe, K. & Shibuya, H. 2003. Negative regulation of Wnt signalling by HMG2L1, a novel NLK-binding protein. *Genes Cells,* 8**,** 677-84.

Yamamoto, T. S., Takagi, C. & Ueno, N. 2000. Requirement of Xmsx-1 in the BMP-triggered ventralization of Xenopus embryos. *Mech Dev,* 91**,** 131-41.

Yang, L., O'neill, P., Martin, K., Maass, J. C., Vassilev, V., Ladher, R. & Groves, A. K. 2013. Analysis of FGF-dependent and FGF-independent pathways in otic placode induction. *PLoS One,* 8**,** e55011.

Yang, L., Zhang, H., Hu, G., Wang, H., Abate-Shen, C. & Shen, M. M. 1998. An early phase of embryonic Dlx5 expression defines the rostral boundary of the neural plate. *J Neurosci,* 18**,** 8322-30.

Yntema, C. L. 1933. Experiments on the determination of the ear ectoderm in the embryo of Ambystoma punctatum. . *J Exp Zool* 317-357.

Yntema, C. L. 1937. An experimental study of the origin of the

cells which constitute the VIIth and VIIIth cranial ganglia and nerves in the embryo of Amblystoma punctatum. . *J. Exp. Zool.***,** 75-101.

Yntema, C. L. 1939. Self differentiation of heterotopic ear ectoderm in the embryo of Ambystoma punctatum. *J Exp Zool***,** 1-17.

Yntema, C. L. 1943. An experimental study on the origin of

the sensory neurones and sheath cells of the IXth and Xth cranial nerves in Amblystoma punctatum. *J. Exp. Zool.***,** 93-119.

Zelarayan, L. C., Vendrell, V., Alvarez, Y., Dominguez-Frutos, E., Theil, T., Alonso, M. T., Maconochie, M. & Schimmang, T. 2007. Differential requirements for FGF3, FGF8 and FGF10 during inner ear development. *Dev Biol,* 308**,** 379-91.

Zentner, G. E., Tesar, P. J. & Scacheri, P. C. 2011. Epigenetic signatures distinguish multiple classes of enhancers with distinct cellular functions. *Genome Res,* 21**,** 1273-83.

Zhang, B., Day, D. S., Ho, J. W., Song, L., Cao, J., Christodoulou, D., Seidman, J. G., Crawford, G. E., Park, P. J. & Pu, W. T. 2013. A dynamic H3K27ac signature identifies VEGFA-stimulated endothelial enhancers and requires EP300 activity. *Genome Res,* 23**,** 917-27.

Zhang, J. & Jacobson, A. G. 1993. Evidence that the border of the neural plate may be positioned by the interaction between signals that induce ventral and dorsal mesoderm. *Dev Dyn,* 196**,** 79-90.

Zhang, J., Talbot, W. S. & Schier, A. F. 1998. Positional cloning identifies zebrafish one-eyed pinhead as a permissive EGF-related ligand required during gastrulation. *Cell,* 92**,** 241-51.

Zhang, T., Ranade, S., Cai, C. Q., Clouser, C. & Pignoni, F. 2006. Direct control of neurogenesis by selector factors in the fly eye: regulation of atonal by Ey and So. *Development,* 133**,** 4881-9.

Zhang, Y., Knosp, B. M., Maconochie, M., Friedman, R. A. & Smith, R. J. 2004. A comparative study of Eya1 and Eya4 protein function and its implication in branchio-oto-renal syndrome and DFNA10. *J Assoc Res Otolaryngol,* 5**,** 295-304.

Zheng, W. 2003. The role of Six1 in mammalian auditory system development. *Development,* 130**,** 3989-4000.

Zhou, X., Hollemann, T., Pieler, T. & Gruss, P. 2000. Cloning and expression of xSix3, the Xenopus homologue of murine Six3. *Mech Dev,* 91**,** 327-30.

Zhu, C. C., Dyer, M. A., Uchikawa, M., Kondoh, H., Lagutin, O. V. & Oliver, G. 2002. Six3-mediated auto repression and eye development requires its interaction with members of the Groucho-related family of co-repressors. *Development,* 129**,** 2835-49.

Zilinski, C. A., Shah, R., Lane, M. E. & Jamrich, M. 2005. Modulation of zebrafish pitx3 expression in the primordia of the pituitary, lens, olfactory epithelium and cranial ganglia by hedgehog and nodal signaling. *Genesis,* 41**,** 33-40.

Znosko, W. A., Yu, S., Thomas, K., Molina, G. A., Li, C., Tsang, W., Dawid, I. B., Moon, A. M. & Tsang, M. 2010. Overlapping functions of Pea3 ETS transcription factors in FGF signaling during zebrafish development. *Dev Biol,* 342**,** 11-25.

Zou, D., Silvius, D., Fritzsch, B. & Xu, P. X. 2004. Eya1 and Six1 are essential for early steps of sensory neurogenesis in mammalian cranial placodes. *Development,* 131**,** 5561-72.

Zou, D., Silvius, D., Rodrigo-Blomqvist, S., Enerback, S. & Xu, P. X. 2006. Eya1 regulates the growth of otic epithelium and interacts with Pax2 during the development of all sensory areas in the inner ear. *Dev Biol,* 298**,** 430-41.

Zuber, M. E., Perron, M., Philpott, A., Bang, A. & Harris, W. A. 1999. Giant eyes in Xenopus laevis by overexpression of XOptx2. *Cell,* 98**,** 341-52.

Zwilling, E. 1941. The determination of the otic vesicle in Rana pipiens. *Journal of Experimental Zoology* 333-342.

Zygar, C. A., Cook, T. L. & Grainger, R. M., Jr. 1998. Gene activation during early stages of lens induction in Xenopus. *Development,* 125**,** 3509-19.

9. Appendix

9.1 Expression profiles of known and new genes involved in PPR and otic development

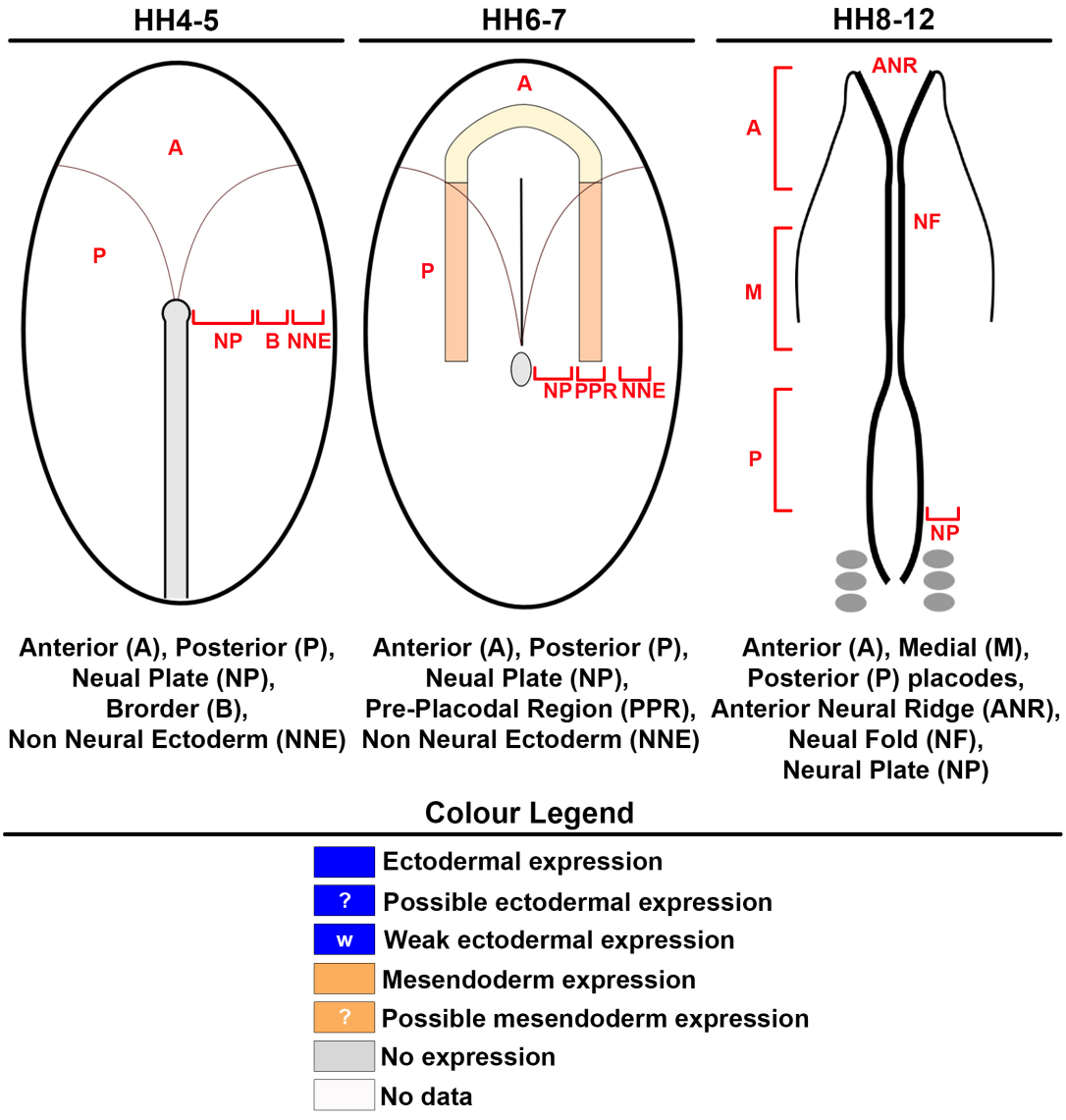

Figure 9.1 Schematic of the regions mainly analysed during the *in situ* hybridisation screening at different embryonic stages.

Table 9.1 Summary of the expression pattern of known and new genes at different developmental stage.

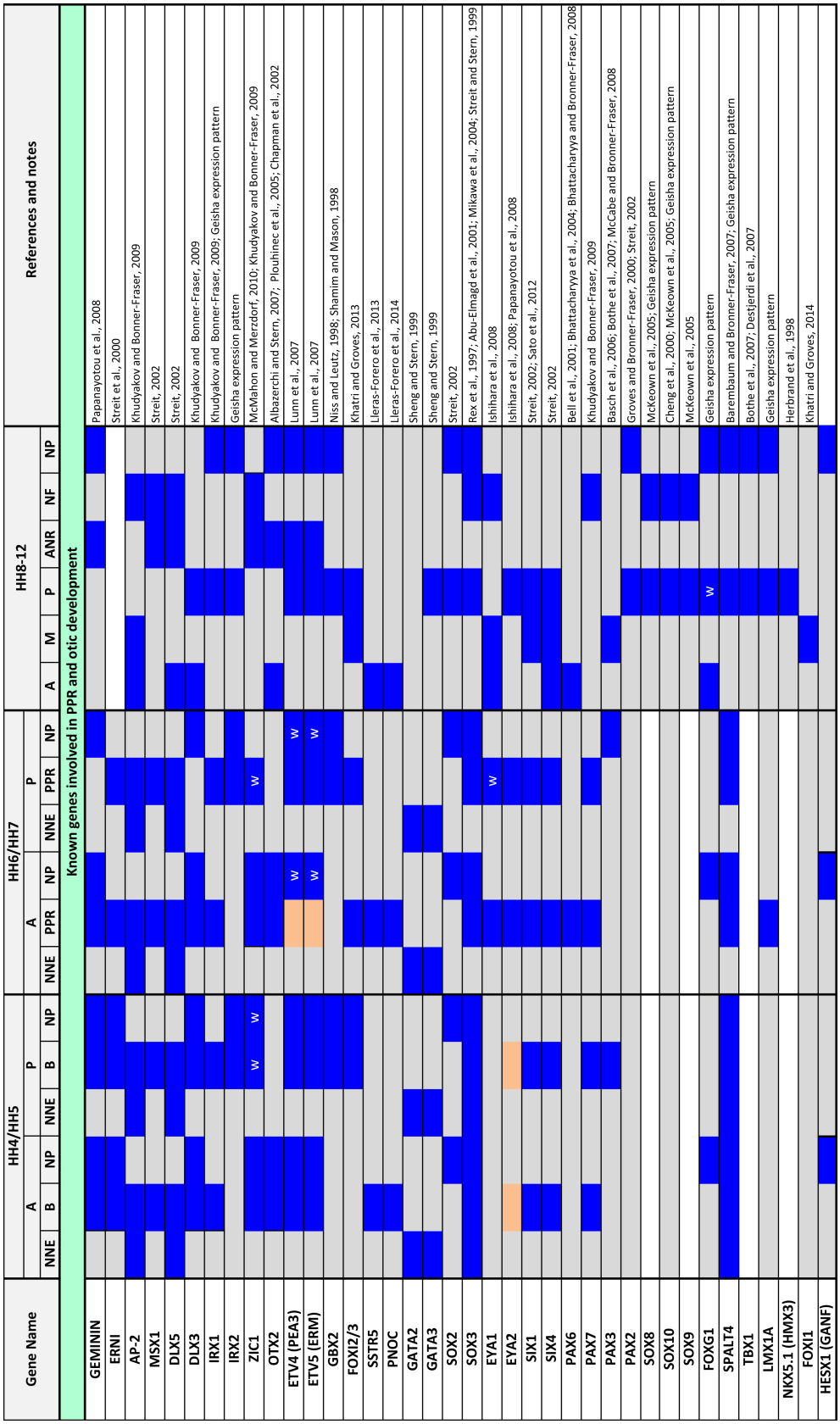

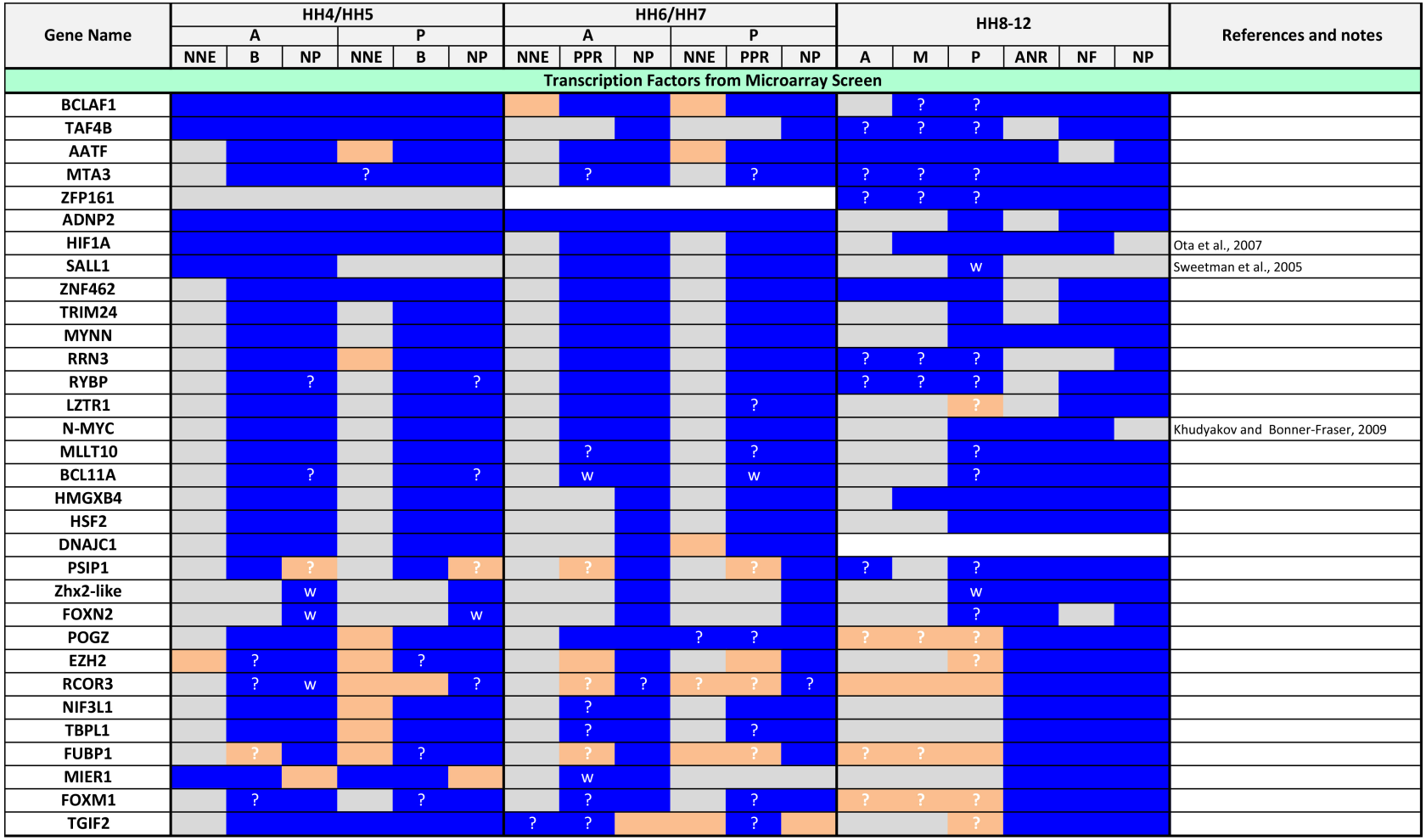
Gene Name
HH4/HH5
A
P
NNE
B
NP
NNE
B
NP
HH6/HH7
A
NNE
PPR
NP
P
NNE
PPR
NP
HH8-12
A
M
P
ANR
NF
NP
References and notes
Transcription Factors from Microarray Screen
BCLAF1
TAF4B
AATF
MTA3
ZFP161
ADNP2
HIF1A
Ota et al., 2007
SALL1
Sweetman et al., 2005
ZNF462
TRIM24
MYNN
RRN3
RYBP
LZTR1
N-MYC
Khudyakov and Bonner-Fraser, 2009
MLLT10
BCL11A
HMGXB4
HSF2
DNAJC1
PSIP1
Zhx2-like
FOXN2
POGZ
EZH2
RCOR3
NIF3L1
TBPL1
FUBP1
MIER1
FOXM1
TGIF2

Gene Name	HH4/HH5						HH6/HH7						HH8-12						References and notes
	A			P			A			P									
	NNE	B	NP	NNE	B	NP	NNE	PPR	NP	NNE	PPR	NP	A	M	P	ANR	NF	NP	
Transcription Factors from Microarray Screen																			
EAF2																			
NSD1													?	?	?				
MORC2		?	?		?	?									?				
YEATS4								?			?								
E2F8		w			w			?	?		?	?							
SP4																			
TOX3								?										?	
ZFHX1B (SIP1)																			Sheng et al., 2003
DBX2		?	?		?	?									?				
STOX2		?		?	?								w						
ZNF423 like		?	?		?	?													
ING5																			
ZNF217				?															
NFKB1	?			?															
SP8																			Kawakami et al., 2004; Neural crest gene
DLX6																			Brown et al., 2005
Signalling Molecules from Microarray Screen																			
HOMER2																			
CXCL14																			
KREMEN1																			
FSTL4				?										?					
GPR160		?			?			?	w			w							
Chromatin modifing enzymes from Microarray Screen																			
DNMT3A																			
DNMT3B														?					
WHSC1													w	w					
SETD2																			

9.2 Level of gene expression quantified by NanoString

Table 9.2 Normalised level of expression of Cnt and +FGF2 samples after 6 hours of culture analysed using the PPR NanoString probe set.

Genes	6 HRS										
	- FGF2				+ FGF2				Fold Change	P-Value	Results
	1	2	3	AVG	1	2	3	AVG			
AATF	0.0037	0.0035	0.0056	**0.0042**	0.0043	0.0038	0.0056	**0.0046**	**1.0768**	**0.723**	
ADNP2	0.0030	0.0034	0.0031	**0.0032**	0.0027	0.0022	0.0024	**0.0024**	**0.7592**	**0.017**	
AP-2	0.0332	0.0383	0.0182	**0.0299**	0.0187	0.0233	0.0081	**0.0167**	**0.5599**	**0.155**	
AXIN2	0.0021	0.0014	0.0017	**0.0017**	0.0018	0.0017	0.0028	**0.0021**	**1.2188**	**0.412**	
BCL11A	0.0000	0.0000	0.0000	0.0000	0.0000	0.0000	0.0000	0.0000	**No expressed**		**LOW**
BCL2	0.0011	0.0011	0.0015	**0.0012**	0.0012	0.0008	0.0017	**0.0012**	**0.9870**	**0.956**	
BCL7A	0.0067	0.0054	0.0072	**0.0064**	0.0075	0.0050	0.0068	**0.0064**	**0.9973**	**0.986**	
BMP4	0.0015	0.0012	0.0031	**0.0019**	0.0037	0.0029	0.0035	**0.0033**	**1.7310**	**0.097**	
CCND1	0.0102	0.0080	0.0118	**0.0100**	0.0097	0.0121	0.0155	**0.0124**	**1.2422**	**0.293**	
CDKN1B	0.0009	0.0019	0.0009	**0.0012**	0.0011	0.0017	0.0011	**0.0013**	**1.0416**	**0.900**	
CHD7	0.0049	0.0046	0.0050	**0.0048**	0.0065	0.0051	0.0079	**0.0065**	**1.3462**	**0.116**	
CITED2	0.0039	0.0017	0.0077	**0.0044**	0.0036	0.0040	0.0059	**0.0045**	**1.0159**	**0.972**	
CNTNAP5	0.0023	0.0011	0.0026	**0.0020**	0.0022	0.0013	0.0023	**0.0019**	**0.9374**	**0.828**	
CXCL14	0.0002	0.0003	0.0004	**0.0003**	0.0183	0.0224	0.0098	**0.0168**	**60.9579**	**0.011**	**UP**
CXXC6-like	0.0002	0.0002	0.0002	**0.0002**	0.0002	0.0001	0.0002	**0.0002**	**0.9634**	**0.871**	
DACH1	0.0021	0.0015	0.0022	**0.0020**	0.0014	0.0014	0.0022	**0.0017**	**0.8546**	**0.468**	
DBX2	0.0001	0.0003	0.0000	**0.0002**	0.0002	0.0002	0.0001	**0.0002**	**1.0078**	**0.991**	
DLX3	0.0012	0.0022	0.0005	**0.0013**	0.0006	0.0008	0.0002	**0.0005**	**0.4070**	**0.216**	
DLX5	0.0071	0.0117	0.0044	**0.0077**	0.0025	0.0046	0.0009	**0.0027**	**0.3438**	**0.100**	
DLX6	0.0050	0.0088	0.0028	**0.0055**	0.0017	0.0034	0.0006	**0.0019**	**0.3467**	**0.138**	
DNAJC1	0.0041	0.0028	0.0054	**0.0041**	0.0043	0.0030	0.0049	**0.0041**	**0.9960**	**0.987**	
DNMT3A	0.0000	0.0000	0.0000	0.0000	0.0000	0.0000	0.0000	0.0000	**No expressed**		**LOW**
DNMT3B	0.0144	0.0107	0.0188	**0.0146**	0.0121	0.0109	0.0152	**0.0127**	**0.8687**	**0.510**	
E2F8	0.0000	0.0000	0.0000	0.0000	0.0000	0.0000	0.0000	0.0000	**No expressed**		**LOW**
ECE1	0.0030	0.0039	0.0030	**0.0033**	0.0028	0.0035	0.0032	**0.0032**	**0.9637**	**0.759**	
EEF1A1	0.1545	0.1571	0.1358	**0.1491**	0.1644	0.1471	0.1400	**0.1505**	**1.0091**	**0.897**	
ERNI	0.0327	0.0801	0.0319	**0.0483**	0.0249	0.0782	0.0295	**0.0442**	**0.9156**	**0.870**	
ETV4	0.0000	0.0000	0.0000	0.0000	0.0000	0.0000	0.0000	0.0000	**No expressed**		**LOW**
ETV5	0.0027	0.0020	0.0042	**0.0030**	0.0071	0.0059	0.0086	**0.0072**	**2.4085**	**0.014**	**UP**
EYA1	0.0008	0.0007	0.0002	**0.0005**	0.0006	0.0004	0.0002	**0.0004**	**0.7983**	**0.629**	
EYA2	0.0047	0.0056	0.0018	**0.0040**	0.0056	0.0107	0.0010	**0.0057**	**1.4232**	**0.603**	
EZH2	0.0102	0.0080	0.0104	**0.0095**	0.0099	0.0085	0.0099	**0.0094**	**0.9888**	**0.912**	
FSTL4	0.0017	0.0019	0.0011	**0.0016**	0.0008	0.0010	0.0004	**0.0007**	**0.4745**	**0.043**	**DOWN**
FOXG1	0.0000	0.0000	0.0000	0.0000	0.0000	0.0000	0.0000	0.0000	**No expressed**		**LOW**
FOXI1	0.0000	0.0000	0.0000	0.0000	0.0000	0.0000	0.0000	0.0000	**No expressed**		**LOW**
FOXI3	0.0033	0.0079	0.0045	**0.0052**	0.0135	0.0173	0.0090	**0.0133**	**2.5301**	**0.044**	**UP**
FOXM1	0.0010	0.0007	0.0008	**0.0009**	0.0008	0.0008	0.0007	**0.0008**	**0.9116**	**0.362**	
FOXN2	0.0013	0.0009	0.0015	**0.0012**	0.0014	0.0010	0.0018	**0.0014**	**1.1789**	**0.518**	
GAPDH	0.3344	0.3229	0.2802	**0.3125**	0.3002	0.3107	0.2762	**0.2957**	**0.9462**	**0.435**	
GATA2	0.0067	0.0161	0.0036	**0.0088**	0.0007	0.0020	0.0008	**0.0011**	**0.1294**	**0.112**	
GATA3	0.0020	0.0043	0.0006	**0.0023**	0.0005	0.0009	0.0001	**0.0005**	**0.2314**	**0.184**	
GBX2	0.0009	0.0006	0.0046	**0.0020**	0.0096	0.0058	0.0146	**0.0100**	**4.9055**	**0.049**	**UP**
GEMININ	0.0016	0.0014	0.0015	**0.0015**	0.0017	0.0014	0.0014	**0.0015**	**0.9936**	**0.938**	
GPR160	0.0003	0.0003	0.0003	**0.0003**	0.0001	0.0001	0.0001	**0.0001**	**0.4380**	**0.004**	**DOWN**
HDAC1	0.0048	0.0053	0.0060	**0.0054**	0.0049	0.0046	0.0058	**0.0051**	**0.9530**	**0.646**	
HESX1	0.0010	0.0013	0.0028	**0.0017**	0.0161	0.0069	0.0108	**0.0113**	**6.5834**	**0.025**	**UP**
HEY1	0.0025	0.0025	0.0030	**0.0026**	0.0033	0.0063	0.0033	**0.0043**	**1.6365**	**0.171**	
HEY2	0.0002	0.0002	0.0002	**0.0002**	0.0018	0.0012	0.0013	**0.0015**	**7.6980**	**0.002**	**UP**
HIF1A	0.0123	0.0127	0.0133	**0.0128**	0.0130	0.0140	0.0124	**0.0131**	**1.0258**	**0.576**	
HMGXB4	0.0011	0.0009	0.0010	**0.0010**	0.0015	0.0010	0.0012	**0.0012**	**1.2017**	**0.254**	
HMX3	0.0000	0.0000	0.0000	0.0000	0.0000	0.0000	0.0000	0.0000	**No expressed**		**LOW**
HOMER2	0.0021	0.0030	0.0015	**0.0022**	0.0024	0.0034	0.0013	**0.0024**	**1.0785**	**0.835**	
HPRT1	0.0027	0.0026	0.0032	**0.0028**	0.0029	0.0027	0.0031	**0.0029**	**1.0319**	**0.688**	
HSF2	0.0030	0.0024	0.0039	**0.0031**	0.0035	0.0026	0.0039	**0.0033**	**1.0783**	**0.696**	
ING5	0.0008	0.0011	0.0009	**0.0009**	0.0013	0.0011	0.0014	**0.0013**	**1.3461**	**0.069**	
IRX1	0.0014	0.0029	0.0012	**0.0018**	0.0013	0.0023	0.0013	**0.0016**	**0.8763**	**0.732**	
IRX2	0.0011	0.0013	0.0025	**0.0016**	0.0005	0.0006	0.0009	**0.0006**	**0.3977**	**0.099**	
IRX3	0.0157	0.0117	0.0168	**0.0147**	0.0087	0.0095	0.0103	**0.0095**	**0.6452**	**0.031**	**DOWN**
KERATIN19	0.0026	0.0040	0.0016	**0.0027**	0.0023	0.0031	0.0013	**0.0023**	**0.8226**	**0.606**	
KREMEN1	0.0003	0.0005	0.0003	**0.0004**	0.0002	0.0003	0.0003	**0.0003**	**0.7655**	**0.307**	
LEF1	0.0026	0.0025	0.0023	**0.0025**	0.0036	0.0023	0.0033	**0.0030**	**1.2417**	**0.230**	
LMX1A	0.0000	0.0000	0.0000	0.0000	0.0000	0.0000	0.0000	0.0000	**No expressed**		**LOW**
LMX1B	0.0085	0.0019	0.0091	**0.0065**	0.0055	0.0014	0.0061	**0.0043**	**0.6702**	**0.479**	

Genes	6 HRS										
	- FGF2				+ FGF2				Fold Change	P-Value	Results
	1	2	3	AVG	1	2	3	AVG			
LRP11	0.0029	0.0062	0.0013	**0.0035**	0.0018	0.0030	0.0008	**0.0019**	0.5373	0.366	
LZTR1	0.0000	0.0000	0.0000	0.0000	0.0000	0.0000	0.0000	0.0000	No expressed		LOW
MEF2D	0.0021	0.0031	0.0021	**0.0024**	0.0021	0.0028	0.0026	**0.0025**	1.0354	0.832	
MIER1	0.0011	0.0010	0.0019	**0.0014**	0.0013	0.0009	0.0014	**0.0012**	0.8838	0.648	
MLLT10	0.0005	0.0003	0.0013	**0.0007**	0.0011	0.0007	0.0014	**0.0011**	1.5458	0.331	
MORC2	0.0020	0.0019	0.0033	**0.0024**	0.0024	0.0020	0.0037	**0.0027**	1.1211	0.684	
MSX1	0.0218	0.0101	0.0281	**0.0200**	0.0240	0.0216	0.0212	**0.0223**	1.1145	0.690	
MTA3	0.0000	0.0000	0.0000	0.0000	0.0000	0.0000	0.0000	0.0000	No expressed		LOW
MYNN	0.0019	0.0017	0.0028	**0.0021**	0.0023	0.0021	0.0030	**0.0024**	1.1527	0.501	
N-MYC	0.0091	0.0032	0.0152	**0.0092**	0.0102	0.0076	0.0117	**0.0098**	1.0716	0.867	
NFKB1	0.0028	0.0043	0.0020	**0.0031**	0.0022	0.0033	0.0022	**0.0025**	0.8249	0.523	
NPAS3	0.0000	0.0000	0.0000	0.0000	0.0000	0.0000	0.0000	0.0000	No expressed		LOW
NSD1	0.0000	0.0000	0.0000	0.0000	0.0000	0.0000	0.0000	0.0000	No expressed		LOW
OTX2	0.0067	0.0063	0.0109	**0.0080**	0.0035	0.0067	0.0034	**0.0045**	0.5700	0.134	
PAX2	0.0010	0.0000	0.0007	**0.0006**	0.0095	0.0024	0.0052	**0.0057**	9.9495	0.070	
PAX3	0.0000	0.0000	0.0000	0.0000	0.0000	0.0000	0.0000	0.0000	No expressed		LOW
PAX6	0.0047	0.0072	0.0021	**0.0047**	0.0006	0.0011	0.0000	**0.0006**	0.1177	0.052	
PAX7	0.0000	0.0000	0.0000	0.0000	0.0000	0.0000	0.0000	0.0000	No expressed		LOW
PCNA	0.0238	0.0244	0.0271	**0.0251**	0.0211	0.0224	0.0243	**0.0226**	0.9006	0.142	
PDLI4	0.0052	0.0036	0.0063	**0.0050**	0.0052	0.0065	0.0061	**0.0059**	1.1760	0.373	
PHF10	0.0059	0.0054	0.0056	**0.0056**	0.0060	0.0057	0.0054	**0.0057**	1.0147	0.731	
PHF20	0.0059	0.0058	0.0071	**0.0063**	0.0059	0.0051	0.0066	**0.0059**	0.9362	0.549	
PNOC	0.0024	0.0027	0.0013	**0.0021**	0.0020	0.0021	0.0005	**0.0016**	0.7341	0.450	
POGZ	0.0017	0.0017	0.0012	**0.0015**	0.0017	0.0015	0.0013	**0.0015**	0.9717	0.823	
PSIP1	0.0050	0.0042	0.0070	**0.0054**	0.0054	0.0039	0.0058	**0.0050**	0.9252	0.707	
PTPRU	0.0006	0.0005	0.0005	**0.0005**	0.0004	0.0004	0.0003	**0.0004**	0.7099	0.004	DOWN
RRN3	0.0000	0.0000	0.0000	0.0000	0.0000	0.0000	0.0000	0.0000	No expressed		LOW
RX1	0.0000	0.0000	0.0000	0.0000	0.0000	0.0000	0.0000	0.0000	No expressed		LOW
RYBP	0.0029	0.0027	0.0028	**0.0028**	0.0028	0.0022	0.0028	**0.0026**	0.9237	0.393	
SALL1	0.0242	0.0324	0.0344	**0.0304**	0.0253	0.0259	0.0367	**0.0293**	0.9658	0.841	
SALL4	0.0045	0.0036	0.0058	**0.0046**	0.0040	0.0038	0.0052	**0.0043**	0.9319	0.704	
SDHA	0.0045	0.0046	0.0045	**0.0045**	0.0046	0.0046	0.0055	**0.0049**	1.0882	0.248	
SETD2	0.0036	0.0031	0.0075	**0.0047**	0.0046	0.0034	0.0084	**0.0055**	1.1496	0.749	
SIX1	0.0044	0.0060	0.0016	**0.0040**	0.0032	0.0045	0.0015	**0.0031**	0.7687	0.590	
SIX3	0.0010	0.0014	0.0014	**0.0013**	0.0010	0.0005	0.0003	**0.0006**	0.4660	0.054	
SIX4	0.0037	0.0044	0.0029	**0.0036**	0.0038	0.0037	0.0030	**0.0035**	0.9665	0.816	
SMAD6	0.0000	0.0000	0.0000	0.0000	0.0000	0.0000	0.0000	0.0000	No expressed		LOW
SOX10	0.0004	0.0002	0.0001	**0.0002**	0.0000	0.0000	0.0000	0.0000	0.0000	0.114	
SOX2	0.0041	0.0013	0.0111	**0.0055**	0.0044	0.0017	0.0092	**0.0051**	0.9343	0.926	
SOX3	0.0018	0.0022	0.0045	**0.0028**	0.0023	0.0022	0.0049	**0.0031**	1.1011	0.826	
SOX9	0.0004	0.0001	0.0003	**0.0003**	0.0002	0.0001	0.0001	**0.0001**	0.4324	0.165	
SP4	0.0024	0.0020	0.0028	**0.0024**	0.0024	0.0021	0.0028	**0.0024**	1.0279	0.835	
SSTR5	0.0021	0.0021	0.0006	**0.0016**	0.0001	0.0000	0.0000	**0.0000**	0.0278	0.032	DOWN
STOX2	0.0024	0.0012	0.0023	**0.0020**	0.0016	0.0011	0.0016	**0.0014**	0.7248	0.256	
TAC1	0.0000	0.0000	0.0000	0.0000	0.0000	0.0000	0.0000	0.0000	No expressed		LOW
TBL1XR1	0.0035	0.0028	0.0058	**0.0040**	0.0039	0.0033	0.0051	**0.0041**	1.0246	0.931	
TBX1	0.0002	0.0000	0.0002	**0.0001**	0.0019	0.0002	0.0012	**0.0011**	7.7991	0.120	
TBX2	0.0000	0.0000	0.0000	0.0000	0.0000	0.0000	0.0000	0.0000	No expressed		LOW
TBX3	0.0001	0.0004	0.0000	**0.0002**	0.0000	0.0000	0.0000	0.0000	0.0000	0.176	
TGIF2	0.0052	0.0054	0.0047	**0.0051**	0.0038	0.0043	0.0044	**0.0042**	0.8192	0.034	
TOX3	0.0003	0.0003	0.0009	**0.0005**	0.0003	0.0003	0.0007	**0.0005**	0.9070	0.856	
TP53	0.0072	0.0076	0.0076	**0.0075**	0.0072	0.0074	0.0084	**0.0077**	1.0264	0.650	
TRIM24	0.0038	0.0035	0.0042	**0.0038**	0.0032	0.0034	0.0030	**0.0032**	0.8354	0.050	
WHSC1	0.0069	0.0071	0.0083	**0.0074**	0.0062	0.0056	0.0070	**0.0063**	0.8427	0.127	
YEATS4	0.0029	0.0030	0.0050	**0.0036**	0.0032	0.0025	0.0061	**0.0039**	1.0836	0.828	
ZFHX1B	0.0040	0.0001	0.0053	**0.0031**	0.0038	0.0010	0.0055	**0.0035**	1.1147	0.871	
ZHX2	0.0029	0.0017	0.0032	**0.0026**	0.0047	0.0022	0.0046	**0.0039**	1.4800	0.257	
ZIC1	0.0005	0.0000	0.0004	**0.0003**	0.0002	0.0000	0.0002	**0.0001**	0.4604	0.359	
ZIC2	0.0162	0.0016	0.0208	**0.0129**	0.0170	0.0066	0.0221	**0.0152**	1.1823	0.767	
ZIC3	0.0111	0.0016	0.0212	**0.0113**	0.0153	0.0072	0.0275	**0.0167**	1.4748	0.547	
ZNF217	0.0125	0.0117	0.0184	**0.0142**	0.0146	0.0144	0.0216	**0.0169**	1.1895	0.446	
ZNF423	0.0104	0.0038	0.0126	**0.0089**	0.0113	0.0056	0.0129	**0.0099**	1.1111	0.788	
ZNF462	0.0101	0.0071	0.0117	**0.0096**	0.0122	0.0090	0.0169	**0.0127**	1.3183	0.315	

Table 9.3 Normalised level of expression of Cnt and +FGF2 samples after 6 hours of culture analysed using the otic NanoString probe set

Genes	6 HRS										
	Cnt				+ FGF2				Fold Change	P-Value	Results
	1	2	3	AVG	1	2	3	AVG			
AFF4	0.0040	0.0041	0.0039	**0.0040**	0.0047	0.0048	0.0050	**0.0048**	1.2054	0.0024	
ARID3A	0.0047	0.0055	0.0040	**0.0047**	0.0080	0.0081	0.0079	**0.0080**	1.6894	0.0019	UP
ARID3C	0.0029	0.0036	0.0021	**0.0029**	0.0025	0.0021	0.0027	**0.0025**	0.8570	0.4369	
ATN1	0.0045	0.0044	0.0047	**0.0045**	0.0045	0.0046	0.0049	**0.0047**	1.0235	0.4925	
AXIN2	0.0016	0.0021	0.0018	**0.0018**	0.0020	0.0024	0.0017	**0.0020**	1.1143	0.4473	
BACH2	0.0007	0.0008	0.0006	**0.0007**	0.0009	0.0010	0.0009	**0.0010**	1.3674	0.0159	
BAZ1A	0.0001	0.0001	0.0001	**0.0001**	0.0002	0.0002	0.0002	**0.0002**	1.8484	0.0023	UP
BCL2	0.0008	0.0006	0.0008	**0.0007**	0.0009	0.0010	0.0009	**0.0009**	1.2923	0.0285	
BCL7A	0.0042	0.0036	0.0048	**0.0042**	0.0044	0.0045	0.0047	**0.0045**	1.0895	0.3511	
BLIMP1	0.0079	0.0062	0.0086	**0.0076**	0.0062	0.0056	0.0061	**0.0060**	0.7890	0.0995	
BMP4	0.0014	0.0023	0.0020	**0.0019**	0.0042	0.0045	0.0039	**0.0042**	2.2087	0.0019	UP
BMP7	0.0000	0.0000	0.0000	**0.0000**	0.0000	0.0000	0.0000	**0.0000**	No expressed		LOW
BRD1	0.0027	0.0028	0.0027	**0.0027**	0.0029	0.0028	0.0028	**0.0028**	1.0357	0.0574	
BRD2	0.0097	0.0104	0.0108	**0.0103**	0.0102	0.0105	0.0103	**0.0103**	1.0032	0.9249	
BRD4	0.0001	0.0001	0.0001	**0.0001**	0.0001	0.0001	0.0001	**0.0001**	1.0344	0.7881	
BRD7	0.0073	0.0071	0.0072	**0.0072**	0.0074	0.0069	0.0072	**0.0072**	0.9983	0.9424	
BRN3	0.0000	0.0000	0.0000	**0.0000**	0.0000	0.0000	0.0000	**0.0000**	No expressed		LOW
CBX1	0.0075	0.0070	0.0085	**0.0077**	0.0074	0.0075	0.0083	**0.0077**	1.0089	0.8979	
CBX3	0.0101	0.0102	0.0104	**0.0102**	0.0104	0.0109	0.0116	**0.0110**	1.0753	0.0889	
CBX4	0.0005	0.0006	0.0003	**0.0004**	0.0012	0.0010	0.0007	**0.0009**	2.1347	0.0413	UP
CCND1	0.0065	0.0059	0.0059	**0.0061**	0.0123	0.0130	0.0097	**0.0117**	1.9059	0.0056	UP
CD151	0.0000	0.0000	0.0000	**0.0000**	0.0000	0.0000	0.0000	**0.0000**	No expressed		LOW
CDH1	0.0054	0.0060	0.0038	**0.0050**	0.0041	0.0032	0.0039	**0.0037**	0.7353	0.1311	
CDH2	0.0027	0.0015	0.0027	**0.0023**	0.0022	0.0023	0.0019	**0.0021**	0.9278	0.7171	
CDH6	0.0017	0.0009	0.0046	**0.0024**	0.0037	0.0059	0.0059	**0.0052**	2.1418	0.1132	
CDKN1B	0.0023	0.0029	0.0018	**0.0023**	0.0024	0.0025	0.0024	**0.0024**	1.0322	0.8160	
CHCHD8	0.0000	0.0000	0.0000	**0.0000**	0.0000	0.0000	0.0000	**0.0000**	No expressed		LOW
CHD2	0.0022	0.0021	0.0020	**0.0021**	0.0029	0.0032	0.0027	**0.0030**	1.4093	0.0067	
CHD7	0.0052	0.0051	0.0051	**0.0051**	0.0075	0.0077	0.0078	**0.0077**	1.4944	0.0000	
MAF2	0.0000	0.0000	0.0000	**0.0000**	0.0000	0.0000	0.0000	**0.0000**	No expressed		LOW
CNOT4	0.0002	0.0003	0.0002	**0.0002**	0.0003	0.0004	0.0003	**0.0003**	1.3589	0.0622	
COL11A1	0.0005	0.0005	0.0005	**0.0005**	0.0003	0.0003	0.0003	**0.0003**	0.5961	0.0014	
CRYSTALLIN	0.0000	0.0000	0.0000	**0.0000**	0.0000	0.0000	0.0000	**0.0000**	No expressed		LOW
CTNNB1	0.0252	0.0273	0.0233	**0.0253**	0.0220	0.0226	0.0223	**0.0223**	0.8840	0.0643	
CUX1	0.0002	0.0002	0.0002	**0.0002**	0.0001	0.0002	0.0002	**0.0002**	0.9017	0.4721	
CXCL14	0.0000	0.0002	0.0002	**0.0001**	0.0206	0.0172	0.0174	**0.0184**	131.1218	0.0001	UP
CYP26A	0.0102	0.0011	0.0104	**0.0073**	0.0037	0.0029	0.0024	**0.0030**	0.4135	0.2405	
CYP26C1	0.0089	0.0017	0.0100	**0.0069**	0.0068	0.0054	0.0049	**0.0057**	0.8280	0.6789	
DACH1	0.0011	0.0010	0.0007	**0.0009**	0.0012	0.0011	0.0012	**0.0012**	1.2212	0.1773	
DACH2	0.0014	0.0017	0.0014	**0.0015**	0.0007	0.0006	0.0008	**0.0007**	0.4680	0.0021	
DAPK3	0.0082	0.0094	0.0077	**0.0084**	0.0077	0.0077	0.0087	**0.0080**	0.9544	0.5564	
DLX3	0.0013	0.0018	0.0010	**0.0013**	0.0004	0.0003	0.0006	**0.0005**	0.3465	0.0265	
DLX5	0.0110	0.0128	0.0095	**0.0111**	0.0026	0.0022	0.0029	**0.0026**	0.2299	0.0010	DOWN
DLX6	0.0110	0.0128	0.0083	**0.0107**	0.0022	0.0016	0.0019	**0.0019**	0.1759	0.0025	DOWN
DNMT1	0.0036	0.0037	0.0034	**0.0036**	0.0030	0.0029	0.0029	**0.0030**	0.8263	0.0037	
DNMT3A	0.0000	0.0000	0.0000	**0.0000**	0.0000	0.0000	0.0000	**0.0000**	No expressed		LOW
DNMT3B	0.0159	0.0135	0.0165	**0.0153**	0.0143	0.0145	0.0141	**0.0143**	0.9335	0.3290	
DTX4	0.0029	0.0031	0.0019	**0.0026**	0.0020	0.0021	0.0017	**0.0019**	0.7405	0.1520	
EBF2	0.0000	0.0000	0.0000	**0.0000**	0.0000	0.0000	0.0000	**0.0000**	No expressed		LOW
EED	0.0014	0.0013	0.0015	**0.0014**	0.0018	0.0016	0.0015	**0.0016**	1.1402	0.1012	
EN2	0.0001	0.0001	0.0004	**0.0002**	0.0006	0.0007	0.0019	**0.0011**	5.7318	0.1003	
EPHA4	0.0010	0.0006	0.0019	**0.0012**	0.0054	0.0057	0.0054	**0.0055**	4.7522	0.0004	UP
EPHB1	0.0010	0.0011	0.0009	**0.0010**	0.0012	0.0011	0.0009	**0.0011**	1.0756	0.5439	
ETS1B	0.0020	0.0026	0.0026	**0.0024**	0.0009	0.0009	0.0009	**0.0009**	0.3660	0.0021	
ETS2	0.0008	0.0012	0.0009	**0.0010**	0.0016	0.0017	0.0017	**0.0017**	1.7169	0.0028	UP
ETV4	0.0001	0.0000	0.0001	**0.0001**	0.0030	0.0028	0.0023	**0.0027**	36.1662	0.0002	UP
ETV5	0.0020	0.0021	0.0023	**0.0021**	0.0077	0.0074	0.0080	**0.0077**	3.6242	0.0000	UP
EYA1	0.0003	0.0004	0.0002	**0.0003**	0.0001	0.0002	0.0002	**0.0002**	0.5801	0.1783	
EYA2	0.0016	0.0012	0.0017	**0.0015**	0.0032	0.0027	0.0040	**0.0033**	2.2308	0.0101	UP
EZH2	0.0055	0.0046	0.0062	**0.0054**	0.0061	0.0060	0.0061	**0.0061**	1.1186	0.2333	
EZRIN	0.0013	0.0017	0.0013	**0.0014**	0.0025	0.0026	0.0026	**0.0025**	1.7760	0.0011	UP
FEZ1	0.0016	0.0018	0.0014	**0.0016**	0.0013	0.0013	0.0013	**0.0013**	0.8209	0.0676	
FGF16	0.0003	0.0001	0.0001	**0.0001**	0.0003	0.0005	0.0005	**0.0004**	2.8716	0.0607	
FGFR3	0.0163	0.0160	0.0186	**0.0170**	0.0032	0.0027	0.0031	**0.0030**	0.1756	0.0001	DOWN
FGFR4	0.0045	0.0045	0.0040	**0.0043**	0.0030	0.0018	0.0022	**0.0023**	0.5448	0.0085	
FOXC1	0.0000	0.0000	0.0000	**0.0000**	0.0000	0.0000	0.0000	**0.0000**	No expressed		LOW
FOXD3	0.0003	0.0000	0.0037	**0.0013**	0.0042	0.0043	0.0030	**0.0038**	2.8639	0.1169	
FOXG1	0.0000	0.0000	0.0000	**0.0000**	0.0000	0.0000	0.0000	**0.0000**	No expressed		LOW
FOXI1/2	0.0000	0.0000	0.0000	**0.0000**	0.0000	0.0000	0.0000	**0.0000**	No expressed		LOW
FOXI3	0.0061	0.0108	0.0080	**0.0083**	0.0194	0.0158	0.0230	**0.0194**	2.3480	0.0106	UP
FOXP1	0.0028	0.0027	0.0028	**0.0028**	0.0044	0.0043	0.0040	**0.0042**	1.5203	0.0004	UP
FOXP4	0.0035	0.0036	0.0024	**0.0032**	0.0039	0.0041	0.0047	**0.0042**	1.3339	0.0790	
FRZB	0.0023	0.0015	0.0021	**0.0020**	0.0017	0.0020	0.0013	**0.0016**	0.8377	0.3491	
FSTL4	0.0016	0.0014	0.0009	**0.0013**	0.0006	0.0004	0.0004	**0.0005**	0.3568	0.0130	
FZD1	0.0049	0.0049	0.0040	**0.0046**	0.0034	0.0036	0.0034	**0.0035**	0.7567	0.0259	
FZD2	0.0007	0.0007	0.0004	**0.0006**	0.0002	0.0002	0.0003	**0.0003**	0.4108	0.0156	
FZD7	0.0181	0.0151	0.0173	**0.0168**	0.0334	0.0327	0.0318	**0.0326**	1.9405	0.0001	UP

Genes	6 HRS										
	Cnt				+ FGF2						
	1	2	3	AVG	1	2	3	AVG	Fold Change	P-Value	Results
GAPDH	0.2108	0.2036	0.2093	**0.2079**	0.1970	0.2032	0.1928	**0.1977**	**0.9506**	**0.0521**	
GATA2	0.0177	0.0283	0.0116	**0.0192**	0.0011	0.0008	0.0007	**0.0009**	**0.0461**	**0.0201**	**DOWN**
GATA3	0.0046	0.0067	0.0026	**0.0046**	0.0007	0.0008	0.0012	**0.0009**	**0.1958**	**0.0352**	**DOWN**
GBX2	0.0006	0.0012	0.0008	**0.0009**	0.0150	0.0200	0.0134	**0.0161**	**18.0965**	**0.0015**	**UP**
GLI1	0.0006	0.0006	0.0005	**0.0006**	0.0004	0.0003	0.0003	**0.0003**	**0.4983**	**0.0054**	
GLI2	0.0025	0.0024	0.0017	**0.0022**	0.0012	0.0013	0.0012	**0.0013**	**0.5768**	**0.0227**	
GLI3	0.0040	0.0023	0.0060	**0.0041**	0.0070	0.0062	0.0072	**0.0068**	**1.6481**	**0.0734**	
GRHL2	0.0069	0.0097	0.0046	**0.0071**	0.0023	0.0016	0.0020	**0.0020**	**0.2787**	**0.0263**	
HAS2	0.0038	0.0055	0.0029	**0.0041**	0.0015	0.0010	0.0019	**0.0015**	**0.3621**	**0.0317**	
HAT1	0.0008	0.0008	0.0008	**0.0008**	0.0009	0.0008	0.0007	**0.0008**	**1.0199**	**0.7657**	
HDAC1	0.0047	0.0048	0.0048	**0.0048**	0.0048	0.0046	0.0047	**0.0047**	**0.9777**	**0.1287**	
HDAC2	0.0360	0.0343	0.0355	**0.0353**	0.0361	0.0345	0.0359	**0.0355**	**1.0064**	**0.7644**	
HELLS	0.0104	0.0105	0.0107	**0.0105**	0.0113	0.0109	0.0110	**0.0111**	**1.0536**	**0.0148**	
HES4	0.0116	0.0116	0.0116	**0.0116**	0.0078	0.0078	0.0073	**0.0076**	**0.6558**	**0.0000**	
HES5	0.0000	0.0000	0.0000	**0.0000**	0.0000	0.0000	0.0000	**0.0000**	**No expressed**		**LOW**
HESX1	0.0009	0.0004	0.0006	**0.0007**	0.0136	0.0094	0.0121	**0.0117**	**17.7880**	**0.0008**	**UP**
HEY1	0.0012	0.0013	0.0007	**0.0011**	0.0014	0.0015	0.0011	**0.0013**	**1.2634**	**0.2344**	
HIPK1	0.0063	0.0061	0.0056	**0.0060**	0.0069	0.0071	0.0066	**0.0069**	**1.1444**	**0.0239**	
HIPK3	0.0009	0.0008	0.0008	**0.0008**	0.0010	0.0009	0.0011	**0.0010**	**1.2143**	**0.0349**	
HMG1	0.0277	0.0304	0.0301	**0.0294**	0.0149	0.0141	0.0163	**0.0151**	**0.5136**	**0.0002**	
HMX3	0.0000	0.0000	0.0000	**0.0000**	0.0000	0.0000	0.0000	**0.0000**	**No expressed**		**LOW**
HOMER2	0.0022	0.0024	0.0016	**0.0021**	0.0026	0.0023	0.0026	**0.0025**	**1.2220**	**0.1427**	
HOXA1	0.0001	0.0008	0.0003	**0.0004**	0.0008	0.0011	0.0009	**0.0009**	**2.2858**	**0.0874**	
HOXA2	0.0000	0.0000	0.0000	**0.0000**	0.0000	0.0000	0.0000	**0.0000**	**No expressed**		**LOW**
HOXA3	0.0000	0.0000	0.0000	**0.0000**	0.0000	0.0000	0.0000	**0.0000**	**No expressed**		**LOW**
HOXB1	0.0000	0.0002	0.0001	**0.0001**	0.0009	0.0013	0.0009	**0.0011**	**10.9404**	**0.0026**	**UP**
HPRT1	0.0016	0.0015	0.0016	**0.0016**	0.0019	0.0017	0.0017	**0.0017**	**1.1132**	**0.0900**	
ID1	0.0028	0.0023	0.0030	**0.0027**	0.0042	0.0042	0.0053	**0.0045**	**1.6846**	**0.0122**	**UP**
ID2	0.0183	0.0180	0.0229	**0.0197**	0.0124	0.0127	0.0149	**0.0133**	**0.6748**	**0.0229**	
ID4	0.0043	0.0054	0.0041	**0.0046**	0.0027	0.0036	0.0043	**0.0035**	**0.7623**	**0.1543**	
IRX1	0.0061	0.0072	0.0038	**0.0057**	0.0047	0.0048	0.0034	**0.0043**	**0.7586**	**0.2783**	
IRX2	0.0021	0.0026	0.0012	**0.0020**	0.0006	0.0007	0.0004	**0.0005**	**0.2717**	**0.0218**	
IRX3	0.0131	0.0107	0.0124	**0.0121**	0.0081	0.0084	0.0060	**0.0075**	**0.6200**	**0.0114**	
IRX4	0.0000	0.0000	0.0000	**0.0000**	0.0000	0.0000	0.0000	**0.0000**	**No expressed**		**LOW**
IRX5	0.0015	0.0014	0.0011	**0.0013**	0.0005	0.0004	0.0003	**0.0004**	**0.3034**	**0.0019**	
JAG1	0.0009	0.0009	0.0010	**0.0010**	0.0003	0.0004	0.0003	**0.0003**	**0.3201**	**0.0001**	
KDM1A	0.0045	0.0040	0.0047	**0.0044**	0.0051	0.0051	0.0055	**0.0052**	**1.1826**	**0.0291**	
KDM2A	0.0017	0.0017	0.0017	**0.0017**	0.0017	0.0017	0.0017	**0.0017**	**1.0074**	**0.5534**	
KERATIN19	0.0111	0.0150	0.0098	**0.0120**	0.0069	0.0069	0.0095	**0.0078**	**0.6507**	**0.0792**	
KERATIN8	0.0043	0.0056	0.0028	**0.0042**	0.0034	0.0035	0.0032	**0.0034**	**0.7972**	**0.3380**	
KLF7	0.0004	0.0005	0.0008	**0.0006**	0.0011	0.0014	0.0014	**0.0013**	**2.3463**	**0.0076**	**UP**
KRM1	0.0002	0.0002	0.0001	**0.0002**	0.0000	0.0001	0.0000	**0.0000**	**0.2461**	**0.0145**	**DOWN**
KROX20	0.0000	0.0000	0.0000	**0.0000**	0.0000	0.0000	0.0000	**0.0000**	**No expressed**		**LOW**
LDB1	0.0026	0.0027	0.0025	**0.0026**	0.0024	0.0026	0.0026	**0.0025**	**0.9811**	**0.6170**	
LEF1	0.0030	0.0041	0.0031	**0.0034**	0.0061	0.0069	0.0062	**0.0064**	**1.9036**	**0.0022**	**UP**
LFNG	0.0032	0.0039	0.0027	**0.0032**	0.0030	0.0032	0.0032	**0.0031**	**0.9670**	**0.7794**	
LMX1A	0.0000	0.0000	0.0000	**0.0000**	0.0000	0.0000	0.0000	**0.0000**	**No expressed**		**LOW**
LMX1B	0.0086	0.0039	0.0111	**0.0079**	0.0030	0.0023	0.0025	**0.0026**	**0.3323**	**0.0695**	
MAFA	0.0007	0.0006	0.0009	**0.0008**	0.0003	0.0003	0.0003	**0.0003**	**0.3697**	**0.0091**	
MECOM	0.0000	0.0000	0.0000	**0.0000**	0.0000	0.0000	0.0000	**0.0000**	**No expressed**		**LOW**
MEIS1	0.0025	0.0039	0.0035	**0.0033**	0.0024	0.0033	0.0030	**0.0029**	**0.8715**	**0.4466**	
MLL2	0.0015	0.0015	0.0015	**0.0015**	0.0018	0.0016	0.0017	**0.0017**	**1.1126**	**0.0281**	
MLL5	0.0000	0.0000	0.0000	**0.0000**	0.0000	0.0000	0.0000	**0.0000**	**No expressed**		**LOW**
MSI1	0.0031	0.0027	0.0025	**0.0028**	0.0078	0.0072	0.0058	**0.0069**	**2.4907**	**0.0025**	**UP**
MSX1	0.0101	0.0091	0.0158	**0.0117**	0.0096	0.0127	0.0116	**0.0113**	**0.9698**	**0.8841**	
MYB	0.0005	0.0006	0.0007	**0.0006**	0.0005	0.0006	0.0006	**0.0005**	**0.9432**	**0.6582**	
NELL1	0.0015	0.0017	0.0008	**0.0013**	0.0009	0.0008	0.0008	**0.0008**	**0.6250**	**0.1595**	
NFKB1	0.0029	0.0035	0.0017	**0.0027**	0.0020	0.0018	0.0018	**0.0018**	**0.6802**	**0.1932**	
N-MYC	0.0041	0.0026	0.0048	**0.0038**	0.0084	0.0074	0.0062	**0.0074**	**1.9275**	**0.0180**	**UP**
NOTCH1	0.0061	0.0055	0.0068	**0.0061**	0.0025	0.0027	0.0023	**0.0025**	**0.4111**	**0.0007**	
NR2F2	0.0003	0.0003	0.0002	**0.0003**	0.0001	0.0001	0.0001	**0.0001**	**0.3878**	**0.0192**	
NR-CAM	0.0003	0.0002	0.0003	**0.0003**	0.0003	0.0003	0.0003	**0.0003**	**1.1421**	**0.2736**	
OTOG	0.0000	0.0000	0.0000	**0.0000**	0.0000	0.0000	0.0000	**0.0000**	**No expressed**		**LOW**
OTOL1	0.0000	0.0000	0.0000	**0.0000**	0.0000	0.0000	0.0000	**0.0000**	**No expressed**		**LOW**
OTX2	0.0059	0.0036	0.0038	**0.0045**	0.0034	0.0020	0.0019	**0.0024**	**0.5445**	**0.0761**	
PAX2	0.0004	0.0001	0.0010	**0.0005**	0.0073	0.0079	0.0129	**0.0094**	**18.5807**	**0.0082**	**UP**
PAX3	0.0000	0.0000	0.0000	**0.0000**	0.0000	0.0000	0.0000	**0.0000**	**No expressed**		**LOW**
PAX6	0.0088	0.0101	0.0055	**0.0081**	0.0002	0.0001	0.0002	**0.0001**	**0.0167**	**0.0044**	**DOWN**
PAX7	0.0000	0.0000	0.0000	**0.0000**	0.0000	0.0000	0.0000	**0.0000**	**No expressed**		**LOW**
PCNA	0.0133	0.0128	0.0141	**0.0134**	0.0112	0.0117	0.0122	**0.0117**	**0.8714**	**0.0201**	
PDLIM4	0.0021	0.0022	0.0025	**0.0023**	0.0022	0.0019	0.0022	**0.0021**	**0.9334**	**0.3633**	
PHOX2b	0.0000	0.0000	0.0000	**0.0000**	0.0000	0.0000	0.0000	**0.0000**	**No expressed**		**LOW**
PLAG1	0.0016	0.0015	0.0015	**0.0015**	0.0016	0.0016	0.0017	**0.0016**	**1.0480**	**0.1601**	
PNOC	0.0024	0.0035	0.0025	**0.0028**	0.0016	0.0010	0.0018	**0.0015**	**0.5196**	**0.0367**	
PTCH1	0.0013	0.0016	0.0011	**0.0013**	0.0010	0.0009	0.0008	**0.0009**	**0.6946**	**0.0543**	
RAI1	0.0017	0.0016	0.0017	**0.0017**	0.0030	0.0025	0.0022	**0.0025**	**1.5311**	**0.0169**	**UP**
FZD7	0.0181	0.0151	0.0173	**0.0168**	0.0334	0.0327	0.0318	**0.0326**	**1.9405**	**0.0001**	**UP**

Genes	6 HRS										
	Cnt				+ FGF2				Fold Change	P-Value	Results
	1	2	3	AVG	1	2	3	AVG			
RARB	0.0025	0.0031	0.0019	**0.0025**	0.0005	0.0005	0.0006	**0.0005**	0.2164	0.0049	DOWN
RARG	0.0014	0.0016	0.0012	**0.0014**	0.0012	0.0013	0.0010	**0.0012**	0.8711	0.3188	
RASA1	0.0007	0.0008	0.0006	**0.0007**	0.0008	0.0006	0.0008	**0.0007**	1.0182	0.8861	
RERE	0.0038	0.0037	0.0037	**0.0037**	0.0037	0.0036	0.0038	**0.0037**	0.9939	0.7114	
RFX4	0.0000	0.0000	0.0000	**0.0000**	0.0000	0.0000	0.0000	**0.0000**	No expressed		LOW
ROBO1	0.0010	0.0010	0.0014	**0.0011**	0.0017	0.0017	0.0017	**0.0017**	1.4994	0.0149	
ROBO2	0.0058	0.0058	0.0061	**0.0059**	0.0050	0.0034	0.0052	**0.0045**	0.7656	0.0687	
RXRG	0.0007	0.0008	0.0008	**0.0008**	0.0002	0.0002	0.0002	**0.0002**	0.2397	0.0005	DOWN
SALL1	0.0283	0.0287	0.0199	**0.0257**	0.0288	0.0318	0.0227	**0.0278**	1.0827	0.6169	
SALL4	0.0029	0.0026	0.0025	**0.0026**	0.0019	0.0020	0.0016	**0.0018**	0.6976	0.0117	
SCML2	0.0010	0.0009	0.0010	**0.0010**	0.0009	0.0010	0.0010	**0.0010**	1.0292	0.6002	
SDHA	0.0034	0.0032	0.0034	**0.0033**	0.0034	0.0032	0.0031	**0.0033**	0.9792	0.5915	
SEMA4D	0.0008	0.0008	0.0005	**0.0007**	0.0012	0.0011	0.0010	**0.0011**	1.5590	0.0160	UP
SEMA7A	0.0000	0.0000	0.0000	**0.0000**	0.0000	0.0000	0.0000	**0.0000**	No expressed		LOW
SETD2	0.0033	0.0027	0.0031	**0.0030**	0.0050	0.0050	0.0042	**0.0047**	1.5472	0.0064	UP
SETDB1	0.0034	0.0033	0.0034	**0.0034**	0.0040	0.0038	0.0037	**0.0038**	1.1448	0.0060	
SETMAR	0.0000	0.0000	0.0000	**0.0000**	0.0000	0.0000	0.0000	**0.0000**	No expressed		LOW
SIP1	0.0007	0.0003	0.0015	**0.0008**	0.0019	0.0020	0.0016	**0.0018**	2.2066	0.0562	
SIX1	0.0026	0.0029	0.0012	**0.0022**	0.0008	0.0008	0.0013	**0.0010**	0.4441	0.0942	
SIX3	0.0013	0.0009	0.0010	**0.0011**	0.0016	0.0003	0.0005	**0.0008**	0.7399	0.5558	
SIX4	0.0027	0.0030	0.0025	**0.0027**	0.0028	0.0028	0.0031	**0.0029**	1.0702	0.4000	
SLIT1	0.0041	0.0036	0.0050	**0.0042**	0.0012	0.0010	0.0014	**0.0012**	0.2850	0.0018	
SLIT2	0.0005	0.0006	0.0006	**0.0006**	0.0003	0.0004	0.0005	**0.0004**	0.7395	0.1130	
SLIT3	0.0014	0.0016	0.0012	**0.0014**	0.0010	0.0010	0.0015	**0.0011**	0.8144	0.2372	
SMARCC1	0.0037	0.0037	0.0036	**0.0036**	0.0038	0.0039	0.0035	**0.0038**	1.0285	0.4567	
SMOC1	0.0000	0.0000	0.0000	**0.0000**	0.0000	0.0000	0.0000	**0.0000**	No expressed		LOW
SMYD2	0.0017	0.0016	0.0017	**0.0017**	0.0018	0.0019	0.0017	**0.0018**	1.0955	0.1007	
SNAIL1	0.0006	0.0008	0.0004	**0.0006**	0.0018	0.0016	0.0012	**0.0015**	2.5417	0.0136	UP
SNAIL2	0.0040	0.0017	0.0160	**0.0072**	0.0006	0.0009	0.0017	**0.0011**	0.1464	0.2390	
SOHO1	0.0000	0.0000	0.0000	**0.0000**	0.0002	0.0002	0.0003	**0.0002**	10.0300	0.0019	UP
SOX1	0.0001	0.0002	0.0000	**0.0001**	0.0000	0.0000	0.0000	**0.0000**	0.3712	0.2869	
SOX10	0.0000	0.0000	0.0000	**0.0000**	0.0000	0.0000	0.0000	**0.0000**	No expressed		LOW
SOX13	0.0033	0.0029	0.0040	**0.0034**	0.0077	0.0070	0.0072	**0.0073**	2.1583	0.0006	UP
SOX2	0.0055	0.0032	0.0060	**0.0049**	0.0063	0.0064	0.0043	**0.0057**	1.1592	0.5226	
SOX3	0.0010	0.0010	0.0007	**0.0009**	0.0012	0.0014	0.0009	**0.0012**	1.3157	0.1755	
SOX8	0.0016	0.0015	0.0032	**0.0021**	0.0013	0.0014	0.0018	**0.0015**	0.7117	0.3420	
SOX9	0.0001	0.0000	0.0002	**0.0001**	0.0001	0.0001	0.0001	**0.0001**	0.6033	0.3956	
SP8	0.0000	0.0000	0.0000	**0.0000**	0.0000	0.0000	0.0000	**0.0000**	No expressed		LOW
SPRY1	0.0001	0.0001	0.0001	**0.0001**	0.0092	0.0090	0.0107	**0.0097**	121.7940	0.0001	UP
SPRY2	0.0006	0.0004	0.0014	**0.0008**	0.0301	0.0337	0.0355	**0.0331**	40.6826	0.0000	UP
SREBF2	0.0059	0.0060	0.0048	**0.0056**	0.0082	0.0090	0.0072	**0.0082**	1.4591	0.0164	
SSTR2	0.0001	0.0001	0.0001	**0.0001**	0.0002	0.0003	0.0004	**0.0003**	2.8581	0.0364	UP
SUV39H1	0.0002	0.0002	0.0002	**0.0002**	0.0002	0.0002	0.0002	**0.0002**	1.0499	0.3328	
TBX10	0.0000	0.0000	0.0000	**0.0000**	0.0000	0.0000	0.0000	**0.0000**	No expressed		LOW
TBX2	0.0000	0.0000	0.0000	**0.0000**	0.0000	0.0000	0.0000	**0.0000**	No expressed		LOW
TCF7L1	0.0024	0.0023	0.0023	**0.0024**	0.0027	0.0024	0.0028	**0.0026**	1.1197	0.0610	
TCF4	0.0027	0.0021	0.0022	**0.0023**	0.0030	0.0031	0.0032	**0.0031**	1.3327	0.0166	
TEAD3	0.0022	0.0024	0.0017	**0.0021**	0.0024	0.0024	0.0022	**0.0023**	1.1093	0.4035	
TFAP2A	0.0406	0.0427	0.0440	**0.0424**	0.0185	0.0148	0.0210	**0.0181**	0.4263	0.0003	
TFAP2C	0.0113	0.0159	0.0085	**0.0119**	0.0030	0.0034	0.0033	**0.0032**	0.2709	0.0157	
TLE1	0.0011	0.0009	0.0017	**0.0012**	0.0011	0.0013	0.0009	**0.0011**	0.9050	0.6931	
TRIM28	0.0069	0.0074	0.0060	**0.0068**	0.0055	0.0057	0.0054	**0.0055**	0.8131	0.0386	
TRIM3	0.0018	0.0022	0.0016	**0.0019**	0.0018	0.0017	0.0019	**0.0018**	0.9538	0.6597	
TRIM71	0.0050	0.0055	0.0060	**0.0055**	0.0075	0.0083	0.0084	**0.0081**	1.4678	0.0036	
TSHZ1	0.0000	0.0000	0.0000	**0.0000**	0.0000	0.0000	0.0000	**0.0000**	No expressed		LOW
VGLL2	0.0002	0.0003	0.0001	**0.0002**	0.0000	0.0000	0.0000	**0.0000**	0.0000	0.0700	
WHSC1	0.0046	0.0046	0.0051	**0.0047**	0.0050	0.0048	0.0052	**0.0050**	1.0539	0.2489	
WHSC1L1	0.0038	0.0041	0.0039	**0.0039**	0.0036	0.0037	0.0036	**0.0036**	0.9239	0.0464	
ZBTB16	0.0009	0.0008	0.0010	**0.0009**	0.0003	0.0003	0.0003	**0.0003**	0.3865	0.0006	
ZFHX3	0.0014	0.0014	0.0011	**0.0013**	0.0007	0.0006	0.0009	**0.0007**	0.5377	0.0119	
ZNF384	0.0014	0.0016	0.0014	**0.0015**	0.0014	0.0015	0.0014	**0.0014**	0.9952	0.9326	
ZNF385C	0.0021	0.0020	0.0016	**0.0019**	0.0026	0.0023	0.0031	**0.0027**	1.3938	0.0577	
ZNF423	0.0072	0.0063	0.0093	**0.0076**	0.0096	0.0111	0.0115	**0.0107**	1.4140	0.0431	
ZNF521	0.0057	0.0051	0.0068	**0.0058**	0.0075	0.0090	0.0081	**0.0082**	1.4013	0.0257	
ZNF534	0.0021	0.0023	0.0021	**0.0022**	0.0019	0.0017	0.0019	**0.0018**	0.8551	0.0247	
ZNF618	0.0010	0.0010	0.0010	**0.0010**	0.0009	0.0009	0.0008	**0.0009**	0.8761	0.0108	

Table 9.4 Normalised level of expression of Cnt and +FGF2 samples after 12 hours of culture analysed using the PPR NanoString probe set.

Genes	12 HRS										
	Cnt				+ FGF2				Fold Change	P-Value	Results
	1	2	3	AVG	1	2	3	AVG			
AATF	0.0045	0.0061	0.0044	**0.0050**	0.0044	0.0046	0.0044	**0.0044**	**0.8911**	**0.3957**	
ADNP2	0.0019	0.0022	0.0026	**0.0022**	0.0027	0.0016	0.0018	**0.0020**	**0.9182**	**0.6551**	
AP-2	0.0230	0.0061	0.0327	**0.0206**	0.0239	0.0084	0.0245	**0.0189**	**0.9203**	**0.8701**	
AXIN2	0.0042	0.0031	0.0034	**0.0036**	0.0009	0.0011	0.0010	**0.0010**	0.2709	0.0011	DOWN
BCL11A	0.0000	0.0000	0.0000	0.0000	0.0000	0.0000	0.0000	0.0000	No expressed		LOW
BCL2	0.0011	0.0013	0.0010	**0.0011**	0.0014	0.0017	0.0014	**0.0015**	**1.3177**	**0.0751**	
BCL7A	0.0064	0.0079	0.0069	**0.0071**	0.0067	0.0087	0.0072	**0.0075**	**1.0654**	**0.5745**	
BMP4	0.0013	0.0007	0.0007	**0.0009**	0.0023	0.0022	0.0010	**0.0018**	1.9873	**0.1173**	
CCND1	0.0107	0.0140	0.0089	**0.0112**	0.0098	0.0075	0.0092	**0.0088**	**0.7867**	**0.2192**	
CDKN1B	0.0008	0.0008	0.0009	**0.0008**	0.0010	0.0009	0.0012	**0.0010**	**1.2051**	**0.1012**	
CHD7	0.0055	0.0061	0.0057	**0.0057**	0.0067	0.0074	0.0062	**0.0067**	**1.1736**	**0.0644**	
CITED2	0.0031	0.0041	0.0028	**0.0033**	0.0042	0.0042	0.0042	**0.0042**	**1.2620**	**0.0823**	
CNTNAP5	0.0009	0.0019	0.0007	**0.0012**	0.0008	0.0010	0.0008	**0.0009**	0.7349	**0.4646**	
CXCL14	0.0003	0.0002	0.0006	**0.0003**	0.0045	0.0039	0.0051	**0.0045**	12.9594	0.0003	UP
CXXC6-like	0.0001	0.0002	0.0002	**0.0002**	0.0001	0.0002	0.0001	**0.0001**	0.7175	**0.2092**	
DACH1	0.0018	0.0020	0.0018	**0.0019**	0.0017	0.0021	0.0021	**0.0020**	**1.0651**	**0.4620**	
DBX2	0.0001	0.0002	0.0002	**0.0001**	0.0002	0.0006	0.0003	**0.0004**	2.5434	**0.1883**	
DLX3	0.0007	0.0002	0.0013	**0.0008**	0.0008	0.0002	0.0010	**0.0006**	**0.8363**	**0.7778**	
DLX5	0.0060	0.0015	0.0080	**0.0052**	0.0047	0.0010	0.0040	**0.0032**	0.6211	**0.4278**	
DLX6	0.0050	0.0011	0.0071	**0.0044**	0.0047	0.0008	0.0037	**0.0031**	0.6988	**0.5636**	
DNAJC1	0.0031	0.0038	0.0030	**0.0033**	0.0032	0.0042	0.0031	**0.0035**	**1.0578**	**0.6853**	
DNMT3A	0.0000	0.0001	0.0000	**0.0000**	0.0000	0.0000	0.0000	**0.0000**	No expressed		LOW
DNMT3B	0.0141	0.0171	0.0111	**0.0141**	0.0132	0.0123	0.0112	**0.0123**	**0.8720**	**0.3808**	
E2F8	0.0000	0.0000	0.0000	**0.0000**	0.0000	0.0000	0.0000	**0.0000**	No expressed		LOW
ECE1	0.0023	0.0021	0.0028	**0.0024**	0.0031	0.0025	0.0027	**0.0028**	**1.1514**	**0.2268**	
EEF1A1	0.1362	0.1479	0.1566	**0.1469**	0.1431	0.1786	0.1649	**0.1622**	**1.1040**	**0.2681**	
ERNI	0.0606	0.0365	0.0206	**0.0392**	0.0508	0.0301	0.0338	**0.0382**	**0.9745**	**0.9434**	
ETV4	0.0000	0.0000	0.0000	**0.0000**	-0.0001	0.0000	0.0000	**0.0000**	No expressed		LOW
ETV5	0.0034	0.0054	0.0026	**0.0038**	0.0077	0.0088	0.0073	**0.0079**	2.0780	0.0113	UP
EYA1	0.0005	0.0004	0.0004	**0.0004**	0.0006	0.0003	0.0007	**0.0006**	**1.2756**	**0.3367**	
EYA2	0.0051	0.0025	0.0068	**0.0048**	0.0067	0.0020	0.0095	**0.0060**	**1.2553**	**0.6497**	
EZH2	0.0094	0.0112	0.0108	**0.0104**	0.0103	0.0093	0.0108	**0.0102**	**0.9754**	**0.7355**	
FSTL4	0.0006	0.0009	0.0009	**0.0008**	0.0010	0.0006	0.0008	**0.0008**	**1.0403**	**0.8360**	
FOXG1	0.0004	0.0004	0.0002	**0.0003**	0.0009	0.0014	0.0011	**0.0011**	3.2056	0.0122	UP
FOXI1	0.0000	0.0000	0.0000	**0.0000**	-0.0001	0.0000	0.0000	**0.0000**	No expressed		LOW
FOXI3	0.0030	0.0008	0.0028	**0.0022**	0.0117	0.0028	0.0137	**0.0094**	4.2678	**0.1030**	
FOXM1	0.0010	0.0011	0.0012	**0.0011**	0.0011	0.0008	0.0011	**0.0010**	**0.8859**	**0.3253**	
FOXN2	0.0014	0.0016	0.0013	**0.0014**	0.0012	0.0015	0.0012	**0.0013**	**0.9091**	**0.3636**	
GAPDH	0.3648	0.3249	0.3685	**0.3527**	0.2944	0.2750	0.3164	**0.2953**	**0.8371**	0.0353	
GATA2	0.0040	0.0004	0.0048	**0.0031**	0.0005	0.0001	0.0004	**0.0003**	0.1072	**0.1119**	
GATA3	0.0008	0.0002	0.0017	**0.0009**	0.0012	0.0004	0.0012	**0.0009**	**1.0187**	**0.9749**	
GBX2	0.0018	0.0020	0.0012	**0.0017**	0.0168	0.0243	0.0035	**0.0149**	9.0044	**0.0948**	
GEMININ	0.0012	0.0017	0.0020	**0.0016**	0.0010	0.0011	0.0015	**0.0012**	0.7449	**0.2331**	
GPR160	0.0002	0.0004	0.0002	**0.0003**	0.0002	0.0001	0.0002	**0.0002**	0.6628	**0.2677**	
HDAC1	0.0046	0.0045	0.0048	**0.0046**	0.0059	0.0050	0.0050	**0.0053**	**1.1372**	**0.1227**	
HESX1	0.0014	0.0024	0.0007	**0.0015**	0.0154	0.0451	0.0220	**0.0275**	18.1373	0.0447	UP
HEY1	0.0045	0.0034	0.0049	**0.0043**	0.0092	0.0035	0.0089	**0.0072**	1.6865	**0.2031**	
HEY2	0.0001	0.0002	0.0000	**0.0001**	0.0004	0.0004	0.0002	**0.0003**	3.3649	0.0445	UP
HIF1A	0.0141	0.0122	0.0148	**0.0137**	0.0143	0.0104	0.0139	**0.0128**	**0.9359**	**0.5809**	
HMGXB4	0.0009	0.0010	0.0010	**0.0010**	0.0011	0.0011	0.0011	**0.0011**	**1.1143**	0.0222	
HMX3	0.0000	0.0000	0.0000	**0.0000**	-0.0001	0.0000	0.0000	**0.0000**	No expressed		LOW
HOMER2	0.0021	0.0011	0.0028	**0.0020**	0.0031	0.0013	0.0029	**0.0025**	**1.2338**	**0.5674**	
HPRT1	0.0027	0.0032	0.0024	**0.0028**	0.0027	0.0027	0.0027	**0.0027**	**0.9792**	**0.8242**	
HSF2	0.0032	0.0040	0.0030	**0.0034**	0.0031	0.0039	0.0030	**0.0033**	**0.9786**	**0.8732**	
ING5	0.0008	0.0007	0.0009	**0.0008**	0.0008	0.0008	0.0007	**0.0008**	**0.9550**	**0.4962**	
IRX1	0.0012	0.0015	0.0015	**0.0014**	0.0019	0.0006	0.0016	**0.0014**	**0.9793**	**0.9459**	
IRX2	0.0008	0.0010	0.0006	**0.0008**	0.0011	0.0004	0.0006	**0.0007**	**0.8634**	**0.6492**	
IRX3	0.0095	0.0091	0.0106	**0.0097**	0.0047	0.0024	0.0059	**0.0043**	0.4474	0.0087	DOWN
KERATIN19	0.0017	0.0009	0.0021	**0.0016**	0.0016	0.0013	0.0019	**0.0016**	**1.0335**	**0.9048**	
KREMEN1	0.0008	0.0005	0.0008	**0.0007**	0.0003	0.0004	0.0002	**0.0003**	0.3983	0.0141	DOWN
LEF1	0.0034	0.0032	0.0041	**0.0036**	0.0015	0.0015	0.0015	**0.0015**	0.4190	0.0019	DOWN
LMX1A	0.0000	0.0000	0.0000	**0.0000**	0.0000	0.0000	0.0000	**0.0000**	No expressed		LOW
LMX1B	0.0075	0.0065	0.0058	**0.0066**	0.0082	0.0120	0.0085	**0.0095**	**1.4361**	**0.0927**	

Genes	12 HRS										
	Cnt				+ FGF2				Fold Change	P-Value	Results
	1	2	3	AVG	1	2	3	AVG			
LRP11	0.0022	0.0014	0.0051	**0.0029**	0.0033	0.0006	0.0044	**0.0028**	**0.9528**	**0.9353**	
LZTR1	0.0001	0.0001	0.0001	**0.0000**	0.0001	0.0001	0.0001	**0.0000**	**No expressed**		**LOW**
MEF2D	0.0017	0.0016	0.0018	**0.0017**	0.0017	0.0016	0.0019	**0.0018**	**1.0500**	**0.5026**	
MIER1	0.0011	0.0016	0.0012	**0.0013**	0.0012	0.0013	0.0012	**0.0012**	**0.9351**	**0.5682**	
MLLT10	0.0005	0.0011	0.0009	**0.0008**	0.0007	0.0009	0.0004	**0.0007**	**0.8228**	**0.5507**	
MORC2	0.0019	0.0024	0.0023	**0.0022**	0.0017	0.0025	0.0020	**0.0021**	**0.9580**	**0.7628**	
MSX1	0.0157	0.0088	0.0128	**0.0124**	0.0140	0.0111	0.0084	**0.0112**	**0.8986**	**0.6488**	
MTA3	0.0000	0.0001	0.0001	**0.0000**	0.0000	0.0001	0.0000	**0.0000**	**No expressed**		**LOW**
MYNN	0.0022	0.0024	0.0020	**0.0022**	0.0021	0.0026	0.0023	**0.0023**	**1.0525**	**0.5733**	
N-MYC	0.0118	0.0220	0.0090	**0.0142**	0.0076	0.0049	0.0058	**0.0061**	**0.4276**	**0.1123**	
NFKB1	0.0023	0.0014	0.0040	**0.0025**	0.0029	0.0017	0.0029	**0.0025**	**0.9915**	**0.9811**	
NPAS3	0.0000	0.0000	0.0000	**0.0000**	0.0000	0.0001	0.0000	**0.0000**	**No expressed**		**LOW**
NSD1	0.0000	0.0000	0.0000	**0.0000**	0.0000	0.0000	0.0000	**0.0000**	**No expressed**		**LOW**
OTX2	0.0069	0.0198	0.0058	**0.0108**	0.0048	0.0044	0.0081	**0.0058**	**0.5326**	**0.3391**	
PAX2	0.0040	0.0119	0.0018	**0.0059**	0.0123	0.0119	0.0095	**0.0112**	**1.9085**	**0.1678**	
PAX3	0.0000	0.0000	0.0000	**0.0000**	-0.0001	0.0000	0.0000	**0.0000**	**No expressed**		**LOW**
PAX6	0.0048	0.0118	0.0083	**0.0083**	0.0041	0.0005	0.0038	**0.0028**	**0.3344**	**0.0773**	
PAX7	0.0000	0.0000	0.0000	**0.0000**	-0.0001	0.0000	0.0000	**0.0000**	**No expressed**		**LOW**
PCNA	0.0247	0.0321	0.0283	**0.0284**	0.0260	0.0234	0.0271	**0.0255**	**0.8991**	**0.3014**	
PDLI4	0.0067	0.0045	0.0059	**0.0057**	0.0059	0.0047	0.0044	**0.0050**	**0.8791**	**0.4366**	
PHF10	0.0053	0.0065	0.0062	**0.0060**	0.0056	0.0057	0.0058	**0.0057**	**0.9481**	**0.4190**	
PHF20	0.0061	0.0073	0.0063	**0.0066**	0.0059	0.0065	0.0062	**0.0062**	**0.9438**	**0.4170**	
PNOC	0.0018	0.0007	0.0024	**0.0016**	0.0010	0.0005	0.0012	**0.0009**	**0.5658**	**0.2770**	
POGZ	0.0012	0.0016	0.0016	**0.0014**	0.0012	0.0014	0.0016	**0.0014**	**0.9809**	**0.8669**	
PSIP1	0.0050	0.0085	0.0058	**0.0064**	0.0062	0.0063	0.0057	**0.0061**	**0.9447**	**0.7576**	
PTPRU	0.0003	0.0006	0.0005	**0.0005**	0.0005	0.0003	0.0005	**0.0004**	**0.8470**	**0.5584**	
RRN3	0.0000	0.0000	0.0000	**0.0000**	0.0000	0.0000	0.0000	**0.0000**	**No expressed**		**LOW**
RX1	0.0000	0.0000	0.0000	**0.0000**	-0.0001	0.0000	0.0000	**0.0000**	**No expressed**		**LOW**
RYBP	0.0022	0.0023	0.0023	**0.0022**	0.0023	0.0022	0.0024	**0.0023**	**1.0209**	**0.5632**	
SALL1	0.0148	0.0100	0.0164	**0.0137**	0.0240	0.0277	0.0180	**0.0232**	**1.6923**	**0.0493**	**UP**
SALL4	0.0031	0.0053	0.0034	**0.0039**	0.0042	0.0039	0.0037	**0.0040**	**1.0136**	**0.9440**	
SDHA	0.0043	0.0050	0.0046	**0.0046**	0.0044	0.0046	0.0042	**0.0044**	**0.9583**	**0.4500**	
SETD2	0.0030	0.0053	0.0028	**0.0037**	0.0043	0.0049	0.0034	**0.0042**	**1.1267**	**0.6304**	
SIX1	0.0021	0.0023	0.0029	**0.0024**	0.0031	0.0024	0.0043	**0.0032**	**1.3269**	**0.2523**	
SIX3	0.0026	0.0042	0.0012	**0.0026**	0.0042	0.0133	0.0062	**0.0079**	**2.9994**	**0.1425**	
SIX4	0.0030	0.0022	0.0032	**0.0028**	0.0031	0.0031	0.0033	**0.0032**	**1.1336**	**0.2989**	
SMAD6	0.0000	0.0000	0.0000	**0.0000**	-0.0001	0.0000	0.0000	**0.0000**	**No expressed**		**LOW**
SOX10	0.0094	0.0014	0.0106	**0.0071**	0.0008	0.0001	0.0008	**0.0006**	**0.0799**	**0.0868**	
SOX2	0.0029	0.0072	0.0018	**0.0040**	0.0066	0.0118	0.0061	**0.0081**	**2.0562**	**0.1644**	
SOX3	0.0026	0.0063	0.0019	**0.0036**	0.0023	0.0024	0.0017	**0.0021**	**0.5836**	**0.3362**	
SOX9	0.0009	0.0008	0.0013	**0.0010**	0.0002	0.0001	0.0001	**0.0001**	**0.1314**	**0.0050**	**DOWN**
SP4	0.0020	0.0026	0.0024	**0.0023**	0.0023	0.0028	0.0025	**0.0025**	**1.0960**	**0.3584**	
SSTR5	0.0005	0.0001	0.0010	**0.0005**	0.0003	0.0000	0.0002	**0.0002**	**0.3647**	**0.2722**	
STOX2	0.0016	0.0020	0.0013	**0.0016**	0.0013	0.0013	0.0016	**0.0014**	**0.8490**	**0.3080**	
TAC1	0.0000	0.0000	0.0001	**0.0000**	0.0000	0.0000	0.0000	**0.0000**	**No expressed**		**LOW**
TBL1XR1	0.0039	0.0051	0.0036	**0.0042**	0.0038	0.0046	0.0041	**0.0042**	**0.9903**	**0.9409**	
TBX1	0.0003	0.0005	0.0001	**0.0003**	0.0000	0.0003	0.0007	**0.0003**	**1.0966**	**0.9038**	
TBX2	0.0000	0.0000	0.0000	**0.0000**	0.0000	0.0000	0.0000	**0.0000**	**No expressed**		**LOW**
TBX3	0.0000	0.0000	0.0000	**0.0000**	0.0000	0.0000	0.0000	**0.0000**	**No expressed**		**LOW**
TGIF2	0.0039	0.0039	0.0040	**0.0040**	0.0042	0.0038	0.0042	**0.0040**	**1.0213**	**0.5999**	
TOX3	0.0008	0.0008	0.0008	**0.0008**	0.0006	0.0007	0.0005	**0.0006**	**0.7553**	**0.0126**	
TP53	0.0085	0.0080	0.0081	**0.0082**	0.0094	0.0083	0.0093	**0.0090**	**1.0966**	**0.0988**	
TRIM24	0.0025	0.0036	0.0032	**0.0031**	0.0026	0.0029	0.0031	**0.0029**	**0.9175**	**0.5097**	
WHSC1	0.0069	0.0088	0.0074	**0.0077**	0.0067	0.0066	0.0072	**0.0068**	**0.8890**	**0.2257**	
YEATS4	0.0027	0.0045	0.0033	**0.0035**	0.0026	0.0044	0.0028	**0.0033**	**0.9469**	**0.8216**	
ZFHX1B	0.0046	0.0066	0.0034	**0.0049**	0.0025	0.0041	0.0024	**0.0030**	**0.6139**	**0.1593**	
ZHX2	0.0024	0.0031	0.0025	**0.0027**	0.0027	0.0031	0.0025	**0.0028**	**1.0299**	**0.7820**	
ZIC1	0.0006	0.0011	0.0001	**0.0006**	0.0008	0.0031	0.0009	**0.0016**	**2.6304**	**0.2871**	
ZIC2	0.0115	0.0151	0.0073	**0.0113**	0.0146	0.0191	0.0098	**0.0145**	**1.2803**	**0.4160**	
ZIC3	0.0093	0.0168	0.0046	**0.0102**	0.0097	0.0166	0.0087	**0.0117**	**1.1446**	**0.7509**	
ZNF217	0.0100	0.0111	0.0104	**0.0105**	0.0151	0.0159	0.0131	**0.0147**	**1.3986**	**0.0099**	
ZNF423	0.0093	0.0107	0.0074	**0.0091**	0.0125	0.0132	0.0106	**0.0121**	**1.3234**	**0.0790**	
ZNF462	0.0113	0.0186	0.0144	**0.0148**	0.0154	0.0126	0.0129	**0.0137**	**0.9251**	**0.6563**	

Table 9.5 Normalised level of expression of Cnt and +FGF2 samples after 24 hours of culture analysed using the PPR NanoString probe set.

Genes	24 HRS										
	Cnt				+ FGF2				Fold Change	P-Value	Results
	1	2	3	AVG	1	2	3	AVG			
AATF	0.0029	0.0033	0.0036	**0.0033**	0.0038	0.0041	0.0045	**0.0041**	1.2609	0.0367	
ADNP2	0.0024	0.0021	0.0024	**0.0023**	0.0014	0.0022	0.0028	**0.0021**	0.9336	0.7327	
AP-2	0.0235	0.0192	0.0180	**0.0203**	0.0218	0.0109	0.0243	**0.0190**	0.9374	0.7895	
AXIN2	0.0009	0.0027	0.0023	**0.0020**	0.0007	0.0008	0.0006	**0.0007**	0.3633	0.0849	
BCL11A	0.0000	0.0000	0.0000	0.0000	0.0000	0.0000	0.0000	0.0000	No expressed		LOW
BCL2	0.0011	0.0009	0.0009	**0.0009**	0.0017	0.0017	0.0015	**0.0016**	1.6985	0.0015	UP
BCL7A	0.0049	0.0047	0.0051	**0.0049**	0.0068	0.0066	0.0061	**0.0065**	1.3189	0.0032	
BMP4	0.0008	0.0008	0.0007	**0.0008**	0.0011	0.0011	0.0016	**0.0013**	1.6671	0.0424	UP
CCND1	0.0054	0.0058	0.0070	**0.0061**	0.0097	0.0089	0.0117	**0.0101**	1.6661	0.0132	UP
CDKN1B	0.0016	0.0015	0.0013	**0.0015**	0.0013	0.0009	0.0014	**0.0012**	0.8346	0.2749	
CHD7	0.0042	0.0048	0.0044	**0.0045**	0.0073	0.0071	0.0059	**0.0068**	1.5194	0.0082	UP
CITED2	0.0024	0.0030	0.0029	**0.0028**	0.0048	0.0051	0.0049	**0.0049**	1.7631	0.0006	UP
CNTNAP5	0.0003	0.0006	0.0006	**0.0005**	0.0006	0.0005	0.0002	**0.0004**	0.7824	0.5067	
CXCL14	0.0003	0.0000	0.0000	**0.0001**	0.0011	0.0008	0.0016	**0.0012**	13.4003	0.0125	UP
CXXC6-like	0.0002	0.0002	0.0002	**0.0002**	0.0001	0.0001	0.0002	**0.0002**	0.9509	0.8607	
DACH1	0.0012	0.0018	0.0018	**0.0016**	0.0013	0.0017	0.0020	**0.0017**	1.0572	0.7672	
DBX2	0.0000	0.0001	0.0001	**0.0000**	0.0004	0.0008	0.0003	**0.0005**	10.1516	0.0655	
DLX3	0.0013	0.0009	0.0009	**0.0011**	0.0006	0.0001	0.0010	**0.0006**	0.5617	0.1919	
DLX5	0.0043	0.0031	0.0030	**0.0034**	0.0030	0.0012	0.0030	**0.0024**	0.7013	0.2271	
DLX6	0.0031	0.0023	0.0027	**0.0027**	0.0022	0.0011	0.0027	**0.0020**	0.7489	0.2691	
DNAJC1	0.0031	0.0026	0.0027	**0.0028**	0.0029	0.0033	0.0036	**0.0033**	1.1740	0.1031	
DNMT3A	0.0000	0.0000	0.0000	0.0000	0.0000	0.0000	0.0000	0.0000	No expressed		LOW
DNMT3B	0.0101	0.0085	0.0102	**0.0096**	0.0064	0.0118	0.0092	**0.0092**	0.9524	0.7952	
E2F8	0.0000	0.0000	0.0000	0.0000	0.0000	0.0000	0.0000	0.0000	No expressed		LOW
ECE1	0.0027	0.0021	0.0023	**0.0024**	0.0027	0.0032	0.0035	**0.0031**	1.3298	0.0592	
EEF1A1	0.1540	0.1629	0.1577	**0.1582**	0.1854	0.1667	0.1497	**0.1673**	1.0573	0.4408	
ERNI	0.0622	0.0813	0.0669	**0.0701**	0.0381	0.0741	0.0798	**0.0640**	0.9122	0.6885	
ETV4	0.0000	0.0000	0.0000	0.0000	0.0000	0.0000	0.0000	0.0000	No expressed		LOW
ETV5	0.0006	0.0010	0.0011	**0.0009**	0.0060	0.0065	0.0060	**0.0062**	6.9235	0.0000	UP
EYA1	0.0015	0.0013	0.0014	**0.0014**	0.0013	0.0007	0.0016	**0.0012**	0.8578	0.5246	
EYA2	0.0008	0.0022	0.0022	**0.0017**	0.0056	0.0029	0.0117	**0.0067**	3.9289	0.1316	
EZH2	0.0078	0.0082	0.0076	**0.0079**	0.0103	0.0091	0.0096	**0.0097**	1.2285	0.0105	
FSTL4	0.0006	0.0006	0.0006	**0.0006**	0.0056	0.0035	0.0020	**0.0037**	6.1225	0.0398	UP
FOXG1	0.0001	0.0001	0.0002	**0.0001**	0.0007	0.0015	0.0016	**0.0012**	8.8222	0.0213	UP
FOXI1	0.0000	0.0000	0.0000	0.0000	0.0000	0.0000	0.0000	0.0000	No expressed		LOW
FOXI3	0.0016	0.0014	0.0009	**0.0013**	0.0059	0.0026	0.0150	**0.0079**	6.1088	0.1514	
FOXM1	0.0006	0.0006	0.0007	**0.0006**	0.0013	0.0007	0.0008	**0.0009**	1.4276	0.2230	
FOXN2	0.0011	0.0011	0.0010	**0.0011**	0.0012	0.0012	0.0011	**0.0012**	1.1244	0.0166	
GAPDH	0.4333	0.3897	0.3987	**0.4072**	0.3609	0.3068	0.3207	**0.3295**	0.8091	0.0207	
GATA2	0.0106	0.0045	0.0038	**0.0063**	0.0004	0.0001	0.0004	**0.0003**	0.0455	0.0499	DOWN
GATA3	0.0023	0.0013	0.0020	**0.0019**	0.0016	0.0012	0.0027	**0.0018**	0.9568	0.8883	
GBX2	0.0011	0.0007	0.0010	**0.0009**	0.0172	0.0404	0.0083	**0.0220**	23.6444	0.0926	
GEMININ	0.0007	0.0008	0.0010	**0.0008**	0.0010	0.0009	0.0013	**0.0011**	1.2903	0.1446	
GPR160	0.0001	0.0002	0.0001	**0.0001**	0.0001	0.0001	0.0002	**0.0001**	1.0981	0.7875	
HDAC1	0.0044	0.0034	0.0038	**0.0039**	0.0045	0.0038	0.0046	**0.0043**	1.1117	0.3186	
HESX1	0.0005	0.0003	0.0004	**0.0004**	0.0018	0.0043	0.0015	**0.0025**	6.2155	0.0705	
HEY1	0.0051	0.0045	0.0056	**0.0051**	0.0083	0.0063	0.0171	**0.0106**	2.0875	0.1719	
HEY2	0.0000	0.0000	0.0001	**0.0000**	0.0001	0.0001	0.0003	**0.0002**	8.0720	0.0933	
HIF1A	0.0102	0.0094	0.0098	**0.0098**	0.0135	0.0103	0.0133	**0.0123**	1.2596	0.0756	
HMGXB4	0.0005	0.0007	0.0007	**0.0006**	0.0009	0.0008	0.0007	**0.0008**	1.2948	0.0741	
HMX3	0.0000	0.0000	0.0000	0.0000	0.0000	0.0000	0.0000	0.0000	No expressed		LOW
HOMER2	0.0022	0.0014	0.0016	**0.0017**	0.0034	0.0017	0.0042	**0.0031**	1.8010	0.1480	
HPRT1	0.0022	0.0022	0.0026	**0.0023**	0.0030	0.0029	0.0028	**0.0029**	1.2516	0.0205	
HSF2	0.0021	0.0029	0.0029	**0.0026**	0.0029	0.0039	0.0040	**0.0036**	1.3736	0.0985	
ING5	0.0008	0.0007	0.0008	**0.0007**	0.0007	0.0008	0.0008	**0.0008**	1.0434	0.5218	
IRX1	0.0033	0.0025	0.0028	**0.0028**	0.0017	0.0036	0.0030	**0.0028**	0.9791	0.9256	
IRX2	0.0022	0.0015	0.0015	**0.0017**	0.0043	0.0054	0.0022	**0.0040**	2.2992	0.0840	
IRX3	0.0040	0.0061	0.0077	**0.0060**	0.0016	0.0025	0.0034	**0.0025**	0.4209	0.0443	DOWN
KERATIN19	0.0050	0.0022	0.0020	**0.0031**	0.0008	0.0007	0.0019	**0.0011**	0.3695	0.1350	
KREMEN1	0.0022	0.0012	0.0012	**0.0015**	0.0005	0.0004	0.0004	**0.0004**	0.2775	0.0314	DOWN
LEF1	0.0041	0.0053	0.0055	**0.0050**	0.0021	0.0015	0.0017	**0.0018**	0.3517	0.0021	DOWN
LMX1A	0.0000	0.0000	0.0000	0.0000	0.0000	0.0000	0.0000	0.0000	No expressed		LOW
LMX1B	0.0038	0.0053	0.0049	**0.0047**	0.0038	0.0048	0.0021	**0.0036**	0.7609	0.2864	

Genes	24 HRS										
	Cnt				+ FGF2				Fold Change	P-Value	Results
	1	2	3	AVG	1	2	3	AVG			
LRP11	0.0021	0.0027	0.0031	**0.0026**	0.0016	0.0006	0.0029	**0.0017**	0.6548	0.2773	
LZTR1	0.0000	0.0000	0.0000	0.0000	0.0000	0.0000	0.0000	0.0000	No expressed		LOW
MEF2D	0.0022	0.0012	0.0012	**0.0015**	0.0009	0.0011	0.0011	**0.0011**	0.6944	0.2425	
MIER1	0.0009	0.0009	0.0008	**0.0009**	0.0012	0.0012	0.0010	**0.0011**	1.2573	0.0238	
MLLT10	0.0010	0.0010	0.0007	**0.0009**	0.0008	0.0007	0.0010	**0.0008**	0.9581	0.7993	
MORC2	0.0016	0.0019	0.0018	**0.0018**	0.0018	0.0024	0.0021	**0.0021**	1.1849	0.1276	
MSX1	0.0066	0.0117	0.0144	**0.0109**	0.0053	0.0056	0.0052	**0.0054**	0.4935	0.0723	
MTA3	0.0000	0.0000	0.0000	0.0000	0.0000	0.0000	0.0000	0.0000	No expressed		LOW
MYNN	0.0015	0.0017	0.0020	**0.0017**	0.0022	0.0023	0.0022	**0.0022**	1.3212	0.0258	
N-MYC	0.0031	0.0074	0.0092	**0.0066**	0.0055	0.0081	0.0069	**0.0068**	1.0366	0.9095	
NFKB1	0.0024	0.0017	0.0020	**0.0020**	0.0020	0.0019	0.0026	**0.0021**	1.0578	0.7283	
NPAS3	0.0000	0.0000	0.0000	0.0000	0.0000	0.0000	0.0000	0.0000	No expressed		LOW
NSD1	0.0000	0.0000	0.0000	0.0000	0.0000	0.0000	0.0000	0.0000	No expressed		LOW
OTX2	0.0009	0.0060	0.0043	**0.0038**	0.0018	0.0013	0.0029	**0.0020**	0.5275	0.3242	
PAX2	0.0000	0.0002	0.0005	**0.0002**	0.0101	0.0131	0.0081	**0.0104**	45.2476	0.0022	UP
PAX3	0.0000	0.0000	0.0000	0.0000	0.0000	0.0000	0.0000	0.0000	No expressed		LOW
PAX6	0.0058	0.0090	0.0088	**0.0079**	0.0016	0.0021	0.0035	**0.0024**	0.3039	0.0098	DOWN
PAX7	0.0000	0.0000	0.0000	0.0000	0.0000	0.0000	0.0000	0.0000	No expressed		LOW
PCNA	0.0184	0.0242	0.0237	**0.0221**	0.0297	0.0279	0.0289	**0.0288**	1.3032	0.0257	
PDLI4	0.0038	0.0027	0.0024	**0.0030**	0.0047	0.0044	0.0041	**0.0044**	1.4832	0.0369	
PHF10	0.0044	0.0047	0.0043	**0.0044**	0.0050	0.0042	0.0054	**0.0049**	1.0928	0.3119	
PHF20	0.0056	0.0057	0.0052	**0.0055**	0.0062	0.0057	0.0052	**0.0057**	1.0335	0.5857	
PNOC	0.0002	0.0002	0.0003	**0.0002**	0.0007	0.0004	0.0007	**0.0006**	2.5635	0.0185	UP
POGZ	0.0012	0.0017	0.0014	**0.0014**	0.0016	0.0017	0.0016	**0.0016**	1.1460	0.2547	
PSIP1	0.0040	0.0056	0.0053	**0.0050**	0.0046	0.0059	0.0063	**0.0056**	1.1274	0.4092	
PTPRU	0.0002	0.0002	0.0002	**0.0002**	0.0004	0.0003	0.0004	**0.0004**	1.9317	0.0038	UP
RRN3	0.0000	0.0000	0.0000	0.0000	0.0000	0.0000	0.0000	0.0000	No expressed		LOW
RX1	0.0000	0.0000	0.0000	0.0000	0.0000	0.0000	0.0000	0.0000	No expressed		LOW
RYBP	0.0016	0.0015	0.0016	**0.0016**	0.0021	0.0019	0.0020	**0.0020**	1.2449	0.0069	
SALL1	0.0125	0.0073	0.0083	**0.0094**	0.0075	0.0139	0.0104	**0.0106**	1.1357	0.6302	
SALL4	0.0030	0.0028	0.0025	**0.0028**	0.0028	0.0037	0.0043	**0.0036**	1.3014	0.1475	
SDHA	0.0031	0.0039	0.0038	**0.0036**	0.0036	0.0041	0.0042	**0.0040**	1.1156	0.2491	
SETD2	0.0018	0.0018	0.0022	**0.0019**	0.0026	0.0033	0.0030	**0.0030**	1.5464	0.0112	UP
SIX1	0.0013	0.0016	0.0023	**0.0017**	0.0042	0.0038	0.0100	**0.0060**	3.4511	0.1010	
SIX3	0.0010	0.0020	0.0015	**0.0015**	0.0025	0.0059	0.0018	**0.0034**	2.2562	0.2121	
SIX4	0.0028	0.0026	0.0029	**0.0028**	0.0030	0.0029	0.0036	**0.0031**	1.1402	0.1718	
SMAD6	0.0000	0.0000	0.0000	0.0000	0.0000	0.0000	0.0000	0.0000	No expressed		LOW
SOX10	0.0241	0.0184	0.0163	**0.0196**	0.0050	0.0044	0.0056	**0.0050**	0.2546	0.0035	DOWN
SOX2	0.0018	0.0029	0.0036	**0.0027**	0.0050	0.0092	0.0035	**0.0059**	2.1516	0.1527	
SOX3	0.0011	0.0020	0.0023	**0.0018**	0.0013	0.0028	0.0024	**0.0022**	1.2029	0.5497	
SOX9	0.0001	0.0004	0.0001	**0.0002**	0.0001	0.0000	0.0001	**0.0001**	0.4300	0.2840	
SP4	0.0013	0.0017	0.0016	**0.0015**	0.0022	0.0020	0.0018	**0.0020**	1.3070	0.0497	
SSTR5	0.0002	0.0001	0.0001	**0.0001**	0.0001	0.0000	0.0001	**0.0001**	0.7938	0.7215	
STOX2	0.0008	0.0009	0.0013	**0.0010**	0.0011	0.0017	0.0014	**0.0014**	1.3828	0.1653	
TAC1	0.0000	0.0000	0.0000	0.0000	0.0000	0.0000	0.0000	0.0000	No expressed		LOW
TBL1XR1	0.0042	0.0042	0.0042	**0.0042**	0.0049	0.0039	0.0044	**0.0044**	1.0432	0.5638	
TBX1	0.0000	0.0001	0.0003	**0.0001**	0.0003	0.0009	0.0013	**0.0008**	8.3538	0.0781	
TBX2	0.0000	0.0000	0.0000	0.0000	0.0000	0.0000	0.0000	0.0000	No expressed		LOW
TBX3	0.0011	0.0003	0.0003	**0.0005**	0.0073	0.0017	0.0049	**0.0046**	8.4467	0.0674	
TGIF2	0.0044	0.0049	0.0056	**0.0050**	0.0033	0.0046	0.0045	**0.0041**	0.8253	0.1901	
TOX3	0.0006	0.0007	0.0008	**0.0007**	0.0010	0.0009	0.0005	**0.0008**	1.1647	0.4818	
TP53	0.0094	0.0087	0.0092	**0.0091**	0.0100	0.0091	0.0098	**0.0096**	1.0527	0.2177	
TRIM24	0.0018	0.0020	0.0022	**0.0020**	0.0029	0.0026	0.0026	**0.0027**	1.3646	0.0127	
WHSC1	0.0066	0.0071	0.0069	**0.0069**	0.0071	0.0076	0.0082	**0.0076**	1.1082	0.0917	
YEATS4	0.0026	0.0029	0.0026	**0.0027**	0.0024	0.0029	0.0026	**0.0026**	0.9773	0.7691	
ZFHX1B	0.0067	0.0055	0.0060	**0.0061**	0.0029	0.0030	0.0024	**0.0028**	0.4551	0.0010	DOWN
ZHX2	0.0024	0.0022	0.0020	**0.0022**	0.0024	0.0023	0.0017	**0.0021**	0.9774	0.8478	
ZIC1	0.0005	0.0013	0.0020	**0.0013**	0.0003	0.0015	0.0002	**0.0006**	0.5004	0.3466	
ZIC2	0.0030	0.0083	0.0078	**0.0064**	0.0067	0.0127	0.0049	**0.0081**	1.2751	0.5771	
ZIC3	0.0013	0.0052	0.0061	**0.0042**	0.0040	0.0071	0.0021	**0.0044**	1.0434	0.9342	
ZNF217	0.0102	0.0087	0.0083	**0.0091**	0.0123	0.0132	0.0121	**0.0126**	1.3835	0.0067	
ZNF423	0.0050	0.0070	0.0077	**0.0066**	0.0104	0.0130	0.0086	**0.0107**	1.6227	0.0518	
ZNF462	0.0103	0.0128	0.0118	**0.0116**	0.0125	0.0157	0.0138	**0.0140**	1.2047	0.1105	

Table 9.6 Normalised level of expression of DMSO and SU5402 samples after 6 hours of culture analysed using the PPR NanoString probe set.

Genes	6 HRS										
	DMSO				SU5402				Fold Change	P-Value	Results
	1	2	3	AVG	1	2	3	AVG			
AATF	0.0048	0.0044	0.0038	**0.0043**	0.0041	0.0043	0.0031	**0.0038**	**0.8889**	**0.3651**	
ADNP2	0.0025	0.0017	0.0015	**0.0019**	0.0028	0.0013	0.0006	**0.0015**	**0.8160**	**0.6539**	
AP-2	0.0136	0.0137	0.0155	**0.0143**	0.0155	0.0118	0.0141	**0.0138**	**0.9663**	**0.7181**	
AXIN2	0.0028	0.0025	0.0026	**0.0026**	0.0037	0.0032	0.0034	**0.0034**	**1.3023**	**0.0079**	UP
BCL11A	0.0000	0.0000	0.0000	0.0000	0.0000	0.0000	0.0000	0.0000	**No expressed**		LOW
BCL2	0.0013	0.0013	0.0011	**0.0012**	0.0011	0.0012	0.0010	**0.0011**	**0.9108**	**0.3493**	
BCL7A	0.0056	0.0058	0.0059	**0.0058**	0.0059	0.0066	0.0061	**0.0062**	**1.0762**	**0.1202**	
BMP4	0.0028	0.0020	0.0021	**0.0023**	0.0032	0.0019	0.0015	**0.0022**	**0.9497**	**0.8456**	
CCND1	0.0182	0.0145	0.0114	**0.0147**	0.0148	0.0174	0.0110	**0.0144**	**0.9792**	**0.9152**	
CDKN1B	0.0013	0.0012	0.0013	**0.0012**	0.0014	0.0014	0.0013	**0.0014**	**1.1261**	**0.0327**	
CHD7	0.0047	0.0048	0.0050	**0.0048**	0.0043	0.0047	0.0043	**0.0044**	**0.9193**	**0.0672**	
CITED2	0.0068	0.0058	0.0044	**0.0057**	0.0074	0.0085	0.0081	**0.0080**	**1.4191**	**0.0359**	UP
CNTNAP5	0.0005	0.0005	0.0005	**0.0005**	0.0005	0.0005	0.0005	**0.0005**	**0.9395**	**0.1963**	
CXCL14	0.0010	0.0008	0.0010	**0.0009**	0.0004	0.0005	0.0003	**0.0004**	**0.4421**	**0.0033**	DOWN
CXXC6-like	0.0002	0.0002	0.0002	**0.0002**	0.0003	0.0003	0.0001	**0.0002**	**1.0920**	**0.7630**	
DACH1	0.0044	0.0042	0.0047	**0.0044**	0.0055	0.0054	0.0046	**0.0052**	**1.1726**	**0.0699**	
DBX2	0.0001	0.0001	0.0001	**0.0001**	0.0001	0.0001	0.0001	**0.0001**	**1.0048**	**0.9847**	
DLX3	0.0004	0.0004	0.0007	**0.0005**	0.0005	0.0003	0.0005	**0.0004**	**0.8651**	**0.6266**	
DLX5	0.0038	0.0036	0.0053	**0.0042**	0.0036	0.0024	0.0048	**0.0036**	**0.8480**	**0.5028**	
DLX6	0.0025	0.0020	0.0021	**0.0022**	0.0013	0.0008	0.0009	**0.0010**	**0.4551**	**0.0069**	DOWN
DNAJC1	0.0036	0.0039	0.0031	**0.0035**	0.0041	0.0039	0.0024	**0.0035**	**0.9856**	**0.9351**	
DNMT3A	0.0000	0.0000	0.0000	0.0000	0.0000	0.0000	0.0000	0.0000	**No expressed**		LOW
DNMT3B	0.0133	0.0126	0.0062	**0.0107**	0.0131	0.0101	0.0059	**0.0097**	**0.9036**	**0.7540**	
E2F8	0.0000	0.0000	0.0000	0.0000	0.0000	0.0000	0.0000	0.0000	**No expressed**		LOW
ECE1	0.0045	0.0036	0.0033	**0.0038**	0.0046	0.0035	0.0024	**0.0035**	**0.9201**	**0.6961**	
EEF1A1	0.1563	0.1509	0.1979	**0.1683**	0.1612	0.1630	0.2099	**0.1781**	**1.0577**	**0.6786**	
ERNI	0.0578	0.0282	0.0473	**0.0444**	0.0580	0.0345	0.0492	**0.0473**	**1.0633**	**0.8115**	
ETV4	0.0000	0.0000	0.0000	0.0000	0.0000	0.0000	0.0000	0.0000	**No expressed**		LOW
ETV5	0.0038	0.0032	0.0019	**0.0030**	0.0015	0.0013	0.0014	**0.0014**	**0.4670**	**0.0463**	DOWN
EYA1	0.0010	0.0008	0.0005	**0.0008**	0.0006	0.0007	0.0004	**0.0005**	**0.7125**	**0.2364**	
EYA2	0.0035	0.0040	0.0033	**0.0036**	0.0014	0.0019	0.0016	**0.0016**	**0.4535**	**0.0015**	DOWN
EZH2	0.0101	0.0102	0.0095	**0.0099**	0.0099	0.0112	0.0082	**0.0098**	**0.9881**	**0.9013**	
FSTL4	0.0019	0.0014	0.0016	**0.0016**	0.0020	0.0017	0.0019	**0.0019**	**1.1461**	**0.2619**	
FOXG1	0.0000	0.0000	0.0000	0.0000	0.0000	0.0000	0.0000	0.0000	**No expressed**		LOW
FOXI1	0.0000	0.0000	0.0000	0.0000	0.0000	0.0000	0.0000	0.0000	**No expressed**		LOW
FOXI3	0.0075	0.0064	0.0056	**0.0065**	0.0038	0.0027	0.0021	**0.0028**	**0.4370**	**0.0076**	DOWN
FOXM1	0.0007	0.0010	0.0012	**0.0010**	0.0009	0.0012	0.0017	**0.0013**	**1.3301**	**0.2883**	
FOXN2	0.0014	0.0012	0.0010	**0.0012**	0.0014	0.0013	0.0009	**0.0012**	**0.9781**	**0.8982**	
GAPDH	0.3017	0.3385	0.3600	**0.3334**	0.3160	0.3394	0.3526	**0.3360**	**1.0079**	**0.9024**	
GATA2	0.0058	0.0069	0.0090	**0.0072**	0.0109	0.0089	0.0103	**0.0101**	**1.3959**	**0.0612**	
GATA3	0.0023	0.0026	0.0024	**0.0024**	0.0030	0.0018	0.0014	**0.0021**	**0.8513**	**0.4841**	
GBX2	0.0088	0.0102	0.0036	**0.0075**	0.0048	0.0048	0.0027	**0.0041**	**0.5444**	**0.1807**	
GEMININ	0.0013	0.0013	0.0012	**0.0013**	0.0012	0.0011	0.0009	**0.0011**	**0.8692**	**0.1910**	
GPR160	0.0003	0.0003	0.0002	**0.0003**	0.0002	0.0002	0.0003	**0.0002**	**0.9515**	**0.6788**	
HDAC1	0.0046	0.0048	0.0052	**0.0049**	0.0048	0.0051	0.0052	**0.0050**	**1.0363**	**0.4652**	
HESX1	0.0008	0.0009	0.0008	**0.0009**	0.0004	0.0005	0.0004	**0.0004**	**0.5137**	**0.0006**	DOWN
HEY1	0.0041	0.0053	0.0037	**0.0044**	0.0037	0.0046	0.0038	**0.0040**	**0.9274**	**0.5966**	
HEY2	0.0025	0.0022	0.0019	**0.0022**	0.0019	0.0010	0.0009	**0.0013**	**0.5707**	**0.0635**	
HIF1A	0.0111	0.0119	0.0136	**0.0122**	0.0109	0.0119	0.0128	**0.0119**	**0.9740**	**0.7451**	
HMGXB4	0.0010	0.0010	0.0009	**0.0009**	0.0009	0.0008	0.0006	**0.0008**	**0.8376**	**0.1568**	
HMX3	0.0000	0.0000	0.0000	0.0000	0.0000	0.0000	0.0000	0.0000	**No expressed**		LOW
HOMER2	0.0015	0.0019	0.0014	**0.0016**	0.0013	0.0014	0.0012	**0.0013**	**0.8354**	**0.1812**	
HPRT1	0.0041	0.0035	0.0033	**0.0036**	0.0038	0.0035	0.0032	**0.0035**	**0.9617**	**0.6660**	
HSF2	0.0029	0.0027	0.0022	**0.0026**	0.0024	0.0021	0.0012	**0.0019**	**0.7355**	**0.1583**	
ING5	0.0015	0.0012	0.0010	**0.0013**	0.0013	0.0011	0.0010	**0.0011**	**0.8861**	**0.4281**	
IRX1	0.0045	0.0034	0.0026	**0.0035**	0.0037	0.0018	0.0012	**0.0022**	**0.6306**	**0.2441**	
IRX2	0.0018	0.0026	0.0011	**0.0018**	0.0018	0.0024	0.0022	**0.0021**	**1.1481**	**0.5998**	
IRX3	0.0190	0.0177	0.0087	**0.0151**	0.0155	0.0161	0.0143	**0.0153**	**1.0126**	**0.9568**	
KERATIN19	0.0036	0.0023	0.0032	**0.0030**	0.0036	0.0023	0.0027	**0.0029**	**0.9402**	**0.7620**	
KREMEN1	0.0003	0.0003	0.0002	**0.0003**	0.0004	0.0002	0.0001	**0.0002**	**0.8692**	**0.6650**	
LEF1	0.0037	0.0036	0.0027	**0.0033**	0.0036	0.0035	0.0019	**0.0030**	**0.8997**	**0.6319**	
LMX1A	0.0000	0.0000	0.0000	0.0000	0.0000	0.0000	0.0000	0.0000	**No expressed**		LOW
LMX1B	0.0023	0.0020	0.0025	**0.0023**	0.0025	0.0020	0.0028	**0.0024**	**1.0779**	**0.5587**	

Genes	6 HRS										
	DMSO				SU5402				Fold Change	P-Value	Results
	1	2	3	AVG	1	2	3	AVG			
LRP11	0.0011	0.0011	0.0009	**0.0010**	0.0010	0.0010	0.0008	**0.0009**	**0.9236**	**0.3925**	
LZTR1	0.0000	0.0000	0.0000	0.0000	0.0000	0.0000	0.0000	0.0000	**No expressed**		**LOW**
MEF2D	0.0030	0.0026	0.0025	**0.0027**	0.0025	0.0019	0.0020	**0.0021**	**0.7849**	**0.0767**	
MIER1	0.0011	0.0010	0.0010	**0.0010**	0.0011	0.0012	0.0012	**0.0012**	**1.1405**	**0.0474**	
MLLT10	0.0013	0.0008	0.0010	**0.0010**	0.0015	0.0020	0.0005	**0.0014**	**1.2927**	**0.5367**	
MORC2	0.0026	0.0028	0.0024	**0.0026**	0.0028	0.0038	0.0024	**0.0030**	**1.1516**	**0.4106**	
MSX1	0.0162	0.0154	0.0165	**0.0160**	0.0206	0.0149	0.0139	**0.0164**	**1.0249**	**0.8587**	
MTA3	0.0000	0.0000	0.0000	0.0000	0.0000	0.0000	0.0000	0.0000	**No expressed**		**LOW**
MYNN	0.0022	0.0022	0.0019	**0.0021**	0.0023	0.0022	0.0020	**0.0022**	**1.0221**	**0.6931**	
N-MYC	0.0116	0.0101	0.0071	**0.0096**	0.0105	0.0109	0.0058	**0.0091**	**0.9453**	**0.8140**	
NFKB1	0.0018	0.0018	0.0012	**0.0016**	0.0015	0.0012	0.0011	**0.0013**	**0.7951**	**0.2183**	
NPAS3	0.0000	0.0000	0.0000	0.0000	0.0000	0.0000	0.0000	0.0000	**No expressed**		**LOW**
NSD1	0.0000	0.0000	0.0000	0.0000	0.0000	0.0000	0.0000	0.0000	**No expressed**		**LOW**
OTX2	0.0030	0.0032	0.0027	**0.0030**	0.0025	0.0031	0.0038	**0.0031**	**1.0588**	**0.6931**	
PAX2	0.0004	0.0002	0.0001	**0.0002**	0.0001	0.0000	0.0000	**0.0000**	**0.1547**	**0.0679**	
PAX3	0.0000	0.0000	0.0000	0.0000	0.0000	0.0000	0.0000	0.0000	**No expressed**		**LOW**
PAX6	0.0002	0.0002	0.0004	**0.0003**	0.0009	0.0006	0.0006	**0.0007**	**2.3296**	**0.0314**	**UP**
PAX7	0.0000	0.0000	0.0000	0.0000	0.0000	0.0000	0.0000	0.0000	**No expressed**		**LOW**
PCNA	0.0220	0.0281	0.0293	**0.0264**	0.0232	0.0266	0.0275	**0.0258**	**0.9749**	**0.8125**	
PDLI4	0.0062	0.0056	0.0064	**0.0061**	0.0061	0.0061	0.0058	**0.0060**	**0.9888**	**0.7992**	
PHF10	0.0065	0.0060	0.0071	**0.0065**	0.0065	0.0074	0.0057	**0.0065**	**0.9979**	**0.9816**	
PHF20	0.0065	0.0065	0.0063	**0.0064**	0.0066	0.0076	0.0066	**0.0069**	**1.0816**	**0.1717**	
PNOC	0.0009	0.0005	0.0004	**0.0006**	0.0004	0.0001	0.0002	**0.0002**	**0.4267**	**0.1424**	
POGZ	0.0019	0.0017	0.0017	**0.0018**	0.0018	0.0015	0.0017	**0.0017**	**0.9339**	**0.3010**	
PSIP1	0.0050	0.0067	0.0050	**0.0056**	0.0056	0.0067	0.0046	**0.0056**	**1.0126**	**0.9378**	
PTPRU	0.0009	0.0006	0.0010	**0.0008**	0.0007	0.0006	0.0008	**0.0007**	**0.8699**	**0.4839**	
RRN3	0.0000	0.0000	0.0000	0.0000	0.0000	0.0000	0.0000	0.0000	**No expressed**		**LOW**
RX1	0.0000	0.0000	0.0000	0.0000	0.0000	0.0000	0.0000	0.0000	**No expressed**		**LOW**
RYBP	0.0024	0.0024	0.0018	**0.0022**	0.0023	0.0023	0.0016	**0.0021**	**0.9296**	**0.6259**	
SALL1	0.0265	0.0313	0.0185	**0.0255**	0.0281	0.0252	0.0180	**0.0238**	**0.9334**	**0.7416**	
SALL4	0.0060	0.0056	0.0043	**0.0053**	0.0063	0.0070	0.0034	**0.0056**	**1.0497**	**0.8391**	
SDHA	0.0053	0.0047	0.0044	**0.0048**	0.0054	0.0052	0.0037	**0.0047**	**0.9881**	**0.9291**	
SETD2	0.0046	0.0040	0.0024	**0.0037**	0.0035	0.0035	0.0030	**0.0033**	**0.9025**	**0.6263**	
SIX1	0.0108	0.0067	0.0040	**0.0072**	0.0076	0.0057	0.0036	**0.0056**	**0.7862**	**0.5377**	
SIX3	0.0001	0.0000	0.0002	**0.0001**	0.0000	0.0000	0.0000	**0.0000**	**0.1637**	**0.1805**	
SIX4	0.0052	0.0044	0.0032	**0.0043**	0.0048	0.0036	0.0030	**0.0038**	**0.8919**	**0.5882**	
SMAD6	0.0000	0.0000	0.0000	0.0000	0.0000	0.0000	0.0000	0.0000	**No expressed**		**LOW**
SOX10	0.0000	0.0000	0.0000	**0.0000**	0.0000	0.0000	0.0000	**0.0000**	**1.2596**	**0.7753**	
SOX2	0.0026	0.0040	0.0012	**0.0026**	0.0027	0.0042	0.0033	**0.0034**	**1.3101**	**0.4379**	
SOX3	0.0034	0.0033	0.0023	**0.0030**	0.0041	0.0043	0.0035	**0.0039**	**1.3119**	**0.1004**	
SOX9	0.0001	0.0001	0.0002	**0.0001**	0.0001	0.0002	0.0000	**0.0001**	**0.9557**	**0.9398**	
SP4	0.0018	0.0021	0.0021	**0.0020**	0.0017	0.0022	0.0020	**0.0020**	**0.9782**	**0.8173**	
SSTR5	0.0004	0.0002	0.0002	**0.0003**	0.0002	0.0001	0.0002	**0.0002**	**0.6787**	**0.3960**	
STOX2	0.0015	0.0018	0.0007	**0.0013**	0.0014	0.0011	0.0007	**0.0011**	**0.8133**	**0.5662**	
TAC1	0.0000	0.0000	0.0000	0.0000	0.0000	0.0000	0.0000	0.0000	**No expressed**		**LOW**
TBL1XR1	0.0051	0.0047	0.0042	**0.0046**	0.0047	0.0052	0.0043	**0.0048**	**1.0228**	**0.7832**	
TBX1	0.0018	0.0014	0.0002	**0.0012**	0.0003	0.0003	0.0001	**0.0002**	**0.1852**	**0.1188**	
TBX2	0.0000	0.0000	0.0000	0.0000	0.0000	0.0000	0.0000	0.0000	**No expressed**		**LOW**
TBX3	0.0003	0.0003	0.0008	**0.0005**	0.0002	0.0003	0.0002	**0.0002**	**0.4933**	**0.1810**	
TGIF2	0.0059	0.0060	0.0041	**0.0054**	0.0064	0.0052	0.0034	**0.0050**	**0.9364**	**0.7702**	
TOX3	0.0004	0.0005	0.0004	**0.0004**	0.0004	0.0007	0.0006	**0.0006**	**1.2877**	**0.2459**	
TP53	0.0061	0.0062	0.0064	**0.0062**	0.0064	0.0051	0.0062	**0.0059**	**0.9468**	**0.4432**	
TRIM24	0.0034	0.0039	0.0033	**0.0035**	0.0035	0.0043	0.0040	**0.0039**	**1.1199**	**0.2385**	
WHSC1	0.0086	0.0094	0.0060	**0.0080**	0.0093	0.0093	0.0066	**0.0084**	**1.0449**	**0.8028**	
YEATS4	0.0036	0.0045	0.0037	**0.0039**	0.0034	0.0051	0.0034	**0.0040**	**1.0043**	**0.9797**	
ZFHX1B	0.0039	0.0039	0.0026	**0.0035**	0.0034	0.0052	0.0040	**0.0042**	**1.2192**	**0.3235**	
ZHX2	0.0026	0.0024	0.0024	**0.0025**	0.0026	0.0028	0.0022	**0.0026**	**1.0364**	**0.6556**	
ZIC1	0.0002	0.0003	0.0002	**0.0002**	0.0002	0.0004	0.0004	**0.0003**	**1.3549**	**0.2140**	
ZIC2	0.0085	0.0108	0.0047	**0.0080**	0.0088	0.0100	0.0075	**0.0088**	**1.0946**	**0.7146**	
ZIC3	0.0182	0.0193	0.0093	**0.0156**	0.0149	0.0201	0.0194	**0.0182**	**1.1639**	**0.5110**	
ZNF217	0.0145	0.0148	0.0149	**0.0148**	0.0151	0.0161	0.0145	**0.0152**	**1.0307**	**0.4146**	
ZNF423	0.0099	0.0104	0.0049	**0.0084**	0.0081	0.0104	0.0056	**0.0081**	**0.9559**	**0.8761**	
ZNF462	0.0095	0.0098	0.0081	**0.0091**	0.0087	0.0091	0.0064	**0.0081**	**0.8851**	**0.3433**	

Table 9.7 Normalised level of expression of DMSO and SU5402 samples after 12 hours of culture analysed using the PPR NanoString probe set.

Genes	12 HRS										
	DMSO				SU5402				Fold Change	P-Value	Results
	1	2	3	AVG	1	2	3	AVG			
AATF	0.0042	0.0045	0.0042	**0.0043**	0.0038	0.0039	0.0038	**0.0038**	**0.8991**	0.0119	
ADNP2	0.0011	0.0015	0.0019	**0.0015**	0.0020	0.0013	0.0020	**0.0018**	**1.1937**	**0.4467**	
AP-2	0.0119	0.0147	0.0120	**0.0129**	0.0134	0.0109	0.0133	**0.0125**	**0.9736**	**0.7966**	
AXIN2	0.0037	0.0033	0.0029	**0.0033**	0.0035	0.0037	0.0041	**0.0037**	**1.1329**	**0.1832**	
BCL11A	0.0000	0.0000	0.0000	0.0000	0.0000	0.0000	0.0000	0.0000	**No expressed**		**LOW**
BCL2	0.0012	0.0011	0.0010	**0.0011**	0.0009	0.0010	0.0009	**0.0009**	**0.8251**	0.0493	
BCL7A	0.0074	0.0067	0.0064	**0.0068**	0.0060	0.0062	0.0061	**0.0061**	**0.8981**	**0.0865**	
BMP4	0.0016	0.0022	0.0022	**0.0020**	0.0025	0.0021	0.0022	**0.0023**	**1.1448**	**0.3111**	
CCND1	0.0124	0.0138	0.0115	**0.0125**	0.0147	0.0148	0.0115	**0.0136**	**1.0885**	**0.4322**	
CDKN1B	0.0012	0.0013	0.0014	**0.0013**	0.0014	0.0014	0.0016	**0.0015**	**1.1191**	**0.2026**	
CHD7	0.0059	0.0055	0.0053	**0.0056**	0.0047	0.0051	0.0050	**0.0049**	**0.8829**	0.0384	
CITED2	0.0050	0.0045	0.0043	**0.0046**	0.0062	0.0067	0.0048	**0.0059**	**1.2780**	**0.1089**	
CNTNAP5	0.0004	0.0005	0.0003	**0.0004**	0.0004	0.0004	0.0002	**0.0003**	**0.8526**	**0.5620**	
CXCL14	0.0008	0.0010	0.0012	**0.0010**	0.0003	0.0008	0.0006	**0.0005**	0.5462	**0.0830**	
CXXC6-like	0.0002	0.0002	0.0003	**0.0002**	0.0002	0.0003	0.0003	**0.0003**	**1.2531**	**0.1817**	
DACH1	0.0037	0.0036	0.0040	**0.0038**	0.0051	0.0043	0.0047	**0.0047**	**1.2451**	0.0264	
DBX2	0.0001	0.0002	0.0002	**0.0002**	0.0001	0.0001	0.0002	**0.0001**	0.7106	**0.2903**	
DLX3	0.0004	0.0005	0.0008	**0.0006**	0.0005	0.0006	0.0009	**0.0007**	**1.1880**	**0.5236**	
DLX5	0.0025	0.0030	0.0025	**0.0027**	0.0022	0.0020	0.0022	**0.0021**	**0.8013**	0.0395	
DLX6	0.0011	0.0019	0.0011	**0.0013**	0.0011	0.0007	0.0006	**0.0008**	0.5903	**0.1445**	
DNAJC1	0.0031	0.0034	0.0032	**0.0032**	0.0029	0.0027	0.0028	**0.0028**	**0.8850**	0.0254	
DNMT3A	0.0000	0.0000	0.0000	0.0000	0.0000	0.0000	0.0000	0.0000	**No expressed**		**LOW**
DNMT3B	0.0087	0.0117	0.0113	**0.0105**	0.0125	0.0104	0.0104	**0.0111**	**1.0512**	**0.6732**	
E2F8	0.0000	0.0000	0.0000	0.0000	0.0000	0.0000	0.0000	0.0000	**No expressed**		**LOW**
ECE1	0.0031	0.0038	0.0042	**0.0037**	0.0034	0.0029	0.0036	**0.0033**	**0.8874**	**0.3268**	
EEF1A1	0.1630	0.1339	0.1551	**0.1507**	0.1484	0.1488	0.1585	**0.1519**	**1.0081**	**0.9017**	
ERNI	0.0387	0.0605	0.0756	**0.0583**	0.1211	0.1069	0.1068	**0.1116**	1.9155	0.0104	**UP**
ETV4	0.0000	0.0000	0.0000	0.0000	0.0000	0.0000	0.0000	0.0000	**No expressed**		**LOW**
ETV5	0.0025	0.0024	0.0019	**0.0023**	0.0009	0.0007	0.0006	**0.0007**	0.3258	0.0018	**DOWN**
EYA1	0.0017	0.0011	0.0009	**0.0012**	0.0011	0.0012	0.0008	**0.0011**	**0.8586**	**0.5413**	
EYA2	0.0057	0.0046	0.0026	**0.0043**	0.0023	0.0029	0.0010	**0.0021**	0.4814	**0.1010**	
EZH2	0.0114	0.0112	0.0106	**0.0111**	0.0101	0.0101	0.0098	**0.0100**	**0.9018**	0.0141	
FSTL4	0.0010	0.0006	0.0007	**0.0008**	0.0010	0.0007	0.0008	**0.0008**	**1.0783**	**0.6915**	
FOXG1	0.0002	0.0002	0.0002	**0.0002**	0.0002	0.0001	0.0002	**0.0002**	**0.7648**	0.0263	
FOXI1	0.0000	0.0000	0.0000	0.0000	0.0000	0.0000	0.0000	0.0000	**No expressed**		**LOW**
FOXI3	0.0026	0.0042	0.0030	**0.0033**	0.0026	0.0016	0.0019	**0.0020**	0.6274	**0.0955**	
FOXM1	0.0016	0.0012	0.0009	**0.0012**	0.0008	0.0011	0.0008	**0.0009**	0.7427	**0.2200**	
FOXN2	0.0013	0.0014	0.0012	**0.0013**	0.0013	0.0012	0.0012	**0.0013**	**0.9663**	**0.4604**	
GAPDH	0.3696	0.3577	0.3732	**0.3669**	0.3072	0.3325	0.3411	**0.3270**	**0.8912**	0.0236	
GATA2	0.0035	0.0047	0.0070	**0.0051**	0.0091	0.0075	0.0104	**0.0090**	1.7602	0.0431	**UP**
GATA3	0.0010	0.0022	0.0035	**0.0022**	0.0024	0.0015	0.0027	**0.0022**	**0.9802**	**0.9584**	
GBX2	0.0046	0.0048	0.0033	**0.0042**	0.0024	0.0021	0.0017	**0.0021**	0.4940	0.0152	**DOWN**
GEMININ	0.0011	0.0011	0.0013	**0.0012**	0.0010	0.0010	0.0012	**0.0010**	**0.8802**	**0.1912**	
GPR160	0.0003	0.0002	0.0001	**0.0002**	0.0001	0.0003	0.0001	**0.0002**	0.7291	**0.5291**	
HDAC1	0.0050	0.0052	0.0048	**0.0050**	0.0045	0.0045	0.0044	**0.0045**	**0.8924**	0.0159	
HESX1	0.0006	0.0005	0.0004	**0.0005**	0.0004	0.0004	0.0004	**0.0004**	0.7495	**0.0639**	
HEY1	0.0044	0.0052	0.0033	**0.0043**	0.0033	0.0037	0.0024	**0.0032**	0.7301	**0.1469**	
HEY2	0.0011	0.0015	0.0016	**0.0014**	0.0011	0.0008	0.0011	**0.0010**	0.6969	**0.0822**	
HIF1A	0.0160	0.0138	0.0117	**0.0138**	0.0125	0.0125	0.0112	**0.0121**	**0.8735**	**0.2620**	
HMGXB4	0.0009	0.0008	0.0009	**0.0008**	0.0007	0.0008	0.0009	**0.0008**	**0.9313**	**0.2821**	
HMX3	0.0000	0.0000	0.0000	0.0000	0.0000	0.0000	0.0000	0.0000	**No expressed**		**LOW**
HOMER2	0.0009	0.0014	0.0012	**0.0012**	0.0011	0.0011	0.0009	**0.0010**	**0.8851**	**0.4332**	
HPRT1	0.0029	0.0030	0.0033	**0.0031**	0.0027	0.0029	0.0034	**0.0030**	**0.9738**	**0.7705**	
HSF2	0.0029	0.0033	0.0031	**0.0031**	0.0028	0.0025	0.0025	**0.0026**	**0.8448**	0.0285	
ING5	0.0009	0.0009	0.0011	**0.0009**	0.0009	0.0009	0.0011	**0.0009**	**0.9908**	**0.9313**	
IRX1	0.0014	0.0025	0.0032	**0.0023**	0.0024	0.0015	0.0021	**0.0020**	**0.8544**	**0.5960**	
IRX2	0.0010	0.0011	0.0009	**0.0010**	0.0015	0.0014	0.0008	**0.0012**	**1.2685**	**0.3018**	
IRX3	0.0115	0.0134	0.0097	**0.0116**	0.0145	0.0147	0.0089	**0.0127**	**1.1001**	**0.6211**	
KERATIN19	0.0017	0.0019	0.0032	**0.0023**	0.0028	0.0026	0.0059	**0.0038**	1.6618	**0.2689**	
KREMEN1	0.0004	0.0004	0.0008	**0.0005**	0.0005	0.0004	0.0013	**0.0007**	1.3610	**0.5486**	
LEF1	0.0044	0.0043	0.0048	**0.0045**	0.0044	0.0046	0.0057	**0.0049**	**1.0895**	**0.4071**	
LMX1A	0.0000	0.0000	0.0000	0.0000	0.0000	0.0000	0.0000	0.0000	**No expressed**		**LOW**
LMX1B	0.0033	0.0029	0.0018	**0.0027**	0.0029	0.0026	0.0023	**0.0026**	**0.9699**	**0.8750**	

Genes	12 HRS										
	DMSO				SU5402				Fold Change	P-Value	Results
	1	2	3	AVG	1	2	3	AVG			
LRP11	0.0007	0.0007	0.0007	**0.0007**	0.0006	0.0007	0.0005	**0.0006**	0.8545	0.0894	
LZTR1	0.0000	0.0000	0.0000	0.0000	0.0000	0.0000	0.0000	0.0000	No expressed		LOW
MEF2D	0.0019	0.0024	0.0026	**0.0023**	0.0022	0.0019	0.0023	**0.0021**	0.9339	0.5412	
MIER1	0.0013	0.0012	0.0011	**0.0012**	0.0012	0.0012	0.0011	**0.0012**	0.9659	0.6187	
MLLT10	0.0008	0.0006	0.0008	**0.0007**	0.0007	0.0007	0.0010	**0.0008**	1.0906	0.5864	
MORC2	0.0022	0.0021	0.0022	**0.0022**	0.0026	0.0024	0.0025	**0.0025**	1.1422	0.0139	
MSX1	0.0170	0.0207	0.0196	**0.0191**	0.0202	0.0181	0.0295	**0.0226**	1.1829	0.3952	
MTA3	0.0000	0.0000	0.0000	0.0000	0.0000	0.0000	0.0000	0.0000	No expressed		LOW
MYNN	0.0023	0.0024	0.0022	**0.0023**	0.0020	0.0022	0.0019	**0.0020**	0.8712	0.0565	
N-MYC	0.0107	0.0130	0.0121	**0.0119**	0.0118	0.0117	0.0110	**0.0115**	0.9623	0.5700	
NFKB1	0.0012	0.0017	0.0015	**0.0014**	0.0012	0.0010	0.0011	**0.0011**	0.7652	0.0798	
NPAS3	0.0000	0.0000	0.0000	0.0000	0.0000	0.0000	0.0000	0.0000	No expressed		LOW
NSD1	0.0000	0.0000	0.0000	0.0000	0.0000	0.0000	0.0000	0.0000	No expressed		LOW
OTX2	0.0025	0.0022	0.0007	**0.0018**	0.0026	0.0033	0.0008	**0.0022**	1.2282	0.6838	
PAX2	0.0031	0.0015	0.0003	**0.0017**	0.0001	0.0002	0.0001	**0.0001**	0.0792	0.1273	
PAX3	0.0000	0.0000	0.0000	0.0000	0.0000	0.0000	0.0000	0.0000	No expressed		LOW
PAX6	0.0008	0.0020	0.0010	**0.0013**	0.0009	0.0015	0.0011	**0.0012**	0.9264	0.8281	
PAX7	0.0000	0.0000	0.0000	0.0000	0.0000	0.0000	0.0000	0.0000	No expressed		LOW
PCNA	0.0302	0.0273	0.0258	**0.0278**	0.0221	0.0238	0.0226	**0.0228**	0.8214	0.0234	
PDLI4	0.0047	0.0053	0.0033	**0.0044**	0.0043	0.0043	0.0028	**0.0038**	0.8638	0.4795	
PHF10	0.0066	0.0060	0.0062	**0.0063**	0.0062	0.0059	0.0062	**0.0061**	0.9729	0.4894	
PHF20	0.0076	0.0067	0.0069	**0.0071**	0.0061	0.0067	0.0060	**0.0063**	0.8855	0.0797	
PNOC	0.0004	0.0007	0.0003	**0.0004**	0.0003	0.0003	0.0002	**0.0002**	0.5482	0.1501	
POGZ	0.0018	0.0016	0.0018	**0.0017**	0.0016	0.0015	0.0017	**0.0016**	0.9093	0.1703	
PSIP1	0.0063	0.0069	0.0057	**0.0063**	0.0053	0.0059	0.0051	**0.0055**	0.8621	0.1020	
PTPRU	0.0007	0.0007	0.0008	**0.0007**	0.0007	0.0007	0.0006	**0.0007**	0.9012	0.3195	
RRN3	0.0000	0.0000	0.0000	0.0000	0.0000	0.0000	0.0000	0.0000	No expressed		LOW
RX1	0.0000	0.0000	0.0000	0.0000	0.0000	0.0000	0.0000	0.0000	No expressed		LOW
RYBP	0.0022	0.0024	0.0022	**0.0023**	0.0020	0.0020	0.0019	**0.0020**	0.8687	0.0073	
SALL1	0.0160	0.0197	0.0180	**0.0179**	0.0207	0.0174	0.0186	**0.0189**	1.0558	0.5201	
SALL4	0.0041	0.0043	0.0038	**0.0041**	0.0045	0.0042	0.0039	**0.0042**	1.0239	0.6926	
SDHA	0.0046	0.0051	0.0052	**0.0050**	0.0043	0.0044	0.0050	**0.0046**	0.9178	0.2179	
SETD2	0.0035	0.0034	0.0029	**0.0033**	0.0032	0.0037	0.0029	**0.0033**	1.0018	0.9847	
SIX1	0.0066	0.0060	0.0035	**0.0054**	0.0055	0.0053	0.0026	**0.0045**	0.8399	0.5593	
SIX3	0.0000	0.0000	0.0000	**0.0000**	0.0000	0.0000	0.0000	**0.0000**	6.3438	0.2402	
SIX4	0.0032	0.0033	0.0030	**0.0031**	0.0030	0.0027	0.0029	**0.0029**	0.9186	0.1094	
SMAD6	0.0000	0.0000	0.0000	0.0000	0.0000	0.0000	0.0000	0.0000	No expressed		LOW
SOX10	0.0009	0.0011	0.0007	**0.0009**	0.0003	0.0002	0.0003	**0.0003**	0.2775	0.0042	DOWN
SOX2	0.0023	0.0023	0.0008	**0.0018**	0.0026	0.0029	0.0010	**0.0021**	1.2155	0.6505	
SOX3	0.0021	0.0024	0.0018	**0.0021**	0.0026	0.0029	0.0019	**0.0024**	1.1559	0.4085	
SOX9	0.0002	0.0002	0.0002	**0.0002**	0.0002	0.0001	0.0002	**0.0002**	0.8752	0.5150	
SP4	0.0023	0.0020	0.0018	**0.0021**	0.0018	0.0018	0.0017	**0.0018**	0.8620	0.1124	
SSTR5	0.0001	0.0001	0.0000	**0.0001**	0.0001	0.0001	0.0000	**0.0000**	0.6993	0.7198	
STOX2	0.0012	0.0017	0.0014	**0.0014**	0.0015	0.0013	0.0014	**0.0014**	0.9921	0.9421	
TAC1	0.0000	0.0000	0.0000	0.0000	0.0000	0.0000	0.0000	0.0000	No expressed		LOW
TBL1XR1	0.0052	0.0052	0.0047	**0.0050**	0.0048	0.0053	0.0046	**0.0049**	0.9674	0.5700	
TBX1	0.0017	0.0009	0.0006	**0.0010**	0.0004	0.0004	0.0004	**0.0004**	0.3856	0.1278	
TBX2	0.0000	0.0000	0.0000	0.0000	0.0000	0.0000	0.0000	0.0000	No expressed		LOW
TBX3	0.0004	0.0004	0.0010	**0.0006**	0.0001	0.0002	0.0013	**0.0006**	0.9204	0.9163	
TGIF2	0.0033	0.0047	0.0057	**0.0046**	0.0052	0.0043	0.0054	**0.0050**	1.0924	0.6143	
TOX3	0.0005	0.0005	0.0006	**0.0005**	0.0005	0.0005	0.0004	**0.0005**	0.8754	0.2703	
TP53	0.0071	0.0072	0.0076	**0.0073**	0.0073	0.0071	0.0077	**0.0074**	1.0074	0.8348	
TRIM24	0.0032	0.0031	0.0030	**0.0031**	0.0032	0.0030	0.0031	**0.0031**	0.9933	0.8139	
WHSC1	0.0080	0.0087	0.0079	**0.0082**	0.0072	0.0071	0.0068	**0.0070**	0.8522	0.0127	
YEATS4	0.0041	0.0036	0.0040	**0.0039**	0.0038	0.0037	0.0039	**0.0038**	0.9756	0.5439	
ZFHX1B	0.0060	0.0051	0.0031	**0.0047**	0.0047	0.0058	0.0037	**0.0047**	1.0064	0.9784	
ZHX2	0.0030	0.0030	0.0023	**0.0028**	0.0027	0.0026	0.0022	**0.0025**	0.9120	0.4317	
ZIC1	0.0006	0.0003	0.0003	**0.0004**	0.0006	0.0005	0.0005	**0.0005**	1.3186	0.2883	
ZIC2	0.0096	0.0104	0.0050	**0.0083**	0.0118	0.0112	0.0064	**0.0098**	1.1798	0.5646	
ZIC3	0.0121	0.0114	0.0061	**0.0099**	0.0121	0.0132	0.0067	**0.0107**	1.0816	0.7855	
ZNF217	0.0127	0.0120	0.0106	**0.0118**	0.0120	0.0123	0.0104	**0.0116**	0.9822	0.8183	
ZNF423	0.0101	0.0100	0.0075	**0.0092**	0.0104	0.0101	0.0085	**0.0097**	1.0500	0.6800	
ZNF462	0.0110	0.0108	0.0101	**0.0106**	0.0092	0.0096	0.0091	**0.0093**	0.8735	0.0148	

Table 9.8 Normalised level of expression of DMSO and SU5402 samples after 24 hours of culture analysed using the PPR NanoString probe set.

Genes	24 HRS										
	DMSO				SU5402				Fold Change	P-Value	Results
	1	2	3	AVG	1	2	3	AVG			
AATF	0.0041	0.0044	0.0030	**0.0039**	0.0031	0.0026	0.0027	**0.0028**	0.7205	0.0737	
ADNP2	0.0014	0.0016	0.0007	**0.0012**	0.0010	0.0015	0.0012	**0.0012**	0.9964	0.9892	
AP-2	0.0126	0.0109	0.0171	**0.0135**	0.0137	0.0083	0.0105	**0.0108**	0.8015	0.3358	
AXIN2	0.0023	0.0025	0.0018	**0.0022**	0.0034	0.0025	0.0030	**0.0029**	1.3367	0.0947	
BCL11A	0.0000	0.0000	0.0000	0.0000	0.0000	0.0000	0.0000	0.0000	No expressed		LOW
BCL2	0.0015	0.0014	0.0017	**0.0015**	0.0013	0.0017	0.0013	**0.0014**	0.9405	0.5814	
BCL7A	0.0065	0.0066	0.0062	**0.0065**	0.0057	0.0053	0.0049	**0.0053**	0.8239	0.0143	
BMP4	0.0010	0.0008	0.0011	**0.0010**	0.0012	0.0024	0.0013	**0.0016**	1.6890	0.1540	
CCND1	0.0170	0.0134	0.0124	**0.0143**	0.0145	0.0108	0.0142	**0.0132**	0.9235	0.5872	
CDKN1B	0.0014	0.0013	0.0019	**0.0015**	0.0018	0.0025	0.0026	**0.0023**	1.4904	0.0840	
CHD7	0.0054	0.0057	0.0061	**0.0057**	0.0050	0.0048	0.0042	**0.0047**	0.8138	0.0235	
CITED2	0.0032	0.0037	0.0033	**0.0034**	0.0045	0.0044	0.0046	**0.0045**	1.3230	0.0025	UP
CNTNAP5	0.0003	0.0004	0.0002	**0.0003**	0.0003	0.0001	0.0002	**0.0002**	0.6474	0.1435	
CXCL14	0.0021	0.0025	0.0016	**0.0021**	0.0021	0.0023	0.0020	**0.0022**	1.0407	0.7709	
CXXC6-like	0.0002	0.0003	0.0001	**0.0002**	0.0002	0.0002	0.0002	**0.0002**	1.0805	0.6793	
DACH1	0.0019	0.0017	0.0023	**0.0020**	0.0029	0.0038	0.0028	**0.0032**	1.6150	0.0329	UP
DBX2	0.0007	0.0006	0.0003	**0.0005**	0.0002	0.0002	0.0001	**0.0002**	0.3198	0.0690	
DLX3	0.0006	0.0004	0.0008	**0.0006**	0.0009	0.0010	0.0014	**0.0011**	1.8910	0.0593	
DLX5	0.0014	0.0010	0.0029	**0.0017**	0.0017	0.0013	0.0015	**0.0015**	0.8485	0.6770	
DLX6	0.0006	0.0006	0.0010	**0.0007**	0.0005	0.0002	0.0004	**0.0003**	0.4799	0.1205	
DNAJC1	0.0033	0.0032	0.0024	**0.0029**	0.0023	0.0021	0.0019	**0.0021**	0.7085	0.0509	
DNMT3A	0.0000	0.0000	0.0000	0.0000	0.0000	0.0000	0.0000	0.0000	No expressed		LOW
DNMT3B	0.0099	0.0094	0.0049	**0.0081**	0.0081	0.0076	0.0069	**0.0075**	0.9363	0.7686	
E2F8	0.0000	0.0000	0.0000	0.0000	0.0000	0.0000	0.0000	0.0000	No expressed		LOW
ECE1	0.0032	0.0031	0.0022	**0.0028**	0.0027	0.0028	0.0023	**0.0026**	0.9233	0.5533	
EEF1A1	0.1587	0.1466	0.1813	**0.1622**	0.1750	0.1527	0.1614	**0.1631**	1.0053	0.9468	
ERNI	0.0725	0.0598	0.1088	**0.0804**	0.1042	0.2490	0.2047	**0.1860**	2.3137	0.0801	
ETV4	0.0000	0.0000	0.0000	0.0000	0.0000	0.0000	0.0000	0.0000	No expressed		LOW
ETV5	0.0014	0.0020	0.0017	**0.0017**	0.0005	0.0006	0.0004	**0.0005**	0.2936	0.0024	DOWN
EYA1	0.0012	0.0012	0.0011	**0.0012**	0.0015	0.0006	0.0012	**0.0011**	0.9069	0.7052	
EYA2	0.0024	0.0027	0.0036	**0.0029**	0.0015	0.0002	0.0018	**0.0011**	0.3952	0.0441	DOWN
EZH2	0.0095	0.0099	0.0077	**0.0090**	0.0076	0.0073	0.0068	**0.0072**	0.8002	0.0660	
FSTL4	0.0003	0.0005	0.0005	**0.0004**	0.0003	0.0002	0.0003	**0.0003**	0.6251	0.1625	
FOXG1	0.0002	0.0004	0.0002	**0.0003**	0.0003	0.0002	0.0002	**0.0002**	0.6967	0.1724	LOW
FOXI1	0.0000	0.0000	0.0000	0.0000	0.0000	0.0000	0.0000	0.0000	No expressed		LOW
FOXI3	0.0008	0.0006	0.0020	**0.0012**	0.0005	0.0003	0.0004	**0.0004**	0.3737	0.1823	
FOXM1	0.0008	0.0008	0.0012	**0.0009**	0.0008	0.0005	0.0007	**0.0007**	0.7350	0.1517	
FOXN2	0.0014	0.0015	0.0010	**0.0013**	0.0011	0.0015	0.0010	**0.0012**	0.9273	0.6721	
GAPDH	0.3801	0.4058	0.3790	**0.3883**	0.3665	0.3119	0.3253	**0.3346**	0.8616	0.0447	
GATA2	0.0034	0.0022	0.0036	**0.0031**	0.0095	0.0079	0.0101	**0.0092**	2.9992	0.0015	UP
GATA3	0.0018	0.0013	0.0021	**0.0018**	0.0020	0.0018	0.0024	**0.0021**	1.1630	0.3770	
GBX2	0.0042	0.0037	0.0029	**0.0036**	0.0013	0.0004	0.0008	**0.0008**	0.2206	0.0037	DOWN
GEMININ	0.0011	0.0011	0.0008	**0.0010**	0.0009	0.0005	0.0006	**0.0007**	0.6548	0.0708	
GPR160	0.0001	0.0002	0.0001	**0.0001**	0.0001	0.0001	0.0001	**0.0001**	0.6473	0.1475	
HDAC1	0.0044	0.0041	0.0045	**0.0043**	0.0040	0.0040	0.0040	**0.0040**	0.9242	0.0452	
HESX1	0.0004	0.0005	0.0006	**0.0005**	0.0003	0.0003	0.0003	**0.0003**	0.5409	0.0092	DOWN
HEY1	0.0028	0.0043	0.0043	**0.0038**	0.0026	0.0032	0.0029	**0.0029**	0.7584	0.1583	
HEY2	0.0004	0.0002	0.0006	**0.0004**	0.0004	0.0010	0.0007	**0.0007**	1.7537	0.2226	
HIF1A	0.0115	0.0125	0.0136	**0.0125**	0.0114	0.0106	0.0100	**0.0107**	0.8504	0.0599	
HMGXB4	0.0008	0.0008	0.0007	**0.0007**	0.0008	0.0008	0.0006	**0.0008**	1.0122	0.8897	
HMX3	0.0000	0.0000	0.0000	0.0000	0.0000	0.0000	0.0000	0.0000	No expressed		LOW
HOMER2	0.0015	0.0015	0.0016	**0.0015**	0.0013	0.0009	0.0012	**0.0011**	0.7227	0.0236	DOWN
HPRT1	0.0027	0.0028	0.0026	**0.0027**	0.0025	0.0032	0.0027	**0.0028**	1.0300	0.7220	
HSF2	0.0030	0.0035	0.0020	**0.0028**	0.0020	0.0019	0.0015	**0.0018**	0.6333	0.0883	
ING5	0.0009	0.0010	0.0007	**0.0009**	0.0009	0.0008	0.0007	**0.0008**	0.9421	0.6523	
IRX1	0.0034	0.0026	0.0025	**0.0028**	0.0022	0.0010	0.0023	**0.0018**	0.6444	0.1243	
IRX2	0.0017	0.0016	0.0016	**0.0016**	0.0013	0.0004	0.0011	**0.0009**	0.5666	0.0508	
IRX3	0.0089	0.0087	0.0057	**0.0077**	0.0100	0.0076	0.0084	**0.0087**	1.1190	0.5027	
KERATIN19	0.0036	0.0021	0.0030	**0.0029**	0.0066	0.0091	0.0075	**0.0078**	2.6759	0.0047	UP
KREMEN1	0.0019	0.0014	0.0008	**0.0014**	0.0028	0.0016	0.0017	**0.0021**	1.5021	0.2296	
LEF1	0.0064	0.0059	0.0055	**0.0059**	0.0069	0.0046	0.0050	**0.0055**	0.9362	0.6465	
LMX1A	0.0000	0.0000	0.0000	0.0000	0.0000	0.0000	0.0000	0.0000	No expressed		LOW
LMX1B	0.0023	0.0044	0.0022	**0.0030**	0.0032	0.0006	0.0017	**0.0019**	0.6308	0.3523	

Genes	24 HRS										
	DMSO				SU5402				Fold Change	P-Value	Results
	1	2	3	AVG	1	2	3	AVG			
LRP11	0.0010	0.0009	0.0008	**0.0009**	0.0006	0.0003	0.0007	**0.0005**	0.5753	0.0228	DOWN
LZTR1	0.0000	0.0000	0.0000	0.0000	0.0000	0.0000	0.0000	0.0000	No expressed		LOW
MEF2D	0.0018	0.0015	0.0019	**0.0017**	0.0017	0.0026	0.0020	**0.0021**	1.2318	0.2127	
MIER1	0.0013	0.0012	0.0012	**0.0013**	0.0011	0.0012	0.0011	**0.0011**	0.9012	0.0543	
MLLT10	0.0010	0.0015	0.0006	**0.0010**	0.0009	0.0011	0.0010	**0.0010**	0.9639	0.8940	
MORC2	0.0020	0.0021	0.0019	**0.0020**	0.0019	0.0023	0.0017	**0.0020**	0.9796	0.8102	
MSX1	0.0111	0.0097	0.0048	**0.0085**	0.0133	0.0080	0.0114	**0.0109**	1.2779	0.3871	
MTA3	0.0000	0.0000	0.0000	0.0000	0.0000	0.0000	0.0000	0.0000	No expressed		LOW
MYNN	0.0022	0.0022	0.0019	**0.0021**	0.0021	0.0021	0.0018	**0.0020**	0.9316	0.2946	
N-MYC	0.0095	0.0100	0.0047	**0.0081**	0.0061	0.0040	0.0044	**0.0048**	0.6004	0.1538	
NFKB1	0.0011	0.0011	0.0010	**0.0011**	0.0008	0.0012	0.0008	**0.0010**	0.8907	0.4546	
NPAS3	0.0000	0.0000	0.0000	0.0000	0.0000	0.0000	0.0000	0.0000	No expressed		LOW
NSD1	0.0000	0.0000	0.0000	0.0000	0.0000	0.0000	0.0000	0.0000	No expressed		LOW
OTX2	0.0002	0.0020	0.0004	**0.0009**	0.0004	0.0000	0.0003	**0.0003**	0.3031	0.3578	
PAX2	0.0006	0.0021	0.0008	**0.0012**	0.0001	0.0001	0.0002	**0.0001**	0.0910	0.0827	
PAX3	0.0000	0.0000	0.0000	0.0000	0.0000	0.0000	0.0000	0.0000	No expressed		LOW
PAX6	0.0036	0.0030	0.0011	**0.0026**	0.0022	0.0003	0.0014	**0.0013**	0.5128	0.2449	
PAX7	0.0000	0.0000	0.0000	0.0000	0.0000	0.0000	0.0000	0.0000	No expressed		LOW
PCNA	0.0251	0.0283	0.0252	**0.0262**	0.0199	0.0150	0.0167	**0.0172**	0.6569	0.0074	DOWN
PDLI4	0.0036	0.0034	0.0048	**0.0040**	0.0029	0.0021	0.0029	**0.0026**	0.6660	0.0626	
PHF10	0.0056	0.0055	0.0048	**0.0053**	0.0053	0.0051	0.0043	**0.0049**	0.9215	0.3611	
PHF20	0.0064	0.0065	0.0059	**0.0063**	0.0061	0.0056	0.0051	**0.0056**	0.8968	0.1294	
PNOC	0.0004	0.0002	0.0004	**0.0003**	0.0002	0.0002	0.0005	**0.0003**	0.9026	0.7962	
POGZ	0.0018	0.0017	0.0015	**0.0017**	0.0016	0.0014	0.0014	**0.0015**	0.8861	0.1439	
PSIP1	0.0060	0.0063	0.0043	**0.0055**	0.0046	0.0036	0.0039	**0.0041**	0.7304	0.1065	
PTPRU	0.0009	0.0007	0.0008	**0.0008**	0.0006	0.0006	0.0007	**0.0007**	0.8418	0.1371	
RRN3	0.0000	0.0000	0.0000	0.0000	0.0000	0.0000	0.0000	0.0000	No expressed		LOW
RX1	0.0000	0.0000	0.0000	0.0000	0.0000	0.0000	0.0000	0.0000	No expressed		LOW
RYBP	0.0020	0.0020	0.0015	**0.0018**	0.0017	0.0017	0.0015	**0.0016**	0.8914	0.3092	
SALL1	0.0086	0.0061	0.0063	**0.0070**	0.0061	0.0047	0.0057	**0.0055**	0.7838	0.1762	
SALL4	0.0025	0.0030	0.0017	**0.0024**	0.0019	0.0022	0.0017	**0.0019**	0.8034	0.3093	
SDHA	0.0049	0.0047	0.0039	**0.0045**	0.0039	0.0041	0.0035	**0.0038**	0.8519	0.1336	
SETD2	0.0026	0.0026	0.0020	**0.0024**	0.0023	0.0022	0.0022	**0.0022**	0.9373	0.4897	
SIX1	0.0035	0.0047	0.0036	**0.0039**	0.0046	0.0011	0.0042	**0.0033**	0.8356	0.6070	
SIX3	0.0000	0.0000	0.0000	**0.0000**	0.0000	0.0000	0.0001	**0.0000**	-2.3275	0.3936	
SIX4	0.0024	0.0026	0.0023	**0.0025**	0.0029	0.0025	0.0023	**0.0026**	1.0456	0.6266	
SMAD6	0.0000	0.0000	0.0000	0.0000	0.0000	0.0000	0.0000	0.0000	No expressed		LOW
SOX10	0.0109	0.0127	0.0112	**0.0116**	0.0097	0.0014	0.0033	**0.0048**	0.4111	0.0572	
SOX2	0.0026	0.0026	0.0010	**0.0021**	0.0010	0.0002	0.0009	**0.0007**	0.3245	0.0755	
SOX3	0.0038	0.0032	0.0018	**0.0029**	0.0012	0.0005	0.0013	**0.0010**	0.3422	0.0431	DOWN
SOX9	0.0001	0.0001	0.0001	**0.0001**	0.0001	0.0001	0.0002	**0.0001**	1.2976	0.1467	
SP4	0.0020	0.0022	0.0020	**0.0021**	0.0019	0.0013	0.0013	**0.0015**	0.7264	0.0588	
SSTR5	0.0000	0.0000	0.0000	**0.0000**	0.0000	0.0000	0.0000	**0.0000**	1.0652	0.9121	
STOX2	0.0013	0.0012	0.0007	**0.0011**	0.0011	0.0010	0.0008	**0.0009**	0.8872	0.5910	
TAC1	0.0000	0.0000	0.0000	0.0000	0.0000	0.0000	0.0000	0.0000	No expressed		LOW
TBL1XR1	0.0051	0.0055	0.0044	**0.0050**	0.0045	0.0042	0.0046	**0.0044**	0.8876	0.1735	
TBX1	0.0006	0.0014	0.0008	**0.0010**	0.0005	0.0003	0.0003	**0.0004**	0.3911	0.0775	
TBX2	0.0000	0.0000	0.0000	0.0000	0.0000	0.0000	0.0000	0.0000	No expressed		LOW
TBX3	0.0008	0.0003	0.0012	**0.0008**	0.0014	0.0044	0.0022	**0.0027**	3.4891	0.1092	
TGIF2	0.0045	0.0043	0.0030	**0.0039**	0.0049	0.0056	0.0043	**0.0049**	1.2530	0.1716	
TOX3	0.0008	0.0008	0.0006	**0.0008**	0.0006	0.0002	0.0005	**0.0004**	0.5492	0.0378	DOWN
TP53	0.0084	0.0078	0.0080	**0.0081**	0.0084	0.0087	0.0080	**0.0084**	1.0339	0.3644	
TRIM24	0.0025	0.0027	0.0021	**0.0024**	0.0024	0.0024	0.0022	**0.0023**	0.9583	0.6368	
WHSC1	0.0080	0.0083	0.0052	**0.0072**	0.0056	0.0043	0.0047	**0.0049**	0.6841	0.0935	
YEATS4	0.0038	0.0040	0.0028	**0.0035**	0.0032	0.0032	0.0031	**0.0032**	0.9054	0.4257	
ZFHX1B	0.0071	0.0064	0.0061	**0.0065**	0.0058	0.0031	0.0041	**0.0043**	0.6621	0.0556	
ZHX2	0.0025	0.0023	0.0024	**0.0024**	0.0020	0.0014	0.0018	**0.0017**	0.7172	0.0169	DOWN
ZIC1	0.0017	0.0019	0.0003	**0.0013**	0.0020	0.0004	0.0016	**0.0013**	1.0055	0.9922	
ZIC2	0.0072	0.0079	0.0027	**0.0060**	0.0058	0.0011	0.0033	**0.0034**	0.5718	0.2960	
ZIC3	0.0066	0.0051	0.0031	**0.0049**	0.0047	0.0015	0.0046	**0.0036**	0.7361	0.4226	
ZNF217	0.0093	0.0100	0.0098	**0.0097**	0.0088	0.0104	0.0096	**0.0096**	0.9933	0.9007	
ZNF423	0.0088	0.0084	0.0046	**0.0073**	0.0065	0.0034	0.0043	**0.0048**	0.6525	0.1914	
ZNF462	0.0125	0.0118	0.0109	**0.0117**	0.0116	0.0098	0.0090	**0.0101**	0.8650	0.1502	

9.3 Size, quantification of the concentration and sequence quality of the ChIP-seq samples

Input (Cnt ChIP-seq)

A. Ladder

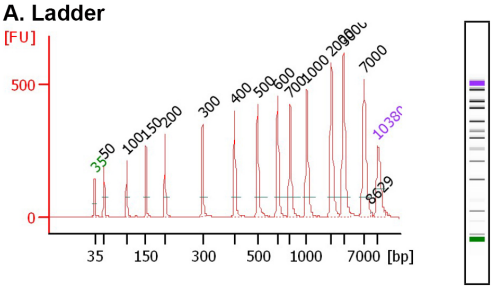

B. Before Amplification

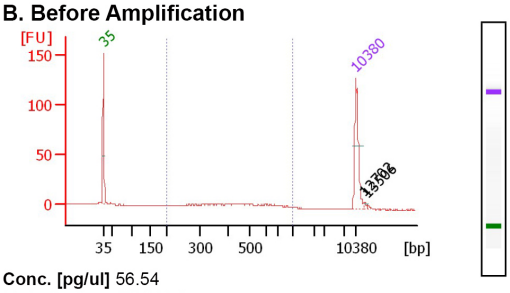

Conc. [pg/ul] 56.54
Molarity [pmol/l] 211.7

C. Post Amplification

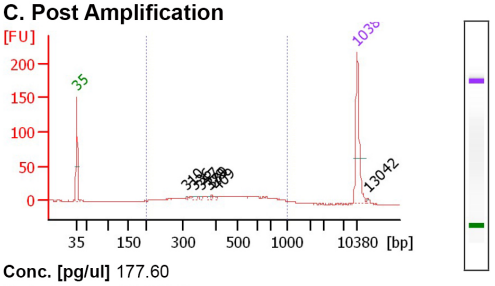

Conc. [pg/ul] 177.60
Molarity [pmol/l] 683.3

D. DNA Library

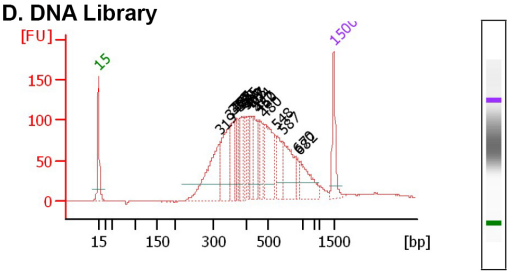

E. Per base quality sequence (Forward)

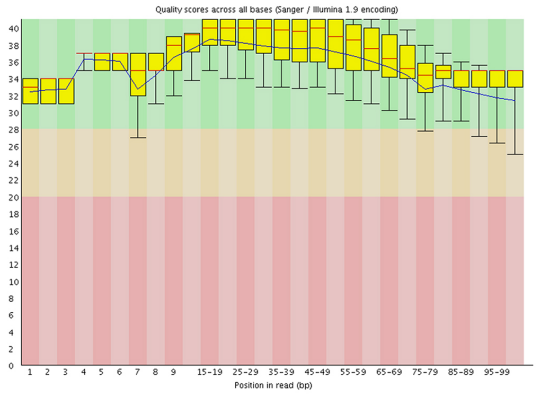

Trimming: 5' 9bp

F. Per base quality sequence (Reverse)

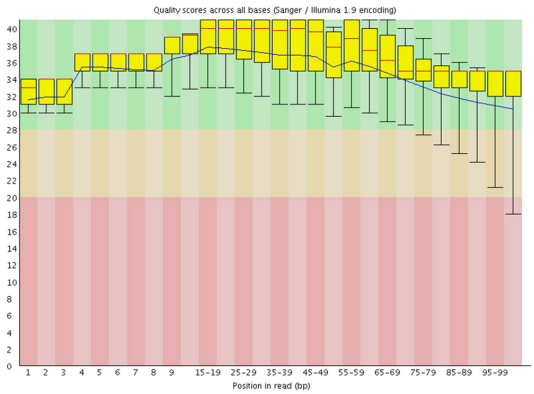

Trimming: 5' 9bp

Extimated duplication: 53%
Uniquely aligned sequences: 19,293,100

H3K4me1 (Cnt ChIP-seq)

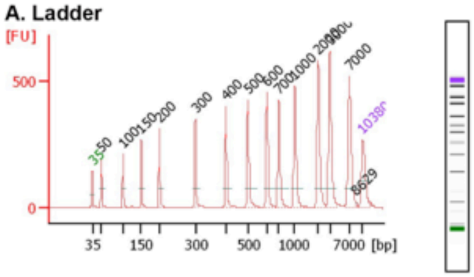

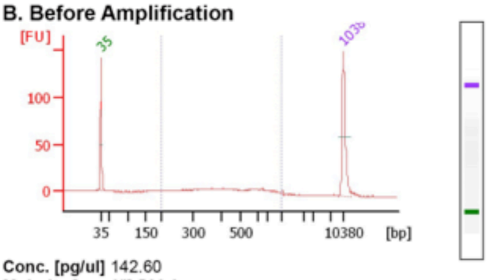

Conc. [pg/ul] 142.60
Molarity [pmol/l] 568.9

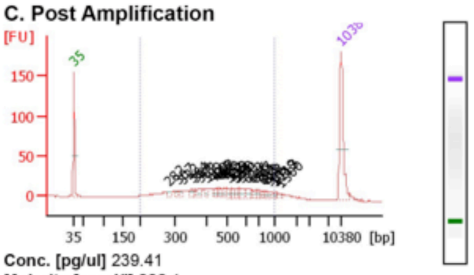

Conc. [pg/ul] 239.41
Molarity [pmol/l] 898.1

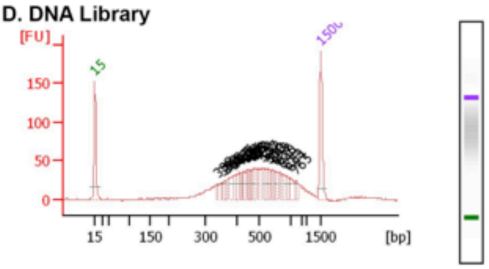

E. Per base quality sequence (Forward)

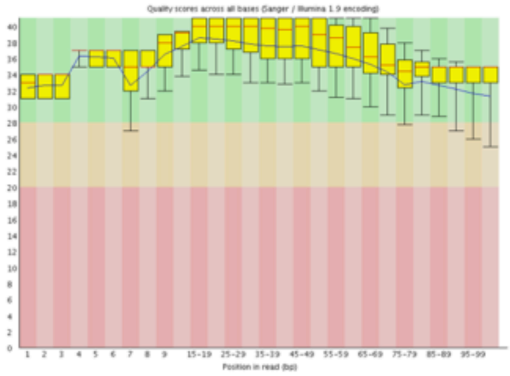

Trimming: 5' 9bp

F. Per base quality sequence (Reverse)

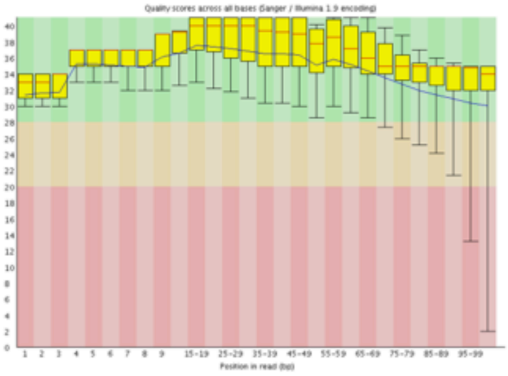

Trimming: 5' 9bp and 3' 5bp

Extimated duplication: 70%
Uniquely aligned sequences: 29,426,130

H3K27ac (Cnt ChIP-seq)

A. Ladder

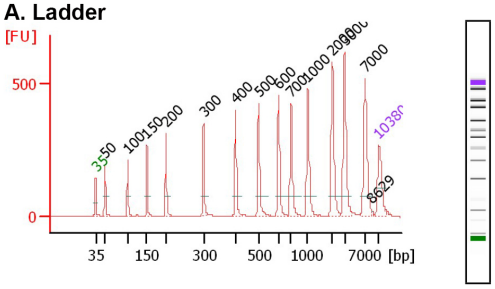

B. Before Amplification

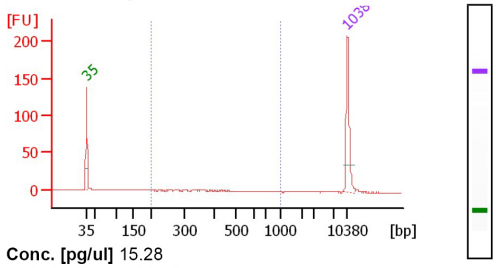

Conc. [pg/ul] 15.28
Molarity [pmol/l] 62.6

C. Post Amplification

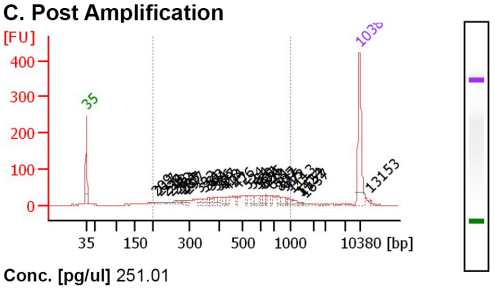

Conc. [pg/ul] 251.01
Molarity [pmol/l] 927.9

D. DNA Library

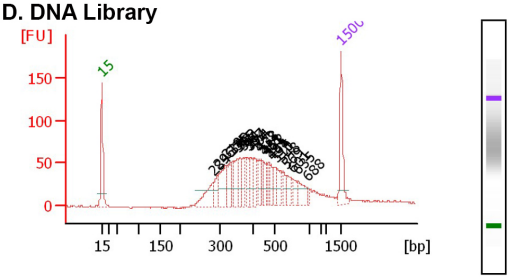

E. Per base quality sequence (Forward)

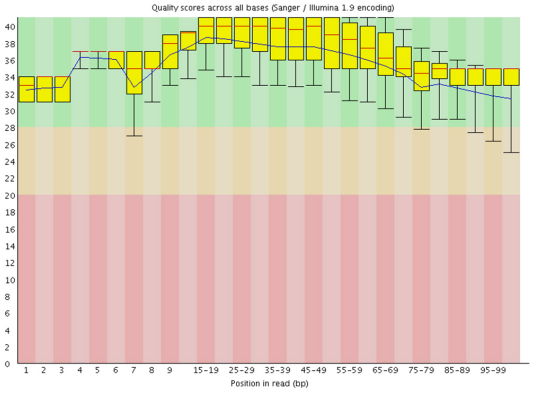

Trimming: 5' 9bp

F. Per base quality sequence (Reverse)

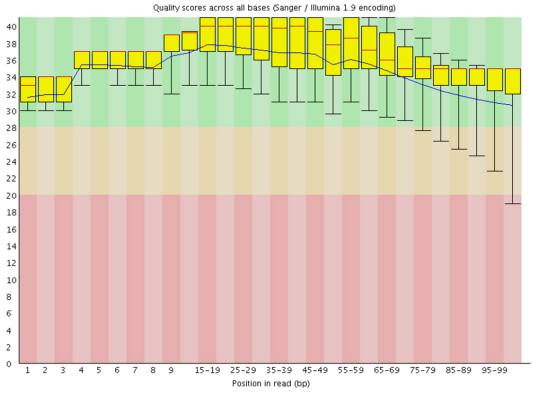

Trimming: 5' 9bp

Extimated duplication: 40%
Uniquely aligned sequences: 45,118,942

H3K27me3 (Cnt ChIP-seq)

A. Ladder

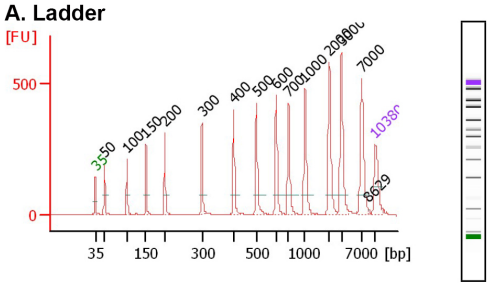

B. Before Amplification

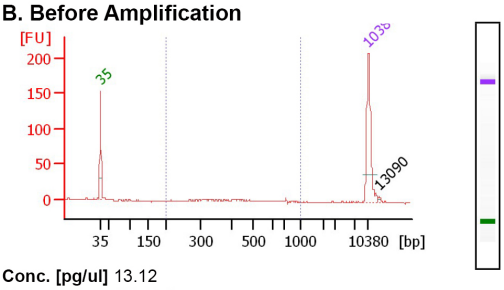

Conc. [pg/ul] 13.12
Molarity [pmol/l] 48.3

C. Post Amplification

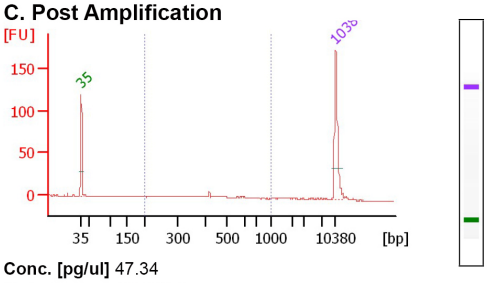

Conc. [pg/ul] 47.34
Molarity [pmol/l] 189.9

D. DNA Library

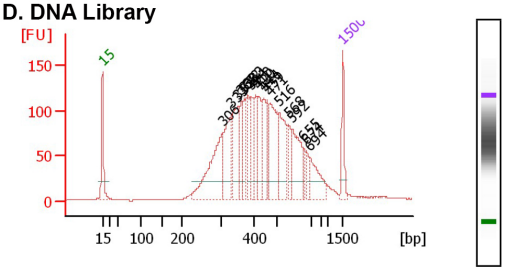

E. Per base quality sequence (Forward)

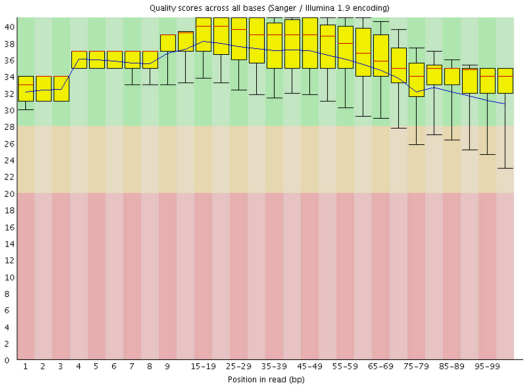

Trimming: 5' 9bp

F. Per base quality sequence (Reverse)

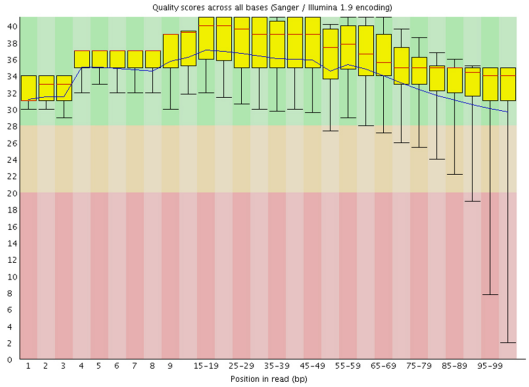

Trimming: 5' 9bp and 3' 10bp

Extimated duplication: 40%
Uniquely aligned sequences: 13,516,136

Input (+FGF ChIP-seq)

A. Ladder

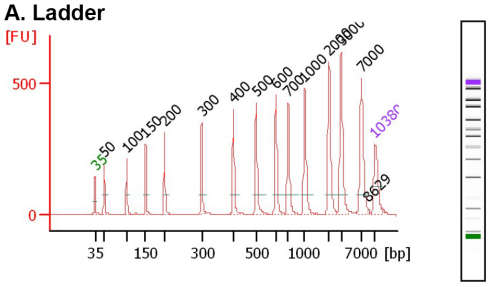

B. Before Amplification

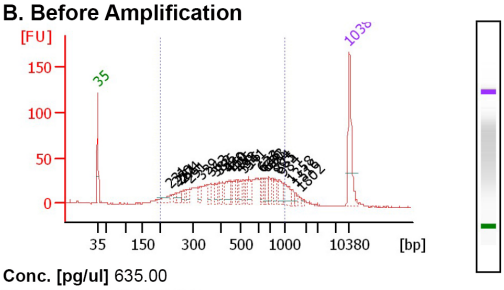

Conc. [pg/ul] 635.00
Molarity [pmol/l] 2,371.5

C. Post Amplification

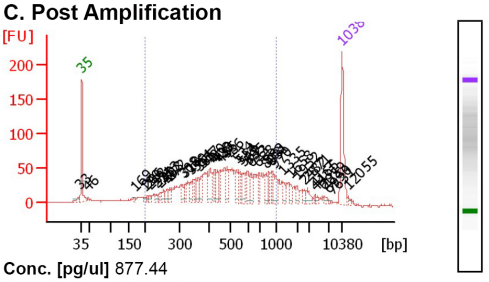

Conc. [pg/ul] 877.44
Molarity [pmol/l] 3,226.6

D. DNA Library

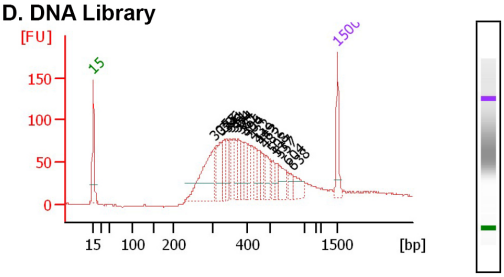

E. Per base quality sequence (Forward)

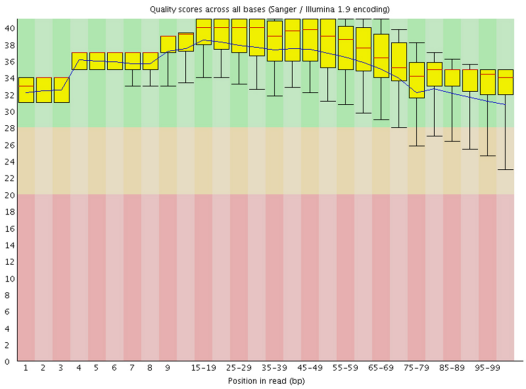

Trimming: 5' 9bp

F. Per base quality sequence (Reverse)

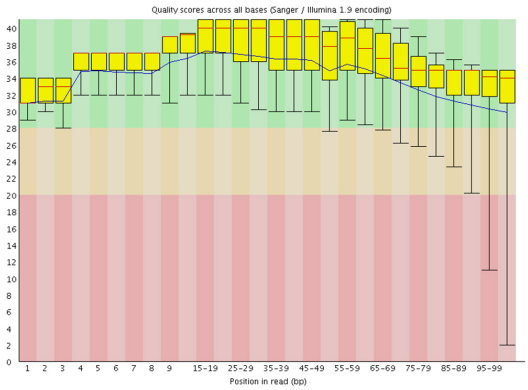

Trimming: 5' 9bp and 3' 5bp

Extimated duplication: 19%
Uniquely aligned sequences: 27,876,916

H3K4me1 (+FGF ChIP-seq)

A. Ladder

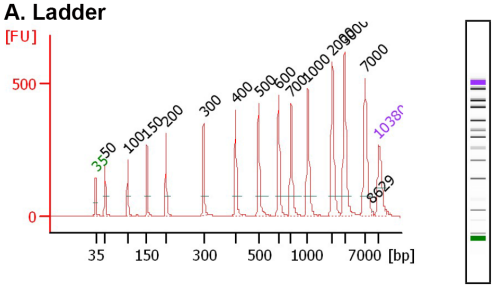

B. Before Amplification

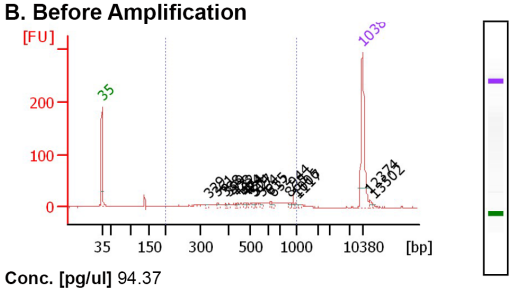

Conc. [pg/ul] 94.37
Molarity [pmol/l] 330.0

C. Post Amplification

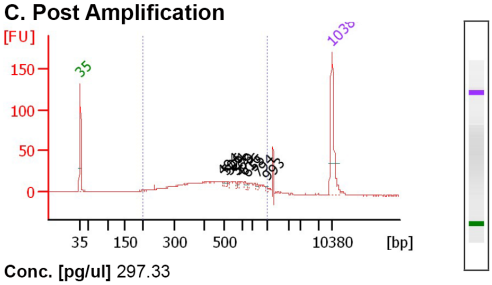

Conc. [pg/ul] 297.33
Molarity [pmol/l] 1,109.8

D. DNA Library

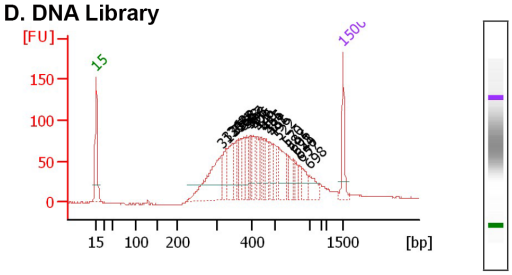

E. Per base quality sequence (Forward)

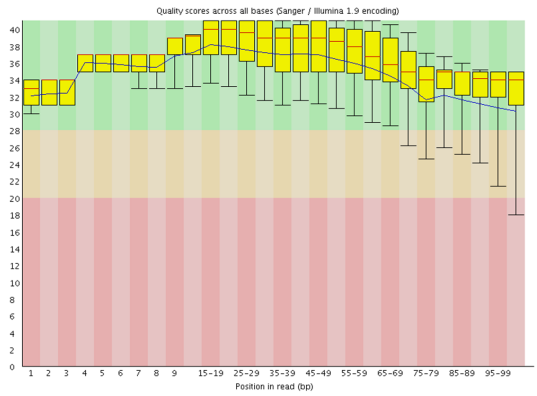

Trimming: 5' 9bp

F. Per base quality sequence (Reverse)

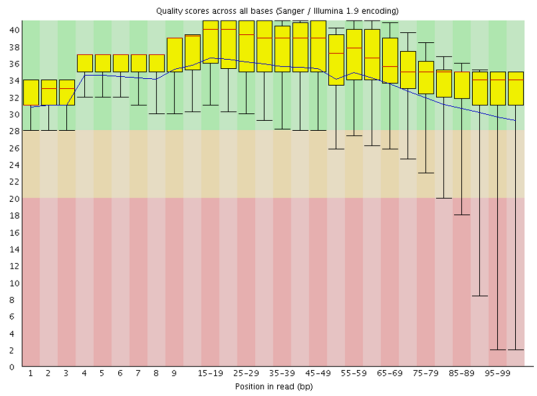

Trimming: 5' 9bp and 3' 15bp

Extimated duplication: 46%
Uniquely aligned sequences: 30,796,840

H3K27ac (+FGF ChIP-seq)

A. Ladder

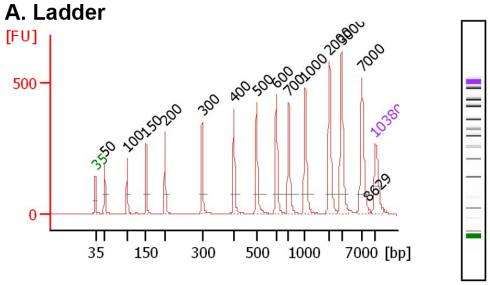

B. Before Amplification

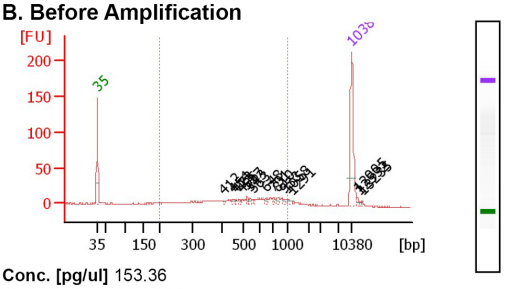

Conc. [pg/ul] 153.36
Molarity [pmol/l] 540.2

C. Post Amplification

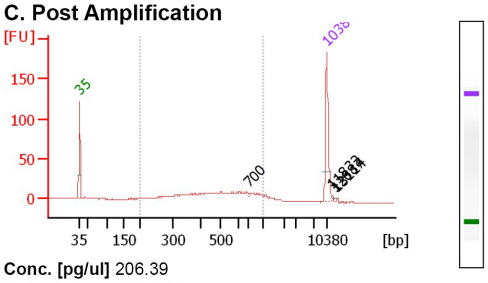

Conc. [pg/ul] 206.39
Molarity [pmol/l] 724.3

D. DNA Library

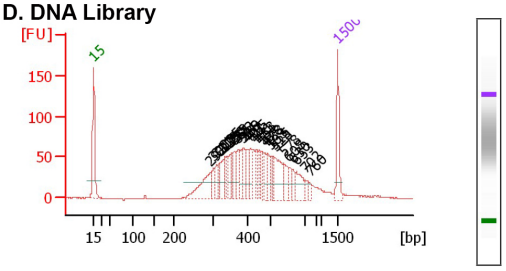

E. Per base quality sequence (Forward)

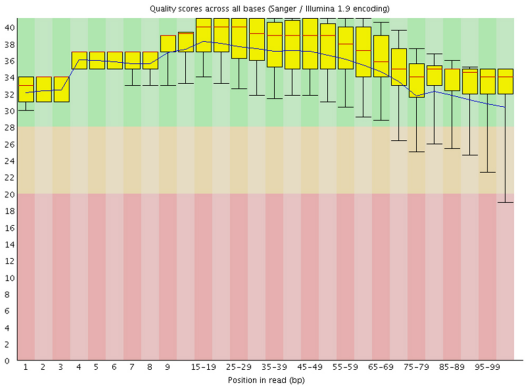

Trimming: 5' 9bp

F. Per base quality sequence (Reverse)

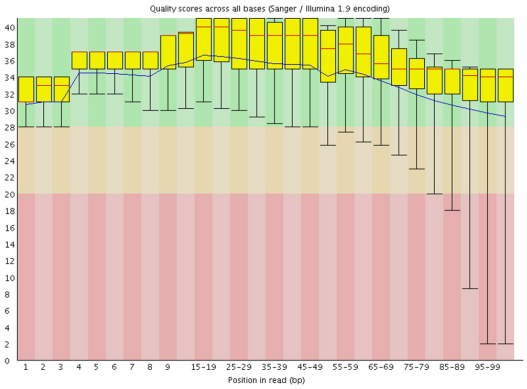

Trimming: 5' 9bp and 3' 15bp

Extimated duplication: 38%
Uniquely aligned sequences: 37,692,634

H3K27me3 (+FGF ChIP-seq)

A. Ladder

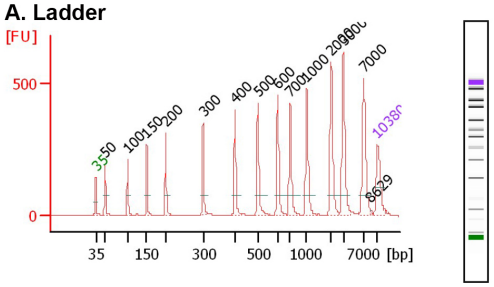

B. Before Amplification

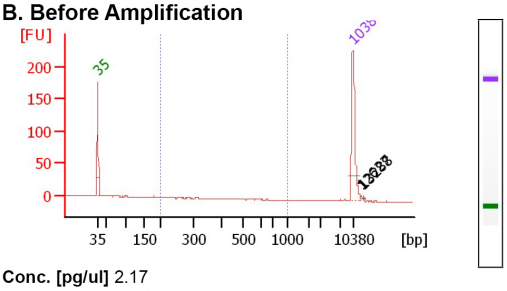

Conc. [pg/ul] 2.17
Molarity [pmol/l] 11.7

C. Post Amplification

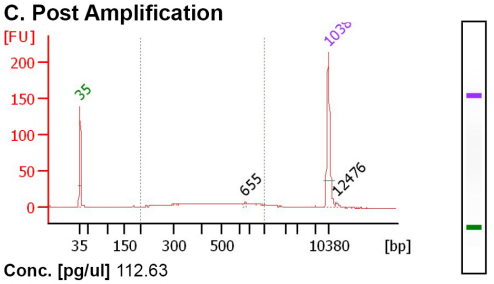

Conc. [pg/ul] 112.63
Molarity [pmol/l] 418.2

D. DNA Library

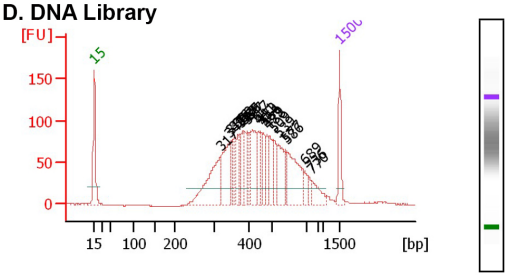

E. Per base quality sequence (Forward)

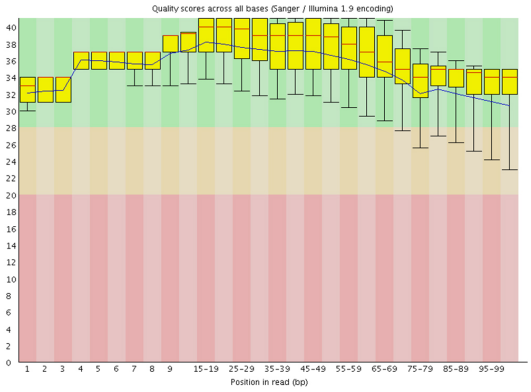

Trimming: 5' 9bp

F. Per base quality sequence (Reverse)

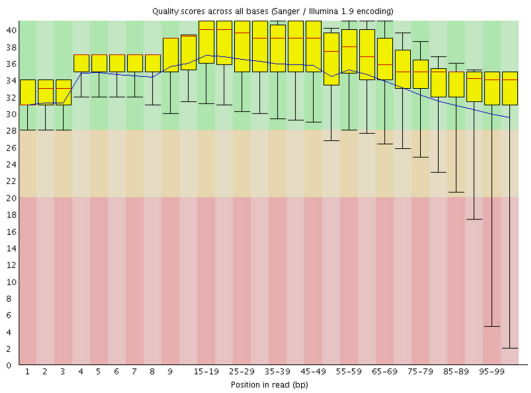

Trimming: 5' 9bp and 3' 10bp

Extimated duplication: 55%
Uniquely aligned sequences: 25,987,262

Figure 9.2 Quantification of the concentration and sequence quality of the ChIP-seq samples.

(A) Ladder profile from Bioanalyser. Estimation of the concentration and size of the pull-down fragments: **(B)** before amplification, **(C)** after amplification and **(D)** post-library preparation. **(E-F)** Plot of the sequence quality obtained by the software FastQC. The x-axis represents the bais-pair (bp) position in the read, while the y-axis rapresents the quality score. Bases with a score falling in the green (score between 40 and 28) and the orange area (score of 28-20) are considered to be optimal however bases in the red area (score below 20) were trimmed. The trimming values from the 5' and 3' are reported below each plot. The first 9bp at 5' were trimmed to avoid contamination of primer/adaptor sequences. Estimation of the percentage of sequence duplication is reported at the end of the figure together with the count of uniquely aligned sequences. At least 10,000,000 reads were unique in each sample; this was sufficient to perform the downstream analysis.